American Journal Of
Engineering Research

AJER

American Journal of Engineering Research

American Journal of Engineering Research

Editorial Board

American Journal of Engineering Research (AJER)

CONTENTS

Analysis and Simulation of Dihydrate Process for the Production of Phosphoric Acid (Reactor Section)

Ms.G.Bharathi kannamma, Dr.D.Prabhakaran, Dr.T.Kannadasan
M. Tech Scholar, Department of Chemical Engineering, Coimbatore Institute of Technology
Associate Professor, Department of Chemical Engineering, Coimbatore Institute of Technology
Professor and Head, Department of Chemical Engineering, Coimbatore Institute of Technology

Abstract: - The simulation model has been examined using experimental data obtained from a phosphoric acid plant. The predicted results are in very good agreement with the experimental data with a relative absolute error of less than 4.2%. To solve the simulation model, sequential modular approach (tearing streams employed) is used to obtain the recycle stream and conversion parameters by employing Genetic algorithm and Standard Least Square Optimization. The effect of various parameters on the conversion has been made to find the optimum operating conditions of the phosphoric acid plant for a given phosphate rock feed flow rate, chemical composition, and particle size distribution. The effect of varying reactor(s) temperature, sulfuric acid feed rate, agitator–impeller speed, ratio of slurry recycle to feed rate, and ratio of return acid to feed rate have been investigated.

Keywords: - *Analysis and simulation, Dihydrate process, Phosphoric acid, Effect of parameters*

I.   INTRODUCTION

Phosphoric acid is an important intermediate chemical product. It is mainly used for the manufacturing of fertilizers. Production capacity for phosphoric acid yielded about 33 million tons of P_2O_5. About 90% of world P_2O_5 consumption involves the fertilizer industry. There is a steadily growing demand for phosphate fertilizers. The phosphoric acid production is directly linked to the phosphate fertilizer consumption. Phosphoric acid is produced in industrial scale when a phosphorous containing mineral reacts with a mixture of sulphuric and phosphoric acids. The main by-product of this reaction is the formation of calcium sulphate (gypsum) crystals, which are separated by filtration from phosphoric acid at the end of the process together with other by-products formed during the reaction. The phosphoric acid production process involves intense interactions among solid and liquid components and is sensitive to a number of factors such as mineral characteristics, reactant compositions and process temperature conditions.

Gioia et al. (1977) developed a mathematical model for the hemi-hydrate process for the production phosphoric acid from calcareous phosphates. The multi-reactor mathematical model is based on material and population balances. The Gioia et al. (1977) model consists of N-CSTRs in series (dissolution–crystallizer reactors). In their model, the phosphate rock, the sulfuric acid and the recycle from the filter (return acid) are all fed to the first reactor. The model remains at a theoretical level as no comparisons are made with industrial or experimental data. The analysis presented in this paper will be based, as much as possible, on the general results and methods of transport phenomena, chemical kinetics, and population balances. The model will then be used to find the operating conditions. The existing published work on phosphoric acid production modeling reveals (Gioia et al., 1977; Shakourzadeh et al., 1980; Yeo et al., 1991; Cho et al., 1996) several common characteristics. However, they fall short of providing design flexibility as they are explicitly oriented towards the design case they are expected to emulate. The sets of mathematical equations employed for the representation of the processing tasks are case-specific, hence requiring the manual addition of terms in case that new design options (i.e. streams, materials, processes, etc.) are considered in the performed design calculations.

In this present work simulation modeling has been used and model-based computer program developed to simulate a three-CSTR pilot plant leaching process of phosphate rock with sulfuric acid and recycled phosphoric acid for the production of phosphoric acid and precipitation of calcium sulfate di-hydrate as a

byproduct. To solve the simulation model, sequential modular approach method is used to obtain the recycle stream and conversion parameters by employing Genetic algorithm and Standard Nonlinear Least Square Optimization. The effect of various parameters on the conversion has been made to find the optimum operating conditions of the phosphoric acid plant for a given phosphate rock feed flow rate, chemical composition, and particle size distribution.

II.   PROCESS DESCRIPTION

Almost all phosphoric acid needed for the fertilizer industry is produced by wet processes. In many of these processes, the raw phosphate ore is converted into phosphoric acid and calcium sulfate di-hydrate (gypsum) by adding a mixed solution of sulfuric and phosphoric acids to the reactor. The main process used in industrial practice for phosphoric acid production is the "wet method", which includes single-stage and re-crystallization processes. The single-stage processes consist of a single reaction-crystallization step and the most common routes for phosphoric acid production in this case are the di-hydrate and hemi-hydrate processes. Using the wet method, phosphoric acid is produced in reactors that facilitate the mixing and contact of phosphate rock with an aqueous solution of sulfuric and phosphoric acid. The phenomenon can be described by the following two-stage reaction:

$$Ca_3(PO_4)_2 \cdot CaF_2 + 6H_3PO_4 \rightarrow 4Ca(H_2PO_4)_2 + 2HF$$
$$Ca(H_2PO_4)_2 + H_2SO_4 + nH_2O \rightarrow 2H_3PO_4 + CaSO_4 \cdot nH_2O$$
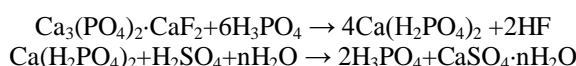
Where, the gypsum product can be di-hydrate (n = 2), hemi-hydrates (n = 0.5) or anhydrite (n = 0).

However, many other side reactions are involved, among which is the reaction of calcium carbonate whose content in the phosphate rock determines to a great extent the crystal size of the apatite. In the first stage hydrogen ions from recycled phosphoric acid attack the phosphate ore particles (represented by fluorapatite) to form mono-calcium phosphate ($Ca(H_2PO_4)_2$). In the second stage, the formed mono-calcium phosphate reacts with sulfuric acid to form phosphoric acid and insoluble calcium sulfate (gypsum). As the phosphate ore particles dissolve in the reactor, super-saturation of calcium sulfate occurs, leading to gypsum crystallization that involves phenomena such as nucleation and crystal growth. The slurry produced from the reaction section is lead to a filter where the solid calcium sulfate crystals are mechanically separated from the produced liquid phosphoric acid. As the phosphate ore particles dissolve in the reactor, supersaturation of calcium sulfate occurs, thereby leading to gypsum crystallization that involves both nucleation and crystal growth. The form in which the calcium sulfate crystallizes (i.e., type of process) depends on the reaction temperature and on the acid concentration in the reaction system itself. At a temperature range of 70–80°C and moderate acid concentrations, the calcium sulfate crystallizes in the gypsum (di-hydrate: $CaSO_4.2H_2O$) form, as it is the case in this work. At higher acid concentrations and temperatures (>80°C), the hemi hydrate CaSO4.2H2O formed, and at still higher acid concentrations and temperatures (90–100°C), the anhydrite ($CaSO_4$) is formed.

1.1. Analysis of the Di-hydrate Wet Process

The mathematical model used in this work represents a 10–16 kg/h capacity pilot plant used to produce phosphoric acid by the di-hydrate process. The pilot plant consists of three isothermal CSTRs (R_1, R_2 and R_3) and one filter–feed tank (R_4), all connected in series. The suspension mixture overflows from one reactor to another. These reactors represent the core of the plant where chemical reactions, crystallization, and other phenomena take place. The reactant fluid that is made of a suspension of solid particles in a liquid is kept under relatively high speed of agitation in order to keep even the largest particles suspended.

The experimental set-up for the di-hydrate process is shown in Figure 1. It consists mainly of three subsystems: the feeding, reaction, and filtration subsystems. The feeding subsystem consists of two parts: one for the phosphate ore and the other for sulfuric acid feed and recycle phosphoric acid to the reactor. The four tanks are interconnected via the recycle slurry pump in order to ensure perfect mixing inside the reaction section (which will be considered as a continuous stirred tank reactor (CSTR) during the theoretical analysis and modeling). The filtration section receives the hot slurry in order to produce the final required phosphoric acid and at the same time enables the successive washing operation of the cake to enhance the P_2O_5 recovery and to handle the recycle acid (return acid) required by the reaction subsystem.

The phosphate rock feed (F_F) is fed to the first reactor (R_1). Sulfuric acid feed (F_A) and return acid from the filter (F_R) are mixed together in a mixing box and introduced into the third reactor (R_3). In this way, most of the water soluble P_2O_5 losses can be recovered back into the process by circulating part of the dilute filtrate (acid) back to previous stages of filter washing and the remaining part for the dilution of concentrated sulfuric acid feed before it enters the reactor(s). As recommended, large amount of slurry (F_{RS} is recycled from the third reactor to the first. The fluorine gas evolved during reaction (as SiF_4 and HF) as well as CO_2 gas coming from decomposition of carbonates and oxidation of organic matter are vented to the atmosphere or discarded to a suitable scrubbing system in industrial plants. The overall gas mass flow rate from reactor or tank j is $V_g(j)$. CO_2 gas may form

some kind of foam on the reaction surface in the reactors, so a defoamer is added in small amounts to control the foam formed during processing. The output stream from the third reactor, F_3, is introduced to the filter feed tank (R_4), which provides a constant head of slurry for the filtration process. A stream of makeup water, F_V, may be added to compensate for water losses through evaporation from the reactors (no makeup water is used here). Washing water, F_W, is added to the filter, which is the last step in the process, where gypsum stream, F_G, and product acid stream, F_P, are obtained. Some of the product acid is recycled as a return acid, F_R, to the third reactor (R_3) as mentioned before for reaction initiation. No additional cooling by artificial means (air or vacuum cooling) is required here, because the excess heat released from the reactions is just sufficient to cover the natural heat loss.
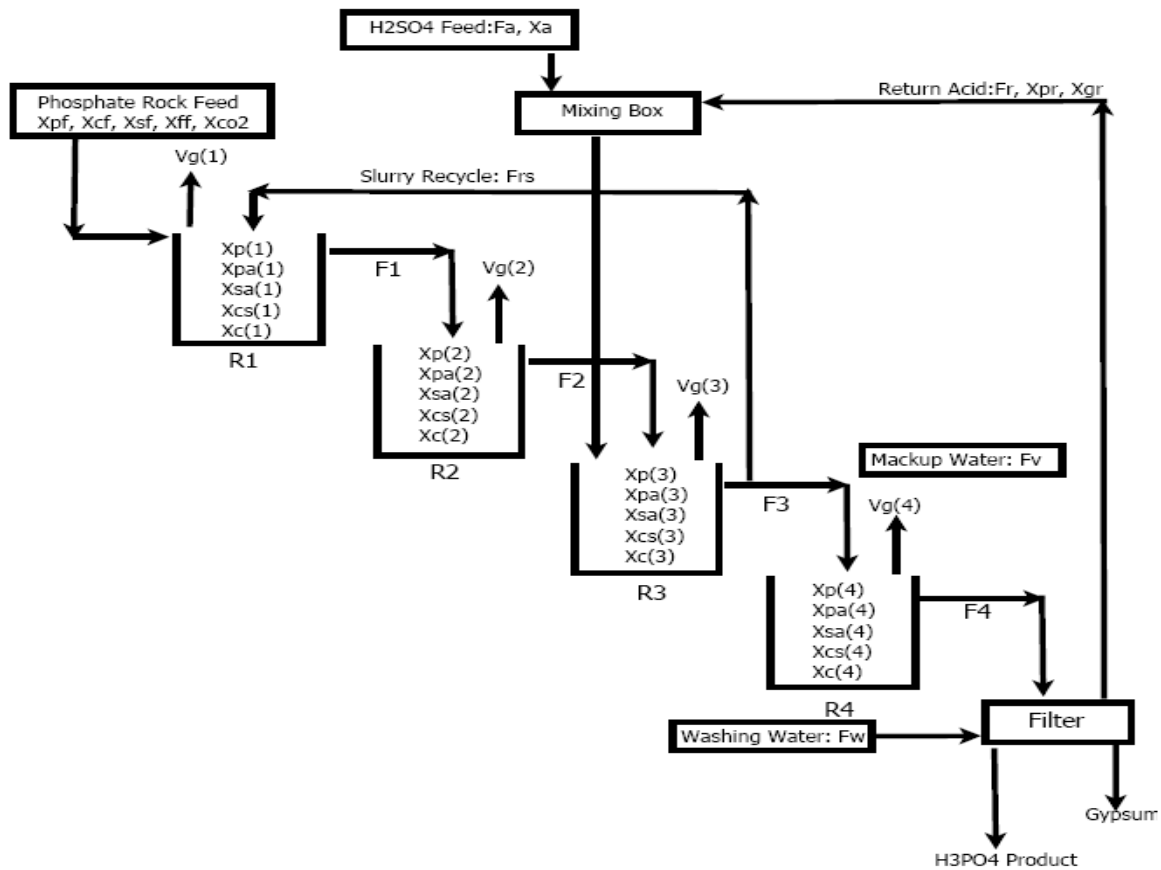
Fig. 1. Flow sheet for the pilot plant production of phosphoric acid

1.2. Model Formulation

The process consists of a reaction on the phosphate particles by sulfuric acid producing a solution mainly composed of calcium sulfate and phosphoric acid. The stoichiometry of the overall dissolution reaction depends on the chemical composition of the phosphate rock. The calcium sulfate separates by crystallizing as $CaSO_4.2H_2O$ if the values of the temperature and composition (H_3PO_4 and H_2SO_4) existing in the solution. The reactant fluid is made up of a suspension of solid particles in a liquid (slurry), the use of continuous stirred tank reactors (CSTR) is most appropriate. In this work, we are mainly interested in the reactor–crystallizer where dissolution and crystallization take place.

A flow pattern characterized by perfect macro-mixing and segregation for solid particles has been postulated. Perfect macro-mixing implies an exit age distribution function, $E_j(t)$ given by

$$E_j(t) = \frac{1}{t_{avg}} \exp\left(\frac{-t}{t_{avg}}\right) \tag{1}$$

Where t is the dissolution time of a single particle (h). t_{avg} is the mean residence time (h) defined as "mass of slurry in reactor j/mass flow rate of suspension to reactor j

$$t_{avg} = \frac{m}{W_s} = \frac{\rho V}{W_s} \tag{2}$$

Where, m is the mass of slurry in reactor (kg), W_s the total mass flow rate into reactor (kg/h), V the reactor volume (m^3), and ρ the density of reaction mixture (kg/m^3).

1.2.1. Dissolution Mechanism

The phosphate rock particles are spherical in shape, one can visualize the following steps occurring during the dissolution of the phosphate rock

i) At the solid/liquid interface, the salts that are contained in the mineral dissolve and dissociate. At this interface, thermodynamic equilibrium whose conditions are regulated by the solubility products is postulated.

ii) The reactant H^+, derived from H_2SO_4 dissociation, diffuses from the core of the liquid toward the liquid/solid interface.

iii) H^+ ions react with the main constituents of the rock. Neglecting other minor reactions, the main reactions taking place in the liquid phase are

$$PO_4^{3-} + 3H^+ \longrightarrow H_3PO_4$$
$$F^- + H^+ \longrightarrow HF$$
$$CO_3^{2-} + 2H^- \longrightarrow H_2CO_3$$
$$H_2CO_3 \longrightarrow H_2O + CO_2$$
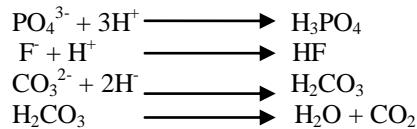
All reaction products diffuse back into the main body of the liquid.

The above reactions occur by proton transfer mechanism and therefore can be assumed to be instantaneous with respect to diffusion. The overall dissolution process is thus controlled by the diffusion of reactants toward a reaction plane. This situation is analogous to that encountered in the process of gas absorption with instantaneous chemical reaction.

1.2.2. Mass Transfer Co-efficient

$$\ln\left(\frac{2rK_L(r)}{D_v Sc^{0.33}}\right) = 0.479\ln\left(\frac{6r}{D_T}\right) + 0.359\ln Re - 0.533 \qquad (3)$$

$$K_L\left(\frac{D_T^{0.479}}{0.69219 D_v Sc^{0.33} Re^{0.359}}\right) = \left(\frac{1}{R_{avg}}\right)^{0.521} \qquad (4)$$

Here $r = R_{avg}$

$$B = \frac{0.69219 D_v Sc^{0.33} Re^{0.359}}{D_t^{0.479}} \qquad (5)$$

Substitute (5) in (4)

$$K_L = B\left(\frac{1}{R_{avg}}\right)^{0.521} \qquad (6)$$

1.2.3. Dissolution Time for Single Particle

$$t = \frac{-\emptyset_M \rho_M \, \alpha}{C_{SA}(j)} \int_{R_{avg}}^{r} \frac{dr}{K_L} \qquad (7)$$

$$A = \frac{-\emptyset_M \rho_M \, \alpha}{C_{SA}(j)} \qquad (8)$$

The shape factor is defined here as the ratio of the surface area of a sphere of volume equal to that of the particle to the surface area of the particle. The value here accounts for all species in the phosphate rock that react with sulfuric acid

Substitute A and B in equation in (7)

$$t = \frac{A}{B}\int_{R_{avg}}^{r} r^{0.521} dr$$

$$t = 0.65746\frac{A}{B}\left(r^{1.521} - R_{avg}^{1.521}\right) \qquad (9)$$

$$U_t = 0.6574\frac{A}{B} \qquad (10)$$

For Complete Dissolution $r = 0$, $t = T_R$

$$T_R = -U_t R_{avg}^{1.521} \qquad (11)$$

The conversion degree, X, for a single spherical particle is given by

$$1 - x = \left(\frac{r}{R}\right)^3 \qquad (12)$$

For particles of common radius R entering reactor j, the degree of conversion is given by

$$X_j(R) = 1 - \int_0^\infty (1 - X_j) E_j(t) dt \qquad (13)$$

$$= 1 - \int_0^{T_R} \left(\frac{r}{R}\right)^3 E_j(t) dt \qquad (14)$$

By considering the size distribution of the feed, the actual degree of conversion in reactor j is given by

$$X_j = 1 - \int_0^{R_{max}} f_{j-1}(R) \left\{ \int_0^{T_R} \left(\frac{r}{R}\right)^3 E_j(t) dt \right\} dR \qquad (15)$$

The input size distribution function, can be approximated by

$$f_0(R) = e^{-R^\beta} \int_{R_{min}}^R e^{t^\beta} dt \qquad (16)$$

The exponent is a constant characteristic of particle size distribution (β in this work is assumed to be equal to unity). R_{min} and R_{max} (the minimum and maximum radii of the particles) are to be evaluated from the size distribution of the actual feed.

$$f_0(R) = e^{-R} \int_{R_{min}}^R e^t dt \qquad (17)$$

$$E_j(t) = \frac{1}{t_{avg}} \exp\left[-U_t \frac{(r^{1.521} - R_{avg}^{1.521})}{t_{avg}} \right] \qquad (18)$$

Differentiating and substituting (17) and (18) in equation (15), the conversion is

$$= \left[\begin{array}{c} \int_0^{R_{max}} e^{-R} \left\{ 1 - \exp\left(U_t\left(R_{min}^{1.521} - R^{1.521}\right)\right)\right\} \int_R^0 \frac{1.521 U_t}{t_{avg}} \left(\frac{r}{R}\right)^3 r^{0.521} \\ \exp\left(\frac{-U_t(r^{1.521} - R^{1.521})}{t_{avg}}\right) dr dR \end{array} \right]$$

III.   ANALYSIS OF RESULTS AND DISCUSSION

The parametric study carried out in this work using the pilot plant mathematical model and presented below, covers the effect of reaction temperature, sulfuric acid feed flow rate, agitator–impeller speed, and slurry recycle and return acid flow rates. Table 1 shows some model-predicted results vs. pilot-plant experimental data. It is clear that the predicted values are close enough to the experimental data and the absolute relative error range is 0.4–4.2%.

Table 1. Comparison between Experimental values and Model values

QUANTITY	EXPERIEMENTAL VALUE	MODEL VALUE	RELATIVE ERROR
H_3PO_4 Mass Fraction	0.4095	0.3919	4.2979
H_2SO_4 Mass Fraction	0.0355	0.0347	2.2535
$CaSO_4$ Mass Fraction	0.2881	0.2853	0.9718
CaO Mass Fraction	0.0050	0.0049	0.4000
Conversion, X_3	97.5000	95.1300	2.4307

3.1. Effect of Reaction Temperature

The temperature range of 70–80∘C has been considered here, since as mentioned earlier, the calcium sulfate crystallizes in the di-hydrate form in this range. The overall conversion of the process, represented by conversion in Reactor 3, only slightly increases with the increase in temperature. The effect of temperature on calcium sulfate formation in Reactor 3 is more pronounced, the rate of formation of calcium sulfate start high then reaches a steady value as temperature increases. This is due to the fact that a calcium sulfate layer formed on the outer surface of the phosphate particles hinders the rate of reaction. The Figure 2 shows clearly the effect of temperature on conversion in reactor 3.
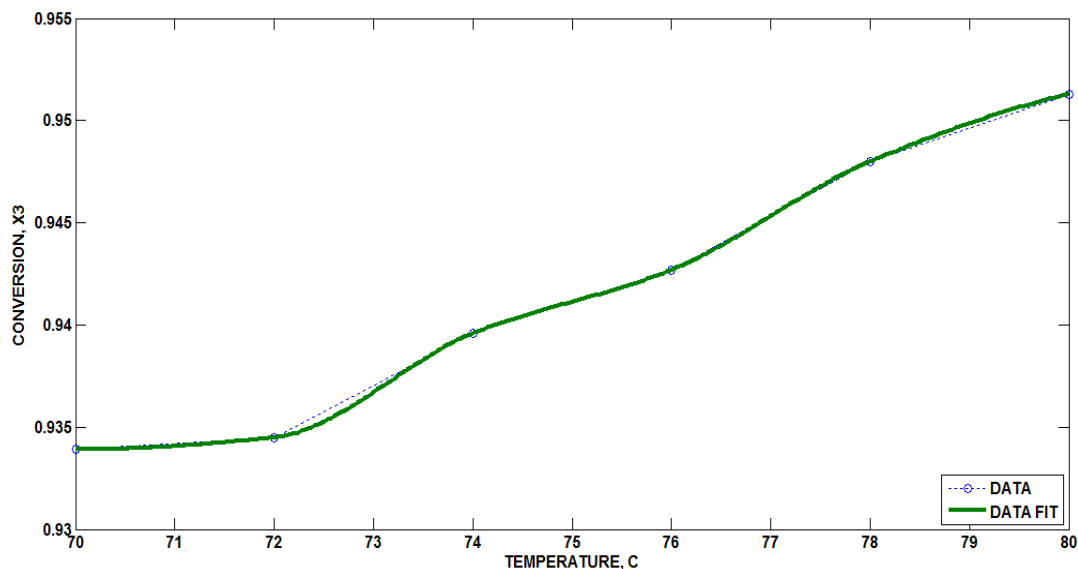
Fig.2. Effect of temperature on conversion in reactor 3

3.2. Effect of Agitator–Impeller Speed

It is expected that by increasing the agitator–impeller speed the dense layer coating the phosphate rock core to break down and it will be removed by the reaction solution. This will give the phosphate core further chance to react and cause the rate of reaction as well as the overall conversion to increase. Upon increasing the impeller speed from 5000 to 10 000 rph, X_3 increased from 94.1 to 95.7% (see Fig. 3). As a result, the complete dissolution time of a single phosphate particle decreased from 0.84 to 0.66 min when the impeller speed was increased from 5000 to 10000 rph. On the other hand, increasing the impeller speed will bring the calcium sulfate crystals to collide with each other thus forming larger crystals with higher nuclei population densities increasing the crystal growth rate to a higher limit will make filtration harder and consumes a lot of power. Also filtration rate decreases with the increase of nucleation rate.
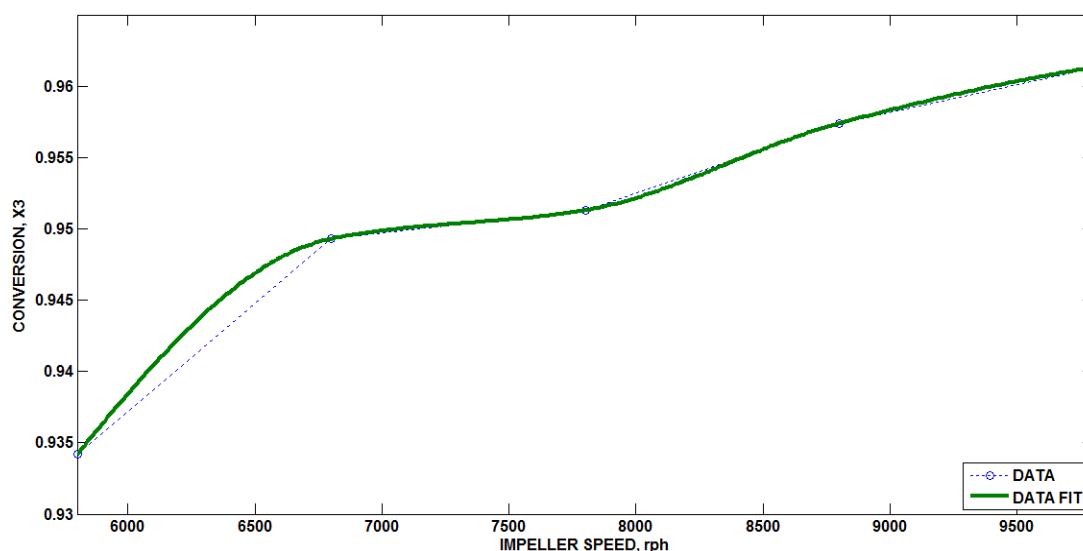
Fig.3. Effect of impeller speed on conversion in reactor 3

3.3. Effects of Slurry Recycle Flow Rate

Upon increasing the slurry recycle flow rate, it has been noticed from Figure 4 that the overall conversion, phosphoric acid concentration increase until they reach some upper limit, after which the dense calcium sulfate layer probably coats the phosphate rock core thus preventing the acid solution from reaching the core surface. The effect of slurry recycle on the complete dissolution time of a single phosphate particle in Reactors 1 and 3 is clear that this dissolution time is sharply decreasing for Reactor 1 and almost constant for Reactor 3, and it becomes almost constant at higher slurry recycle flow rates of about 700 kg/h and above.
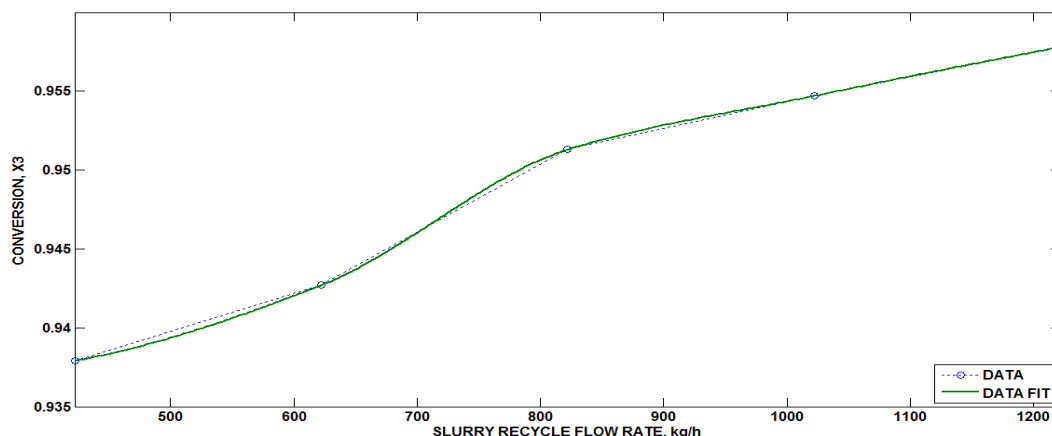
Fig.4. Effect of slurry flow rate on conversion in reactor 3

3.4. Effect of Return Acid Flow Rate

The return acid from the filter, whose composition is mainly phosphoric acid (about 18.4% P_2O_5) is very important for the initiation of the reaction. It reacts with the phosphate rock to form a soluble mono-calcium phosphate compound which in turn reacts with sulfuric acid to form phosphoric acid and calcium sulfate. By increasing the return acid flow rate, the reaction rate will increase until it reaches a maximum, beyond which rock blinding occurs and the particles are prevented from further reaction with the acid solution. Conversion in Reactor 3 has been obtained, as shown (at F_{RA} between 24 and 32 kg/h). The same is true for the dissolution rate of the phosphate rock as shown. The complete dissolution time of a single particle has a flat minimum for the same return acid flow rate range. The Figure 5 shows clearly the impact of return acid flow rate in conversion in reactor 3.
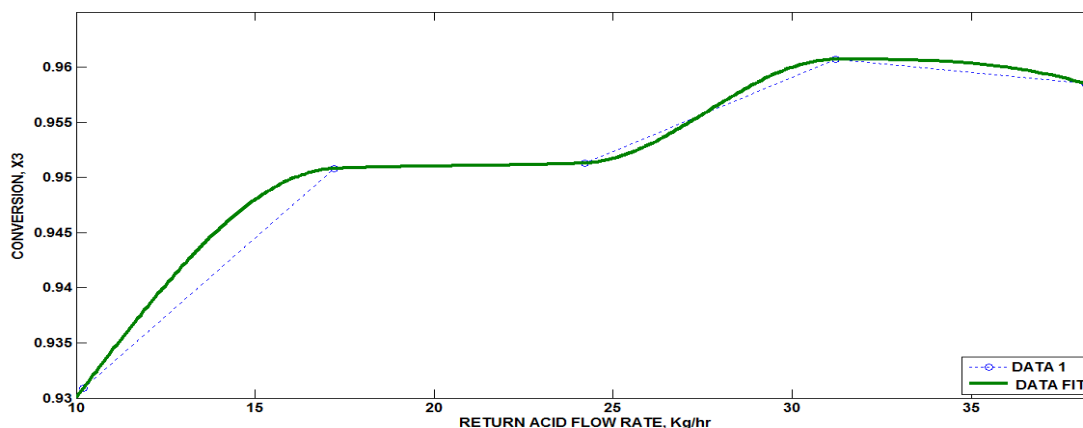
Fig.5. Effect of return acid flow rate on conversion in reactor 3

IV.   CONCLUSION

In this present work a model-based computer program is developed to simulate a three-CSTR pilot plant leaching process of phosphate rock with sulfuric acid for the production of phosphoric acid and precipitation of sulfate di-hydrate as a byproduct. This work is an illustration of the application of the principles of chemical engineering to the analysis of real processes. Solving this simulation model has showed that, the knowledge of these principles is sufficient to get a reasonable description of what is going on in the "real life" process. This kind of work is very important in saving time and effort required for conducting pilot plant or industrial plant experiments. The model equation is solved by employing genetic algorithm (GA) followed by standard nonlinear least square (lsqnonlin) optimization method. The results of the simulated model have been found to represent the behavior of the process in a very good manner, with an absolute relative error of less than 4.2% from real pilot plant results. Effects of the recycle acid from washing filter cake and the slurry recycle ratio were examined.

For the specific feed studied in this work, a reactor temperature of 80°C, a slurry recycle to feed ratio of 80, and a return acid to feed ratio of 2.5 have been found to give best results. The optimum conditions for sulfuric acid feed rate and agitation speed as operating parameters, are determined only from power limitations and the economics of the plant itself. The effect of initial size of phosphate rock particles on coating is not considered in this work. This may be considered as future investigation.

REFERENCES

[1]. R.L. Gilbert, and E.C. Moreno, Dissolution of phosphate rock by mixtures of sulfuric and phosphoric acids, Ind. Eng. Chem. Process. Des. Dev., 4 (1965), 368–371.

[2]. A.B. Amin, and M.A. Larson, Crystallization of calcium sulfate from phosphoric acid, Ind. Eng. Chem. Process. Des. Dev., 7 (1968), 133–137.

[3]. F. Gioia, G. Mura and A. Viola, Analysis, simulation, and optimization of the hemihydrate process for the production of phosphoric acid from calcareous phosphorites, Ind. Eng. Chem. Process. Des. Dev.,16 (1977), 390–399.

[4]. K. Shakourzadeh, R. Bloise and F. Baratin, Modeling of a wet-process phosphoric acid reactor: influence of phosphate rock impurities, in: Proceedings of the Second International Congress on Phosphorus Compounds, April 21–25, (1980), Boston, MA, 443–455.

[5]. M. Jansen, A. Waller, J. Verbiest, R.C. Van Landschoot and G.M. Van Rosmalen, Incorporation of phosphoric acid in calcium sulphate hemihydrate from a phosphoric acidprocess ,Industrial Crystallization, Vol. 84, Elsevier, Amsterdam, 1984.

[6]. P. Becker, Phosphates and Phosphoric Acid Raw Materials, Technology and Economics of the Wet Process, 2nd ed., Marcel Dekker, NY, 1989.

[7]. Y.K. Yeo, Y.S. Cho, W.H.B. Park and K. Moon, Simulation of the dehydrate process for the production of the phosphoric acid, Kor. J. Chem. Eng., 8 (1991), 23–32.

[8]. T.F. Al- Fariss, S.M. Abdul Razik, Nayef M. Ghasem, F. A. Abdelaleem and Said S. E. H. Elnashaie, Computer program for the mass and heat balance calculations for the wet process phosphoric acid (hemi-hydrate) and its applications to Saudi phosphate rock, fertilizer research, 35 (1993), 169-175.

[9]. Y.S. Cho, Y.K. Yeo, W.H.B. Park and K. Moon, Modelling and simulation of a wet hemihydrate phosphoric acid process, Kor. J. Chem. Eng., 13 (1996), 585–595.

[10]. P.M. Mathias, C. Chau-Chyun and M.Walters, Modelling the complex chemical reactions and mass transfer in a phosphoric acid reactor, in: Proceedings of the Joint China/USA Chemical Engineering Conference, Beijing, China, 2000.

[11]. S.I. Abu-Eishah and N.M. Abu-Jabal, Parametric study on the production of phosphoric acid by the dehydrate process, Chem. Eng. J., 81 (2001), 231–250.

[12]. O. Bennouna and T. Bounahmidi, Steady State Simulation of Phosphoric acid Concentration Process, Marcel Dekker, Inc, 2002.

[13]. Athanasios, Papadopoulos and P. Seferlis, Generic modelling, design and optimization of industrial phosphoric acid production processes, Chemical Engineering and Processing, 48 (2009), 493–506.

Research Paper   Open Access

Using of natural patterns in urban design &planning (Case study: Mashhad meddle area)

Mohammad rahim Rahnama, Samaneh Sherkat, Mohammad Homaeefar
Assistant Professor Geography &Urban Planning department, Ferdowsi University, Mashhad, Iran
PhD Scholar Department of Geography &Urban Planning, Ferdowsi University, Mashhad, Iran
PhD Scholar Department of Geography and Urban Planning, Ferdowsi University, Mashhad, Iran

Abstract: - Meddle area of Mashhad is important area due to gardens, macro land uses and open & green spaces. Using of natural adaptable patterns in order to promoting urban environmental quality. Also have been done comprehensive and master plans in order to improving quality. The purpose of research is improving urban environmental quality and creating relation between natural structure and spatial –physical structures. Research method is "descriptive- analyzed". The process of research is analyzing of some patterns such as: mosaic pattern, branch pattern and etc. on the other hand, has been tried, determination better factor for approaching sustainable city. Analyzing natural pattern is important for strengthening urban factors. The findings show, using from forms, physical structure, and natural shape create appropriate urban environment.

Keywords: *natural models, branch pattern, background pattern, mosaic pattern, native city, west central area*

I.   INTRODUCTION

Natural environment has been concluded from all of elements, natural process in every aspects such as landscape and viewpoint, shape of earth, plant cover and etc. also , it could be analyzed as value models such as basic models , earth shape model , landscape model , ecosystem model and etc (bell , 1999: 26) . These models and process have value factors, such as sustainability, various, beautifully and etc. so, they are as the best models. Indeed, natural environment, viewpoints create peaceful spaces (Lang, 2003: 87).

Cites growth inharmonious, due to developing and physical changes. So, there aren't physical environment quality in our cites. This process has been resulted physical and spatial models. Today, physical models don't support quantity and quality condition for residents. Thus, physical changes, decrease environment quality and create many problems (mehdizadeh, 2004:105). Cities haven't value spaces due to don't applicability with needs of residents, requests and behaviors models, also don't applicability with environmental and natural conditions. Also don't use from natural factors such as viewpoint, sun and etc.

The main problem is mentioned criteria and values in design models and urban planning, don't provide needs of residents both quality and quantity aspects. On the other hand, it decreases quality of natural environment (special in large cities). There are reduction of quality in many cites. They are:

Don't use from values and opportunity of natural environment such as winter ray, don't appropriate urban infrastructure especial in transportation , don't exist urban security system in crisis condition such as sail , earthquake , don't responsibility functional spaces and etc . They are begging new problems in cites now.

In this research, have been studied better models in design and urban planning that adapt with natural models in city. There are many gardens and land uses in Middle area in Mashhad. So this district has appropriate potential for creating open and green spaces that adapt by natural condition.

Research purpose

Total purpose in this research is, adapting physical condition of middle district with natural models in urban planning and urban design. So subdivided are:
-    introducing various natural models in urban planning and urban design
-    Measuring, compatibility of middle area by mentioned models.

- Proposing appropriate model for middle area in Mashhad.
-

Research method
This research is "descriptive –analytical". So, has been analyzed physical structure of studied area. Also, research method includes seven parts. They are:
- documental and liberality studies in order to introducing natural models in urban planning
- evaluation studied area with mentioned patterns
- creating plan and geography information (GIS) in order to update information

So, at first was considered proposed natural models in order to using from natural factors and approaching development models. Then, was analyzed mentioned area in several aspects. At finally, was compared studied area by considered model and finding challenges.
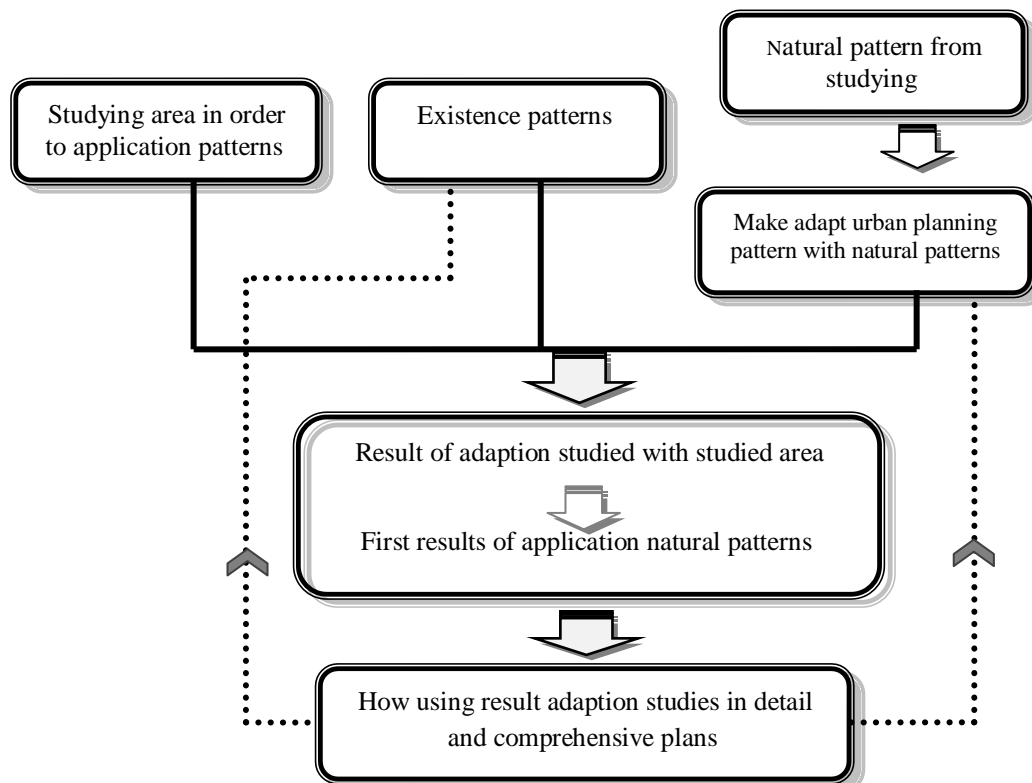
Figure (1): method research

II.   THEORETICAL BASIS

1.1. Adaptability natural models
The world isn't random. There are models in every place. Indeed, we use from them every day. Models has been seen in wide scale, also many options has been used from natural. One of the basic challenges is, understanding these processes and relation between them. Indeed, there are complex relations between processes that understanding is difficult (bell, 1999: 22).

Models could be defined by some worlds such as: orient, shape, fabric, density, and color, view forces, continuous, repetition, similarity, cohesion and etc.   Analyzing of patterns was done through studying of place and classification of natural phenomenon that they have as like as patterns.
Therefore have been analyzed natural pattern in four parts (main parts). They are:
1. **Basic natural pattern:** pitter Stevens has proposed patterns and relevance between processes in patterns in natural book (Patterns in nature, 1974). Also, he has divided patterns and natural element in various scales in four parts. They are: 1- spiral pattern, 2- curve pattern, 3- junction pattern, 4- mosaic pattern. Each pattern has special factors (bell, 1999: 38).
2. **Earth shape patterns:** these patterns emphasis on hemisphere by using natural factors such as: repetition, coherence and etc (bell, 1999: 38).

3. **Aesthetic of natural environment (landscape):** this pattern consider identity of natural places, also it define space. Indeed, it is several sensitive between human and natural environment. These relations are, various and complex, coherence, several scales and forces (Mak hark, 2008: 30).

4. **landscape synthetic patterns :** landscape include several patterns , such as : shape , structure , elements and etc . All of the landscape consists of them (Matluk, 2001:24). Landscape patterns have been consisted of concept of landscape language, means, landscape conversation (between details and residents), processes and natural forms, networks (Aspyrn, 1998:19).

The first finding that has been concluded from considering and analyzing of natural patterns and quality factors has been shown in table 1.

Table1: adaptive results of natural pattern in manufacture environment

Using in artifact environment (urban planning and urban design patterns)	Natural environment patterns	
	Using of pattern	Basic patterns in natural environment
Approaching to maximum capacity in limit spaces and completing urban spaces	Using of needle plants in order to utilization from light of sun	spiral pattern	Basic patterns
Adapting urban edge from flexible curve patterns and curve line	continuous flow by inharmonic cover plants	curve pattern	
Creating balance in terrific flows (v/c)	There is junction traits and hierarchy traits	junction pattern	
Composition functional element in several scales , mosaic patterns	There is understandable framework according to understandable mosaic	mosaic pattern	
- Creating density structure - Creating physical building in order to identity	Earth shape is according to natural pattern Also , determining land uses	Earth shape patterns	
Using from water element	There is identity of natural places , also there is coherence between natural elements	Aesthetic of natural environment	
Using from natural structure in order to developing physical form	Appropriate form of landscape elements such as : mosaic , tunnels , path, background	Landscape patterns	
Creating various physical in relation wind , sun , temperature	Landscape language is special words such as water, soil. indeed it is as alive element for creating various condition in natural environment (Bahraini , 1996:22)		
Creating harmonic spaces (shape , construction , density)	There is structure and shape in landscape (structure were led to understanding environment) (Biken, 1998, 35).		

1.2. Research history & functional samples of natural patterns

Generally, there is regard to natural in previous years in urban systems (Magtif, 2009, 53). In this research, was considered some concepts such as: green city, ecology city, sustainable city and etc (Bahraini, 2004: 65). Indeed, green city approach or native city have used functional samples and natural patterns in urban environment. These patterns emerge in green space networks patterns, native city, and sustainable city. On the other hand, there is one paper that has been done natural patterns and has changed to applied model. Other paper has been studied natural and objective concepts.

1.2.1.   Mosaic patterns (new strategies in urban design)

Mosaic patterns have been seen in every where in all of the earth. Also, this patterns understandable for every one. These patterns have been seen in various scales.

Figure (1): natural earth mosaic

Re: Başer & Kubat 2007, A New Landscape Design Strategy, Kadıky – Istanbul

Conceptual framework of natural environment in inside and outside ecosystems. Always, one same conceptual framework could be used in urban environment or could be created sustainable urban viewpoint. So, designer should be explored structure in natural environment and creating sustainable city. Kadıkoy is one the city in Istanbul that conceptual framework of urban environment is based on mosaic pattern for approaching urban sustainable viewpoint. These patterns are used relation open spaces networks, shape of path. Also, this pattern is defined as continues components (Baser&kubat, 2007).

Figure 2: proposed green and open spaces according to mosaic pattern
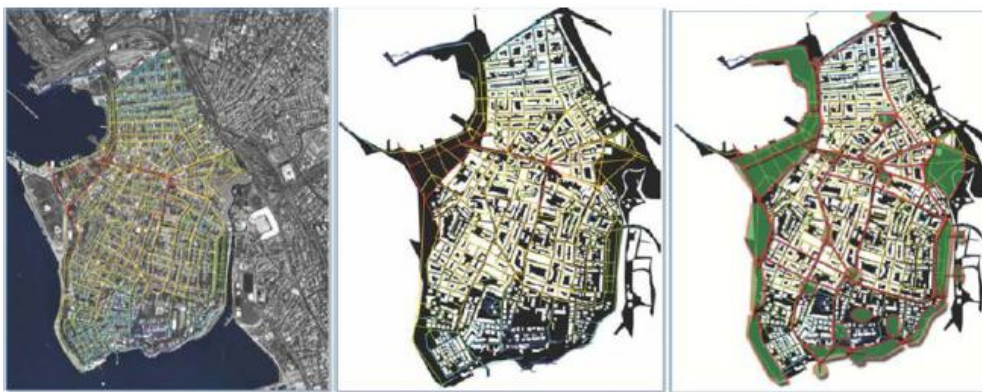
Re: Başer & Kubat 2007, A New Landscape Design Strategy, Kadıköy – İstanbul

1.2.2. Green space and networks pattern
Gatraple project (green network project) (2008), was done trough hierarchy of green networks in order to improving environmental quality (landscape pattern & natural environment elements).

Figure 3: Proposed green space network pattern of Gatrapel city
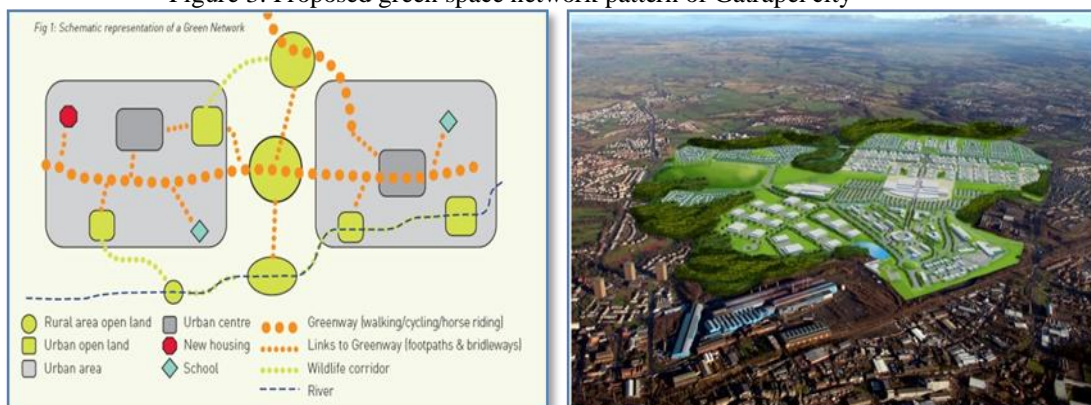
Re: Farrar, Gowkthrapple regeneration, Greenspace & Green Network 2008
Also, other city such as Kirkols has been used nodes and green corridors and has been used from opportunities.

1.2.3. Urban sustainable form

Done studied for sustainability (Urban design for sustainability 2008) is, appropriate method for having sustainable cites. Therefore, was studied design theory and urban sustainable models in order to development of compact green city. In this research has been done, coherence between natural and manufacture environment by using functional coherence, improving green nods (Helsinki& Schulz, 2006), strengthening appropriate density ,appropriate green structure ,making integrated structure , developing neighborhoods centers , designing green structures & urban viewpoint , creating identity , improving design and management of structures and green nods as continues elements between old and new structures (Land use consultant , 2008) .

Figure 4 : detail of urban green structure (Green network in Kirklees)
Re: Başer & Kubat 2007, A New Landscape Design Strategy, Kadıköy – İstanbul

III.   STUDIED AREA

Mashhad has been located between Hezar Masjed & Binaloud Mountains. The city is located at 36.20º North latitude and 59.35º East longitude, in the valley of the Kashaf River near Turkmenistan, between the two mountain ranges of Binalood and Hezar-masjed. Mashhad divided 7 parts in planning based on environmental, physical, economical, social indicators (Farnahad consultant, 2008). This area consists of natural and physical opportunities. Thus, middle area is one of the main economical and physical areas in Mashhad. This area has some factors. Such as:

-    appropriate place in urban spatial space
-    appropriate relation between with natural area such as Binalood mountain
-    consisting of structure and various physical fabrics
-    centralization of activities in urban scale
-    there is value environmental such as : gardens , canals
-    there is the most network in this area due to holly shrine
-    there is problems about urban spaces and physical structure , so it is necessary urban planning

Figure 5: proposed planning area in Mashhad metropolitan
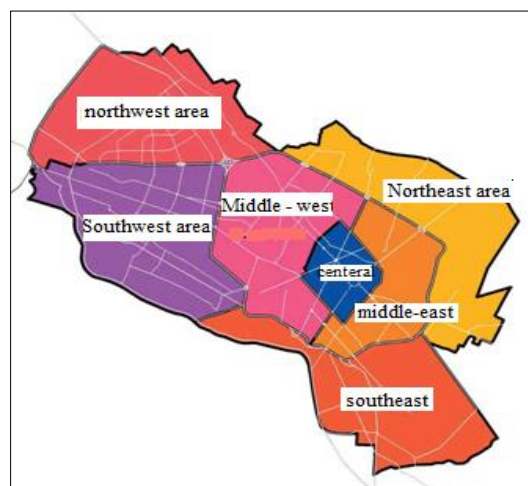
2.1. Studied area in urban natural structure

The area is 3207 hectare (11%).also; it located a side Binalood Mountain and Kohsangi (natural element). According to, there is channel structure in this area (Prsomash consultant, 2008:67). So, studied area has appropriate position in Mashhad metropolitan. South mountains create value landscape in this area. Also, there is appropriate slope in studied area (90 meter difference of height). There are various temperatures due to different weather. They effect on urban environment quality.

2.2. Studied area in urban functional structure

Studied area has spatial position in Mashhad city. There is a lot of land uses and services and populations in area. So, development of area is led to progressing that other area of Mashhad. Also, there is diversity construction due to western and central newly constructed. In this area, 37% of lands consist of residential zone and other parts consist of other land uses that have been dispersed in area. Due to the most land uses are non residential, so it show important of studied area as services zone in Mashhad city.

2.3. Studied area in urban physical structure

Studied area has been located in center of Mashhad .its developed fabric are related to after 1957 decade. There is corridor axis in south boundary of studied area. Studied area has been located between raster fabric of western area and central fabric. Totally, it have special place in metropolitan. Centralization of height building in this area, dispersion of land uses , centralization of macro physical lands are important factors for developing Mashhad city .

Figure 6: functional structure of Mashhad central area
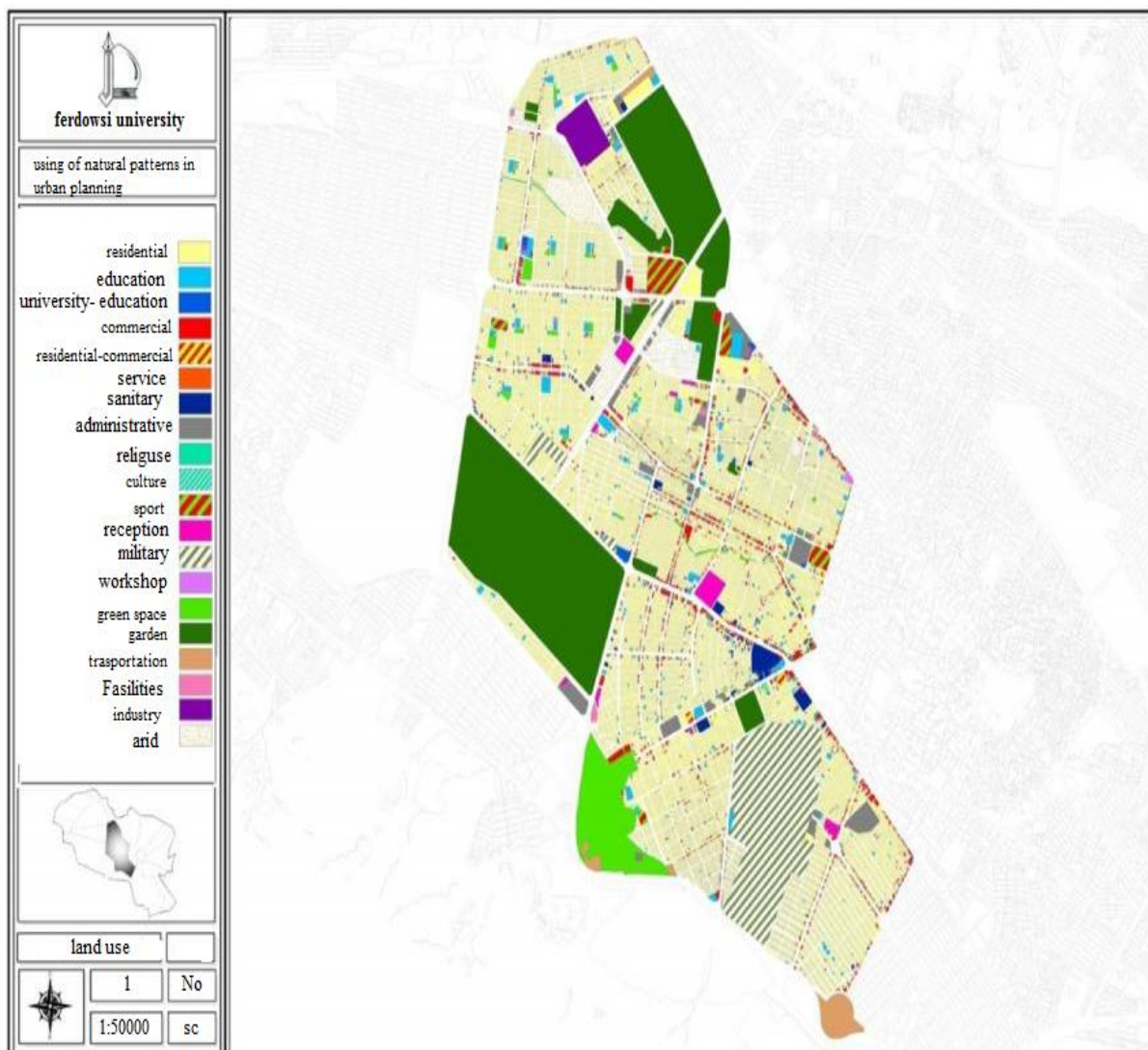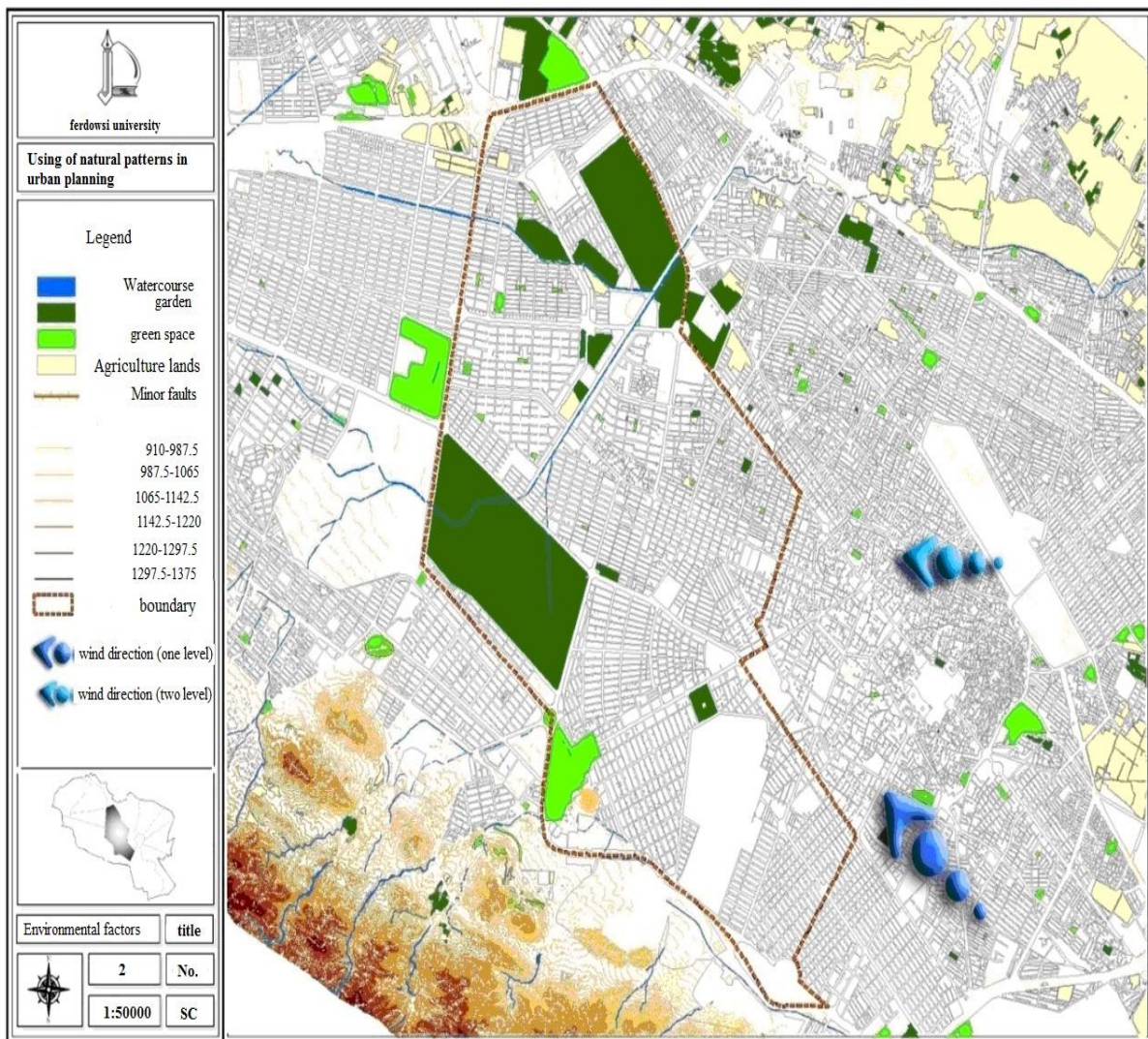
Figure 7: environmental structure of Mashhad central area

IV.   CONCLUSION & DISCUSSION

According to research method, was considered structure of central area and was proposed as plans. Also, were proposed adaptable and functional models in urban and design planning. So, are proposed finding of analyzing natural models and influents of them.

3.1. Natural structure in order to development of shape and physical form

Structure and natural form are led to shape and form. On the other hand create limitations. So, city as manufacture environment has relation with natural structure. Indeed, the city would be determined developing and evolution.

Mashhad consist of potential group that could be developed and create sustainable landscape for residents. So, adaptability of condition forms by natural environment is very important.

3.2. Composition functional elements in some scales in mosaic networks

Totally, environment consists of some mosaic pattern in different scales. This pattern consists of hierarchy structure (Bell, 1999: 38). According to models , the structure of studied area are :
-   green mosaic
-   functional mosaic in neighborhood and district scale
-   urban functional mosaic

These areas provide services and functional and uses that, are led to developing urban spaces. On the other hand mosaic pattern have ability to complete vacant land use.

3.3. Complete physical and spatial dissociation in order to spiral pattern (green space network)

Spiral model is consequence of development in limit environment in order to utilization of natural conditions (terener, 1999:65).

According to factors area, are used from this model in order to completing green space network as spiral rings of green space. This pattern relate to structure and natural networks. So the results of Continuous green space networks are green axes, potential green spots and etc. natural pattern are led to utilization and balanced dispersion n studied area. Also, it complete spatial dispersion in this zone

3.4. Physical structure that has been resulted from earth slope (open space network as background)

Totally, mountain structure is created Based on earth shape. This factor are led to balanced condition in this area or every where (Bell, 1999: 178). Using of pattern has been done relation background. Utilization of spots potential are led to improved quality of urban environment .

Using of natural patterns in urban planning

legend

Functional area consist of district, Region , city . also they have harmonies

Influence spot on Studied area

Existed harmonic mosaic

Potential spot in order to Completing of existed mosaic

functional structure base on mosaic pattern — Title

4 — NO.

SC

2. Mosaic pattern
Composition of functional elements in scale range

Using of natural patterns in urban planning

Legend

green space network

appropriate spots in order to compelet vacand lands

green and open apots

potential spot in order to compeleting spiral patterns

Spiral rings

3. Completing of spatial and physical dispersion
For approaching spiral patterns

4. natural patterns of earth shape

تطبیق الگوهای طبیعی زمینه و مارپیچ بر ساختار کالبدی و فضای سبز حوزه — عنوان نقشه

۵ — شماره نقشه

مقیاس

3.5. Adaptation shape and physical form in combination with climatic factors such as wind

Each form shows existed limitation and process in exist condition. Shapes and forms are various due to environment factors such as: wind, sun and etc (Spearman, 1998: 243). Also, urban fabrics should be adapted environmental condition. For example orient of wind is one of the most important factors for land uses. So, the land uses should be located in appropriate location that should be matched by environmental condition.

3.6. Branching pattern and codification structure based on studied area

This pattern is led to arrange natural elements. Often, this pattern is created by junction of rivers or other natural elements (Bell, 1999: 38). It is necessary for creating of balance terrific flows in our cites. By using of model was determined capacity of urban path.

3.7. Adaptability of urban watercourse, follows, edges from flexible screw model

Screw model is flexible pattern that create harmonic viewpoints, such as: plant cover, opposite edges and etc. this pattern define soft edge as physical edge, separated edge. Totally, are used for arranging potential edge. Therefore, this pattern useful in solving landscape problems in urban environment. Flexible screw model, codify density structure in cites.

3.8. Corridors and Walking routes network models between functional mosaics

Landscape structures are analyzed by description of detail elements such as: mosaics, canals and etc. indeed, the path relate between mosaics (Spearman, 1998: 191). By using mosaic patterns could be codified corridors and canals. Thus, based on pattern, has been proposed some path that have located between mosaic patterns. They are:
Natural tunnels (green axes), walking ways (entertainment-commercial), green path or bicycle path

3.9. Natural environmental quality patterns by flow networks

Viewpoint and landscape emerge beautiful environment due to special identity foe each landscape (Spearman, 1998:70). This pattern is used in order to identity for environment. On the other hand, it should be improved other factors such as religion or natural quality. Generally, this pattern strengthens urban identity.

3.10. Adaptability water flow path pattern by main axes

All of the natural viewpoints consist of special elements. These patterns determine landscape language (Lind, 1996: 23). By using these patterns, could be provided natural quality in urban spaces. So by utilization of natural location could be revived rain water. Also could be reserved natural sources.
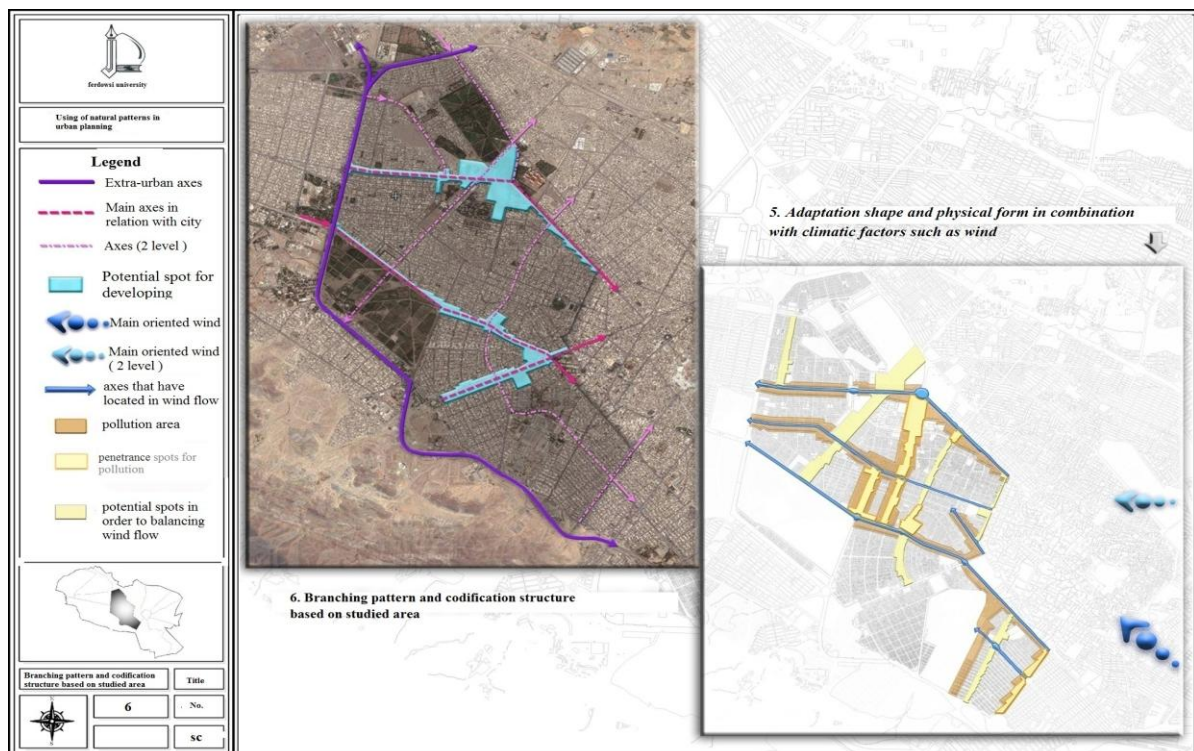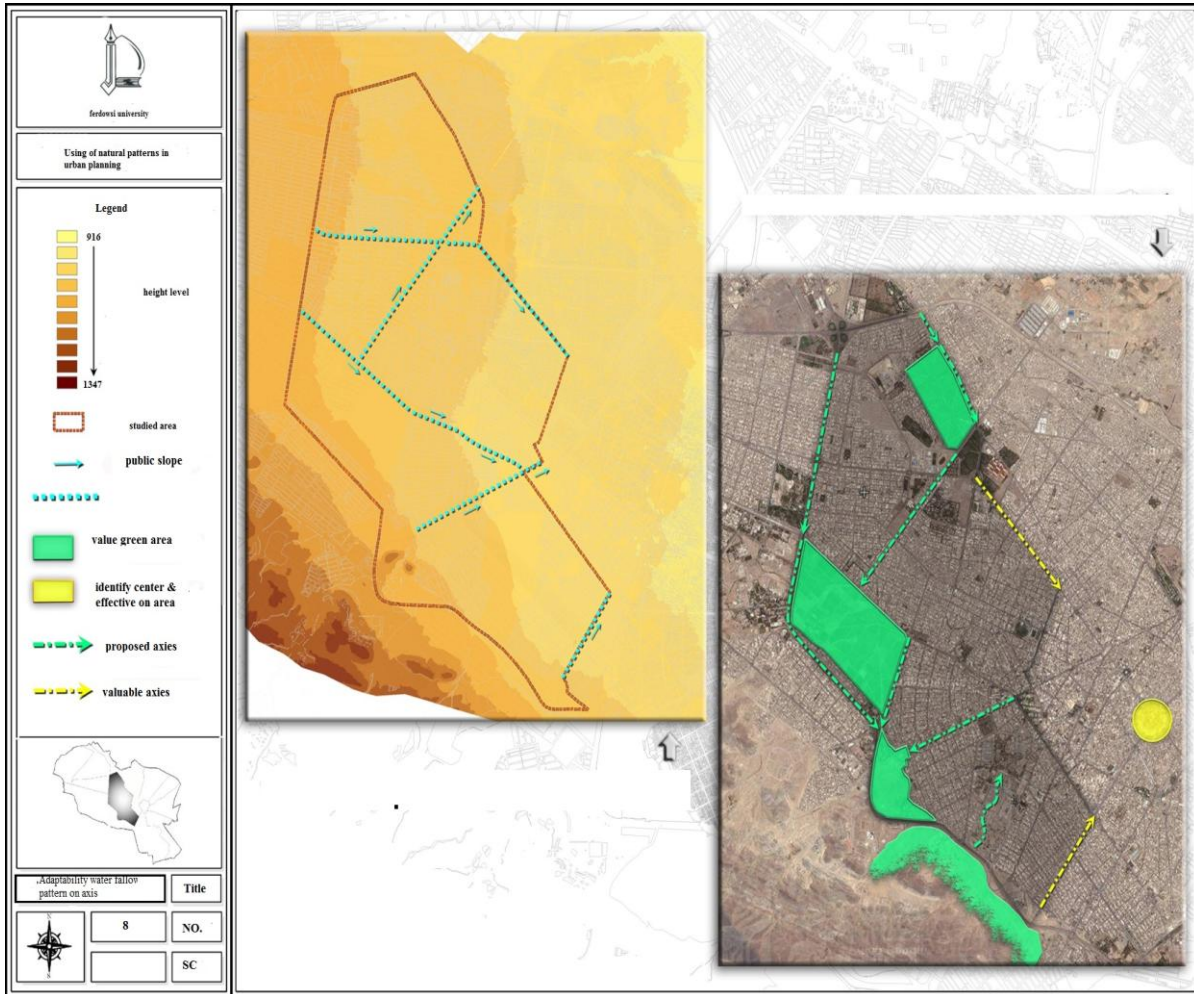
At finally by analyzing of natural models, was determined functional patterns in urban planning and urban design. Table 2 shows, natural models according to function in details plan or comprehensive plans.

Table 2: using natural models in urban planning and urban design in studied area

Functional in urban design	Functional in proposing developed models	Functional case	Basic natural models	
Open and green space networks such as nods and green axes	Dispersion functional spot in studied area	Completing spatial and physical dispersion in order to approaching spiral model	Basic models (spiral)	1
Walking natural path	There is spot that have density potential	Adaptability of urban watercourse, follows, edges from screw model	Basic models (screw)	2
- Dividing region according to main structure - Hierarchy network	Main network relation to city	Branching pattern and codification structure based on studied area	Basic models (branchy	3
-creating neighborhoods - creating functional system	Total functional structure relation to city	Mosaic model in composition functional elements	Basic models(mosaic)	4
-	Creating density spots	Physical structure from resulting earth shape	Landscape model	5
Creating special identity	-	Natural environmental quality patterns by flow networks	Beautifully natural environment model	6
Completing special green network	-	Adaptability water flow path pattern by main axes	Landscape model	7
-	Density and physical structure	Natural structure in order to completing urban form	Earth shape model	8
Creating spots without pollution	-	Adaptability shape and form with climatic factors	Earth shape model	9
Natural access network	-	Corridor networks and walking path between mosaic	Landscape model	10

V.   PROPOSING NATURAL DEVELOPMENT MODEL

At finally, have been proposed strategies in different structure. According table 2, each model have clear results. So, based on data and finding could be anticipated natural development models for studied area. The main subjects in this research are:

- improving the role of studied area in Mashhad city with relation urban network
- design of functional structure that it consist of centers and activities axes according to mosaic framework
- design of physical structure according to urban spatial structure
- completing urban terrific networks in relation other parts
- design urban networks according to branch pattern

This development model would be used in future for studied area .
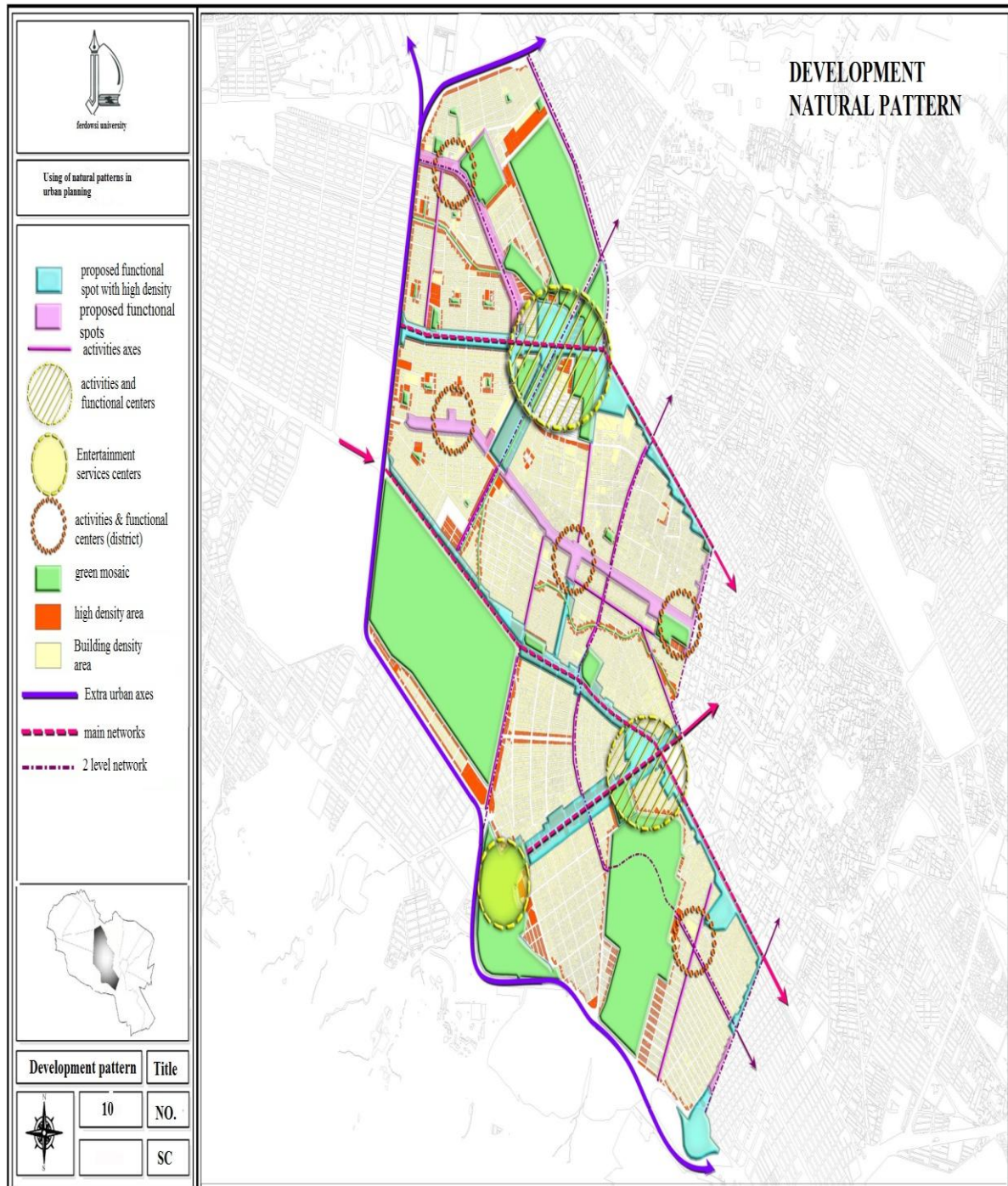
Figure 10: proposed natural development pattern

REFERENCES

[1]　Arbier an & Higenz Catrin , land use planning for developing lands , Bahraini keyvan Karimi, Tehran University Press, 2003

[2]　Spierman , landscape language, Bahraini H. and B. Aminzadeh, Tehran University Press, 2007

[3]　Bahrain, SH. Healthy City Project, World Health Organization and the need for strict implementation of the Islamic Republic of Iran, Journal of Environmental Studies: Environmental Studies Series, No. 17. Winter. 1998

[4]　Bahraini Hussain, urban planning, expectations, Tehran University, Summer 2005

[5]　Simon Bell, perception, perspective, pattern, process, translate, B. Aminzadeh, Tehran University 2004

[6]　Edmund Bacon, Design of Cities, translated by Farzaneh Taheri, Research Center of Planning and Architecture 1989

[7]　Parsomash sustainable pattern of development of mid-western city of Mashhad, 2008

[8]　8- Tom Turner, City as Landscape, translated by F. Nourian, processing enterprises and urban planning (affiliated to Tehran Municipality),

[9]　Farnahad, landscape and metropolitan development pattern wax Mashhad, in Persian date 2010

[10]　Jon Lang, Creating Architectural Theory, translated by A. Objective oven, Tehran University Press, 2004

[11]　Gunnar Lind, water and city B translations teacher center. Research of Urban Planning and Architecture 1999

[12]　Matlak John L., Introduction to Landscape Design and Environment, Department of Education, the parks and green spaces in Tehran in 1999

[13]　Magtyf Cliff urban design based on sustainable development, translation Narcissus Publications, 2009

[14]　Ian Mc Harg, Design with Nature, translated by Abdul Wahab Mohammad, Jihad, Mashhad University Press,

[15]　Viler SM. and Beatles T Wheeler, sustainable urban development, Urban Studies Center publications are translated into real Kianoush Zaker and Architecture Department of Housing and Urban Development, 2010

[16]　Hedman Richard and Andrew, urban design principles, translated by R. and A. Rezazadeh born, University of Science and Technology 2010

[17]　A New Landscape Design Strategy For Creating Continuous, Perceptible and Productive Urban Green , a case study of Kadıköy – İstanbul , Bahar Başer & Ayşe Sema Kubat 2007

[18]　Gowkthrapple regeneration ,Greenspace & Green Network Study , Final report , by Irronside Farrar , November 2008

[19]　Developing a Green Network in Kirklees , Kirklees Council Environment Unit , 2007

[20]　Encouraging walking, the role of urban design , Experiences of the EU- ECOCITY project , Uwe Schubert & Franz Skala , Vienna- Austria 2008

[21]　Urban Design for Sustainability: Learning from Helsinki, Carol Schulz, The Sir George Pepler International Award: 2006

[22]　Green Network Strategy Ravenscraig byLand Use Consultants, December 2008 (2008)

Research Paper   Open Access

Studies on the Mechanical and Water uptake Properties of Some Polyolefins / Corn Starch Blends (1)

Ifeoma Perpetua Oragwu and Isaac Ogbennaya Igwe
Department of Polymer and Texile Engineering, Federal University of Technology, Owerri, Nigeria.

Abstract: - Corn starch blends of high density- and low density polyethylene have been prepared by injection moulding technique. Maleic anhydrides- graft-polyethylene was used as a compatibilizers. The effect of corn starch content on the blends was evaluated by mechanical property measurements and water uptake tests. Results indicated that the tensile strength of the blends decreased with increase in corn starch contents. While the elongation at break of low density polyethylene-corn starch blends decreased with increase in starch content, the elongation at break of high density polyethylene/corn starch blends first decreased with increase in starch content, up to 7.25 wt %, and there-after, decreased with further increase in corn starch contents. The addition of maleic anhydride-graft-polyethylene was found to improve the tensile strength and elongation at break of the blends. Both the compatibilized and uncompatibilized blend absorbed water, the amount of which increased with increase in corn starch content, and immersion period; and tended to level off after the fourth day of immersion in water. The amount of water absorbed by the blends was appreciably decreased on incorporation of maleic anhydride-graft-polyethylene into the blends.

I.   INTRODUCTION

Starch is a natural polymer which is referred to as a polysaccharide. It is produced by all green plants, and consists of two distinct molecules, the amylose (linear polymer), and amylopectin(branched- polymer) *[1]*. Starch from various botanical sources are among the most abundant, renewable and inexpensive natural biopolymers. Using starch to partially replace synthetic plastics will not only reduce the dependence on petroleum-based plastics, but also reduce plastic wastes. It is common knowledge, however, that biodegradable plastics from starch cannot compete with conventional petroleum-based plastics because of their poor mechanical properties *[2]*. Most recently, starch has received maximum attention in the preparation of biodegradable plastics, especially for one time use plastics, because it is the most abundant, degradable, low cost natural polymer. It is equally available throughout the year. Partial substitution of synthetic plastics with materials like starch provides not only cheap filler but also biodegradation properties to the final products [3]. Thus, the addition of starch to synthetic plastics like polypropylene *[4]*, poly (vinyl alcohol) *[5]*, high density polyethylene *[6,7]*, and linear low density polyethylene*[8 ,9]*, has been reported to enhance their biodegradability . In blends of starch with synthetic polymers such as polystyrene, and polypropylene, the hydrophilic nature of starch leads to poor adhesion (miscibility) with the synthetic polymers, which are hydrophobic in nature. To improve their compatibility, various attempts had been made to modify either starch or the synthetic polymer,*[10]*. It has been found that plasticisers, coupling agents, or modified starch only partially improved the dispersion of starch in the synthetic polymer such as polyethylene, and their interfacial properties because of their limited interaction,*[11,12]*. Another approach was to use poly(ethylene-co-acrylic), poly(ethylene-co-vinylalcohol) or oxidized polyethylene ascompatibilizer in polyethylene-starch composites, but the composites had unsatisfactory mechanical properties,*[13,14]*. Another method to improve the miscibility of phases in starch- polyethylene blends is the chemical modification of the hydroxyl groups of the starch to induce hydrophilicity into it. Octenyl succinate starch metal ion complexes were combined with polyethylene to create a biodegradable plastic with good tensile strength*[15]*. As part of our effort to investigate the biodegradation of high and low density polyethylene/corn starch blends, we report here, the effect of maleic

anhydride-graft-polyethylene as a compatibilizer on some properties of high- and low density polyethylene / corn starch blends.

II.   MATERIALS AND METHODS

2.1   Materials
The high- and low density polyethylene used in this study were obtained from Ceeplast Industries, Aba, Nigeria. The density of the polymers are 0.97, and 0.952 g /cm^3 respectively. They have melt flow indexes of 9.0 g/10 mins, at 230 ^{0}C and 2.0 g/10mins at 190 ^{0}C respectively. The corn starch was obtained from the Crop Science Department, Anambra State University, Uli, Nigeria. The starch was dried at 120 ^{0}C for 24 hrs, to a moisture content of < 1.5 % prior to sample preparation. The maleic anhydride-graft-polyethylene (MA-g-PE) was purchased from FINLAB Chemicals, Owerri, Nigeria. It is a product of Sigma Aldrich, USA and it's viscosity is between 1,700.00 to 4,500 cps at 140 ^{0}C.

2.2   Sample Preparation
The high-, and low density polyethylene blends of corn starch were prepared by thoroughly mixing the weighed amounts of the polymer with appropriate corn starch quantities (0, 2.5, 5.0, 7.25, 10.0, 12.50, and 15.0 wt %). The high-, or low density polyethylene was melted and homogenized with the corn starch in an injection moulding machine .The blends were extruded as sheets. Similarly, high-, or low density polyethylene blends in the presence of the compatibilizer, maleic anhydride-g-polyethylene (MA-g-PE) were prepared as described above. The compatibilizer level was 10.00 wt % based on the weight of corn starch in the blend.

2.3   Testing on the Blends
The tensile properties of the dumbbell-shaped samples of the blends were measured according to the ASTM D 638 specification. The elongation at break(EB) was also recorded along the meter rule pointer at 200 – 100 mm. The Rockwell hardness (ASTM D 785), and specific gravity (ASTM D 792) properties of the blends were determined using standard methods.

2.4   Water Uptake
The blends specimens were dried at 85 ^{0}C in an oven until a constant weight was attained prior to immersion. The water uptake tests were performed to last for a period of six weeks. Weight gains were recorded by periodic removal of the specimens from the water. Water adhering on the surface of the specimens were carefully removed with filter paper before weighing on a balance with a precision of 1 mg . The percentage of water uptake at different times (W_t) was calculated according to the equation:

$$W_t (\%) = W_2 \_ W_1 / W_1 \times 100 \qquad\qquad (1)$$

where W_1 and W_2 are the weights of the dried sample and the samples after immersion time, t .

III.   RESULTS AND DISCUSSSIONS

The tensile properties of high density polyethylene and low density polyethylene/corn starch blends with and without maleic anhydride-graft-polyethylene are shown in **Figure 1**. When the corn starch content increased, the tensile strength of the blends decreased, presumably because of incompatibility of the polyolefins and corn starch. It is probable that the inclusion of corn starch in the polyolefin matrices caused a very significant stress concentration. In effect, fracture could be initiated from the weak interface of the blends, due to their envisaged poor interfacial adhesion, thus resulting in reduced tensile properties. *Thakore et al [3],* who investigated low density polyethylene/potato starch or starch acetate blends found that the tensile strength of the blends decreased with increased starch or starch acetate content. The higher tensile strength of high density polyethylene as compared to low density polyethylene is attributed to the former's higher density, lack of branching, and stronger intermolecular force of attraction that exists in its chains according to *Karyn [16].* Similarly, *Lin et al [2]* who investigated low density polyethylene/corn starch blends found results in similar to ours.
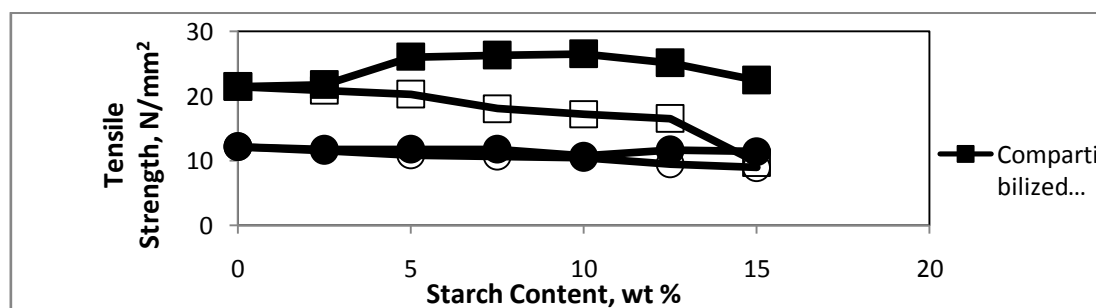
Figure 1: Plot of tensile strength versus corn starch content for compatibilized and uncompatibilized HDPE, and LDPE Corn Starch Blends.

      The plots show that the tensile strength of high density polyethylene/ corn starch blends were in all cases higher than those of low density polyethylene/starch blends, with the determined tensile strength of high density polyethylene(21.98 Nm^{-2}) being higher than that of low density polyethylene (12.17 Nm^{-2}). When the compatibilizer (MA-g-PE) was added to the polyolefin blends, the tensile properties of the blends were increased and two types of behaviours can be observed;

      (i) the tensile strength of the high density polyethylene/corn starch blends were greatly increased at maleic anhydride-graft-polyethylene contents, 4.0 wt % based on 10 % corn starch content, and thereafter, decreased after MA-g-PE content, 4.0 wt.%. The decrease in the tensile strength of compatibilized high density polyethylene, after the addition of   4.0wt % maleic anhydride-graft-polyethylene is probably due to the molecular morphology of HDPE near the surface or in the bulk of the plastic phase *Sanadi et al, [19].* Transcrystallization and changes in the apparent strength of the bulk matrix can result to changes in the contribution of the matrix to the composites strength

      (ii) the tensile strength of the low density polyethylene / corn starch content were gradually increased, were in all cases were smaller than that of the unblended LDPE within the MA-g-PE content investigated. It is believed that MA-g-PE increased the adhesion between the polyolefin matrices and the corn starch filler. The improved interfacial adhesion between the polyolefins and corn starch has a positive impact on the stress transfer, thus reducing the chance of interfacial debonding, and leading to improved tensile strength properties. The above results further support the assumption that the interaction between starch and MA-g-PE was a chemical one between the hydroxyl groups in corn starch and anhydride groups in MA-g-PE, because, a polar interaction between them would not improve their properties to any significant extent. In contrast to our results, *Matzinos et al [17]* who characterized LDPE/starch blends, reported an increase in the strength of the blends with starch contents of up to 50 wt % starch after which the tensile strength of the blends decreased with any further increased in starch content.

Figure 2:   Plot of Elogation at Break versus Corn Starch Content for Compartibilized and Uncompartibilized HDPE and LDPE Corn Starch Blends
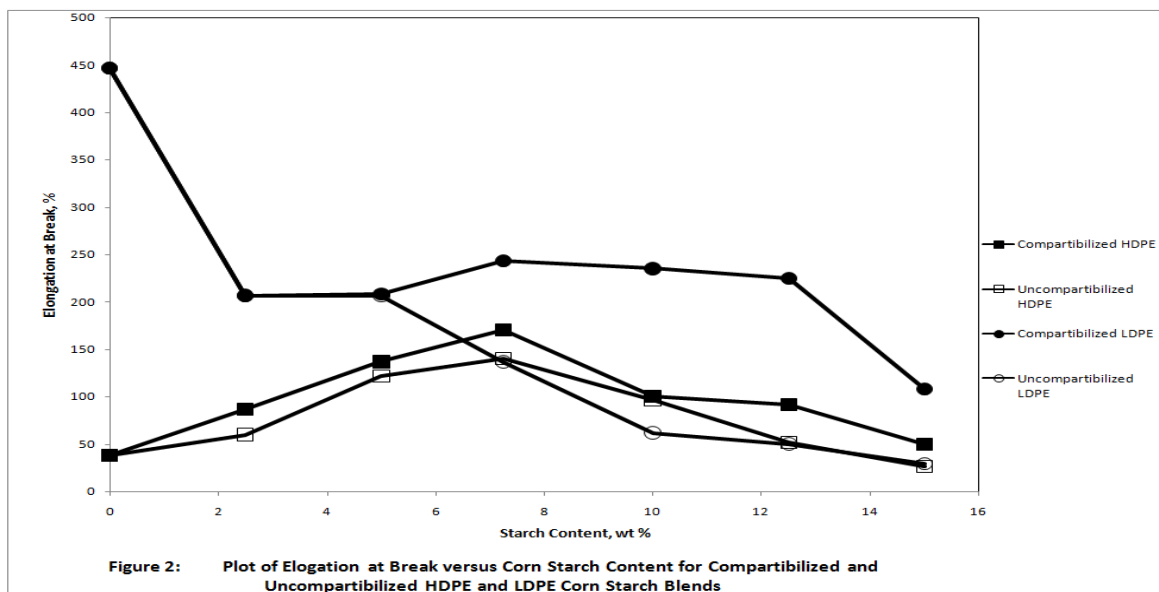
      The elongation at break obtained for the various blends are obtained in figure 2.

The two polyolefin blends of corn starch were observed to behave differently with increasing starch content:

(i)   when corn starch content was increased, the elongation at break of LDPE/corn starch blends decreased, presumably because of the heterogeneous dispersion of starch in LDPE matrix, and the incompatibility of LDPE and starch. A similar behaviour was also observed with LLDPE /starch films *Evangelista et al [10]. Thakore et al [3],* had also reported a decrease in elongation at break of LDPE /potato starch blends with increase in potato starch content. In synthetic polymer blends, the addition of the immiscible component to a ductile matrix generally decreases the elongation properties considerably at break point *Paul, et al [18].*

(ii)   the elongation at break for HDPE/corn starch blends was observed to increase with increase in starch content, up to 7.25 wt % of starch, and thereafter, decreased with further increase in corn starch content. Similar behaviour was also noticed in the variation of tensile strength of HDPE / corn starch blends with corn starch content.

When MA-g-PE was added to the polyolefin /corn starch blends, the elongation at break of the resulting blends were further improved. The following observations are however noteworthy:

(i) the elongation at break of HDPE /corn starch blends increased with increase in MA-g-PE content, up to 30 wt % and thereafter, decreased with any further increase in the MA-g-PE content. However, the resulting decrease in elongation at break values are greater when compared to the uncompatibilized blends.

(ii) between 1.0 wt % and 2.0 wt % of MA-g-PE content, the elongation at break increased, after which it decreased with further increase in MA-g-PE content.

Thakore et al [3] in their studies found that the elongation at break of LDPE/starch acetate and LDPE/starch blends increased with increase in starch acetate, and starch contents, in the blends reached a maximum, and thereafter decreased. This increase in elongation at break was attributed to the improved plasticity of starch acetate.

Figure 3:   Plot of Water Uptake versus Immersion Time for Compartibilized and Uncompartibilized HDPE, and Corn Starch Blends

Figure 4:   Plot of Water Uptake versus Immersion Time for Compartibilized and Uncompartibilized LDPE, and Corn Starch Blends
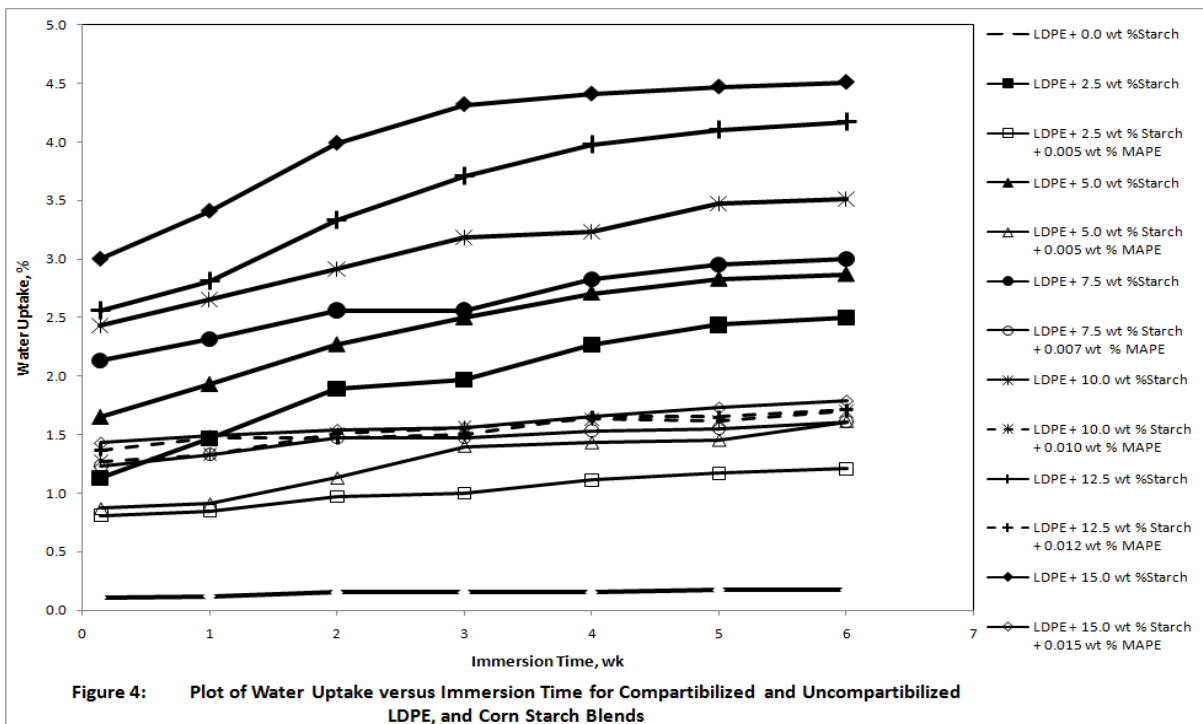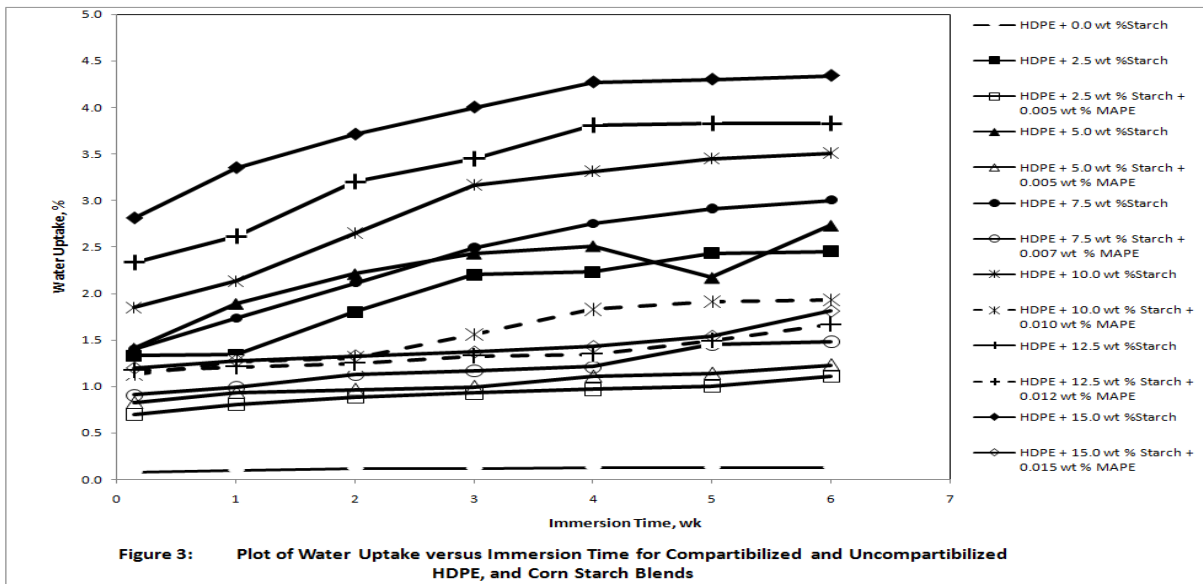
Figure 4: Plot of water uptake and immersion time for compatibilized and uncompatibilized LDPE /corn starch blends.

The water uptake for uncompatibilized and compatibilized polyolefin blends are illustrated in Figures **3** and **4** respectively. The figures show progressive increase in the amount of water absorbed by HDPE-, and LDPE/starch blends with increase in the amount of starch incorporated into the polyolefins, and period of water absorption. For most of the blends, the amount of water absorbed tended to level off (i.e. equilibrium absorption) after the fourth day of immersion in water. The negligible amount of water absorbed by HDPE, and LDPE tended to remain fairly constant throughout the duration of the experiment. These polyolefins are hydrophobic. The water uptake in the blends are due to the presence of hydrophilic starch particles in the blends. Starch particles possess an abundant of hydroxyl groups in their molecules and which are available for interactions with water molecules. Thus, water molecules can saturate the surface of the polyolefin/corn starch blends easily and penetrate into the composites through voids which result in higher water uptake in a short immersion period as reported by *Sanadi, et al, and Danjija et al, [20, 21].*

Figures **3** and **4** show that the compatibilized polyolefin blends absorbed less water when compared to the uncompatibilized blends. Thus, at each corn starch content in the blend considered, the compatibilized polyolefin blends absorbed less water when compared to the uncompatibilized blends. This is attributed to the improved adhesion obtained between the corn starch and polyolefins in the presence of MA-g- PE which reduces the water penetration into the blends.

The water absorbed by LDPE /corn starch blends is observed to be higher than those absorbed by HDPE/corn starch blends. LDPE has a high degree of short chain branching in its molecule *Katchy, [22],* and which has the capacity to loosen up the main chain structure thereby allowing the water molecules to penetrate more easily. This fac**t may** account in parts for the observed high amount of water absorbed by LDPE, and its blends when compared to HDPE and its blends.

IV.   CONCLUSION

Corn starch has been used to prepare blends of high density polyethylene, and low density polyethylene. When the starch content increased, the tensile strength of the blends decreased. The elongation at break(EB) of the blends was found to behave differently with increase in starch content. For LDPE, the EB of the blends decreased with increase in starch content , while for HDPE, the EB of the blends first increased with increase in starch content, up to 7.25 wt **%,** and thereafter, decreased with any further increase in starch content.
HDPE-, LDPE/corn starch are two- medium blend, therefore, MA-g-PE was used to improve the adhesion between the polyolefins and corn starch. The tensile strength and elongation at break of the blends were therefore improved with the addition of MA-g-PE as   compatibilizer. The water uptake for both the uncompatibilized and compatibilized blends increased with the increase in corn starch content. However, the quantity of water absorbed by the compatibilized blends was in all cases lower than the uncompatibilized blends.

REFERENCES

[1].   Ratanakamnuan, U. and Aht-Ong, D. *Photobiodegradation of Low Density Polyethylene/Banana Starch Films*, Journal of Applied Polymer Science, 100, 2725 -2736 , 2006.

[2].   Lin, W., Wang ,Y. J. and Sun, Z. *Effects of Polyethylene-graft- maleic anhydride on Thermal Properties, Morphology, and Tensile Properties of Low Density Polyethylene and Corn Starch Blends*, Journal of Applied Polymer Science, 88, 2904 -2911, 2003.

[3].   Thakore,L.M., Iyer, S., Desai, A. Lele,A. and Desvi, S. *Morphology Thermomechanical Properties, and Biodegradability of Low Density Polyethylene /Starch Blends,* Journal of Applied Polymer Science, 74, 2791- 2802, 1999.

[4].   Zuchowska, D., Steller, R., and Meissner, W., *Polymer Degradation and   Stabilization*, Journal of Applied Science, 60 , 471- 480 , 1998.

[5].   Tudorachi, N., Cascaval,C.N., Rusu, M., Pruteanu, M. *Testing of Polyvinyl Alcohol and starch Mixtures as Biodegradable Polymer Materials,* 19, 785-799, 2000.

[6].   Kang,B.G., Yoon,S.H., Lee,S.H., Yie, J.E., Yoon, B.S., and Suh,M., *Studies on the Physical Properties of Modified Starch Filled High Density Polyethylene,* Journal of Applied Polymer Science, 60, 1977 – 1984, 1998.

[7].   Sailaja, R.R.N. and Chanda,M., *Use of Polyethylene-co-Vinyl Alcohols as Compatibilizer in LDPE /Thermoplastic Tapioca Starch Blends,* Journal of Applied Polymer Science, 86,12, 3126-3134,2002.

[8].   Chandra, R. And Rustgi, R., *Biodegradation of maleated linear low density polyethylene and starch blends,* Polymer Degradation and Stability journal, 56, 2, 185-202, 1997.

[9].   Tatjana, I., Janis, Z., IIze, E., Martin, K., Robert, M., *Mechanical Properties of Injection-moulded Binary Blends of Polyethylene with small addition of liquid crystalline Polymer*, Journal of Applied Science, 122 ,(6), 3564-3568, 2011 .

[10].　Evangelista, R.L., Nikolov, N.L., Sung, W., Jane,J. And Gelina, R.J. *Synthesis and Properties of Starch Based Biomaterial,* Industrial Engineering and Chemical Research, 30, 60, 1841-1846, 2008.

[11].　Lui, W., Wang, Y.J., and Sun, Z., *LDPE-Starch Blends Using Amylase, Journal of Applied Effect of Polyethylene grafted Maleic Anhydride (MA-g-PE) on Thermal Properties, Morphology and Tensile Properties of Low Density Polyethylene (LDPE) and Corn* Starch *Blends.* Journal of Applied Polymer Science, 88, (13),2904 -2911, 2003.

[12].　Sagar, A. G., and Merril, E.W*., Biodegradability Studies on Polymer Science,*58, 1647- 1658, 1995.

[13].　Willet, J. L., *Water Sorption and Diffusion in Starch/Polyolefins Blends*, Journal of Polymer Engineering and Science 35, 14 ,1184 -1190, 2004.

[14].　Prinos, J., Bikiaris ,D., Theologidis, S., and Panayiotou, C*., Infra- red Spectroscopy Methods reveal Hydrogen Bonding and Interaction between Components in Polymer Blends*, Journal of Applied Science, 97, (3,5), 813–821, 1998.

[15].　Pyuish, B.S. and Bandopadhyay, S., Jayesh,R.B*., Enviromentally degradable starch filled low density polyethylene Polymer* Degradation and Stability 47, (2), Journal of Material Processing Technology, 47, (2), 165 -173 ,1991.

[16].　Karyn, M. *What is High Density Polyethylene*, Wise Greek Publishers, London, 2010.

[17].　Matzinos,P., Bikiaris, D., Kokkou, S., and Panayiotou, C. *Processing and Characterization of LDPE / Starch Products*, Journal Applied Polymer Science, 79, 2548- 2557, 2001.

[18].　Paul, D.R., Vison, C. E. and Locke, C. E*., Compatibilization of Commingled Plastics with Maleic Anhydride modified Polyethylene and Ultraviolet Pre-Irradiation, of Polymer,* journal of Engineering and Science, 108, (4) 2597–2603, 2008.

[19].　Sanadi, A.R., Caulfield, D.F., Jacobson, R. E. and Rowell, R.M., *Renewable Agricultural Fibres as Reinforcing Fillers in Plastics : Mechanical Properties of Kenaf Fibres-Polypropylene Composites*, Industrial Engineering and Chemical Research , 34 (5), 1889 -1896 ,

[20].　Sanadi, I.D. Hunt, J.F., Caulfield, D. F., Kovacsvolgyi, G. and Detree,B., *High Fibre-Low Matrix Composites: Kenaf Fibre/Propylene*, The Sixth International Conference on Wood/Fibre Plasti-Composites, USA, 121-124, 15-16, May 2001.

[21].　Danjija, I. D., Nawang, R., Ishiaku, U. S., Ismail, H., Mohd, Ishak, Z.A.M. Degradation Studies and Moisture Uptake of Sago- Starch Filled Linear Low Density Polyethylene Composites, 25,75-81, 2001.

[22].　Katchy , E.M. Principles of Polymer Science, EL' Demark, Ltd, Enugu, 2000.

Research Paper   Open Access

Engineering creativity by using computer aided Mindmap

Imran Mahmud[1], Yousuf M Islam[2] , Shahriar Rawshon[3]
[1](Department of Software Engineering, Daffodil International University, Bangladesh)
[2](Department of Computer Science and Engineering, Daffodil International University, Bangladesh)
[3](College of Business Administration, International University of Business Agriculture and Technology, Bangladesh)

Abstract : Creativity is a high-level cognitive process which has given rise to research in various fields such as education. This paper shows a research on how Mind Mapping helps tertiary level students in Bangladesh to explore their creativity. It also focuses on use of Mind mapping in a learning environment which requires an enhanced way of thinking, learning and presenting. A research framework and a conceptual framework were developed to conduct this research. Based on the framework a case study will be followed by a qualitative and quantitative study on a group of students. The case study aims to compare student's performance before the use of mind map and the change after using it. Result of the research shows that use of Mind Mapping enhances the learning capacity in terms of number of ideas generated as well as improves presentation focus.. This research paper will facilitate the students, teachers and the researchers who seek ways to enhance the tertiary level educational experience.

Keywords: **-** *Creativity, Educational technology, Engineering education, Learning Method, Mind mapping*

I.   INTRODUCTION
What is creativity? It was discussed in [1] that there are two broad types of creativity, improbabilist and impossibilist. Improbabilist creativity involves novel combinations of familiar ideas. The deeper type of creativity involves METCS: the Mapping, Exploration, and Transformation of Conceptual Spaces. It is impossibilist, in that totally new ideas may be generated which – with respect to the particular conceptual space concerned – could not have been generated before. In the current research, the improbabilist type of creativity is looked at, in particular, whether students in a developing country university experience *increased* combination of their own ideas, both in terms of increased number of ideas generated and the resulting synthesis of ideas, before and after the use of a technique called Mind Mapping.

Developed by Tony Buzan in 1970, Mind Mapping is a revolutionary technique for capturing ideas on a horizontal surface. In [2] it was found the use of mind mapping for understanding case studies very useful among post graduate EMBA students. Mind mapping can be used in every activity where thought, planning, recall or creativity is involved (See [3]). A mind map allows a user to record a great deal of information in the form of linked ideas with keywords and images. Essentially, a user records or inscribes gathered information on a page while showing the relationships between the concepts involved. An example of a basic mind map drawn to organize this paper is shown in Fig.1.
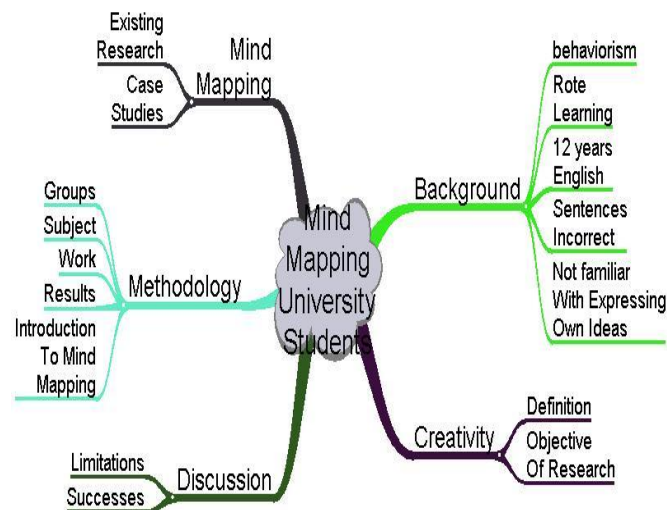
Fig.1 An example of a basic mind map

The mind map in Fig. 1 shows an attempt at organizing the paper currently being written. The branches only show two levels of linked ideas. There is no limit to the number of levels that can be added. In addition to keywords, visual images that represent key the key ideas can also be used.

"Using Mind Mapping as a study technique": (e.g. [4]) shows that retention and recall are better among students when mind maps were used as a study technique. However, they point out that the users must be motivated towards the use of mind maps, i.e. the students must enjoy using it and obviously be conversant in their use. It was studied whether mind mapping can be used as a pre-writing strategy to help explore and generate ideas for writing (see [5]). Author suggests that Mind Mapping tend to help students plan in the following ways:

- to find clearer focus;
- to have better organization of ideas;
- to have clearer ideas;
- to have better ordering of ideas;
- to include more relevant and appropriate ideas;
- to delineate more ideas;
- to have better paragraphing.

In [6] suggests a report which found similar improved results while using another type of mind tool, called Concept Mapping (See also [7]). Nurses used concept mapping to record and understand patient profiles. These nurses performed better than nurses that simply used the regular nursing plan guidelines. It appears therefore that use of tools that allow linking concepts help idea generation and focus.

For the present study, the students are from a developing country, Bangladesh. For both teaching and learning the behaviorism model is widely followed, i.e. student is given information that he/she is required to memorize and reproduce in quizzes and exams. The student is even required to memorize a variety of essays and reproduce one of these essays in the final exams. Essays given by the teacher often contain grammatical and spelling errors. The essays are memorized together with these errors and reproduced exactly. The result is that when students arrive at tertiary level they are not only unable to express independent thought, their sentence construction is random, i.e. mistakes in sentence making are not consistent. To understand the nature of mistakes, a batch of 18 students, studying in the first year first semester of a Computer Science degree were asked to write about a real incident in their lives that deeply affected them. To engage the students, the teacher first related a story in her own life and then got volunteer students to relate stories. Finally, students were paired and asked to verbally relate their stories to each other before finally writing their own story. All stories were collected, the total number of sentences counted and types of mistakes analyzed. It shows that 63.5% of the sentences written had a variety of errors. Further analysis revealed that those who write correct sentences use simple sentence structures, i.e. single verb sentences. When such students attempt to express more complex ideas, they run into trouble. Individual students were then collected and when asked to express the same ideas again the mistakes encountered were different. As the students do not have practice in independent sentence making, the mistakes made are random. It is with these types of students that the current research is designed. The test is to see whether mind mapping can help these students generate ideas for their presentations and assignments

II.   RESEARCH QUESTION AND OBJECTIVES

To answer this question we have several objectives to fill up
- Identify the level of improvements of after using mindmap?
- How does creativity express in mindmap?
- Was the mind map technique effective in enhancing students' creative thinking and problem solving skills?
- What impacts the students after using mind mapping?
- Impacts on student's knowledge compared to paper-based mind mapping and conventional teaching method?

III.   METHODOLOGY

Creativity assessment efforts might be qualitative, quantitative, or both. Analyzing qualitative data is a process which considers relevant contextual issues, possible biases, and values; it is concerned more with discerning the meaning of information rather than with formulating and testing statistical hypotheses, although there exists possibilities of statistical scores for creativity through mathematical means. A research process framework was developed by the researchers and that is shown on Fig 2
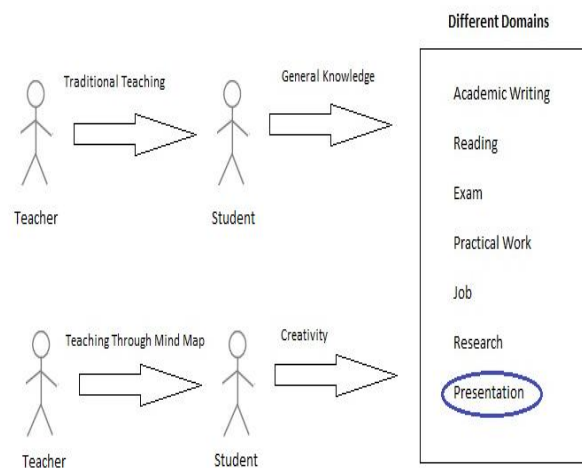
Fig 2: Research Frame work

IV.   EXPERIMENTAL DESIGN

1) Equipments
Some equipment like pen, pencil, marker, papers, and white board were introduced in this research study.

2) Procedure
In the research 11 students of Department of Agriculture from International University of Business Agriculture and Technology (IUBAT), Bangladesh were chosen and the research timeline was in between on January 2011 to April 2011.

First of all, lecturer discussed about importance of ICT in various sectors which is appropriate for this experiment using traditional teaching method with simple PowerPoint presentation. At that moment, students had no idea about any mapping techniques. After the lesson, teacher asked the students to make a presentation of uses of ICT tools in agricultural sector. When their writing is completed then teacher introduced different types of mapping techniques specially paper based mindmap. In the second part of this experiment, students worked for presentation using mind map with same topic.

V.   RESULT AND FINDINGS

After the experiment, the result is quite impressive; researchers found that without the knowledge of mindmap, students focused average of 7 point of interest (POI) or different sectors of using ICT in agriculture in their writing. But after having the concept of mindmap, no of sectors or point of interest(POI) increased as an average of 13 which is almost double than their previous writing.

TABLE 1 : Calculation of Experiment

	Mean	Standard Deviation
Total POI (Without Mindmap)	7	1.891810606
Total POI (With Mindmap)	13	9.052631579

In the chart, it was clearly visible that, standard deviation of students writing without help of mindmap they have covered relevance sectors is 1.81. That means most of the students covered relevant areas of 5.11—8.89 which is even less than the average of sector covered by students writing after using mindmap.
In our two sets of 20 measurements, both data sets gave a mean of consistently 7 and 13, but both groups size were small. How confident can we be that if we repeated the measurements thousands of times, both groups would continue to give a mean of 7 and 13
To estimate this, we calculated the standard error of the mean (S.E.M. or S_{x-bar}) using the equation

$$S_{\overline{x}} = \frac{S}{\sqrt{n}}$$

Where **S** was the standard deviation and **n** was the number of measurements.
- In our first data set, the student not using mind map S.E.M. was .42

$S_{x=s/\sqrt{n}}$

$S_{x=}1.89/\sqrt{20} = 1.89/4.47 = .42$
- In the second group the student using mind map S.E.M. it was .67

$S_{x=s/\sqrt{n}}$

$S_{x=3/\sqrt{20}=3/4.47=.67}$

95% confidence limits,
It turned out that there was a 68% probability that the "true" mean value of any effect being measured falls between +1 and −1 standard error (S.E.M.). Since this was not a very strong probability, most workers preferred to extend the range to limits within which they can be 95% confident that the "true" value lies. This range is roughly between −2 and +2 times the standard error.
So
- for our first group, .42 x 2 = .84
- for our second group, .67 x 2 = 1.34
So
- If our first group was representative of the entire population, we were 95% confident that the "true" mean lied somewhere between 6.16 and 7.84 (7 ± .84 or $6.16 \leq 7 \leq 7.84$).
- For our second group, we were 95% confident that the "true" mean lied somewhere between 11.66 and 14.34 (13 ± 1.34 or $11.66 \leq 13 \leq 14.34$).

Put another way, when the mean was presented along with its 95% confidence limits, the workers were saying that there is only a 1 in 1.34 chance that the "true" mean value was outside those limits. Put still another way: the probability (**p**) that the mean value lied outside those limits is less than 1 in 1.34 (**p** = <0.05).
According to Chebyshev's theorem, the interval (7, 19) can be written as (13-2*3, 13+2*3) which is same as (Mean -k*SD, Mean +k*SD), where k =6/3=2.
According to Chebyshev's theorem, at least 1 - (1/k-squared) of the measurements will fall within (Mean - k*SD, Mean +k*SD)
But 1 - (1/k-squared) = 1 - (1/2^2) = 1 − 0.25= 0.75
Thus 75 percent of the values will fall between 7 and 19 for a data set with mean of 13 and standard deviation of 2.
That result said that the 75 percent possibility was that the average student using the mind map can generate more ides than the traditional system with 2 standard deviation.
According to Empirical rule, approximately 95% of the measurements (data) will fall within two standard deviation of the mean. Therefore (Mean -2*SD, Mean +2*SD) = (13-2*3, 13+2*3) = (7, 19) will contain 95 % of the observations.
Thus the two values are 7 and 19. That result said that the 95 percent possibility is that the average student using the mind map can generate more ides than the traditional system with 2 standard deviation.
As a result, researchers concluded the research with a positive view on Mindmap and from the experiments to

shows that it is really a powerful tool to improve academic tasks of students; in another word it increases the level of creativity of students. This research will help the researchers of the field of contemporary research, academic research, academic reading, academic writing, poster presentation, academic presentation, and innovative teaching and learning methodologies.

REFERENCES

[1]   Boden, M.A. (1994). Précis of the creative mind: myths and mechanisms. Behavioral and Brain Sciences, 17, pp 519-531. doi: 10.1017/S0140525X0003569X

[2]   Mento, A.J., Martinelli, P. and Jones, R.M. (1999). Mind Mapping in Executive Education: Applications and Outcomes. The Journal of Management Development, Vol 18, Issue 4, ISSN 0262-1711, retrieved April 2011 from http://www.fuzz2buzz.com /files/mm_executive_ education_applications _outcomes_ Figs.pdf.

[3]   Buzan, T. (1989), Use Both Sides of Your Brain, 3rd ed., Plenum, New York, NY.

[4]   Farrand, P., Hussain, F. and Hennessy, E. (2002). The efficacy of the `mind map' study technique. Medical Education. 36: 426–431. doi: 10.1046/j.1365-2923.2002.01205.x

[5]   Chan, W. (2004). The effectiveness of using Mind Mapping skills in enhancing secondary one and secondary four students writing in a CMI school. HKU Thesis Online. Retrieved from http://hub.hku.hk/bitstream/10722/31749/1/FullText.pdf.

[6]   Wheeler, L.R. and Collins, S.K.R. (2003).The influence of concept mapping on critical thinking in baccalaureate nursing students. Journal of Professional Nursing. Vol. 19, Issue 6, Pages 339-346, DOI: 10.1016/S8755-7223(03)00134

[7]   Clayton, L.H. (2006) Concept Mapping: An Effective, Active Teaching-Learning Method. Nursing Education Perspectives: July 2006, Vol. 27, No. 4, pp. 197-203

Research Paper   Open Access

Buckling Analysis of Woven Glass Epoxy Laminated Composite Plate

M Mohan Kumar[1], Colins V Jacob [2], Lakshminarayana N [2], Puneeth BM [2], M Nagabhushana[2]

[1]*STTD, National Aerospace Laboratories, Bangalore, India*
[2] *Department of Mechanical Engineering, Visvesvaraya Technological University, Karnataka, India*

Abstract: Buckling behavior of laminated composite plates subjected to in-plane loads is an important consideration in the preliminary design of aircraft components. The sizing of many structural subcomponents of the aircraft structures is often determined by stability constraints. The objective of the current study is to understand the influence of the length-to-thickness ratio, the aspect ratio, the fiber orientation and the cut-out shapes on the buckling load for the glass epoxy laminated composite plate in clamped-free-clamped-free configuration by FE analysis using MSC.Patran/Nastran. Initially, buckling analysis was carried out on aluminum plates, both; experimentally and numerically; for the two different geometric configurations to predict the critical buckling load and the test results were compared with the FEA predictions, to check the validity of the analysis methodology. The same methodology was further followed for analyzing the buckling behavior of the composite plates. The results shows the effect of orientation of fiber, aspect ratio, cut-out shape and length-to-thickness ratio on the buckling of the glass epoxy laminated composite plate.

Keywords: - *Plate buckling, woven glass epoxy laminate, length-to-thickness ratio, aspect ratio, fiber orientation, cut-out shapes*

I.   INTRODUCTION

Development of new applications using composites is accelerating due to the requirement of materials with unusual combination of properties that cannot be met by conventional monolithic materials. Actually, composite materials are capable of covering this requirement in all means because of their heterogeneous nature. Properties of composite arise as a function of its constituent materials, their distribution and the interaction among them and as a result an unusual combination of material properties can be obtained.

Laminated composites are gaining wider use in mechanical and aerospace applications due to their high specific stiffness and high specific strength. Fiber-reinforced composites are used extensively in the form of relatively thin plate, and consequently the load carrying capability of composite plate against buckling has been intensively considered by researchers under various loading and boundary conditions. Due to the excellent stiffness and weight characteristics, composites have been receiving more attention from engineers, scientists, and designers. During operation, the composite laminate plates are commonly subjected to compression loads that may cause buckling if overloaded. Hence their buckling behaviors are important factors in safe and reliable design of these structures.

There are few studies on optimal design of simply supported rectangular plates laminated to composite material and subjected to uniaxial compressive loading [1,5]. Numerical results are presented for optimal-design plates laminated of glass/epoxy, boron/epoxy, and carbon/epoxy composite materials. Initially, few studies were made on thin-walled structures which are having high strength coupled with the ease of manufacturing and the relative low weight. However, thin-walled structures have the characteristic of susceptibility of failure by instability or buckling. It is therefore important to the design engineer that accurate methods are available to determine the critical buckling strength [8].

A procedure for determining the buckling load of the aluminum rectangular plate is carried out where

buckling loads are determined from different experiment methods and were compared with the theoretical buckling loads and also various formulation based on the first-order shear deformation theory and von-Karman-type nonlinearity to estimates the critical/buckling loads of laminated composite rectangular plates under in-plane uniaxial and biaxial loadings. Different combinations of simply supported, clamped and free boundary conditions were considered [5, 11]. Also, the influence of boundary conditions on the buckling load for rectangular plates was studied [2]. Numerical and experimental studies were conducted to investigate the effect of boundary conditions, length/thickness ratio, and ply orientation on the buckling behavior of E-glass/epoxy composite plates under in-plane compression load.

It was found that most of the studies were focused on unidirectional fiber. Industry driven woven fibers are being increasingly used in many industries. Hence more importance is give on its structural behavior. It also indicates that the interaction among stacking sequence, cutout shape and length/thickness ratio on the buckling behavior of woven fiber laminated composites are needed to investigate in more detail. The aim of performing this work is to extend the knowledge of the structural behavior of woven fabric composites subject to compressive load which is lacking. The main objective of this study is to carry out buckling analysis of symmetrically and laminated composite plates under clamped-free–clamped-free boundary condition. The effects on buckling load by cut out size, length/thickness ratio, ply orientation and cut-out shapes are investigated.

II.   EXPERIMENTAL STUDY

Experimental studies were carried on the following two Al-plate configurations to find out the critical buckling load:

- Rectangular Al 2024 T3 plate (300×200×1.6 mm)
- Square Al 2024 T3 plate (300×300×1.6mm)

This experimental study was carried out to validate the buckling results obtained from FEA, so that the same analysis methodology can be followed for the buckling analysis of woven fabric composite plates. The experiment comprises of an aluminum plate clamped on two longitudinal ends on an INSTRON 1341 testing machine of 50KN capacity and kept free at the other two. Then it was loaded in axial compression. Clamped boundary conditions were simulated along the top and bottom edges, restraining 50mm length and the test specimens were mounted on the testing machine through the mechanical fixtures. The top fixture was held fixed during the test whereas the bottom fixture was moved by servo hydraulic cylinder.

Figure 1: Buckling test setup and onset of buckling in rectangular aluminum plate

As the load was increased the dial gauge needle started moving and at a particular value of the load applied, there was a sudden large movement of the needle and thus the 1st mode buckling was observed. The load corresponding to this point is the critical buckling load of the plate.

The same test procedure was repeated, similarly, for the square aluminum plate and under the similar loading conditions, the dial gauge showed sudden large movement of the needle due to the large out-of-plane deformation of the plate and thus the 1st mode buckling was observed. The load vs. displacement curve was plotted and the load at which the initial part of the curve deviated from linearity was taken as the Critical buckling load.

Figure 2: Buckling test setup and onset of buckling in square aluminum plate

III.   FINITE ELEMENT ANALYSIS

3.1 FE Buckling Analysis of Aluminum 2024-T3 Plates

In this study, linear static buckling analysis was carried out on both aluminum plates and for the woven fabric laminated composite plates using MSC.Patran and MSC.Nastran package to estimate critical buckling load in order to study the influence of length-to-thickness ratio, the ply orientation, cut out shape and the aspect ratio on the buckling behavior of the woven fabric laminated composite plate.

Here QUAD4 shell elements of 1 mm global edge length were used to mesh the model and the total number of elements was around 60,000 with 60500 nodes. The solution was found using Solution Sequence 105 under Buckling solution type employing the Lanczos extraction method for the 1st mode buckling i.e. for the 1st Eigen value.
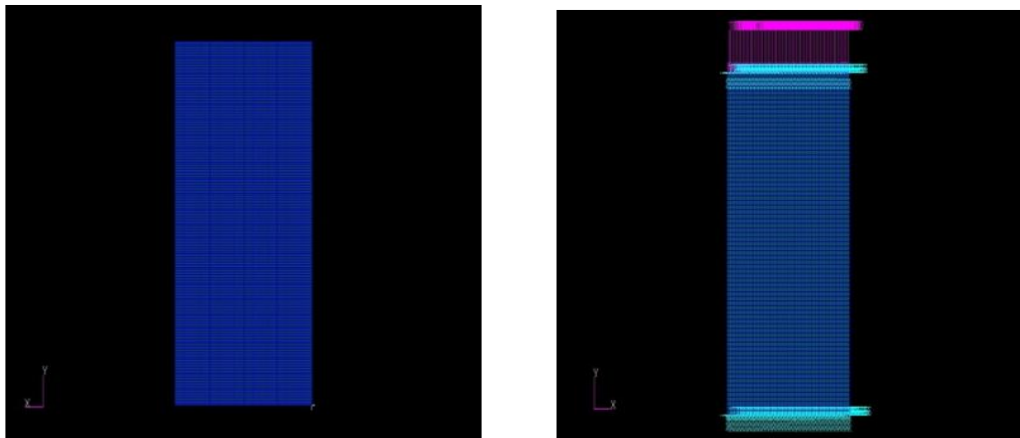
Figure 3: FE model and Boundary conditions applied for the square aluminum plate

3.2 FE Buckling Analysis of Composite Plates

Following the validity for the correctness of the methodology used for the analysis of the aluminum plate, the same procedure was followed for the analysis of the composite plates. The mechanical properties of the analyzed specimens were $E_{11} = 7700$ N/mm^2, $E_{22} = 7700$ N/mm^2, $\nu = 0.12$ and $G_{12} = 2810$ N/mm^2.

The widths of the plates were kept constant while varying the lengths so as to study the effect of aspect ratio on the buckling behavior. Also the thicknesses were varied for the same lengths of the plates so as to study the effect of length-to-thickness ratio. Since woven fabric composite plates were considered for the analysis, the orientation of the fiber which was initially kept 0° was then changed to the 30°/-30° alignment and to 45°/-45°, in order to study the effect of fiber orientation as well.

The analysis was carried out considering the plate to be two-dimensional orthotropic laminate and the composite to be laminated. Also the loading the plate was carried along the fiber direction in the FE analysis. Also, in order

to study the effect of the cut-out shapes on buckling behavior, three different cut-out shapes, namely, circular, square, and rectangular were analyzed for $[0]_{12}$ plates keeping the cut-out area constant as 962 mm^2.

a. Without cut-out   b. Circular cut-out

c. Square cut-out   d. Rectangular cut-out
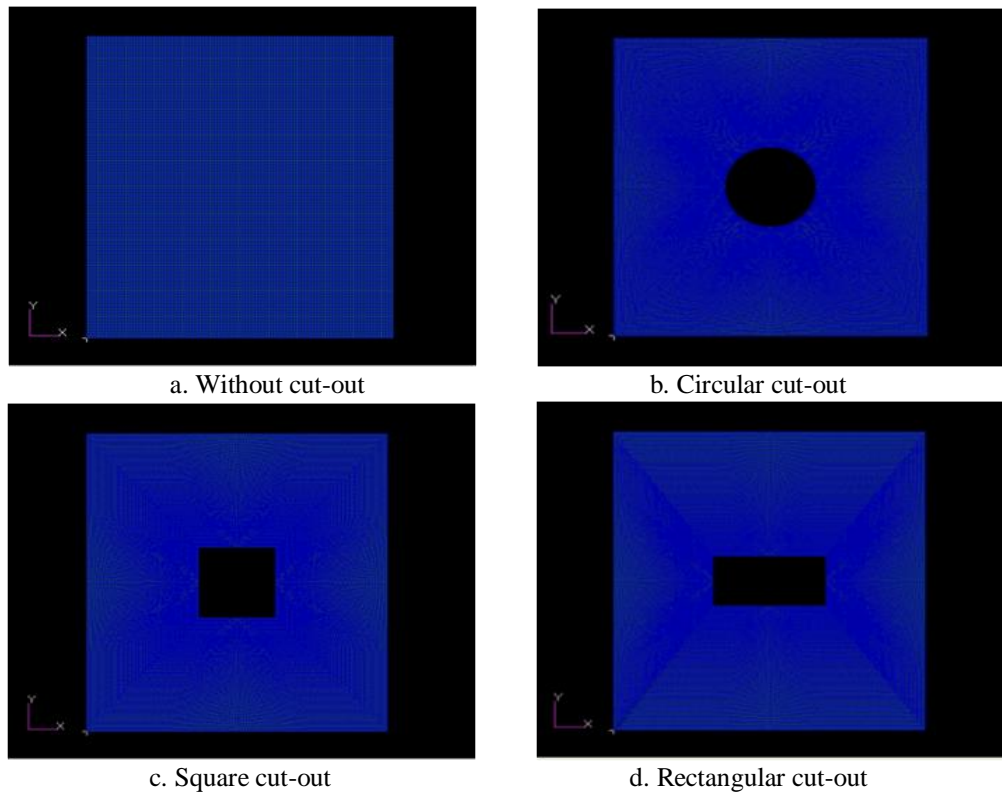
Figure 4: FE model of composite plates with different cut-out shapes

IV.   RESULT AND DISCUSSION

4.1 Buckling Results for Aluminum 2024-T3 plates

The experimental analysis of the two aluminum plates yielded the load vs. displacement curve with the displacement on the x- axis and the load on the y-axis. That critical buckling load point was determined from the intersection of two tangents drawn from the pre-buckling and post-buckling regions. From the graph shown in the Figure- 5, it can be seen that for the rectangular aluminum plate, the load becomes constant at 2.26 kN. This represents the 1st mode buckling of the specimen after which the plate is considered failed. Since the thickness of the plate is very small, the plate shows a large deflection for small increment in the load.

Also, the FE analysis result for the buckled shape of the rectangular aluminum plate is shown in the Figure 6. It is observed that the critical buckling load for the rectangular specimen is determined as 2.52 kN.
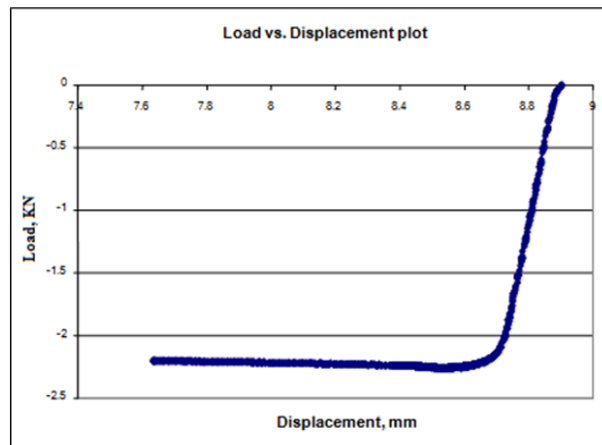
Figure 5: Load vs. out-of-plane displacement graph for rectangular aluminum plate
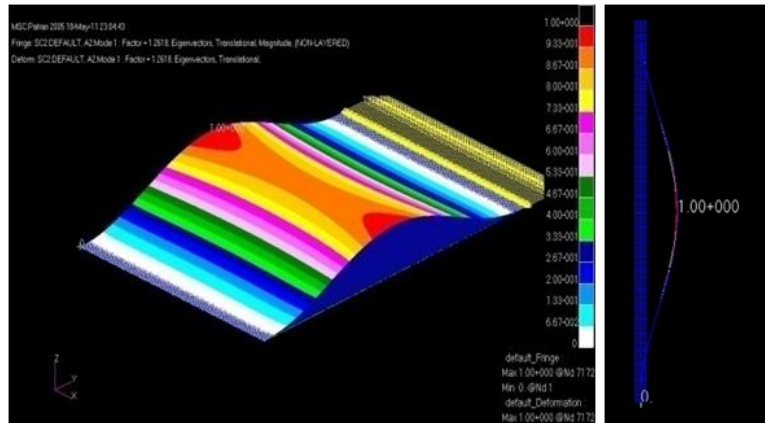
Figure 6: Buckled shape of the rectangular aluminum plate

Similarly, the load vs. out-of-plane displacement for square aluminum plate is shown in the figure-7. From the graph, it can be observed that the 1st mode buckling load is 2.87 kN.
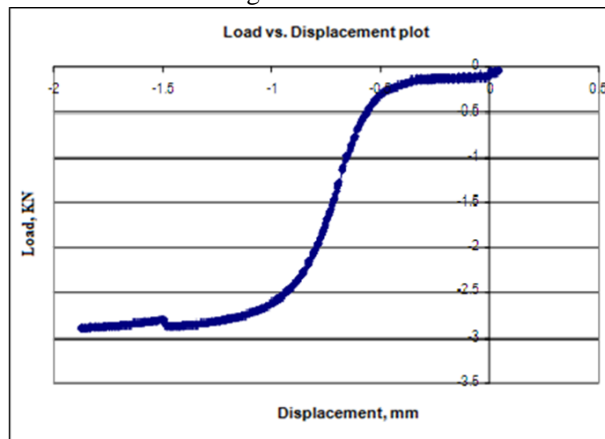
Figure 7: Load vs. out-of-plane displacement graph for square aluminum plate

The FE analysis result for the buckled shapes of the square aluminum plate is shown in the figure 8. It is observed that the critical buckling load for the square specimen is determined as 3.24 kN.
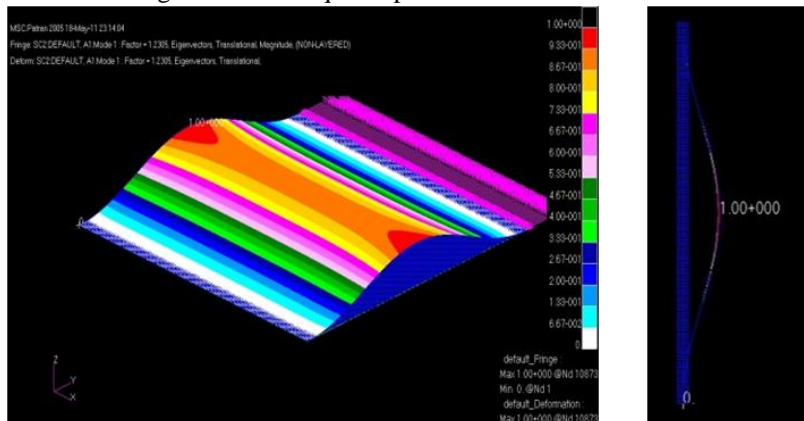
Figure 8: Buckled shape of the square aluminum plate

Table I: Buckling Results for Aluminum Plates

Plate Type	Length (mm)	Width (mm)	Thickness (mm)	Expt P_{cr} (KN)	FE Pcr (KN)
Rectangle	300	200	1.6	2.24	2.52
Square	300	300	1.6	2.52	3.24

4.2 Buckling Results for Composite Plates
        The laminated composite plates were analyzed for determining the critical buckling load. The effect of length-to-thickness ratio, aspect ratio, fiber orientation and cut-out shapes on the buckling load for the woven glass epoxy laminated composite plate is studied.

4.2.1 Effect of Length-to-Thickness (a/t) ratio on Buckling Load
        In this study the thickness of the plate was increased by increasing number of layers as shown in the figure 9. Here the length-to-thickness ratio was varied between 33.77 and 98.48. We can observe that the numerical results show that the variation in buckling load is very sensitive to the thickness and the buckling load decreases with increase in length to thickness ratio.
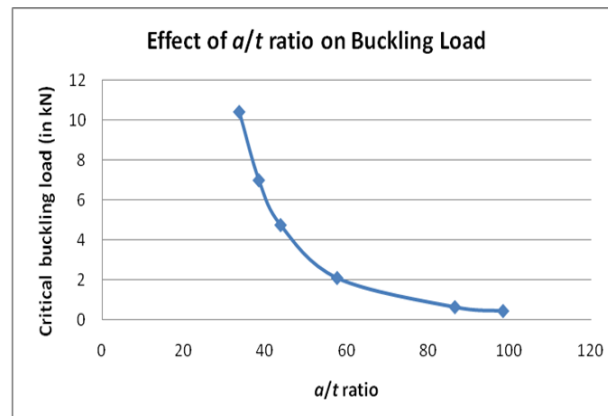
Figure 9: Buckling load vs. length-to-thickness (a/t) ratio

4.2.2 Effect of Aspect (a/b) ratio on Buckling Load
        In this study, the laminated plates were evaluated at three different aspect ratios. The buckling load decreases continuously with increasing aspect ratio but the rate of decrease is not uniform It is observed that buckling load was maximum for aspect ratio 1.08 and minimum for aspect ratio 1.67. The aspect ratio and buckling load was plotted along x- and *y*- axis as shown in figure 10. From the graph, it is observed that the buckling load is decreases with the increase in the aspect ratio.
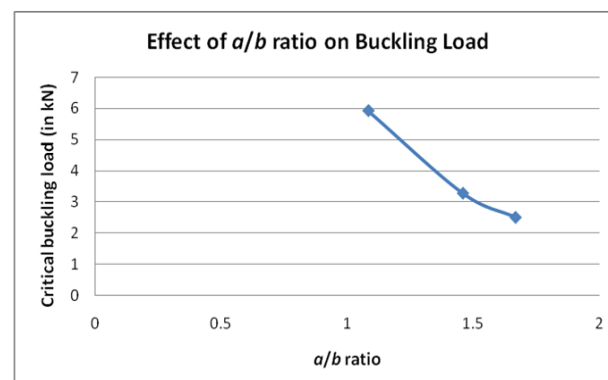
Figure 10: Buckling load vs. aspect (a/b) ratio

4.2.3 Effect of Fiber Orientation on Buckling Load
        In this study the buckling load of composite plates with different fiber orientation was determined. The result shows the decreasing trend of the buckling load with increase in the fiber orientation. The maximum buckling load occurred for 0° fiber orientation. The variation of buckling load with fiber orientation is shown in figure 11. From the figure, it is observed that with the increase in fiber orientation, the buckling load decreases.

4.4.4 Effect of Cut-out Shapes on Buckling Load
        In this section, in order to understand the effects of circular, square and rectangular shaped cut-outs on buckling load, plates with these cut-out shapes of equal areas were considered. From the Table 2, it can be

observed buckling load generally decreases with the presence of cut-out. The plate with rectangular cut-out gives the least buckling load of 7.23 kN and for the one with the circular cut-out, the highest buckling load was observed with 7.89 kN.
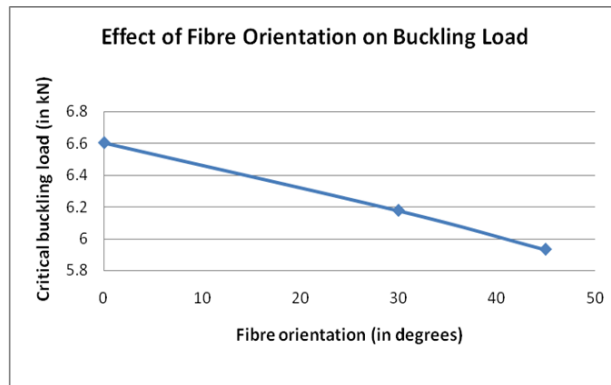
Figure 11: Buckling load vs. fiber orientation

a. Without cut-out   b. Circular cut-out

c. Square cut-out   d. Rectangular cut-out
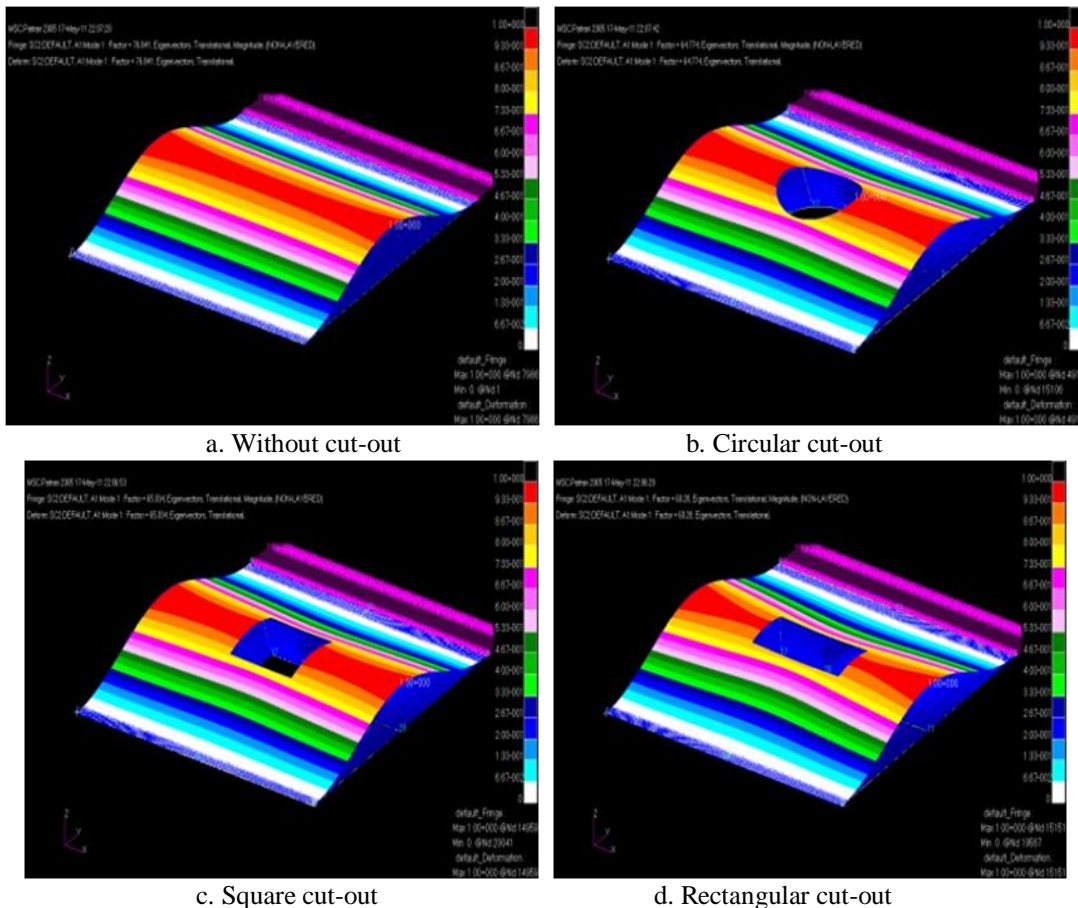
Figure 12: Buckling behavior of composite plates with different cut-out shapes

Table II: Critical buckling loads for the various cut-out shapes

Sl. no.	Cut-out shapes	Length, a (in mm)	Width, b (in mm)	Thickness, t (in mm)	Critical buckling load, P_{cr} (in kN)
1	No cut-out	130	120	3.7	9.221
2	Circular	130	120	3.7	7.899
3	Square	130	120	3.7	7.804
4	Rectangular	130	120	3.7	7.234

V. CONCLUSION

This study considers the buckling response of rectangular laminated composite plates with clamped-free-clamped-free boundary conditions. For this, a linear buckling analysis was initially carried out on aluminum plates of two different configurations to estimate critical buckling load and the predicted FE results were verified with the results obtained from the buckling tests conducted. Further, the same analysis methodology was followed to estimate the critical buckling load for various woven fabric laminated composite plates to study the influence of length-to-thickness ratio, the aspect ratio, the ply orientation and the cut-out shapes on its buckling behavior. From the present experimental and numerical studies, the following conclusions are the following conclusions may be drawn based on the results obtained in this investigation made:

1. It was noted that variations in length-to-thickness ratio affects the critical buckling load. The buckling load decreases as the a/t ratio increases. The rate of decrease of buckling load is not uniform with the rate of increase of a/t ratio.
2. As the aspect ratio increases, the critical buckling load of the plate decreases. When the aspect ratio changed from 1.0 to 1.7. The rate of change of buckling load with a/b ratio is almost uniform.
3. It was seen that the different fiber orientation angles affected the critical buckling load adversely. With the increase in the fiber angle, the buckling load decreased. The plate with $[0]_8$ layup had the highest buckling load and the plate with $[45]_8$ layup had the least.
4. The reduction of the buckling load due to the presence of a cut-out is found to be significant. It is noted that the presence of cut-out lowers the buckling load and it varies with the cut-out shape. The plate with circular cut-out yielded to the greatest critical buckling load while the rectangular cut-out failed for the lowest buckling load.

VI. ACKNOWLEDGEMENTS

REFERENCES

[1] Chainarin Pannok and Pairod Singhatanadgid; "Buckling analysis of composite laminate rectangular and skew plates with various edge support conditions"; The 20th Conference of Mechanical Engineering Network of Thailand, 2006.

[2] Shukla K.K., Nath, Y., and Kreuzer, E., "Buckling and transient behavior of layered composite plates under thermo-mechanical loading", ZAMM, 85, No.3, 163-175, 2005.

[3] Q. Han and G. Lu, "Torsional buckling of a double-walled carbon nanotube embedded in an elastic medium"; Eur. J. Mech. A/Solids 22; pp. 875–883, 2003.

[4] Wang Gang, Liu Hai Yan, Ning Jian Guo; "Dynamic Buckling in a Rod Having Finite Length Due to Axial Impact"; Journal of Beijing Institute of Technology; 2002-03.

[5] Chavanan Supasak and Pairod Singhatanadgid; "A Comparison of Experimental Buckling Load of Rectangular Plates Determined from Various Measurement Method"; The 18th Conference of Mechanical Engineering Network of Thailand; 2002.

[6] Shun-Fa Hwang and Shu-Mao Huang; "Postbuckling behavior of composite laminates with two delaminations under uniaxial compression"; Composite Structures, Volume 68, Issue 2; 2001.

[7] Chattopadhyay A. and Radu, A. G., "Dynamic Instability of Composite Laminates Using a Higher Order Theory," Computers and Structures, Vol. 77, 453-460, 2000.

[8] Fok, "Applied Theory of Thin Plates to Engineering Structures", 1984.

[9] A.W. Leissa, "Buckling of composite plates", 1976, Pg. 51-66.

[10] Stephen P. Timoshenko and Kriger, "Theory of Plates and Shells", 2nd Ed., McGraw-Hill International Edition, 1959.

[11] Frederic Y.M. Wan, "On Lateral Buckling of End-loaded Cantilevers with Transverse Shear Deformations", Solid Mechanics and Its Applications, 2002, Volume 88, 343-356.

[12] R. Von Mises; Treatise on Saint-Venant's Principle; Bull. AMS; 51; 555-562; 1945.

[13] Euler, "Treatise on Column Flexural Buckling"; 1759.

[14] Brush, D. O. and Almroth, B. O.; "Buckling of bars, plates, and shells"; McGraw-Hill, New York; 1975.

Research Paper   Open Access

Assessment of Infiltration rate of a Tank Irrigation Watershed of Wellington reservoir, Tamilnadu, India.

Srinivasan.K[1] and Poongothai.S[2]

[1]Assistant Professor, [2]Professor, Department of Civil Engineering, Annamalai University Annamalainagar, India,

Abstract: - A Study was attempted to assess the infiltration rate of a tank irrigated Wellington watershed of Tamilnadu, India. Different types of soil samples have been collected from 30 locations spread uniformly over study area in order to examine the infiltration rate of soils and its impact on the overall crop production process. Double ring infiltrometer was used to carry out the experimental study. Infiltration rates were taken at 0 to70 minutes of 10 minutes intervals. The assessment or determination of infiltration rate was processed by laboratory analysis of soil samples for the particle size distribution. The infiltration rates were well above the recommended values for crop production. This will help improve the structure and restore soil potentials. Apart from these, suitability evaluation of land in order to effectively categorize soils on the basis of their potential for optimal use could as well be imperative.

Key Words: - Double ring infiltrometers, Land use, Soil type and texture, Steady state infiltration and surface irrigation.

I.   INTRODUCTION

Precipitation, upon falling on the soil surface, wets it, fills depressions and penetrates into the soil. This water replenishes the soil moisture deficiency with the excess moving downward by force of gravity through seepages or percolation to build up the water table [3]. The phenomenon of infiltration has been variously defined; it entails a process of water movement from surface soil into the ground. This water is said to have the potentials of penetrating into the lower soil profile [8], [16]. Besides, it carries with it some amount of nutrients [11], [2]. Infiltration is the term applied to the process of water entry into the soil. The rate of infiltration determines. The time at which superficial water appears on the soil surface. The amount of runoff that will form over the soil surface during rainfall or irrigation. If the rate of infiltration is limiting, the entire water balance in the root zone will be affected. Infiltration is the process by which water enters the soil. It separates water into two major hydrologic components - surface runoff and subsurface recharge. The assessment of runoff risk has assumed an increased importance because of concerns about the associated pollution hazards. Accurate determination of infiltration rates is essential for reliable prediction of surface runoff. As environmental impact assessments are concerned with long-term effects, it is essential that the infiltration data on which they are based should be reasonably stable over decades. For planning purposes it is essential to know the stability of infiltration data for the infiltration capacity of individual soils is adequate to cope with the anticipated hydrologic loads. A high infiltration rate is generally desirable for plant growth and the environment. In some cases, soils that have unrestricted water movement through their profile can contribute to environmental concerns if misapplied nutrients and chemicals reach groundwater and surface water resources via subsurface flow. In India also, very few studies have been reported that focused on infiltration based rainfall simulator experiment [1], [17]. [12]- [14] have measured run-off and sediment yield over a period of 2–3 years from micro-watersheds in Kumaun Himalaya under the natural rainfall conditions but studies based on simulated rainfall are very rare in the country. A few studies had been carried out by [15], [9], [19], [20] for estimating the infiltration rates in various basins in different parts of India using double ring infiltrometers.

Infiltration of water into the soil has important impact in the overall functioning of the variable land – based activities. It has significant tradeoffs for environmental sustainability, food security, biodiversity stability and

susceptibility of soil to adverse environmental conditions. Two factors can greatly undermine availability of water for sustainable crops production *viz*: low water table and impervious layer. The former may be due to excessive infiltration which is often a function of soil characteristic while the later may be largely due to clay deposit that can cause crusting below the soil surface. Infiltration of water into the soil has important impact in the overall functioning of the variable land – based activities. It has significant tradeoffs for environmental sustainability, food security, biodiversity stability and susceptibility of soil to adverse environmental conditions. Two factors can greatly undermine availability of water for sustainable crops production *viz*: low water table and impervious layer. The former may be due to excessive infiltration which is often a function of soil characteristic while the later may be largely due to clay deposit that can cause crusting below the soil surface. The study of infiltration rates come in handy in many hydrological problems such as runoff estimation, soil moisture budgeting and in irrigation planning. Infiltration has an important place in the hydrological cycle. Detailed study of Infiltration process meets the following purposes.

(i)   Estimation of peak rates and volumes of runoff in planning of tams, culverts and bridges etc.,
(ii)   Estimation of surface runoff and overland flow.
(iii)   Planning of watershed engineering
(iv)   Estimation of groundwater recharge
(v)   Assessment of soil moisture deficits and planning irrigation and drainage system etc.,

II.   METHODOLOGY

There are four commonly employed methods and instruments for the measurement of infiltration, namely double infiltrometers; ponding; blocked recirculating infiltrometer; and a deduction of infiltration from evaluation of the advance phase and the tail-water [18]. The ring infiltrometer methods are usually applied in Vellar River basin, while the other two are suitable for furrow irrigation. In a homogenous one-layer soil, water flows relatively uniformly in the vertical direction, with very little lateral drainage. So, measurements done with a single ring infiltrometer could be as accurate as that obtained from a double ring infiltrometer. The soils in the Wellington reservoir area have developed as a result of annual deposition of different layers of sediments. In such multiple layered soils, significant lateral water flow is inevitable and hence, a double ring infiltrometer is preferable. As shown in (Fig.1).water in the outer ring moistens a large surrounding area, creating a buffer to effectively minimize any flow of water from the inner ring in a horizontal direction. Table1. Steady infiltration rates for general soil texture groups in very deeply wetted soil [4]
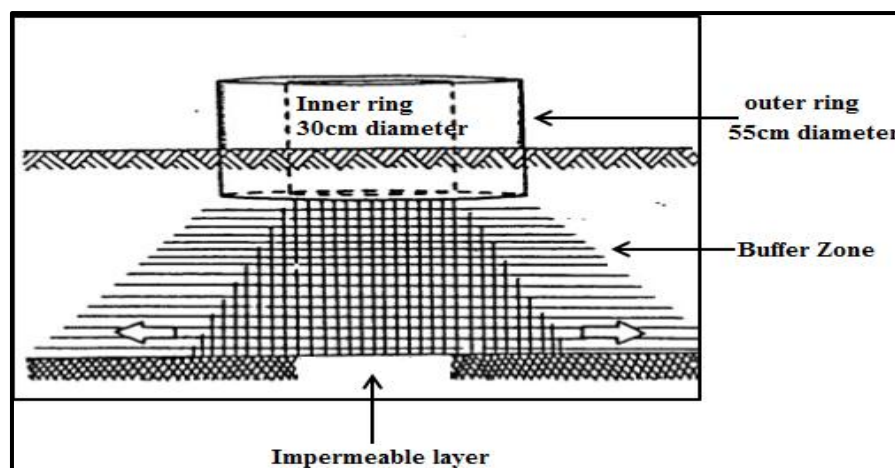
Fig1. Buffering the lateral flow below an double ring infiltrometer [18]

The Study Area

The study area considered is Wellington reservoir watershed which is located in the Tittakudi taluk (Fig 2). It lies between the longitudes of $11°21'$ to $11°31'$ E and latitudes of $78°57'$ to $79°28'$N. The present study area occupies an aerial extent of 100 sq.km and the relief ranges from 62 m to 121 m above MSL. As of 2001 India Census, Tittagudi had a population of 20,734. In this taluk, agriculture area is 823.74 km^2. The study area receives an average rainfall of 1100 mm with more than 80% of the rainfall received during the NE monsoon. The minimum and maximum temperature ranges between 20°C and 34°C in the month of January and May respectively. River Vellar flows in the southern part of the study area. Geomorphologically the area consists of old flood plains, pediments, duricrust and pediments covered by forest land [22]. Black soil is predominant soil type in this area and main occupation of the area is agriculture. The groundwater level of the study area ranges

from 2m to 8m bgl (below ground level). The Wellington Reservoir is located in Vellar Basin across a tributary stream Periya Odai of Vellar River. The Reservoir was constructed during 1913-1923 and irrigates an ayacut of 11,200 Hectare. It receives regulated supply diverted from Vellar River at Tholudur regulator and an additional catchment area of 129 (Km)^2 of its own during North East Monsoon. Paddy, Sugarcane is the major crops grown in and around wellington ayacut.
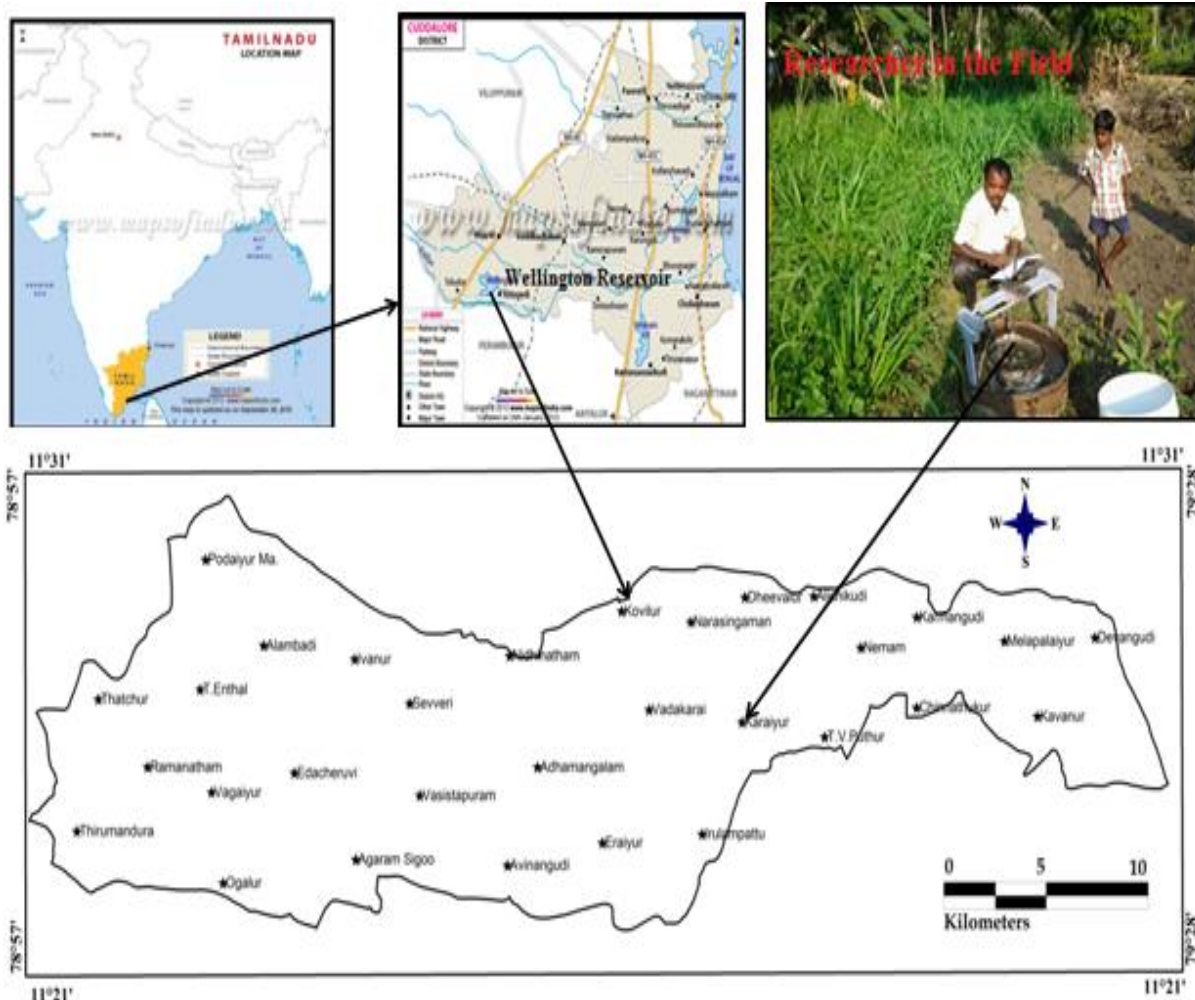
Fig: 2 Study area location map

III.   RESULTS AND DISCUSSIONS

The major soils that were identified from soil type maps are well sand, poor sand, poor clay and well clay. (Fig. 3-6)shown in the infiltration rate curves for well sand, poor sand, poor clay and well clay soils, respectively. The measured steady state infiltration rates for the selected soil types are presented in (Table 4) and Steady state infiltration rates for the study area (Fig 8). The initial infiltration rates range from 8.4 – 46.8, 13.2-46.8, 7.2 - 36 and 5.4 – 58.8 cm/hour (Fig. 3-6) while steady state infiltration rates ranges of cultivated land [10] 8.4 – 19.2, 13.2 – 21, 7.2 - 18 and 5.4 – 30 cm/hour, respectively for well sand, poor sand, poor clay and well clay soils, respectively (Table 4). Generally, the lower the initial soil moisture content is, the higher the initial soil infiltration rate will be [7]. This explains the high initial infiltration rates for all the soil types, since the initial soil moisture was expected to be low due to dry soils in winter when the experiments were conducted. The infiltration rate curves for the study area are exponential and asymptotic and are adequately described by the existing infiltration models such as [5]. Infiltration is rapid through large continuous pores at the soil surface and slows as pores become smaller. Steady-state infiltration rates typically occur when soil is nearly saturated and are listed for varying textural classes in (Table 1). These are average values and should not be generalized for all soil types. Guideline of basic infiltration rates infiltration classification for various soil types discussed in (Table 2) and according of [6] basic infiltration rate cm/hr, ratings of infiltration rate for surface irrigation Table 3.

TABLE: 1. STANDARD VALUES OF STEADT STATE INFILTRATION FOR GENERAL SOIL TEXTURE GROUPS [4]

Soil Type	Steady Infiltration Rate (in/hr)
Sands	> 0.8
Sandy and silty soils	0.4 - 0.8
Loams	0.2 - 0.4
Clays	0.04 - 0.2
Sodic clayey soils	< 0.04

TABLE 2: GUIDELINE BASIC INFILTRATION RATES FOR VARIOUS SOIL TYPES (THOMAS ET AL., 2004)

Soil type	Basic infiltration rate in mm hr-1	Infiltration class
Sand	> 30	Very rapid
Sandy loam	20 to 30	Moderately rapid to rapid
Loam to silt loam	10 to 20 Moderately slow to moderately rapid	Moderately slow to moderately rapid
Clay loam	5 to 10	Slow to moderately slow
Clay	1 to 5	Very slow to slow

TABLE: 3 RATINGS OF INFILTRATIONS RATE FOR SURFACE IRRIGATION [6]

Basic infiltration rate cm/hr	Sustainability for surface irrigation.
< 0.1	Unsuitable (too slow) but suitable for rice
0.1 – 0.3	Marginally suitable (too slow), marginally suitable for rice
0.3 -0.7	Suitable; unsuitable for rice
0.7 -3.5	Optimum
3.5-6.5	Suitable
6.5-12.5	Marginally suitable (too rapid) small basin Reflowed
12.5-25.0	Suitable only under special condition very small basins reflowed
>25.	Unsuitable (too rapid) recommended for overhead method only

TABLE 4: Measured Steady State Infiltration Rates For Selected Soil Types

Soil type	Site	Steady state infiltration rate (cm/hour)
Well sand	1. M.Pudaiyur 2. Thatcher	8.40 19.2
Poor sand	3. Aalambadi 4. T.Enthal 5. Vagaiyur 6. Ramanatham 7. Edaicheruvai 8. Ivanur	21 15 20.4 15 13.2 13.2
Poor Clay	9. Cinnathukurichi 10. Kavanur 11. Karmangudi 12. Devangudi	16.8 7.2 10.8 18
Well Clay	13. Vasistapuram 14. Sevveri 15. Ogalur 16. Thirumandurai 17. Agaram Sigoor 18. Alichigudi 19. Deevalur 20. Vadagarai 21. Narasingamangalam 22. Kovilur 23. Nithinatham 24. Aathamangalam 25. Avinangudi 26. Eraiyur 27. Irulampattu 28. Karaiyur 29. TV.Puthur 30. Nemam	9.6 17.4 22.8 12 5.4 12 22.8 15.6 25.2 10.8 19.2 18 24 10.8 10.8 13.2 30 9.6

Figure 3: Infiltration curve for Well Sand
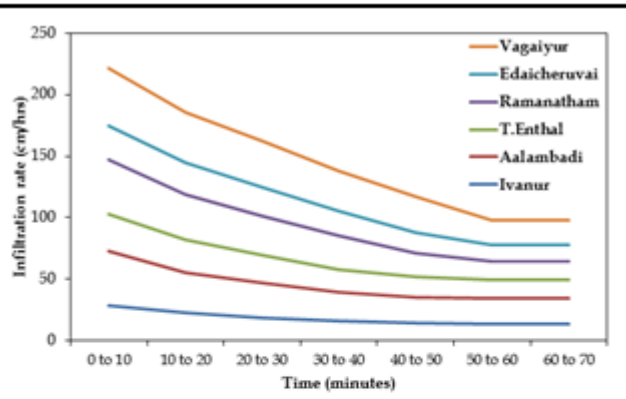
Figure 4: Infiltration curve for Poor Sand
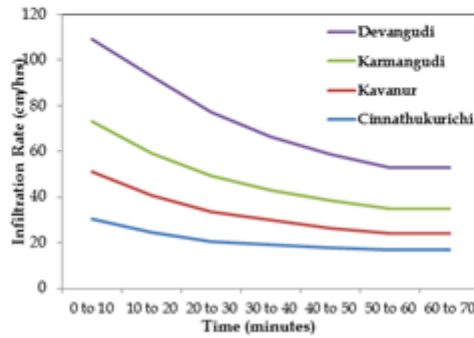
Figure 5: Infiltration curve for Poor Clay
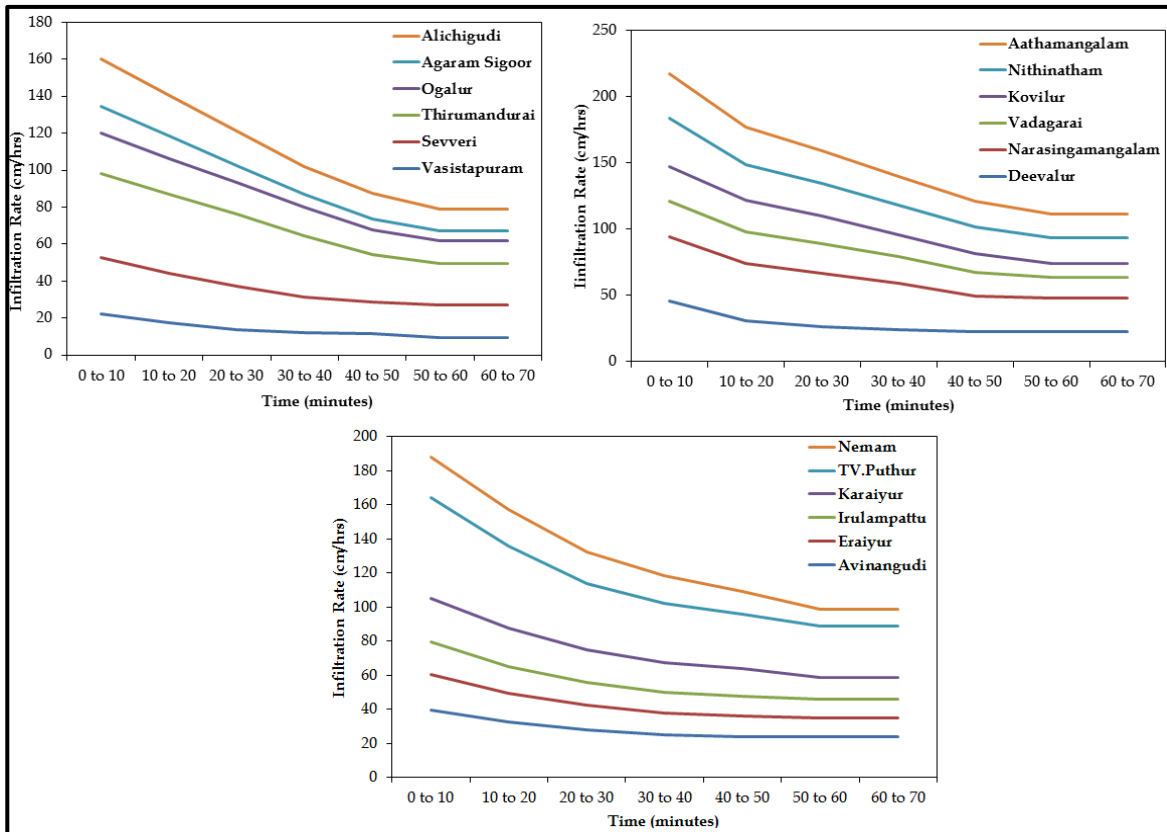
Figure 6: Infiltration rate curves for Well Clay

SOILS AND LANDUSE

The study area is broadly classified into 7 soil types. They are sandyclayloam, sandy clay, sandy loam, silt clay, sandloam, clay and sand. The soil groups are shown in (Fig.7). The main crops grown in the area are paddy and sugarcane. The entire northern part is covered by agriculture especially more than two crop. The broad landuse/cover distribution in the wellington reservoir is shown in (Fig.9).
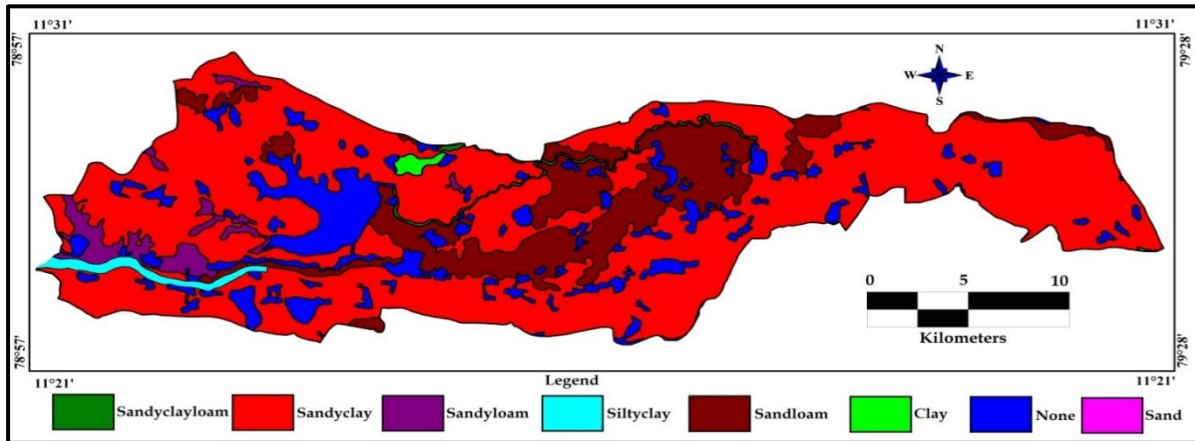
Fig: 7. Soil group map
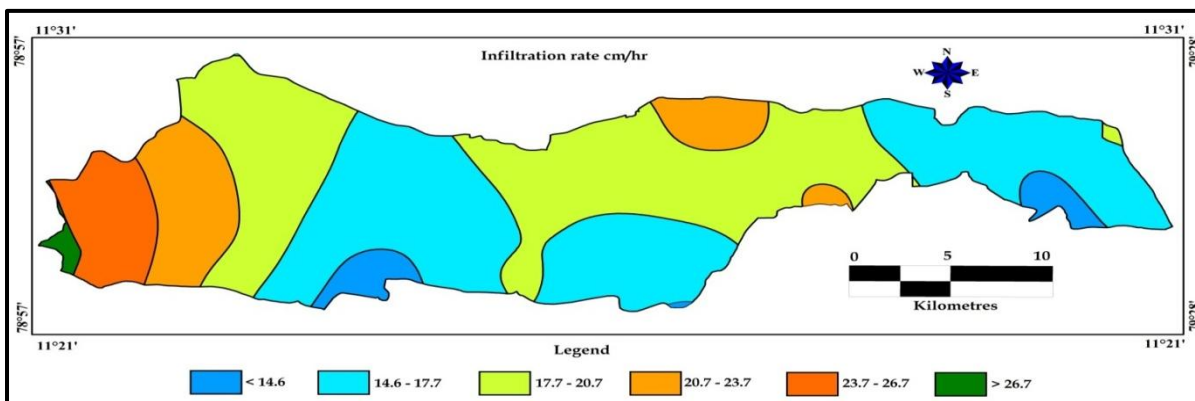
Fig: 8. Infiltration rate of the study area
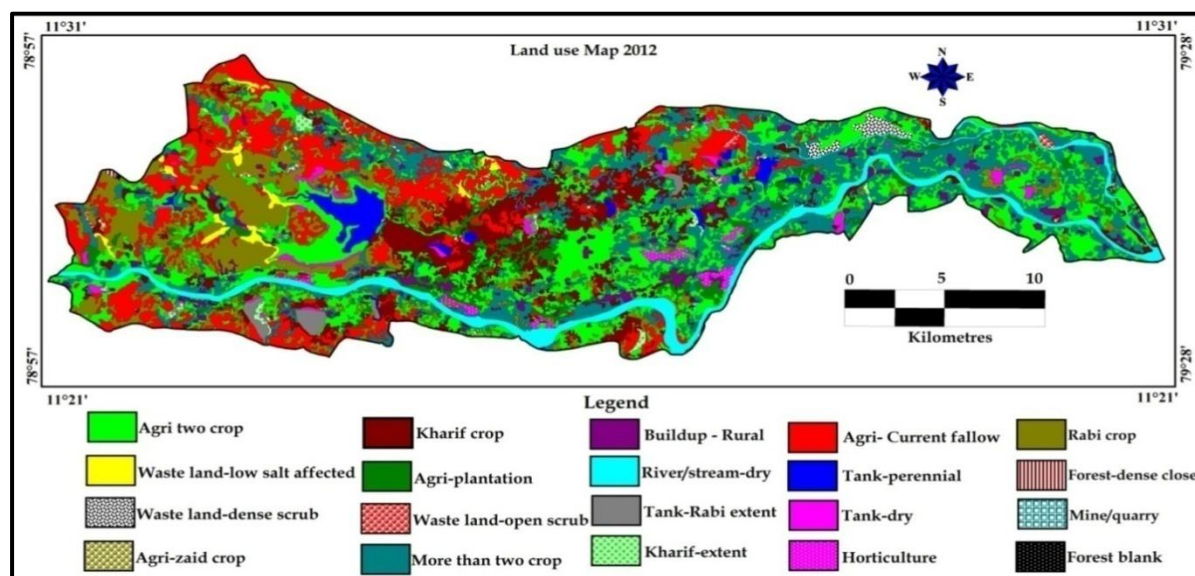
Fig: 9. Landuse/cover map of the Study area

IV.   CONCLUSIONS

The current study determined steady state infiltration rates of different soil types in selected areas of Wellington reservoir in Tittagudi taluk, Cuddalore district, Tamilnadu. Well sand, poor sand, poor clay and well were identified and their steady state infiltration rates ranged from 8.4 – 19.2, 13.2 – 21, 7.2 - 18 and 5.4 – 30 cm/hour, respectively. Well sand soil has the highest initial and steady infiltration rates due to the fact that it has coarse texture and large porous spaces which promote fast infiltration. The measured infiltration rates were higher than the basic values which were attributed to local variations in soil structure. The infiltration rate curves determined are asymptotic and are adequately described by existing infiltration models such as [5]. The measured infiltration rates are significant in prediction of surface runoff, saturated hydraulic conductivity of surface layers and groundwater recharge, and developing or selecting efficient irrigation methods. Studies on infiltration rates of soils are required in solving many hydrological problems such as runoff estimation, soil moisture budgeting irrigation planning, landuse planning and management. This research shows that vegetation cover is one of the most important factors that accelerates infiltration rate and thus reduces overland flow which and ultimately in turns conserves the soil. The area is unsuitable for surface irrigation due to its high infiltration capacity. It is recommended that human activities in the form of deforestation, bush burning and grazing by livestock should be discouraged, while in this area; planting of trees on barren lands should be encouraged to reduce erosion.

V.   ACKNOWLEDGMENT

VI.   AUTHOUR INDEX

K.Srinivasan got him B.E in Civil Engineering in Madras University (SRM Engineering College, Chennai in 2000) and M.E. in Water Resources engineering and management, Annamalai University, Annamalainagar, Tamilnadu, India in 2005. Currently working as an Assistant Professor of Civil Engineering, Engineering wing DDE, Annamalai Univeristy, Annamalainagar, Tamilnadu, India.

REFERENCES

[1].   A. Bhardwaj and R.Singh "Development of a portable rainfall simulator infiltrometer for infiltration, runoff and erosion studies," *Agricultural Water Management*, 22, pp. 235–248, 1992.

[2].   P.K.Chhonkar, S.Bhadrary and T.J.Purakayastha, "Phytore-mediation of heavy metal contaminated soils," *Monographs, Dehion of soil science & Agricultural chemistry*, IARI, New Delhi 2005.

[3].   J. Diamond, "Bulk Density Determination of Chlonroche Country Soil," *Irish Geography*, (36) 2, 2004.

[4].   D. Hillel "Introduction to soil physics," *Academic Press, San Diego*, CA, 1982.

[5].   R.E. Horton "An approach towards a physical interpretation of infiltration capacity," *Soil Science Society of America*, Vol. 5, USA, 1940.

[6].   J.R.Landon "Booker tropical soil manual," A handbook for soil survey and agricultural land evaluation in tropics and sub-tropics," *Longman Science & Technology*, London, UK, ISBN: 0470205210, 474 pp. 1991.

[7].   M. Lili, V. F. Bralts, P.Yinghua, L.Han and L.Tingwu "Methods for measuring soil infiltration," *State of the art, Int J Agric & Biol Eng.* 1(1), pp 22-30. (2008).

[8].   T. J. Marshall Soil Physics. Cambridge, *Cambridge University Press*. 2002.

[9].   Omkar and E Patwari "Infiltration studies in Jammu region," *NIH, Roorkee report*, TR – 163. 1993.

[10].   G.E.Osuji, M.A.Okon, M.C.Chukwuma and I.I.Nwarie "Infiltration Characteristics of Soils under Selected Land Use Practices in Owerri, Southeastern Nigeria," *Nwarie World Journal of Agricultural Sciences* 6 (3), pp 322-326, 2010.

[11].   R.K. Rattan, S. P.Datta, P.K. Chhonkar, K.Suribabu, and A. K. Sing "Long-term impact of irrigation with sewage effluents on heavy metal content in soils, crops and groundwater a case study," *Agriculture, Ecosystems & Environment* 109, pp 310 – 322. 2005.

[12].   J.S.Rawat and S.P.Rai "Pattern and intensity of erosion in the environmentally stressed Khulgad watershed," *Kumaun Himalaya, J. Geol. Soc. India*, 50, pp 331–338. 1997.

[13].   Rawat J S and Rawat M S 1994. "Accelerated erosion and denudation in the Nana Kosi watershed, central Himalaya, India," *Part I: Sediment Load*; Mt. Res. Dev. 14 25–38.

[14].   J.S.Rawat, M.M.Haigh and M.S.Rawat "Hydrological response of a Himalayan pine forest micro-watershed," Preliminary results; *Proc. Int. Symp on Hydrology of mountainous Areas*, Simla 28–30, pp 235–258. 1992.

[15]. J.S.Rawat, P.K.Purandara and S.Chandrakumar "Infiltration studies in the Malaprapa and Ghataprapa catchments*," NIH, Roorkee report,* CS – 105. 1993.

[16]. T.Shanley "Infiltration Rate Assessment of Soils Capacity to accept Rainfall,".2004.

[17]. R. Singh, N. Panigrahy and G .Philip "Modified rainfall simulator infiltrometer for infiltration, runoff and erosion studies," *Agricultural Water Management* 41, pp167–175. 1999.

[18]. K.L.Smedema, F.W.Voltman and W.D.Rycroft "Modern land drainage: Planning, design and management of agricultural drainage," *A.A. Balkema Publishers, Taylor and Francis*, the Netherlands, pp 446. 2004.

[19]. P.Soni and S.R.Singh "Average infiltration from cylinder infiltrometer test," *Indian Soc of Agri. Engineers*, 24th annual convection held at PKV, (Akols India). 1988.

[20]. P.Soni, S.Naithani and H.N.Matur "Infiltration studies under different vegetation cover," *Indian J of Forestery*, Vol 8(3), pp 170 – 173. 1985.

[21]. W.L.Thomas, G.S.Robert, R.T.Richard and W.N.Howard "Soil water monitoring and measurement," *A Pacific Northwest Publication*, Washington State University, Oregon, Idaho [online]. Available at http://cru.cahe.wsu.edu/CEPublications, 2004.

[22]. G.R, Senthilkumar, "Hydrogeological investigations in Tittagudi Taluk, Cuddalore, Tamil Nadu, S. India," *Unpublished thesis of Annamalai University*, pp. 23-27.2006.

Research Paper	Open Access

Natural convection of the localized heat sources of T-shaped nanofluid-filled enclosures

M. A. Mansour, A. Y. Bakier, M. A. Y. Bakier
Department of Mathematics, Faculty of Sciences, Assiut University, Assiut, Egypt

Abstract: - Natural convection fluid flow and heat transfer inside T-shaped enclosures filled with Cu-Water nanofluid has been investigated numerically using finite difference method. A parametric study was conducted and effects of pertinent parameters such as Rayleigh number, the aspect ratio of the T-shaped enclosure, and the volume fraction of the Cu nanoparticles on the flow and temperature fields and the rate of heat transfer inside the enclosure were investigated. It was found from the obtained results that the mean Nusselt number increased with increase in Rayleigh number and volume fraction of Cu nanoparticles regardless aspect ratio of the enclosure. Moreover the obtained results showed that the rate of heat transfer increased with decreasing the aspect ratio of the cavity. Also it was found that the rate of heat transfer increased with increase in nanoparticles volume fraction. Also at low Rayleigh numbers, the effect of Cu nanoparticles on enhancement of heat transfer for narrow enclosures was more than that for wide enclosures.

Keywords: - *Natural convection, nanofluid, T-shaped cavity, Nusselt number, Rayleigh number.*

I.   INTRODUCTION

Nanofluid, which is a mixture of nano-sized particles (nanoparticles) suspended in a base fluid, is used to enhance the rate of heat transfer via its higher thermal conductivity compared to the base fluid. Mahmoodi [1] investigated numerically free convection of Cu-water nanofluid in L-shaped and C-shaped cavities. He found that effect of presence of nanoparticles on heat transfer enhancement is more apparent for narrow L-shaped and C-shaped cavities.

Many researchers have simulated the heat removal mechanism by means of natural convection in enclosures heated from below [3, 4]. More recently, Cheikh et al. [5] studied natural convection in a square enclosure heated from below and cooled from above for a variety of thermal boundary conditions at the top and sidewalls. They carried out their simulation for two different lengths of the heat source and various Rayleigh numbers. They argued that the maximum temperature of the heat source did not change significantly for the diffusion dominated cases whereas decreased rather rapidly with Rayleigh number for convection dominated regimes.

In most natural convection studies, the base fluid in the enclosure has a low thermal conductivity, which limits the heat transfer enhancement. However, the continuing miniaturization of electronic devices requires further heat transfer improvements from an energy saving viewpoint. An innovative technique, which uses a mixture of nanoparticles and the base fluid was first introduced by Choi [6] in order to develop advanced heat transfer fluids with substantially higher conductivities. The resulting mixture of the base fluid and nanoparticles having unique physical and chemical properties is referred to as a nanofluid. It is expected that the presence of the nanoparticles in the nanofluid increases the thermal conductivity and therefore substantially enhances the heat transfer characteristics of the nanofluid.

Eastman et al. [7], Xie et al. [8] showed that higher thermal conductivity can be achieved in thermal systems utilising nanofluids. In recent years thermophysical properties of nanofluids have been investigated by many researchers [9-14]. Investigation of different applications of nanofluids can be found in literature such as forced convection of nanofluids (Namburu et al. [16], Santra et al. [17] and Strandberg and Das [18]), boiling heat transfer of nanofluids (Das et al. [19]) and mixed convection of nanofluids (Akbarinia and Behzadmehr

[20], Akbari et al. [21], Ghaffari et al. [22], Mahmoodi [23] and Arefmanesh and Mahmoodi [24]).There are a number of recent studies on free convection inside cavities containing nanofluid. Khanafer et al. [25] investigated numerically the problem of free convection of nanofluid in rectangular cavities with cold right wall, hot left wall and insulated horizontal walls. They found that the rate of heat transfer increased with increase in nanoparticles volume fraction. Since the free convection heat transfer of nanofluids in the thermal engineering applications will be extending the existing knowledge, the authors are motivated by interest in investigation of the effects of a nanofluid in the laminar free convection heat transfer in T-shaped enclosures. The most convenient application of T-shaped enclosures can be cooling of some electronic parts in the manufactures. Using the nanofluids the efficiency of the cooling can be enhanced. In the present study the governing equations in terms of primitive variables in Cartesian coordinate system are discretized using the finite difference method. The effects of aspect ratio of enclosure, nanoparticles volume fraction and Rayleigh number on the flow and temperature fields and heat transfer characteristics are discussed.

In the present paper natural convection fluid flow and heat transfer of Cu-water nanofluid inside T-shaped enclosure was studied numerically and the effects of the Rayleigh number, aspect ratio of enclosure and volume fraction of the nanoparticles on flow pattern, temperature field and rate of heat transfer were investigated.

II.　　MATHEMATICAL MODELING

$$\frac{\partial u}{\partial x} + \frac{\partial v}{\partial y} = 0 \tag{1}$$

$$u\frac{\partial u}{\partial x} + v\frac{\partial u}{\partial y} = -\frac{1}{\rho_{nf}}\frac{\partial p}{\partial x} + \frac{\mu_{nf}}{\rho_{nf}}(\frac{\partial^2 u}{\partial x^2} + \frac{\partial^2 u}{\partial y^2}) \tag{2}$$

$$u\frac{\partial v}{\partial x} + v\frac{\partial v}{\partial y} = -\frac{1}{\rho_{nf}}\frac{\partial p}{\partial y} + \frac{\mu_{nf}}{\rho_{nf}}(\frac{\partial^2 v}{\partial x^2} + \frac{\partial^2 v}{\partial y^2}) + \frac{(\rho\beta)_{nf}}{\rho_{nf}}g(T-T_C) \tag{3}$$

$$u\frac{\partial T}{\partial x} + v\frac{\partial T}{\partial y} = \alpha_{nf}(\frac{\partial^2 T}{\partial x^2} + \frac{\partial^2 T}{\partial y^2}) \tag{4}$$

$$\rho_{nf} = (1-\varphi)\rho_f + \varphi\rho_s \tag{5}$$

$$(\rho c_p)_{nf} = (1-\varphi)(\rho c_p)_f + \varphi(\rho c_p)_s \tag{6}$$

$$(\rho\beta)_{nf} = (1-\varphi)(\rho\beta)_f + \varphi(\rho\beta)_s \tag{7}$$

$$\alpha_{nf} = \frac{k_{nf}}{(\rho c_p)_{nf}} \tag{8}$$

$$\beta_{nf} = \frac{(1-\varphi)(\rho\beta)_f + \varphi(\rho\beta)_s}{(1-\varphi)\rho_f + \varphi\rho_s} \tag{9}$$

$$\mu_{eff} = \frac{\mu_f}{(1-\varphi)^{2.5}} \tag{10}$$

$$\frac{k_{nf}}{k_f} = \frac{(k_s + 2k_f) - 2\varphi(k_f - k_s)}{(k_s + 2k_f) + \varphi(k_f - k_s)} \tag{11}$$

$$X = \frac{x}{H}, Y = \frac{y}{H}, U = \frac{uH}{\alpha_f}, V = \frac{vH}{\alpha_f}, P = \frac{pH^2}{\rho_{nf}\alpha_f^2}, \theta = \frac{T-T_C}{T_H - T_C} \tag{12}$$

$$\frac{\partial U}{\partial X} + \frac{\partial V}{\partial Y} = 0 \tag{13}$$

$$U\frac{\partial U}{\partial X} + V\frac{\partial U}{\partial Y} = -\frac{1}{\rho_{nf}}\frac{\partial P}{\partial X} + \frac{\mu_{nf}}{\rho_{nf}\alpha_f}(\frac{\partial^2 U}{\partial X^2} + \frac{\partial^2 U}{\partial Y^2}) \tag{14}$$

$$U\frac{\partial V}{\partial X} + V\frac{\partial V}{\partial Y} = -\frac{1}{\rho_{nf}}\frac{\partial P}{\partial Y} + \frac{\mu_{nf}}{\rho_{nf}\alpha_f}(\frac{\partial^2 V}{\partial X^2} + \frac{\partial^2 V}{\partial Y^2}) + \frac{(\rho\beta)_{nf}}{\rho_{nf}\beta_f}Ra\,Pr\,\theta \tag{15}$$

$$U\frac{\partial \theta}{\partial X} + V\frac{\partial \theta}{\partial Y} = \frac{\alpha_{nf}}{\alpha_f}(\frac{\partial^2 \theta}{\partial X^2} + \frac{\partial^2 \theta}{\partial Y^2}) \tag{16}$$

$$Ra = \frac{g\beta_f(T_h - T_C)H^3}{\alpha_f \nu_f}, \quad \Pr = \frac{\nu_f}{\alpha_f} \tag{17}$$

$$\begin{cases} on\ walls: \begin{cases} a\,b, c\,d, g\,h: U = V = 0, \partial\theta/\partial y = 0 \\ f\,e: \begin{cases} U = V = 0, \partial\theta/\partial y = 1, D - 0.5*B \le X \le D + 0.5*B \\ U = V = 0, \partial\theta/\partial y = 0, Otherwise \end{cases} \\ on\ walls\ a\,h, b\,c: U = V = 0, \theta = 0 \\ \\ on\ walls\ d\,e, f\,g: U = V = 0, \partial\theta/\partial x = 0 \end{cases} \tag{18}$$

$$Nu_{local} = \frac{hH}{k_f} \tag{19}$$

$$h = \frac{q_w}{T_h - T_C} \tag{20}$$

$$k_{nf} = -\frac{q_w}{\partial T/\partial Y}\ on\ wall\ f\,e \tag{21}$$

$$Nu_l = -(\frac{k_{nf}}{k_f})\frac{\partial \theta}{\partial Y}\ on\,wall\,f\,e \tag{22}$$

$$Nu_m = (\int_{D-0.5*B}^{D+0.5*B} Nu_l\,dX\big|_{Y=1}) \tag{23}$$

III. NUMERICAL METHOD AND VALIDATION

In this investigation, the finite difference method (Mansour et al. [26]) was employed to solve the governing equations with the boundary conditions. Central difference quotients were used to approximate the second derivatives in both the-XandY-directions. Then, the obtained discretized equations are solved using a Gauss-Seidel iteration technique (Grosan et al.[27]; Singh and Venkateshan [28]). The solution procedure is iterated until the following convergence criterion is satisfied:

$$\sum_{i,j}|\chi_{i,j}^{new} - \chi_{i,j}^{old}| \le 10^{-7}$$

where χ is the general dependent variable. The numerical method was implemented in FORTRAN software. In order to verify the accuracy of present method, the obtained results in special cases are compared with the results obtained by Walker and Homsy [29], Gross et al.[30], Manole and Lage [31]. Table 2 shows a good agreement was found between the present results and the results obtained by the previous works. These favorable comparisons lend confidence in the numerical results to be reported subsequently.

The finite difference method uses four sets of grids: 36×36, 66×66, 96×96, and 126×126 as shown in Table 3. There is a good agreement was found between 66 × 66 and 126× 126 grids, so the numerical computations were carried out for 66 × 66 and 126× 126 grid nodal points.

IV. RESULTS AND DISCUSSION

The results are presented in terms of streamlines, isotherms, average Nusselt number and local Nusselt number. Fig. 2 illustrates effect of increase in AR on flow pattern and temperature distribution inside the enclosures filled with pure fluid ($\phi = 0$) at $Ra = 10^5$. As can be seen from the streamlines in the figure, for $AR =$ 0.3 the fluid is heated by the sources and expands as it moves downward. Then the fluid is cooled by the cold ribs and compressed as it moves upward. Hence, there is a symmetrical behavior for the stream lines. The isotherms for this aspect ratio are condensed adjacent to the top of the cavity, because the top wall has a

maximum effect in heating the fluid. Moreover as the T-shaped enclosure becomes narrower the local Rayleigh number and buoyancy force in the top region of the cavity. The corresponded isotherms show that for *AR*= 0.9 thermal stratification occurs in the gaps over the cold rib. Also it must be noted that when the aspect ratio of the cavity increases, the isotherms becomes more evenly distributed on the top of the cold rib. From the observed result maximum and minimum limits are found for developing the Rayleigh-Bénard cells in the gap between the source and the cold rib. Also it can be considered that the walls *cd* and *gh* work as temperature pumps in the cavity, that is for *AR*<0.6, where its effect is clear.

Fig. 3 shows the streamlines and isotherms inside the T – shape enclosure filled with pure fluid at *AR*=0.3, *D*=.5, Ra=10^5, and for various lengths of heat source. There is no great change among the contours. Only one thing can be noticed, as B is small, as heat transfer is obvious.

Fig. 4 shows streamlines and isotherms inside the T – shape enclosure filled with pure fluid (ϕ =0.0) at Ra=10^5, *AR*=0.3, *B*=1/3 and for different heat source locations. The symmetric behavior decays as the source moving away from the middle.

Fig. 5 shows streamlines and isotherms inside the T– shape enclosure filled with nanofluid (ϕ =0.1) at Ra=10^5, *B*=1/3, *D*=.5 for different aspect ratios of enclosure. There isn't great change from pure case.

Fig. 6 shows streamlines and isotherms at Ra=10^5, *AR*=0.3 and for different heat source lengths. It is clear that the heat transfer is very week and takes its huge value at B=0.6.

Fig. 7 shows streamlines and isotherms inside the T – shape enclosure filled with nanofluid at Ra=10^5, *AR*=0.3, *D*=.5, *B*=1/3 and for various values of solid volume fraction. The effect of (ϕ) is week as seems from contours.

Fig. 8 shows streamlines and isotherms inside the T – shape enclosure filled with nanofluid at Ra=10^5, *AR*=0.3, D=.5, B=1/3 and for various nonoparticles. As seems from contours, the various nanofluids don't have great different from each others.

Fig.9. presented the profiles of (a) θ_s -X curves for different solid volume fractions, it's clear that the source temperature decreases as the solid volume fraction increases. Also, the profiles are symmetric around the middle of the top wall where the curves reach to its unique maximum values, while in the ends there are its two minimum points. Fig. 9(b) shows the variations of local Nusselt number along the heat source for different solid volume fractions. It is obvious that the curves inverse the previous curves in (a).

Fig. 10 shows the variation of the local Nusselt number along the heat source for different heat source lengths. It is shown that the profiles are symmetric. Generally, the heat transfer decreases as the heat source length increases, and the curve becomes more flat.

Fig. 11 shows the profiles of Nu$_m$-ϕ for various heat source lengths, it confirms that the average Nusselt number increases as the solid volume fraction increases. But it decreases as *B* increases.

Fig. 12 shows the profiles of Nu$_m$-ϕ for various aspect ratios, *AR*, it can be noticed that the average Nusselt number decreases as *AR* increases. It is can verified that there is no effect for *AR* in pure case. However, the effect of the aspect ratio increases and can be more obviousness as the solid volume fraction increases.

Fig. 13 shows the profiles of Nu$_m$-ϕ for various Rayleigh number, for Ra<5x10^5 the rate is nearly congruent, often the average Nusselt number increases as Raleigh number increases.

Fig. 14 shows variation of average Nusselt number with heat source location at various aspect ratios where *B*=1/3, *Ra*=10^5 and ϕ =0.1. it can verified from the curves that the effect of the location of heat source increases greatly, as the aspect ratio increases. So there is a huge difference at *AR*=0.9, while the change tend to be zero at *AR*=.3.

Fig.15 presents the effects of the length of heat source on its average Nusselt number for different aspect ratios. As stated, the heat transfer decreases as the heat source length increases. The difference between the end-point and the start-point decreases as *AR* increases.

Fig. 16 shows the profile of local Nusselt number along the heat source for different types of nanofluids. Profiles are obtained for all nanofluids with the lowest Nusselt number for the middle of the heat source. It is clear that the smallest values for *Nu$_s$* are on the curve of pure water; conversely, the biggest values are on curve of TiO$_2$. Table 1 shows that TiO$_2$ has the lowest

value of thermal conductivity compared to other nanoparticles, hence, it has the lowest values of Nusselt number. Cu and Ag, on the other hand, have the highest values. In addition, the thermal conductivity of Al$_2$O$_3$ is approximately one tenth of Cu and Ag (Table 1), thus, the Nusselt number for Al$_2$O$_3$ is lower than that for Cu and Ag. Fig. 23 presents the variation of average Nusselt number with solid volume fraction.

Table 4 shows that changing nanotypes does not affect both Nu$_m$ and maximum temp., but that is not for

stream function values. Cu and Ag decrease ψ_{max} values. On the contrary, the other types are. Rayleigh number has not significant effect on Nu_m and θ_{max} but it enhances the stream values. Table 5 displays the effect of aspect ratio which supplies both ψ_{max} and θ_{max}, but it decreases the average Nusselt nuber values.

V.   CONCLUSION

Natural convection in a partially heated enclosure from bottom and top, filled with different types of nanofluids has been numerically investigated by finite difference method. The effects on the enclosure cooling performance of Rayleigh number, solid volume fraction, heat source length and location and the type of nanofluid are studied.The increase of Rayleigh numbers strengthens the natural convection flows which results in the reduction of heat source temperature. Also the increase of solid volume fraction of nanoparticles causes the heat source maximum temperature to decrease particularly at low Rayleigh numbers where conduction is the main heat transfer mechanism. The increase of heat source length increases the heat transfer to the nanofluid and therefore, increases the surface temperature of the heat source and the strength of natural convection circulating cells within the enclosure. As the heat source moves from the left wall towards the middle of the bottom wall of the enclosure, at low Rayleigh numbers, the heat source maximum temperature continuously increases. At high Rayleigh number, minimum rate of heat transfer occurs from top wall and its minimum occurs from the bottom wall while at low Rayleigh number similar rates heat transfer from top and bottom walls are observed.
As the T-shaped enclosure becomes narrower, the rate of heat transfer increases. Also as the Rayleigh number increases, the rate of heat transfer increases for a constant AR.

REFERENCES

[1]   Mostafa Mahmoodi, Seyed Mohammad Hashemi, Numerical study of natural convection of a nanofluid in C-shaped enclosures, International Journal of Thermal Sciences 55 (2012) 76-89.
[2]   I. Sezai, A.A. Mohamad, Natural convection from a discrete heat source on the bottom of a horizontal enclosure, Int. J. Heat Mass Transf. 43 (2000) 2257–2266.
[3]   M. Corcione, Effects of the thermal boundary conditions at the sidewalls upon natural convection in rectangular enclosures heated from bellow and cooled from above, Int. J. Therm. Sci. 42 (2003) 199–208.
[4]   B. Calgagni, F. Marsili, M. Paroncini, Natural convective heat transfer in square enclosures heated from below, Appl. Therm. Eng. 25 (2005) 2522–2531.
[5]   N.B. Cheikh, B.B. Beya, T. Lili, Influence of thermal boundary conditions on natural convection in a square enclosure partially heated from below, Int. Comm. Heat Mass Transf. 34 (2007) 369–379.
[6]   S.U.S. Choi, Enhancing thermal conductivity of fluids with nanoparticles. ASME Fluids Eng Div 1995, 231, 99–105.
[7]   J.A. Eastman, S.U.S. Choi, S. Li, W. Yu, L.J. Thompson, Anomalously increased effective thermal conductivities of ethylene glycol-based nanofluids containing copper nanoparticles, Appl. Phys. Lett. 78 (6) (2001) 718–720.
[8]   H.Q. Xie, H. Lee, W. Youn, M. Choi, Nanofluids containing multiwalled carbon nanotubes and their enhanced thermal conductivities, J. Appl. Phys. 94 (8) (2003) 4967–4971.
[9]   S. Jana, A. Salehi-Khojin, W.H. Zhong, Enhancement of fluid thermal conductivity by the addition of single and hybrid nano-additives, Thermochimica Acta 462 (1–2) (2007) 45–55.
[10]   S.M. Aminossadati, B. Ghasemi, Natural convection cooling of a localised heat source at the bottom of a nanofluid-filled enclosure, European Journal of Mechanics B/Fluids 28 (2009) 630–640.
[11]   H.U. Kang, S.H. Kim, J.M. Oh, Estimation of thermal conductivity of nanofluid using experimental effective particle volume, Exp. Heat Transfer 19 (2006) 181-191.
[12]   V. Velagapudi, R.K. Konijeti, C.S.K. Aduru, Empirical correlation to predict thermophysical and heat transfer characteristics of nanofluids, Thermal Sci. 12 (2008) 27-37.
[13]   C. Murugesan, S. Sivan, Limits for thermal conductivity of nanofluids, Thermal Sci. 14 (2010) 65-71.
[14]   A.K. Nayak, R.K. Singh, P.P. Kulkarni, Measurement of volumetric thermal expansion coefficient of various nanofluids, Tech. Phys. Lett. 36 (2010) 696-698.
[15]   M.M. Papari, F. Yousefi, J. Moghadasi, H. Karimi, A. Campo, Modeling thermal conductivity augmentation of nanofluids using diffusion neural networks, Int. J. Thermal Sci. 50 (2011) 44-52.
[16]   P.K. Namburu, D.K. Das, K.M. Tanguturi, R.S. Vajjha, Numerical study of turbulent flow and heat transfer characteristics of nanofluids considering variable properties, Int. J. Thermal Sci. 48 (2009) 290-302.
[17]   A.K. Santra, S. Sen, N. Chakraborty, Study of heat transfer due to laminar flow of copperewater nanofluid through two isothermally heated parallel plates, Int. J. Thermal Sci. 48 (2009) 391-400.
[18]   R. Strandberg, D.K. Das, Finned tube performance evaluation with nanofluids and conventional heat transfer fluids, Int. J. Thermal Sci. 49 (2010) 580-588.

[19]　S.K. Das, N. Putra, W. Roetzel, Pool boiling characterization of nano-fluids, Int. J. Heat Mass Tranf. 46 (2003) 851-862.

[20]　A. Akbarinia, A. Behzadmehr, Numerical study of laminar mixed convection of a nanofluid in horizontal curved tubes, Appl. Thermal Eng. 27 (2007) 1327-1337.

[21]　M. Akbari, A. Behzadmehr, F. Shahraki, Fully developed mixed convection in horizontal and inclined tubes with uniform heat flux using nanofluid, Int. J. Heat Fluid Flow 29 (2008) 545-556.

[22]　O. Ghaffari, A. Behzadmehr, H. Ajam, Turbulent mixed convection of a nanofluid in a horizontal curved tube using a two-phase approach, Int. Comm. Heat Mass Trans. 37 (2010) 1551-1558.

[23]　M. Mahmoodi, Mixed convection inside nanofluid filled rectangular enclosures with moving bottom wall, Thermal Sci. 15 (2011) 889-903.

[24]　A. Arefmanesh, M. Mahmoodi, Effects of uncertainties of viscosity models for Al2O3ewater nanofluid on mixed convection numerical simulations, Int. J. Thermal Sci. 50 (2011) 1706-1719.

[25]　K. Khanafer, K. Vafai, M. Lightstone, Buoyancy-driven heat transfer enhancement in a two-dimensional enclosure utilizing nanofluid, Int. J. Heat Mass Tran. 46 (2003) 3639-3653.

[26]　M.A.Mansour, A.J. Chamkha, R.A.Mohamed , M.M.Abd El-Aziz , S.E.Ahmed, MHD natural convection in an inclined cavity filled with a fluid saturated porous medium with heat source in the solid phase. Nonlinear Anal. 15(2010)55–70.

[27]　T.Grosan , C.Revnic, I.Pop, D.B.Ingham, Magnetic field and internal heat generation effects on the freeconvection in a rectangular cavity filled with a porous medium. Int. J. Heat Mass Transf. 52(2009)1525–1533.

[28]　B.V.Ratish Kumar, P.V.S.N.Murthy, P.Singh, Free convection heat transfer from an isothermal wavy surface in a porous enclosure. Int. J. Numer. Meth. Fluids 28(1998)633–661.

[29]　K.L.Walker, G.M.Homsy, Convection in a porous cavity. J. Fluid Mech. 87(1978)449–474.

[30]　R.J.Gross , M.R.Bear , C.E.Hickox, The application of flux-corrected transport (FCT) to high Rayleigh number natural convection in a porous medium. In: Proceedings of 8th International Heat Transfer Conference, San Francisco, CA, USA, (1986).

[31]　D.M.Manole, J.L.Lage, Numerical benchmark results for natural convection in a porous medium cavity. In:Proceedings of the ASME Conference on Heat and Mass Transfer in Porous Media, HTD, 216 (1992) 55–60.

[32]　M.Haajizadeh , A.F.Ozguc and C.L.Tien, Natural convection in a vertical porous enclosure with internal heat generation, *Int. J. Heat Mass Transfer*, 27(1984)1893–190.
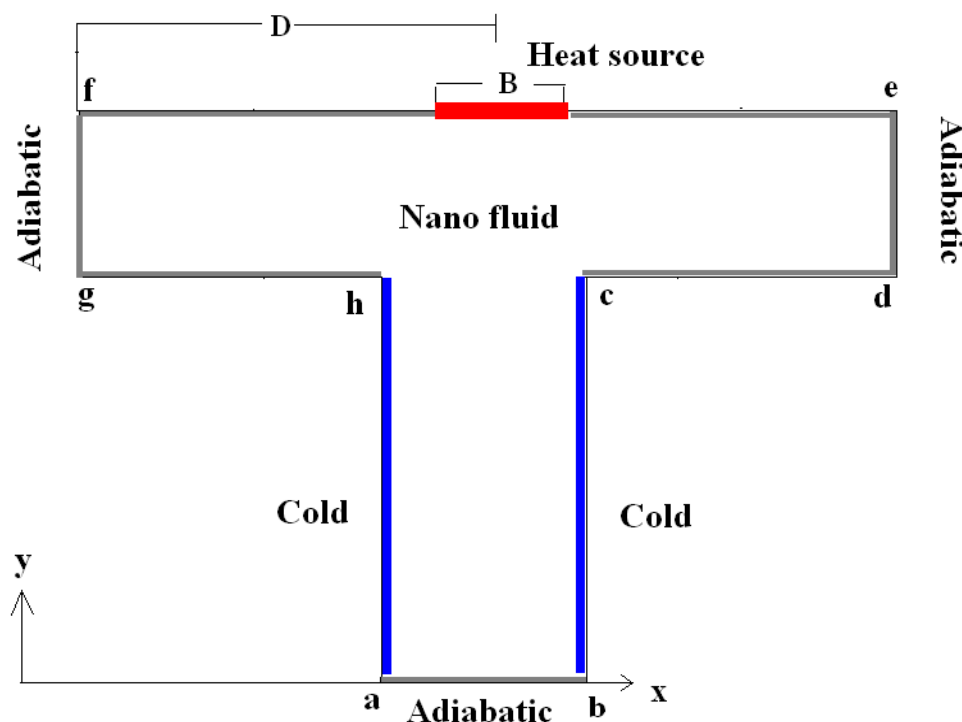
Fig. 1 Physical model of the prblem.
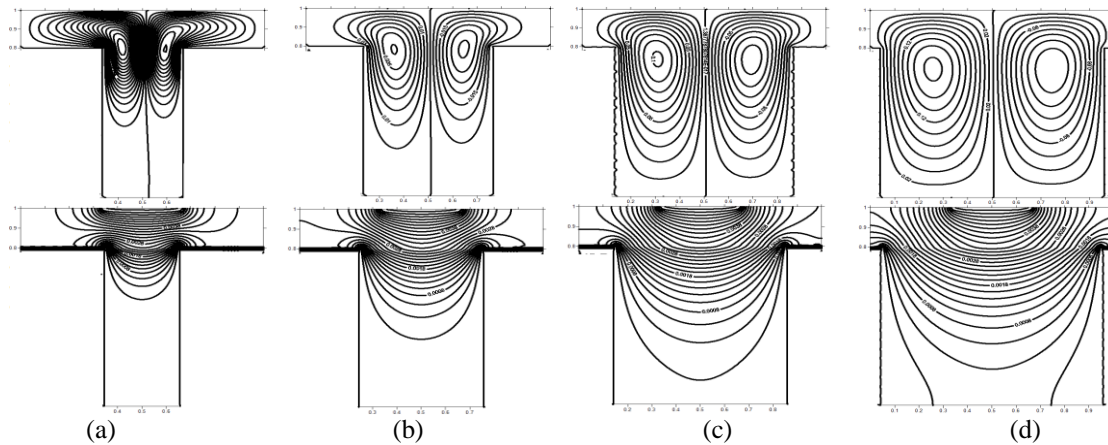
Fig. 2 Streamlines (top) and isotherms (down) inside the T – shape enclosure filled with pure fluid (ϕ =0.0) at Ra=10^5, B=1/3, D=.5, (a) AR=.3, (b)AR=.5, (c)AR=.7, (d)AR=.9
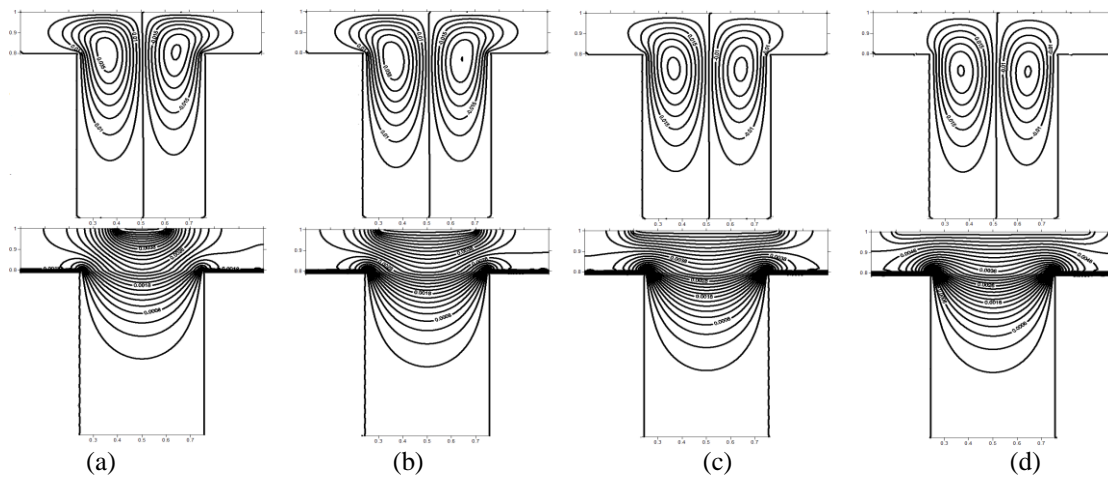
Fig. 3 Streamlines (top) and isotherms (down) inside the T – shape enclosure filled with pure fluid (ϕ =0.0) at Ra=10^5, AR=0.5, D=.5, (a) B=.2, (b) B=.4, (c)B=.6, (d)B=.8
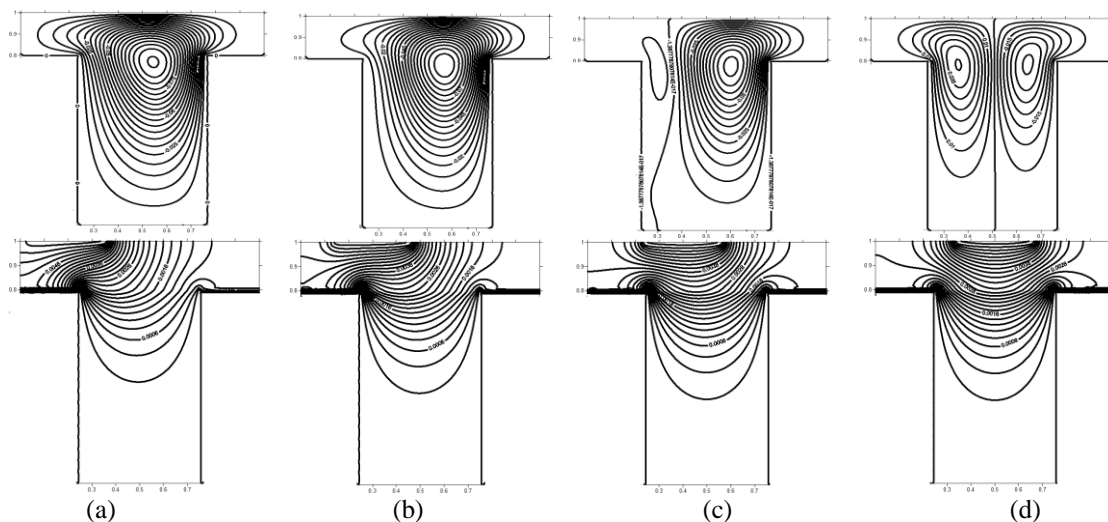
Fig. 4 Streamlines (top) and isotherms (down) inside the T – shape enclosure filled with pure fluid (ϕ =0.0) at AR=0.5, Ra=10^5,B=1/3.,(a) D=.2, (b) D=.3, (c) D=.4, (d) D=.5
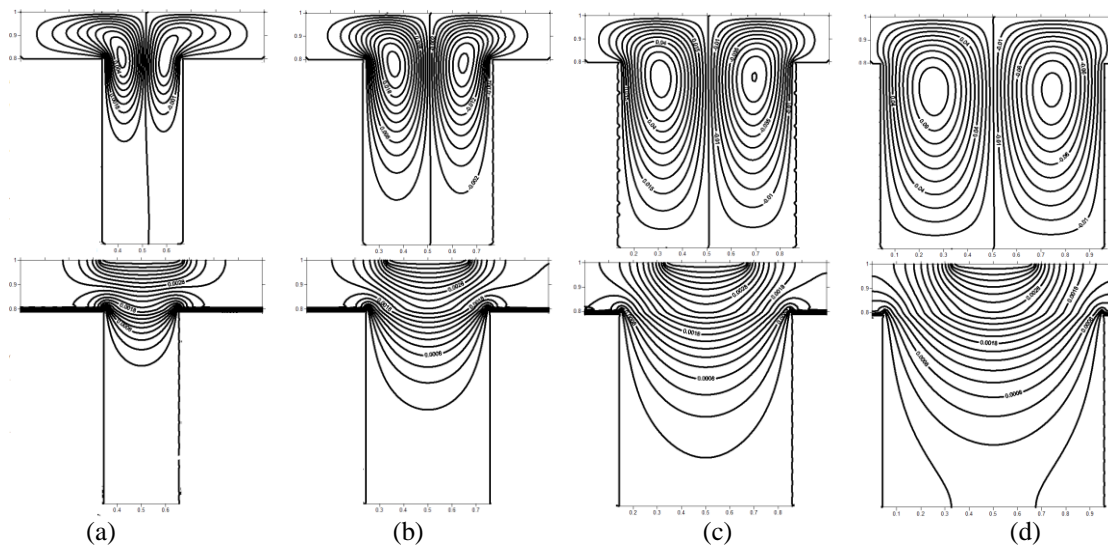
Fig. 5 Streamlines (top) and isotherms (down) inside the T − shape enclosure filled with nanofluid (ϕ =0.1) at Ra=10^5, B=1/3, D=.5, (a) AR=.3, (b) AR=.5, (c) AR=.7, (d) AR=.9.
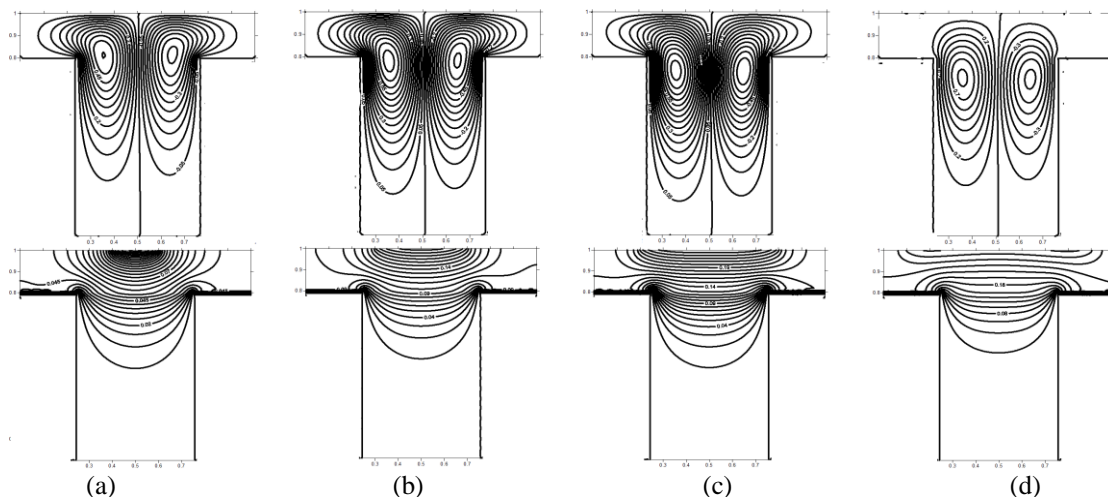
Fig. 6 Streamlines (top) and isotherms (down) inside the T − shape enclosure filled with nanofluid (ϕ =0.1) at Ra=10^5, AR=0.5, D=.5, (a) B=0.2, (b) B=0.4, (c) B=0.6, (d) B=0.8.
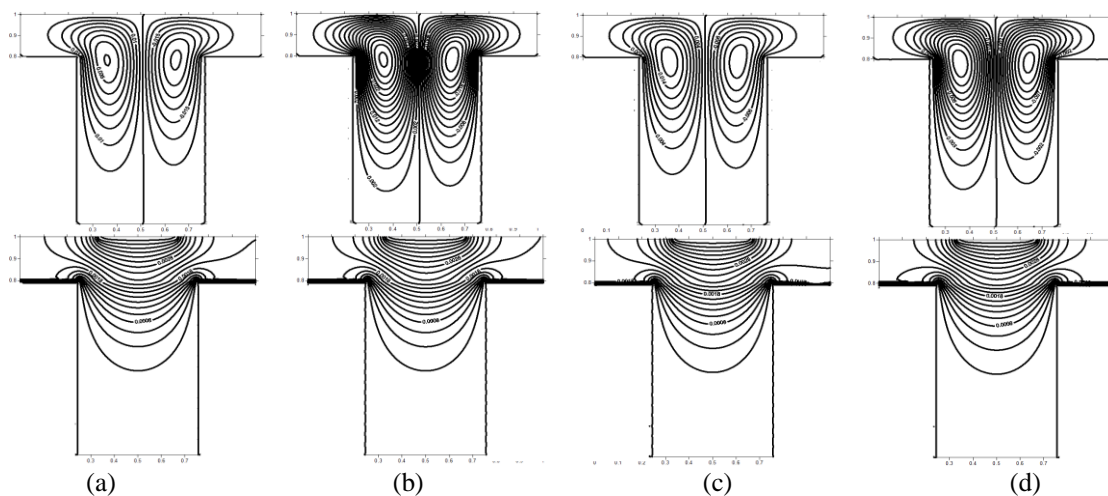
Fig. 7 Streamlines (top) and isotherms (down) inside the T − shape enclosure filled with nanofluid at Ra=10^5, AR=0.5, D=.5, B=1/3., (a) ϕ =0.0, (b) ϕ =.05, (c) ϕ =0.1, (d) ϕ =0.2
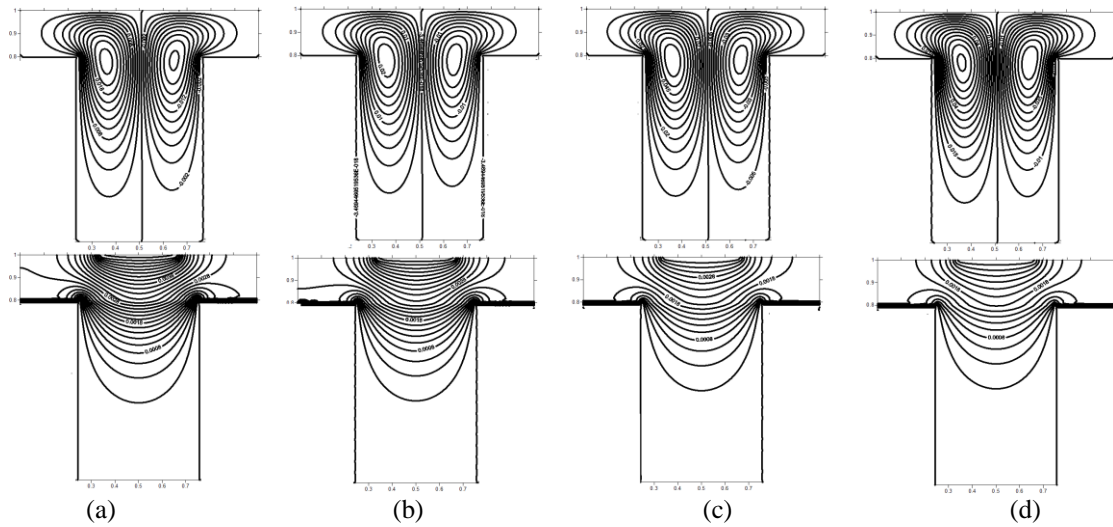
Fig 8. Streamlines (top) and isotherms (down) inside the T – shape enclosure filled with nanofluid at Ra=10^5, AR=0.5, D=.5, B=1/3., ϕ =0.1 ,(a) Cu-water,(b) Ag-Water,(c) Al$_2$O$_3$-Water,(d) Ti O$_2$-Wter
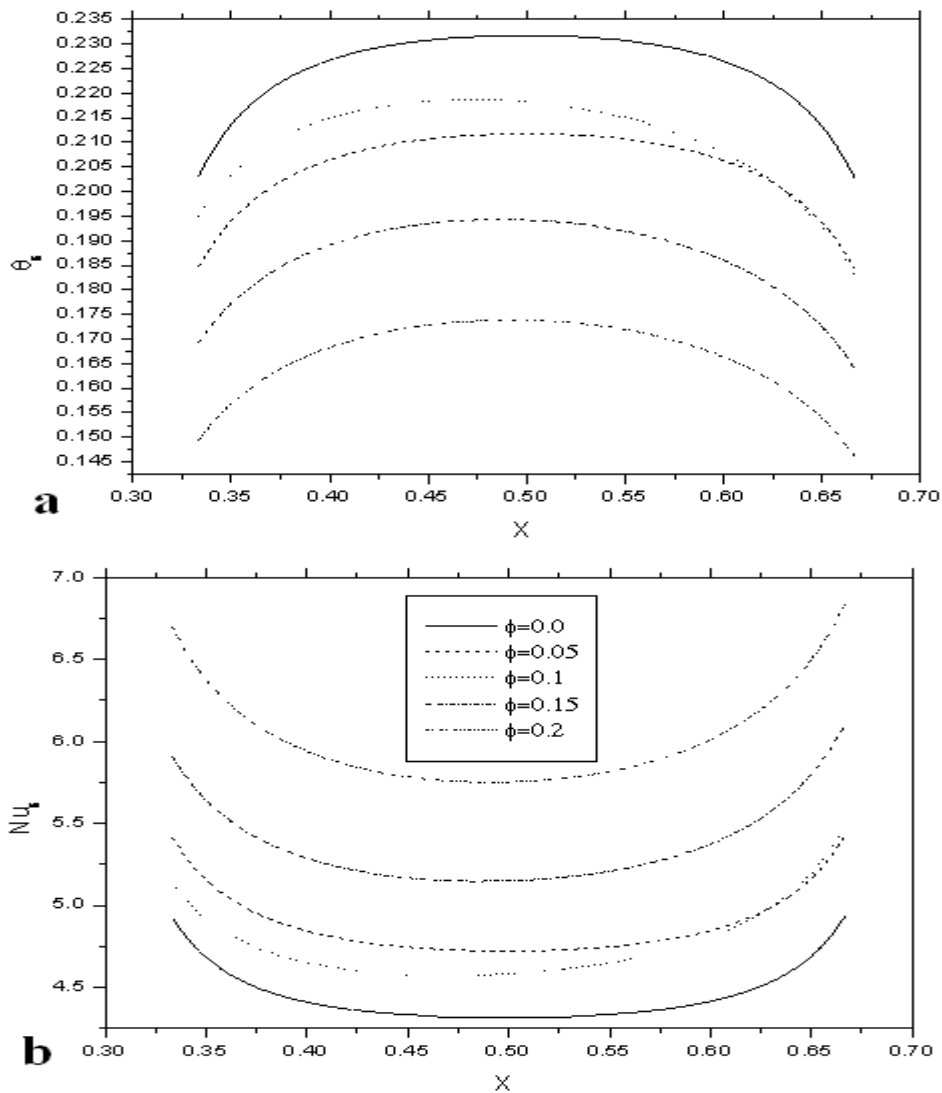
Fig.9. a) Profile of source temperature along the heat source for various solid volume fraction,
b) Profile of local Nusselt number along the heat source for various solid volume fraction (Cu-Water, D=0.5, Ra=10^5, B=1/3 and AR=0.5)
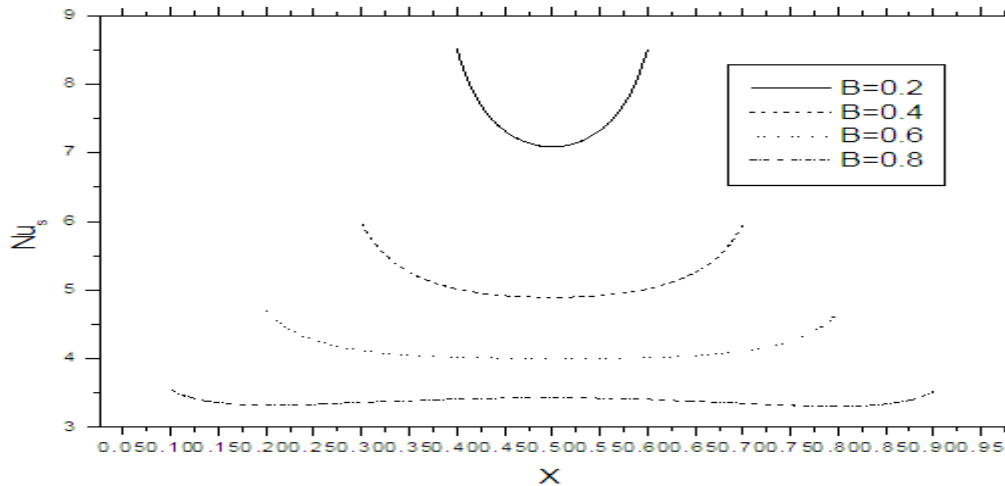
Fig.10. Variation of local Nusselt number along the heat source at the top for various heat source lengths (Cu-Water, D=0.5, Ra=10^5 and AR=0.5).
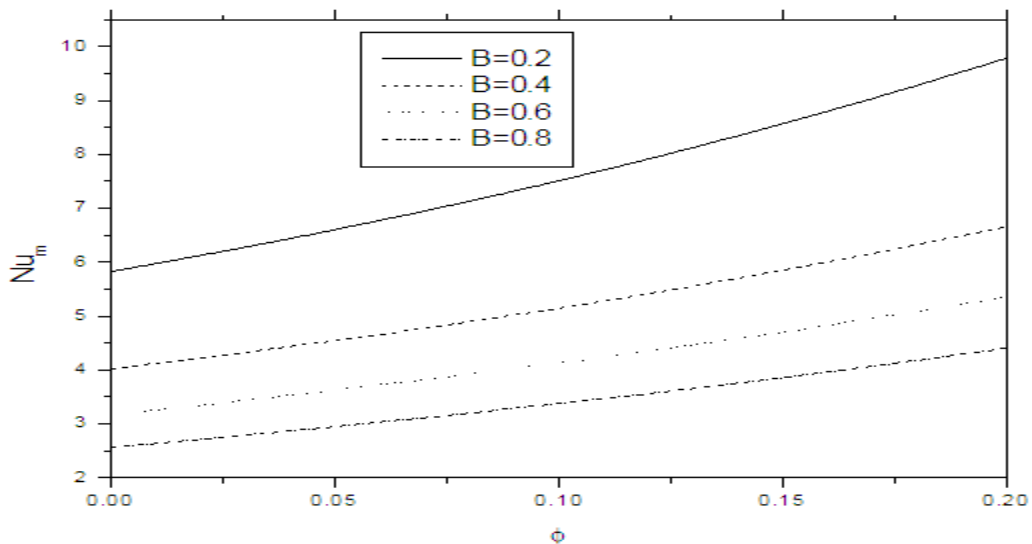
Fig.11. Variation of average Nusselt number with solid volume fraction at various heat source lengths (Cu-Water, D=0.5, Ra=10^5 and AR=0.5).
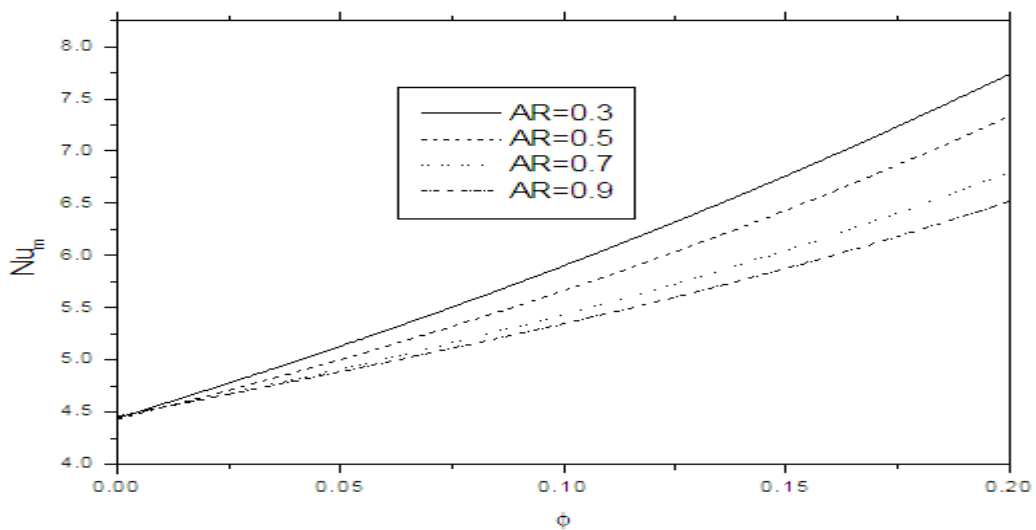
Fig.12. Variation of average Nusselt number with solid volume fraction at various aspect ratios (Cu-Water, D=0.5, Ra=10^5 and B=1/3.).
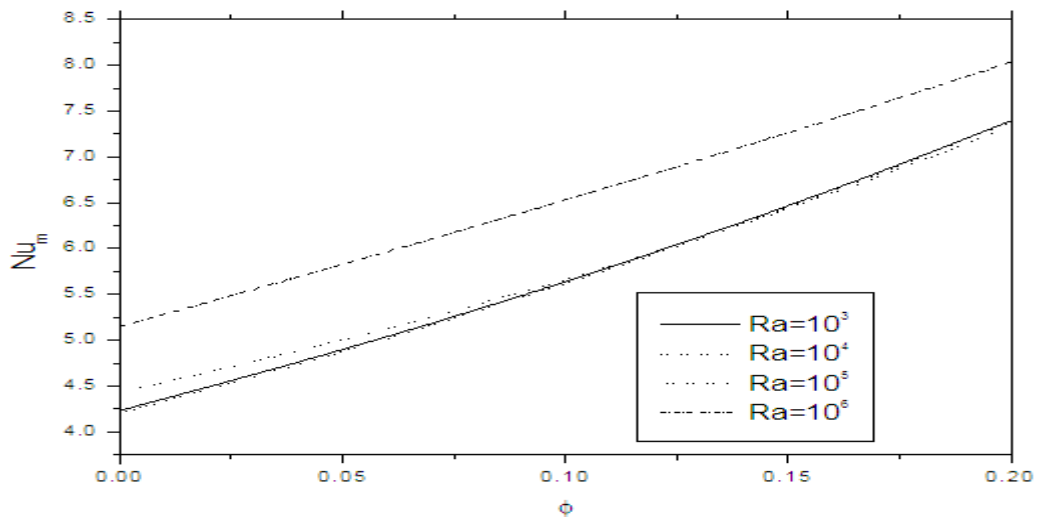
Fig.13. Variation of average Nusselt number with solid volume fraction at various Rayleigh numbers (Cu-Water, D=0.5, AR=0.5 and B=1/3.).
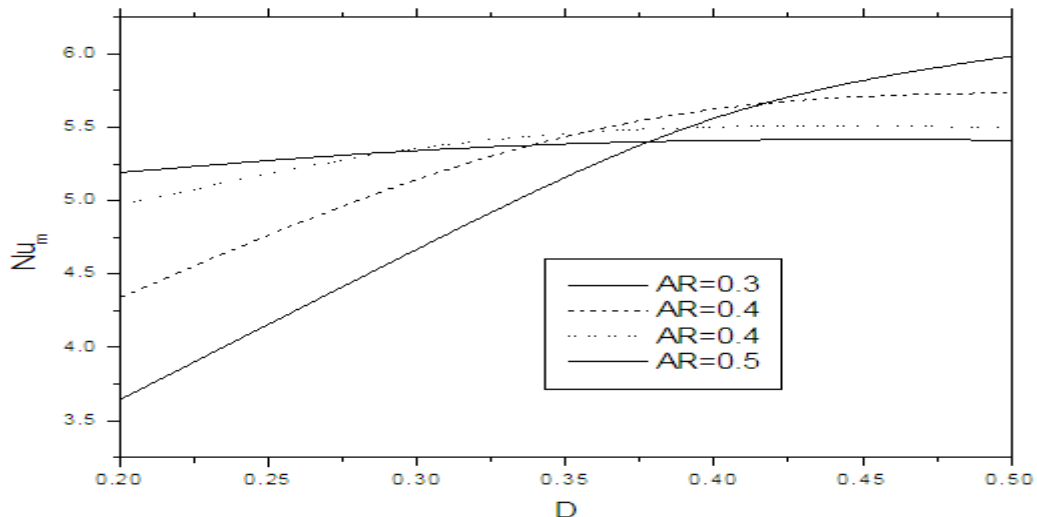
Fig.14. Variation of average Nusselt number with heat source location at various aspect ratios (Cu-Water, B=1/3., B=1/3,Ra=10^5 and ϕ =0.1).
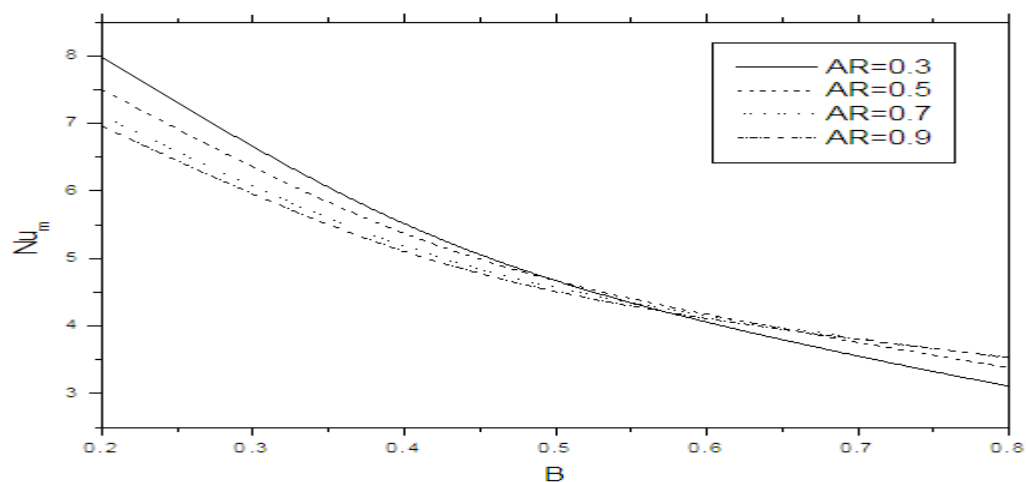
Fig.15. Variation of average Nusselt number with heat source length at various aspect ratios (Cu-Water, B=1/3., B=1/3,Ra=10^5 and ϕ =0.1).
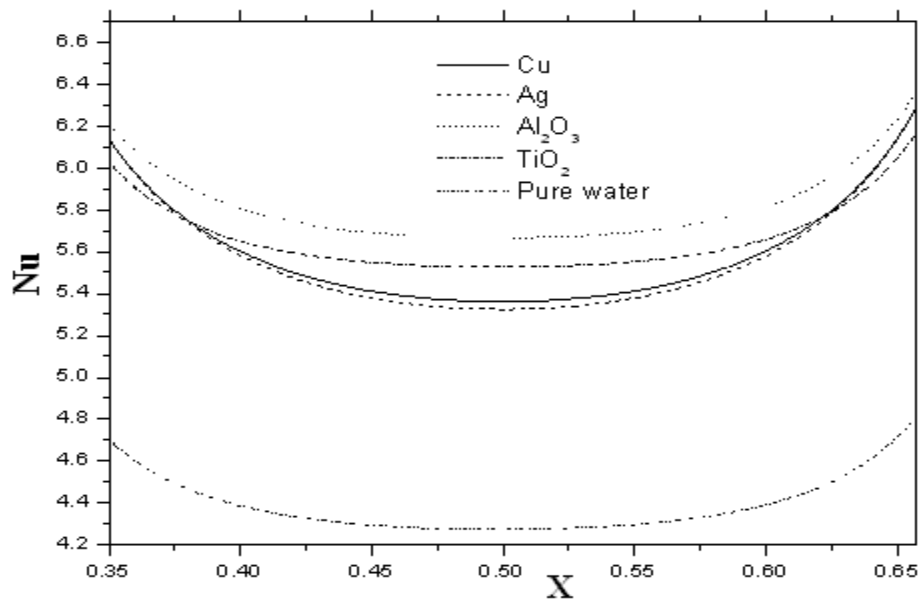
Fig.16. Variation of local Nusselt number along the heat source at the top for different types of nanofluid (D=0.5, B=1/3,Ra=10^5 and AR=0.5).

Table 1. Thermo-physical properties of water and nanoparticles.

	Pure water	Copper(Cu)	Silver (Ag)	Alumina Al₂O₃	Titanium Oxide (TiO₂)
$\rho(kgm^{-3})$	997.1	8933	10500	3970	4250
$C_p(Jkg^{-1}K^{-1})$	4179	385	235	765	686.2
$k(Wm^{-1}K^{-1})$	0.613	401	429	40	8.9538
$\beta(K^{-1})$	21×10^{-5}	1.67×10^{-5}	1.89×10^{-5}	0.85×10^{-5}	0.9×10^{-5}

Table 2. Comparison of ψ_{max} and θ_{max} .

Ra	Haajizadeh et al.[32]		Grosan et al.[27]		Present Work	
	ψ_{max}	θ_{max}	ψ_{max}	θ_{max}	ψ_{max}	θ_{max}
10	0.078	0.130	0.079	0.127	0.0799	0.1272
10^3	4.880	0.118	4.833	0.116	4.8266	0.117

Table 3. Grid independency results

	Nu_m	θ_{max}	ψ_{max}
36x36	3.413	0.990	0.587
66x66	4.757	0.973	7.725
96x96	4.684	0.990	6.024
126x126	5.241	0.983	10.676

Table 4.Results for the base case (φ=0.1, AR=0.3, B=1/3., D=.5).

Ra	nanotypes	Nu_m	θ_{max}	ψ_{max}
10^3	Cu	5.639	0.194	0.01
	Ag	5.640	0.194	0.01
	AL_2O_3	5.572	0.196	0.027
	TiO_2	5.3633	0.204	0.03
10^4	Cu	5.6179	0.194	0.099
	Ag	5.6211	0.194	0.093
	AL_2O_3	5.5359	0.195	0.241
	TiO_2	5.3272	0.202	0.266
10^5	Cu	5.6599	0.187	0.691
	Ag	5.6385	0.188	0.681
	AL_2O_3	5.8706	0.177	1.166
	TiO_2	5.7126	0.181	1.203
10^6	Cu	6.5310	0.157	1.897
	Ag	6.4705	0.158	1.968
	AL_2O_3	6.8025	0.150	2.548
	TiO_2	6.5903	0.155	2.582

Table 5.Results for the base case (φ=0.1, AR=0.3, Ra=10^5, D=.5).

AR	nanotypes	Nu_m	θ_{max}	ψ_{max}
0.3	Cu	5.898	0.17982	0.19475
	Ag	5.899	0.18011	0.18820
	AL_2O_3	5.856	0.17869	0.37906
	TiO_2	5.646	0.18489	0.40310
0.5	Cu	5.66	0.18653	0.69135
	Ag	5.638	0.18784	0.68099
	AL_2O_3	5.871	0.17651	1.16578
	TiO_2	5.713	0.18097	1.20345
0.7	Cu	5.43	0.19207	1.34306
	Ag	5.369	0.19474	1.35531
	AL_2O_3	5.914	0.17439	1.97483
	TiO_2	5.792	0.17787	2.00221
0.9	Cu	5.345	0.19429	1.94181
	Ag	5.263	0.19756	1.98595
	AL_2O_3	5.927	0.17418	2.66769
	TiO_2	5.812	0.17750	2.68667

Research Paper   Open Access

The fundamental formulas for vertices of convex hull

Md. Kazi Salimullah[1], Md. Khalilur Rahman[2*], Md. Mojahidul Islam[3]
1. Department of Computer Science and Engineering, Islamic University, Kushtia, Bangladesh.
2. Associate Professor, Department of Applied Physics, Electronics and Communication Engineering, Islamic University, Kushtia, BangladeshAuthor.
3. Assistant Professor, Department of Computer Science and Engineering, Islamic University, Kushtia, Bangladesh.

Abstract: - This paper represents four formulas for solution of convex hull problem. It aims to analyze how many points are vertices out of total input points, how many vertices lie on a horizontal or vertical lines, position of vertices and number of vertices on lower and higher lines(horizontal or vertical).

Keywords: - Jarvis's March method, horizontal line (HL), vertical line(VL), vertices , Convex Hull(CH).

I.   INTRODUCTION
Convex hull is a part of computational geometry. Convex hull of a set S of points is the smallest convex polygon P for which each point in S is either on the boundary of P or in its interior. We denote the convex hull of S by CH(S). Convexity has a number of properties that makes convex polygons easier to work with than arbitrary polygons. For example, every diagonal of a convex polygon is a chord, every vertex of convex polygon is convex (that means its interior angle is less than or equal to 180 degree). There are some methods generated for solving convex hull problem. Among these methods Graham Scan method[1], Jarvis's March method[1], Divide and Conquer method[2], Incremental method[3] and Prune-Search methods[4] are remarkable. Number of horizontal line indicates the number of different values of y among the input points. Number of vertical line indicates the number of different values of x among the input points. The end points where two segments meet are called it vertices. The vertices of a polygon are classified as convex or reflex. A vertex is convex if the interior angle at the vertex--through the polygon interior—measures less than or equal to 180 degrees. A vertex is reflex otherwise (its interior angle measures greater than180 degrees).

II.   DESCRIPTION
Statement of formulas
i)   Every vertices of the convex hull must be the starting or ending points (among input points) of any horizontal or vertical line.
ii)   For top and bottom horizontal line or leftmost and rightmost vertical line the starting and ending points are must be vertices of desired convex hull.
iii) The highest number of vertices in one line (horizontal or vertical) is less than or equal to two.
iv)   If the number of lines(horizontal or vertical) is K at which all the points lie then the total number of vertices is less than or equal to 2K.

III.   PROOF OF FORMULAS
1st Formula
Every vertices of the convex hull must be starting or end points of any HL or VL.

Proof

Given a set of input points $P = \{P_1, P_2, P_3, -----P_{10}\}$. Let all the points that lies in 3 HL or 3VL: The objective of this formula is to prove the vertices are starting or end points of any HL or VL. These point are shown in following figure.
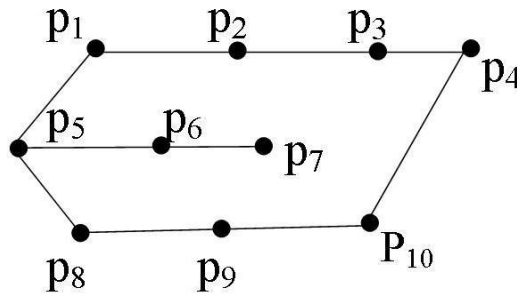
According to definition of convex hull all the input points will be enclosed by smallest polygon and the edge by connecting any two points in inside the polygon and the interior angle of the vertex which will be less than or equal to 180^0.

From the above figure it is seen that by connecting p_1 and p_4 the point p_2 and p_3 can be included into the polygon. By connecting p_5 and p_7 the point p_6 can be included into the polygon. By connecting p_8 and p_{10} the point p_9 can be included into the polygon. So, the desired vertices exist among P_7 which is not a vertex because the edge $P_4 P_{10}$ is then outside the polygon. P_6 can not be vertex because then the point P_5 and P_7 are outside the polygon. So the desired convex hull among these points is $P_1 P_5 P_8$ $P_{10} P_4$. All these vertex points are either starting or end points among these 3 HL.

Example

Let there are 31 points are in 7 HL. The point are (5,17), (10,17), (14,17), (17,17), (20, 17), (25, 17), (-5, 13), (3, 13), (13,13), (19, 13), (27, 13), (10, 10), (2, 7) (6, 7), (11, 7), (17,7), (22, 7), (-2, 5), (15, 5), (25, 5), (1, 4), (4, 4), (8, 4), (6, 7), (11, 7), (17, 7) (22, 7), (-2, 5), (15, 5), (25, 5), (1,4), (4, 4), (8, 4), (13, 4), (9, 4), (21, 4), (2, 2), (5, 2), (9, 2), (16,2), (19, 2). By applying Jarvis's march method the desired convex hull is (2,2), (19,2), (25,5), (27, 13), (25, 17), (5, 17), (-5, 13), (-2, 5). Which is shown in Figure2. From the Figure it seen that all these vertices are either starting point or end point of any HL. So the first formula is proved (under the above discussion).
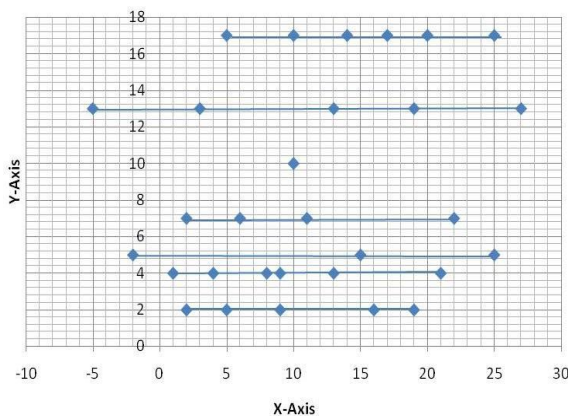
Figure1: Input points
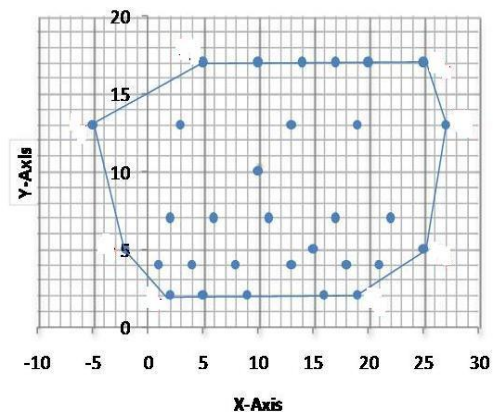
Figure2: Convex hull

2nd Formula

For top and bottom HL or leftmost(LM) and rightmost(RM) VL the starting and the end points must be vertices of the desired CH.

Proof

From the first formula, it is proved that vertices will exist among starting and end points of HL or VL. Let there are two points in top HL. Let these two points are vertices. To prove it at first it is considered that LM point is not a vertex. Since it is an input point to include into CH it needs another point at left side of LM point or upside of LM point, since there is no point at the left side of LM point and there is no point up of the LM

point. So if the LM point is included into the CH then LM point will be a vertex. Again it is considered that RM point is not a vertex. Since RM point is an input point so to include the RM point into CH it needs another point at right side of RM point at the same line or up of the RM point. But it is the top HL so there is no point up of the RM point and there is no another point at the right side of RM point. So RM point also will be a vertex. Similarly for Bottom HL it can be shown that starting and end points of Bottom HL are also vertices. If there is one point in both top HL and bottom HL then that point is vertex. For both top HL and bottom HL then that point is vertex. For both LM VL and RM VL it is also shown that starting and end points are vertices.

Example
From the first example, the vertex points are (2.2), (19,2), (25,5), (27,13), (25, 17), (5,17) (-5, 13) and (-2, 5). The leftmost point of the top HL is (5, 17) and the right most point (25, 17) which are vertices of the desired CH.
The leftmost point is the bottom HL is (2, 2) and the rightmost point is (19,2) which are the vertices of the desired CH. So the second formula is proved.

3rd Formula
The number of vertices in one HL or VL is less than or equal to two.

Proof
This formula gives the concept of highest no of vertices in one HL or VL. Let there are 3 HL or VL and each HL or VL has n no. of points that means it is given 3n no of input points; they are:

$$P_{11}, \ P_{12}, \ P_{13}, \text{--------} \ P_{1n}$$
$$P_{21}, \ P_{22}, \ P_{23}, \text{--------} \ P_{2n}$$
$$P_{31}, \ P_{32}, \ P_{33}, \text{--------} \ P_{3n}$$

According to first law, the vertices of the desired convex hull will be included among $P_{11}, \ P_{1n}, \ P_{21}, \ P_{2n},$ $P_{31}, \ P_{3n}$ are vertices of the desired CH. Now in middle line, the starting and end point are P_{21} and P_{2n}. If there is any vertex in this line then that point is either P_{21} and P_{2n}. Because if P_{22} or P_{23} or ---- or P_{2n-1} is vertex then the condition of the convexity will be broken. Moreover, by connecting starting and end points we can include all the points in that line into CH.

Example
From Figure2 it seen that the no. of vertices in first HL=2, in second HL the no. of vertices =2, In 3rd HL the no. of vertices = 0. In 4th HL the no. of vertices=0, In 5th HL the no. of vertices= 2, In 6th HL the no. of vertices = 0, In 7th HL the no. of vertices =2. Each line has highest no. of vertices 2. So from the discussion, the third formula is proved. (counting order of HL from up to down).

4th formula
If the number of the HL or VL is k then the number of vertices less than or equal to 2k.

Proof
This formula gives the concept about the highest no of vertices into among input points. It is related with the no. of line (VL or HL) at which all the input points exist. From 3rd formula it is proved that in one line there exist highest 2 vertices. So if the no of line (HL or VL) is K then highest no. of vertices are 2k. Among these the starting and end points in top and bottom HL or leftmost and rightmost VL are vetices by 2nd formula. But the starting and end point of other HLs or VLs may not be vertices because other HLs or VLs exist among top and bottom HLs or leftmost and rightmost VLs. If all starting and end points are vertices then total no. of vertices will be 2k otherwise less than 2k.

Example
In Figure2, there are 7 HLs. 1st line has 2, second has 2, 3rd has 0, 4th has 0, 5th has 2, 6th has 0 and 7th has 2 no. of vertices. So total no. of vertices = 2+2+0+0+2+0+2=8 which is less than 14. So the 4th formula is also proved.

Applications
By applying these formulas the complexity of any convex hull algorithm can be decreased as remarkable rate. Since it is proved that the vertices of the CH are must be starting and end points of any HL or VL. So by analyzing only the starting and end points of all HLs or VLs it can determined the desired Convex Hull. That means if the total no of line is equal to K then analyzing only 2k no. of points can be determined the desired convex hull although there exists Kn no. of points (each line has n points). If there exists h no. of

vertices among this input point then the new complexity of Jarvis's march method will be 2kh after applying these formulas. Whereas present complexity of Jarvis's march method is Khn, that is so larger than 2kh. Since starting and end points of top and bottom HL or leftmost and rightmost VL are vertices so the CH can be determined more easily which is shown in "A new technique for solving convex hull problem"[5]. Another advantage is it can check easily a point is inside or outside of the CH and merging of two convex hull.

Results and Discussion

Now these four formulas are proved for different convex hull. In the table number of horizontal line is expressed as HL.

Number of points	Number of lines=k	Highest Number of vertices =2k	Input points	Total number of vertices	Vertices	1st formula	2nd formula	3rd formula	4th formula
8	HL=2	4	(2,1),(5,1),(9,1),(12,1), (-2,5), (2,5), (8,5), (10,5)	4	(2,1),(12,1), (-2,5) ,(10,5)	True	True	True	True
10	HL=3	6	(-1,7), (4,7), (6,7), (10,7), (1,2),(5,2),(7,2), (-5,1), (1,1), (10,1)	4	(-5,1), (10,1), (-1,7), (10,7)	True	True	True	True
15	HL=4	8	(-6,3),(-3,3),(0,3),(5,3), (2,5), (4,5), (10,5), (12,5), (15,5), (5,10) (7,10),(10,10),(15,10), (1,12), (5,12)	6	(-6,3),(5,3), (15,5),(15,10), (1,12),(5,12)	True	True	True	True
20	HL=4	8	(-6,3),(-3,3),(0,3),(5,3), (10,3), (-10,5), (4,5), (10,5), (12,5), (15,5) (-10,10),(5,10),(7,10), (10,10),(15,10) (-2,12),(0,12),(1,12),(5,12), (7,12)	8	(-6,3), (10,3), (-10,5), (15,5), (-10,10), (15,10), (-2,12), (7,12)	True	True	True	True
15	HL=5	10	(1,2),(4,2),(10,2), (-5,6), (5,6), (12,6), (1,10), (3,10), (5,10), (-3,15)(3,15),(4,15), (6,18),(10,18), (13,18)	7	(1,2),(10,2), (-5,6),(12,6), (-3,15),(6,18), (13,18)	True	True	True	True

From the above table it is seen that for all the inputs, four formulas are true. So it can be said that for any input four formulas are true.

IV. CONCLUSION

These four formulas can be applied for any convex hull problem. So it can be said these formulas are successful formulas for solution of convex hull problem. These formulas describe the fundamental characteristics of vertices of convex hull.

REFERENCES

[1]. Thomas H. Cormen, Charles E. Leiserson, Ronald L.Rivest, Clifford Stein; *Introduction to Algorithms,* The MIT Press, McGraw-Hill Book Company, Second edition, pp. 947-961

[2]. Michael J. Laszlo. *Computational Geometry and Computer graphics in C++,* Prentice-Hall of India private Ltd, Eastern Economy Edition, pp.203-208

[3]. Michael J. Laszlo; *aforesaid*, pp.139-145

[4]. Thomas H. Cormen et al; *aforesaid*, pp.189-192

[5]. Md. Kazi Salimullah, Md. Khalilur Rahman; A new technique for solving convex hull problem; *International Journal of Engineering Research And Technology(IJERT)*, vol-2, issue-5, May2013, India

Research Paper	Open Access

Organizational analysis of the number of failures of integral components of the circuits – OE Spinning machine based on mechanical oscillations in observed time of their exploitation from aspect of their reliability

Professor dr. Slobodan Stefanović[1], Professor dr. Radoje Cvejić[2], Professor dr. Radojko Lojaničić[3]

[1]High School of Applied Professional Studies of Vranje, Serbia
²Associate Professor, Faculty of strategic and operational management, Belgrade, Serbia
[3]Associate Professor, Faculty of strategic and operational management, Belgrade

Summary: Reliability of integral components of system for winding coils with finished yarn with OE spinning machine is performed analytically by showing the mathematical transfer functions through the final equation value of reliability based on the partial values of reliability.These final transfer functions are obtained based on the formed sub-methods as follows: Pre method (1) that consists in the fact that for the obtained exploitation data on failures, because of the high level of mechanical osillations, define the empirical function of density of distribution $\lambda_e(t)$ and empirical reliability function $R_e(t)$ and pre method (2) that was used for the selection of statistical reliability distribution of the analysed circuit components which corresponds best to the obtained data on failures that occurred due to the influence of high level of mechanical oscillations in the exploitation of their work. Based on these sub methods are obtained final forms of curve $f(G_{NK}(t), t)$ that determines the shape of the statistical distribution of the analyzed system reliability.

Keywords: *number of failures, OE – spinning machine, winding coils system, reliability, dependency of the reliability curve.*

I.   INTRODUCTION - INTRODUCTION – DESCRIPTION OF COMPLEX FOR COIL WINDING WITH FINISHED YARN

System of power transmission of the system for coil winding with finished yarn is shown in Figure 1. and consists the following parts and components which are classified based on the spun yarn which is obtained by spinning from the rotor (turbine) and on its way to the coil on which is winding.

YARN THAT IS OUT OF MECHANISM FOR PARAFFIN
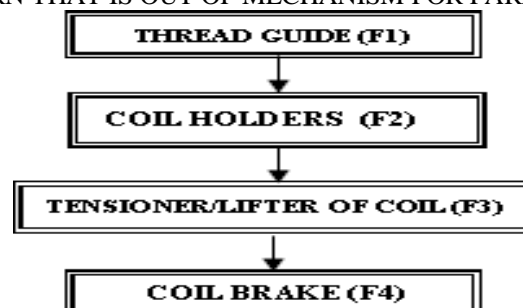
Figure (1). System of transmission for winding coils with finished yarn

THREAD GUIDE (F1) – serves for evenly and safely winding of yarn on cone coil. His movement is rectilinear with feedback gait, the number of cycles is 120/ per minute. It is made from a special type of ceramic with a metallic sheathing resistant on the occurrence of friction. Installation and removal are very simple (Fig. 2).
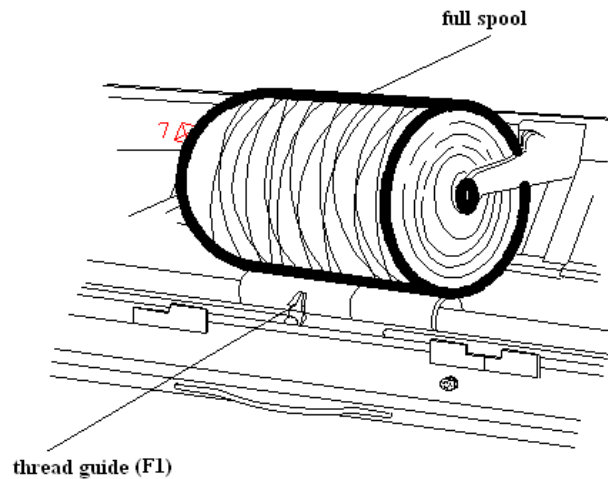
Fig. (2). System for the winding coil with finished yarn – the front part of the complex

COIL HOLDERS (F2) – serves for centering and evenly circular rotation of coil when winding. Holders are made from a special type of polymer, they are special forms placed on the rolled bearings. When bearings breakdown, because of dust in it, leads to its malfunction and fracture of the inset of coil holder (Fig. 3).

TENSIONER/LIFTER OF COIL (F3) – is system of springs and levers that is used for disposal of full coils on a conveyor belt. System of springs is unstrained at coil winding with yarn, while at the full coils the same is activated and divides the full coil from coverings on which coil leans while rolling on (Fig. 3).

COIL BRAKE (STOPPING OF COILS WHEN YARN BREAKS) (F4) – is a system that consists from roller shape coverings on which coil leans while rollin on, as well as from the lever that activates while tying the broken yarn (Fig. 3).

THREAD GUIDE (F1) – serves for evenly and safely winding of yarn on cone coil. His movement is rectilinear with feedback gait, the number of cycles is 120/ per minute. It is made from a special type of ceramic with a metallic sheathing resistant on the occurrence of friction. Installation and removal are very simple.
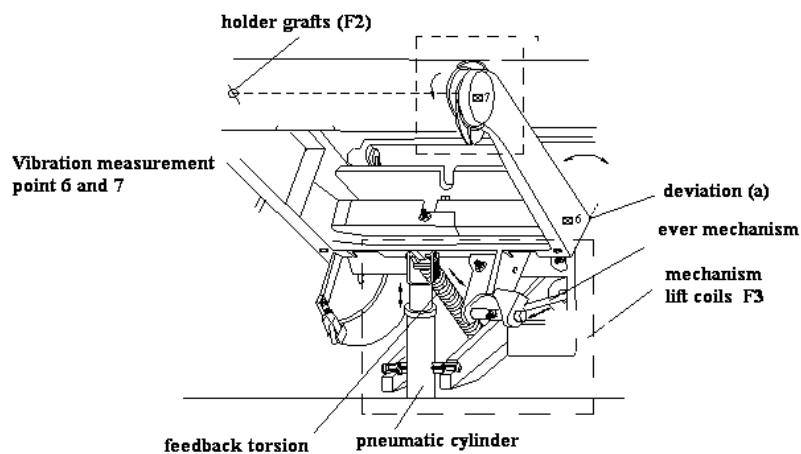
Fig. (3). System for winding coils with finished yarn – rear of the complex

COIL HOLDERS (F2) – serves for centering and evenly circular rotation of coil when winding. Holders are made from a special type of polymer, they are special forms placed on the rolled bearings. When bearings breakdown, because of dust in it, leads to its malfunction and fracture of the inset of coil holder.

TENSIONER/LIFTER OF COIL (F3) – is system of springs and levers that is used for disposal of full coils on a conveyor belt. System of springs is unstrained at coil winding with yarn, while at the full coils the same is activated and divides the full coil from coverings on which coil leans while rolling on (Fig. 3).

COIL BRAKE (STOPPING OF COILS WHEN YARN BREAKS) (F4) – is a system that consists from roller shape coverings on which coil leans while rollin on, as well as from the lever that activates while tying the broken yarn.

II. THEORETICAL ANALYSIS OF THE SYSTEM

Analyzed circuits at the beginning of the exploitation, did not have a big number of failures of their components, but there was a lack of precision in their installation that lead to a certain arrest, and it can be said that these are not early failures in initial work of circuits but disadvantages when starting OE – spinning machine in its exploitative work.

From established state of work of OE – spinning machine gradually came to tear of the circuit components, and in conjunction with that, to increased levels of mechanical oscillations that led to cancellation of some of their components.The first failures have occurred about 13 000 hours of work on the integral components of analyzed circuits of OE – spinning machine. From this period there is a rapid growth of failure of their integral components, and for this period can be said that it is a period of their unstable work. This can be displayed with dependency diagram of the number of failures N FAILURES (N OTKAZA) in the function of the exploitation time t (Figure 4.).
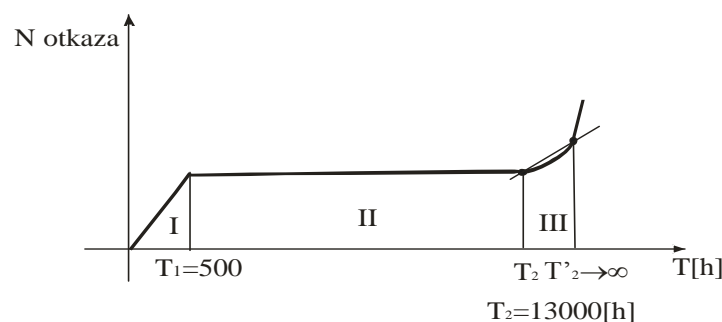
Figure (4). Dependency area of the number of failures of analyzed circuit components based on the increased level of mechanical oscillations in the function of their time of exploitation work without the use of preventive maintenance technology

On figure 4. can clearly see three areas where failures occur, as follows:

The area of initial work of the circuit $0 \div (t_1)$, *(I area of exploitation);*

The area of initial work of the circuit $(t_1 \div t_2)$, *(II area of exploitation);*

The area of initial work of the circuit $\left(t_2 < t'_2 < t'_2 \to \infty\right)$, *(III area of exploitation).*

Failure analysis of the integral components of analyzed circuits will be concentrated in the areas of their unstable work because then it come to their intensification . If with t_1 - mark the time by which the analyzed circuit was initiating his work, and with t_2 time by which the analyzed circuit had work without failure (exploitation-established circuit with the area of allowed risk of work – safe work) then each time interval after the time t_2 is interval of his unstable work $t'_2 > t_2$, that is, interval of the risk.

In figure 5. is presented dependency of number of failures N FAILURES (N OTKAZA) in the function of exploitation time t of integral components of analyzed circuits on which were implemented procedures of preventive maintenance technology.
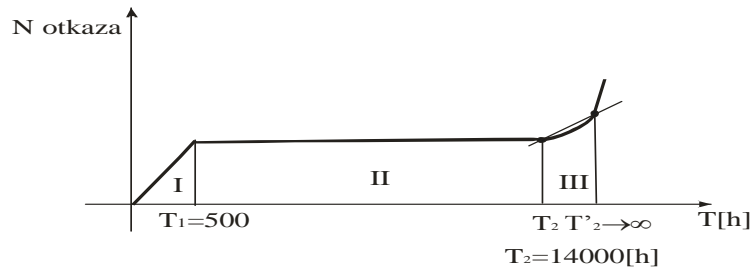
Figure 5. Dependency area of the number of failures of analyzed circuit components based on the increased level of mechanical oscillations in the function of their time of exploitation work with the use of preventive maintenance technology

III.   RELIABILITY OF THE WORK OF ANALYZED CIRCUIT COMPONENTS OF OE- SPINNING MACHINE

Determination of the reliability of the work of integral components is taken as a part of the collective concept of security functioning and its performance. The starting point was the quality of service of OE - spinning machines that includes:
- Performance of use (availability and stability performance),
- Availability performance (performance of: reliability, maintainability and logical support of maintenance).

So that the listed performances could ensure safety of functioning of the work of OE – spinning machine, it was necessary to link the reliability of his work and the process of preventive maintenance technology.

To determine the reliability of the integral components of the analyzed circuit, will use the data on failures that occurred due to the impact of increased levels of mechanical oscillations (vibrations) and have been recorded from the exploitation of their work (Table 1).

Table 1. Total number of failures on integral components of the analyzed circuits on which are not implemented procedures of preventive maintenance technology and on those on which were implemented

Ordinal number	Name of the integral component of the circuit	Number of failures of integral components on which were not implemented procedures of preventive maintenance technology	Number of failures of integral components on which were implemented procedures of preventive maintenance technology
8.	Thread guide (F1)	21	20
9.	Coil holder (F2)	114	92
12.	Coil brake (F4)	2	2

IV.   RELIABILITY OF WORK OF COMPONENTS OF ANALYZED COMPLEX OF OE –SPINNING MACHINE WITH METHOD OF ANALYSES OF FAULT TREE

Determination of the reliability of work of constituent components is taken as part of the collective security of functioning and its performance. Started from the quality of service of OE - spinning machines that includes:
- Performance of use (performance of availability and stability),
- Performance of availability (performance: reliability, maintainability and maintenance logical support).

To ensure the safety of the listed performance function of assembly OE - spinning it was necessary to link the reliability of their work procedures and implementation of preventive maintenance technology.
To determine the reliability of the constituent components of the analzyed complex, used the data on failures that occurred due to the impact of increased levels of mechanical oscillations (vibration) and have been recorded from the exploitation of their work.

For the analysis of data to determine the reliability of components analyzed complex, it was used the following pre methode which consists in this: that for the obtained exploitation data on failures, because of the influence of high level of mechanical oscillations, define the empirical density function $f_e(t)$, empirical function of failure intensity $\lambda_e(t)$ and empirical function of reliability $R_e(t)$.

This sub method for the determination of the main functions in the analysis of the reliability of integral parts and components of complex, were chosen based on the analysis of data on failures incurred because of

increased levels of mechanical oscillations obtained in the exploitation of their work, and are the most practical way to determine the reliability of their work. As the analysis of the data of reliability, will determined density function failure $f_e(t)$, function of failure intensity $\lambda_e(t)$ and function of reliability $R_e(t)$, based on which will be determined reliability of the work of components of analyzed complexes.

For a more complete analysis of the reliability of the components of the analyzed complex, shall be determined safe function of their work.

If we have (n) connected components of complex in the system of power transmission of OE - spinning machines for which we analyze the reliability, starting from the period for $t = 0$, than at any point of time (t_i) it will be $n_i(t_i)$ of the complex that are not cancel. In this case, the empirical density function of failure $f_e(t)$, can be determined from the form:

$$fe(t) = \frac{\dfrac{n_i(t_i) - n_i(t_i + \Delta t_i)}{n}}{\Delta t_i} = \frac{n_i(t_i) - n_i(t_i + \Delta t_i)}{n \cdot \Delta t_i} \qquad (4.1)$$

where : $t_i \le t \le \Delta t_i$.

Empirical function of failure intensity $\lambda_e(t)$, is equal to the quotient of ratio of the number of failures in the time interval Δt_i and the number of circuits that are not canceled at the beginning of the interval, with the length of the time interval Δt_i.

This function is determined by the empirical formula:

$$\lambda e(t) = \frac{\dfrac{n_i(t_i) - n_i(t_i + \Delta t_i)}{n_1(t_i)}}{\Delta t_i} = \frac{n_i(t_i) - n_i(t_i + \Delta t_i)}{n_1(t_i) \cdot \Delta t_i} \qquad (4.2)$$

where : $t_i \le t \le \Delta t_i$.

The difference between the empirical density of failure $f_e(t)$, and empirical functions of failure $\lambda_e(t)$ is in the speed of happening the failure. Empirical density of the failure is overall speed failure happenings, while the empirical function of failure intensity, current speed of failure happening. Empirical reliability function $R_e(t)$ represents the probability of no failure work of connected components of analyzed complex (n) during the time *t*.

This is represented by the form:

$$R_e(t) = \frac{n_1}{n}, \qquad (4.3)$$

where:

$n_1(t)$ - number of the correct complexes or components of complexes at the end of the time interval *Δti;* $n(t)$ - total number of components of the analyzed complex.

Presented patterns in determining empirical functions: failure density $f_e(t)$, function failure $\lambda_e(t)$ and reliability $R_e(t)$, will be applied in determining the approximate reliability of the work of analyzed complex components.

Concretely computation of these functions will be shown in determining the reliability of the work of analyzed complex components on which have not been applied technology of preventive maintenance procedures and the ones on which these procedures are implemented.

V. DETERMINATION OF CORRECTION VALUES OF THE RELIABILITY OF THE INTEGRAL COMPONENTS WORK OF ANALYZED COMPLEX BASED ON THE EMPIRICAL (EXPLOITATION) DATA

Since are defined exploitation values of reliability that are expressing approximate values of reliability of integral components work of analyzed complex with maximum safety (areas of their safe work time and areas of reduction of their reliability) for their more precise determination it was used determination of their

correction values.
Correction values of reliability from empirical (exploitation) data are shown in pictures from 7, and their tabular values are shown within these pictures.

Correction values of reliability are obtained by dividing the empirical density function of the empirical values $\left(f_e(t)\right)$ and function of failure intensity $\left(\lambda_e(t)\right)$ for the time interval of the exploitation work of complex components (analysis included exploitation work time of integral componentsof the complex in the period $13000 \le \Delta t_i \le 21000\,\text{hours}$) (Fig. 7.) and is determined by the expression:

$$P_i(t) = \frac{f_{e_i}(t)}{\lambda_{e_i}(t)}. \tag{5.1}$$

VI.　　DETERMINATION OF STATISTICAL METHODS RELIABILITY DISTRIBUTION OF THE ANALYZED CIRCUIT

To determine the statistical method of reliability distribution is necessary to create models and to determine transmission function of the reliability of the analyzed curcuit. For determining table of the transfer functions of the circuit for the coil winding with finished yarn $G_{NK}(t)$ correction values of reliability are used $P_i(t)$.

Formation of models included the layout of circuit components according to processing of the yarns, that is, according to the order of components in the fault tree.

The components are sequential arranged on the circut, from the thred guide to the mechanism for disposal of the coils with finished yarn at the circuit for coil winding with finished yarn.

For these reasons, the model of the block diagram is shown. In this model, approach to solving the obtaining of transfer function is reduced to reduction of the diagram blog.

Based on the obtained final expressions of transfer functions of the analyzed circuit ($G_p(t)_{NK}$ - for winding coils with finished yarn), and in it replacing the values of component reliability $P_i(t)$ for time intervals $13000(\text{h}) \le \Delta t_i \le 20000(\text{h})$ tabular values are obtained for significance of reliability zones, from which is constructed the curve of reliability of transfer function of analyzed circuit.

Model of the block diagram of reliability of transfer function at the circuit for coil winding with finished yarn. Model of the block diagram of reliability of transfer function at the circuit for coil winding with finished yarn is shown in Figure 6.
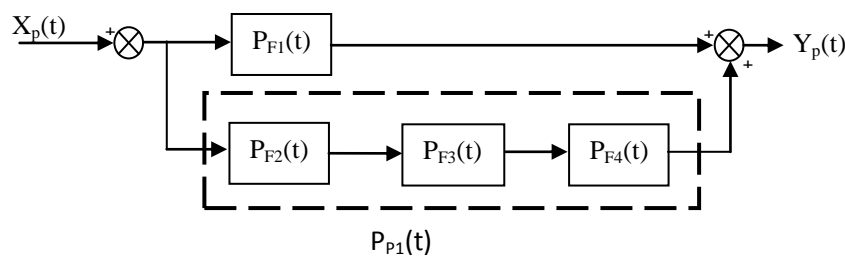
Figure (6). Initial model of the block diagram of reliability of transfer function at the circuit for coil winding with finished yarn

Step I - Determination of partial blocks of reliability $P_{P1}(t) = P_{F2}(t) \cdot P_{F3}(t) \cdot P_{F4}(t)$. (Figure 7.)
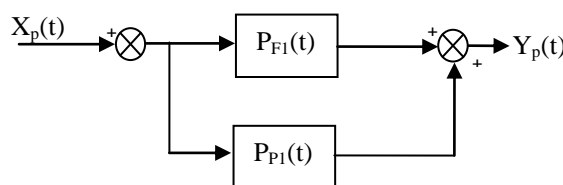
Figure (7). Picture of partial blocks of reliability

Step II – Determination of the overall transfer function of reliability of the circuit for winding coil with finished yarn:

$$G_{NK}(t)_P = \frac{Y_P(t)}{X_P(t)} = P_{F1}(t) + P_{P1}(t) = P_{F2}(t) \cdot P_{F3}(t) \cdot P_{F4}(t) + P_{F1}(t)$$　　　(6.1)

VII.　　CONCLUSION – FORMATION OF TABLE VALUE OF TRANSFER FUNCTION OF CIRCUIT FOR WINDING COIL WITH FINISHED YARN $G_p(t)_{NK}$

　　Tables are set up based on the final expressions of transmission functions of reliability depending on the time interval of circuits.

　　Based on the obtained results, a graphical representation of dependence is performed $f(G_p(t)_{NK}, t)$. (Figure 8.). Display of values of transmission function of reliability of the circuit for winding coils with finished yarn was performed in tables over constructed graphics of transfer function and is shown in Figure 8.

Remark: Shaded areas $P_i(t)$ have included values $P_i(t) \geq 0,5$ because values below this limit are not taken into consideration (include areas where repairs of the circuit should be made, which will be discussed in more detail in determining the value of the reliability in cases of selected statistical distribution).

Curve, $f(G_p(t)_{NK}, t)$ corresponds by its form to long-normal curves, and therefore for choice of statistical reliability distribution should be taken **long-normal distribution.**

Reliability values $P_i(t)$		transfer function of reliability for the coil winding assembly the finished yarn $G_p(t)_{NK}$
1,0		2,0
0,9		1,63
0,8	shaded areas represent the ultimate limit of satisfactory reliability in the analysis	1,312
0,7		1,043
0,6		0,816
0,5		0,625
0,4		0,464
0,3		0,327
0,2		0,208
0		0,101
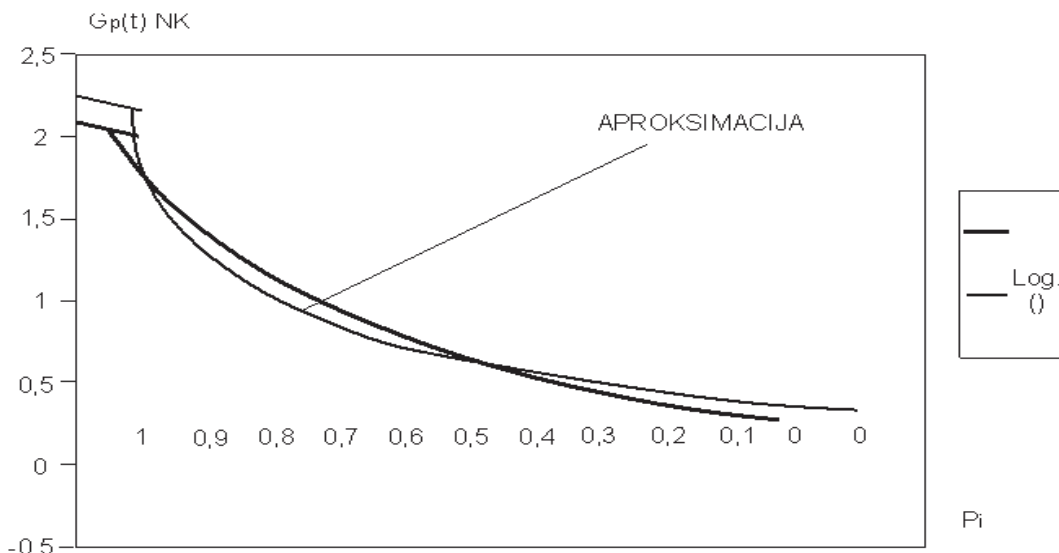
Figure (8). Graph of transfer function of circuit for coil winding with finished yarn with approximation $G_P(t)_{NK}$

REFERENCES

[1]   Adamović Ž., Stefanovic, S., Procedures for the implementation of control of mechanical vibrations and method of collection of the data on technical systems, XVIII Yugoslav conference with international participation "Noise and Vibration", Faculty of Occupational Safety, Niš, 2002.

[2]   S. Stefanovic, THE ANALYSIS OF FUNCTIONING OF BASIC COMPONENTS OF OE - TECHNICAL SYSTEM, INTERNATIONAL JOURNAL OF ENGINEERING, Tome XI (Year 2013). Fascicule 1. str. 237-244, ISSN 1584 – 2665, ANNALS of Faculty Engineering Hunedoara, Romania.

[3]   S. Stefanovic, DETERMINATION OF THE VALUE OF SELECTED OSCILLATION FREQUENCY MEASUREMENT POINT ANALYZED PARTS OE SPINNING - On the box spinning, PRIYANKA RESEARCH JOURNAL PUBLICATION, International Journal of Mechanical Engineering Research and Development (IJMERD) ISSN 2248-9347, India, (2012). Journal Impact Factor (2011) - 0.9278 Calculated by GISI.

[4]   Barlow, G., Proshan, F., Statistical Theory of Reliability and Life Testing Probability Models, Holt, Richard of Winston Inc.., New York, 1975.Deanzer, W., Systems Engineering, Verlag industril Org., Zurich, 1979.

[5]   Nakajima, S., "TPM Developement INPLEMENTING PROGRAM TOTAL productive maintenence" productivit Press, Cambridge, Massachutsetts, Norwalk, Connecticut, 1989.

[6]   Prasad, B., "CONCURRENT ENGINEERING-INTEGRATED PRODUCT AND PROCESS ORGANIZATION", Vol. 1, Prentice-Hill, New Jersey, 1996.ROTOR Spiner, GMB, RIETERR, 1995.

[7]   Stefanovic, S., DETERMINATION OF THE VALUE OF SELECTED OSCILLATION FREQUENCY MEASUREMENT POINT ANALYZED PARTS OE SPINNING - On the box spinning, International Journal of Mechanical Engineering Research and Development (IJMERD), PRIYANKA RESEARCH JOURNAL PUBLICATION. INDIA, 2012.

[8]   Stefanovic, S., Ugrenović, M., Productivity modern spinning machines, depending on the parameters of diagnostic failure in power transmission systems, Journal TEHDIS no. 1/2002., Belgrade.

[9]   S. Stefanović, RESERCH INTO THE CAUSES OF INACCURACIES OF COMPONENTS OF COMPLEX FOR COIL WINDING WITH FINISHED YERN AT OE. Lucrarea trimisă redacţiei Metalurgia International a fost acceptată spre publicare în numărul 2013., ISSN 1582 – 2214, "METALURGIA INTERNATIONAL" is introduced in THOMSON SCIENTIFIC MASTER JOURNAL LIST, letter M, position 440. vol. 18 SPECIAL ISSUE NO. 8, str. 96 – 101 (2013).

[10] S. Stefanovic, DETERMINATION OPERATION TIME RISK OF BOX SPINNING COMPONENTS - OE SPINNING MACHINE, American Journal of Engineering Research (AJER) ISSN : 2320-0847, Volume-XX, Issue-4, (2013).

Research Paper   Open Access

Optimization of Conditions for the Preparation of Activated Carbon from Mango Nuts using HCl

Kwaghger, A[1*] and Ibrahim J.S[2]
[1,2]Department of Mechanical Engineering, University of Agriculture, Makurdi, Nigeria.

Abstract: - Activated carbon was prepared from mango nuts by chemical activation method using HCl herein referred to as MNAC. The effect of experimental variables; temperature, concentration, impregnation ratio and carbonization time on the quality of the activated carbon- surface area, carbon yield and ash content were investigated. The response surface methodology (RSM) technique was used to optimize the production conditions. The influence of the studied production parameters on the activated carbon produced was investigated using the analysis of variance (ANOVA) to identify the significant variables. The optimum preparation conditions for preparation of the MNAC were obtained a follows: carbonization temperature of 212.1°C, HCl concentration of 100%, 30 min resident time and 1ml/g mix ratio. This resulted in the activated carbon with 5.92% ash content, 1142.3 m^2/g surface area and 63.2% carbon yield. It was observed that the experimental values obtained were in good agreement with the values predicted by the model with relatively small errors between the predicted and the actual values (0.33, 0.18 and 1.94 for ash content, surface area and carbon yield respectively).

Keywords: - *Activated carbon, Conditions, HCl, Mango nuts, Optimization.*

I.   INTRODUCTION

Mango, *magnifera indica,* is a major waste in Makurdi, the capital city of Benue state especially during its harvesting season as farmers from different part of the state find a ready market in Makurdi.The edible part of mango is the peel and the fibrous material. The pit is not a consumable part of mango and is usually discarded as waste. Mango has become and economically important species since its demand domestically and for export has increased tremendously. Due to the high consumption of the edible part, massive amount of mango nut are disposed causing gradual fermentation and subsequent release of odour [1]. To make better use of cheap and abundant agricultural waste, it is proposed to convert mango nut waste into activated carbon. This conversion will address problems of unwanted agricultural wastes been converted into useful, value- added adsorbent and also the use of agriculture by- products to represent potential source of adsorbent which will largely address problems of waste management. However, not many studies have been reported on converting mango nut into activated carbon. Some relevant studies found in literature were reported by other authors [2-5]. A challenge in activated carbon production is to produce very specific carbons which are suitable for certain application. The most important characteristics of an activated carbon is it adsorption capacity which is highly influenced by the preparation conditions [6]. In assessing the effect of the treatments on quality attribute, the use of an adequate experimental design is particularly important. Response Surface Methodology (RSM) has been found to be a useful tool to study the interaction of two or more variables [7]. Optimization of experimental conditions using RSM has widely been applied in various processes; however, its application in activated carbon production is rare. Some previous studies reported using RSM in optimizing the production of activated carbon with other agricultural wastes were reported by other authors [7- 10]. As far as known, no study has been carried out using RSM approach in analysing the production process of activated carbon with mango using HCl as activating agent.

In the present study, the optimal experimental conditions required to obtain adequate activated carbon with desirable properties in terms of carbon yield, surface area and ash content, which are critical in determining a good quality activated carbon for a wide range of adsorption applications were determined. A modelling technique was applied to relate the experimental conditions of the activation process with properties

of activated carbon. A good quality activated carbon should have low ash content as possible. Faust and Aly [11], suggests that typical values of ash content should be in the range of 5 – 6% and about 85 – 90% for carbon content. As the carbon content of the activated carbon increase, the surface area also increases. High carbon content value is desired to achieve high surface area. Bacaoui *et al*, [8] reported that for economic viability, activated carbon should have a carbon yield of 10- 20% and a surface area of 1000- 1300 m^2/g. Using olive-waste cake waste, Ahmad and Alrozi [12] reported a carbon yield of 20.76%; Aloko and Adebayo [13] reported 1620m^2/g surface area, 148.20% ash content and 29.24% carbon yield using mango peel; Sahu *et al* [10] reported a carbon yield value of 46.08% using Tamarind wood; Hameed *et al*, [14] reported a carbon yield of 17.96% and a surface area of 1141m^2/g. The inorganic material contained in activated carbon is measured as the ash content and this value should be in range of 2-10 % [15]. The ash content generally gives a good idea about the inorganic constituents associated with carbon obtained by different carbonization methods. Low value of ash content indicates that the inherent carbon in the starting material is high [16]. Soleimani and Kaghazchi [17] reported that activated carbon with high ash content is undesirable because it reduces the absorption capacity and mechanical strength of activated carbon.

The main objective of the paper is to determine the suitable experimental conditions; carbonization temperature, activation time, concentration and impregnation ratio required to prepare activated carbons from mango nuts for effective use in a variety of adsorption application. Also, to select indigenous raw materials of agricultural origin (mango seeds), explore the potential of producing activated carbons from mango nut wastes and carry out studies to explore the possibility of obtaining high quality activated carbons.

II.   MATERIALS AND METHODS.

2.1 Preparation of the activating agent (HCl). 25, 50 and 75 *ml* of hydrochloric acid was added to 75, 50 and 25 *ml* of distilled water to obtain 25, 50 and 75 % volume concentrations of acid activating agent respectively. For 100 % volume concentration, no distilled water was added (it was used undiluted) so that it remained in 100 % volume concentration [18].

2.2 Preparation and carbonization of mango seeds. In the preparation of the mango seeds, the procedure is described hence was follows. First, the dried mango nuts collected were cracked using hammer and the seeds were then removed from the nuts and were dried under sun light at room temperature for two weeks after which they were crushed using laboratory mortar and pestle. The resulting particles were again sun-dried for 5 hours to remove any residual moisture left in them. The particles were then sieved using *6mm* sieve size and used for the rest of the experimental work. The sieved samples were then impregnated with different concentrations of the activation agents (25%, 50%, 75% and 100%). 50*g* of the samples was measured and impregnated (mixed) with 50*ml*, 100*ml*, 150*ml* and 200*ml* of the various activating agents to obtain ratios of 1:1, 1:2, 1:3 and 1:4 *ml/g* respectively. The impregnated samples were left at room temperature for 24 hours. After impregnation, the excess solutions were filtered off and the remaining material dried for three days at room temperature. Finally the resulting samples were carbonized in a pre- heated furnace at temperatures of 200, 400, and 600°C for durations of 30, 60, 90 and 120 minutes. The activated carbons were rinsed with distilled water, dried at 750°C temperature for 1 hour in the furnace and crushed to obtain particle sizes of *3mm* by passing the crushed carbon through sieve size 300*μm*. Care was taken to ensure the material was not forced through the sieve by hand pressure.

2.3 Characterizations of the products

Ash Content Determination: The ash content of MKAC produced was determined by the standard test method for ash content- ASTM D2866-94. A crucible was pre- heated in a furnace to about 500°C, cooled in a desiccator and weighed. 1.0g of MKAC was transferred into the crucible and reweighed (oven dry weight). The crucible and sample were then placed in the furnace and temperature was raised to 500°C. The sample was removed and allowed to cool in a desiccator to room temperature and reweighed (ash weight). The ash content was calculated using equation 1.

$$Ash\ content(\%) = \frac{Ash\ weight(g)}{Over\ dry\ weight(g)} \times 100 \qquad\qquad (1)$$

Surface Area Determination: The diameter (assuming spherical shape) of the activated carbon was obtained by passing the crushed carbon through sieve size of 300μm and the external surface area was calculated by the relation;

$$Surface\ area,\ S_A = \frac{6(cm^2/g)}{B_d P_d} \qquad\qquad (2)$$

B_b = bulk density
P_d = particle size (particle diameter)
A measuring cylinder was weighed, and then filled with the prepared sample of MKAC and gently tamped until no change in the level of the sample was observed. The volume occupied by the packed sample was recorded as V_s, if W_c is the weight of the empty cylinder and W, the weight of the cylinder and sample, then, weight of the

sample W_s was obtained by $W_s = W - W_c$ [20]

The bulk density was calculated using equation 3.

$$B_d\left(\frac{g}{mL}\right) = \frac{W_s}{V_s} \tag{3}$$

Where V_s, is the volume occupied by the packed sample

Activated Carbon Yield
The dried weight, W_{ca} of each carbon sample was determined and the carbon yield (CY) was calculated as follows;

$$Carbon Yield = \frac{W_{ca}}{W_f} \times 100\% \ [21] \tag{4}$$

Where, W_{ca} = oven dried weight of carbon sample,
W_f = weight of carbon retrieved from the furnace.

III.　　RESULTS

Table 1: ANOVA for ash content (HCl)

Source	F	P
Regression	52.12	0.000
Linear	129.35	0.000
Temp	457.08	0.000
Conc	14.94	0.000
Time	29.37	0.000
Ratio	16.00	0.000
Square	38.73	0.000
Temp*Temp	121.36	0.000
Conc*Conc	24.75	0.000
Time*Time	4.12	0.043
Ratio*Ratio	4.69	0.031
Interaction	9.55	0.000
Temp*Conc	8.49	0.004
Temp*Time	20.09	0.000
Temp*Ratio	19.06	0.000
Conc*Time	0.60	0.440
Conc*Ratio	9.07	0.003
Time*Ratio	0.00	0.961

Table 2: ANOVA for surface area (HCl)

Source	F	P
Regression	31.65	0.000
Linear	62.56	0.000
Temp	94.34	0.000
Conc	2.76	0.097
Time	130.65	0.000
Ratio	22.49	0.000
Square	14.49	0.000
Temp*Temp	10.64	0.001
Conc*Conc	27.05	0.000
Time*Time	17.33	0.000
Ratio*Ratio	2.96	0.086
Interaction	22.48	0.000
Temp*Conc	15.06	0.000
Temp*Time	74.14	0.000
Temp*Ratio	15.89	0.000
Conc*Time	13.10	0.000
Conc*Ratio	6.76	0.010
Time*Ratio	9.91	0.002

Table 3: ANOVA for carbon yield (HCl)

Source	F	P
Regression	16.75	0.000
Linear	21.52	0.000
Temp	20.75	0.000
Conc	0.04	0.840
Time	65.17	0.000
Ratio	0.12	0.726
Square	25.58	0.000
Temp*Temp	4.70	0.031
Conc*Conc	93.88	0.000
Time*Time	3.66	0.056
Ratio*Ratio	0.10	0.756
Interaction	7.69	0.000
Temp*Conc	28.78	0.000
Temp*Time	12.70	0.000
Temp*Ratio	3.75	0.053
Conc*Time	0.26	0.610
Conc*Ratio	0.45	0.502
Time*Ratio	0.21	0.651
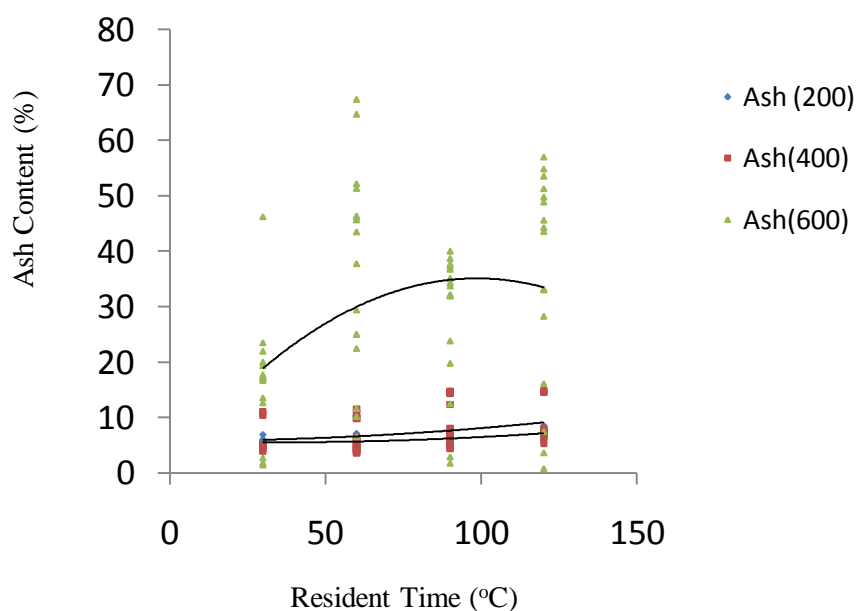
Fig. 1: Effect of Resident Time on Ash Content at the studied Temperatures (HCl)
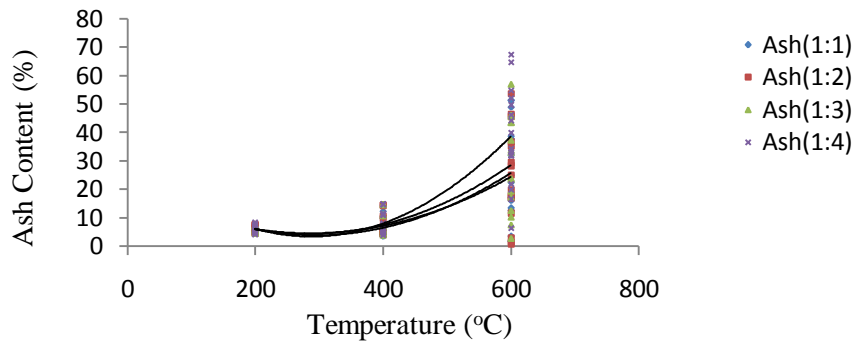
Fig. 2: Effect of Temperature on Ash Content at the studied Impregnation Ratios (HCl)
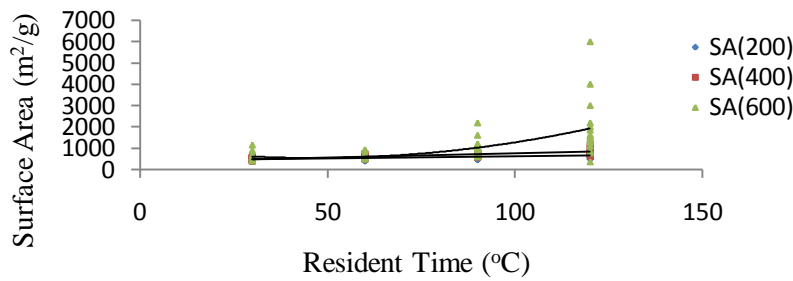
Fig. 3: Effect of Resident Time on Surface Area at the studied Temperature (HCl)
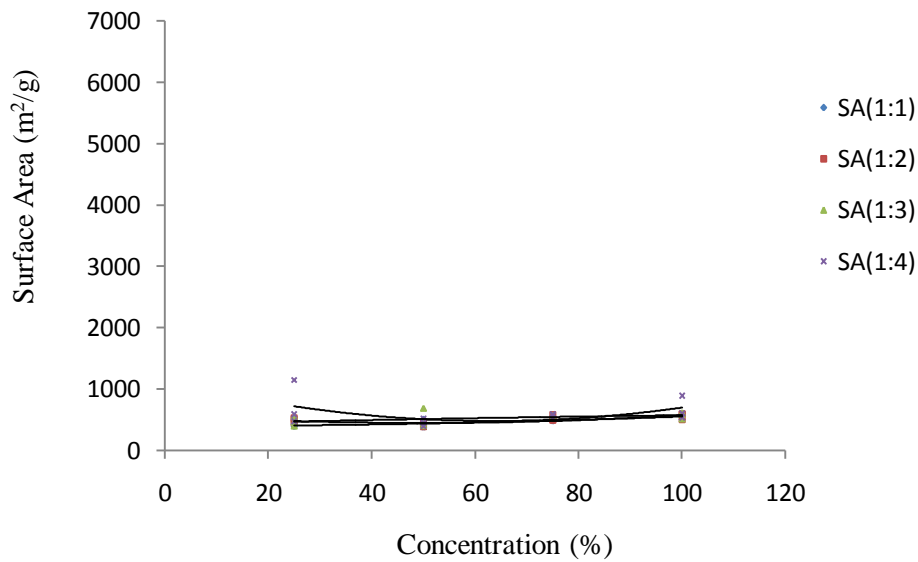
Fig. 4: Effect of Concentration on Surface Area at the studied Impregnation Ratios (HCl)
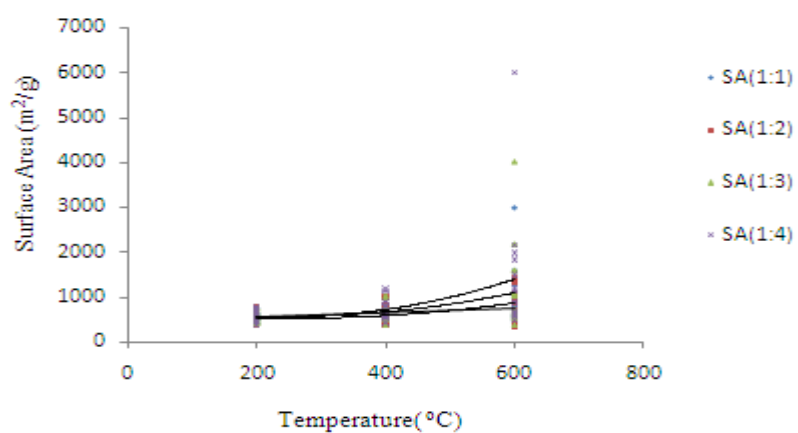
Fig. 5: Effect of Temperature on Surface Area at the studied Impregnation ratios (HC1)
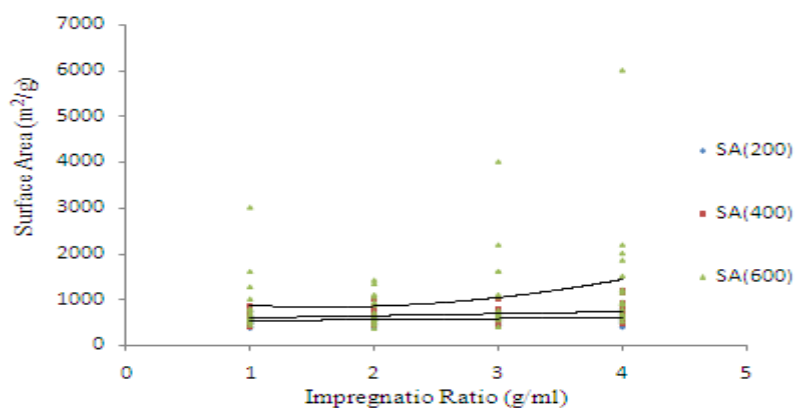
Fig. 6: Effect of Impregnatio Ratio on Surface Area at the studied Temperatures (HC1)
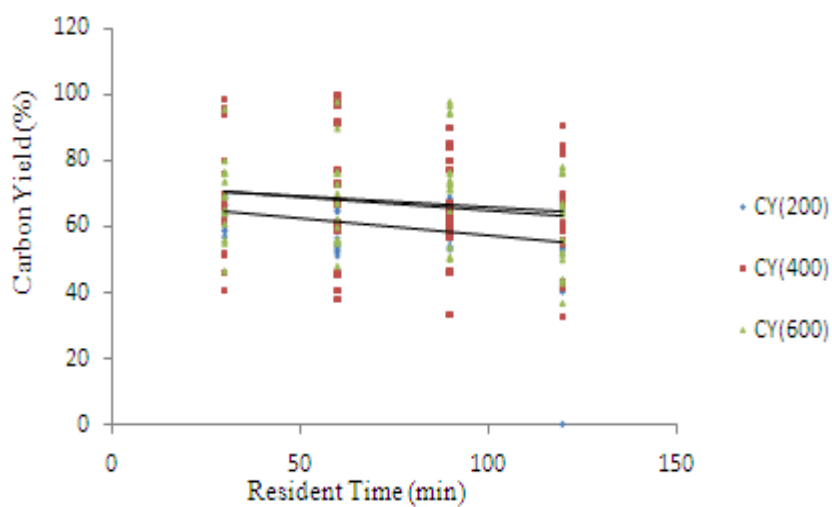
Fig. 7: Effect of Resident Time on Carbon Yield at the studied Temperature (HC1)
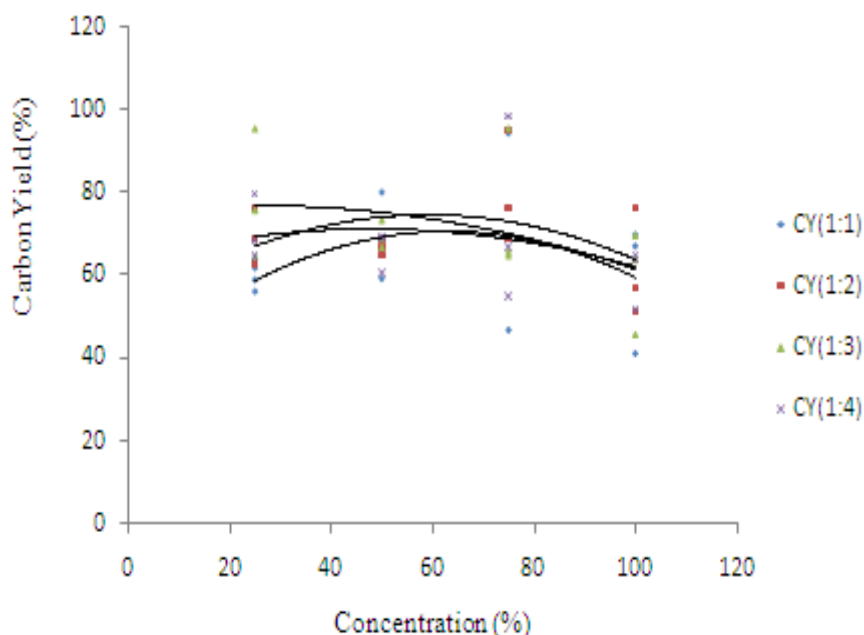
Fig. 8: Effect of Concentration on Carbon Yield at the studied Impregnation Ratios (HCl)

Table 4: Software generated conditions responses at optimal global conditions with desirability

Activating Agent	Ash Content (%)	Surface Area (m^2/g)	Carbon Yield (%)
HCl	5.92	1142.3	63.27
(Desirability)	(1)	(0.903850)	(1)

Table 5: Model validation analysis

Temp.(%)	Conc.(%)	RT(min)	IR(ml/g)	Ash (%)		SurfaceArea (m^2/g)		Carbon Yield (%)	
				Prtd.	Extl.	Prtd.	Extl.	Prtd.	Extl.
212.1	100	30	1	5.92	5.90	1142.3	1140.2	63.27	64.5

Prtd = Predicted value
Extl = Experimental value
RT = Resident Time
IR = Impregnation Ratio

IV. DISCUSSION

Fig. 1 shows the effects of residence time on ash content at the various temperatures studied. The interaction of temperature and time was observed to be significant as seen in the ANOVA for ash content in Table 1, with a P- value of 0.000. This indicates that the effect of temperature on ash content depends on the residence time. It was observed that the ash content of the MNAC increases with increase in residence time at all the temperatures studied, showing significant quadratic relationship with ash content (P- value of 0.043). Generally, ash content increases as the carbonization temperature increases. At 600°C however, ash content starts to decrease. The ANOVA for ash content indicates that, the interaction of temperature and impregnation ratio was significant with a P- value of 0.000. This suggests that the effect of temperature on ash content was

also dependent on the impregnation ratio. Also, Table 1 suggests that impregnation ratio has significant quadratic relationship with ash content with a P- value of 0.031. The quadratic coefficient for impregnation ratio was -4.9546 indicating that as the impregnation ratio increases the ash content decreases. A similar trend was observed by Usmani *et al*, [22]. They observed that increasing the impregnation ratio gradually decreases the ash content using $CaCl_2$ as the activating agent. KCl however showed no effect. Generally HCl, $ZnCl_2$ and $CaCl_2$, have good ash reduction action especially on raw materials of vegetable origin.

　　　Fig. 2 shows the effect of temperature on ash yield at all levels of impregnation ratios studied. It was observed that ash output increases as the temperature increases at all impregnation ratios. Temperature effect on ash content at the various mix ratios was however discussed in the paragraph above. The ANOVA for ash content in Table 1 shows that the interaction of temperature and mix ratio is significant (P- value of 0.000). This suggests that the effect of temperature on ash content depends on the mix ratio. The increase in ash yield was however within accepted range of 5-6% when activation was carried out at lower temperatures. This observation could be due to the highly corrosive nature of HCl on the precursor such that longer activation became detrimental to targeted yield of carbon. Longer activation durations intensify dehydration and elimination reactions increasing volatiles in the system resulting in ash increase [23]. The trend observed was consistent with results of Adel *et al*, [24] using HCl. In their report, the ash yield increases from (20.79-21.95) for rice husk while the ash content for beans husk decreased from (1.63-1.48). The discrepancies could be due to the lignocellulosic content of the precursors used. The nature of the result could be traced to the fact that the low boiling point of the activating agent (HCl) caused it to vaporize easily leaving a dry precursor thus enhancing burn-off yielding ash as the duration of carbonization increases. Also the difference in behaviour could be due to the different lignocellulosic composition of the precursor thus reacting differently when in contact with the activating agent. According to the other studies, the difficulties arising from the complex composition of lignocellulosic materials and the activating agents as well as from the large number of complex reactions involved in the pyrolysis process makes it difficult to achieve precise models describing pyrolysis mechanism [5]. The interaction of temperature and concentration was significant with a P-value of 0.004 as seen in Table 1. This suggests that the effect of temperature on ash content also depends on the concentration which in turn depends on the impregnation ratio. Generally, the effect of the studied parameters on ash content can be said to be synergistic with all the parameters contributing significantly to the ash content of the MNAC produced. In Table2 the ANOVA for surface area suggests that the model is significant with the linear, quadratic and interaction terms all significant. Table 2 also indicates that the interactions of temperature and concentration, temperature and time, temperature and ratio, concentration and time, concentration and ratio as well as time and ratio are all significant with P- values of 0.000, 0.000 0.000, 0.000, 0.010 and 0.002 respectively. This observation suggests that the effect of temperature on ash content depends on both the concentration of HCl as well as the impregnation ratio. The effect of concentration on surface area depends on carbonization temperature and impregnation ratio and the effect of carbonization time on the ash content depends on the impregnation ratio. Fig. 3 shows the effect of carbonization time on the surface area at the temperatures studied. The Fig. indicates that as the carbonization duration increase, the surface area also increases. The increase was observed to be gradual at lower temperatures of 200 and 400°C. However, at 600°C, the increase was sharp. In Table 2, resident time and carbonization temperature play decisive role in the surface area of MNAC produced. This observation was similar to that of Tan [6] using KOH as activating agent. Generally, as the temperature rises and duration in the furnace increases, the C- HCl and C- CO_2 reaction rates increase resulting in increasing devolatilization which further develop the rudimentary pore structure in the char and also enhance the existing pores thus creating higher surface area and higher porosities. Besides, the increase in temperature also caused the CO_2 and the surface metal complexes to further gasify the carbon leading to widening of mesopore to macropore [23]. Fig. 4 shows the effect of concentration on the surface area at the ratios studied. The Fig. shows a little increase, though significant, in surface area as the concentration increases. However, it was observed from the graph that within the concentrations used in the research, no maximum point was reached. In Fig. 7, the increasing trend of surface area observed can be explained by the fact that carbon gasification was enhanced by increase in impregnation ratio and residence time thus causing the removal of carbon atoms on pore walls, which increase surface area [25]. Fig. 5 shows the effect of temperature on surface area at the studied residence time. The ANOVA for surface area in Table 2 suggests that the interaction of temperature and impregnation ratio was highly significant (P- value of 0.000). This indicates that, the effect of temperature on surface area was largely due to the resident ratio. The increase of temperature and impregnation ratio enhances the existing pores leading to higher surface area and higher absorption rates. In Fig. 5, surface area was observed to increase with increasing temperature. This observation could probably be due to drastic expansion of the carbon material leading to the creation of large surface area. Similar results were obtained by Diao *et al*,[26] using sorghums, they found that, for temperatures lower than 500°C, microporous carbons with small surface areas were observed, however, at temperature of 600°C, high surface areas were observed. Prahas *et al*, [27] also observed similar results. They found that as temperature and impregnation ratio increase the

surface area also increases. The optimum activation temperature for higher surface area was found to be 450°C for coconut shells impregnated with phosphoric acid [28] and 500°C for rubber wood dust [29]. The observation in the present work could probably be due to the depolymerization of cellulose in the reaction as concentration increases resulting in tar formation. The temperature of activation has significant effects on the development of carbon's porous networks and should just be enough to eliminate all the moisture and most of volatile components in the precursor to cause pores to develop. Since the end of the volatile evolution marks the formation of the basic pore structure, activation should be limited up to a point. Higher temperatures cause enlargement of pores at the expense of the surface area. Also, control of the activation temperature is of economic interest since shorter durations are generally desired as this is equivalent to reduction in energy consumption. Fig. 6 shows the increase of surface area with increasing impregnation ratio. It was found that the highest surface area was obtained at ratio 1:4 for temperature of 600°C. At temperatures of 200 and 400°C, only a gradual increase in surface area was observed after undergoing activation process, it was expected that the volatile matter content decreases significantly whereas the fixed carbon content increases. This observation could have been due to pyrolytic effect at high temperature where most of the organic substance have degraded and discharged both as gas and liquid tars living the material with high carbon purity [6].

The ANOVA for carbon yield in Table 3 suggests that the regression model was significant. All the levels of the model, linear quadratic and interaction terms, were significant with P- values 0.000 for each. The interactions of temperature and concentration, time and temperature as well as temperature and ratio were significant with P- values of 0.000, 0.000 and 0.053 respectively. The quadratic effects of temperature and concentration were also significant with P- values of 0.031 and 0.000 respectively. Fig. 7 shows the effect of residence time on carbon yield using HCl at the temperatures studied. The Fig. suggests the linear relationship of time with carbon yield. It shows that carbon yield decreases as the residence time increases at all temperatures of activation studied. The interaction of time and temperature was also significant. This could be because longer carbonization durations mean higher probability of the carbon to be exposed to the steam atmosphere; hence higher chance for the activation reaction to take place. Based on the activation, higher temperature and longer reaction time means more carbon will react and more gasification will occur that will increase the ash content with extra reactions taking place, more carbon will be consumed and there will be low carbon yield [30]. Similar trends were observed by Chan *et al*, [30] using HCl and tyres precursor, Adel *et al* [24] using Rice husk and beans husk with HCl activation agent. However the yield obtained using HCl was higher than fixed carbon of the mango nuts. Essentially, mango nuts are complex composite material formed of natural polymers (cellulose, lignin and hemicellulose) during carbonization at high temperatures; these polymeric structures decompose and liberate most of the non-carbon elements, mainly hydrogen, oxygen and nitrogen in form of liquid (tars) and gasses leaving behind a rigid carbon skeleton in the form of aromatic sheet strips. The presence of HCl during activation promotes depolymerization, dehydration and redistribution of constituents' biopolymers and also favours the conversion of aliphatic to aromatic compounds thus increasing the yield of carbon yield [25].

The observation in Fig. 7 agrees with that observed by Sundaryanto *et al*, [31] where activated temperature was found to play an important role in the yield of activated carbon. The increase in temperature would release increasing volatiles as a result of intensifying dehydration, which HCl is noted for, elimination reaction and increase C-HCl reaction rates, thereby resulting in decreasing carbon yield [32- 33]. Indeed, the increase in temperature and time quickens the gasification reactions of carbon and therefore, attack the amorphous component which obstructs the pores causing decrease in carbon yield [8]. Sentorun- Shalaby *et al* [34] observed that at higher activation temperatures, activation of apricot stones becomes more extensive resulting in lower solid yield with more widened porous structure. The yield of activated carbon prepared from fir wood was also found to decrease gradually with carbonization duration. However, impregnation ratio promoted the yield of activated carbons. Similar trends were observed by Prahas *et al*,[27] although they used H_3PO_4 and Jack fruit peel waste as precursors. The observed result for carbon yield in the present work could be because; the reaction of lignocelluloses with HCl begins as soon as the components are mixed. The acid first attack hemicelluloses and lignin because cellulose is more resistant to acid hydrolysis [35]. Here, the acids will hydrolyse glycosidic linkages in lignocellulosic and cut aryl ether bond in lignin. These reactions are accompanied by further chemical transformations that include dehydration, degradation and condensation. As the temperature increase, aromatic condensation reactions also take place among the adjacent molecules which results in the activation of gaseous products, from hydro-aromatic structure of carbonized char leading to decrease carbon yield. Similar observation was reported by Adel *et al,* [24] using rice husk, when temperature was increases from 80-120°C using HCl as activating agent. However an increase in carbon yield was observed when they used HCl and beans husk. The differences would be due to the original lignocellulosic content and elemental composition of precursors used.

It is worthy of note in Figs. 2 and 5 that while ash yield was much at 600°C, carbon yield decreased at this same temperature and surface area increases at 600°C. Figs. 1, 3 and 7 show relationships of ash content

surface area and carbon yield with time. Many researchers reported that there will be a drop in surface area after certain decrease of ash content. It was observed that the surface area of carbon produced will start to decrease when the ash content reached around 50% and up to 68% [36- 38]. Also, when there is a collapse in the micro pores, this might lower surface area but at the same time there is micro pore and meso pore formation which would increase the surface area [30]. As a result, the overall surface area increases despite high ash yield.

Fig. 8 shows the effect of concentration on the carbon yield at the various ratios considered. The interaction effect of concentration and ratio as seen in Table 3 was not significant (P-value = 0.45). The quadratic effect of concentration on surface area is significant with a P- value of 0.022. The Fig. suggests that surface area increase to a point where average concentration is 55% beyond which the surface area begins to drop. It was observed from the ANOVA in Table 3 that, for carbon yield, impregnation ratio generally did not show any significant contribution to carbon yield at both linear and quadratic levels. The interaction of temperature and ratio was almost not significant with a P- value of 0.053.

4.1 Prediction equations for HCl.

Response Surface Methodology (RSM) which is a collection of mathematical and statistical technique that is useful for modelling and analysis of problems in which a response of interest is influenced by several variables [38]. A 2FI (two factor interaction) polynomial regression model was developed to analyse the factor interaction and to identify the significant factors contributing to the model. The surface area, carbon yield and ash content are utilized in the quadratic model according to the propositions of the software. Analysis of variance was carried out to justify the adequacy of the model. The final empirical models for ash content, surface area and carbon yield respectively are shown in equations (5), (6) and (7). The suitability and quality of the model developed was evaluated using the correlation coefficient R^2 which are 66% for equation 5 above, 55% for equation 6 and 39% for equation 7. The high values of R^2 indicate good agreement between experimental data and the model prediction [39]. The coefficient with one factor represents the effect of the particular factor; while the coefficient with two factors and those with second- order terms represent the interaction between two factors and quadratic effect respectively. The positive sign in front of the terms indicates synergistic effect, whereas negative sign indicates antagonistic effect

$$ASH=9.9970+11.5905TEMP+2.2958CONC+3.2186TIME+2.3756RATIO+10.3445TEMP^2-4.9546CONC^2-2.0221TIME^2+2.1572RATIO^2+2.1192TEMP*CONC+3.2600TEMP*TIME+3.1752TEMP*RATIO+0.6154CONC*TIME-2.3991CONC*RATIO-0.0385TIME*RATIO \quad (5)$$

$R^2 = 66\%$

$$SA=382.21+236.48TEMP-44.31CONC+304.84TEMP+126.47RATIO+137.55TEMP^2+232.61CONC^2+186.19TEMP^2+76.90RATIO^2-126.75TEMP*CONC+281.25TEMP*TIME+130.19TEMP*RATIO-129.50CONC*TIME-93.05CONC*RATIO+112.67TIME*RATIO \quad (6)$$

$R^2 = 55\%$

$$CY=70.0662-4.6502TEMP-0.2257CONC-9.0287TEMP+0.3921RATIO+3.8343TEMP2-18.1731CONC2-3.5889TIME2-0.5832RATIO2-7.3487TEMP*CONC-4.8825TEMP*TIME-2.6534TEMP*RATIO+0.7653CONC*TIME-1.007CONC*RATIO-0.6797TIME*RATIO \quad (7)$$

$R^2 = 39\%$

Low R^2 value for ash could be due to due to difficulty in handling combustion processes, however agreeable carbon yield of 63.27% was obtained as carbon yield from the raw materials.

4.2 Process optimization.

In the production of commercial activated carbons, high quality products are expected in terms of high surface area, high carbon yield and low ash content for effective adsorption capacity and economic viability.

However, to optimize all these responses under the same condition is difficult since the interest regions of factors are different. This is because, while higher carbon yield and surface area are desirable, ash content has to be low for a good quality activated carbon. In order to compromise between these three responses, the function of desirability was employed using MINITAB version 16 software as shown in table 4. The experimental conditions with the highest desirability were selected to be verified. The MNAC was then prepared using the experimental conditions given in table 5 including the predicted and experimental values. The optimal activated carbon using preparation conditions as: 212.1^{o}C carbonization temperature, 100% concentration of HCl, 30 min resident time and 1ml/g mix ratio which resulted in 5.92% ash content, 1142.3m^2/g surface area and 63.27% carbon yield. It was observed that the experimental values obtained were in good agreement with the values predicted from the model, with relatively small errors between the predicted and the actual values as seen in Table 5, which were only 0.33, 0.18 and 1.94 respectively for ash content, surface area and carbon yield. Through the process optimization, mango nut was proved to be a potential precursor for production of activated carbons with high surface area, high carbon yield and low ash content as required.

V.   CONCLUSION

Mango nuts are good precursor for the production of activated carbons with characteristic high quality. The RSM methodology is an appropriate tool to study the optimization of the activation process of preparing activated carbons to be used in a given technological process. In the present paper, the optimization was done to obtain activated carbons from mango nuts with high surface, high carbon yield, low ash content suitable for adsorption applications. The experimental parameters analysed were temperature, concentration, and carbonization time and impregnation ratio. The optimal activated carbon was obtained using preparation conditions as: 212.1^{o}C carbonization temperature, 100% concentration of HCl, 30 min resident time and 1ml/g mix ratio which resulted in 5.92% ash content, 1142.3 m^2/g surface area and 63.27% carbon yield which are quite satisfactory and suitable for a wide range of adsorption applications.

REFERENCES

[1]. S. Okonogi, C. Duangrat, S. Anuchpreeda, S. Tachakittirungrod and S. Chowwanapoonpohn S, Comparison of antioxidant capacities and cytotoxicities of certain fruit peels. *Food Chem. 103, 2007, 839- 846.*

[2]. D. G. Akpen, I. L. Nwaogazie, and T.G. Leton, Optimization of conditions for the removal of colour from waste water by mango seed shells based activated carbons. *Indian J. Sc. & Tech. Vol 4; no.8 2011.*

[3]. M. Ajmal, R. Mohammad, Y. Yusuf, and A. Ahmed, Adsorption behaviour of Cadmium, Zinc, Nickel and Lead from aqueous solutions by MagniferaIndica seed shell. *Indian J. Env.Hlth. 40 (1),1998, 15-26.*

[4]. K. V Kumar, and A. Kumaran, Removal of methylene blue by mango seed kernel powder. *Biochem. Eng. J. 27, 2005, 83-93*

[5]. M. P. Elizalde- Gonzalez and V. Hernandez- Montoya, Characterization of mango pit as raw material in the preparation of activated carbons for wastewater treatment. *Biochem. Eng. J. 36, 2007, 230- 238.*

[6]. I. A. W. Tan, A. L. Ahmad, and B. H. Hameed, Preparation of activated carbon from coconut husk: Optimization study on removal of 2, 4, 6- trichlorophenol using response surface area method. *J. of Haz.Mater. 153, 2008, 709- 717*

[7]. F. Karacan, U. Ozden, and S. Karacan, Optimization of manufacturing conditions for activated carbons from Turkish lignite by chemical activation using surface response methodology. *Apl. Thermal Eng. 27 (7), 2007, 1212- 1218*

[8]. A. Bacaoui, A. Yaacoubi, A. Dahbi, C. Bennouna, R. Phantanluu, F. J. Maldonado- Hodar, J. Rivera and C. Moreno- Castilla, Optimization of conditions for the preparation of activated carbons from olive-waste.*Carbon.39, 2001, 425- 432.*

[9]. R. Azargohar and A. K. Dalai, Production of activated carbon from luscar char: Experimental and modelling studies, *Micropor. Mesopor. Mater 85, 2005, 219- 225*

[10]. J. N. Sahu, J. Achrya, and B. C. Meikap, Optimization of production conditions for activated carbons from Tamarind wood by zinc chloride using response surface methodology. *Bioresour. Technol. 101, 2010,1974- 1982*

[11]. S. D. Faust and O. M. Aly*Chemistry of Water Treatment*, (Butterwort Pub. Woburn, 1983)

[12]. M. A. Ahmad and R. Alrozi, Optimization of preparation conditions for mangosteen peel- based activated carbons for the removal of remazol brilliant blue R using response surface methodology. *Chemical.Engr. J. 165, 2010, 883- 890.*

[13]. D. F. Aloko and G. A. Adebayo, Production and characterization of activated carbons from agricultural waste. *J. Eng. Applied Sci.2 (2), 2008, 440-444.*

[14]. B. H. Hameed, I. A. W Tan and A. L. Ahmad, Preparation of oil palm empty fruit bunch- based activated carbon for removal of 2, 4, 6- trichlorophenol: Optimization using response surface methodology. *Journal of Hazardous Mat.164, 2009, 1316- 1324.*

[15]. T. Yang and A. C. Lua, Characteristics of activated carbons prepared from pistachio-nut Shells by physical activation. *Journal of Colloid andInterface Sci. Vol. 267, Issue 2, 2003, 408-417.*

[16]. S. Karthikeyan , P. Sivakumar and P. N. Palanisamy, Novel activated carbons from agricultural wastes and their characterization. *E- Journal of Chem. Vol. 5, 2008, 409- 426.*

[17]. M. Soleimani and T. Kaghazchi, Agricultural waste conversion to activated carbon by chemical activation with phosphoric acid.*Chem. Eng. Technol. 30, 2007, 649- 654.*

[18]. Laboratory solution preparation guide.(2008).

[19]. S. S. Dara, *Experiments and Calculations in Engineering Chemistry*, (S. Chand and Co. Ltd. New-Delhi1991)

[20]. M. Ahmedna , M. M. Johns, S. J. Clark, W. E. Marshall and M. M. Rao, Potential of agricultural by-product based activated carbon for use in raw sugar discolorization. *Journal of Sci. Food and Agric. 75, 1997, 117-124.*

[21]. O. P. Fapetu, Production of carbon from biomass for industrial and metallurgical processes. *Nigerian Journal of Eng. Manag.1, 2000, 34- 37.*

[22]. T. H. Usmani, T. W. Ahmad and A. H. K. Yousufzai, Preparation and liquid- phase characterization of granular activated carbon from rice husk. *Bioresour.Technol. 30, 1994, 31- 35.*

[23]. F. U. Wu and R. L. Teng, Preparation of highly porous carbon from fir wood by KOH etching and CO_2 gasification for adsorption of dyes and phenols from water. *Journal of Colloid Interface Sci. 294, 2006, 21- 30.*

[24]. A. M. Adel, Z. H. Abd El- Wahab, A. A. Ibrahim and M. T. Al- Shemy, Characterization of microcrystalline cellulose prepared from lignocellulosic materials. Part I. Acid catalysed hydrolysis. *Bioresour. Technol. 101, 2010, 4446- 4455*

[25]. H. Teng, M. A. Serio, M. A. Whjtowicz, R. Bassilaki and P. R. Solomon, Reprocessing of used tyres in to activated carbon and other products. *Ind. Eng. Chem. Res. 34(9), 1996, 3102- 3113*

[26]. Y. Diao, W. P. Walawender, and L.T. Fan, Activated carbons prepared from phosphoric acid activation of grain sorghum. Bioresour. Technol. 81,2002, 45- 52.

[27]. D. Prahas, Y. Kartika, N. Indraswati and S. Ismadji, Activated carbon from jackpeel waste by H_3PO_4 chemical activation: Pore structure and surface chemistry characterization. *Chem. Eng. Journal 140, 2008, 32-42.*

[28]. J. Laine, A. Calafat, and M. Labady, Preparation and characterisation of activated carbons from coconut shell impregnated with phosphoric acid. *Carbon.27, 1989, 191- 195.*

[29]. C. Srinivasakannan and M. B. Zailani, Production of activated carbon from rubber wood sawdust. *Biomass & Bioenergy. 27,2004, 89- 96.*

[30]. O. S. Chan, W. H. Cheung and G. McKay, Preparation and characterisation of demineralised tyre derived activated carbon. *Carbon.49, 2006, 4674- 4687.*

[31]. Y. Sundaryanto, S. B. Hartono, W. Irawaty, H. Hindarso and S. Ismadji, High surface area activated carbon prepared from cassava peel by chemical activation. *Bioresour.Technol. 97, 2006, 734- 739.*

[32]. A. C. Lua, and T. Yang, Effect of activating temperature on the textural and chemical properties of potassium hydroxide activated carbon prepared from pistachio- nut shell. *Journal of Colloid Sci. 274, 2004,594- 601.*

[33]. D. Adinata, W. M. A. W. Daud and M. K. Aroua, Preparation and characterization of activated carbon from palm shell by chemical activation with K_2CO_3. *Bioresour. Technol. (98), 2007, 145-149.*

[34]. C. Sentorun- Shalaby, M. G. Ucak- Astarhoglu, L. Artok and C. Sarici, Preparation and characterization of activated carbons by one- step steam pyrolysis/ activation from apricot stones. *Micropor.Mesopor.Mater. 88, 2006, 126-134*

[35]. M. Jagtoyen, and F. Derbyshire, Activated carbon from yellow poplar and white oak by H_3PO_4 activation. *Carbon. 36, 1998, 1085-1097.*

[36]. J. F. Gonzalez, M. J. Encimar, C. M. Gonzalez- Garcia, E. Sabio, A. Ramiro and J. L. Canito, Preparation of activated carbons from used tyres by gasification with steam and carbon dioxide. *Appl. Surf. Sci.252 (17), 2006, 5999- 6004.*

[37]. T. Xu and X. Liu, Peanut shell activated carbon: characterisation, surface modification and adsorption of Pb^{2+} from aqueous solution. *China Journal of Chem. Eng. 16(3), 2008, 406- 407.*

[38]. S.Q. Li, Q. Yao, S. E. Wen, Y. Chi and J. H. Yan, Properties of pyrolytic chars and activated carbons derived from pilot- scale pyrolysis of used tyre. *Journal of Air Waste Manag.Assoc. 55(9), 2005, 1315- 1341.*

[39]. D.C Montgomery, D.C. *Design and analysis of experiments,* (5th ed. John Wiley and Sons, New York. USA 2001).

Research Paper	Open Access

Development of Decision Support Software for Matching Tractor-Implement System Used on Iranian Farms

Rasoul Loghmanpour zarini[1], Asadollah Akram[2], Reza Alimardani[3], Reza Tabatabaekoloor[4]

[1, 2, 3]*(Department of Agricultural Machinery, Collage of Agricultural Engineering and Technology, University of Tehran, Iran)*
[4]*(Department of Farm Machinery, Sari Agricultural Science and Natural Resources University, Sari, Iran)*

Abstract:- A decision support software (DSS) was developed in Visual Basic 6.0 programming language for matching and selecting implements with tractors and time management of farm operations. The proper selection and matching of tractor and implements is now become very important and difficult in Iran because of availability of variety of tractor models and powers ranging from 5.5 to 60 kW and variety of implement sizes. The purpose of this study was development software for mechanized operation and its application in paddy's farms. The developed DSS was tested with a case study to demonstrate the flexibility of the software. This software has databases including variety of tractor models and implements sizes, existing data from five climatology stations from 1990 to 2010, tractors and implements performance and soil and operation conditions for the zone of this study. Tractors and implements were selected and matched for paddy fields by developed DSS. Finally, tillage operation in paddy fields was managed with selected tractors and implements. Use of DSS in this study indicated that tractors with power less than 35 kW are able to complete the tillage operations (plowing, harrowing and puddling) for paddy fields lower than 40 hectares. Also, results indicate that energy consumption for tillage operation on paddy's farms in case study was 17.36 percentages less than other paddies.

Keywords: - *Agricultural Mechanization, Decision Support Software, Energy use, Paddy cultivation, Tractor*

I. INTRODUCTION

The selection of proper tractor and its matching implements has now become more difficult than ever before. The matching and selection of a tractor-implement system involves many decision-making processes that depend on different factors. These factors include tractor and implement specifications, soil conditions (firm, tilled or soft) and operation conditions (depth and speed operation), etc.

Decision support systems (DSS) are defined as an interactive computer-based system intended to help decision makers utilize data and models in order to identify and solve problems and make decisions [1]. A correct matching of tractor-implement system would result in decreased power losses, improved efficiency of operation, reduced operating costs and optimum utilization of capital on fixed costs [2]. Currently, researchers are involved in developing decision support systems/computer programs/models that are effective and simple to access [3, 4, 5, 6, 7, 8, 9, 10, 11, 12, 13, 14, 15]. Siemens et al. [16] formulated a farm machinery selection and management program written in C language. The output included a list of machinery with prices and annual use, work schedule, cost of operation and the total machinery related costs. Butani and Singh [17]; Singh and Chandraratne [18] developed a decision support system (DSS) for optimization of farm machinery systems with the flexibility to incorporate regional variations in crops and cropping practices, farm characteristics, size of the farm equipment and cost of the resources and output. The DSS utilized least cost method for optimization of farm machinery system. Zoz [7] described a methodology for predicting tractor field performance based on drawbar performance for 4WD tractor. Grisso and Perumpral [19] demonstrated the use of spreadsheet for matching tractors and implements. They predicted tractor performance and implement draft based on the Brixius model and ASABE Standard D 497.5, respectively. They concluded that the optimization of weight distribution for maximum power delivery efficiency, computation of field capacity and fuel consumption was possible with

the use of spreadsheet. Singh et al. [20] developed a model based on DSS for farm management. The model was developed for Indian farmers to access online interactive and flexible information for their farm management. They concluded that the model would help farmers in increasing productivity by raising the yield/hectare of food grains thus leading to their economic growth.

Sahu and Raheman [21] developed a decision support system in Visual Basic 6.0 programming language for matching tillage implements with 2WD tractors for predicting the field performance of tractor–implement system. Most of the developed DSS predict tractor field performance based on ASABE standards and other models and are supported by data of only a few tractors and implements [19, 20, 21, 22]. Only a few researchers in developed countries directed their effort to develop appropriate procedure for matching of tractors and implements based on estimated power requirement and power availability taking into consideration the terrain and equipment factors [1, 13].

Mehta et al. [23] developed a DSS for selection of tractor-implement system and used it on Indian farms. They calculated PTO power requirement of tractor for implements with various soil and operation conditions. They concluded that DSS helps in selection of a tractor or an implement of particular size farm various makes and models of commercially available tractors and implements. A few other researchers mentioned the general procedures for matching of tractor and implement on the basis of power availability and power required by considering the soil factor, unit draft, field efficiency, tractive efficiency and transmission efficiency [13, 24, 25, 26].

In this study a decision support software (DSS) for Iranian farms conditions was developed using Visual Basic 6.0 as programming language and Microsoft Access as database, which helps in the selection of implements and matching tractors and implements to increase production and productivity in Iranian farms and usage in mechanization cooperative.

II.   MATERIALS AND METHODS
2.1 Development of decision support system (DSS)

Decision support software was developed in Visual Basic 6.0 programming language. This software is suitable for matching and selecting implements with tractors and for time management of farm operations. Database for the software was developed by Microsoft Access 2007. The complete DSS was divided into four modules; if the tractor is available, find out the optimum matching size of the equipment; if the equipment is available, find out the optimum size of tractor requirement; if the tractor and equipment are available, find out the best offer for better application and management of required days for all operations. The program starts with a window such as Fig. 1 and ends with the final result required by the user. The overall structure of the program is shown in Fig. 2.

Fig. 1. Main menu of DSS (window of program starting).
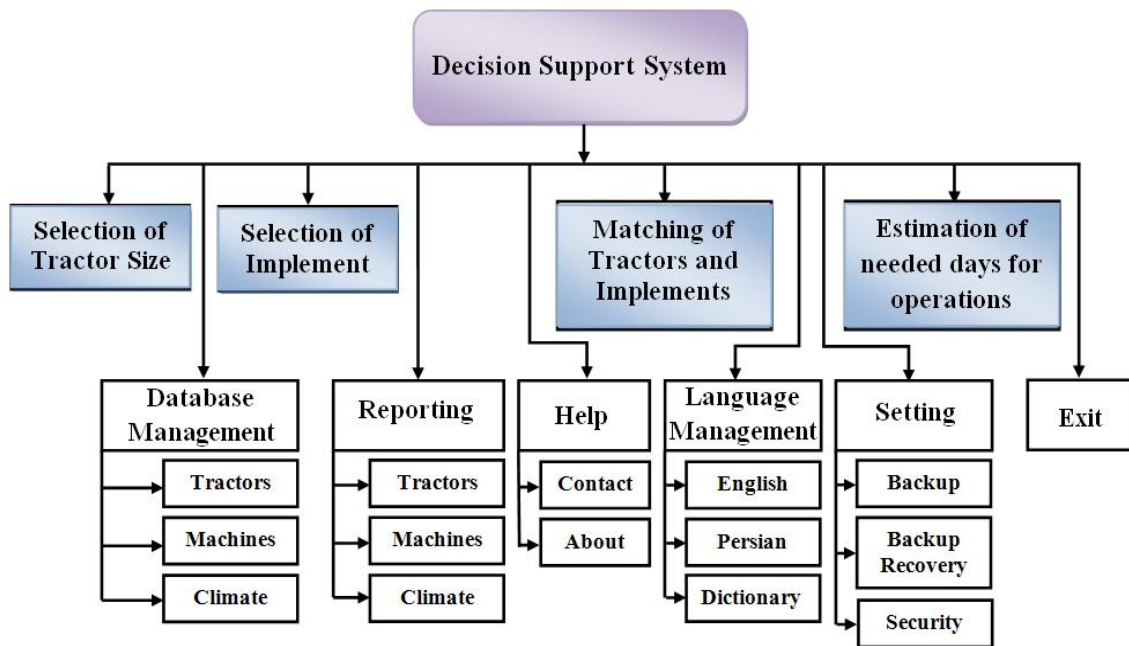
Fig. 2. Overall structure of developed DSS.

The software was developed for mechanization cooperative. These cooperatives were created to provide mechanization services for farmers. These services in Iran are included mechanized operations, consulting about using of tractor and farm machinery and management of them. The complete structure of software for purpose of this study was divided into four main modules (Fig. 3). These four modules are very important in each mechanization cooperative in Iran.
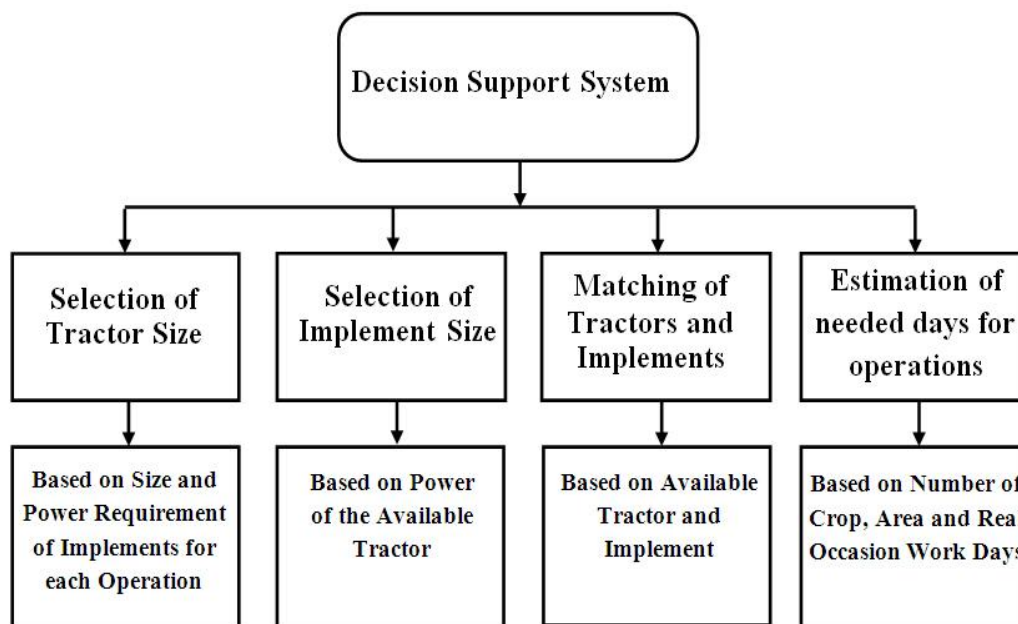
Fig. 3. Description of the DSS for four main modules.

2.2 Selection of tractor

The power requirement of a tractor for different field operations can be calculated after getting the preliminary details regarding land holding, total available working time, soil conditions and type of operations [27]. Selection of a tractor was calculated by Eq. (1) [28].

The logic of selection for this module was based on selection of different tractors (2WD, 4MFWD and 4WD) by manager for each operation.

The typical speed and the draft requirement for various implements, field operations and soil conditions are given in Table 1.

$$P_{PTO} = \frac{Speed \times D \times W \times SF}{2} \qquad (1)$$

Where P_{PTO} is PTO power requirement for implement (kW), S is speed of operation (km h^{-1}), D is draft per unit of implement width (kN), W is width of implement and SF is soil factor that depends on tractor and soil type. The amounts of SF are shown in Table 2.

All tractors that exist in Iran were placed in software database. Also, database has good flexibility for changing data.

Table 1. Draft, recommended speed and field efficiency for various implements [27, 29].

Implements/equipment	Draft per metre of width, kN	Typical speed, km/h	Field efficiency, %
M B plough (200 mm depth)			
Heavy clay soil	15.70	4.5	80
Heavy soil	13.73	5.0	80
Medium soil	10.30	5.0	80
Light soil	6.87	6.0	80
One way disc plough			
Heavy soil	5.90	6.0	80
Medium soil	4.41	6.0	80
Light soil	2.94	6.0	80
Offset or heavy tandem disc harrow			
Heavy soil	5.90	6.0	80
Medium soil	4.91	6.0	80
Light soil	3.73	6.0	80
Duck foot cultivator			
Heavy soil	4.41	6.0	80
Medium soil	2.94	6.0	80
Light soil	1.47	6.0	80
Seed drill			
Heavy soil	1.47	5.0	70
Medium soil	0.88	5.0	70
Light soil	0.49	5.0	70
Planter			
Heavy soil	1.47	5.0	70
Medium soil	1.72	5.0	70
Light soil	1.77	5.0	70

Table 2. Soil factors for different types of tractor and soil Jain & [27, 29].

		Tractor Type		
		2WD	4MFWD	4WD
	Firm	1.64	1.54	1.52
Soil Type	**Tilled**	1.75	1.61	1.56
	Sandy	2.13	1.82	1.67

Fig. 4 shows the theoretical flowchart of tractor selection in this software. Selection of tractor size is based on implement size and power requirement for each operation.

2.3 Selection of implement sizes

The required width of implement can be calculated by knowing the available time, operating speed and power available for field operation. Type of soil (firm, tilled or soft) is important for calculation of required implement width. In this software, selection of implement size was done based on power of the available tractor. The maximum implement width calculated by Eq. (2) that was based on Eq. (1) [28].

$$Max.\ W. = \frac{PTO\ Power \times 21.58}{S \times D \times SF}$$

(2)

Where Max. W. is maximum implement width (m) that can work with available PTO power, soil type, working speed and draft per unit of implement width. Also, SF is soil factor that depends to the tractor and soil types (Table 2). Theoretical flowchart for implement selection in this software is shown in Fig. 5.
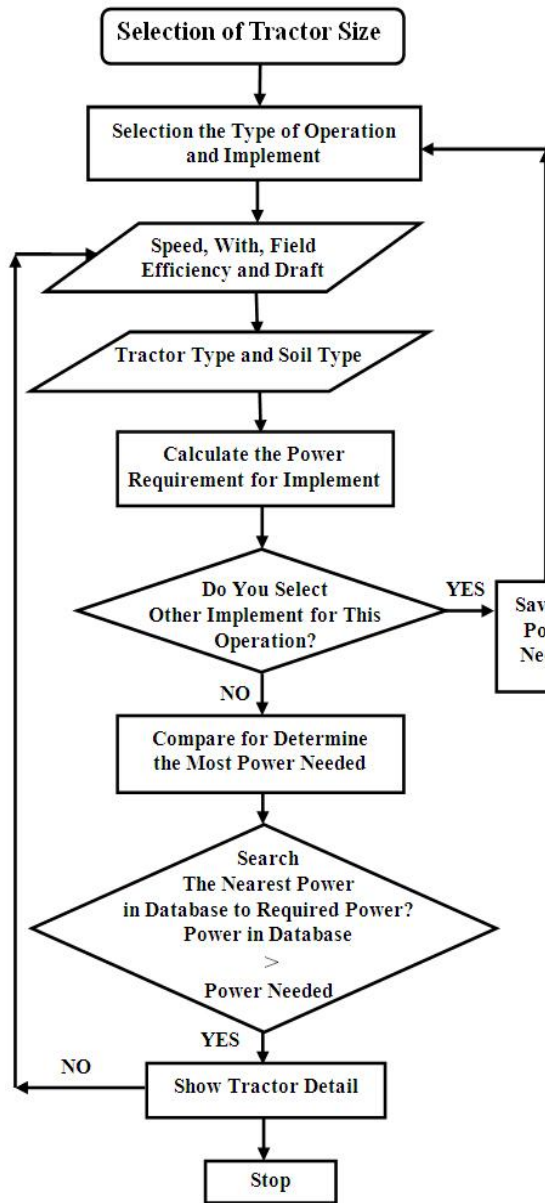
Fig. 4. Selection of tractor for various soil and operation conditions.
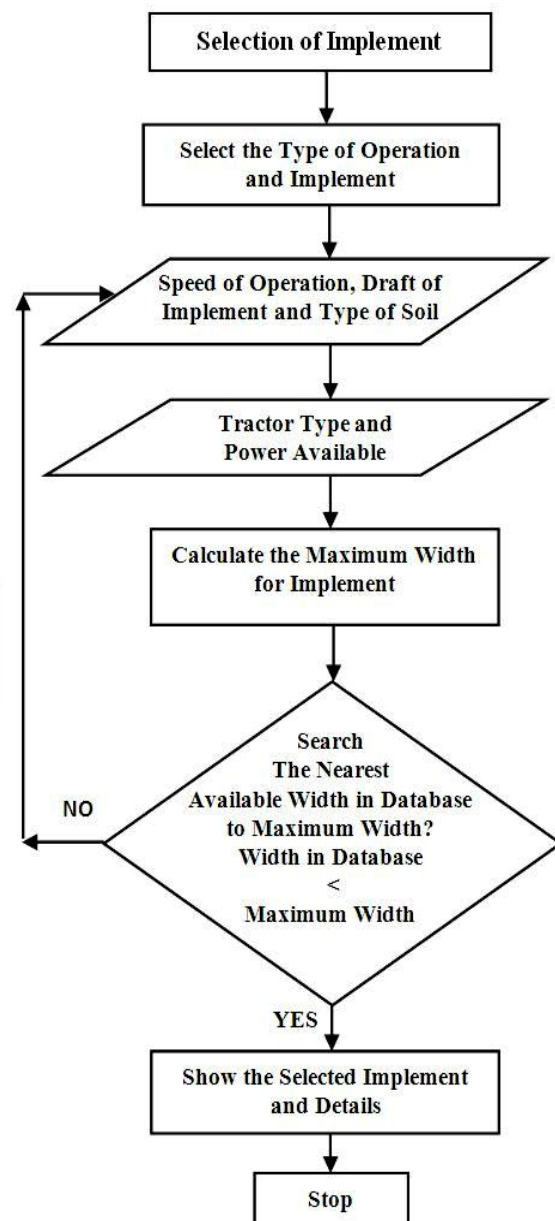
Fig. 5. Selection of implement for various soil and operation conditions.

2.4 Matching of tractors and implements

The correct matching of machinery should result in increased efficiency of operations, less operating costs, and optimum use of capital on fixed costs [13]. A decision support software (DSS) was developed for selecting the tractor and its matching equipment and vice versa for different soils and operating conditions. In this software, the purpose of this item was that whether the selection of tractor – implement system for the past agronomy- year's data is correct or not? If the answer was not, the software offers suggestions to manager for better matching of tractors – implement system. This software gives the manager three solutions for better matching of tractors – implement system. Fig. 6 shows flowchart for matching of tractors – implement system.

Solution includes maximum speed, maximum width and required power. Maximum width was calculated by the past agronomy-year's data and Eq. (2). The required power was calculated by available implement data in the past agronomy- year's data and Eq. (1).
The maximum speed calculated by the past agronomy- year's data and Eq. (3) [28].

$$Max.\ S. = \frac{PTO\ Power \times 28.94}{W \times D \times SF} \qquad (3)$$

Where Max. S. is maximum workable speed; PTO power is available power; W is available implement width; D is draft per unit of implement width in the past agronomy- year's data and SF is soil factor that depends on the tractor and soil types (Table 2).
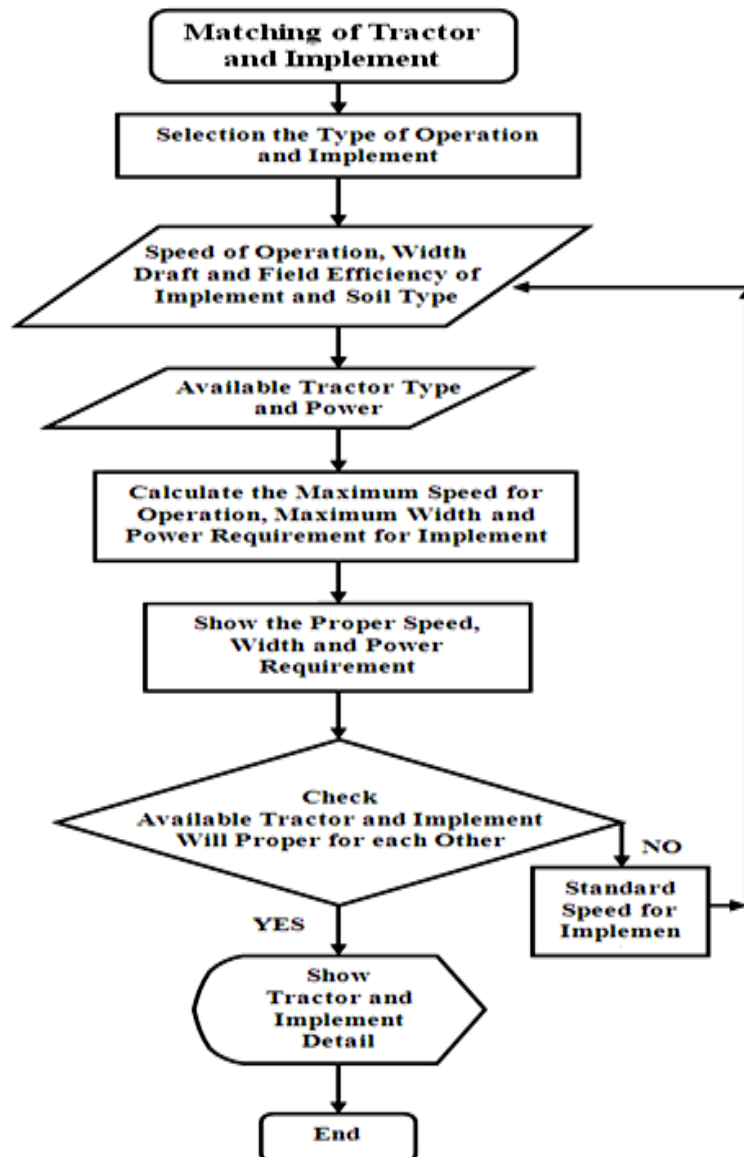
Fig. 6. Flowchart for matching of tractors – implement system.

Manager by these suggestions can select the proper tractor – implement system and improve the operation efficient, energy consumption and reduce the operations cost.

2.4 Estimating of needed days for operations

The prediction of weather constraints, especially wet days, represents an important tool for farmers and people working in agricultural activities to improve the agricultural-system efficiency. Optimum planning and scheduling of field work such as tillage and harvesting can reduce crop production losses [30]. Fig. 7 shows estimation of needed days for operations by software.

In this study, software can determine the required field days and manage it. It is very necessary for manager to know that how many days are required for each operation. This software by weather stations data's can determine really available days for each operation. The total field days needed was calculated by Eqs. (4) and (5). The real available days was calculated by Eqs. (6); (7) and (8). It is logical that real available days should be more than field days needed.

Field days needed for each implement (Hectare per day) = (Fe × W × S × T × N) / 10   (4)

Where: Fe= Field efficiency of current implement (%); W= Current implement width (m); S= Current implement speed (km h^{-1}); T= Available time per day (h); N= Number of operation by current implement
Total field days needed (Day) = Sum of Area of crop (hectare) / Field days needed for all each implement   (5)
Available days for operation = Existing days from start to end of operation   (6)
Pwd = Sd + (0.5 × Cd) + (0.25 × Pcd) + (0.125 × Rd)   (7) [31]
Where: Pwd= Possibility of working days for each month; Sd= Sunny days in current month; Cd= Cloudy days in current month; Pd= Partly cloudy days in current month; Rd= Rainy days in current month Real available days for operation = Pwd × Available days for each working month   (8)

Manager should change the selected tractor (power), implements (width, speed or other implements with better field efficiency) or available time per day if real available days for operation lower than total field days needed for operation, though the software offers suggestions to the manager.

III.   RESULTS AND DISCUSSION

The case considered to validate the developed DSS for selection of tractor–implement system is presented in this section. To illustrate the above selection criteria, a case of growing a major crop was considered in a year for tillage operation (Paddy field) in a 30 ha farm in tilled soil. This case study was performed in Mazandaran province of Iran and managed by mechanization cooperative.

3.1 Paddy cultivation

The recommended time for tillage operation in Mazandaran province of Iran are given in Table 3. The weed control operation is usually done by hand or by releasing ducks in rice paddies in Mazandaran province. The power requirement for tillage operation was calculated by this software and its scheduling opportunity managed. The tillage operation usually starts by plowing (Depth= 10-15cm) and will be continue by harrowing operation. Tillage operation will be finish by puddling operation for paddy cultivation. One plowing operation in 40 ha (total area) and two harrowing operations in 40 ha i.e. 80 ha were required before puddling operation for paddy cultivation. Two puddling operations were recommended before transplantation. Time available usually is 8 h per day and actual available time was determined by data of five weather stations.

Table 3. Recommended times for tillage operation in paddy fields.

Operations	Scheduling Opportunity		
Tillage or Seed bed preparation	1 December to 30 December (Plowing)	20 February to 10 March (Harrowing)	1 April to 30 April (Puddling)
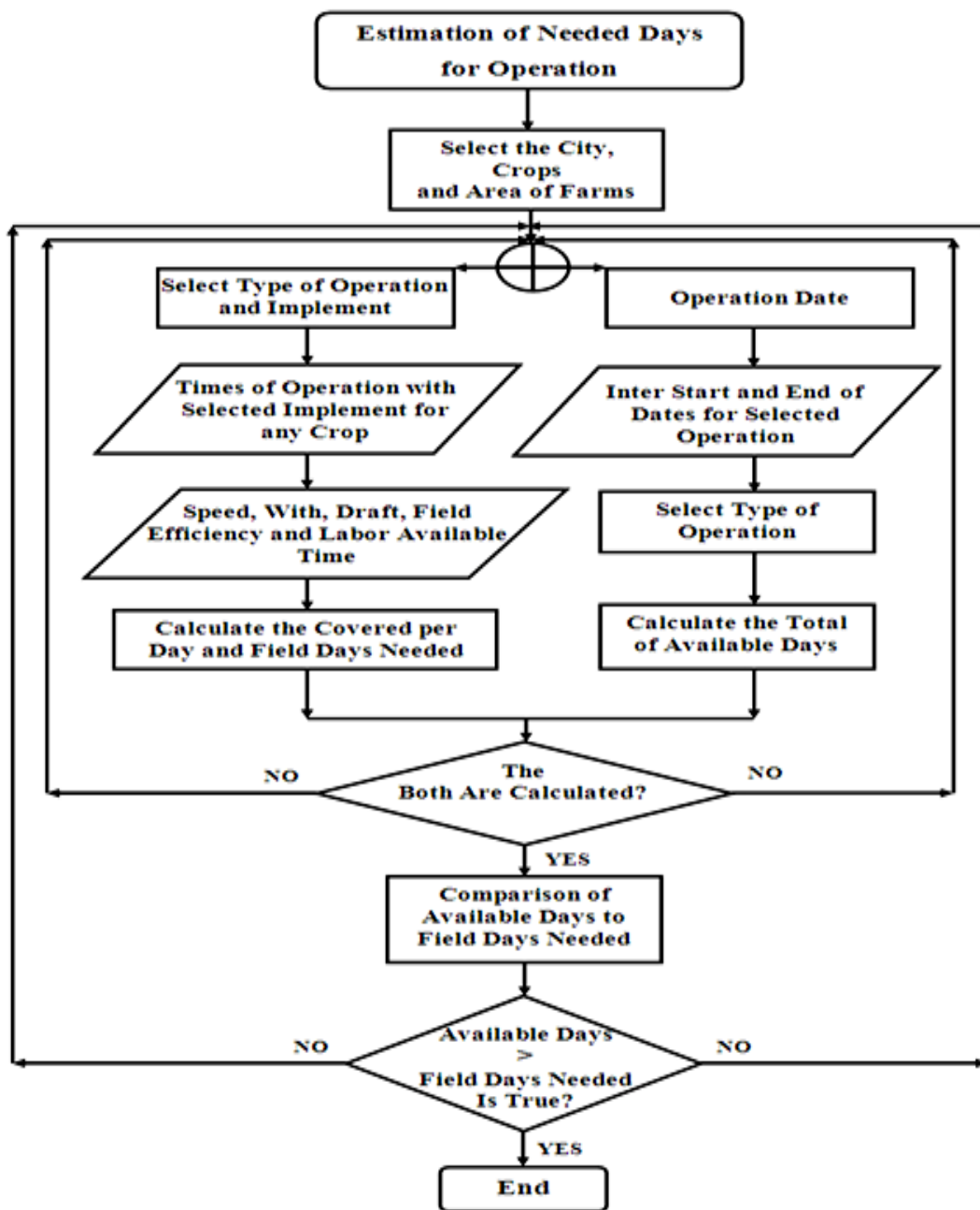
Fig. 7. Flowchart for estimation of needed days and really available days for each operation.

3.2 Selection of implement size according to actual available time

At the first stage, actual available time was predicted by time available and recommended times (Table 3) for operations by DSS. It was calculated by Eqs. (6); (7) and (8). According to the recommended times, time available for plowing operation was 30 days. Also, times available for harrowing and puddling operations were 48 and 29 days, respectively (Table 3). For determining the optimum size of implement, which can complete the operation in available time, it needs to know how many days is the real available time for operation. Figures 8, 9 and 10 illustrate the real available times for plowing, harrowing and puddling operations, respectively.

According to predictions, actual available times for plowing, harrowing and puddling operations were 18.9, 31.27 and 17.36 days, respectively. DSS was selected proper implements for actual available times. All implements selected can complete the operations in recommended times. Fig. 11 shows the proper size of implements selected for plowing, harrowing and puddling operations. All implements selected were existed in mechanization cooperative of case study.

Fig. 8. Prediction of real available time for plowing.

Fig. 9. Prediction of real available time for harrowing.

Fig. 10. Prediction of real available time for puddling.

The moldboard plow, Harrow disc and rotivator were selected for plowing operation, harrowing and puddling operations. According to the Fig. 11, field days needed were lower than real available times for each operation. Available implements size for plowing operation were 0.6, 0.9 and 1.2 m. Operation speed and field efficiency for moldboard plow was taken as 6 km/h and 75%, respectively (Table 1). A moldboard plow with width of 0.6 m was selected by DSS. Work days needed for plowing operation was calculated 18.51 days (say 19 days) or 152 h by Eq. (4). Also, a harrow disc was selected with width of 1.5 m among three sizes (0.8, 1.1 and 1.5 m) for harrowing operation. Two harrowing operations in 40 ha i.e. 80 ha were required before puddling operations. Field days needed for harrowing operations was calculated 12.69 days (say 13 days) or 104 h by Eq. (4). Two puddling operations in 40 ha i.e. 80 ha were required for puddling operation. Work days needed for puddling operations was calculated 16.56 days (say 17 days) or 136 h by Eq. (4). A rotivator with width of 1.15 m was selected by DSS among three available sizes (0.75, 0.9 and 1.15 m) for puddling operation. Work days needed for puddling operations was calculated 16.56 days (say 17 days) or 136 h by Eq. (4).
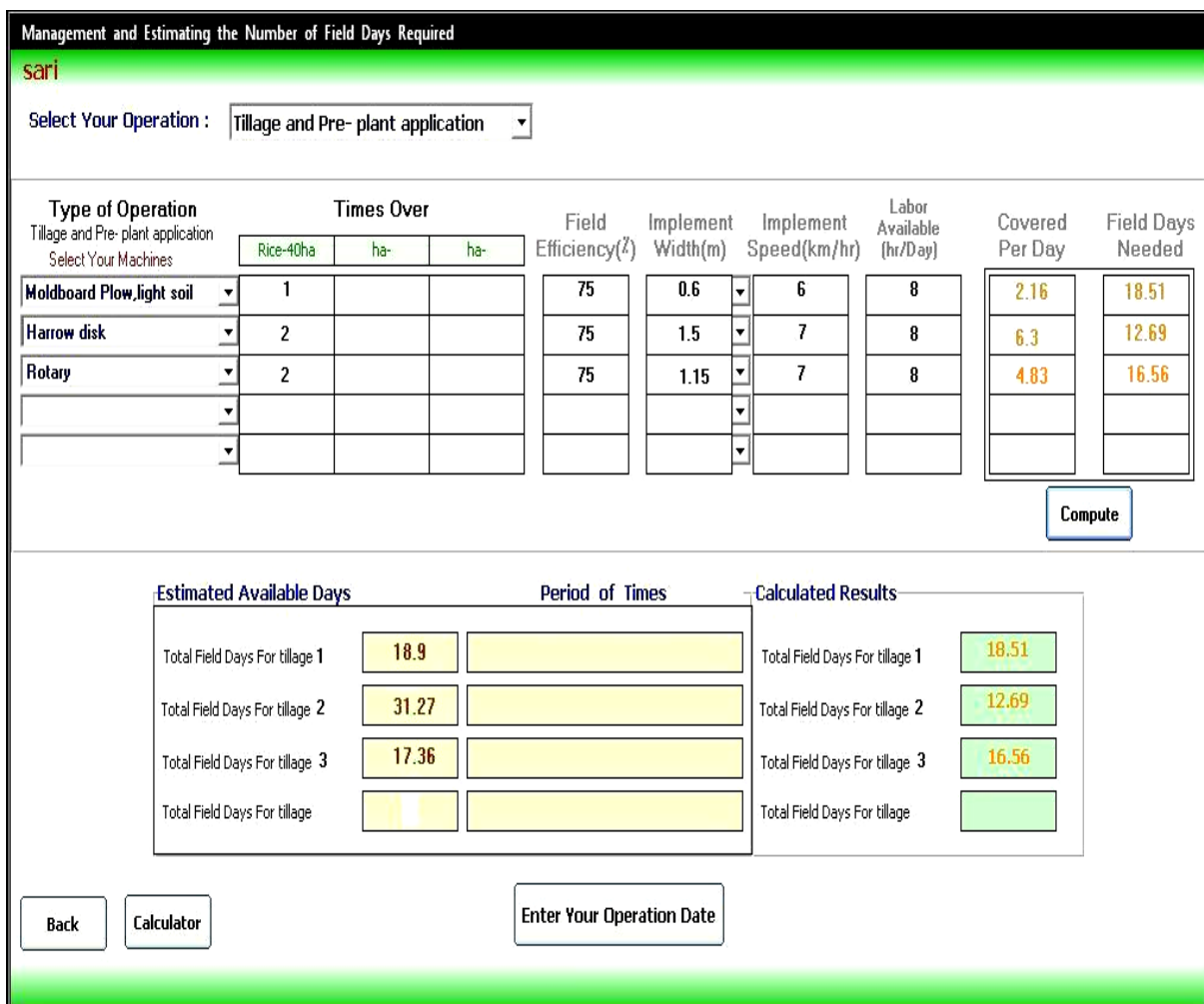
Fig. 11. Selection of proper implement size by comparison of real available times with field days needed.

3.3 Selection of tractor sizes for each operation

A tractor must be sized for job. On farms with one principal field tractor, that job is usually primary tillage. Even when it is known how much power is needed for a given field operation, knowing the size of tractor to use still presents a problem. When matching a tractor and implement, three important factors must be considered:

a. The tractor must not be overloaded or early failure of components will occur.
b. The implement must be pulled at the proper speed or optimum performance cannot be obtained.
c. The soil conditions and their effects on machine performance must be considered.

After selection of implement size for each operation, proper tractor sizes were selected by DSS. Tractors were selected from mechanization cooperative and they were available. Selection of proper and

optimum tractor size is very important for mechanization cooperative. To prevent waste of energy and capital, most proper tractor size should be selected. Fig. 12 shows the selection of tractor for plowing operation. PTO power required was calculated by Eq. (1). Similarly, PTO power for harrowing and puddling operations were calculated.

Fig. 12. Selection of tractor size for plowing operation.

According to the Fig. 12, a tractor was selected for moldboard plow with width of 0.6 m and other data from Table 1. Type of selected tractor was 2WD among 2WD, 4WD and 4MFWD tractors. Also, soil type was selected soft among the firm, tilled and soft soils. Finally the required PTO power was calculated 14.61 kW and was searched by DSS for find nearer tractor size to it according to Fig. 4. By clicking on "View Process", a new form opens for show of selected tractors. Fig. 13 shows the selected tractors for each operation. According to Fig. 13, DSS was selected three tractors for each operation. Always, selected tractors were existed in database or mechanization cooperative. The form of Fig. 13 includes two frames. The upper frame shows maximum power required in all operations. The maximum power required shows by green text. For this study, maximum power required was related to puddling operation. DSS was selected a tractor with ITM 942 model, a tractor with Darvana 604 model and a tractor with Universal model for plowing, harrowing and puddling operations. Power needed for plowing operation was 14.61 kW and power of selected tractor for it was about 15 kW. Also, the selected tractors for harrowing and puddling operations had power about 25 kW and 35 kW, respectively. Fig. 13 shows an image for selected tractors by clicking on "View Image".
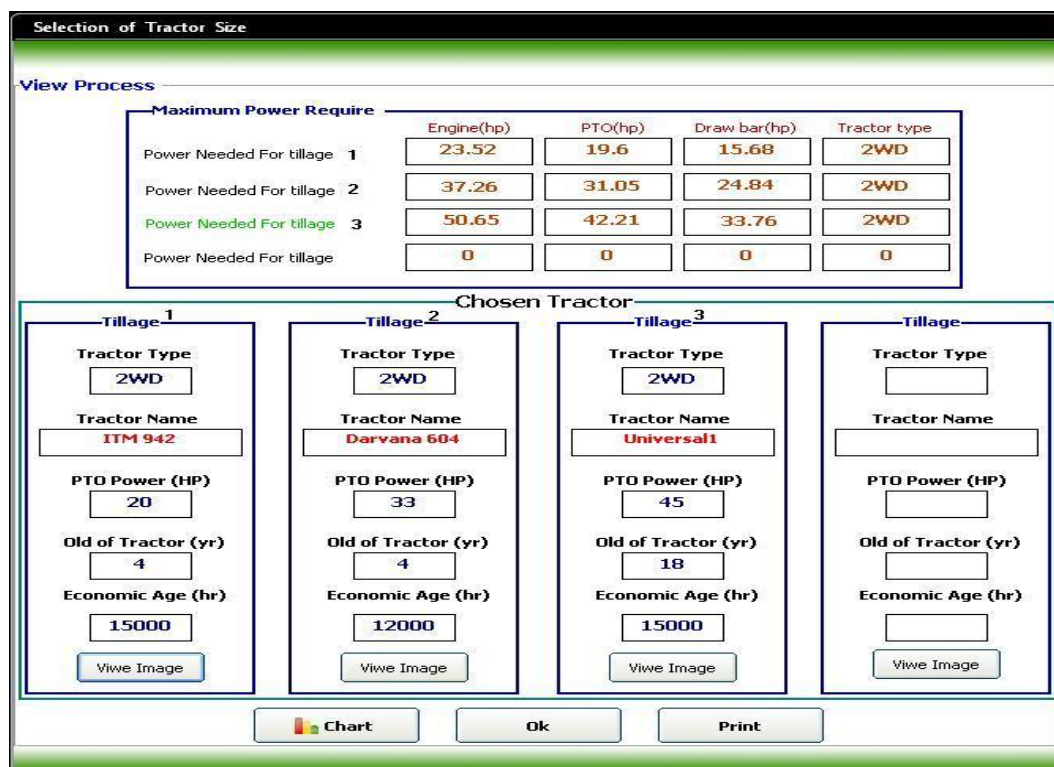
Fig. 13. Selected tractors for each operation.

Finally, the average of energy consumption in tillage operation for case study paddies was calculated and compared with other paddies. Energy inputs for calculation were Tractor and machines, diesel fuel and labour. Amounts of energy use on case study paddies were placed in group 1 and other paddies were placed in group 2. Results of amounts of energy consumption for tillage operation on 2 groups of paddies show in Table 4.

Table 4. Energy consumption in tillage operation on 2 groups of study.

Inputs	Energy use in group 1 (MJ ha^{-1})	Energy use in group 2 (MJ ha^{-1})
Tractor and machines	254.3	305.5
Diesel fuel	1005.2	1124.5
Labour	75.8	185.8

Results in table 4 show that energy use for paddies of group 1 that developed DSS used for them was lower than paddies of group 2. Results indicate that energy consumption on paddies of case study was 17.36 percentages less than other paddies. Most of the difference in energy inputs was labour with 59.2 percentages. This result shows that selection and matching of tractors and implement on paddies of case study was improper. It will increase the energy consumption and decrease the economic profitability.

IV.   CONCLUSION

The purpose of this study was creation of Decision Support Software for Mechanized operation and its utilization for Iranian farms. The following conclusions can be drawn from the study:

1. The DSS provides flexibility to either select an implement to match the tractor or to select a tractor to match the implement based on various soil and operating parameters.
2. The DSS helps to manager to know that the selected tractor and implement based on the past agronomy-years data is proper or not.
3. The developed DSS manages the operations times and predict the real available time without the geographical restrictions.
4. Use of this software can help farmers and mechanization cooperative in selection of the right size of tractor–implement system based on soil, weather and operating parameters.
5. Use of DSS shows that tractors with power less than 35 kW are able to complete the tillage operations (plowing, harrowing and puddling) for paddy cultivation.

6. Use of developed DSS can reduce the energy consumption in agricultural operation. In this study, energy consumption on paddies of case study was 17.36 percentages less than other paddies.

V.   ACKNOWLEDGEMENTS

REFERENCES

[1]   Power, D.J., 1999. Decision support systems glossary. http://dssre-sources.com/books/48.php. 2009.04.18.
[2]   Taylor, R., Schrock, M., Wertz, K., 1991. Getting themost fromyour tractor. http://www.oznet.ksu. edu/library/ageng2/mf588.pdf. 2003.06.05.
[3]   Gee-Clough, D., McAllister, M., Pearson, G., Evernden, D.W., 1978. The empirical prediction of tractor-implement field performance. J. Terramech. 15(2):81–94.
[4]   Ozkan, E., Edwards, W.M., Saulmon, A., 198). A Machinery Selection Model for Farmer Decision Making. ASAE, 89-1018. ASAE, St. Joseph, MI.
[5]   Upadhyaya, S.K., Williams, T.H., Kemble, L.J., Collins, N.E., 1984. Energy requirement for chiseling in coastal plain soils. Trans. ASAE, 27(6):1643-1649.
[6]   Brixius, W.W., 1987. Traction Prediction Equations for Bias Ply Tires. ASAE, 87-1622. ASAE, St. Joseph, MI.
[7]   Zoz, F.M., 1987. Predicting Tractor Field Performance (Updated). ASAE, 87-1623. ASAE, St. Joseph, MI.
[8]   Colvin, T.S., McConnell, K.L., Catus, B.J., 1989. TERM: a computer model for field simulation. Trans. ASAE, 32(2), 391-396.
[9]   Evans, M.D., Clark, R.L., Manor, G., 1989. A Traction Prediction and Ballast Selection Model. ASAE, 89-1054. ASAE, St. Joseph, MI.
[10]   Grisso, R.D., Al-Hamed, S.A., Taylor, R.K., Zoz, F.M., 1992. Demonstrating tractor performance trends using Lotus templates. Applied Engineering in Agriculture, 8(6):733-738.
[11]   Al-Hamed, S.A., Grisso, R.D., Zoz, F.M., Von Bargen, H., 1994. Tractor performance spreadsheet for radial tires. Computers and Electronics Agriculture, 10(1):45-62.
[12]   Harrigan, T.M., Rotz, C.A., 1994. Draft of Major Tillage and Seeding Equipment. ASAE, 94-1533. ASAE, St. Joseph, MI.
[13]   Gould, N.S., Lund, R.D., Hill, J., 1999. Matching tractors and implements-the economic way. http://www.agekon.com/Machsem/Webroom1.html. 2003.08.24.
[14]   Al-Hamed, S.A., Al-Janobi, A.A., 2001. A program for predicting tractor performance in Visual C++. Computers and Electronics Agriculture, 31(2):137-149.
[15]   ASAE standards. 2001. D497. 4. Agricultural Machinery Management Data. ASAE, St. Joseph, MI.
[16]   Siemens, J., Hambarg, K., Tyrrell, T., 1990. A machinery selection and management program. Journal of Production Agriculture. 3(2):212-219.
[17]   Butani, K.M., Singh, G., 1994. Decision support system for the selection of agricultural machinery with a case study in India. Computer and Electronics in Agriculture, 10(2):91-104.
[18]   Singh, G., Chandraratne, I.W.D.T., 1995. Decision support system for crop planning and equipment selection for developing countries. International Agricultural Engineering Journal, 4(1&2):17-27.
[19]   Grisso, R., Perumpral, J., 2006. Spreadsheet for matching tractors and implements. ASABE, 061085. MI: St. Joseph.
[20]   Singh, M., Singh, P., Singh, S.B., 2008. Decision support system for farm management. Proceeding of World Academic Science, Engineering and Technology, 29:346-9.
[21]   Sahu, R.K., Raheman, H., 2008. A decision support system on matching and field performance prediction of tractor-implement system. Computers and Electronics in Agriculture, 60:76-86.
[22]   Suarez de Cepeda, M., Recio, B., Rubio, F., 2004. Decision support system for farms mechanization. ASAE/CSAE meeting, 043040. MI: St. Joseph.
[23]   Mehta, C.R., Karan Singh, M.M., 2011. A decision support system for selection of tractor–implement system used on Indian farms. Journal of Terramechanics, 48:65-73.
[24]   Downs, H.W., Taylor, R.K., Al-Janobi, A.A., 1990. A decision aid for optimizing tractor-implement system. In: Proceedings of the ASAE Winter Meeting, USA, pp. 18-21.
[25]   Downs, H.W., Hansen, R.W., 1998. Equipment: selecting energy-efficient tractor. http://www.colostate .edu/pubs/farmgt/05007.pdf. 2003.08.06.
[26]   Powell, G., 2001. Selection and matching of tractor and implements. http://www.pdi.gld.gov.au /fieldcrops/3492.html.2003.04.04.
[27]   Jain, S.C., Philip, G., 2003. Farm machinery-an approach. 1st ed. Delhi: Standard Publishers Distributors.
[28]   Edwards, W., 2009. Ag.D.M. File A3-28, Matching Tractor Power and Implement Size http://www.extension.iastate.edu/agdm/decisionaidscd.html#mach. 2009.10.01.
[29]   IS 9164, 1979. Guide for estimating cost of farm machinery operation. New Delhi: Bureau of Indian Standards.
[30]   Ozkan, E., Edwards, W.M., Saulmon, A., 1984. A Machinery Selection Model for Farmer Decision Making. ASAE Paper No. 89-1018. ASAE, St. Joseph, MI.
[31]   Witiney, B., 1988. Choosing and Using Farm Machinery. Longman Scientific and Technical. New York. USA. 442pp.

Research Paper   Open Access

Experimental Study of Umts Radio Signal Propagation Characteristics by Field Measurement

Isabona Joseph[1], Konyeha. C.C[2]
1&2Department of Basic Sciences, Benson Idahosa University, PMB.1100, Benin City, Nigeria

Abstract: - Knowledge of propagation characteristics in the mobile channel is important to the design, analysis and optimisation of a cellular system. Such need is of great concern to achieve higher quality standards, lower overall running cost, minimize transmit power, better covering of different areas with different environmental situations. Thus, received signal prediction models play an important role in the RF coverage optimization and efficient use of the available resources in wireless communication. As the demand of location based services (LBS) increases in non-line of site (NLOS) environment, a robust received signal prediction model is needed to enhance the accuracy of the LBS techniques. This paper presents a large scale received signal prediction model for various types of propagation environment from field measured signal data. Based on the experimental data obtained, path loss exponent and standard deviation of signal strength variability are determined. It is shown that the values of these parameters vary from study location to location in the coverage area. The results indicate that different empirical models for mean signal strength should be used in different regions of the coverage area for cellular network planning.

I.   INTRODUCTION

Universal Mobile Telecommunication Systems (UMTS) is one of Third Generation (3G) standards. It is an upgrade from GSM via GPRS and EDGE. The standardization work for UMTS is carried out by Third Generation Partnership Project (3GPP) [1][2]. It aims at providing global roaming. It also inculcates various multimedia services for voice, data and video at increased data rates of 384 kbps while moving and 2 Mbps when stationary at specific locations. It also has greater capacity with higher efficiency than first and second generation systems and it can also work in conjugation with Internet protocol. Higher bandwidth here enables a wide range of applications for both customers and business. For the consumer it provides video streaming, TV broadcast, video calls, video clips – news, music, sports, enhanced gaming, chat, location services etc and for business it provides high speed teleporting access, sales force automation ,video conferencing and real-time financial information.

Signal propagation prediction models used in GSM 900/1800 systems are not one to one applicable UMTS due to frequency differences [3]. Path loss prediction models used in GSM system should be extended to find suitable expression for 2100MHz. Another important difference between UMTS and GSM systems in terms of radio propagation is the difference in the carrier spacing which is 5 MHz in UMTS system and 200 kHz GSM system. For this reason, UMTS system is more vulnerable to frequency selective fading than GSM systems.

Particularly, as wireless signal traverse the path from a transmitter to a receiver, they will be diffracted, scattered, and absorbed by the terrain, trees, building, vehicles, people etc. that encompasses the propagation environment. The presence of obstructions along the path may cause signal to experience greater attenuation than it would under free space conditions [4]. Radio signal attenuation and path losses depend on the environment and have been recognized to be difficult to calculate and predict [5].

Past studies of the signal propagation, in both indoor and outdoor environment have used several models with varying degrees of success and or complexity, if we focus on the signals of UMTS; we have to consider the propagation environments we will run into. The quality of coverage of any wireless network design depends on the accuracy of the propagation model, which in turn depends on the factors including distance from the desired base station (BS) and interfering BSs, path loss exponent, shadowing and multipath fading [6], [7].

The propagation characteristics of mobile radio environment are also derived from the field measurement studies [8–10]. Thus, for accurate cellular network design, the propagation models are estimated from signal strength measurement taken in the study area [11], [12].

In this paper, the field measurements of received signal strength (RSS) taken at the frequency of 2100 MHz in a vehicular environment have been analyzed and reported. The received signal levels from the BS were monitored from inside a vehicle moving at a speed of about 30 km/h. Total coverage area chosen for the measurement campaign consisted of a mixture of significantly different propagation environments

II.　　　MATERIALS AND METHOD

Measurement-based Prediction (or MbP) is a unique radio propagation process, which increases the accuracy of conventional propagation model predictions by making use of measured data to improve the model predictions around base station sites. The measurements were conducted from a UMTS network with WCDMA interface transmitters, located BIU Campus, Ugbor Avenue and Gapiona Avenue, all evenly distributed in Government Reservation Area (GRA), Benin City. The driving routes in these different locations are shown in figure 1-3. The measured received signal strength data which is the Received Signal Code Power (RSCP) and transmitter-receiver (T-R) separation distance (d) are recorded in dBm and m. Every measurement points of received signal strength and T-R separation distance are recorded evenly from all the predefined routes of three base stations. Each measurement point is represented in an average of a set of samples taken over a small area (10m^2) in order to remove the effects of fast fading [11].

The data collection tool consisted of ERICSSON TEMS (Test Mobile Systems) Cell-Planner tool with an antenna mounted on a moving vehicle 1.5 meter above ground level, Global Positioning System Receiver Set (GPS system) and a personal computer and a piece of compass. The personal computer houses the operating system and the data collection software (ERICSSON TEMS Investigation 8.0). The personal computer serves as the communication hub for all other equipments in the system. . The GPS operates with global positioning satellites to provide the location tracking for the system during data collection position on a global map which has been installed on the personal computer. The compass help to determine the various azimuth angles of the base station transmitters. Average height of transmit antenna is about 30 – 32 meter above ground level, with the same transmit power. Sampling rate of the collected data, on the average, is about 2 – 3 samples per meter.
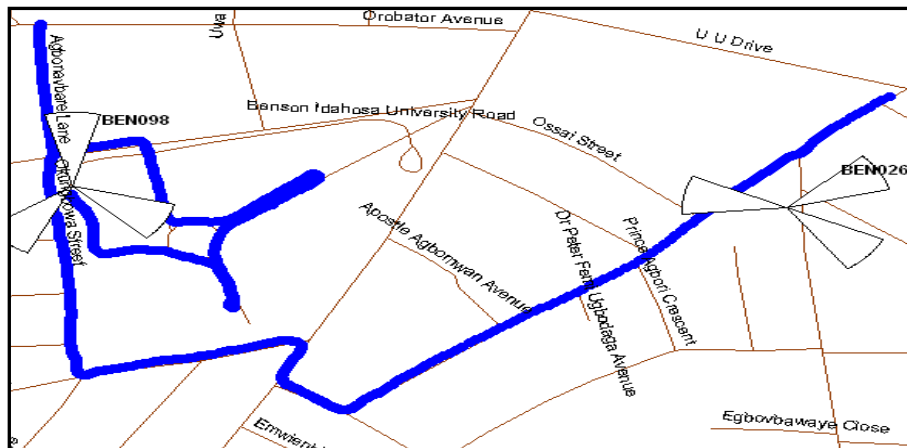
Figure 1: Measurement routes in Ugbor Avenue
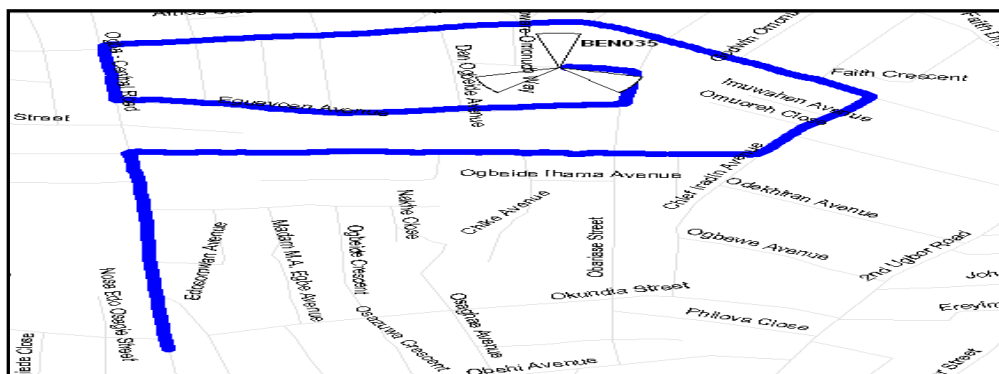
Figure 2: measurement routes in Garpiona Avenue
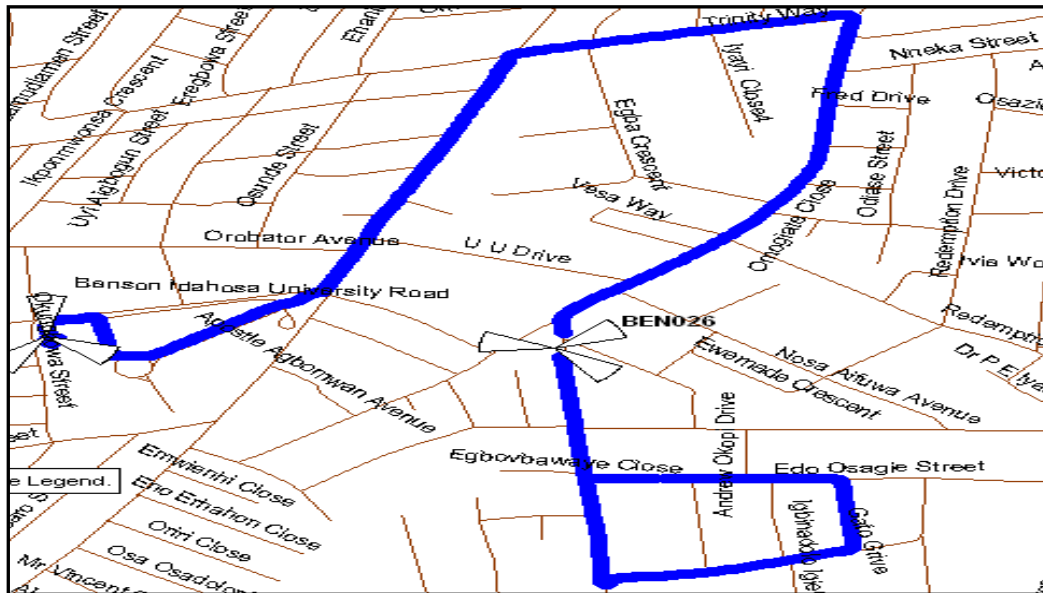
Figure 3: measurement routes in BUI Campus environ

III.   RESULTS AND DISCUSSIONS

III.1.   Modeling of Measured RSS data

Generally, the log-distance propagation model via linear regression is a statistical method often used to make predictions about signal strength from the sample data. In this section, linear regression analysis is carried out on the measured data. In the analysis, simple regression was fitted to the set of data, which is essentially a linear least squares curve fitting procedure. The mean signal strength in dB at mobile station (MS) as a function of distance d from base station (BS is modelled as follows [12], [13]:

$PL (d) = A \log d + C$ (1)

Or it can be written in the known following form:

$PL (d) = 10n \log (d/d_0) + PL (d_0)$ (2)

where *n* is the path loss exponent, and *PL (d_0)* is the reference path loss at distance d_0.

Now, the predicted signal *PL (D)* can be obtained as

$PL (D) = EIRP_T - PL (d)$ (3)

And $EIRP_T = P_T - L_C - G_T$ (4)

Where $EIRP_T$, is the effective isotropic radiated power of the UMTS base station, P_T is the base station transfer output power, L_C is antenna cable loss, and G_T is transmitting antenna gain. These powers, loss, and gain are added in dBm.

From the fitting parameters, *PD (d)* can be obtained as follows

$PD (d) = -A \log d + C = PL (d) = -10n \log d + C$ (5)

Similar to equation (2), the large-scale received signal prediction model *PD (d)* in *decibel* for an arbitrary BS-MS separation (*d*) can be expressed as following:

$PL (d) = PD (d_0) - 10n \log (d/d_0)$ (6)

Where *PL (d_0)* is the reference predicted signal at distance d_0 and it is written as:

$PD (d_0) = C - 10 n \log (d_0)$ (7)

Iii.2   Modeling Of Rss Uncertainty

In reality, the RSS does not have a deterministic behaviour, but present random variables. This is most likely due to the radio hardware imperfection and to the incomplete description of the RF communication link. Regardless of the RSS uncertainty source, it is of great importance to describe and characterizes the RSS uncertainty and distribution. Therefore it is important to explore the RSS uncertainty with respect to the distribution type.

One possible distribution of measured RSS values as reported in [16] and [17] is the Gaussian or normal distribution with probability function (PDF) given by:

$$PDF\sigma, \mu(x) = \frac{1}{\sigma\sqrt{2\pi}} exp(-\frac{x-\mu}{2\sigma^2})^2$$ (8)

Where μ is the signal mean value, σ is the standard deviation and x is the RSS variable, measured.

Iii.3   Discussions

Here, the mean signal strength in dB at MS as a function of distance d from BS is modelled as in equation (5). The regression analysis of the field measurement data has led to a simple one slope characterization for RSS against distance on logarithmic scale as shown in Figure 2, 4 and 6 respectively. The straight line represents the least squares linear regression fit. Applying regression fit on the entire set of the measurement data, it is found that the overall path loss exponent 'n' varies from 1.6 to 3.3 and standard deviation of signal strength variability ' σ_s ' ranged from 5.57-12.09 dB. The variation in propagation characteristics over different regions is a consequence of the terrain profile, man-made structures and environmental features. For a given system parameters, different values of path loss exponent and standard deviation of signal strength variability will cause radically different predicted performance parameters of the cellular networks, particularly the handover performance. Table 1 provides typical values of n under different environments. The value of the path loss exponent is an indicator of how fast energy is lost between transmitter and receiver. The higher the path loss exponent, the faster the signal strength drops with respect to distance, therefore in modeling the propagation of signal for a particular environment, there is the need to determine the path loss exponents for that environment. For $n < 2$ is a measure of the guiding effect of the channel and when $n > 2$ the channel is considered to be scattering energy [14].

Table 1: Pathloss Exponent for different environments [14]

Environment	Pathloss Exponent 'n'
Free Space	2
Urban	4.2
Log-normally shadowing area	2-4
Shadowed Urban	3 to 5
In building line-of sight	1.6 to 1.8
Obstructed in building	4-6
Obstructed factory	2-3
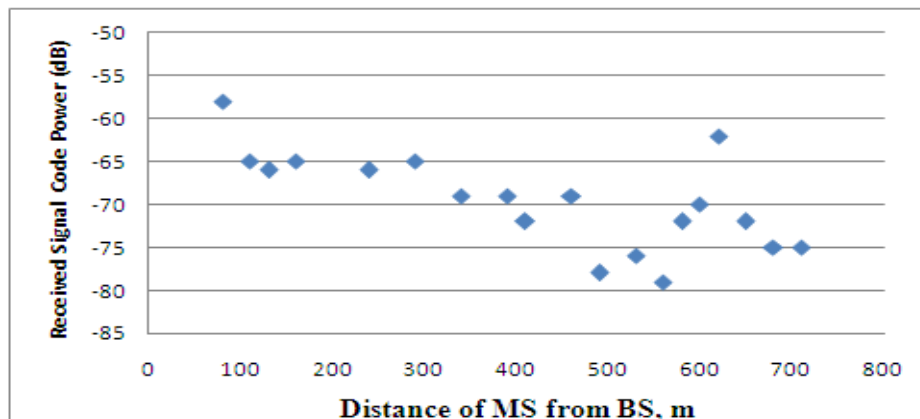
Figure 1: Signal strength data variability in Gapiona Avenue
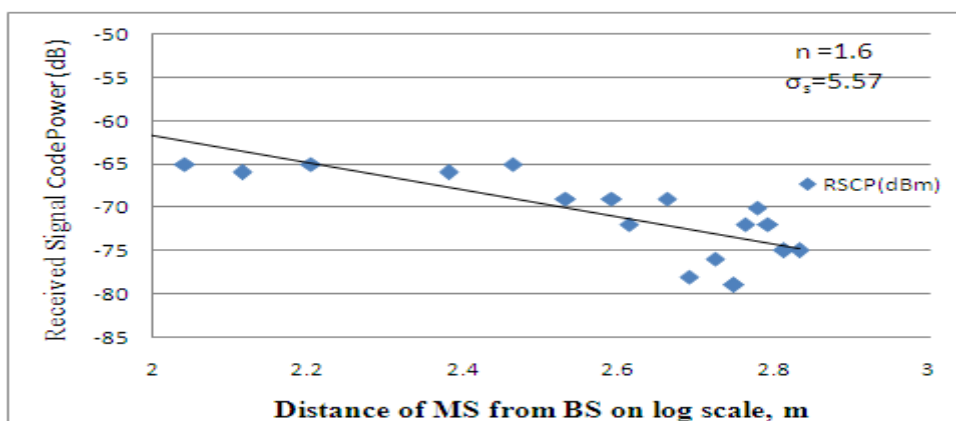
Figure 2: Signal strength data variability and regression fit in Gapiona Avenue
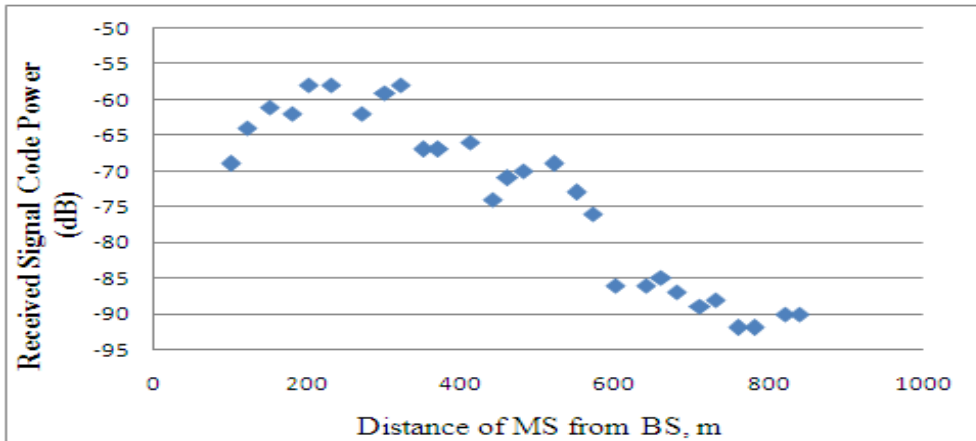
Figure 3: Signal strength data variability in Ugbor Avenue
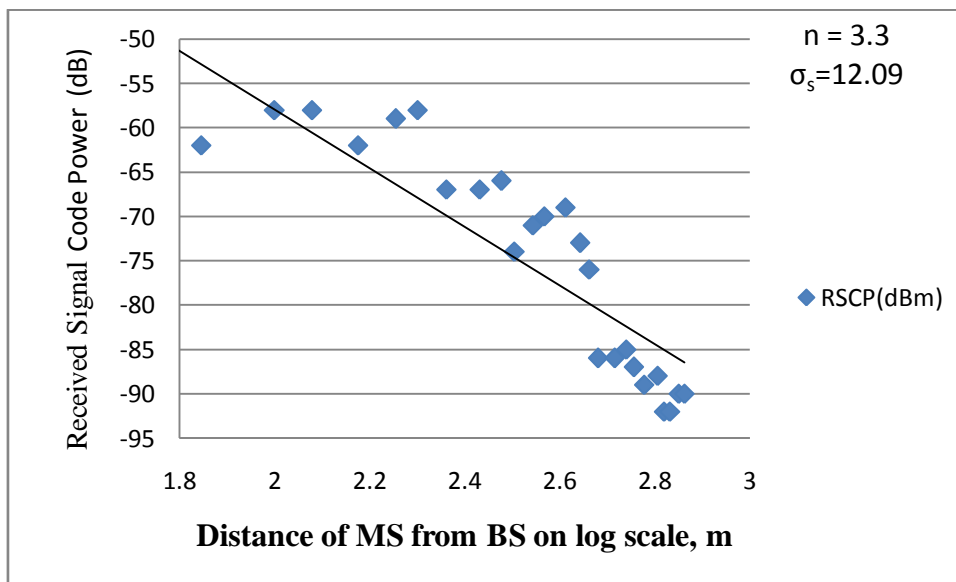
Figure 4: Signal strength data variability and regression fit in Ugbor Avenue
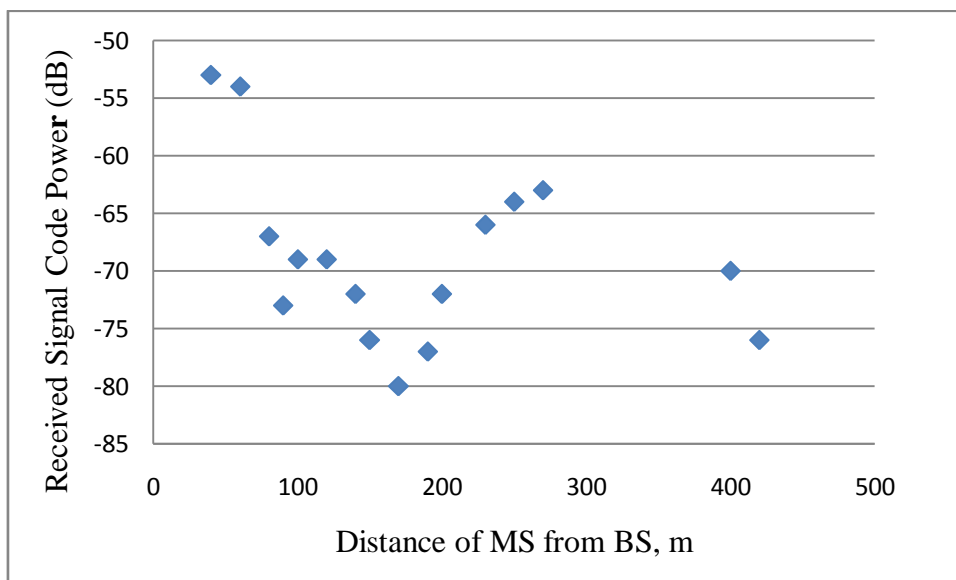
Figure 5: Signal strength data variability in BIU Campus
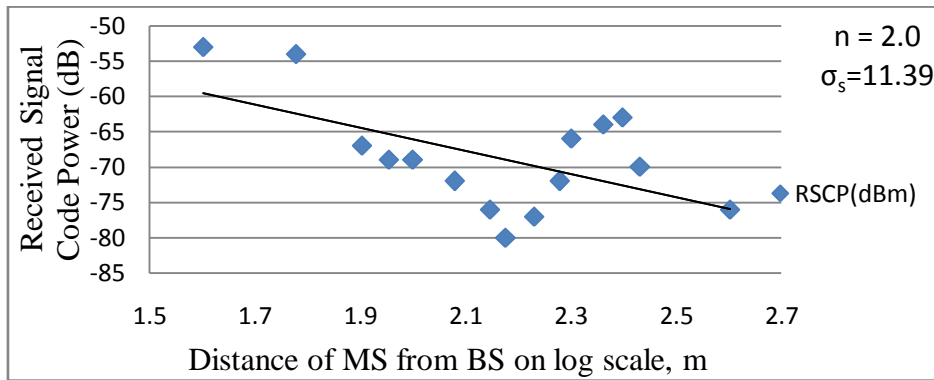
Figure 6: Signal strength data variability and regression fitting in BIU Campus

We also observed from the graphs in figure 1-6 that the radio signals of mobiles closer the BS experiences larger signal attenuation loss values than those far away from the BS in all the study locations. This may be due to different scattering bahaviour of radio signal in the near field and far field regions of the transmitting BS antenna. The term near-field refers to the field pattern that exists close to the antenna, while the term far-field refers to the field pattern at large distances.

Figure 7 (a)-(c) presents the results for three different $PDF\sigma, \mu(x)$ cases, calculated through equation (8). The results demonstrate that our measured RSS values does not follow the Gaussian distribution and this agrees with results reported in [18], but however disagree with the null hypothesis that RSS values does follows Gaussian distribution in [16] and [17].
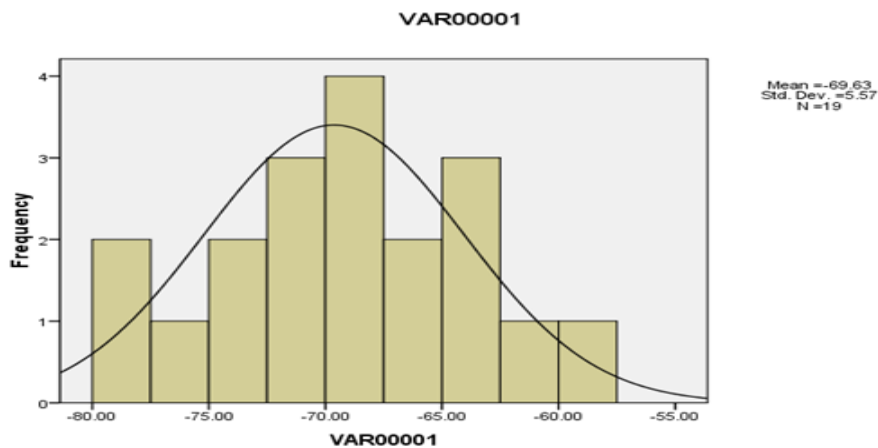
Figure 7 (a): Gaussian distribution of RSS in study location 1
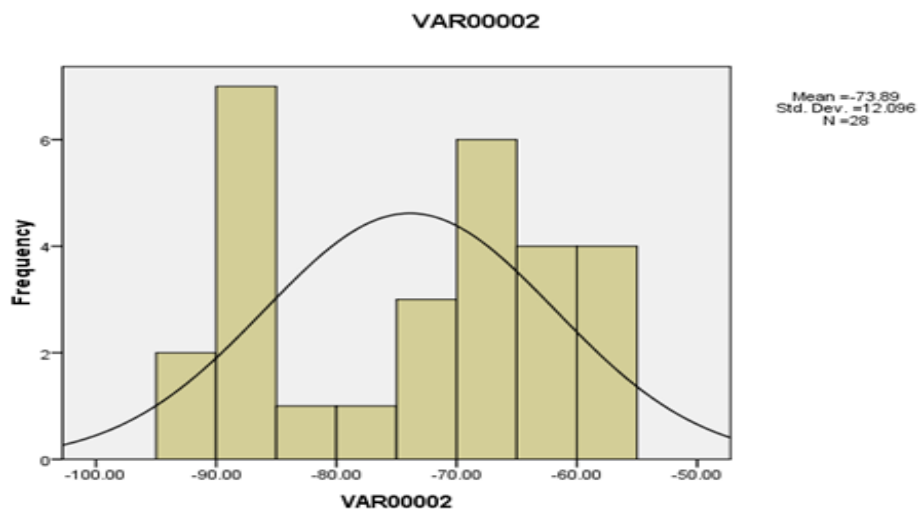
Figure 7(b): Gaussian distribution of RSS in study location 2

VAR00003

Mean = -72.11
Std. Dev. = 11.39
N = 28
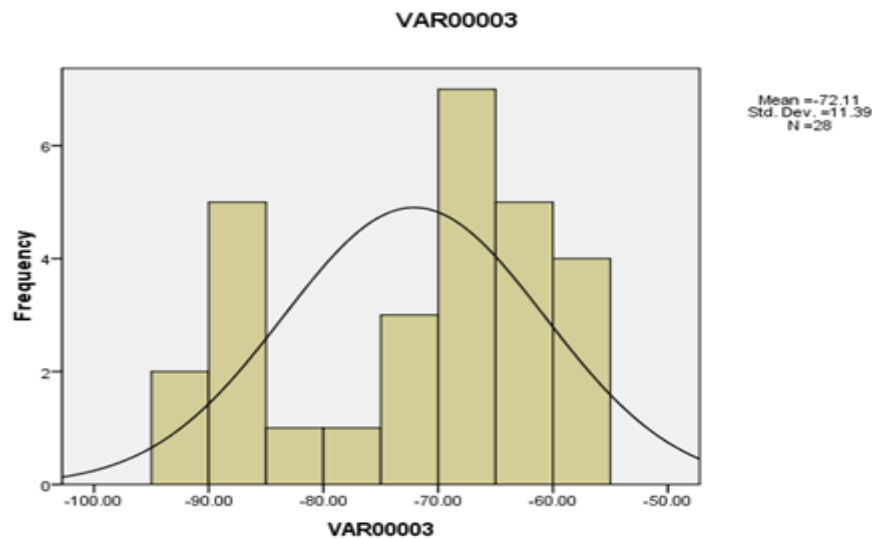
Figure 7 (c): Gaussian distribution of RSS in study location 3

IV.   CONCLUSION

Study of radio wave propagation in different environments is an essential pre requisite for designing mobile communication systems. Radio wave propagation channels are modelled in statistical way using real propagation measurement data. In this paper, the field measurement of received signal power conducted at frequency of 2100 MHz for UMTS network in GRA Benin city, Nigeria and statistical analysis measurement results has been reported. The path loss exponents for different areas are obtained by utilizing the least squares method. The path loss exponents obtained lie in the range from 1.6 to 3.3. The results may be utilized as reference in the system level simulation for network planning and optimizing the design parameters of handover initiation algorithms.

REFERENCES

[1].   Dilpreet K, Pankaj R, and Amanpreet, K (2010) Analysing Quality of Service in UMTS, International Journal of Computer Applications, Vol. 11– No.12, pp 31-34.

[2].   E.M. Saad, O.M. EL-Ghandour and M.K. Jehan (2008), "Evaluation of QoS in UMTS Backbone Network Using Differentiated Services", 25th National Radio Science Conference (NRSC), Egypt, 2008.

[3].   Selim, S.S, Satı ,Y and Fulya C.K (2010), Comparison of Propagation Loss Prediction Models of UMTS for an Urban Areas, 18th Telecommunications forum TELFOR 2010 Serbia, Belgrade, November 23-25, 2010.

[4].   Tarokh, V., (2009). "New Directions in Wireless Communication Research", pg.1, Springer Dordrecht Heidelberg London New York ISBN 978-1-4419-0672-4.

[5].   Terplan, K., Morrwle, P., (1999) "The Telecommunication Handbook", pp. 2-4, IEEE Press, ISBN 0-8493-3137-4.

[6].   W C Jakes, Ed. 'Microwave Mobile Communications'. New York, Wiley, IEEE Press, 1994.

[7].   K Pahlavan, P Krishnamurthy, A Hatami, Y M Makela, J P Pichna R and J Vallstron. 'Handoff in Hybrid Mobile Data Networks'. IEEE Personal Communications, vol 7, April 2000, p 34

[8].   X Zhao, J Kivinen, P Vainikainen and K Skog. 'Propagation Characteristics for Wideband Outdoor Mobile Communications at 5.3 GHz'. IEEE Journal on Selected Areas in Communications, vol 20, no 3, April 2002, p 507 M J Gans, N Amitay, Y S Yeh, T C Damen, R A Valenzuela, Choelhang Cheon and John Lee. 'Propagation Measurements for Fixed Wireless loops (FWL) in a Suburban Region with Foliage and Terrain Blockages'. IEEE Transactions on Wireless Communications, vol 1, no 2, April 2002, p 302.

[9].   M V S N Prasad and R Singh. 'Terrestrial Mobile Communication Train Measurements in Western India'. IEEE Transactions on Vehicular Technology, vol 52, no 3, May 2003, p 671.

[10].   Takahashi, S., Kato, A., Sato, K., Fujise, M., (2004). "Distance dependence of path loss for millimeter wave inter-vehicle communication" IEEE Vehicular Technology pp. 26-30 vol.1.

[11].   Rosu, I. (2000). Small Antennas for High Frequencies, *YO3DAC / VA3IUL,* http://www.qsl.net/va3iul/

[12].   Iida, T., (2002). "Wireless Communication R and D in the science and technology policy In Japan, IEICE Transaction, pp. 419-427.

[13].   Jakes, C. W. (1994) "Microwave Mobile Communications", 1st ed., John Wiley and Sons, New York.

[14].   Kaemarungsi, K. (2006) "Distribution of WLAN Received Signal Strength Indication for Indoor Location Determination," in 1st International Symposium on Wireless Pervasive Computing. IEEE, 2006, pp. 1–6.

[15].   Sheng, Y, Tan, K, Chen, G, Kotz, D. and Campbell, A. (2008) "Detecting 802.11 MAC Layer Spoofing Using Received Signal Strength," in 2008 IEEE INFOCOM - The 27th Conference on Computer Communications. IEEE, pp. 1768–1776.

[16].   Robitzsch, S and L. Murphy (2012) ''Empirical Analysis of Measured 802.11 Receive Signal Strength Values Using Various Atheros Based Mini-PCI Cards'' Available online at: http://pel.ucd.ie/files/pdf

Research Paper   Open Access

Maintenance Scheduling Improvements In Flexible Manufacturing System Supply Chains

S. Craig Littlejohn, Phd.
South Carolina State University

Abstract: - Globalization and competitive markets have created new challenges for modern manufacturers. In the current marketplace, manufacturers must be agile, efficient, and capable of quickly responding to customer demands and changes in the modern manufacturing environment. Manufacturing systems do not exist in isolated environments. Manufacturing systems are always a part of an overall supply chain. The performance of each part of the supply chain has an effect on the performance of every other part of that supply chain. One of the most vital priorities for facilitating good supply chain performance is efficient maintenance scheduling and utilization throughout the supply chain. This article presents a brief discussion on flexibility, as it relates to manufacturing supply chains and general manufacturing environments. Two maintenance scheduling formulations are introduced. These formulations can be applied at any point in a supply chain.

I. INTRODUCTION

This article presents a brief discussion of supply chains for flexible manufacturing systems with a particular focus on an often overlooked aspect for efficient supply chain performance, maintenance scheduling. It is a common belief that Henry Ford created the blueprint for how manufacturing processes should be structured. Two of the most notable characteristics of Ford's process were: item mass production and the vertical integration of all manufacture-related processes. In terms of mass production Ford assumed that the manufacturing marketplace was company centered as opposed to customer centered. A company centered manufacturing marketplace is one in which associated variations and trends are dictated by the desires of the decision makers and designers of a corporate entity. For this kind of manufacturing marketplace, consumer demands are not the driving force behind change. In contrast, change occurs within a customer centered marketplace based on the desires (which are often quite fickle) of consumers. In this kind of marketplace an organization's success is dependent on its ability to quickly respond to customer demands.

The use of vertical integration allowed Ford to control all aspects of the production process. Figure 1 is a flow chart of general activities associated with a manufacturing environment. Suppliers for raw materials used to make Ford products were owned by Ford. Manufacturing and assembly processes associated with Ford products were owned by Ford. Distribution of final Ford products was also controlled by Ford. Some of the potential advantages of vertical integration are: greater overall protection for a company against changes in the marketplace, an increased control over determining the location of the supply chain activities (illustrated in Figure 1), and lower transportation costs. Some of the potential drawbacks of vertical integration are a decreased ability to respond to changes in marketplace demands, less item variety, and greater costs (outsourcing may be cheaper overall in comparison to using resources to produce an item internally).

```
┌─────────────────────────────┐
│        Raw Materials        │
│                             │
└─────────────────────────────┘
               │
               ▼
┌─────────────────────────────┐
│        Manufacturing        │
│                             │
└─────────────────────────────┘
               │
               ▼
┌─────────────────────────────┐
│          Assembly           │
│                             │
└─────────────────────────────┘
               │
               ▼
┌─────────────────────────────┐
│        Distribution         │
│                             │
└─────────────────────────────┘
               │
               ▼
┌─────────────────────────────┐
│        End Customer         │
│                             │
└─────────────────────────────┘
```
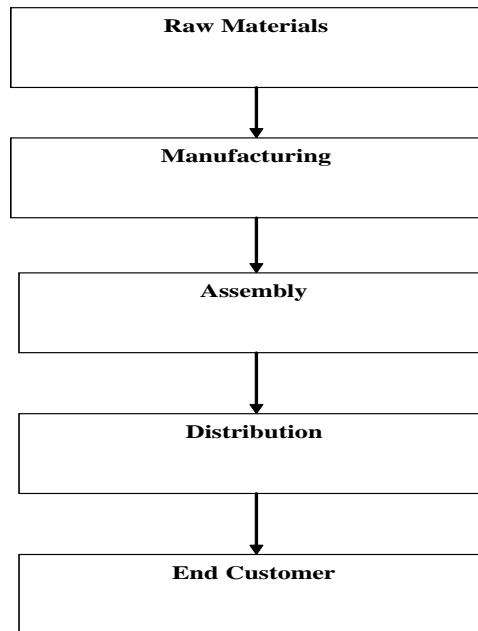
Figure 1 This blueprint was utilized by many for much of the twentieth century (between the decades of 1920 and 1970).

In contrast, one of the defining characteristics of the twenty first century manufacturing environment is that an organization's competitiveness is strongly determined by that organization's ability to respond to changes. The existence of trade blocs and the continuing development of new technology have lead to the globalization/internationalization of modern day manufacturing marketplaces. Organizations must consider that their potential customers are no longer limited to people who live in a certain community, reside in a limited region, or communicate in a particular language. Modern manufacturers must be able to adjust to variations in customer demands (quantity and quality), new technology, and other changes. Flexible manufacturing systems can allow organizations to meet these challenges. The next section of this article will briefly discuss the topic of flexibility from the perspective of the overall manufacturing supply chain.

II. SUPPLY CHAIN FLEXIBILITY

In terms of flexibility within manufacturing environments, much focus is put on the flexibility of the actual manufacturing processes. This section briefly discusses flexibility from the perspective of the overall manufacturing supply chain. (Leslie, Robert, and Rhonda 2003) identify six components for supply chain flexibility. These components are:

1. Operations Flexibility
2. Market Flexibility
3. Logistics Flexibility
4. Supply Flexibility
5. Organizational Flexibility
6. Information Systems Flexibility

Operations flexibility is defined as a manufacturer or service organization's ability to organize assets and operations to be able to respond to changing customer trends at every point in a supply chain. Market flexibility is defined as the ability to build close relationships with customers. This includes the designing, modifying and mass customization of products. Logistics flexibility is having the capabilities to deliver and receive products cost effectively regardless of customer and supplier changes. The ability to alter the organization or structure of the supply chain to respond to demand changes is called, Supply flexibility. Organizational flexibility deals with an organization's ability to match worker skills with the skills required by marketplace demands. Information systems flexibility is defined as an organization's information system being capable of allowing the organization to receive and respond to changes in the marketplace.

(Babu and More 2008) present a fairly thorough review of existing literature covering the topic of Supply Chain Flexibility. Research/evidence in (Fatemi 2010) discusses supply chain flexibility and provides a review of manufacturing flexibility and supply chain flexibility literature. (Sanchez and Perez 2005) and (Grigore 2007) divide supply chain flexibility into two categories: process flexibility and logistics flexibility. Process flexibility is described as the number of product types that can be manufactured by each producer.

Logistics flexibility is described as the ability to get a product to market or the ability to attain material from a supplier. Sanchez and Perez separate these flexibility categories into ten separate dimensions:

a.   Product flexibility
b.   Volume flexibility
c.   Routing flexibility
d.   Delivery flexibility
e.   Trans-shipment flexibility
f.   Postponement flexibility
g.   Sourcing flexibility
h.   Target market flexibility
i.   Launch flexibility
j.   Access flexibility

A summary of the definitions of these dimensions as stated by these writers is now given. Product flexibility is ability to meet customer specification and to make products of varying physical characteristics. Volume flexibility is the ability of an organization to increase or decrease its overall production in response to market changes. Routing flexibility is the ability to process an item in different ways. Delivery flexibility is the ability to adapt lead times according to customer requirements. Trans-shipment flexibility describes the ability to physically relocate stock between supply and demand locations of relatively small distances. Postponement flexibility is defined as the ability to incorporate a customer's product requirements within the later stages of production. Sourcing flexibility refers to an organization not being dependent on any single supplier for any component or raw material. Target market flexibility measures the ability to meet the needs of high priority markets. Launch flexibility is the ability to quickly introduce new products into a market. Access flexibility measures the ability to distribute in a widespread or intensive manner. The following figure gives a visual illustration of these ten flexibility dimensions. It was originally presented in (Sanchez and Perez 2005).
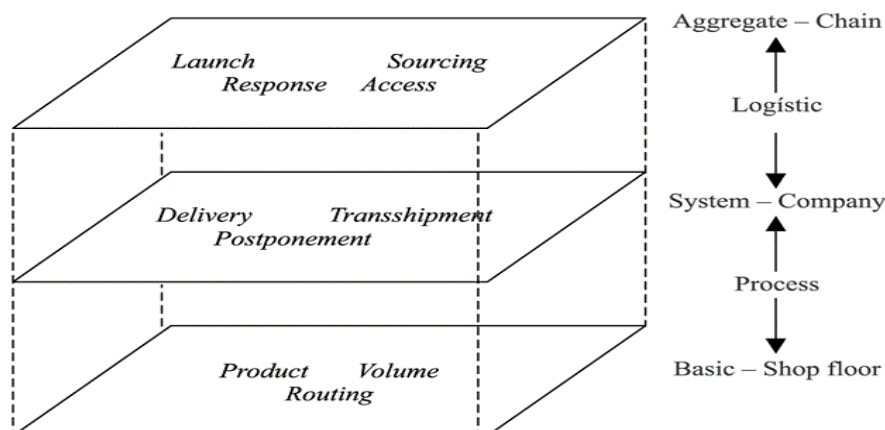
Figure 2: Source (Sanchez and Perez 2005)

Each of these dimensions requires the implementation of well designed maintenance processes for maximum efficiency. This section has briefly discussed some important aspects of manufacturing supply chain flexibility. The next section of this article will discuss the topic of flexible manufacturing systems.

III.   FLEXIBILITY AND MANUFACTURING SYSTEMS

Flexible manufacturing systems are similar to automated production lines. An important difference between the two is that flexible manufacturing systems have capabilities for processing different parts simultaneously. (Inman 2010) says that the origin of the concept of flexible manufacturing systems is in the 1960s. During the 1960s and 1970s (and continuing into the following decades), the priorities of manufacturers began to center around three critical points: product cost, product quality, and product delivery speed. At this time robots, programmable controllers, and other computerized controls were beginning to be used in manufacturing environments for the control of machines. The desire to create both a customizable manufacturing environment that is also agile was essential to the development of flexible manufacturing systems. Currently there is a fourth manufacturing priority, flexibility.

Three classical categories of manufacturing environments are: batch manufacturing, continuous manufacturing, and job manufacturing. Batch manufacturing environments can increase their efficiency and ability to respond to changes in the marketplace by implementation of flexible manufacturing systems. Batch

manufacturing environments produce a designated quantity of a certain item in a series of processes. From a process perspective, the reason for using batch processes is often directly related to machine capacity and process limitations. From an external (marketplace) standpoint, batch manufacturing tends to be more flexible in relation to other manufacturing environments. Batch manufacturing allows for the production of multiple items in a single production line. It is common for companies that produce seasonal products to use batch manufacturing. Also, the costs of discontinuing an unpopular product is much less in batch environments than it is in other manufacturing environments. While batch manufacturing processes can be very useful and productive, they tend to be inefficient. This inefficiency primarily stems from time wasted (i.e. downtime) because of the necessity to reset machines, and change raw materials before each new batch is started. Before the beginning of a new batch, a test output must be completed. This increases the amount of cycle time (time between the completion of one batch and the commencement of the next batch). Maintenance scheduling is very important in these environments, because it can help to decrease the amount of downtime and cycle time that could occur because of equipment or machine breakdown (unscheduled downtime) or scheduled (routine) downtime. In batch manufacturing, work is divided into sections or "breaks" often called workstations. However, continuous manufacturing environments are designed without breaks in the production line. Whereas batch manufacturing is constrained to a specific or finite amount of outputs (number of end products), in theory the number of outputs for a continuous manufacturing environment is infinite. Continuous manufacturing environments are more costly (in large part due to higher required initial capital). They are useful for producing similar items. An example of this is the continuous production of various models of similar automobiles. Because of their design, continuous manufacturing environments require maintenance to be performed while production continues. The design of continuous manufacturing environments may make them more suitable to automation and therefore more easily compatible to flexible manufacturing systems than are batch manufacturing environments. Job manufacturing is production that focuses on the need of a specific customer. The quality requirements for this type of environment are higher than it is in other manufacturing environments. It is more similar to batch manufacturing than it is to continuous manufacturing. The items produced within job manufacturing environments tend to be single and unique. The skills required in these types of manufacturing environments tend to be more specialized in relation to the required skills in other types of manufacturing environments. There is an intrinsic nature of flexibility in job manufacturing. Out of the three manufacturing environments discussed in this section, job manufacturing environments would benefit the least from the application of flexible manufacturing system technology. Job manufacturers can alter products in order to precisely respond to market demands. The next section of this article briefly discusses another type of manufacturing that is becoming more useful in the current marketplace, additive manufacturing.

IV.　　ADDITIVE MANUFACTURING

Additive manufacturing (or additive fabrication) is the process of combining (adding) materials in a layer by layer process in order to make objects from three dimensional data such as CAD drawings. It utilizes batch manufacturing in that multiple products, either similar or dissimilar, can be produced simultaneously. It allows for the construction of objects (both simple and complex) without the need for tools or castings, forgings, or other equipment. This can lead to an overall reduction of expenses to an organization. The use of additive manufacturing can reduce waste and enhance design and engineering processes. Proper utilization of additive technology can allow for the realization of more agile and flexible manufacturing systems. Significant advances have been made to the various additive manufacturing technologies such as stereolithography, laser sintering, and fused deposition. The newest of these technologies is three dimensional printing. Stereolithography was the first additive manufacturing technology. It is used to create a solid object from a three dimensional computer image. The object is constructed one layer at a time. Layers of material are deposited in a bottom to top manner by means of a computer-controlled laser which draws the shape of the object onto the surface of liquid resin (usually). The process in which prototypes and finished items are created from three dimensional drawings through the use of thermoplastics and metals is called laser sintering. In laser sintering the thermoplastics and metals are cured by a high temperature laser. The three dimensional drawings are cross-sectioned into thousands of layers and built up in a layer by layer fashion by the machine being used. Fused deposition modeling (FDM) is a type of additive manufacturing that can be used to create plastic prototyping models and production parts. The FDM process works by extruding layers of plastic from materials such as: polycarbonate, polyphenysulfone, or other material. The models produced by FDM can be assembled or used as normal objects. The term three dimensional printing is often used to include both rapid prototyping and rapid manufacturing. Rapid prototyping products are used for concept modeling primarily for the purpose of measuring if a design meets customer specifications. These products are also sometimes used to determine the fit or compatibly of the modeled product with other parts within its intended system. In contrast, rapid manufacturing products are created for specific application purposes.

The potential advantages of additive manufacturing over other manufacturing categories are:

- Cost reduction
- Lead time reduction
- Minimization of waste
- Greater flexibility for varying designs
- Increased energy efficiency
- Environmentally friendly
- Reduced maintenance costs

Although maintenance costs are reduced in additive manufacturing environments, as with all categories of manufacturing, maintenance is still a vital part of additive manufacturing supply chains. Maintenance must remain a high priority in order to actualize the potential advantages in the above list. The next section of this article will discuss the importance of maintenance in manufacturing supply chains.

V. MAINTENANCE IN SUPPLY CHAINS

In general, maintenance systems are created for the purpose of ensuring the serviceability and safety of equipment or systems so that maximum possible performance levels can be achieved. Scheduling and planning are two (of several) primary functions of the maintenance modeling paradigm. Scheduling is the arrangement of resources to be used and planning is the act of ensuring that resources and tools are in order before the required tasks are to take place. Within the construct of maintenance planning and scheduling, there are two categories. The first category consists of preventive maintenance, routine maintenance, and scheduled overhauls. The second category consists of unscheduled maintenance due to emergencies. Any maintenance schedule should consider both known and unknown circumstances. For regular manufacturing systems, it is vital to maximize the availability of resources at all points of the manufacturing supply chain. Increased availability of resources is even more vital within flexible manufacturing systems than it is in general manufacturing systems. This is because of the necessity of flexible manufacturing systems to be able to quickly respond to various changes. Efficient maintenance systems can be essential in facilitating the creation of manufacturing environments that have high resource availability. The rest of this section presents a brief discussion of an important tool for increasing resource availability at all points in a supply chain, total completion time maintenance scheduling. The consideration now is the minimizing the total completion time scheduling problem for a set of maintenance jobs. Minimization of the total completion time for a set of jobs leads to the overall availability of a set of resources (i.e. machines, vehicles, tools, etc.) being maximized. The United States military refers to this as maximizing the overall fleet availability. This objective is accomplished through intelligent scheduling of maintenance personnel (or maintainers). In this type of environment, a maintenance department with M number of maintenance workers is responsible for performing all maintenance jobs. However, both the number of maintenance workers and the number of operations that can be performed by the maintenance workforce are not varied in a given scenario.

Consider a process in which a set of Q pieces of equipment produces items at a constant rate R per unit time. These pieces of equipment are subject to periodic failure and a crew of maintenance workers is available to maintain the equipment. The approach is to have a schedule for maintenance workers devised so as to maximize the overall availability of these machines during a finite time interval. Availability can be quantified by the total production/work performed by all equipment/resources at the end of the time period. Each maintenance worker has a skill that may or may not be required on a certain resource. This means that each maintenance work order associated with any given equipment does not necessarily require each skill. Each worker has a set speed at which he or she can perform his or her required task.

Examples of these types of problems are presented next. The first example is simplified such that all of the assumptions associated with a general open shop scheduling problem hold. These assumptions are:

1. A job i is *not* allowed to be worked on simultaneously by more than one worker at a time.
2. There are *not* multiple workers for each operation.
3. In situations where multiple workers for each worker type are allowed, identical workers for each worker type have the same processing speed.

Maintenance Scheduling Example Number One

Consider a scenario in which there are 10 systems that each produce $r = 100$ units per hour. Three of the systems are down (i.e., N = 3 jobs) at the beginning of the time horizon ($t = 0$) and the Maintenance Department contains two skilled workers (i.e., M = 2). The Maintenance Department is composed only of machines each of which has one unique operation. The problem is to determine the sequence of processing jobs and/or machine schedules that maximizes the number of available systems of total time horizon $T = 8$ hours (the total length of one scheduling shift) which will be quantified by the total production at the end of the period. Every hour that a system is available during the time horizon is equivalent to 100 units of production by that

system. However, every hour that a system is not available is equivalent to 0 units of production by that system. Three maintenance work orders (or jobs) have been sent to the maintenance department. Let x_{ij} be the assignment of job i to Machine j. Then consider the following information in Table 2 (note that 0 indicates that job i does not need to be processed by worker j).

Table 1: Processing Times

job i	machine j	
	1	2
1	2	0
2	5	3
3	0	1

The above problem will now be solved for this open shop environment using two different rules: shortest processing time and longest processing time. In an open shop environment, the scheduling heuristic is applied to each individual worker.

Shortest Processing Time (SPT) Results

        Shortest processing time scheduling occurs when items are processed in increasing order of their required processing times. When shortest processing time is applied to the above problem, Machine 1 performs maintenance first on Job 1 and then on Job 2. Machine 1 does not have any scheduled maintenance for Job 3. Meanwhile, Machine 2 performs maintenance first on Job 3 and then on Job 2. Machine 2 is not scheduled to perform any maintenance on Job 1. Both workers can work on separate jobs simultaneously. However, for this example a delay scheduling assumption is made. According to the traditional scheduling theory with a delay scheduling implementation, only one worker can work on the same job at a time. Both workers are scheduled to perform work on Job 2. In this example, Machine 2 finishes maintenance on Job 3 before Machine 1 finishes maintenance on Job 1. Therefore, Machine 2 can begin to work on Job 2 first. Machine 1 must wait until Machine 2 completely finishes work on Job 2 before Machine 1 can perform work on Job 2. Figure 3 shows the schedule for each worker and the total completion time for the jobs. The sequencing of jobs on each machine can be seen in Figure 2. The completion times of each job can also be seen in this figure.
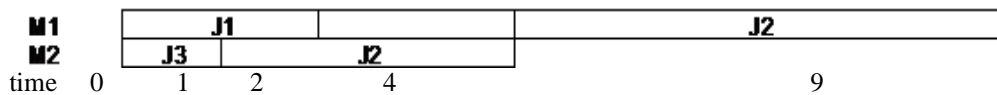
Figure 3: Shortest Processing Time Schedule for Example 1

System uptime (or availability) is assumed to be equal to the total time horizon minus total completion time for each job. The availabilities of each system are as follows: System 1 was made available for six hours, System 2 was made available for zero hours, and System 3 was made available for seven hours. Since every hour of system uptime is equivalent to 100 units of production, then the total production at the end of the time horizon is as follows:
(6 + 7) hours * 100 units/ time horizon in hours = 1300 units.

Longest Processing Time (LPT) Results

        Longest processing time scheduling occurs when items are processed in decreasing order of their required processing times. Both Machine 1 and Machine 2 are scheduled to work on Job 2 at the same time. Since for this example delayed scheduling methods are being used and both workers are not allowed to work simultaneously on the same job, Machine 1 is scheduled to work on Job 2 first because it has the longer scheduled processing time. The processing time of Job 3 for Machine 2 is one hour and the processing time for Machine 1 on Job 2 is five hours. Therefore, Machine 2 can complete Job 3 before Machine 1 has completed Job 2. Because the overall processing time of the jobs is being minimized, Machine 2 is allowed to work on Job 3 first. In other words, idle time is not forced. Job 2 cannot be worked on by Machine 2 until Machine 1 finishes. The scheduling sequences and total completion times based on a delay scheduling assumption are shown in Figure 3.
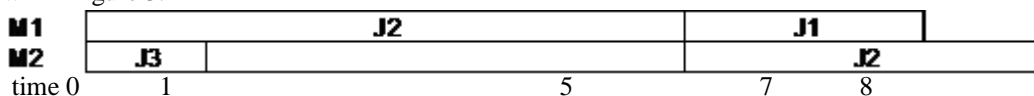
Figure 4: Longest Processing Time Schedule for Example 1

The completion times for the jobs are as follows: Job 1 is 7, Job 2 is 8, and Job 3 is 1. The corresponding availabilities for the three resources are 1, 0, and 7 respectively. Since every hour of resource uptime is equivalent to 100 units of production, then the total production at the end of the time horizon is as follows:
8 hours * 100 units/hour = 800 units.

The above results show that scheduling using shortest processing time (SPT) is preferred over longest processing time scheduling. SPT both minimizes the total completion time of the machine/worker labor, while simultaneously maximizing the total production at the end of the time horizon. This gives a visual illustration that minimizing total completion time is equivalent to maximizing total production.

Maintenance Scheduling Example Number Two

An example of a personnel scheduling problem for maintenance personnel within a manufacturing supply chain is now considered. In order to make an open shop scheduling problem into a personnel scheduling problem, the assumption that states that there cannot be more than one machine/worker at a time at a job (scheduled maintenance task) is relaxed. The previous problem is considered and the new constraint (multiple machines/workers can work on the same job simultaneously) is applied, using the SPT and LPT once again. Figure 4 and Figure 5 give the results for this example.
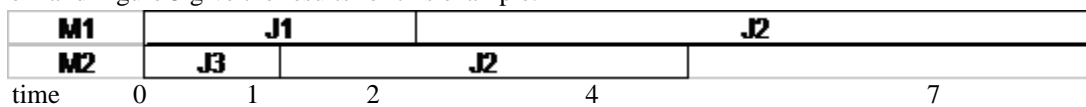
Figure 5. Shortest Processing Time Schedule for Example 2

The availabilities for the three resources are: 6, 1, and 7 for resources 1, 2, and 3, respectively. Since every hour of resource uptime is equivalent to 100 units of production, then the total production at the end of the time horizon is as follows:
(6 + 1+ 7) hours * 100 units/ time horizon in hours = 1400 units
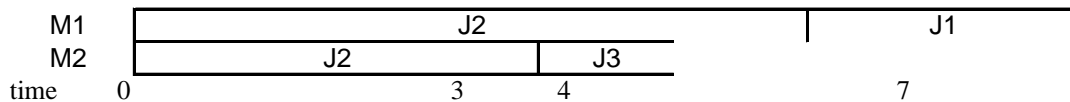
Figure 6. Longest Processing Time Schedule for Example Number Two

The availabilities for the three resources are one, three, and four for systems 1, 2, and 3, respectively. Since every hour of resource uptime is equivalent to 100 units of production, then the total production at the end of the time horizon is as follows:
(1 + 3 + 4) hours * 100 units/hour = 800 units.

The results for the example problems show that SPT sequencing produces better schedules than did the LPT. These results also show that the introduction of the new constraint where multiple workers can work on one job simultaneously actually increases machine availability for both rules. This is representative of maintenance environments which allow for differing maintenance tasks to be performed concurrently. Two such environments are discussed briefly later in this article.

Availability and Total Completion Time

The equivalence of the objectives of maximizing the availability of a collection of systems and minimizing the total completion time associated with repairing resources that are unavailable is now proved mathematically. As in the examples above, resource availability is observed at the beginning of a time period and the availability of a particular system is quantified by the total number of items produced by that system after a time period of length *T*. In this context, availability is measured by the total number of items produced collectively by the systems (resources) during the time interval [0, *T*].

In this situation A_i represents the availability of job i, C_i symbolizes the completion time of job i, p_j is the maintenance processing time for the jth job, and *N* is the total number of jobs. Thus we have: $A_i = T - C_i$.

The maximum availability is $max(\sum_{i=1}^{N}(T - C_i))$. This is equal to both of the following:

$max \sum_{i=1}^{N} T - \sum_{i=1}^{N} C_i$ and $NT - \sum_{i=1}^{N} C_i$. It can also be written as, $max(-\sum_{i=1}^{N} C_i)$ since NT is

constant. Therefore, by duality, $mn \sum_{i=1}^{N} C_i$.

Maintenance Scheduling Environments

(Littlejohn and Stanfield (2005)) discuss two types of maintenance scheduling approaches that are found in manufacturing supply chain environments. In both approaches, the objective is to minimize the total completion time of scheduled jobs. The first approach is identified as, "Total Operation Completion Time Scheduling". This approach is observed when offline maintenance tasks are performed. For these environments, a part that needs work performed on it is removed and replaced by a part that is performing properly. The removed part is worked on at a separate location and only returned to service after maintenance work is completed. The formula presented by Littlejohn and Stanfield for this approach to maintenance is as follows:

$$min \sum_{i=1}^{N} \sum_{j=1}^{T} \sum_{k=1}^{M} \sum_{l=1}^{Z} (N - j + 1) * p_{ijk} * x_{ijkl} \tag{1}$$

$$\sum_{k=1}^{M} \sum_{l=1}^{Z} x_{ijkl} = 1, \forall\, i = 1 \ldots N; j = 1 \ldots T \tag{2}$$

$$\sum_{i=1}^{N} \sum_{j=1}^{T} x_{ijkl} \leq 1, \forall\, k = 1 \ldots M; l = 1 \ldots Z \tag{3}$$

$$x_{ijkl} = 0 \text{ or } 1 \tag{4}$$

Equation (2) ensures that each job and worker has exactly one position at a time. Equation (3) ensures that all positions have at most one job on a worker at a time. Equation (4) is a constraint that explicitly denotes x_{ijkl} as a binary decision variable.

For the second approach, multiple maintenance tasks must be performed in order for a system (ex.: assembly process, transportation truck, etc.) to be classified as ready to be used. The tasks are independent from each other. For example, consider a materials supply truck that is used to transport component machine parts from a supplier to a manufacturing plant. The truck has preventive maintenance scheduled several times a year in the following categories: engine maintenance, tire maintenance, and paint job. Each task can be completed separately from the other tasks. It is also possible for the simultaneous completion of these tasks. Since the truck is not considered ready to be used until all of these tasks are completed, the last task to finish determines the completion time for the system (where in this case the system is the supply truck). This approach is identified as, "Maximum Operation Completion Time Scheduling". The formula they presented for this approach is as follows:

$$min \sum_{i}^{N} IJF_i \tag{5}$$

$$IJF_i = \max(woc_{jkl} * d_{ijkl}), \forall\, i = 1 \ldots N \tag{6}$$

$$woc_{jkl=1} = \sum_{i=1}^{N} t_{ijk} * d_{ijkl}\ \forall\, j = 1 \ldots T; k = 1 \ldots \omega; l = 1 \tag{7}$$

$$woc_{jkl=1} = \sum_{i=1}^{N} t_{ijk} * d_{ijkl} + woc_{jkl-1}\ \forall\, j = 1 \ldots T; k = 1 \ldots \omega; l = 2 \ldots O \tag{8}$$

$$\sum_{k=1}^{\omega} \sum_{l=1}^{O} d_{ijkl} = 1\ \forall\, i = 1 \ldots N; j = 1 \ldots T \tag{9}$$

$$\sum_{i=1}^{N} d_{ijkl} \leq 1\ \forall\, j = 1 \ldots T; k = 1 \ldots \omega; l = 1 \ldots O \tag{10}$$

$$d_{ijkl} = 0 \text{ or } 1 \tag{11}$$

Equation (6) defines the completion time of a job as the maximum of the operation completion times within that job. Equation (7) is used to figure out the time that an operation by worker type j is completed by individual worker k at position l when l is greater than 1. Equation (8) calculates the time that operation j is completed by worker k at position l when $l=1$. Equation (9) ensures that every job is assigned to only one position for a

worker. The next formulation ensures that for every worker type, at most one parallel worker is assigned to any job i. Equation (11) ensures that the decision variable, x_{ijkl} is binary.

This section has discussed maintenance and its importance in manufacturing environments. Two scheduling formulation were presented. These formulations can be used to increase the availability of resources at any point in a supply chain.

VI. CONCLUSION

This article has presented a discussion on flexibility in manufacturing systems. Important issues for consideration in flexible supply chains have been highlighted. The application of flexible manufacturing system technologies can improve the ability of some general manufacturing environments to meet the needs of customers. Maintenance requirements are ubiquitous within the supply chain for any manufacturing environment. Flexible manufacturing environments cannot exist in environments that have view maintenance as a low priority. Efficient maintenance scheduling is an important tool for any manufacturing environment. If properly understood and applied, good maintenance practices can greatly enhance the performance of any manufacturing supply chain and facilitate the creation of genuine flexible manufacturing systems.

REFERENCES

[1]. Angel, Martínez Sánchez; Manuela, Pérez Pérez. (2005). Supply chain flexibility andfirm performance. International Journal of Operations & Production Management,Vol. 25 Number 7.

[2]. Fatemi, Matin (2010). Supply Chain Flexibility: Definition and Review. European Journal of Economics, Finance and Administrative Sciences, Iss: 20.

[3]. Grigore, Simona Daniela. (2007). Supply Chain Flexibility. Romanian Economic Business Review. Vol 2. Iss:1, pp.66-70.

[4]. Inman, A. R.. (2010). Flexible Manufacturing. Encyclopedia of Business, 2nd edition. Available from: http://www.referenceforbusiness.com/management/Ex-Gov/Flexible-Manufacturing.html

[5]. Leslie K. Duclos, Robert J. Vokurka, Rhonda R. Lummus, (2003) A conceptual model of supply chain flexibility. Industrial Management & Data Systems, Vol. 103 Iss: 6, pp.446 – 456.

[6]. Littlejohn, S. Craig; Stanfield, Paul. (2005). Maintenance Worker Scheduling in A Military Environment. Institute for Industrial Engineers Conference.

[7]. More, D., & Babu, A. (2008). Perspectives, practices and future of supply chain flexibility. International Journal of Business Excellence, Vol. 1 Iss: 3, DOI: 10.1504/IJBEX.2008.017885.

Research Paper   Open Access

Indicators of energy efficiency in ammonia productions plants

Flavio V. Tavares, Luciane P. C. Monteiro, Fernando B. Mainier
Programa de Pós-Graduação em Engenharia Química, Escola de Engenharia, Universidade Federal Fluminense, Niterói, RJ, Brazil

Abstract: - This paper presents and analyzes tools for the assessment of energy efficiency in ammonia production plants using key performance indicators (KPI). Monitoring the consumption of inputs in the industry could generate reductions in greenhouse gas emissions while simultaneously producing gains in energy efficiency in industrial operations. The continuous monitoring of performance indicators relative to emissions data and the consumption of natural resources allows for effective and direct intervention, resulting in improvements in production processes and operating practices. The use of such information by operating teams, in conjunction with management actions focused on continuous improvement, could lead to energy efficiency gains, a reduction in greenhouse gas emissions, and make production processes more profitable.

Keywords: - *Ammonia, Energy Efficiency, Greenhouse Gases, Key Performance Indicators (KPI).*

I.   INTRODUCTION

With increasing demands for their products, industrial chemical manufacturers are being subjected to a number of national and international pressures to reduce greenhouse gas emissions. In addition, investors are demanding lower production costs in conjunction with higher production gains. Thus, advances in the control of production processes focused on reducing losses, the strict monitoring of resource consumption, and the energy efficiency of their production processes have become essential activities in the routine operation of chemical production plants.

Data published in 2007 by the Organization for Economic Co-operation and Development (OECD) show that global emissions of greenhouse gases will increase by 50% by 2050, mainly as a result of increased demand for energy and economic growth in large countries with emerging economies. According to the organization, emissions of carbon dioxide (CO_2), one of the main gases causing the greenhouse effect, are expected to grow by 70% by 2050 as a result of increasing energy use [1].

The industrial system is one of the largest energy consumers in Brazil and throughout the world. Energy costs may represent about 10% of the production costs. A common and very important input in the industry is water vapor. This input is used in the generation, transmission and use of energy. Much of the electricity generation in the northern hemisphere uses water vapor as the working fluid in thermodynamic cycles. About 40% of the fossil fuel burned in U.S. industry is used in the generation of steam. The steam generated is, in turn, used in heating processes to concentrate and purify liquids, but it can also be used directly as feedstock [2, 3, 4].

An analysis of steam systems indicates that in a typical industry that does not employ preventive or predictive maintenance techniques, 28% of steam traps have problems. To improve the use of steam, industries must employ an appropriate method for testing steam traps to identify leaks, making repairs or replacing faulty traps when required.

Electricity is an essential input for industrial activity, and ensuring its delivery, quality, safety and affordability is essential for the development of the global economy and the growth of industrial production. Figure 1 shows the electricity consumption in Brazil and in other countries of the world.
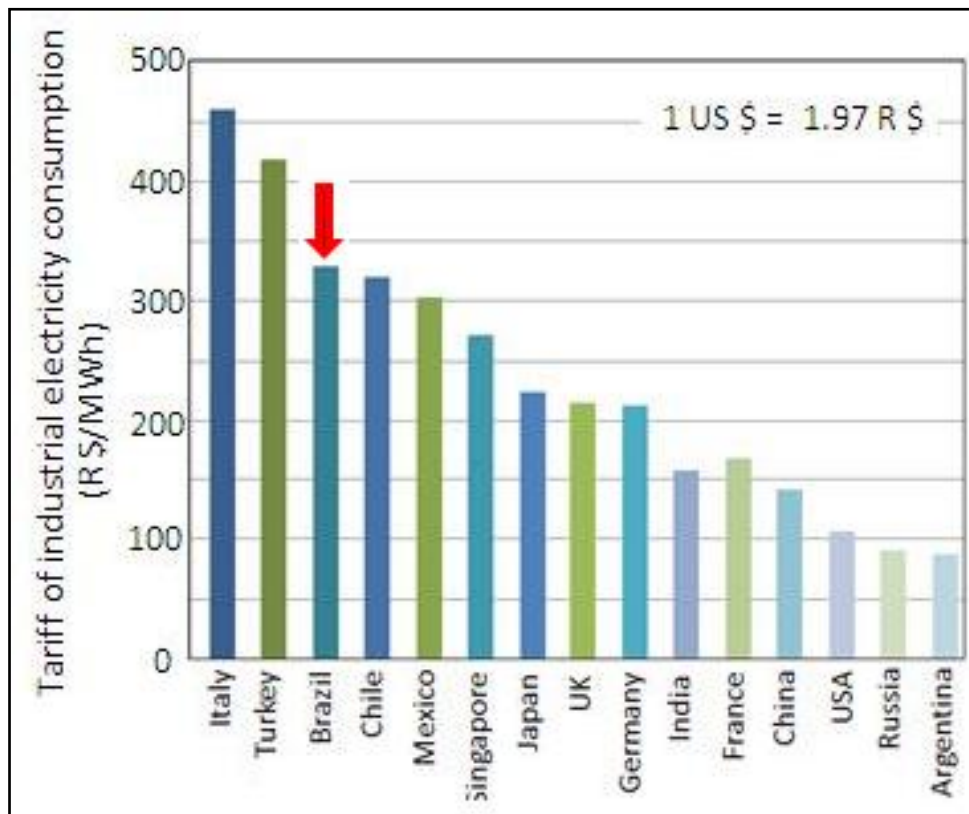
Figure 1- Tariff of industrial electricity consumption based on the Brazilian currency (Real $)

A more detailed analysis of production processes can identify potential areas for reducing manufacturing costs. An interesting strategy for reducing the consumption of inputs focuses on energy efficiency for both new and existing systems. Energy efficiency can be seen as an interesting means of reducing manufacturing costs. It can generate immediate and attractive returns, and may also provide robustness in the sustainability and profitability of operations. An effective management process begins with an analysis of energy consumption and greenhouse gas emissions. The results of such an analysis should be considered in any decision-making processes.

II.   AMMONIA PRODUCTION PROCESS

Ammonia is one of the fundamental raw materials required for modern civilization. The raw materials for the production of ammonia are hydrocarbons, air, and energy, which is essential for all industrial operations. Commonly used energy sources are coal or hydrocarbons, which react with water vapor at high temperatures, and electricity, which is used in the operation of gas compressors. Natural gas (CH_4) is the hydrocarbon used most frequently in ammonia production, with about 80% of current global production being based on natural gas. There are three main types of processes currently used for the production of ammonia:

- steam reforming from natural gas or other light hydrocarbons (natural gas liquids, naphtha);
- partial oxidation of heavy oil or waste oil;
- gasification of coal.

Figure 2 illustrates the steam reforming process of ammonia production.

The natural gas produced in Brazil is contaminated with potentially poisonous sulfur compounds (H_2S). These compounds are typically removed from the natural gas stream, in a process known as desulfurization, using a cobalt molybdenum catalyst [5].

The resulting gas (CH_4), which still contains about 0.1 ppm (parts per million) sulfur after going through this process, is then blended with the steam. This mixture is heated to between 500 and 600 °C and introduced into the main reformer (in some cases, however, an adiabatic pre-reformer precedes the primary reformer).
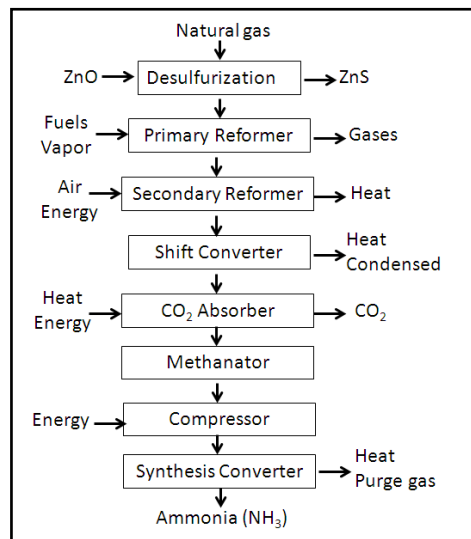
Figure 2 - Flowchart of ammonia production using the steam reforming process

The flue gases leaving the radiant section of the furnace reformer have exit temperatures approaching 1000 °C. Only 50–60% of the fuel heat is directly used in the ammonia production process itself, but the enthalpy of the combustion gases is utilized in the convection section of the reformer for the generation of steam or for other process requirements.

The process gas effluent from the primary reformer is directed to the secondary reformer, which receives the process air intake. The process air serves to enhance the combustion reactions and provide the nitrogen (N_2) necessary for the synthesis reaction. The gas/air mixture exits the secondary reformer at a temperature of 1000 °C, and 99% of the original gas feed is converted. The process gas is then cooled to between 350 and 400 °C and is used to power a steam boiler or a waste heat recovery boiler.

After conversion of CO to CO_2, the gas, which generally contains about 20% CO_2, is subjected to either a chemical or a physical process. The absorption process is followed by adsorption facilitated by a pressure decrease with increasing temperature. CO_2 removed from the process is used mainly for the production of urea, injection wells in crude oil production, dry ice production, and in other industries.

At this point, only small amounts of CO and CO_2 remain in the synthesis gas stream. They must be removed, however, because they are poisonous to catalysts of ammonia synthesis.

In the next step (known as methanation), the small amounts of CO and CO_2 react with a given amount of hydrogen to produce methane (CH_4) and water in a reactor containing a nickel catalyst at a temperature of about 300 °C.

After separation of the condensate, the stream of process gas, called synthesis gas, reaches the ammonia synthesis section. This reaction occurs at pressures that are normally in the range of 100–250 bar. The ammonia synthesis occurs in an exothermic reaction that makes use of iron catalysts at temperatures of 350–550 °C. Because of the high exothermicity of the reaction, a comprehensive and efficient heat exchange mechanism is essential. Only 20–30% of the synthesis gas is converted to ammonia on each pass through the converter. For this reason, a synthesis loop is required, with the ammonia being separated by cooling and condensation, and the effluent vapor being mixed with fresh synthesis gas and returned to the converter.

The cooling and condensation of ammonia is achieved via an auxiliary refrigeration cycle using ammonia vapor in order to achieve satisfactory results at the low concentrations of ammonia gas returned to the converter.

In integrated plants, the ammonia that is synthesized can be used directly in, for example, the production of urea or nitric acid.

III.   USE OF INDICATORS OF ENERGY EFFICIENCY IN INDUSTRY

The energy consumption in industrial processes can be determined by taking the level of activity, the industry structure and energy efficiency into account. Changes in energy consumption in industry are not only determined by energy efficiency in industrial processes but also by other political, economic and environmental factors. Additional factors, such as the production capacity and lifetime of the plant, should be considered in any analysis of energy efficiency [6, 7, 8].

The use of indicators aimed at evaluating the efficiency of processes in industry is growing in importance on a national and global level. The results of an analysis of energy efficiency indicators may be useful in the areas of strategic planning, management and environmental technology, and energy conservation. In practice, it is worth noting that the application of the analysis of these indicators and their relevance in describing the interrelationship between energy efficiency and resources consumed are associated mainly with the economic and political environment within the industry.

The use of indicators can have an impact on production processes. In industry, the analysis of energy efficiency indicators can help define relevant guidelines, such as:

- directing changes in energy consumption
- establishing energy-efficient policies
- indicating structural constraints that have an impact on increasing energy efficiency
- replacing technological processes
- changes in the use and choice of raw materials that are used in manufacturing processes, with the goal of reducing the demand for energy
- serving as a tool to assess goals for environmental policies aimed at the reduction of gaseous emissions

According to Abreu et al [9], indicators commonly used for the analysis of energy efficiency in industry can be subdivided into four groups: thermodynamic, physical-thermodynamic, economic-thermodynamic, and economic. Indicators that can be analyzed according to the laws of thermodynamics are included in the first group. The physical-thermodynamic indicators are also known as specific indicators. They are used to evaluate an input in relation to a particular production output. The third group provides a measure of the final product at market prices relative to thermodynamic units. The fourth group of indicators evaluates the changes caused by energy efficiency, in monetary terms, and can be considered to evaluate both the incoming and outgoing energy of a given process.

Based on thermodynamic laws, energy can be defined as the theoretical maximum useful work obtained when a system is brought to thermal equilibrium with the environment by means of processes in which the system interacts only with its environment [10].

According to Saidur et al [3, 4], the exergy is a direct function of the laws of thermodynamics. A property that determines the potential for useful work in a certain amount of energy in a specific state can be represented by Equation 1,

$$Ex = (H - H_O) - T_O (S - S_O) \qquad \text{(eq. 1)}$$

where the exergy (Ex) is a function dependent on the enthalpy (H) of the entropy (S), the absolute temperature (T) and also of the pressure and composition of the system. The subscripts represent the enthalpy and entropy conditions in the vicinity of the system.

Starting from an exergetic balance for a hypothetical system, it becomes feasible to direct the construction of an indicator. The exergy (Ex) is the difference between the sum of flows entering the exergetic system (ΣEx_e) through sources of fuel and raw materials, their losses (ΣEx_s) and losses that are consumed in the process (ΣEx_c) as represented by Equation 2.

$$Ex = \Sigma Ex_e - \Sigma Ex_s - \Sigma Ex_c \qquad \text{(eq. 2)}$$

The concept of exergy can be useful in analyzing aspects related to the life cycles of products as the exergetic content can determine the flow of energy lost. According to Dincer et al [11], exergy can be considered as a link between the thermodynamic concepts and systems engineering processes in relation to the environment from the viewpoint of energy efficiency.

The literature presents several studies that define and characterize the energy efficiency of industrial processes on the basis of macro indicators, which report on the economy as a whole (macroeconomics), or on the basis of individual industrial sectors with their specific production outputs [12, 13].

IV.   METHODOLOGY

To calculate net energy efficiency, the annual production of ammonia and the energy used in its manufacture were taken into account. All feedstocks (direct and indirect) and fuels consumed in an ammonia production plant were considered in this study.

The energy plots considered in the calculation of the indicators were, among others, those relating to energy for the production of ammonia, the energy used for starting the plant, the energy consumed during unplanned shutdowns, and any reduction in the lifetime of the catalysts (possible deteriorations). We also considered the annual performance against the expense of efficiency projects.

To facilitate the analysis between the different ammonia production plants, it was necessary to develop a basis for comparison. This normalization was performed according to the different configurations of the plants analyzed. The following are some of the considerations that were taken into account:

- imported electricity was converted to its heat equivalent, assuming 40% efficiency based on the lower calorific value of the fuel;
- the import and export of steam corresponding to a 90% conversion efficiency was considered as a reference for saturated steam at 150 °C;
- the baseline for the production of liquid ammonia was considered to be 100% under atmospheric pressure conditions and a temperature of -32 °C;
- the energy used to produce and pump cooling water was considered in the calculation for the share of energy use;
- the amount of energy used to produce and pump feed water for boilers was considered in the calculation for energy use;
- No adjustments were made on the basis of different technologies, climate conditions, catalysts used or operational problems.

To analyze energy efficiency, 50 ammonia production plants and their individual annual product outputs were included in the study. The energy efficiency indicator was calculated according to Equation 3,

$$\eta = (R + C_f + Z)/M_{NH3} \qquad \text{(eq. 3)}$$

where:

η = energy efficiency (GJ/t_{NH3})

R = the conversion of raw materials consumed in equivalent energy, assuming the lower calorific value

C_f = the conversion of fuel used in the process in equivalent energy, assuming the lower calorific value

Z = other energies involved in the process, such as electricity and steam imported, export credit for energy (steam) generation, and pumping water to supply boiler and cooling water

M_{NH3} = ammonia production in metric tons

      The part related to ammonia production was considered to be the maximum daily production at the expense of the production capacity of the plant design. The plants were divided into three categories. Of the 48 conventional plants (plants that utilize steam reforming), 12 were classified as small, with ammonia production values of less than 1000 t/day (metric tons per day), 17 plants were classified as intermediate, with production values of 1000–1500 t/day, and 19 plants producing more than 1500 t/day were classified as large.

V.   RESULTS AND DISCUSSION

      The annual production capacities of the ammonia plants analyzed are shown in Figure 3. The production capacities ranged from 91,000 t/y to 749,800 t/y. The values found in the evaluation of the energy efficiency indicator ranged from 23.8 GJ/t NH_3 to 51.9 GJ/t NH_3. Of the 50 plants analyzed, two used high purity hydrogen as a feedstock. These plants typically have higher levels of efficiency when compared with other plants. The 48 conventional ammonia production plants use various raw materials such as natural gas or heavy oil derived from petroleum fractions.
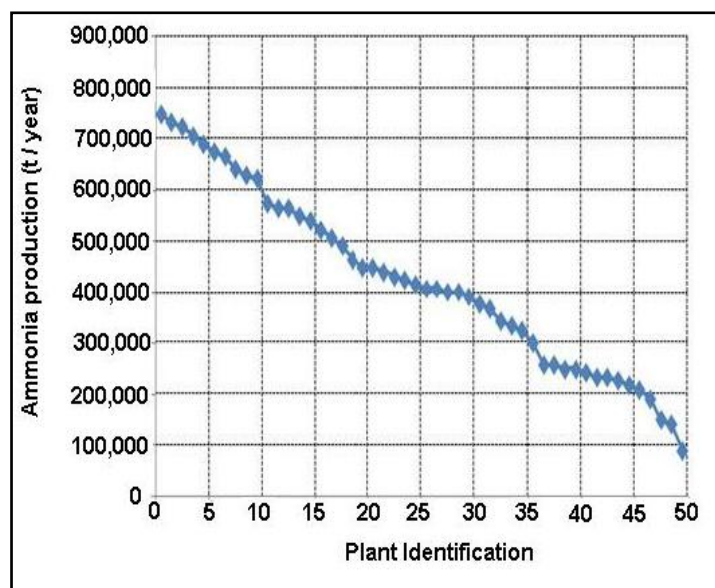
Figure 3 - Annual production of ammonia (metric tons)

Figure 4 shows the energy efficiency indicator for each ammonia plant.
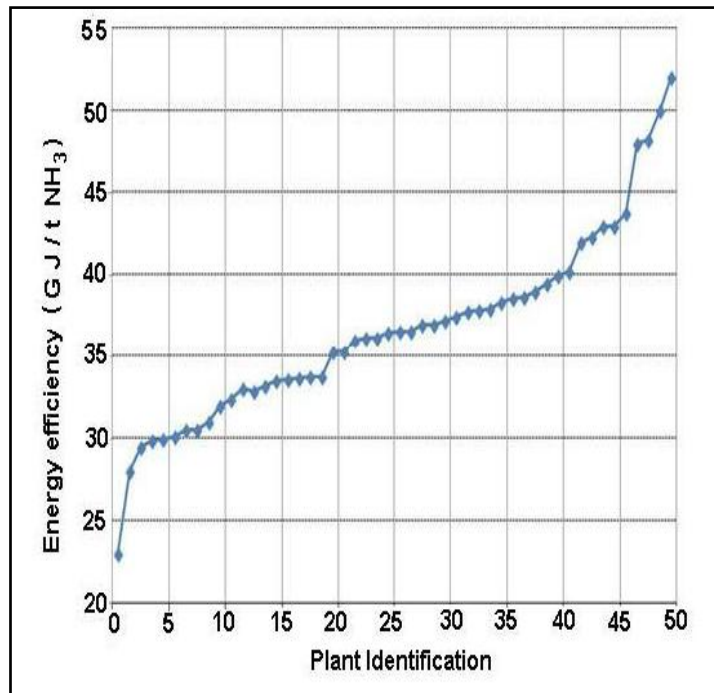
Figure 4 - Energy efficiency (GJ/t NH$_3$) for ammonia production plants

The relationship between capacity and energy efficiency for the 48 conventional ammonia production plants is shown in Figure 5.
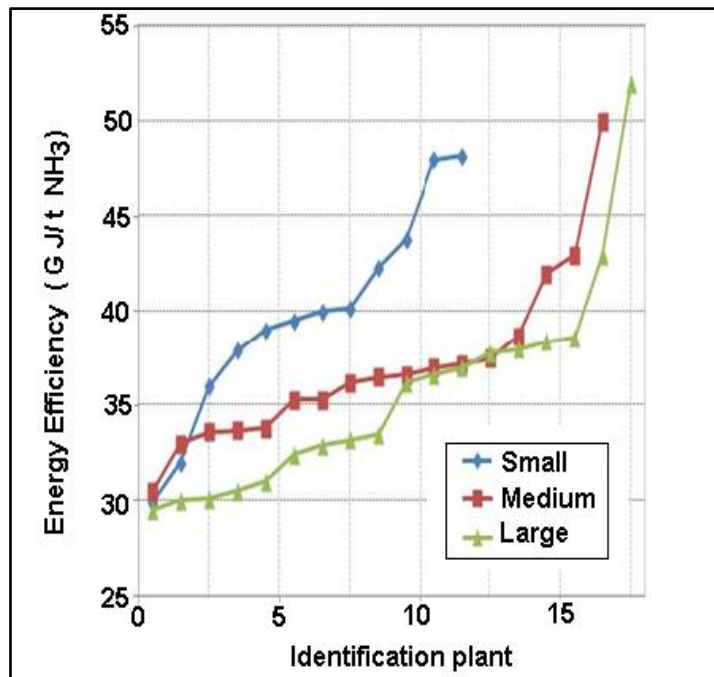
Figure 5 - Energy efficiency (GJ/t NH$_3$) in the capacity of ammonia production plants of varying production capacities

From the analysis of Figure 5 we see that there is a relationship between the production capacity and efficiency of the plants analyzed. In general, plants with higher capacity have higher energy efficiency and plants with smaller capacity are less energy efficient. However, the best plants in each group have energy efficiency rates ranging from 29.5 GJ/t NH$_3$ to 30.6 GJ/t NH$_3$, indicating that plants with a capacity lower than

1000 t/d may still be energy efficient.

Figure 6 shows the calculation of the energy efficiency indicator as a function of the age of each plant. The age of each plant varies from between 1.5 and 39 years. The plants were divided into three categories. Those classified as new are less than 14 years old. Plants between 18 and 29 years old were classified as intermediate, and plants older than 30 years were classified as old.
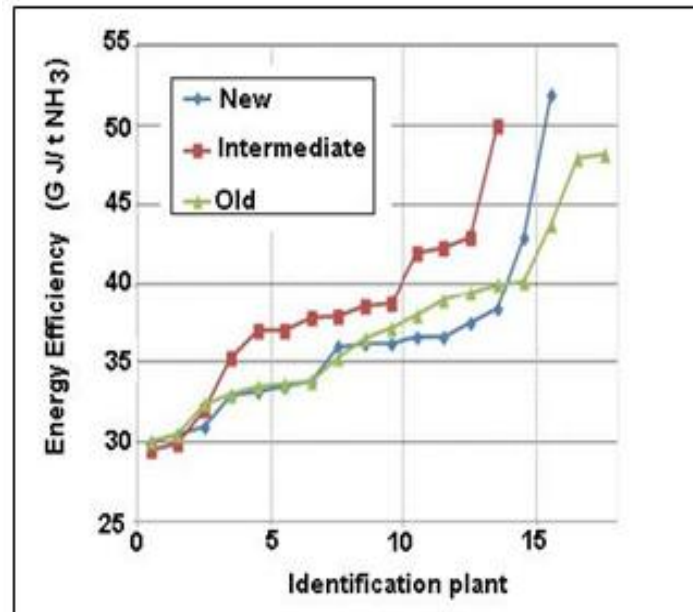
Figure 6 - Energy efficiency as a function of the age of the ammonia production plants

Of the 48 conventional ammonia production plants analyzed, those classified as new showed better average energy efficiency indicators, with a net energy efficiency of 36.0 GJ/t NH_3 for 16 plants analyzed in this group. Plants classified as intermediate (14 plants) displayed an average energy efficiency of 37.7 GJ/t NH_3. The plants classified as old showed an average result of 37.4 GJ/t NH_3.

The best plants in each group have energy efficiency ratings of about 30 GJ/t NH_3. This observation indicates that even plants that have been operational for longer periods of time can, through modifications and improvements in their processes operate at good levels of energy efficiency.

VI.   CONCLUSIONS

This work presents an evaluation of the energy efficiency of ammonia production plants through the use of indicators. Data from 50 ammonia plants were considered in this study. The energy efficiency indicator was based on the annual production of ammonia and took into account the equivalent amounts of energy consumed in the consumption of raw materials, fuels, and other forms present in the process, such as the energy consumption equivalent of the generation and distribution of cooling water, and the import or export of steam, among others.

Comparisons were made on the basis of the designs of the plants and the production processes used. Other comparisons took into account the energy efficiency of the plants. We presented energy efficiency rates as a function of the age of plants and also as a function of annual production. It was found that there is a direct relationship between production capacity and energy efficiency.

REFERENCES

[1]   S. Nakano, A. Okamura, N. Sakurai, M. Suzuki, Y. Tojo, and N. Yamano, *The Measurement of CO₂ Embodiments in International Trade: evidence from the harmonized input-output and bilateral trade database*, Organization for Economic Co-operation and Development (OECD), February, 2009.

[2]   D. Einstein, E. Worrdell and M. Khrushch, *Steam systems in industry: energy use and energy efficiency improvement potentials*, Lawrence Berkeley National Laboratory, 2001.

[3]   R. Saidur, J. U. Ahamed and H. H. Masjuki, Energy, exergy and economic analysis of industrial boilers, *Energy Policy 38, 2010. 2188-2197.*

[4]　R. Saidur, Energy savings and emission reductions in industrial boilers, *Thermal Science, 15, 3, 2011, 705-719.*

[5]　F. B. Mainier, G. C. Sandres and R. J. Mainier, Integrated Management System for in-House Control of Accidental Hydrogen Sulfide Leaks in Oil Refineries, *International Journal of Science and Advanced Technology, volume 2, issue 9, September, 2012, 76-84.*

[6]　E. Worrell, L. Bernstein, J. Roy, L. Price, S. R. Cardan and J. Harnish, Industrial Energy Efficiency and Climate Change Mitigation, Lawrence Berkeley National Laboratory, February, 2009.

[7]　 M. G. Patterson, What is energy efficiency?: concepts, indicators and methodological issues*, Energy Policy 24, 5,1996, 377-390.*

[8]　K. Bunse, M. Vodicka, P. Schönsleben, M. Brülhart and F. O. Ernst, Integrating energy efficiency performance in production management – gap analysis between industrial needs and scientific literature, *Journal of Cleaner Production, 19, 6-7,2011, 667-679.*

[9]　Y. V. Abreu, M. A. G. Oliveira and S. M. G. Guerra, *Energia Sociedade e Meio Ambiente*. Universidad de Malaga, 2009.

[10]　M. E. Toxopeus, E. Lutters and F. Houten, Environmental Indicators & Engineering: an Alternative for Weighting Factors, *13th International Conference on Life Cycle Engineering*, 75, 2006.

[11]　I. Dincer, M. M. Hussain and I. Al-Zaharnah, Analysis of sectorial energy and exergy use of Saudi Arabia, *International Journal of Energy Research, 28, 2004, 205-243.*

[12]　D. Urge-Vorsatz, A. Novikova, S. Koppel and B. Boza-Kiss, Bottom-up of potentials and cost of CO_2 emission mitigation in the buildings sector: insights into missing elements, *Energy Efficiency, 2, 2009, 293-316.*

[13]　 I. Rafiqui, C. Weber, B. Lehmann and A. Voss, Energy efficiency in ammonia production – perspectives and uncertainties, *Energy,* 30, 13, 2005, 2487-2504.

Research Paper   **Open Access**

Proprietary software versus Open Source Software for Education

N. Pankaja[1], Mukund Raj P K[2]
[1]EMRC (Electronic Media Research Center, India)
[2](MLRCC/ University of Mysore, India)

Abstract: - The Internet has brought learning "online" and offers many advantages. It is convenient, available at any time of the day, and can be accessed nearly anywhere in the world. Recently, Cloud computing is all the rage. E-Learning offers tremendous potential to increase the availability and convenience of education. Today, online content is varied and can include: text on a website, digital audio, digital video, animated images, and virtual reality environments. This content can be created in a variety of ways by utilizing a variety of authoring tools and softwares. These days, we observe a movement in higher education leading from proprietary software to open source, for e-learning applications (1) In fact, open source software (OSS) development can provide the necessary flexibility to combine languages, scripts, learning objects and lesson plans, effectively, without the cost and rigidity of proprietary software. In recent years, numerous open access LMS software's have emerged as viable alternatives to costly proprietary and commercial products. Open source software's of Content Management Systems (CMS) and Learning Management System (LMS) are gaining popularity. We weigh the pro's and cons of utilizing the OSS and proprietary software in this paper.

I. INTRODUCTION

The Internet has brought learning "online" and offers many advantages. It is convenient, available at any time of the day, and can be accessed nearly anywhere in the world. E-Learning offers tremendous potential to increase the availability and convenience of education. When e-Learning is made accessible and Section 508 compliant, it enables employees with disabilities to receive equivalent access to training materials used by their peers. As with many types of products and technologies, including those used in e-Learning, people with disabilities may inadvertently be excluded if accessibility is not considered and incorporated into products and technologies. However, accessibility is not only of concern to those with disabilities. The potential for e-Learning expands when developers embrace the widest possible range of individual learning styles, preferences, and abilities. Today, online content is varied and can include: text on a website, digital audio, digital video, animated images, and virtual reality environments. This content can be created in a variety of ways by utilizing a variety of authoring tools and softwares. e-learning means a combination of Content Management System (CMS) and Learning management system (LMS). We shall henceforth call the combination of CMS and LMS a total solution. There are only two choices of a total solution for an educational system – either opt proprietary software or an open source software system. Hence any institution will have to evaluate their choices. The total solution plays an ever increasing and prominent role in the teaching and learning process, paving a new road changing the existing ways of teaching and learning, from a traditional in class way to totally synchronous or asynchronous distant one. While CMS is the front end for the total solution, LMS is the back-end. These days, we observe a movement in higher education leading from proprietary software to open source, for e-learning applications (2). In fact, open source software development can provide the necessary flexibility to combine languages, scripts, learning objects and lesson plans, effectively, without the cost and rigidity of proprietary packages (3) The purpose of this paper is to consider the challenges posed by educational systems into choosing either a proprietary system or an open source systems and the criteria that is to be adopted to choose from either.

II.   SOFTWARE'S AND ITS MODELS

Software (SW) can be shortly defined as the executable code that controls computer behaviour and operations. The term is used, however, to describe a wide range of programming languages, applications, procedures and all related documentation resources. SW also refers to a full cycle of processes from basic architecture to development, packaging and distributing. It is responsible for controlling, integrating, and managing the individual hardware components of a computer system so that other software and the users of the system see it as a functional unit without having to be concerned with the low-level details of the computational system. There are three models of software's for developing any application in computer. They are Freeware, Shareware, Trialware, Proprietary, Public Domain Software and Open Source.

2.1 Freeware

It is provided to be used without any monetary charges. However, severe restrictions of its use, modification and redistribution are still imposed and Source code is not provided. It can be passed on to anyone free of cost.

2.2 Open-source software (OSS)

It is a computer software with its source code made available and licensed with an open-source license in which the copyright holder provides the rights to study, change and distribute the software for free to anyone and for any purpose. Open-source software is very often developed in a public, collaborative manner. Open-source software is the most prominent example of open-source development and often compared to (technically defined) user-generated content or (legally defined) open-content movements

2.3 Proprietary Software

The term proprietary is derived from the Latin word proprietas meaning property. Proprietary Software is computer software licensed under the exclusive legal rights of the copyright holder. Proprietary software is developed by a person or firm who has rights of using existing or developing new tools to create new software. A proprietary software developer sells or provides his creation under some concrete conditions which should be followed in order to avoid any legal issues. In general, these concrete conditions involves usage using software with a purchased license, within the permitted boundaries, no modification allowed, no further re-distributions and no reverse engineering to applied. The main identity of proprietary software is that its source code is always kept secret from outside world. Thus, the internal structure of proprietary software is not exposed. The restrictions on proprietary software are generally imposed through a document called EULA (End-user license agreements) to which users are supposed to agree before using the software. It works just like a contract of usage conditions between the user and vendor. If a user is found indulged in activities leading to the breaking of copyright conditions, the selling authority has the right to impose legal actions against the misusing personal.

2.4 Public Domain Software

The copyright holder donates it to the public. Thus, it is no longer copyrighted and restricted and thus moves towards Open source.

2.5 Shareware

It is generally that version of software which is limited in terms of functionality. Users can download it from internet, uses it with restrictions and then decide to pay for its full version. These can be shared among other people.

2.6 Trialware

It is generally that version of software which is limited in terms of duration of use. User gets the full version of software which can be limited to the usage number of days or usage number of times. After paying and getting registered, the user will get unrestricted access to usage and updates of that software.

III.   PROPRIETARY AND OPEN SOURCE SOFTWARE

Assuming that an educational institute requires developing, implementing and deploying an e-learning solution We will now focus on the OSS and Proprietary software for the purpose of this paper Before we proceed to evaluate OSS and Proprietary software, let us first understand both of them.

3.1 Definition of Proprietary Software:

Software that is distributed under commercial license agreements is usually for fee. The main difference between the proprietary software license and the open source license is that the recipient does not normally receive the right to copy, modify, or redistribute the software without fees or royalty obligations.

Something proprietary is something exclusively owned by someone, often with connotations that it is exclusive and cannot be used by other parties without negotiations. It may specifically mean that something is covered by one or more patents, as in proprietary technology. Proprietary software means that some individual or company holds the exclusive copyrights on a piece of software, at the same time denying other people the access to the software's source code and the right to copy, modify and study the software.

3.2 Definition of Open Source Software:

Software, whose source code is published and made available to the public, enabling anyone to copy, modify and redistribute the source code without paying royalties or fees. Open source code evolves through community cooperation. These communities are composed of individual programmers, users as well as very large companies. Some examples of open source initiatives are GNU/Linux, Eclipse, Apache, Mozilla etc

TABLE 1 – Proprietary versus Open source software

Details	Proprietary Software	Open Source Software
Cost	Varies from a few thousand to a few hundred thousand dollars, depending on the complexity of the system required. This cost is made up of a base fee for software, integration and services and annual licensing/support fees. This cost may be prohibitive for some; however what the user is paying for is a more customized product from a trusted brand that includes higher levels of security and functionality, continuous innovation, a greater ability to scale, on-going training and support and a lower requirement for technical skills.	OSS comes at a low cost because of Open source software. We don't need to get an expensive software or hardware to run the system. Organizations can use this system as long as they like, without thinking of paying any set up, activation, and monthly subscription charges
Service and Support	Service is probably the greatest advantage of using proprietary software. Proprietary software providers offer ongoing support to users, a key selling point for users without technical expertise. If the user manual or guide is not enough, or if a user experiences a problem with the software, there is an immediate point of call to turn to for assistance. There is a certain reduction in the risk undertaken with proprietary software because users are working with companies that are viable, and people with intimate knowledge of the products and services being used should any questions arise. Because service is one of the main reasons users choose proprietary over open source software, many proprietary software providers compete on service, increasing the bargaining power of buyers and thereby increasing customer service levels among providers.	While Service is one of the key issues regarding open source software. Open source software relies on its online community network to deliver learning support via forums and blogs. While there are massive, loyal and engaged online communities that users are turning to. This requires some basic knowledge and skill set from the user to understand feedback from online community and resolve them. Sometimes, the trouble shooting is faster than those of proprietary software. But users who query, should know what their actual problem is, else, they will not receive the right feedback.
Innovation	Proprietary software providers do not allow users to view or alter the source code. While this may be viewed as a disadvantage to some, it ensures the security and reliability of the software. Furthermore, many proprietary software providers customize software for specific users to provide more flexibility while investing in R&D in order to regularly offer new products and upgrades. Proprietary software providers have online user communities that create value by sharing ideas, strategies and best practices through feedback mechanisms such as forums and surveys, which also foster innovation and allow the product to adapt with changing needs. This innovation comes fully tested, and is available to all users of the software. It does not require investment in R&D or the technical understanding of source code, and assistance with implementation is generally part of the package. Because vendors must ensure their software does not become redundant, users also benefit from the type of targeted innovation undertaken- continuous investment in R&D rather than "innovation for innovation's sake", business focused rather than technology focused.	OSS enables innovation by providing users with the freedom and flexibility to adapt the software to suit, without restriction. However, innovation may or may not be passed on to all users of the software. It is a user's prerogative whether they wish to share their innovation with any online communities, and users must be actively participating in these communities to become aware of such innovations. It has been debated whether customized changes to the original source code limit the future support and growth of the software, as these can potentially result in a limited ability to apply future updates, fixes or modules aimed at improving the software, leaving the user with a version that may have irresolvable issues. It is relevant to note that open source software providers in the initial stages generally struggle to attract large scale R&D funding.

Security	There is always a debate on security. Many proprietary software based developed from proprietary operating systems are perceived relatively less secure to those from OSS. But the total solution from proprietary software is viewed as secure because it is developed in a controlled environment by a concentrated team with a common direction. Moreover, the source code may be viewed and edited by the team alone, and is heavily audited, eliminating the risk of back door Trojans and reducing the risk of any bugs or issues with the software.	Open source operating software is perceived as the most secure OS. Linux being a classic example. But total solutions developed from OSS are perceived less secure since the source code is already available freely to all, hence there may be chances for sabotage. Big players using OSS have robust security policies, hence security in big organizations using OSS is not an issue. Earlier, open source software was not always peer reviewed or validated for use. But currently, with the growing importance of OSS, they are reviewed and corrected. Examples of Drupal, wordpress, Joomla etc are there to see.
Usability	Proprietary software generally employs expert usability testing, and as the software is normally aimed at a more targeted audience, and therefore more tailored, usability is generally ranked quite high. In addition, detailed user manuals and guides are provided. This enables faster training and provides an immediate reference, allowing users to move along the learning curve more quickly. Supporting services include seminars, targeted training courses and extensive support to help maximise use of the software. It is also important to note that while many people see proprietary software as "closed", today's proprietary software offers a vast array of mechanisms for enhancement by third party systems and developers	Earlier OSS had been highly criticized for its lack of usability, as generally, the technology is not reviewed by usability experts and does not cater to the vast majority of computer users. Nowadays, OSS is tested by the community for usability and good solutions are being developed globally. Though, open source software does not legally require documentation such as user manuals or guides, hindering the creation of such tools, they are now well documented.
Standards	Describes software interfaces, protocols and electronic formats that are developed by and controlled by a given company and have not been made freely available for adoption by the industry. Some proprietary software uses proprietary standards, i.e. non-public interfaces or electronic formats. When an interface, a protocol or an electronic format is non-public, the owner of the proprietary interface controls it, including when and how the interface changes, who can adopt it, and how it is to be adopted (resulting in user lock-in).	"Open standards" software interfaces, protocols, or electronic formats that are openly documented and have been accepted in the industry through either formal or de facto processes, and which are freely available for adoption by the industry. The open source community has been a leader in promoting and adopting open standards. Some of the success of open source software is due to the availability of worldwide standards for exchanging information, standards that have been implemented in browsers, email systems, file sharing applications, and many other tools. Without open standards it would be impossible to interact and exchange information on the Internet.
Availability	These are available through their respected companies that own the rights to the packages. Sometimes, trial versions are available for free download and testing	These are freely available over the net. Some OSS are also developed into a limited proprietary software with 24X7 support from online community and the developer as well
Transparency	PS does not provide an open look to the internal structure. Only user interfaces are provided to work with it. User cannot know the internal processing and other details.	The source code of OSS is freely available along with the product. Any person can read, modify, build and distribute a modified version of original product. Thus, it gives a transparent look at the core structure of the product.
Reliability	PS is developed by specialized teams at vendor's end only. Only finished products are provided at outlets. Since there is no un-authenticated modification, the outcome is always reliable.	Since OSS are available on a large number of unverified websites and even most of these distributions may be modified by any technologically sound user, all the distributions are reliable in terms of security, robustness, performance. The reason is that is a user adds/modifies some component; it may works good individually, but, may clash with other components and ultimately degrade the product.

- Some Classic examples proprietary software include Microsoft (windows, asp.net, Internet explorer etc), Apple (Macintosh), Google (Gmail, Chrome etc)
- Some classic examples of OSS include Mozilla Firefox, Linux, Android etc

It is evident that for every successful and established open source software, we have an equivalent and sometimes more popular OSS.

IV. POINTS TO PONDER FOR OSS

This leads us to think, why OSS is gaining so much popularity. Why android based smart are phones more popular, why are Joomla, Drupal, Moodle equally popular to proprietary software like Sharepoint, Blackboard etc We now go back to the points the institution has to ponder while making a decision about procurement of a total solution. Some critical criteria are:

1. Budget
2. Stability
3. Flexibility
4. Scalability
5. Usability
6. Life of the solution/ software
7. Security
8. Knowledge base and Self reliance
9. Intellectual Property Rights (IPR)
10. Adaptability to various cross platforms and hardware like mobile, internet, tablet pcs, etc

We have discussed and compared most of these in Table 1.

V. QUICK RECON OF OSS

As a quick recon, we will peruse few points here:

6.1 Budget: Return on Investment (ROI) is critical to all educational institutions. It is becoming more evident that open source software is providing the ROI. It has been noticed that there is a tendency for software companies to over-specify IT solutions. This is an area where OSS precedes, proprietary software vendors.

6.2 Knowledge Base: Implementing an OSS solution requires knowledge base at the User (institution). Without technical know-how – it is difficult to manage OSS. With proprietary software, all help is just a call or email away

6.3 Intellectual Property Rights (IPR): OSS provides an excellent opportunity for the user to claim IPR of the final product, whereas with proprietary software, this is impossible. All said and done, only an Non Disclosure Agreement will provide a security to end user with regards to its practices and final solution. This is an area of growing concern and one of the main factors influencing use of OSS

6.4 Adaptability: The online community is providing many add-ons and plug-ins that enhance the final solution of an OSS, whereas with proprietary solution, this is limited. A glowing example would be the applications for android and joomla etc wrt other proprietary software

VI. WHY USE AN OPEN SOURCE SERVICE

Exactly like the personal computer and the Internet, open source software recently got the attention of the press as a totally new thing that 'suddenly appeared'. Many people believe that the impact of open source software in the information technology industry and in society in general will be huge, and without precedent in its nature, to the point that the current rules by which the software industry behaves will completely change.

Open source Software's: In recent years, numerous open access LMS software's have emerged as viable alternatives to costly proprietary and commercial products. Open source software's of LMS are gaining popularity. Some of the OS softwares are Moodle, Drupal, Wordpress, Blackboard, Joomla etc.

VII. RECENT SUCCESSES OF OSS

Recently OSS has become more of a mainstream product with many companies adopting it in their offices. OSS market share has also grown rapidly making many companies sit up and take notice of the OSS phenomenon.

• IBM recently announced that the company would devote almost $1 billion dollars to support Linux. (Burke, 2000)

• Forrester Research estimates that more than 55% of the world's 2,500 biggest firms use open source software, with almost a quarter using the software in production systems.

• Sun released Star Office, an office suite similar to Microsoft Office, under the GPL license.

To be sure, free/open source software still faces challenges. Both Red Hat and VA Linux, two of the most prominent corporate supporters of Linux, still lose money.

VIII.   OPEN SOURCE ADVANTAGES

9.1 Free Redistribution
The license does not restrict any party from selling or giving away the software as a component of an aggregate software distribution containing programs from several different sources. The license shall not require a royalty or other fee for such sale.

9.2 Source Code
The OSS includes source code, and allows distribution in source code as well as compiled form.

9.3 Derived Works
Most license allow modifications and derived works, and allow them to be distributed under the same terms as the license of the original software.

9.4 No Discrimination against Fields of Endeavour
The license does not restrict anyone from making use of the program in a specific field of endeavour. For example, it may not restrict the program from being used in a business, or from being used for genetic research.

9.5 Is not specific to a Product
The rights attached to the program does not depend on the program's being part of a particular software distribution. If the program is extracted from that distribution and used or distributed within the terms of the program's license, all parties to whom the program is redistributed have the same rights as those that are granted in conjunction with the original software distribution.

9.6 Not Restrict Other Software
The license does not place restrictions on other software that is distributed along with the licensed software. For example, the license does not insist that all other programs distributed on the same medium must be open-source software.

9.7 Technology-Neutral
Most of OSS is technology neutral.

IX.   POPULARITY OF OSS

The basic idea behind the open source movement more people look at the code on the internet, more people read it, more people adapt it, more people redistribute it, more people fix bugs and slowly you have this huge community of people which cannot be employed by a single corporation, all working for the same project and churning out new software at speeds which never could be achieved by conventional software development team. Cost is another factor. OSS is available for download freely. As compared to General idea of open source software, the initial cost of OSS is zero which is very attractive for start-ups and small businesses. Other advantages include reliability and a large number of software engineers working round the clock at no cost to the user. The contributors to the project could be distributed at different corners of the world making support and fixes available round the clock. The other reason for using OSS could be purely based on principles that open source is an ethical business model, all the source code is in the open and none of it is concealed and is good for the client or the user of the software to modify to fit them to their needs rather than depend and wait for the seller of the product to make changes.

X.   GENERAL IDEA OF OPEN SOURCE SOFTWARE

When we talk, in English, about 'free software', there is a dangerous ambiguity, due to 'free' meaning both 'freedom' and 'gratis'. Therefore, in this document, we will use mainly the term 'open source' when referring to users freedom of use, redistribution, etc., and 'gratis software' when referring to zero acquisition cost. The use of the Spanish and French word 'libre', by the way, has been adopted in many environments to refer to open source software, but will not be used here for the sake of uniformity.

XI.   RECENT SUCCESSES

Recently OSS has become more of a mainstream product with many companies adopting it in their offices. OSS market share has also grown rapidly making many companies sit up and take notice of the OSS phenomenon.

• IBM recently announced that the company would devote almost $1 billion dollars to support Linux. (Burke, 2000);

• Forrester Research estimates that more than 55% of the world's 2,500 biggest firms use open source software, with almost a quarter using the software in production systems. (Connor, 2000); • Sun released Star Office, an office suite similar to Microsoft Office, under the GPL license; To be sure, free/open source software still faces challenges. Both Red Hat and VA Linux, two of the most prominent corporate supporters of Linux, still lose money. Microsoft has various code sharing licensing methods under "Shared Source Initiative" program which details around 22 different licenses tailored around different industries and products.

XII.   WHOM OPEN SOURCE WILL HELP

Open source is not something you adopt because it is cool and everybody else seems to do it. If your business is doing absolutely fine in the sense that there are no existing issues that cannot be solved and no future opportunities that cannot be grasped within the traditional software development model, then the open source is probably not for those people.

12.1 Resource Constraint

Businesses usually do not have unlimited resources devoted to their endeavours. It is the responsibility of the management to optimize the allocation of limited resources to maximize profit. Constraints of resources surface in various forms. It prevents a great idea from turning into reality; it hampers the quality of the product due to the lack of proper quality assurance; it forces companies to continue sustained engineering for years to come instead of targeting new markets and developing new products. Open source strategy allows you to enlist an army of outside developers and testers to work for you "for free".

12.2 Strategic competition

When well managed, open source projects can change the landscape of the competition in a way the traditional software. First, there is the "free" factor. By offering a piece of software for free, the usage increases. Then there is the "peer" factor, which further increases the popularity of the free software. When something is popular, wonderful things happen. What you end up with is a product that packs increased functionalities, meets the customer requirements more precisely, is more reliable and integrates well with the rest of the world. In the end, your product competes better among peers, which in turn improves the standing of your company and motivates your employees to produce even better products. If your business faces similar challenges and these benefits are of interest to you, there are a few aspects of open source software that you need to evaluate in order to come to the conclusion whether open source is the right solution.

XIII.   CONCLUSION

In recent years, numerous open access software's have emerged as viable alternatives to costly proprietary and commercial products. Open source software's are gaining popularity. PS and OSS have advantages & disadvantages depending upon the application features they provide. PS have a long lasting stand in the computing era. Open source is fast gaining acceptability and is the future of e-learning. Many world class institutes have adopted Open source. We conclude with the following excerpt from The Guardian, 28 March 2013 (4). "There are clear cost savings available to adopting open source solutions. The University of London Computer Centre hosts Moodle for 2 million students across 150 UK higher and further education providers, many of whom have migrated from a closed source solution...."

REFERENCES

[1].   Coppola C, Neelley E (2004).
[2].   Coppola C, Neelley E (2004).
[3].   Williams, Roy (2003). 2nd European Conference on E-Learning Glasgow Caledonian University, Glasgow, 6–7 November 2003. Academic Conferences Limited.)
[4].   Scott Wilson, Open source in higher education: how far have we come? (the guardian, 28 March 2013)

Research Paper	Open Access

Time and Strain Response of Repeated Ageing Treatments on Recycled Al-Si-Cu Alloy

D.T. GUNDU[1], A. ASHWE[2], P. ADEKA[3]

[1,2,3] *(Department of Mechanical Engineering, University of Agriculture, Makurdi–Nigeria)*

Abstract: - The objective of this study was to investigate the time response of 3-stage artificial ageing treatments on strength properties of recycled Al-Si-Cu alloy with a view to obtaining useful empirical relationships for predicting required treatment cycles. True compressive stress, micro hardness and strain (%) were evaluated in response to ageing time and repeated ageing. The results of compression and hardness tests showed that alloy hardness and compressive stress increased with ageing time, and that these properties also increased with repeated ageing. The results also showed that alloy strain (%) reduced with ageing time and repeated ageing, indicating increasing strength or strain hardening of the alloy with repeated ageing. Using these results, empirical models of the form $\phi_n = \phi_0 e^{\alpha t}$, and $\phi_n = \phi_0 e^{\alpha N}$ are established for predicting the required ageing time and/or number of ageing treatments to raise the strength (or hardness) of an alloy to desired levels to meet service requirements. The strain response of the alloy is modelled as $\varepsilon_n = \varepsilon_0 e^{-\alpha t}$.

Keywords*: - time response, recycled Al-Si-Cu, repeated ageing, strength, hardness, straining*

I. INTRODUCTION

Aluminium alloys have become preferred materials for automotive components because of their light weight and good mechanical properties, offering also better strength to weight ratio materials for these industries [1,2,3]. Aluminium usage provides up to 55% weight savings when compared to steel- which translate into improved fuel economy and reduced greenhouse gas and pollution emission- while offering the same or better stiffness and crashworthiness. Energy savings from light weighting and the resulting increase in-use fuel efficiency far outweigh the energy cost of prime aluminium. However, if the aluminium used is recycled metal, even the energy to produce the metal can be reduced significantly. Re-melting of recycled metal saves almost 95% of the energy required to produce prime aluminium from ore, and thus triggers associated reductions in population and greenhouse emissions from mining, ore refining and melting [4,5]. Although most metals alloy with aluminium, few have sufficient solubility in it. Common addition elements are Mg, Cu, Ti, Na and Sr. Al-Si-Cu alloys within 7-10% silicon and 2-4% copper are mainly used for automotive and airplane parts because of their superior mechanical properties, weldability, castability, and machinability, and also combine high strength, high elongation and very good corrosion resistance.

Metals are generally strengthened by introducing lattice defects which provide obstacles to dislocation motion. The strength and hardness of certain aluminium alloys (and some other metal alloys) may be enhanced by the formation of extreme small and uniformly dispersed second phase particles within the original phase matrix in precipitation or age hardening process. The precipitate particles act as obstacles to dislocation movement and thereby strengthen the heat-treated alloy [1,2,4]. Several aluminium alloys have shown a marked response to age hardening [3,5].
The objective of this study was to investigate the time response of repeated ageing treatments of recycled Al-Si-Cu alloy, with a view of determining its suitability for production of high integrity parts.

II. MATERIALS AND METHODS

Assorted aluminium scraps were collected and cleaned of dirt mainly accumulated dust and trapped oil particles. They were then melted in steel crucibles at 720 °C and cast into round bars of size Ø30mm using galvanized steel moulds. Test specimens of size Ø20mm×25.4mm were machined from the cast. The chemical

(ED-XRFS) composition of the alloy (presented in Table 1) shows that the recycled alloy is an Al-Si-Cu alloy with properties suitable for a wide range of applications; the seemingly high percentage of Fe is partly due to the reaction with the galvanized steel moulds used for casting considering the high melt temperature.

Table 1: Chemical (ED-XRFS) composition (wt. %) of the recycled aluminium alloy

Al	Si	Ca	Sc	Mn	Fe	Ni	Cu	Others
75.2	16.9	0.22	0.15	0.347	1.29	0.160	3.730	0.957

2.1 Solution Treatment

Test specimens were heated to the designated solution treatment temperature, followed by quenching in water at room temperature and finally reheated to the ageing temperature as shown in Fig. 1 [1,3]. Specimens were removed from the furnace at intervals of 15 mins up to a maximum ageing time of 1½ hours. The same procedure was used for 2nd and 3rd stage treatments.
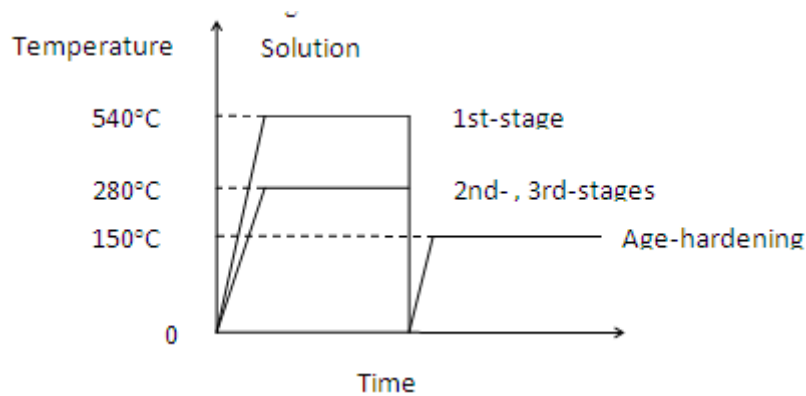
Figure 1: The solution treatment process

2.2 Compression and Hardness Tests

Compression tests were carried out using ELE Compact-1500 compression testing machine. Subsequently, characteristics of strength (hardness, UCS, % strain) were determined. The Vicker's micro-hardness test was carried out on the aged specimens using the Matsuzawa Micro Hardness Tester- Model MHT-1 at a load of 300g with time indentations of 5 seconds.

III.   RESULTS AND DISCUSSION

The experimental results are summarized in Figure 2- 7.

3.1. Compressive Hardness and Strength

The results of compression and hardness tests (Figures 2,3) showed that alloy hardness and compressive stress increased with ageing time following exponential trends. The time response of these strength properties was modelled by the generalized equation (1):

$$\phi_n = \phi_0 e^{\alpha t} \qquad (r^2 \geq 0.9803) \qquad\qquad\qquad (1)$$

where, ϕ_0 - alloy strength property (UCS or HV) preceding ageing treatment; ϕ_n- alloy strength property after ageing; α - the hardening characteristic of the alloy; t - ageing time. The power hardening characteristic of alloy strength n was found to be between 0.002 and 0.0037 for both UCS and HV.
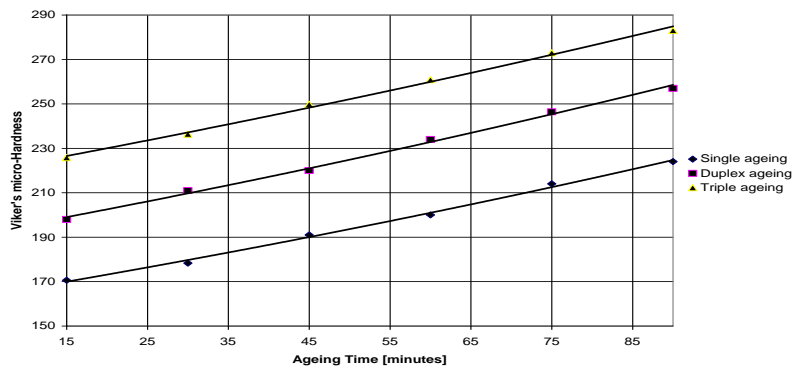
Figure 2: Time response graph of alloy hardness
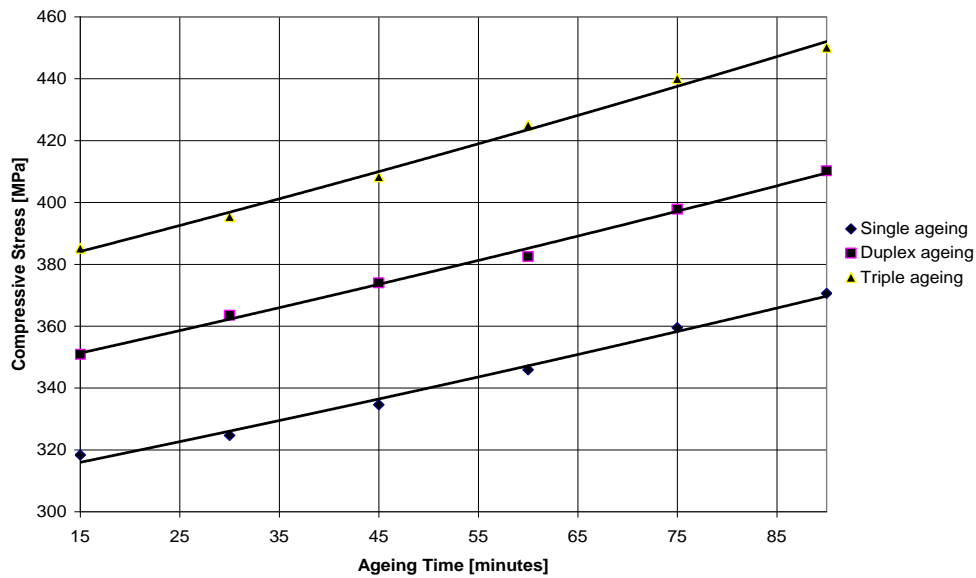
Figure 3: Time response graph of alloy strength

3.2. Time response The trends of Figures 4-5 also show that these properties also increased with repeated ageing. From these plots the relationship between strength properties and number of ageing treatments was modelled by equation (2):

$$\phi_n = \phi_0 e^{\alpha N} \quad (r^2 \geq 0.9890) \tag{2}$$

where α is the hardening characteristic of the alloy, and N – the number of ageing treatments required. The hardening characteristic of the alloy α was found to be between 0.0648 and 0.1329.
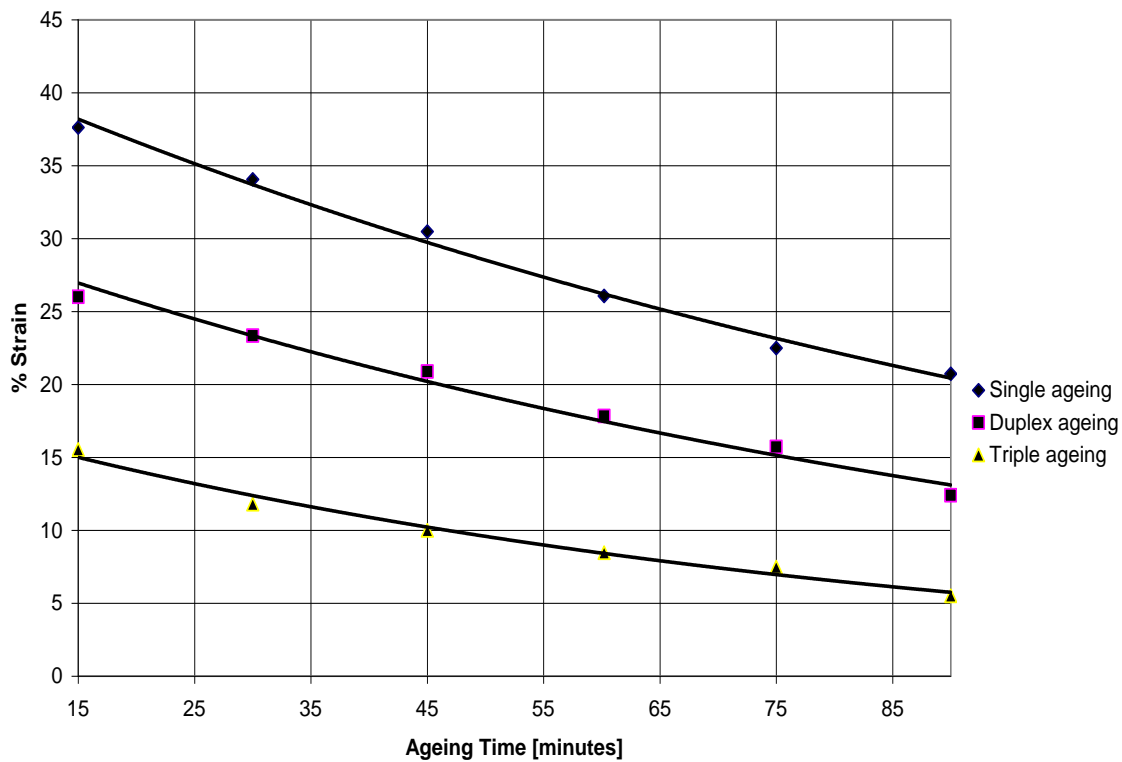
Figure 4: Time response graph of alloy strain
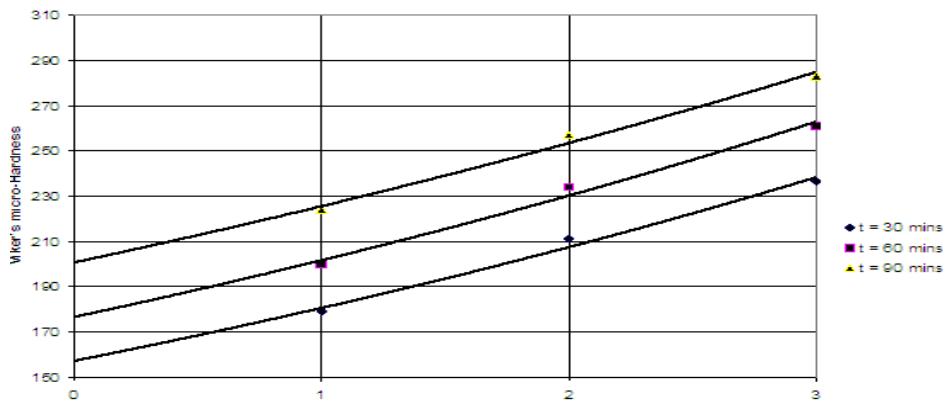
Figure 5: Response graph of alloy hardness with repeated ageing

3.3. Strain response

The results (Figure 6) indicated that the percentage (%) reduction of specimens reduced with increased ageing time. These are indications of increasing strength or strain hardening of the alloy with repeated ageing [3,6]. The time response of % reduction was modelled by equation (3):

$$\varepsilon_n = \varepsilon_0 e^{-\alpha t} \ (r^2 = 0.9803) \tag{3}$$

where the hardening characteristic of the alloy was found to be between 0.0083 and 0.0128. The results (Figure 7) also indicated that % reduction also reduced with repeated ageing. From these plots the relationship between strength properties and number of ageing treatments was modelled by equation (4):

$$\varepsilon_n = \varepsilon_0 e^{-\alpha N} \ (r^2 \geq 0.9728) \tag{4}$$
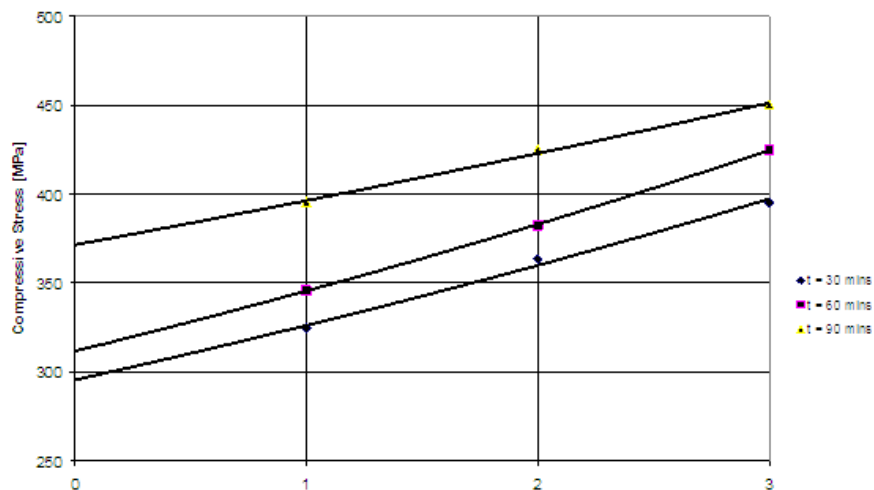
Figure 6: Response graph of alloy strength with repeated ageing
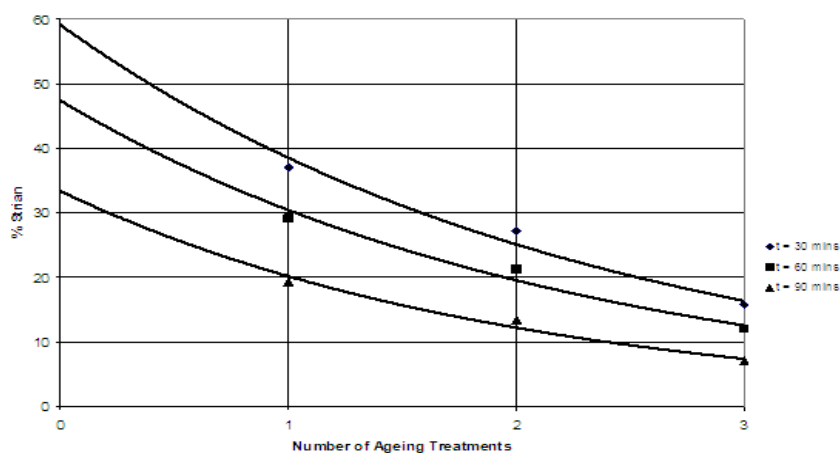
Figure 7: Response graph of strain with repeated ageing treatments

Equations (1) – (3) are similar to empirical models reported in related investigations [5,6] to obtain characteristic curves of the yield stress and tensile strength to predict target strength. Equation (4), previously modelled as a linear relationship in [1], presents a better model for predicting the strain response of the alloy in repeated ageing.

IV.   CONCLUSION

The time required to raise the strength properties to desire levels can be predicted using equations (1) and (3), and the required number of ageing treatments or stages by equations (2) and (4). Strength properties of the recycled aluminium alloy increased with ageing time and repeated (multi-stage) ageing treatments, while the strain induced in the material reduced. The results show that further alloying is possible and the recycled alloy can be further improved, thereby increasing its potential use for production of high integrity parts.

REFERENCES

[1].   D.T. Gundu, S.A. Bam and A. Ashwe. Effect of Multi-Stage Ageing on Strength properties of recycled Al Alloy. International Journal of Engineering Science, 2(2), 2010, 63-67.

[2].   B. Murizam and J.B. Shamsul. Effect of Solution Treatment Temperature on Recycled Aluminium Alloy 319. Proc. International Conference on Strength of Materials – ICoSM2007, 226-228.

[3].   M. Fujda, T. Kvackaj and K. Nagyova. Improvement of MechanicalProperties of ENAW 6082 Aluminium alloy using Equal-Channel Angular Pressing (ECAP) and Post-ECAP Ageing. Journal of Metals, Materials and Minerals, 18, 2008, 81-87.

[4].   A. Gesing and R. Wolanski. Recycling Light Metals from End-of-Life Vehicles. Journal of Materials, 53(11), 2001, 21-23.

[5].   A. Deschamps, D. Dumont, Y. Brechet, C. Sigli and Dubost B. Process modelling of age-hardening aluminium alloys: from microstructure evolution to mechanical and fracture properties. Proc. James T.

Staley Honoray Symposium on Aluminium Alloys, ed. M. Tiryakioglu, ASM International, Materials Park, OH, 2001, 298-305.

[6].   J.F. Nie, B.C. Muddle. On the form of age hardening response in high strength aluminium alloys. Materials Sci. and Eng.: A. Structural Materials: Properties, Microstructure and Processing. Proc. International Conference on the Strength of Materials No. 12 (ICSMA-12), Asolimar, 2001, 319/21, 448-451.

Research Paper   Open Access

Experimental Study of Discharge Characteristics in a Compound Meandering River

Md. Abdullah Al Amin, Dr. Md. S. M. Khan

Assistant Engineer, Bangladesh Water Development Board (BWDB), Bangladesh. Professor,
Dept. of   Water Resources Engineering Bangladesh University of Engineering and Technology (BUET),
(Dhaka- 1000, Bangladesh)

Abstract : - Most of the river flow in the world can be characterized as compound meandering channel in which the discharge distributions are very intricate. Now-a-days engineers, planners as well as researchers are highly interested in predicting precisely and reliably the quantitative estimates of discharge in a compound meandering river. A Laboratory experiment has been performed in a compound meandering channel with symmetric cross-sections having floodplain width ratio of 1, 1.67, 2.33, 3 and depth ratio of 0.20, 0.30, 0.35, 0.40 using the large-scale open air facility in the Department of Water Resources Engineering, Bangladesh University of Engineering and Technology (BUET), Dhaka. Point velocity data have been collected using an ADV (Acoustic Doppler Velocity Meter) for different depth and width ratio at different locations of a compound meandering channel. Cross-sectional discharge is computed by area velocity method from observed velocity profile. The laboratory experiment shows that the discharge always increases with the increase of depth ratio for all the above mentioned cases. At low depth ratio, discharge decreases with the increase of width ratio but for higher depth ratio, discharge increases with the increase of width ratio.

Keywords : - *Acoustic Doppler Velocity meter, Compound Meandering River, Depth Ratio, Discharge Characteristics, Flood Plains, Width Ratio.*

I.   INTRODUCTION

Most of the river flow can be characterized as compound meandering channel flow i.e. consisting of a meandering main channel flanked by one or two side flood plains. In fact, Bangladesh is one of the biggest Deltas in the world which is composed of three major compound river systems in the world, namely the Ganges, the Brahmaputra-Jamuna and the Megna. Proper quantification of the flow parameters for the main channel and flood plain flow of such rivers still has been a subject of considerable research. A systematic study is of utmost importance from the view point of better understanding of the flow phenomena in a compound meandering river. Though Bangladesh is criss-crossed by so many rivers having meandering mechanism i.e. erosion in the outer bend and deposition in the inner bend but unfortunately research documents related to this are hard to come by. Considering the importance and scope for research, the present study is undertaken. Stage-discharge curve in a compound meandering channel plays an important role in controlling floods, solving a variety of river hydraulics and engineering problems, designing stable channels, revetments and artificial waterways. There are limited reports concerning the stage-discharge relationship in a compound meandering channel. Most of the efforts of [1], [2], [3], [4], [5], [6], [7], [8], [9] and [10] were concentrated on the energy loss, different methods for stage-discharge assessment in the compound meandering sections. This study is aimed at understanding the phenomenon of discharge characteristics in a compound meandering channel.

Generally, natural rivers, streams and manmade surface drainage channels often overflow their banks during episodes of high flooding resulting in a huge potential damage to life and property as well as erosion and depositions of sediments. Many rivers have meandering compound channels possessing a main channel, which always carries flow and one or two floodplains, which only carry flow at above bankful stages. It has been established that a strong interaction between the faster moving main channel flow and slower moving floodplain

flow takes place in a compound channel. This interaction results in a lateral transfer of a significant amount of longitudinal momentum which affects the discharge distribution in a channel flow. Discharge in a compound meandering channel is strongly governed by interaction between flow in the main channel and that in the floodplain and are different due to prevailing of different hydraulic conditions in the main channel and floodplain flow.

II. EXPERIMENTAL SETUP AND PROCEDURE

The experimental study has been conducted in the open air facility of Water Resources Engineering Department, Bangladesh University of Engineering and Technology (BUET), Dhaka. The experimental setup is shown in the Fig.1 which consists of two parts, the permanent part and the temporary part. The permanent part is the experimental facility necessary for the storage and regulation of water circulating through the experimental reach. The temporary part is mainly brick walls which are used to vary the floodplain width for different setups. The experimental reach consists of a 670 cm long symmetric compound meandering channel, set at constant bed slope (S_o) 0.001845 with fixed bed and banks and sinuosity ratio (S_r) of 1.20.Water is drawn by the centrifugal pump of discharge capacity 80 l/s from the storage reservoir then it discharges into the u/s reservoir and coveys water to the experimental reach through approach channel of 30m in length and 3.1m in width. To ensure a more smooth flow towards the approach channel guide vanes and tubes are placed between the upstream reservoir and the approach channel which are at right angle to each other. In order to prevent turbulence in the approach channel, PVC pipes (Diffuser) are used. The water regulating function of the downstream end is provided by tail gate. The tail gate rotates around a horizontal axis. It is operated to maintain desired water level in the experimental reach. At the end of the experimental channel, water is allowed to flow freely so that backwater has no effect in the experimental reach. Behind the tail gate, the water falls into the stilling basin and passes through a transition flume which allows water for recirculation. Experiments were performed for four cases i.e. width ratio 1, 1.67, 2.33,3 at four runs i.e. depth ratio Dr =0.2, 0.3, 0.35, 0.4.

Case1: It represents no floodplain condition having width ratio Wr =1 and cross-sectional dimension of the Channel is 45.7cmx42cm.
Case2: It indicates symmetric floodplain width 15.3 cm having width ratio Wr =1.67. The cross-sectional dimension of the main channel is 45.7cmx24.5cm, left floodplain 15.3cm x18 cm and right floodplain 15.3cm x18 cm.
Case3: It indicates symmetric floodplain width 30.5 cm having width ratio Wr=2.33. The cross-sectional dimension of the main channel is 45.7cmx24.5cm, left floodplain 30.5cm x18 cm and right floodplain 30.5cm x18 cm.
Case4: It indicates symmetric floodplain width 45.70 cm having width ratio Wr=3. The cross-sectional dimension of the main channel is 45.7cmx24.5cm, left floodplain 45.7cm x18 cm and right floodplain 45.7cm x18 cm.
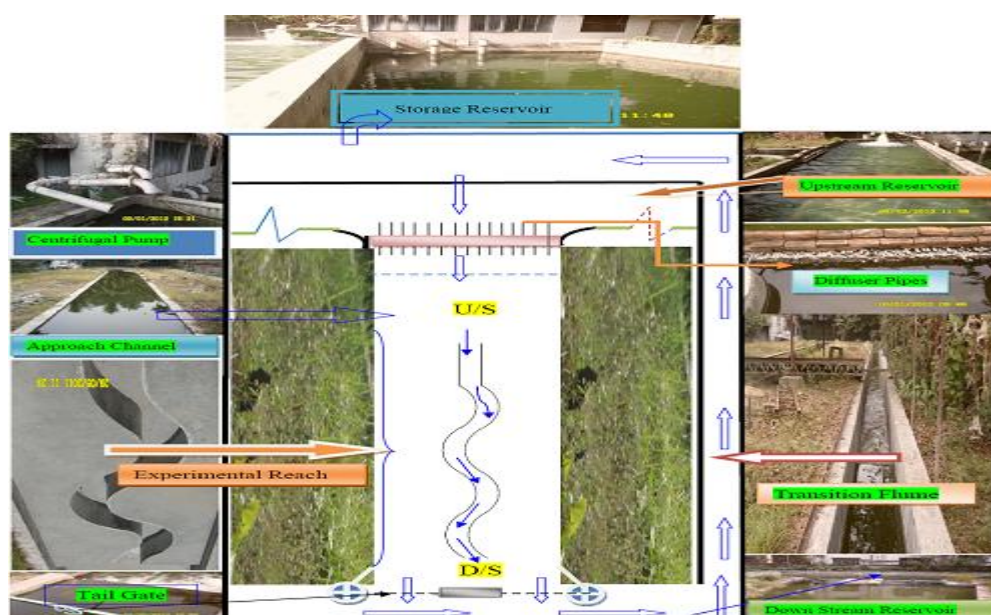
Figure 1: A Schematic Diagram of the Experimental Setup

Point velocities data have been collected by ADV (Acoustic Doppler Velocity meter) at different locations (u/s clockwise bend, u/s crossover, u/s anticlockwise bend etc) of a compound meandering channel. Each location is divided into 19zones starting from left floodplain to right floodplain. The main channel is equally divided into nine zones (zone 1 to zone9), the left floodplain is equally divided into 5zones (zone1 to zone5) and right floodplain is divided into 5 zones (zone1 to zone5). The definition sketch of compound meandering channel is shown in Fig. 2.
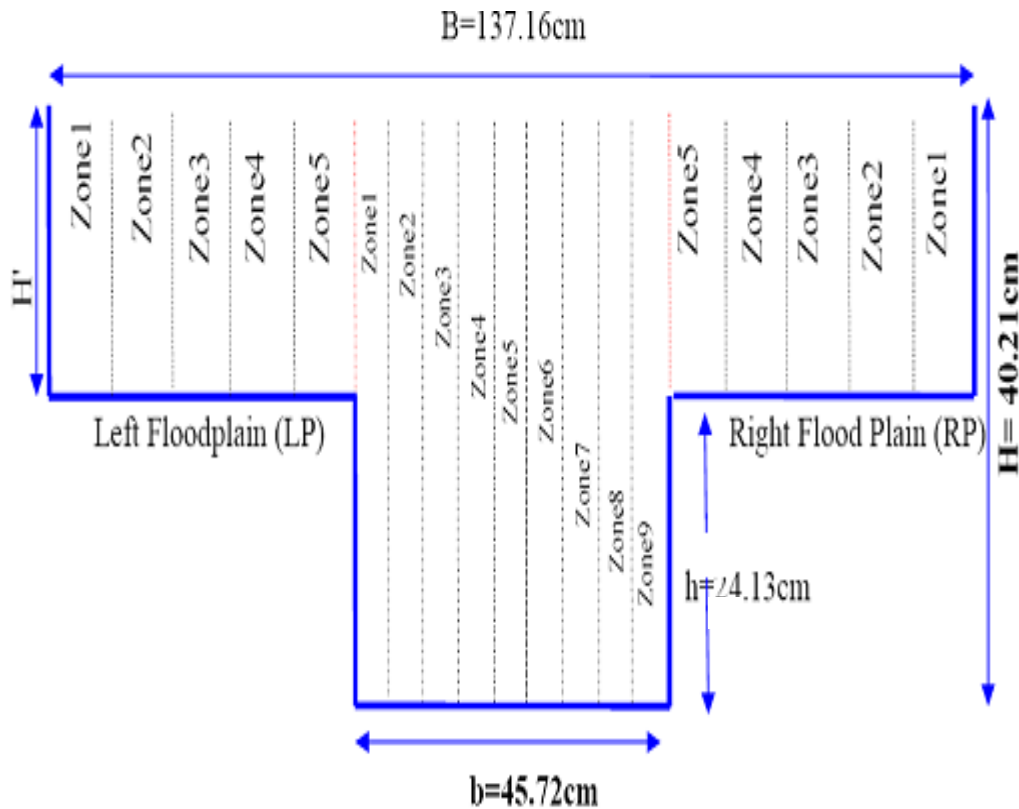
Figure 2: The definition sketch of the compound meandering flow section

In each zone 3D point velocity readings are taken by ADV at five vertical points i.e. 0.1H, 0.2H, 0.4H, 0.6H, 0.8H for main channel and 0.1H',0.2H', 0.4H', 0.6H', 0.8H' for floodplain. Sample of data collection by ADV is shown in the figure 3. In each vertical point 60 seconds point velocity readings are taken and average velocity of 60 seconds point velocity is used for plotting the velocity profile. Cross-sectional discharge is calculated by area velocity method from observed velocity profile. In this method a channel section is subdivided into a number of segments by a number of successive intervals. For all the cross-sections, discharge are calculated separately for the main channel, right and left flood plain; and then total discharge is obtained. The discharge of the segment is calculated as follows

$$\Delta Q_i = \Delta A_i . U_i \qquad\qquad (1)$$

Where ΔQ_i the discharge in the ith segment, ΔA_i is the cross-sectional area of the ith segment and U_i is the average velocity at the ith vertical.
The total discharge is computed as

$$Q = \Sigma \Delta Q_i$$

III.   RESULTS AND DISCUSSIONS

Stage discharge curves with varying width ratios at u/s clockwise bend section, cross-over section and u/s anticlockwise bend section are shown in the Fig. 3, Fig. 4 and Fig. 5. In all cases, the discharge increases with the increase of width ratio for the discharge just above the bank level of the main channel. For the discharges just above the bank level, the retarding influence of the flood plain takes its toll on the overall discharge of the channel. As the depth ratio increases, the retarding effect of the floodplain is counter balanced by the increase in greater flow area provided by the floodplain. So for the higher water level (depth ratio), the discharge increases with the increase in depth of flow.
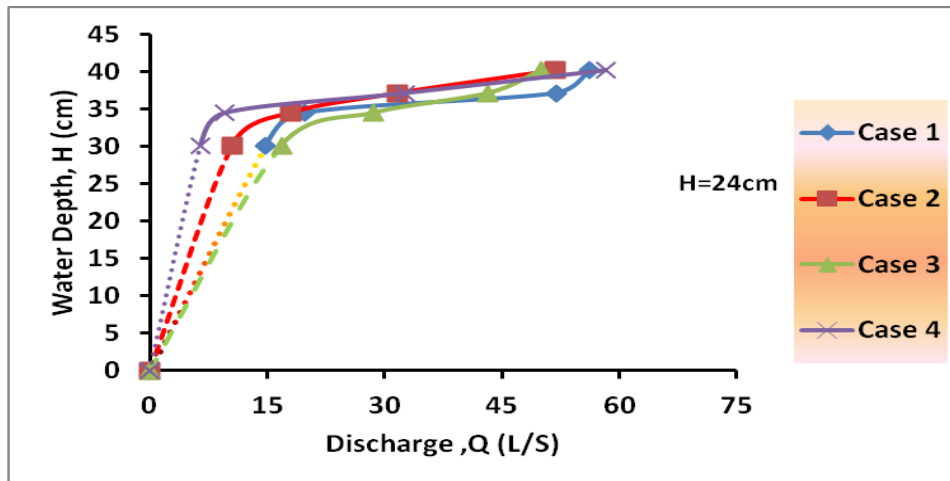
Figure 3: Stage Discharge Curve at U/S Clockwise Bend Section
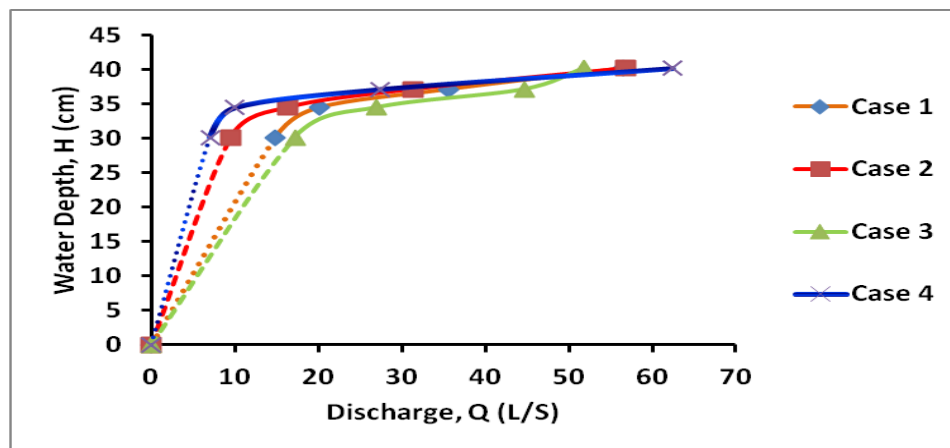
Figure 4: Stage Discharge Curve at U/S Cross-over Section
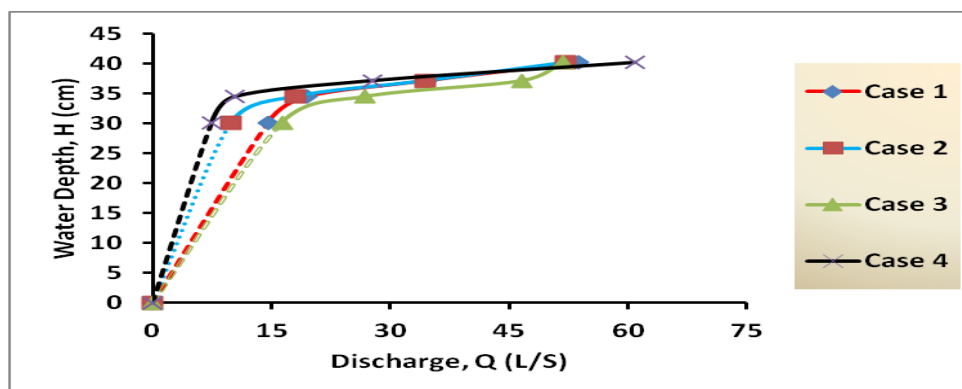
Figure 5: Stage Discharge Curve at U/S Anti-clockwise Bend Section

IV.   CONCLUSIONS

On the basis of this research concerning the discharge characteristics in a compound meandering river with different floodplain width the following conclusions are drawn:

❖ In a compound meandering river, discharge increases with the increase of depth ratio and increasing rate of discharge is more at high water depth ratio. Because at low water depth ratio, the slow moving flow in the floodplain interact with the fast moving main channel flow strongly and considerable momentum exchange takes place. But the intensity of interaction diminishes considerably with the increase of depth ratio.

❖ In a compound meandering river, stage-discharge curve represents straight curve up to in bank flow and curvature nature in the out bank flow.

V.   ACKNOWLEDGEMENTS

Notations

The following symbols are used in this paper ΔA_i = Cross-sectional area of the ith segment B= top width of compound meandering channel b= width of main channel Dr=depth ratio (H-h)/h H= total water depth H'= depth of water above floodplain bed h= height of the main channel ΔQ_i = discharge in the ith segment Q= total discharge S_o= bed slope S_r = sinuosity ratio U_i = average velocity at the ith vertical. Wr = width ratio [B/b]

REFERENCES

[1]   Al-Romaih, J. S. (1996). "Stage discharge assessment in meandering channels," PhD thesis, Univ. of Bradford, U.K.
[2]   Groenhill, R. K., and Sellin, R. H. J. (1993). ''Development of a simple method to predict discharge in compound meandering channels.'' *Proc. Institute Civil Engineers, Water, Merit and Energy*, 101, Water Board, (March), 37–44.
[3]   Muto, Y. (1995). ''Turbulent flow in two stage meander chanenls.'' PhD thesis, Univ. of Bradford, U.K. Patra, K.C., and Kar, S.K., Bhattacharya.A.K. (2004). "Flow and Velocity Distribution in Meandering Compound Channels." Journal of Hydraulic Engineering, ASCE, Vol. 130, No. 5. 398-411.
[4]   Sellin, R. H. J., Ervine, D. A., and Willetts, B. B. (1993). ''Behavior of meandering two stage channels.'' *Proc. of Institute Civil Engineers Water Maritime and Energy*, 101, (June), *Paper No. 10106*, 99–111.
[5]   Shiono, K., and Muto, Y. (1993). ''Secondary flow structure for inbank and overbank flows in trapezoidal meandering channels.'' *Proc., 5th Int. Symp. of Refined Flow Modl. and Turb. Measu.*, Paris (September), 645–652.
[6]   Shiono, K., Muto, Y., Knight, D. W., and Hyde, A. F. L. (1999a). ''Energy losses due to secondary flow and turbulence in meandering channels with over bank flow.'' *J. Hydraul. Res.,* 37(5), 641–664.
[7]   Toebes, G. H., and Sooky, A. A. (1967). ''Hydraulics of meandering rivers with flood plains.'' *J. Waterw. Harbors Div., Am. Soc. Civ. Eng.,* 93(2), 213–236.
[8]   Wark, J. B., and James, C. S. (1994). ''An application of new procedure for estimating discharge in meandering overbank flows to field data.'' *2nd Int. Conf. on River Flood Hydraulics*, March 22–25, Wiley, NewYork, 405–414.
[9]   Willetts, B. B., and Hardwick, R. I. (1993). ''Stage dependency for over bank flow in meandering channels.'' *Proc., Institute of Civil Engineers Water Maritime and Energy*, 101, 45–54.

Research Paper   Open Access

Mhd Unsteady mixed convective flow between twoin finite Vertical Parallel Plates through Porous Medium in Slip flow Regime with Thermal Diffusion

D. Chaudhary, H. Singh, N.C. Jain.
Department of Mathematics, University of Rajasthan, Jaipur 302055, India,

Abstract: - In this paper we have studied a free and forced convective flow of a viscous incompressible fluid through a vertical porous channel bounded by two vertical plates moving with same velocity but in opposite directions, with slip parameters. The temperature and concentration of the plate at y = 0 is considered to be oscillating. Expressions for velocity, temperature, concentration along with skin friction and Nusselt number are obtained and comparative study is made to analyze the effects of different parameters. We observe that increase in velocity slip parameter (h_1) decreases the skin friction. Also, it is noteworthy that Nusselt number is higher for water (Pr = 7) as compared for air (Pr = 0.71).

Keywords: - *Mixed convection, Porous medium, Suction velocity, Thermal diffusion, Unsteady.*

I.   INTRODUCTION

MHD free convection flows are of great interest in a number of industrial applications such as fiber and granular insulation, geothermal systems etc. The science of magneto hydrodynamics (MHD) was concerned with geophysical and astrophysical problems for a number of years. In recent years, the possible use of MHD is to affect a flow stream of an electronically conducting fluid for the purpose of thermal protection, breaking, propulsion, control etc. We also study the mechanism of electronically conducting fluids for example, magma, highly salted water, liquid metals etc. MHD plays an important role in many engineering and industrial problems such as liquid metal cooling, in nuclear reactors, plasma confinement, control of molten iron flow and many others. Mbeledogu et. al. [1] studied an unsteady MHD free convection flow of a compressible fluid past a moving vertical plate. Moreover, influence of viscous dissipation and radiation on unsteady MHD free convection flow past an infinitely heated vertical plate has been studied by Cookey et. al. [2]. On the other hand Singh and Paul [3] studied natural convection between two vertical walls.

During the last decade many research workers have studied mixed convection in channels, which is a phenomenon in many technological processes, such as designs of solar collectors, thermal designs of buildings, air conditioning etc. Barelletta and Celli [4] investigated a mixed convection MHD flow in a vertical channel where as Rajput and Sahu [5] studied a transient free convection MHD flow between two long vertical parallel plates with variable temperature and uniform mass diffusion in a porous medium. Narahari et. al. [6] discussed a transient free convection flow between two long vertical parallel plates with constant heat flux at one boundary. Working on a horizontal channel, Brown and Lai [7] studied correlations for combined heat and mass transfer from an open cavity.

The study of flows through porous medium holds importance in many scientific and engineering applications such as for filteration and purification process, to study the movement of natural gas, water and oil through the oil reservoirs. In view of these applications a series of investigation have been made by Raptis et. al. [8, 9, 10]. Also Geindreau and Auriault [11] studied MHD flows in porous media. On the other hand, Alagoa et. al. [12] investigated radiation and free convection effects of a MHD flow through porous medium between infinite parallel plates. Moreover, Farhad et. al. [13] discussed an accelerated MHD flow in a porous medium with slip condition.

It the present paper, we have analyzed a problem on unsteady free convection MHD flow with mixed convection heat and mass transfer, in a channel filled with porous material, bounded by two vertical parallel plates moving in opposite direction with respect to each other, in slip flow regime. The temperature and mass concentration of the upward moving plate are considered to be oscillating with time. Effects of different parameters entering into the problem are shown graphically on velocity, temperature, concentration, skin friction and Nusselt number. We clearly observe that decrease in velocity slip parameter (h_1) increases the sinusoidal skin friction but it causes the sinusoidal rate of heat transfer to drop.

In many problems like thin film rarefied fluid, fluid containing concentrated suspension, the no slip boundary conditions fails to work. Mankinde and Osalusi [14] have made studies on MHD steady flow in a channel with slip at the permeable boundaries. Moreover, Taneja and Jain [15] discussed MHD flow with slip effects and temperature dependent heat source in a viscous incompressible fluid confined between a long vertical wavy walls and a parallel flat wall.

II.　　FORMULATION OF THE PROBLEM

In two dimensional rectangular Cartesian Coordinate system, we consider an unsteady free convective flow of an incompressible fluid through a vertical channel formed by two parallel plates moving with equal velocity 'U' but in opposite directions, at a distance d apart. The temperature and mass concentration of plate at y = 0, oscillates about a constant non zero mean T_0 and C_0. The suction velocity v_0 and permeability K of the porous medium are taken to be constant.
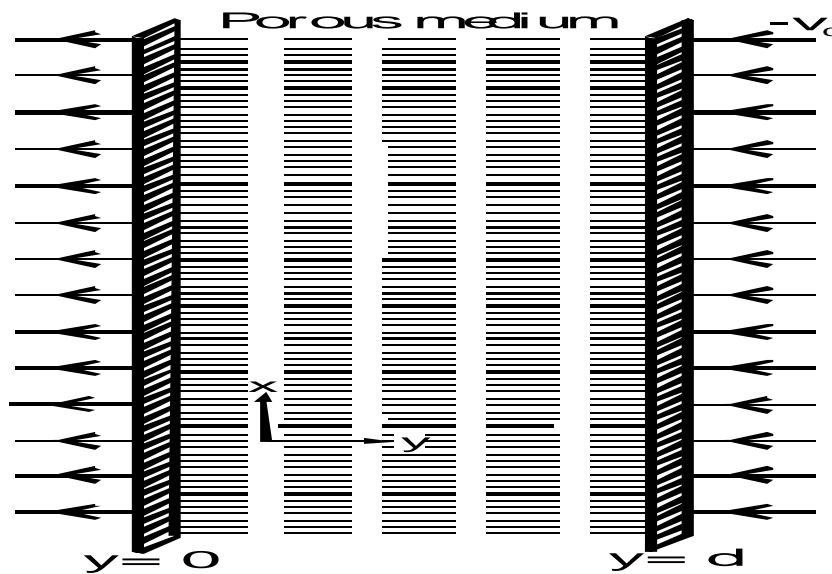
(Figure 1 : Schematic diagram.)

Hence under these conditions, using Boussinesq's approximation, equations governing the flow in the presence of magnetic field of uniform strength B_0, are given by:

Momentum Equation

$$\frac{\partial u}{\partial t} - v_0 \frac{\partial u}{\partial y} = g\beta(T - T_d) + g\beta^*(C - C_d) + \nu \frac{\partial^2 u}{\partial y^2} - \frac{\nu}{K}u - \frac{\sigma B_0^2 u}{\rho} \qquad \ldots(1)$$

Energy Equation

$$\frac{\partial T}{\partial t} - v_0 \frac{\partial T}{\partial y} = \frac{\kappa}{\rho C_p} \frac{\partial^2 T}{\partial y^2} + \frac{S}{\rho C_p}(T - T_d) \qquad \ldots(2)$$

Concentration Equation

$$\frac{\partial C}{\partial t} - v_0 \frac{\partial C}{\partial y} = D \frac{\partial^2 C}{\partial y^2} + D_\ell \frac{\partial^2 T}{\partial y^2} \qquad \ldots(3)$$

where u and v are the components of the velocity in the x and y direction, g is the acceleration due to gravity, β and β^* are the coefficient of volume expansion and species concentration expansion respectively, D is the chemical molecular diffusivity, S is the coefficient of heat source, D_ℓ is coefficient of thermal diffusivity, ρ,

ν, $\square$ and C_p respectively the density, kinematic viscosity, thermal conductivity and specific heat of the fluid at constant pressure. T_d and C_d are the temperature and concentration of the plate at $y = d$.

We assume that the magnetic Reynolds number is small so that the induced magnetic field is negligible. The relevant boundary conditions are:

$$\left.\begin{array}{l} u = U + L_1 \dfrac{\partial u}{\partial y}, \ T = T_0 + \in (T_0 - T_d)e^{i\omega t}, C = C_0 + \in (C_0 - C_d)e^{i\omega t} \ \text{at } y = 0 \\[4mm] u = -U + L_1 \dfrac{\partial u}{\partial y}, \ T = T_d, \qquad\qquad C = C_d \qquad\qquad \text{at } y = d \end{array}\right\} \qquad \ldots(4)$$

where $L_1 \left(\dfrac{2 - m_1}{m_1}\right) L$, L being mean free path and m_1 the Maxwell's reflection coefficient.

On introducing the following non-dimensional quantities:

$$u^* = \frac{u}{U}, \qquad t^* = t\omega, \qquad y^* = y/d$$

$$\omega^* = \frac{\omega d^2}{\nu} \text{(frequency)}, \qquad \theta^* = \frac{T - T_d}{T_0 - T_d},$$

$$C^* = \frac{C - C_d}{C_0 - C_d}, \qquad\qquad\qquad K^* = \frac{K \, v_0^2}{v^2} \text{(Permeability parameter)},$$

$$Pr = \frac{\mu C_p}{\kappa} \text{ (Prandtl number)}, \qquad\qquad \lambda = \frac{v_0 d}{\nu} \text{ (Suction parameter)},$$

$$M = B_0 d \left(\frac{\sigma}{\mu}\right)^{1/2} \text{ (Hartmann number)}, \qquad S^* = \frac{v^2 S}{\kappa \, v_0^2} \text{ (Heat source parameter)},$$

$$Gr = \frac{\nu g \beta (T_0 - T_d)}{U \, v_0^2} \text{(Thermal Grashof number)},$$

$$Gc = \frac{\nu g \beta^* (C_0 - C_d)}{U \, v_0^2} \text{(Mass Grashof number)},$$

$$So = \frac{D_\ell (T_0 - T_d)}{\nu (C_0 - C_d)} \text{ (Soret number)}, \qquad Sc = \frac{\nu}{D} \text{ (Schmidt number)},$$

$$h_1 = \frac{L_1}{d} \text{ (Velocity slip parameter)},$$

in equations (1) to (3), after dropping the asterisks over them they reduce to:

$$\frac{\omega}{\lambda} \frac{\partial u}{\partial t} - \frac{\partial u}{\partial y} = Gr \, \lambda \theta + Gc \, \lambda C + \frac{1}{\lambda} \frac{\partial^2 u}{\partial y^2} - \frac{\lambda}{K} u - \frac{M^2}{\lambda} u \qquad \ldots(5)$$

$$\frac{\omega}{\lambda} \frac{\partial \theta}{\partial t} - \frac{\partial \theta}{\partial y} = \frac{1}{Pr \, \lambda} \frac{\partial^2 \theta}{\partial y^2} + \lambda S \theta \qquad \ldots(6)$$

$$\frac{\omega}{\lambda} \frac{\partial C}{\partial t} - \frac{\partial C}{\partial y} = \frac{1}{Sc \, \lambda} \frac{\partial^2 C}{\partial y^2} + \frac{So}{\lambda} \frac{\partial^2 \theta}{\partial y^2}. \qquad \ldots(7)$$

The corresponding boundary conditions reduce to:

$$\left.\begin{array}{l} u = 1 + h_1 \dfrac{\partial u}{\partial y}, \ \ \theta = 1 + \in e^{it}, \ \ C = 1 + \in e^{it}; \ \text{at } y = 0 \\[4mm] u = -1 + h_1 \dfrac{\partial u}{\partial y}, \ \ \theta = 0, \qquad\quad C = 0 \qquad ; \ \text{at } y = 1 \end{array}\right\} \qquad \ldots(8)$$

III.　　SOLUTION OF THE PROBLEM

Since the amplitude $\in (<<1)$, we represent the velocity, temperature and concentration as:

$$f(y,t) \; = \; f_0(y) \; + \in e^{it} f_1(y) \qquad \ldots(9)$$

where f stands for u, θ and C. With the help of equation (9), the equations (10) to (11) reduces to the following ordinary differential equations by equating like powers of $\in$, neglecting those of $\in^2$ and higher orders:

$$u_0'' + \lambda u_0' - \left(\frac{\lambda^2}{K} + M^2\right) u_0 = -Gr\,\lambda^2\theta_0 - Gc\,\lambda^2 C_0 \qquad \ldots(10)$$

$$u_1'' + \lambda u_1' - \left(\frac{\lambda^2}{K} + M^2 + i\omega\right) u_1 = -Gr\,\lambda^2\theta_1 - Gc\,\lambda^2 C_1 \quad \ldots(11)$$

$$\theta_0'' + Pr\,\lambda\,\theta_0' + Pr\,\lambda^2 S\theta_0 = 0 \quad \ldots(12)$$

$$\theta_1'' + Pr\,\lambda\,\theta_1' + (Pr\,\lambda^2 S - i\,Pr\,\omega)\,\theta_1 = 0 \quad \ldots(13)$$

$$C_0'' + Sc\,\lambda C_0' = -So\,Sc\,\theta_0'' \qquad \ldots(14)$$

$$C_1'' + Sc\,\lambda C_1' - i\omega Sc\,C_1 = -So\,Sc\,\theta_1'' \quad \ldots(15)$$

where the prime denotes differentiation with respect to y.
The corresponding boundary conditions becomes:

$$\left.\begin{array}{l} u_0 = 1 + h_1 u_0', \; u_1 = h_1 u_1'; \theta_0 = 1, \theta_1 = 1; \; C_0 = 1, C_1 = 1; \; \text{at } y \; = \; 0 \\[4pt] u_0 = -1 + h_1 u_0', u_1 = h_1\,u_1'; \theta_0 = 0, \theta_1 = 0; C_0 = 0, C_1 = 0; \; \text{at } y \; = \; 1 \end{array}\right\} \quad \ldots(16)$$

By solving the equations (10) to (15) under boundary conditions (16), we get:

$$\theta_0 = \frac{1}{e^{R_1} - e^{R_2}}\left(e^{R_1 + R_2 y} - e^{R_2 + R_1 y}\right) \qquad \ldots(17)$$

$$\theta_1 = \frac{1}{e^{R_3} - e^{R_4}}\left(e^{R_3 + R_4 y} - e^{R_4 + R_3 y}\right) \qquad \ldots(18)$$

$$C_0 = R_5 e^{R_2 y} + R_6 e^{R_1 y} + R_7 + R_8 e^{-Sc\,\lambda y} \; \ldots(19)$$

$$C_1 = R_{11} e^{R_3 y} + R_{12} e^{R_4 y} + R_{13} e^{R_9 y} + R_{14} e^{R_{10} y} \qquad \ldots(20)$$

$$u_0 = D_1 e^{R_{15} y} + D_2 e^{R_{16} y} - R_{17} e^{R_2 y} + R_{18} e^{R_1 y} + R_{19} - R_{20} e^{-Sc\,\lambda y} \; \ldots(21)$$

$$u_1 = D_3 e^{R_{23} y} + D_4 e^{R_{24} y} - R_{25} e^{R_4 y} + R_{26} e^{R_3 y} - R_{27} e^{R_9 y} - R_{28} e^{R_{10} y} \qquad \ldots(22)$$

Substituting the equations (17) to (22) into (9) for u, θ and C, we have:

$$u(y,t) = D_1 e^{R_{15} y} + D_2 e^{R_{16} y} - R_{17} e^{R_2 y} + R_{18} e^{R_1 y} + R_{19} - R_{20} e^{-Sc\,\lambda y}$$
$$+ \in [D_3 e^{R_{23} y} + D_4 e^{R_{24} y} - R_{25} e^{R_4 y} + R_{26} e^{R_3 y} - R_{27} e^{R_9 y} - R_{28} e^{R_{10} y}]e^{it} \qquad \ldots(23)$$

$$\theta(y,t) = \frac{1}{(e^{R_1} - e^{R_2})}\left(e^{R_1 + R_2 y} - e^{R_2 + R_1 y}\right) + \in \left[\frac{1}{(e^{R_3} - e^{R_4})}\left\{e^{R_3 + R_4 y} - e^{R_4 + R_3 y}\right\}\right]e^{it} \; \ldots(24)$$

$$C(y,t) = \left(R_5 e^{R_2 y} + R_6 e^{R_1 y} + R_7 + R_8 e^{-Sc\,\lambda y}\right) + \in \left(R_1 e^{R_3 y} + R_{12} e^{R_4 y} + R_{13} e^{R_9 y} + R_{14} e^{R_{10} y}\right) e^{it}$$
$$\ldots(25)$$

With convection that the real parts of complex quantities have physical significance in the problem, we have, the main flow velocity which can now be expressed as:

$$u(y,t) \; = \; u_0(y) \; + \in [U_r\,\cos t - U_i \sin t] \qquad \ldots(26)$$

where

$$U_r + i\,U_i \; = \; u_1(y) \text{ and}$$

$$U_r\left[\left(e^{A_9 y} A_{17}\cos B_9 y - e^{A_9 y} B_{17}\sin B_9 y\right) + \left(e^{A_{10} y} A_{18}\cos B_{10} y - e^{A_{10} y} B_{18}\sin B_{10} y\right)\right.$$

$$\left. + \left(e^{A_2 y} B_{11}\sin B_2 y - e^{A_2 y} A_{11}\cos B_2 y\right) + \left(e^{A_1 y} A_{12}\cos B_1 y - e^{A_1 y} B_{12}\sin B_1 y\right)\right.$$

$$+\left(e^{A_3y}B_{13}\sin B_3y - e^{A_3y}A_{13}\cos B_3y\right) + \left(e^{A_4y}B_{14}\sin B_4y - e^{A_4y}A_{14}\cos B_4y\right)\Big]$$

$$U_i = \Big[\left(e^{A_9y}B_{17}\cos B_9y + e^{A_9y}A_{17}\sin B_9y\right) + \left(e^{A_{10}y}B_{18}\cos B_{10}y + e^{A_{10}y}A_{18}\sin B_{10}y\right)$$

$$-\left(e^{A_2y}B_{11}\cos B_2y + e^{A_2y}A_{11}\sin B_2y\right) + \left(e^{A_1y}B_{12}\cos B_1y + e^{A_1y}A_{12}\sin B_1y\right)$$

$$-\left(e^{A_3y}B_{13}\cos B_3y + e^{A_3y}A_{13}\sin B_3y\right) - \left(e^{A_4y}B_{14}\cos B_4y + e^{A_4y}A_{14}\sin B_4y\right)\Big]$$

Hence, the expression for the velocity, for $t = \dfrac{\pi}{2}$, is given by:

$$u\left(y, \frac{\pi}{2}\right) = u_0(y) - \in U_i \qquad \dots(27)$$

Similarly, the expression for the temperature profiles can now be expressed as:

$$\theta(y,t) = \theta_0(y) + \in\big[M_r \cos t - M_i \sin t\big] \qquad \dots(28)$$

where

$$M_r + i\,M_i = \theta_1(y)$$

and

$$M_r = e^{A_1+A_2y}\Big[Z_1\left(\cos B_1\cos B_2y - \sin B_1\sin B_2y\right) + Z_2\left(\sin B_1\cos B_2y + \cos B_1\sin B_2y\right)\Big]$$

$$-e^{A_1y+A_2}\Big[Z_1\left(\cos B_2\cos B_1y - \sin B_2\sin B_1y\right) + Z_2\left(\sin B_2\cos B_1y + \cos B_2\sin B_1y\right)\Big]$$

$$M_i = e^{A_1+A_2y}\Big[Z_1\left(\sin B_1\cos B_2y + \cos B_1\sin B_2y\right) - Z_2\left(\cos B_1\cos B_2y - \sin B_1\sin B_2y\right)\Big]$$

$$-e^{A_1y+A_2}\Big[Z_1\left(\sin B_2\cos B_1y + \cos B_2\sin B_1y\right) - Z_2\left(\cos B_2\cos B_1y - \sin B_2\sin B_1y\right)\Big]$$

Hence, the expression for the temperature for $t = \dfrac{\pi}{2}$ is given by:

$$\theta\left(y, \frac{\pi}{2}\right) = \theta_0(y) - \in M_i \qquad \dots(29)$$

and the expression for the concentration profiles can now be expressed as:

$$C(y,t) = C_0(y) + \in[N_r \cos t - N_i \sin t] \qquad \dots(30)$$

Where $N_r + i\,N_i = C_1(y)$

and

$$N_r = \Big[\left(e^{A_1y}A_5\cos B_1y - e^{A_1y}B_5\sin B_1y\right) + \left(e^{A_2y}A_6\cos B_2y - e^{A_2y}B_6\sin B_2y\right)$$

$$+\left(e^{A_3y}A_7\cos B_3y - e^{A_3y}B_7\sin B_3y\right) + \left(e^{A_4y}A_8\cos B_4y - e^{A_4y}B_8\sin B_4y\right)\Big]$$

$$N_i = \Big[\left(e^{A_1y}B_5\cos B_1y + e^{A_1y}A_5\sin B_1y\right) + \left(e^{A_2y}B_6\cos B_2y + e^{A_2y}A_6\sin B_2y\right)$$

$$+\left(e^{A_3y}A_7\sin B_3y + e^{A_3y}B_7\cos B_3y\right) + \left(e^{A_4y}A_8\sin B_4y + e^{A_4y}B_8\cos B_4y\right)\Big]$$

Hence, the expression for the concentration for $t = \dfrac{\pi}{2}$ is given by:

$$C\left(y, \frac{\pi}{2}\right) = C_0(y) - \in N_i \qquad \dots(31)$$

where

$$R_1 = \frac{-\Pr\lambda + \sqrt{\Pr^2\lambda^2 - 4\Pr\lambda^2 S}}{2}, \qquad R_2 = \frac{-\Pr\lambda - \sqrt{\Pr^2\lambda^2 - 4\Pr\lambda^2 S}}{2}$$

$$R_3 = \frac{-\Pr\lambda + \sqrt{\Pr^2\lambda^2 - 4(\Pr\lambda^2 S - i\Pr\omega)}}{2} = A_1 + iB_1$$

$$R_4 = \frac{-\Pr\lambda - \sqrt{\Pr^2\lambda^2 - 4(\Pr\lambda^2 S - i\Pr\omega)}}{2} = A_2 + iB_2$$

$$R_5 = \frac{-e^{R_1}So\,Sc\,R_2^2}{\left(e^{R_1} - e^{R_2}\right)\left(R_2^2 + Sc\,\lambda\right)}$$

$$R_6 = \frac{e^{R_2}So\,Sc\,R_1^2}{\left(e^{R_1} - e^{R_2}\right)\left(R_1^2 + Sc\,\lambda\right)}, \qquad R_7 = \frac{R_5\left(e^{-Sc\lambda} - e^{R_2}\right) + R_6\left(e^{-Sc\lambda} - e^{R_1}\right) - e^{-Sc\lambda}}{\left(1 - e^{-Sc\,\lambda}\right)}$$

$$R_8 = \frac{R_5\left(e^{R_2} - 1\right) + R_6\left(e^{R_1} - 1\right) + 1}{\left(1 - e^{-Sc\lambda}\right)}, \qquad R_9 = \frac{-Sc\lambda + \sqrt{Sc^2\lambda^2 + 4i\omega Sc}}{2} = A_3 + iB_3$$

$$R_{10} = \frac{-Sc\lambda - \sqrt{Sc^2\lambda^2 + 4i\omega Sc}}{2} = A_4 + iB_4$$

$$R_{11} = \frac{So\,Sc\,R_3^2 e^{R_4}}{\left(e^{R_3} - e^{R_4}\right)\left(R_3^2 + Sc\lambda R_3 - i\omega Sc\right)} = A_5 + iB_5$$

$$R_{12} = \frac{-So\,Sc\,R_4^2 e^{R_3}}{\left(e^{R_3} - e^{R_4}\right)\left(R_4^2 + Sc\lambda R_4 - i\omega Sc\right)} = A_6 + iB_6$$

$$R_{13} = \frac{R_{11}\left(e^{R_{10}} - e^{R_3}\right) + R_{12}\left(e^{R_{10}} - e^{R_4}\right) - e^{R_{10}}}{\left(e^{R_9} - e^{R_{10}}\right)} = A_7 + iB_7$$

$$R_{14} = \frac{R_{11}\left(e^{R_3} - e^{R_9}\right) + R_{12}\left(e^{R_4} - e^{R_9}\right) + e^{R_9}}{\left(e^{R_9} - e^{R_{10}}\right)} = A_8 + iB_8$$

$$R_{15} = \frac{-\lambda + \sqrt{\lambda^2 + 4\left(\dfrac{\lambda^2}{K} + M^2\right)}}{2}$$

$$R_{16} = \frac{-\lambda - \sqrt{\lambda^2 + 4\left(\dfrac{\lambda^2}{K} + M^2\right)}}{2}$$

$$R_{17} = \frac{\lambda^2 e^{R_1}(Gr + Gc\,R_5) - \lambda^2 e^{R_2}Gc\,R_5}{(e^{R_1} - e^{R_2})\left\{R_2^2 + \lambda R_2 - \left(\dfrac{\lambda^2}{K} + M^2\right)\right\}}$$

$$R_{18} = \frac{\lambda^2 e^{R_2}(Gr + Gc\,R_6) - \lambda^2 e^{R_1}Gc\,R_6}{(e^{R_1} - e^{R_2})\left\{R_2^2 + \lambda R_2 - \left(\dfrac{\lambda^2}{K} + M^2\right)\right\}}, \quad R_{19} = \frac{\lambda^2 Gc\,R_7}{\left(\dfrac{\lambda^2}{K} + M^2\right)}$$

$$R_{20} = \frac{\lambda^2 Gc\,R_8}{\left\{Sc^2\lambda^2 - Sc\lambda - \left(\dfrac{\lambda^2}{K} + M^2\right)\right\}}$$

$$R_{21} = 1 + R_{17}(1 - h_1 R_2) + R_{18}(h_1 R_1 - 1) - R_{19} + R_{20}(1 + \lambda h_1 Sc)$$

$$R_{22} = -1 + R_{17}(1 - h_1 R_2)e^{R_2} + R_{18}(h_1 R_1 - 1)e^{R_1} - R_{19} + R_{20}(1 + \lambda h_1 Sc)e^{-Sc\lambda}$$

$$D_1 = \frac{-R_{22} + R_{21}e^{R_{16}}}{\left(e^{R_{16}} - e^{R_{15}}\right)\left(1 - h_1 R_{15}\right)}, \quad D_2 = \frac{R_{22} - R_{21}e^{R_{15}}}{\left(e^{R_{16}} - e^{R_{15}}\right)\left(1 - h_1 R_{16}\right)}$$

$$R_{23} = \frac{-\lambda + \sqrt{\lambda^2 - 4\left(\dfrac{\lambda^2}{K} + M^2 + i\omega\right)}}{2} = A_9 + iB_9$$

$$R_{24} = \frac{-\lambda - \sqrt{\lambda^2 - 4\left(\dfrac{\lambda^2}{K} + M^2 + i\omega\right)}}{2} = A_{10} + iB_{10}$$

$$R_{25} = \frac{Gr\,\lambda^2 e^{R_3} + Gc\,\lambda^2 R_{12}\left(e^{R_3} - e^{R_4}\right)}{\left(e^{R_3} - e^{R_4}\right)\left\{R_4^2 + \lambda R_4 - \left(\dfrac{\lambda^2}{K} + M^2 + i\omega\right)\right\}} = A_{11} + iB_{11}$$

$$R_{26} = \frac{Gr\,\lambda^2 e^{R_4} - Gc\,\lambda^2 R_{11}\left(e^{R_3} - e^{R_4}\right)}{\left(e^{R_3} - e^{R_4}\right)\left\{R_3^2 + \lambda R_3 - \left(\dfrac{\lambda^2}{K} + M^2 + i\omega\right)\right\}} = A_{12} + iB_{12}$$

$$R_{27} = \frac{Gc\,\lambda^2 R_{13}}{\left\{R_9^2 + \lambda R_9 - \left(\dfrac{\lambda^2}{K} + M^2 + i\omega\right)\right\}} = A_{13} + iB_{13}$$

$$R_{28} = \frac{Gc\,\lambda^2 R_{14}}{\left\{R_{10}^2 + \lambda R_{10} - \left(\dfrac{\lambda^2}{K} + M^2 + i\omega\right)\right\}} = A_{14} + iB_{14}$$

$$R_{29} = R_{25}(1 - h_1 R_4) + R_{26}(h_1 R_3 - 1) + R_{27}(1 - h_1 R_9) + R_{28}(1 - h_1 R_{10}) = A_{15} + iB_{15}$$

$$R_{30} = R_{25}(1 - h_1 R_4)e^{R_4} + R_{26}(h_1 R_3 - 1)e^{R_3} + R_{27}(1 - h_1 R_9)e^{R_9}$$
$$+ R_{28}(1 - h_1 R_{10})e^{R_{10}} = A_{16} + iB_{16}$$

$$D_3 = \frac{-R_{30} + R_{29}e^{R_{24}}}{\left(e^{R_{24}} - e^{R_{23}}\right)\left(1 - h_1 R_{23}\right)} = A_{17} + iB_{17}$$

$$D_4 = \frac{R_{30} - R_{29}e^{R_{23}}}{\left(e^{R_{24}} - e^{R_{23}}\right)\left(1 - h_1 R_{24}\right)} = A_{18} + iB_{18}$$

$$A_1 = \frac{-Pr\lambda}{2} + \frac{1}{2\sqrt{2}}\left[\sqrt{\left(Pr^2\lambda^2 - 4Pr\,\lambda^2 S\right)^2 + 16Pr^2\omega^2} + \left(Pr^2\lambda^2 - 4Pr\lambda^2 S\right)\right]^{1/2}$$

$$B_1 = \frac{1}{2\sqrt{2}}\left[\sqrt{\left(Pr^2\lambda^2 - 4Pr\lambda^2 S\right)^2 + 16Pr^2\omega^2} - \left(Pr^2\lambda^2 - 4Pr\,\lambda^2 S\right)\right]^{1/2}$$

$$A_2 = \frac{-Pr\lambda}{2} - \frac{1}{2\sqrt{2}}\left[\sqrt{\left(Pr^2\lambda^2 - 4Pr\lambda^2 S\right)^2 + 16Pr^2\omega^2} + \left(Pr^2\lambda^2 - 4Pr\lambda^2 S\right)\right]^{1/2}$$

$$B_2 = -\frac{1}{2\sqrt{2}}\left[\sqrt{\left(Pr^2\lambda^2 - 4Pr\lambda^2 S\right)^2 + 16Pr^2\omega^2} - \left(Pr^2\lambda^2 - 4Pr\,\lambda^2 S\right)\right]^{1/2}$$

$$A_3 = \frac{-Sc\lambda}{2} + \frac{1}{2\sqrt{2}}\left[\sqrt{\left(Sc^2\lambda^2\right)^2 + 16Sc^2\omega^2} + \left(Sc^2\lambda^2\right)\right]^{1/2}$$

$$B_3 = \frac{1}{2\sqrt{2}}\left[\sqrt{\left(Sc^2\lambda^2\right)^2 + 16Sc^2\omega^2} - \left(Sc^2\lambda^2\right)\right]^{1/2}$$

$$A_4 = \frac{-Sc\lambda}{2} - \frac{1}{2\sqrt{2}}\left[\sqrt{\left(Sc^2\lambda^2\right) + 16Sc^2\omega^2} + \left(Sc^2\lambda^2\right)\right]^{1/2}$$

$$B_4 = -\frac{1}{2\sqrt{2}}\left[\sqrt{\left(Sc^2\lambda^2\right)^2 + 16Sc^2\omega^2} - \left(Sc^2\lambda^2\right)\right]^{1/2}$$

$$A_5 = \frac{P_5P_7 + P_6P_8}{P_7^2 + P_8^2}, \qquad B_5 = \frac{P_6P_7 - P_5P_8}{P_7^2 + P_8^2}$$

$$A_6 = \frac{P_9P_{11} + P_{10}P_{12}}{P_{11}^2 + P_{12}^2}, \qquad B_6 = \frac{P_{10}P_{11} - P_9P_{12}}{P_{11}^2 + P_{12}^2}$$

$$A_7 = \frac{Q_7\left(Q_1 + Q_3 + Q_5\right) + Q_8\left(Q_2 + Q_4 + Q_6\right)}{Q_7^2 + Q_8^2},$$

$$B_7 = \frac{Q_7\left(Q_2 + Q_4 + Q_6\right) - Q_8\left(Q_1 + Q_3 + Q_5\right)}{Q_7^2 + Q_8^2}$$

$$A_8 = \frac{Q_7\left(Q_9 + Q_{11} + Q_{13}\right) + Q_8\left(Q_{10} + Q_{12} + Q_{14}\right)}{Q_7^2 + Q_8^2},$$

$$B_8 = \frac{Q_7\left(Q_{10} + Q_{12} + Q_{14}\right) - Q_8\left(Q_1 + Q_{11} + Q_{13}\right)}{Q_7^2 + Q_8^2}$$

$$A_9 = \frac{-\lambda}{2} + \frac{1}{2\sqrt{2}}\left[\sqrt{\lambda^2 - \frac{4\lambda^2}{K} - 4M^2)^2 + 16\omega^2} + \left(\lambda^2 - \frac{4\lambda^2}{K} - 4M^2\right)\right]^{1/2}$$

$$B_9 = \frac{1}{2\sqrt{2}}\left[\sqrt{\left(\lambda^2 - \frac{4\lambda^2}{K} - 4M^2\right)^2 + 16\omega^2} - \left(\lambda^2 - \frac{4\lambda^2}{K} - 4M^2\right)\right]^{1/2}$$

$$A_{10} = \frac{-\lambda}{2} - \frac{1}{2\sqrt{2}}\left[\sqrt{\left(\lambda^2 - \frac{4\lambda^2}{K} - 4M^2\right)^2 + 16\omega^2} + \left(\lambda^2 - \frac{4\lambda^2}{K} - 4M^2\right)\right]^{1/2}$$

$$B_{10} = \frac{-1}{2\sqrt{2}}\left[\sqrt{\left(\lambda^2 - \frac{4\lambda^2}{K} - 4M^2\right)^2 + 16\omega^2} - \left(\lambda^2 - \frac{4\lambda^2}{K} - 4M^2\right)\right]^{1/2}$$

$$A_{11} = \frac{Q_{15}Q_{17} + Q_{16}Q_{18}}{Q_{17}^2 + Q_{18}^2}, \qquad B_{11} = \frac{Q_{16}Q_{17} - Q_{15}Q_{18}}{Q_{17}^2 + Q_{18}^2}$$

$$A_{12} = \frac{Q_{19}Q_{21} + Q_{20}Q_{22}}{Q_{12}^2 + Q_{22}^2}, \qquad B_{12} = \frac{Q_{20}Q_{21} - Q_{19}Q_{22}}{Q_{21}^2 + Q_{22}^2}$$

$$A_{13} = \frac{Q_{23}Q_{25} + Q_{24}Q_{26}}{Q_{25}^2 + Q_{26}^2}, \quad B_{13} = \frac{Q_{24}Q_{25} - Q_{23}Q_{26}}{Q_{25}^2 + Q_{26}^2}$$

$$A_{14} = \frac{Q_{27}Q_{29} + Q_{28}Q_{30}}{Q_{29}^2 + Q_{30}^2}, \quad B_{14} = \frac{Q_{28}Q_{29} - Q_{27}Q_{30}}{Q_{29}^2 + Q_{30}^2}$$

$$A_{15} = (1 - h_1 A_2) + (B_{11}B_2h_1 + A_{12}(h_1A_1 - 1) - B_{12}B_1h_1 + A_{13}(1 - h_1A_3)$$
$$+ B_{13}B_3h_1 + A_{14}(1 - h_1A_4) + B_{14}B_4h_1$$

$$B_{15} = B_{11}(1 - h_1A_2) - A_{11}B_2h_1 + B_{12}(h_1A_1 - 1) + A_{12}B_1h_1 + B_{13}(1 - h_1A_3)$$
$$- A_{13}B_3h_1 + B_{14}(1 - h_1A_4) - A_{14}B_4h_1$$

$$A_{16} = \left(e^{A_2}\cos B_2\right)\left[A_{11}(1 - h_1A_2) + B_{11}B_2h_1\right] - \left(e^{A_2}\sin B_2\right)\left[B_{11}(1 - h_1A_2)\right.$$
$$- A_{11}B_2h_1\right] + \left(e^{A_1}\cos B_1\right)\left[A_{12}(h_1A_1 - 1) - B_{12}B_1h_1\right] - \left(e^{A_1}\sin B_1\right)\left[B_{12}(h_1A_1 - 1)\right.$$
$$+ A_{12}B_1h_1\right] + \left(e^{A_3}\cos B_3\right)\left[A_{13}(1 - h_1A_3) + B_{13}B_3h_1\right] - \left(e^{A_3}\sin B_3\right)\left[B_{13}(1 - h_1A_3)\right.$$
$$- A_{13}B_3h_1\right] + \left(e^{A_4}\cos B_4\right)\left[A_{14}(1 - h_1A_4) + B_{14}B_3h_1\right]$$
$$- \left(e^{A_4}\sin B_4\right)\left[B_{14}(1 - h_1A_4) - A_{14}B_4h_1\right]$$

$$B_{16} = \left(e^{A_2}\sin B_2\right)\left[A_{11}(1 - h_1A_2) + B_{11}B_2h_1\right] - \left(e^{A_2}\cos B_2\right)\left[B_{11}(1 - h_1A_2)\right.$$
$$- A_{11}B_2h_1\right] + \left(e^{A_1}\sin B_1\right)\left[A_{12}(h_1A_1 - 1) - B_{12}B_1h_1\right] - \left(e^{A_1}\cos B_1\right)\left[B_{12}(h_1A_1 - 1)\right.$$
$$+ A_{12}B_1h_1\right] + \left(e^{A_3}\sin B_3\right)\left[A_{13}(1 - h_1A_3) + B_{13}B_3h_1\right] - \left(e^{A_3}\cos B_3\right)\left[B_{13}(1 - h_1A_3)\right.$$
$$- A_{13}B_3h_1\right] + \left(e^{A_4}\sin B_4\right)\left[A_{14}(1 - h_1A_4) + B_{14}B_3h_1\right]$$
$$+ \left(e^{A_4}\cos B_4\right)\left[B_{14}(1 - h_1A_4) - A_{14}B_4h_1\right]$$

$$A_{17} = \frac{Q_{31}Q_{33} + Q_{32}Q_{34}}{Q_{33}^2 + Q_{34}^2}, \quad B_{17} = \frac{Q_{32}Q_{33} - Q_{31}Q_{34}}{Q_{33}^2 + Q_{34}^2}$$

$$A_{18} = \frac{Q_{35}Q_{37} + Q_{36}Q_{38}}{Q_{37}^2 + Q_{38}^2}, \quad B_{18} = \frac{Q_{36}Q_{37} - Q_{35}Q_{38}}{Q_{37}^2 + Q_{38}^2}$$

$$P_1 = e^{A_1 + A_2 y}(\cos B_1 \cos B_2 y - \sin B_1 \sin B_2 y)$$

$$P_2 = e^{A_1 + A_2 y}(\sin B_1 \cos B_2 y + \cos B_1 \sin B_2 y)$$

$$P_3 = e^{A_1 + A_2 y}(\cos B_2 \cos B_1 y - \sin B_2 \sin B_1 y)$$

$$P_4 = e^{A_1 + A_2 y}(\sin B_2 \cos B_1 y + \cos B_2 \sin B_1 y)$$

$$P_5 = So\, Sc\, e^{A_2}\left[\left(A_1^2 - B_1^2\right)\cos B_2 - 2A_1B_1\sin B_2\right]$$

$$P_6 = So\, Sc\, e^{A_2}\left[\left(A_1^2 - B_1^2\right)\sin B_2 + 2A_1B_1\cos B_2\right]$$

$$P_7 = \left(e^{A_1}\cos B_1 - e^{A_2}\cos B_2\right)\left(A_1^2 - B_1^2 + Sc\lambda A_1\right) - \left(e^{A_1}\sin B_1 - e^{A_2}\sin B_2\right)$$
$$\left(2A_1B_1 + Sc\,\lambda B_1 - \omega Sc\right)$$

$$P_8 = \left(e^{A_1}\sin B_1 - e^{A_2}\sin B_2\right)\left(A_1^2 - B_1^2 + Sc\lambda A_1\right) - \left(e^{A_1}\cos B_1 - e^{A_2}\cos B_2\right)$$
$$\left(2A_1B_1 + Sc\,\lambda B_1 - \omega\, Sc\right)$$

$$P_9 = SoSc\, e^{A_1}\left[2A_2B_2\sin B_1 - \left(A_2^2 - B_2^2\right)\cos B_1\right]$$

$$P_{10} = So\,Sc\,e^{A_1}\left[-2A_2B_2\cos B_1 - \left(A_2^2 - B_2^2\right)\sin B_1\right]$$

$$P_{11} = \left(e^{A_1}\cos B_1 - e^{A_2}\cos B_2\right)\left(A_2^2 - B_2^2 + Sc\lambda A_2\right) - \left(e^{A_1}\sin B_1 - e^{A_2}\sin B_2\right)$$
$$\left(2A_2B_2 + Sc\lambda B_2 - \omega Sc\right)$$

$$P_{12} = \left(e^{A_1}\cos B_1 - e^{A_2}\cos B_2\right)\left(2A_2B_2 + Sc\lambda B_2 - \omega Sc\right) + \left(e^{A_1}\sin B_1 - e^{A_2}\sin B_2\right)$$
$$\left(A_2^2 - B_2^2 + Sc\lambda A_2\right)$$

$$E_1 = \left(e^{A_1}\cos B_1 - e^{A_2}\cos B_2\right),\quad E_2 = \left(e^{A_1}\sin B_1 - e^{A_2}\sin B_2\right)$$

$$Z_1 = \frac{E_1}{E_1^2 + E_2^2},\, Z_2 = \frac{E_2}{E_1^2 + E_2^2}$$

$$Q_1 = A_5\left(e^{A_4}\cos B_4 - e^{A_1}\cos B_1\right) - B_5\left(e^{A_2}\sin B_4 - e^{A_1}\sin B_1\right)$$

$$Q_2 = A_5\left(e^{A_4}\sin B_4 - e^{A_1}\sin B_1\right) + B_5\left(e^{A_4}\cos B_4 - e^{A_1}\cos B_1\right)$$

$$Q_3 = A_6\left(e^{A_4}\cos B_4 - e^{A_1}\cos B_2\right) - B_6\left(e^{A_4}\sin B_4 - e^{A_1}\sin B_2\right)$$

$$Q_4 = A_6\left(e^{A_4}\sin B_4 - e^{A_1}\sin B_2\right) + B_6\left(e^{A_4}\cos B_4 - e^{A_1}\cos B_2\right)$$

$$Q_5 = -e^{A_4}\cos B_4,\quad Q_6 = -e^{A_4}\sin B_4$$

$$Q_7 = (e^{A_3}\cos B_3 - e^{A_4}\cos B_4),\, Q_8 = e^{A_3}\sin B_3 - e^{A_4}\sin B_4$$

$$Q_9 = A_5\left(e^{A_1}\cos B_1 - e^{A_3}\cos B_3\right) - B_5\left(e^{A_1}\sin B_1 - e^{A_3}\sin B_3\right)$$

$$Q_{10} = A_5\left(e^{A_1}\sin B_1 - e^{A_3}\sin B_3\right) + B_5\left(e^{A_1}\cos B_1 - e^{A_3}\cos B_3\right)$$

$$Q_{11} = A_6\left(e^{A_2}\cos B_2 - e^{A_3}\cos B_3\right) - B_6\left(e^{A_2}\sin B_2 - e^{A_3}\sin B_3\right)$$

$$Q_{12} = A_6\left(e^{A_2}\sin B_2 - e^{A_3}\sin B_3\right) + B_6\left(e^{A_2}\cos B_2 - e^{A_3}\cos B_3\right)$$

$$Q_{13} = e^{A_3}\cos B_3,\qquad Q_{14} = e^{A_3}\sin B_3$$

$$Q_{15} = e^{A_1}Gr\lambda^2\cos B_1 + A_6 Gc\lambda^2\left(e^{A_1}\cos B_1 - e^{A_2}\cos B_2\right) - B_6 Gc\lambda^2\left(e^{A_1}\sin B_1 - e^{A_2}\sin B_2\right)$$

$$Q_{16} = e^{A_1}Gr\lambda^2\sin B_1 + B_6 Gc\lambda^2\left(e^{A_1}\cos B_1 - e^{A_2}\cos B_2\right) + A_6 Gc\lambda^2\left(e^{A_1}\sin B_1 - e^{A_2}\sin B_2\right)$$

$$Q_{17} = \left(e^{A_1}\cos B_1 - e^{A_2}\cos B_2\right)\left\{A_2^2 - B_2^2 + \lambda A_2 - \left(\frac{\lambda^2}{K} + M^2\right)\right\}$$
$$-\left(e^{A_1}\sin B_1 - e^{A_2}\sin B_2\right)\left(2A_2B_2 + \lambda B_2 - \omega\right)$$

$$Q_{18} = \left(e^{A_1}\sin B_1 - e^{A_2}\sin B_2\right)\left\{A_2^2 - B_2^2 + \lambda A_2 - \left(\frac{\lambda^2}{K} + M^2\right)\right\}$$
$$+\left(e^{A_1}\cos B_1 - e^{A_2}\cos B_2\right)\left(2A_2B_2 + \lambda B_2 - \omega\right)$$

$$Q_{19} = e^{A_2}Gr\lambda^2\cos B_2 - A_5 Gc\lambda^2\left(e^{A_1}\cos B_1 - e^{A_2}\cos B_2\right) + B_5 Gc\lambda^2\left(e^{A_1}\sin B_1 - e^{A_2}\sin B_2\right)$$

$$Q_{20} = e^{A_2}Gr + \lambda^2\sin B_2 - B_5 Gc\lambda^2\left(e^{A_1}\cos B_1 - e^{A_2}\cos B_2\right) - A_5 Gc\lambda^2\left(e^{A_1}\sin B_1 - e^{A_2}\sin B_2\right)$$

$$Q_{21} = \left(e^{A_1}\cos B_1 - e^{A_2}\cos B_2\right)\left\{A_1^2 - B_1^2 - \lambda A_1\left(\frac{\lambda^2}{K} + M^2\right)\right\}$$
$$-\left(e^{A_1}\sin B_1 - e^{A_2}\sin B_2\right)\left(2A_1B_1 - \lambda B_1 - \omega\right)$$

$$Q_{22} = \left(e^{A_1}\cos B_1 - e^{A_2}\cos B_2\right)\left(2A_1 B_1 + \lambda B_1 - \omega\right) + \left(e^{A_1}\sin B_1 - e^{A_2}\sin B_2\right)$$

$$\cdot\left[A_1^2 - B_1^2 + \lambda A_1 - \left(\frac{\lambda^2}{K} + M^2\right)\right]\Bigg]$$

$$Q_{23} = Gc\,\lambda^2 A_7, \qquad Q_{24} = Gc\,\lambda^2 B_7$$

$$Q_{25} = A_3^2 - B_3^2 + \lambda A_3 - \left(\frac{\lambda^2}{K} + M^2\right), \quad Q_{26} = \left(2A_3 B_3 + \lambda B_3 - \omega\right)$$

$$Q_{27} = Gc\lambda^2 A_8, \qquad Q_{28} = Gc\lambda^2 B_8$$

$$Q_{29} = A_4^2 - B_4^2 + \lambda A_4 - \left(\frac{\lambda^2}{K} + M^2\right), \quad Q_{30} = \left(2A_4 B_4 + \lambda B_4 - \omega\right)$$

$$Q_{31} = -A_{16} + e^{A_{10}} A_{15}\cos B_{10} - e^{A_{10}} B_{15}\sin B_{10}$$

$$Q_{32} = -B_{16} + e^{A_{10}} A_{15}\sin B_{10} + e^{A_{10}} B_{15}\cos B_{10}$$

$$Q_{33} = \left(1 - h_1 A_9\right)\left(e^{A_{10}}\cos B_{10} - e^{A_9}\cos B_9\right) + \left(h_1 B_9\right)\left(e^{A_{10}}\sin B_{10} - e^{A_9}\sin B_9\right)$$

$$Q_{34} = \left(1 - h_1 A_9\right)\left(e^{A_{10}}\sin B_{10} - e^{A_9}\sin B_9\right) - \left(h_1 B_9\right)\left(e^{A_{10}}\cos B_{10} - e^{A_9}\cos B_9\right)$$

$$Q_{35} = A_{16} - e^{A_9} A_{15}\cos B_9 - e^{A_9} B_{15}\sin B_9$$

$$Q_{36} = B_{16} - e^{A_9} A_{15}\sin B_9 - e^{A_9} B_{15}\cos B_9$$

$$Q_{37} = \left(1 - h_1 A_{10}\right)\left(e^{A_{10}}\cos B_{10} - e^{A_9}\cos B_9\right) + \left(h_1 B_{10}\right)\left(e^{A_{10}}\sin B_{10} - e^{A_9}\sin B_9\right)$$

$$Q_{38} = \left(1 - h_1 A_{10}\right)\left(e^{A_{10}}\sin B_{10} - e^{A_9}\sin B_9\right) - \left(h_1 B_{10}\right)\left(e^{A_{10}}\cos B_{10} - e^{A_9}\cos B_9\right)$$

IV.   SKIN FRICTION AND NUSSELT NUMBER

With the help of velocity and temperature profiles, the important parameters skin friction (C_f) and Nusselt number (Nu) at the plate y = 0 and y = 1 in terms of their amplitude and phase are given as:

Skin Friction

$$\tau_0 = \mu\left(\frac{\partial u}{\partial y}\right)_{y=0} \text{ and } \tau_1 = \mu\left(\frac{\partial u}{\partial y}\right)_{y=1}$$

In non-dimensional form after dropping the asterisks over them

$$(C_f)_{y=0} = \frac{\tau_0 d}{\mu U} = \left(\frac{\partial u_0}{\partial y}\right)_{y=0} + \in | \ J \ | \cos\left(t + \alpha_1\right) \quad ...(32)$$

$$(C_f)_{y=1} = \frac{\tau_1 d}{\mu U} = \left(\frac{\partial u_0}{\partial y}\right)_{y=1} + \in | \ H \ | \cos\left(t + \alpha_2\right) \qquad ...(33)$$

where the sinusoidal skin-friction at plate y = 0

$$C_f^1 = \left(\frac{\partial u_0}{\partial y}\right)_{y=0} = D_1 R_{15} + D_2 R_{16} - R_2 R_{17} + R_1 R_{18} + Sc\lambda R_{20} \quad ...(34)$$

where

$$J \ = \ J_r + i\,J_i = \left(\frac{\partial u_1}{\partial y}\right)_{y=0}, \tan\alpha_1 = \frac{J_i}{J_r}$$

$$J_r = A_9 A_{17} - B_9 B_{17} + A_{10} A_{18} - B_{10} B_{18} - A_2 A_{11} + B_2 B_{11} + A_1 A_{12} - B_1 B_{12}$$

$$-A_3A_{13} + B_3B_{13} - A_4A_{14} + B_4B_{14}$$

$$J_i = A_9B_{17} + B_9A_{17} + A_{10}B_{18} + B_{10}A_{18} - A_2B_{11} - B_2A_{11} + A_1B_{12}$$

$$+B_1A_{12} - A_3B_{13} - B_3A_{13} - A_4B_{14} - B_4A_{14}$$

$$\left(\frac{\partial u_0}{\partial y}\right)_{y=0} = D_1R_{15} + D_2R_{16} - R_2R_{17} + R_1R_{18} + Sc\lambda R_{20}$$

and

$$H = H_r + iH_i = \left(\frac{\partial u_1}{\partial y}\right)_{y=1} , \quad \tan\alpha_2 = \frac{H_i}{H_r}$$

$$H_r = A_9e^{A_9}\left[A_{17}\cos B_9 - B_{17}\sin B_9\right] + e^{A_9}\left[-B_9A_{17}\sin B_9 - B_9B_{17}\cos B_9\right]$$

$$+A_{10}e^{A_{10}}\left[A_{18}\cos B_{10} - B_{18}\sin B_{10}\right] + e^{A_{10}}\left[-B_{10}A_{18}\sin B_{10} - B_{10}B_{18}\cos B_{10}\right]$$

$$+A_2e^{A_2}\left[B_{11}\sin B_2 - A_{11}\cos B_2\right] + e^{A_2}\left[B_2B_{11}\cos B_2 + B_2A_{11}\sin B_2\right]$$

$$+A_1e^{A_1}\left[A_{12}\cos B_1 - B_{12}\sin B_1\right] + e^{A_1}\left[-B_1A_{12}\sin B_1 - B_1B_{12}\cos B_1\right]$$

$$+A_3e^{A_3}\left[B_{13}\sin B_3 - A_{13}\cos B_3\right] + e^{A_3}\left[B_3B_{13}\cos B_3 + B_3A_{13}\sin B_3\right]$$

$$+A_4e^{A_4}\left[B_{14}\sin B_4 - A_{14}\cos B_4\right] + e^{A_4}\left[B_4B_{14}\cos B_4 + B_4A_{14}\sin B_4\right]$$

$$H_i = A_9e^{A_9}\left[B_{17}\cos B_9 + A_{17}\sin B_9\right] + e^{A_9}\left[-B_9B_{17}\sin B_9 + B_9A_{17}\cos B_9\right]$$

$$+A_{10}e^{A_{10}}\left[B_{18}\cos B_{10} + A_{18}\sin B_{10}\right] + e^{A_{10}}\left[-B_{10}B_{18}\sin B_{10} + B_{10}A_{18}\cos B_{10}\right]$$

$$-A_2e^{A_2}\left[B_{11}\cos B_2 + A_{11}\sin B_2\right] - e^{A_2}\left[-B_2B_{11}\sin B_2 + B_2A_{11}\cos B_2\right]$$

$$+A_1e^{A_1}\left[B_{12}\cos B_1 + A_{12}\sin B_1\right] + e^{A_1}\left[-B_1B_{12}\sin B_1 + B_1A_{12}\cos B_1\right]$$

$$-A_3e^{A_3}\left[B_{17}\cos B_3 + A_{13}\sin B_3\right] - e^{A_3}\left[-B_3B_{13}\sin B_3 + B_3A_{13}\cos B_3\right]$$

$$-A_4e^{A_4}\left[B_{14}\cos B_4 + A_{14}\sin B_4\right] - e^{A_4}\left[-B_4B_{14}\sin B_4 + B_4A_{14}\cos B_4\right]$$

$$\left(\frac{\partial u_0}{\partial y}\right)_{y=1} = D_1R_{15}e^{R_{15}} + D_2R_{16}e^{R_{16}} - R_2R_{17}e^{R_2} + R_1R_{18}e^{R_1} + Sc\lambda R_{20}e^{-Sc\lambda}$$

Nusselt Number

$$q_0 = \frac{-L_1}{(T_0 - T_d)}\left(\frac{\partial T}{\partial y}\right)_{y=0} \quad \text{and} \quad q_1 = \frac{-L_1}{(T_0 - T_d)}\left(\frac{\partial T}{\partial y}\right)_{y=1}$$

In non-dimensional form after dropping the asterisk over them

$$(Nu)_{y=0} = h_1\left[\left(\frac{\partial\theta_0}{\partial y}\right)_{y=0} + \in|F|\cos(t+\beta_1)\right] \quad …(35)$$

$$(Nu)_{y=1} = h_1\left[\left(\frac{\partial\theta_0}{\partial y}\right)_{y=1} + \in|R|\cos(t+\beta_2)\right] \quad …(36)$$

where the sinusoidal rate of heat transfer at plate y = 0

$$Nu^1 = \left(\frac{\partial\theta_0}{\partial y}\right)_{y=0} = \frac{1}{e^{R_1} - e^{R_2}}\left(R_2e^{R_1} - R_1e^{R_2}\right) \quad …(37)$$

where

$$F = F_r + iF_i = \left(\frac{\partial\theta_1}{\partial y}\right)_{y=0} , \quad \tan\beta_1 = \frac{F_i}{F_r}$$

$$F_r = e^{A_1}\left[Z_1\left(-B_2\sin B_1\right) + Z_2\left(B_2\cos B_1\right)\right] + A_2e^{A_1}\left[Z_1\left(\cos B_1\right) + Z_2\left(\sin B_1\right)\right]$$

$$-e^{A_2}\left[Z_1\left(-B_1 sinB_2\right)+Z_2 B_1 cosB_2\right]-A_1 e^{A_2}\left[Z_1\left(cosB_2\right)+Z_2\left(sinB_2\right)\right]$$

$$F_i = e^{A_1}\left[Z_1\left(B_2 cosB_1\right)-Z_2\left(-B_2 sinB_1\right)\right]+A_2 e^{A_1}\left[Z_1\left(sinB_1\right)-Z_2\left(cosB_1\right)\right]$$

$$-e^{A_2}\left[Z_1\left(B_1 cosB_2\right)-Z_2\left(-B_1 sinB_2\right)\right]-A_1 e^{A_2}\left[Z_1\left(sinB_2\right)-Z_2\left(cosB_2\right)\right]$$

$$\left(\frac{\partial\theta_0}{\partial y}\right)_{y=0}=\frac{1}{e^{R_1}-e^{R_2}}\left(R_2 e^{R_1}-R_1 e^{R_2}\right)$$

and

$$R = R_r + i\,R_i = \left(\frac{\partial\theta_1}{\partial y}\right)_{y=1}, \quad tan\,\beta_2 = \frac{R_i}{R_r}$$

$$R_r = e^{A_1+A_2}\left[z_1\left(-B_2 cosB_1 sinB_2 - B_2 sinB_1 cosB_2\right)+Z_2\left(-B_2 sinB_1 sinB_2\right.\right.$$

$$+B_2 cosB_1 cosB_2\left]+A_2 e^{A_1+A_2 y}\left[z_1\left(cosB_1 cosB_2 - sinB_1 sinB_2\right)\right.\right.$$

$$+Z_2\left(sinB_1 cosB_2 + cosB_1 sinB_2\right)\right]-e^{A_1+A_2}\left[Z_1\left(-B_1 cosB_2 sinB_1\right.\right.$$

$$-B_1 sinB_2 cosB_1\right)+Z_2\left(-B_1 sinB_2 sinB_1 + B_1 cosB_2 cosB_1\right)\right]$$

$$-A_1 e^{A_1+A_2}\left[Z_1\left(cosB_2 cosB_1 - sinB_2 sinB_1\right)+Z_2\left(sinB_2 cosB_1 + cosB_2 sinB_1\right)\right]$$

$$R_i = e^{A_1+A_2}\left[z_1\left(-B_2 sinB_1 sinB_2 - B_2 cosB_1 cosB_2\right)-Z_2\left(-B_2 cosB_1 sinB_2\,d\right.\right.$$

$$-B_2 sinB_1 sinB_2\right]+A_2 e^{A_1+A_2 y}\left[z_1\left(sinB_1 cosB_2 + cosB_1 sinB_2\right)\right.$$

$$-Z_2\left(cosB_1 cosB_2 - sinB_1 sinB_2\right)\right]-e^{A_1+A_2}\left[Z_1\left(-B_1 sinB_2 sinB_1\right.\right.$$

$$+B_1 cosB_2 cosB_1\right)-Z_2\left(-B_1 cosB_2 sinB_1 - B_1 sinB_2 cosB_1\right)\right]$$

$$-A_1 e^{A_1+A_2}\left[Z_1\left(sinB_2 cosB_1 + cosB_2 sinB_1\right)-Z_2\left(cosB_2 cosB_1 sinB_2 sinB_1\right)\right]$$

$$\left(\frac{\partial\theta_0}{\partial y}\right)_{y=1}=\frac{1}{e^{R_1}-e^{R_2}}\left(R_2 e^{R_1+R_2}-R_1 e^{R_2+R_1}\right)$$

(Table 1. Amplitude | J | and phase α_1 of skin-friction at plate y = 0 for fixed)

S.No.	Gr	Gc	Sc	Pr	λ	h_1	ω	| J |	Tan α_1
1	5.0	2.0	0.6	0.71	5.0	0.05	5.0	3.67263	-0.44213
2	7.0	2.0	0.6	0.71	5.0	0.05	5.0	4.14786	-0.57285
3	7.0	3.0	0.6	0.71	5.0	0.05	5.0	3.84867	-0.47512
4	5.0	2.0	0.94	0.71	5.0	0.05	5.0	3.74312	-0.46314
5	5.0	2.0	0.94	7.0	5.0	0.05	5.0	0.98213	0.43198
6	5.0	2.0	0.6	0.71	5.0	0.0	5.0	4.01254	-0.51254
7	7.0	2.0	0.6	0.71	5.0	0.05	20.0	5.31243	-1.00342
8	5.0	2.0	0.6	0.71	8.0	0.0	5.0	4.82165	-0.75431

Values of K = 1.0, So = 1.0, S = 0.2 and M = 0.5

(Table 2. Amplitude | F | and phase tan β_1 of heat transfer at plate y = 0)

S.No.	Pr	λ	S	ω	| F |	Tan β_1
1	0.71	5.0	0.2	5.0	1.08639	1.00513
2	7.0	5.0	0.2	5.0	6.56256	0.53165
3	0.71	8.0	0.2	5.0	0.74542	2.48025
4	0.71	5.0	0.6	5.0	0.83412	2.15968
5	0.71	5.0	0.2	20.0	2.37215	1.20461

V.   RESULT AND DISCUSSIONS

In order to understand the physical importance of the flow between the two plates, calculations have been carried out for velocity, temperature, concentration, skin friction and the rate of heat transfer. Effects for different values of thermal Grashof number (Gr), mass Grashof number (Gc), permeability parameter (K), Prandtl number (Pr), velocity slip parameter (h_1), frequency (ω), Hartmann number (M), suction parameter ($\Box$), heat source parameter (S), Schmidt number (Sc) and soret number (So) are shown graphically. The values of Prandtl number are chosen as 0.71 and 7, which represent air and water respectively at 20°C. In terms of amplitude and phase, the skin friction and the rate of heat transfer are reported in table 1 and 2 at plate y = 0. Moreover sinusoidal skin friction and Nusselt number are also calculated and shown graphically at the plate y =

0. We fix $\in = 0.02$ $t = \dfrac{\pi}{2}$ throughout our calculations.

In figure 2 and 3 , velocity profiles are plotted against y. From the figures, we observe that on increasing Gr, K, $\Box$, S and So, the velocity of the fluid increases. On the other hand velocity drops on increasing Gc, Pr, h_1, M, $\Box$ and Sc. Here, we notice that velocity remains positive near the plate y = 0 but after some distance it becomes negative, this is due to the fact that our plates are moving in opposite directions, specifically plate at y = 1 is moving downwards. Also, physically increase in the permeability parameter (K) implies that medium becomes more porous that is more fluid can flow through, hence increasing the velocity of the fluid.

S.no.	Gr	Gc	K	Pr	h_1	ω
1	5	2	1	0.71	0.05	5.0
2	7	2	1	0.71	0.05	5.0
3	5	3	1	0.71	0.05	5.0
4	5	2	2	0.71	0.05	5.0
5	5	2	1	7	0.05	5.0
6	5	2	1	0.71	0.0	5.0
7	5	2	1	0.71	0.05	20

(table header: $\in$ =0.02, t= π/2, S = 0.2, Sc = 0.6 , So= 1, M = 0.5, λ = 5)
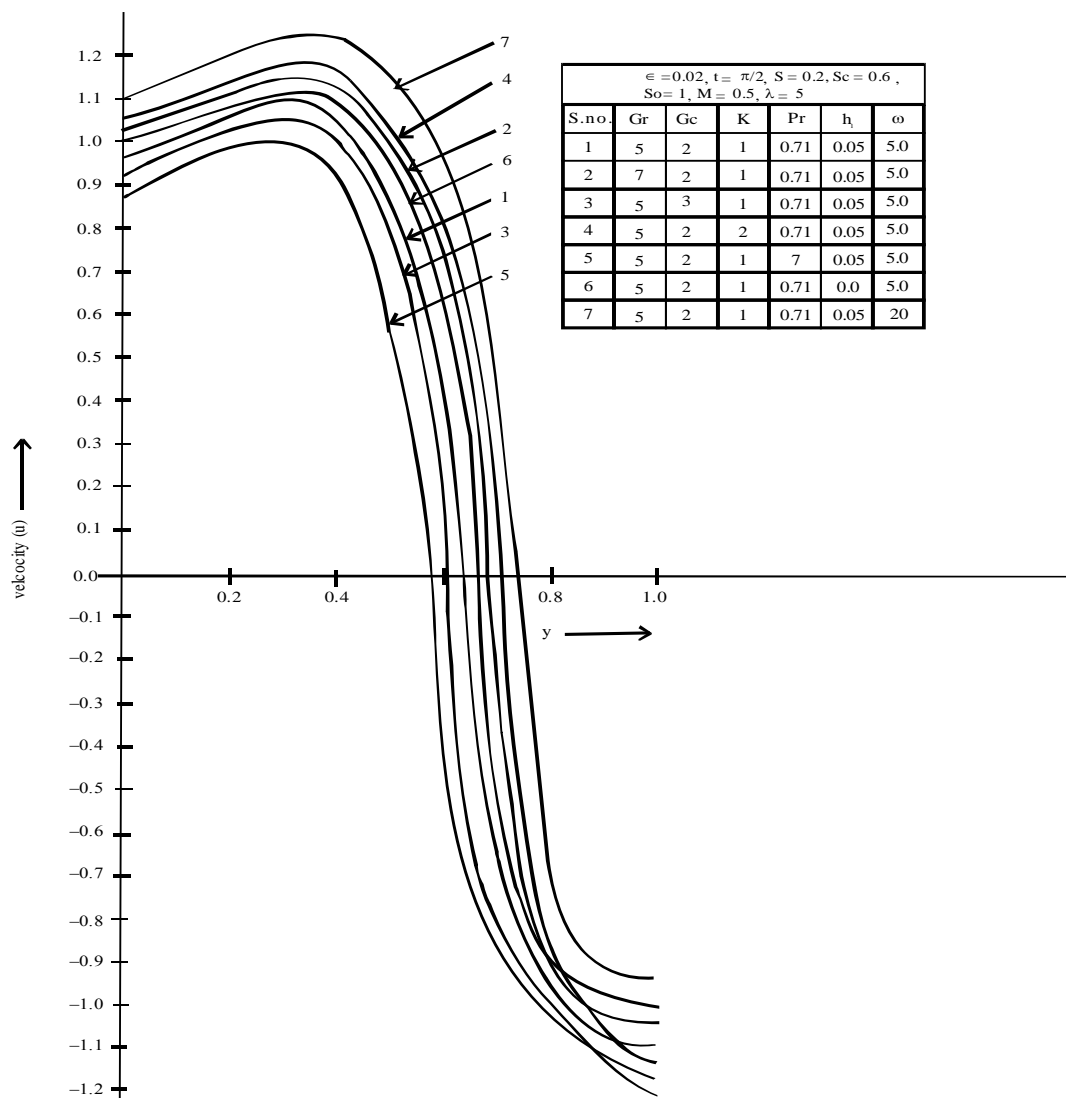
(Figure 2: Velocity profiles plotted against y for different values of Gr, Gc,, K, Pr, h_1 and $\Box$.)
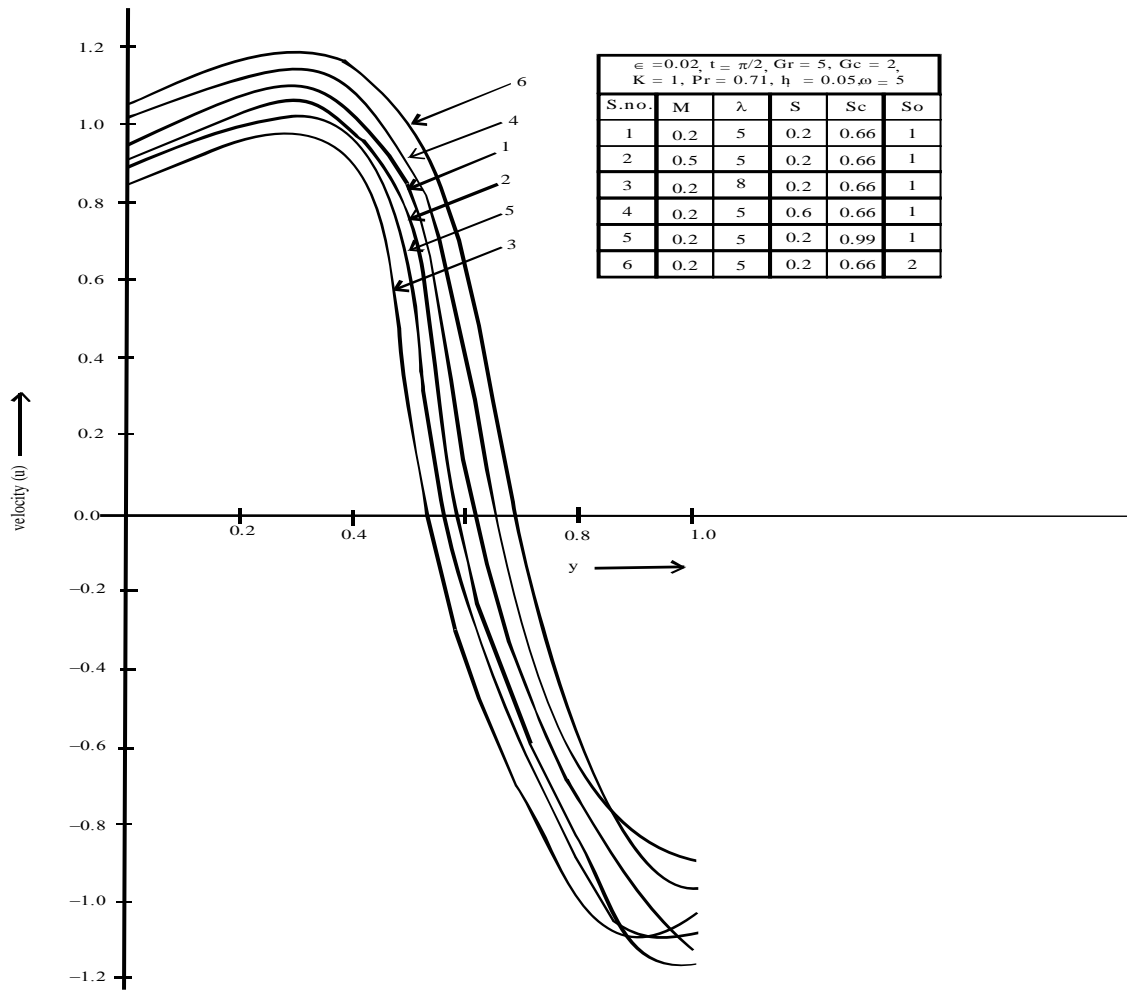
(Figure 3: Velocity profiles plotted against y for different values of M, □ , S, Sc and So.)

$\in$ =0.02, t = $\pi/2$, Gr = 5, Gc = 2, K = 1, Pr = 0.71, ɧ = 0.05,ω = 5					
S.no.	M	λ	S	Sc	So
1	0.2	5	0.2	0.66	1
2	0.5	5	0.2	0.66	1
3	0.2	8	0.2	0.66	1
4	0.2	5	0.6	0.66	1
5	0.2	5	0.2	0.99	1
6	0.2	5	0.2	0.66	2
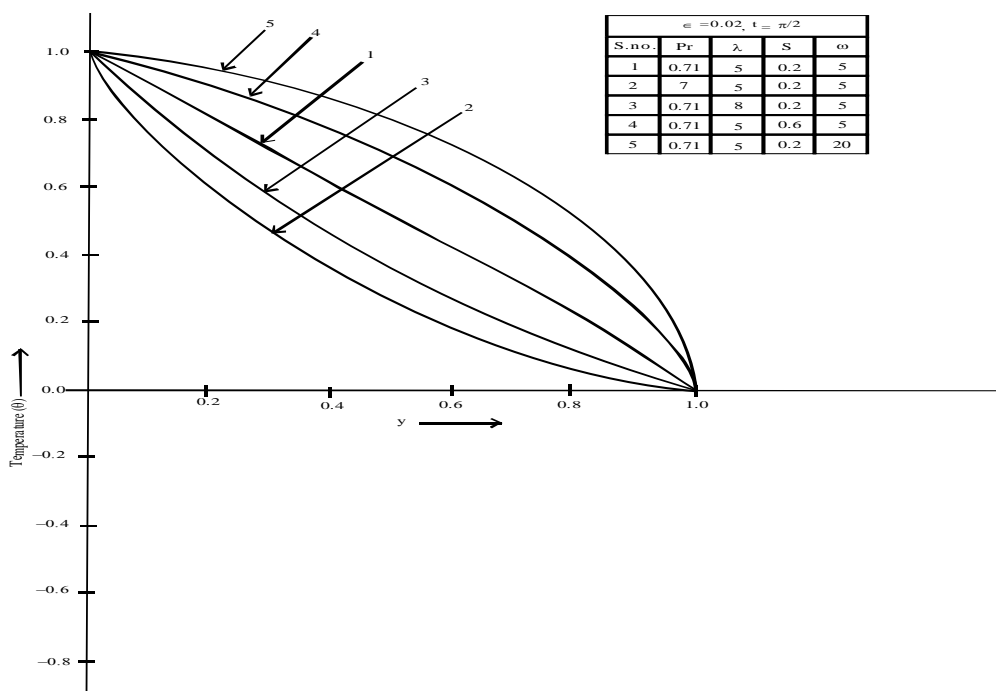
(Figure 4: Temperature profiles plotted against y for different values of Pr, □ , S and □ .)

$\in$ =0.02, t = $\pi/2$				
S.no	Pr	λ	S	ω
1	0.71	5	0.2	5
2	7	5	0.2	5
3	0.71	8	0.2	5
4	0.71	5	0.6	5
5	0.71	5	0.2	20

		∈ = 0.02, t = π/2				
S.no.	Pr	λ	S	ω	Sc	So
1	0.71	5	0.2	5	0.66	1
2	7	5	0.2	5	0.66	1
3	0.71	8	0.2	5	0.66	1
4	0.71	5	0.6	5	0.66	1
5	0.71	5	0.2	20	0.66	1
6	0.71	5	0.2	5	0.94	1
7	0.71	5	0.2	5	0.66	2
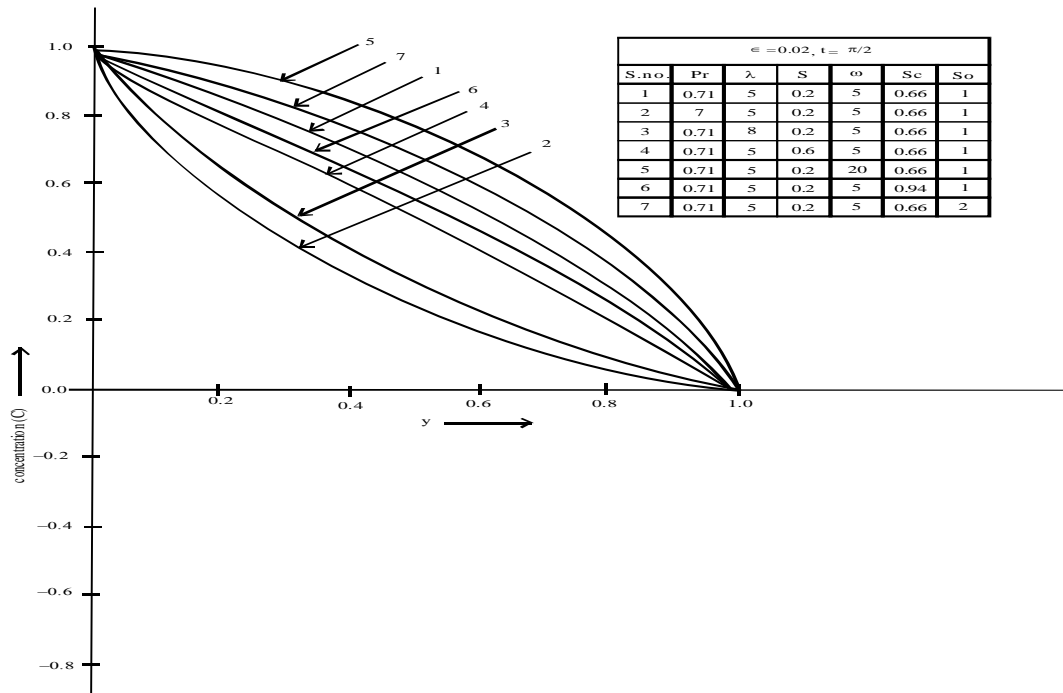
(Figure 5: Concentration profiles plotted against y for different values of Pr, λ, S, ω, Sc and So.)

		K = 1, So = 1, S = 0.2				
S.no	Gr	Gc	Sc	Pr	λ	h_t
1	5	2	0.6	0.71	5	0.05
2	7	2	0.6	0.71	5	0.05
3	7	3	0.6	0.71	5	0.05
4	5	2	0.94	0.71	5	0.05
5	5	2	0.94	7	5	0.05
6	5	2	0.6	0.71	5	0.0
7	7	2	0.6	0.71	8	0.05
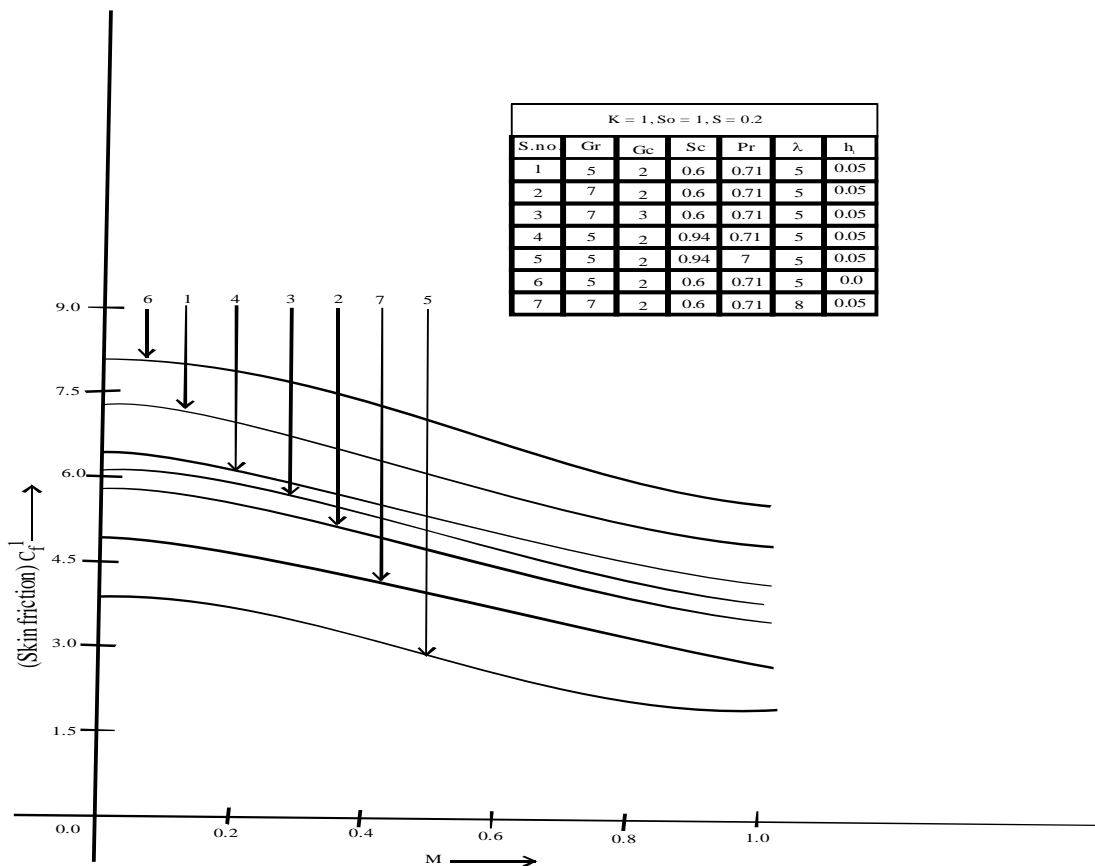
(Figure 6: Sinusoidal skin friction C_f^1 plotted against M at plate y = 0

S.no	Pr	λ	h_1
1	0.71	5	0.05
2	7	5	0.05
3	0.71	8	0.05
4	0.71	5	0.0
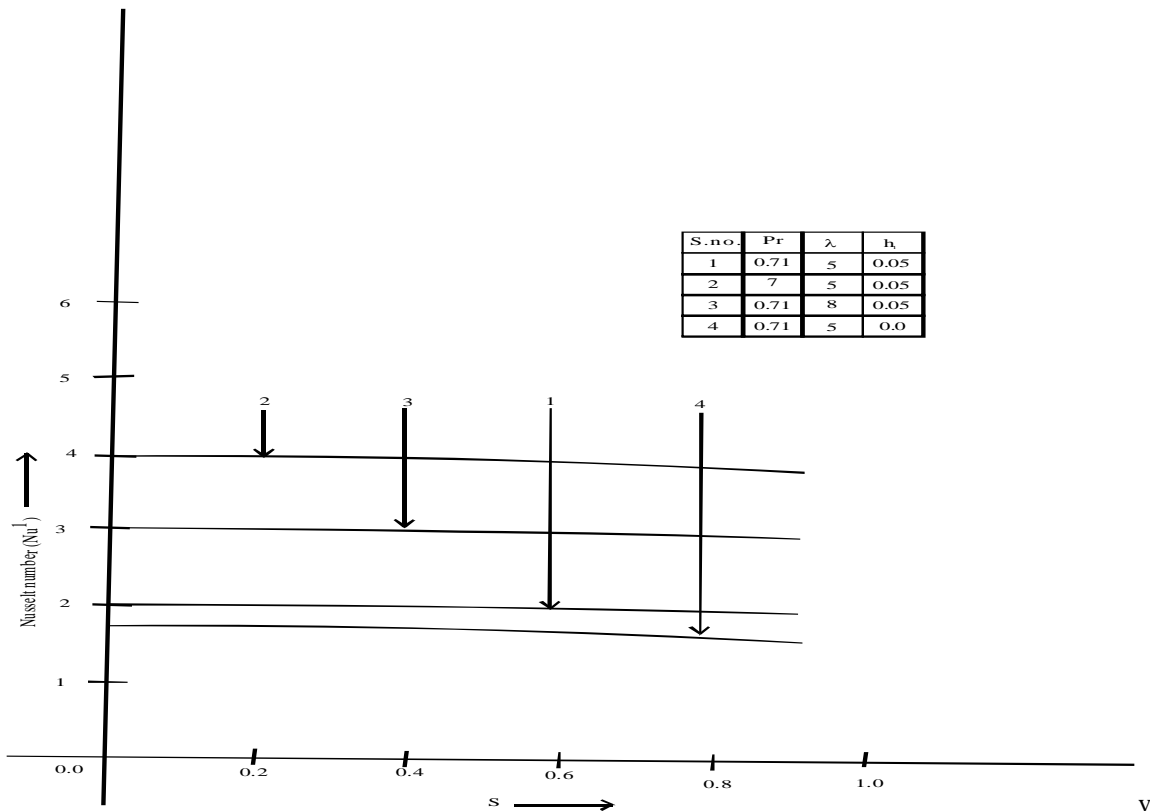
(Figure 7: Sinusoidal rate of heat transfer Nu^1 plotted against S at plate y = 0

Temperature profiles are plotted against y, in figure 4, we observe that on increasing the values of the source parameter (S) and frequency ($\square$), temperature rises, where as on increasing Pr and $\square$, temperature drops. It is noteworthy that as we increase the heat source S i.e. we add heat and hence the temperature rises. In figure 5, concentration profiles are plotted against y. From the figure we observe that concentration profiles are less for higher values of Pr, $\square$, S and Sc. On the other hand for increase in $\square$ and So we get higher concentration profiles.

Table 1, shows the amplitude |J| and phase angle tan $\square_1$ of the skin friction at the plate y = 0, fixing K = 1, So = 1, S = 0.2 and M = 0.5, from the table we observe that when values of $\square$, Gr, Sc and $\square$ are increased, the amplitude |J| increases, but increase in the values of Gc, Pr and h_1 drops the amplitude. The values of tan $\square_1$ shows that there is always a phase lag. Also tan $\square_1$ is higher for water as compared for air. The sinusoidal skin friction at the plate y = 0 is shown in figure 6, fixing K = 1, So = 1 and S = 0.2. From the figure we observe that increasing the values of h_1, $\square$, Gr, Sc and Pr, decreases C_f^1, where as C_f^1 rises with increase in the value of Gc. Physically, increase in the value of velocity slip parameter (h_1) will reduce the friction near the plate hence decreasing C_f^1 since more the slip less will be the friction at the plate. Moreover, skin friction is higher for air (Pr = 0.71) as compared for water (Pr = 7).

Amplitude |F| and phase angle tan $\square_1$, of the rate of heat transfer are shown in Table 2, at the plate y = 0. We observe that when Pr and $\square$ are increased, it increases the amplitude |F| but increase is $\square$ and S decreases it. From the values of tan $\square_1$, we observe that it is less for water as compared for air. This table shows that there always remains a phase lag. Further, the sinusoidal rate of heat transfer at plate y = 0 is shown in figure 7. From the figure we observe increase in $\square$ and h_1, increases Nu^1. Also Nusselt number is higher for water (Pr = 7) as compared for air (Pr = 0.71).

REFERENCES

[1].   Mbeledogu, I.U., Amakiri, A.R.C and Ogulu, A., Unsteady MHD free convection flow of a compressible fluid past a moving vertical plate in the presence of radiative heat transfer. Int. J. Heat and Mass Transfer, 50, 2007, 1668-1674.

[2].   Cookey, C.I., Ogulu, A. and Omubo-Pepple, V.M., Influence of viscous dissipation and radiation on unsteady MHD free convection flow past an infinite heated vertical plate in a porous medium with time

dependent suction. Int. J. of Heat and Mass Transfer, 46, 2003, 2305-2311.

[3]. Singh, A.K. and Paul, T., Transient natural convection between two vertical wall heated/cooled asymmetrically. Int. J. Applied Mechanics and Engineering. 11, 2006, 143-154.

[4]. Bareletta, A. and Celli, M., Mixed convection MHD flow in a vertical channel: effects of Joule heating and viscous dissipation. Int. J. Heat and Mass Transfer, 51(25-26), 2008, 6110-6117.

[5]. Rajput, U.S. and Sahu, P.K., Transient free convection MHD flow between two long vertical parallel plates with variable temperature and uniform mass diffusion in a porous medium. ARPN Journal of Engineering and applied Sciences. 6, 2011, 79-86.

[6]. Narahari, M., Sreenadh, S. and Soundalgekar, V.M., Transient free convectin flow between long vertical parallel plates with constant heat flux at one boundary. J. Thermo Physics and Aeromechanics, 9(2), 2002, 287-293.

[7]. Brown, N. M. and Lai, F.C., correlations for combined heat and mass transfer from an open cavity in a horizontal channel. Int. Comm. In Heat and Mass Transfer, 32 (8), 2005, 1000-1008.

[8]. Raptis, A., Unsteady free convection flow through a porous medium. Int. J. Engin. Sci, 21, 1983, 345-348.

[9]. Raptis, A., Kafousia, N. and Massolas, C., Free convection and mass transfer flow through a porous medium bounded by an infinite vertical porous plate with constant heat flux. ZAMM, 62, 1982, 489-491.

[10]. Raptis, A., Perdikis, G. and Tzivanidis, G., Free convection flow through a porous medium bounded by a vertical surface. J. Phys. D. Appl. Phys. 14, 1981, 99-102.

[11]. Geindreau, C. and Auriault, L. Magnetohydrodynamic flows in porous media. J. of fluid mechanics, 466, 2002, 343-363.

[12]. Alagoa, K.D., Tay, G. and Abbey, T.M., Radiation and free-convection effects of a MHD flow through a porous medium between infinite parallel plates with time-dependent suction. Astrophy. Space. Sci. 260, 1999, 455-468.

[13]. Farhad, A., Norzieha, M, Sharidan, S. and Khan, I., On accelerated MHD flow in a porous medium with slip condition. European J. of Sci. Research, 57 (2), 2011, 293-304.

[14]. Mankinde, O.D. and Osalusi, E., MHD steady flow in a channel with slip at the permeable bopundaries. Rom J. Phys. 51(3-4), 2006, 319-328.

[15]. Taneja, R. and Jain, N.C., MHD flow with slip effects and temperature dependent heat source in a viscous incompressible fluid confined between a long vertical wavy walls and a parallel flat wall. Defence Science Journal, 54, 2004, 21-29.

Research Paper   Open Access

Total Harmonics Distortion Investigation in Multilevel Inverters

Avinash verma, Ruchi shivhare, Sanjeev gupta
Samrat ashoka technological engineering institute Vidisha(mp) india 464001

Abstract*:* The multilevel began with the three level inverter. Use of conventional two – level pulse width modulation (PWM) inverter provide less distorted current and voltage but at cost of higher switching losses due to high switching frequency. Multilevel inverter are emerging as a viable alternative for high power , medium voltage application. This paper compare total harmonics distortion in three level and five level diode clamped multilevel inverter. Diode –clamped three phase topology is considered for study. A sinusoidal PWM technique is used to control the switches of the inverter. Simulation study confirms the reduction in harmonics distortion.

Keywords*: - Harmonics , multilevel inverter , pulse width modulation , Total harmonics distortion*

I.   INTRODUCTION

Wave form of practical inverter are non- sinusoidal and contain certain harmonics. for low –and medium power application, square wave or quasi – square wave form voltage may be acceptable but for high – power application sinusoidal waveform with low distortion are required. Harmonics content present in the output of a dc to ac inverter can be eliminated either by using a filter circuit or by employing pulse width modulation (PWM) techniques. Use of filter has the disadvantage of large size and cost, whereas use of PWM techniques reduces the filter requirement to a minimum or to zero depending on the type of application. Traditional two level high frequency PWM inverter have some drawback, such as production of common mode voltage.[1-3]

Multilevel inverter have found better counter to the conventional two – level pulse width modulation inverter to overcome the above problems. In addition they offer the advantage of less switching stress on eachdevice for high voltage high power application , with a reduced harmonics content at low switching frequency.

A comparative study of five level and seven level diode clamped capacitor clamped and cascade inverter has been presented in [4]. The effect of a passive LC filter on the inverter performance was studied. simulation result indicated reduction in total harmonics distortion (THD) by using higher number of level.

This paper investigates five level inverter and seven level inverter diode clamped three phase inverter on the basic of the THD .an extensive simulation study to optimize the THD content in the line voltage have been presented in this paper.

II.   RELATED WORK

In recent years, industry has begun to demand higher power equipment, which now reaches the megawatt level.Controlled AC drives in themegawatt range are usually connected to the medium-voltage network. Today, it ishard to connect a single power semiconductor switch directly to medium voltage grids. For these reasons, a newfamily of multilevel inverters has emerged as the solution for working with higher voltage levels. Depending onvoltage levels of the output voltage, the inverters can be classified as two-level inverters and multilevel inverters.

The inverters with voltage level 3 or more are referred as multilevel inverters. Multilevel inverters have become attractive recently particularly because of the increased power ratings, improved harmonic performance and reduced EMI emission that can be achieved with the multiple DC levels that are available for synthesis of theoutput voltage. Xiaoming Yuan and Ivo Barbi [1] proposed fundamentals of a new diode clamping multilevelinverter. Bouhali et al[2] developed DC link capacitor voltage balancing in a three phase diode clamped invertercontrolled by a direct space vector of line to line voltages. AnshumanShukla et al [3]

introduced controlschemes for DC capacitor voltages equalization in diode clamped multilevel inverter basedDSTATCOM.Monge et al [4] proposed multilevel diode clamped converter for photovoltaic generators with independentvoltage control of each solar array. Renge and Suryawanshi [5] developed five level diode clamped inverter toeliminate common mode voltage and reduce dv/dt in medium voltage rating induction motor drives. HideakiFujita and Naoya Yamashita [6] discussed performance of a diode clamped linear amplifier. Hatti et al [7]proposed a 6.6-KV transformer less motor drive using a five level diode clamped PWM inverter for energysavings of pumps and blowers. Srinivas in [8] discussed uniform overlapped multi carrier PWM for a six leveldiode clamped inverter. EnginOzdemir et al [9] introduced fundamental frequency modulated six level diodeclamped multilevelinverter for three phase standalone photovoltaic system. BerrezzekFarid and BerrezzekFarid[10] made a study on new techniques of controlled PWM inverters. Anshumanshukla et al [11] proposed flyingcapacitor based chopper circuit for DC capacitor voltage balancing in diode clamped multilevel inverter. Thisliteraturesurvey revealsfew papers only on various PWM techniques and hence this work presents a novelapproach for controlling the harmonics of output voltage of chosen MLI employing sinusoidal switchingstrategies. Simulations are performed using MATLAB-SIMULINK. Harmonics analysis and evaluation ofperformance measures for various modulation indices have been carried out and presented.

III.   MULTILEVEL INVERTER
Neutral Point-Clamped Inverter:

A three-level diode-clamped inverter is shown in Fig. 2(a). In this circuit, the dc-bus voltage is split into three levels by two series-connected bulk capacitors, C1 and C2. The middle point of the two capacitors n can be defined as the neutral point. The output voltage van has three states: Vdc/2, 0, and -Vdc/2. For voltage level Vdc/2, switches S1 and S2 need to be turned on; for -Vdc/2, switches S1' and S2' need to be turned on; and for the 0 level, S2 and S1' need to be turned on.

The key components that distinguish this circuit from a conventional two-level inverter are D1 and D1'. These two diodes clamp the switch voltage to half the level of the dc-bus voltage. When both S1 and S2 turn on, the voltage across a and 0 is Vdc i.e., va0 =Vdc. In this case, D1' balances out the voltage sharing between S1' and S2' with S1' blocking the voltage across C1 and S2' blocking the voltage across C2. Notice that output voltage van is ac, and va0 is dc. The difference between van and va0 is the voltage across C2, which isVdc /2. If the output is removed out between a and 0, then the circuit becomes a dc/dc converter, which has three output voltage levels: Vdc ,Vdc/2, and 0.

(a) seven-level.   (b) Five-level.
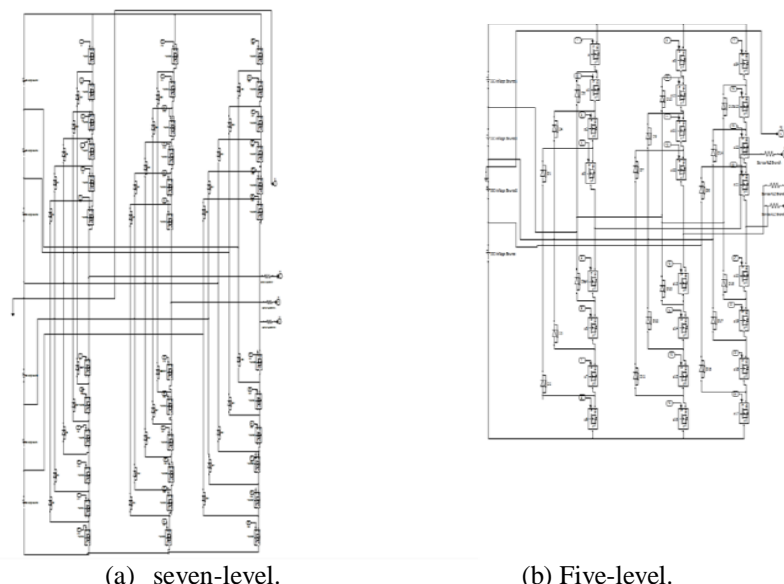
Figure 2 clamped multilevel inverter circuit topologies.

Considering that m is the number of steps of the phase voltage with respect to the negative terminal of the inverter, then the number of steps in the voltage between two phases of the load k isk = 2m+1 (1) and the number of steps p in the phase voltage of a three-phase load in wye connection isp = 2k – 1. (2)

The term multilevel starts with the three-level inverter introduced by Nabae et al. [3]. By increasing the number of levels in the inverter, the output voltages have more steps generating a staircase waveform, which has a reduced harmonic distortion. However, a high number of levels increases the control complexity and introduces voltage imbalance problems.Fig. 2(b) shows a five-level diode-clamped converter in which the dc

bus consists of four capacitors, C1, C2, C3, and C4. For dc-bus voltage Vdc, the voltage across each capacitor is Vdc/4, and each device voltage stress will be limited to one capacitor voltage level Vdc/4 through clamping diodes.To explain how the staircase voltage is synthesized, the neutral point n is considered as the output phase voltage reference point. There are five switch combinations to synthesize five level voltages across a and n.

1) For voltage level Van = Vdc/2, turn on all upper switches S1– S4.
2) For voltage level Van = Vdc/4, turn on three upper switches S2– S4 and one lower switch S1'.
3) For voltage level Van = 0, turn on two upper switchesS3 and S4 and two lower switches S1' and S2'.
4) For voltage level Van = –Vdc/4, turn on one upper switch and three lower switches S1'– S3'.
5) For voltage level Van = –Vdc/2, turn on all lower switches S1'– S4'.

Four complementary switch pairs exist in each phase. The complementary switch pair is defined such that turning on one of the switches will exclude the other from being turned on. In this example, the four complementary pairs are (S1, S1'), (S2, S2'), (S3, S3'), and (S4, S4').

TABLE I. SWITHCING STATES OF THE FIVE LEVEL INVERTER

Va_0	S_1	S_2	S_3	S_4	$S_{1'}$	$S_{2'}$	$S_{3'}$	$S_{4'}$
V5=Vdc	1	1	1	1	0	0	0	0
V4=3Vdc/4	0	1	1	1	1	0	0	0
V3=Vdc/2	0	0	1	1	1	1	0	0
V2=Vdc/4	0	0	0	1	1	1	1	0
V1= 0	0	0	0	0	1	1	1	1

Although each active switching device is only required to block a voltage level of Vdc/(m-1), the clamping diodes must have different voltage ratings for reverse voltage blocking. Using D1'of Fig. 2(b) as an example, when lower devices S2' ~ S4' are turned on, D1' needs to block three capacitor voltages, or 3Vdc/4. Similarly, D2 and D2' need to block 2Vdc/4, and D3 needs to block 3Vdc/4. Assuming that each blocking diode voltage rating is the same as the active device voltage rating, the number of diodes required for each phase will be (m-1) (m-2). This number represents a quadratic increase in m. When m is sufficiently high, the number of diodes required will make the system impractical to implement. If the inverter runs under PWM, the diode reverse recovery of these clamping diodes becomes the major design challenge in high-voltage high-power applications.

IV.   MODULATIONTECHNIQUE

SPWM:

Several multicarrier techniques have been developed to reduce the distortion in multilevel inverters, based on the classical SPWM with triangular carriers. Some methods use carrier disposition and others use phase shifting of multiple carrier signals [7], [8], [9].

The sinusoidal PWM compares a high frequency triangular carrier with three sinusoidal reference signals, known as the modulating signals to generate the gating signals for the inverter switches. This is basically an analog domain technique and is commonly used in power conversion with both analog and digital implementation.The smallest distortion is obtained when the carriers are shifted by an angle of $\theta = 360° \therefore NC = 120°$. A very common practice in industrial applications for the multilevel inverter is the injection of a third harmonic in each cellto increase the output voltage [6], [10]. Another advantageous feature of multilevel SPWM is that the effective switching frequency of the load voltage is three (NC=3) times the switching frequency of each cell, as determined by its carrier signal. This property allows a reduction in the switching frequency of each cell, thus reducing the switching losses.

Proposed SPWM for NPC Multilevel Inverter:

In the SPWM scheme for two-level inverters, each reference phase voltage is compared with the triangular carrier and the individual pole voltages are generated, independent of each other. The SPWM technique, for multilevel inverters, involves comparing the reference phase voltage signals with a number of symmetrical level-shifted carrier waves for PWM generation [11]. It has been shown that for an n-level inverter, n-1 level-shifted carrier waves are required for comparison with the sinusoidal references [11].

When used for an NPCMLI with n number of voltage levels, n-1 number of triangular carrier waves is used. These carrier waves have the same frequency and are arranged on top of each other, so that they together span from maximum output voltage to minimum output voltage [12]. When one carrier wave is crossed by the reference the output wave steps one level up or down with a switch transaction.

V.   RESULT & ANALYSIS

The simulation is carried out using MATLAB/Simulink. Simulation circuit of three phase level NPC isshown in Figure.1. Detailed simulation circuit of each phase is shown in Figure.2. Input is 100V DC .levels inverter output voltage and current in a phase are shown in Figure3. and Figure4.respectively. The phasevoltages and currents in three phase inverter are shown in Figure5. and Figure6.respectively. The line voltagesare shown in Figure7.. The circuit is analyzed for RL load. The FFT analysis result is shown in Figure.8

MATLAB Model for Five level DCMLI:-

The simulation is carried out using MATLAB/Simulink. Simulation circuit of three phase Five level shown in figure 5.13. Detailed simulation circuit shown is figure 5.14. input is 100 v dc. five level inverter output voltage. The FFT analysis is result.

Simulation Result for PWM generating logic PDPWM technique:
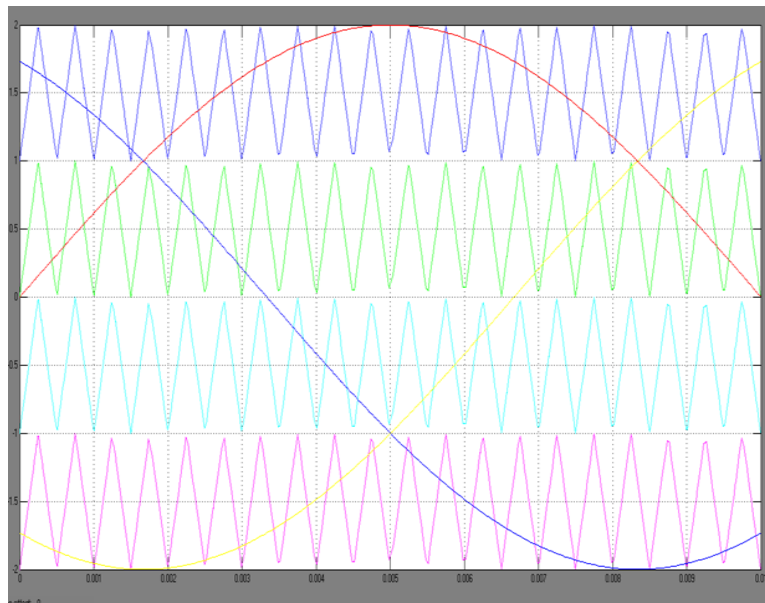
Figure 1Simulation Resultfor PWM generating logic Five Level PDPWM technique (ma = 1 and mf =20)

Simulation Result for Output voltage generated by PDPWM technique:
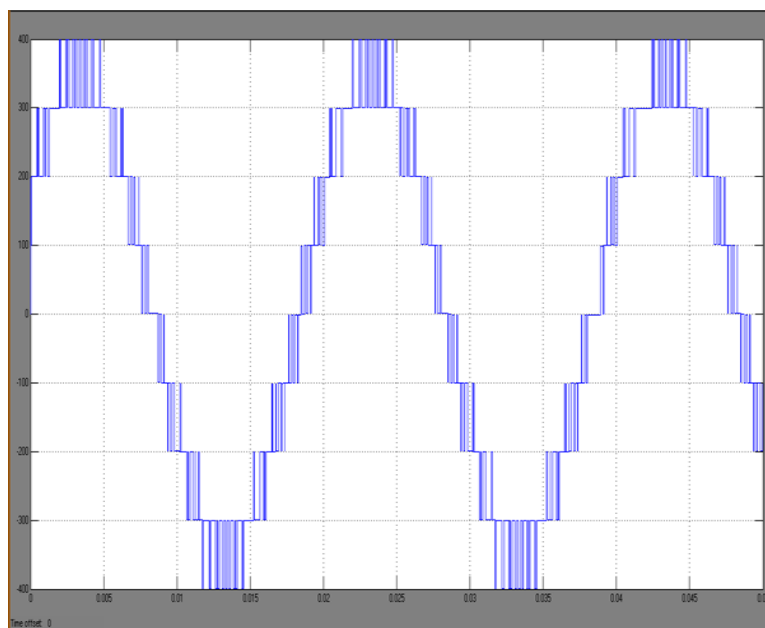
Figure 2Simulation Result for output voltage for Five Level PDPWMtechnique

Phase voltage of Three Phase PDDCMLI:
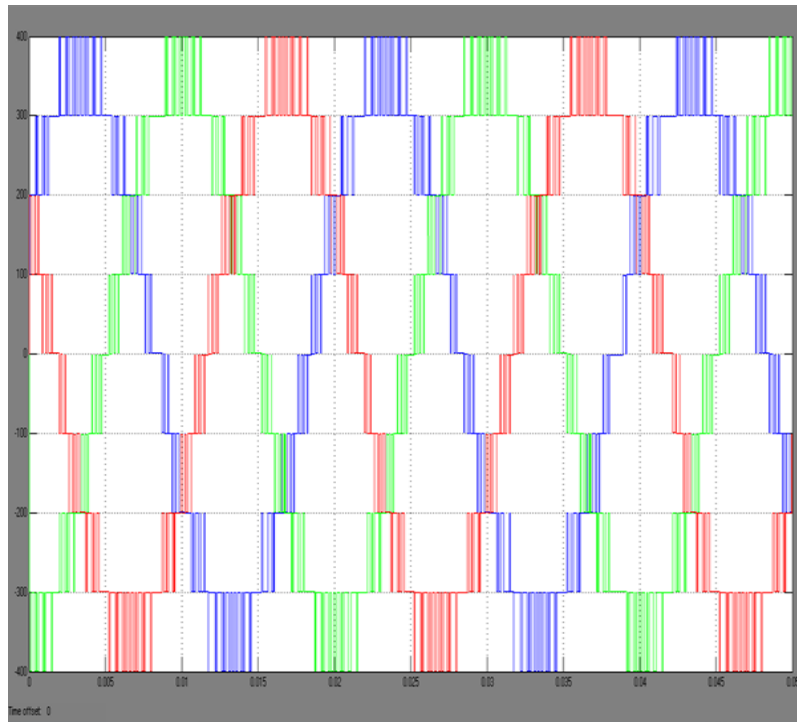
Figure 3Phase voltage of Three Phase Five Level DCMLI

FFT plot for Simulation Result output voltage of PDPWM technique
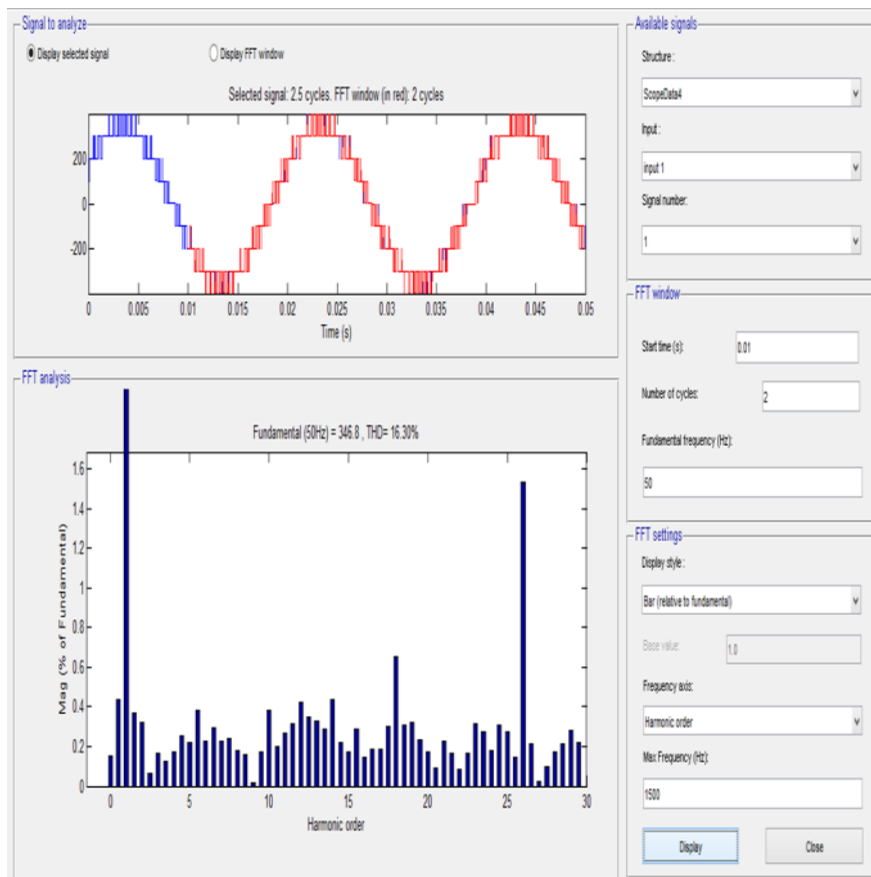
Figure 4FFT plot for Simulation Result output voltage of PDPWM technique

Simulation Result for Seven level PWM generating logic PDPWM technique
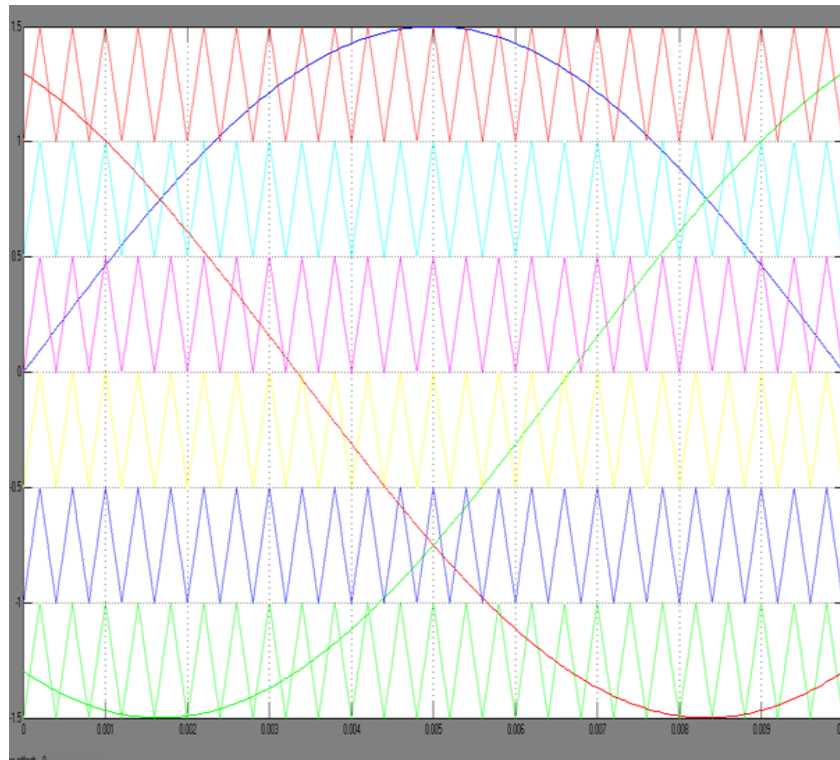
Figure5Simulation Result for PWM generating logic PDPWM technique

Simulation Result for Output voltage generated by PDPWMtechnique
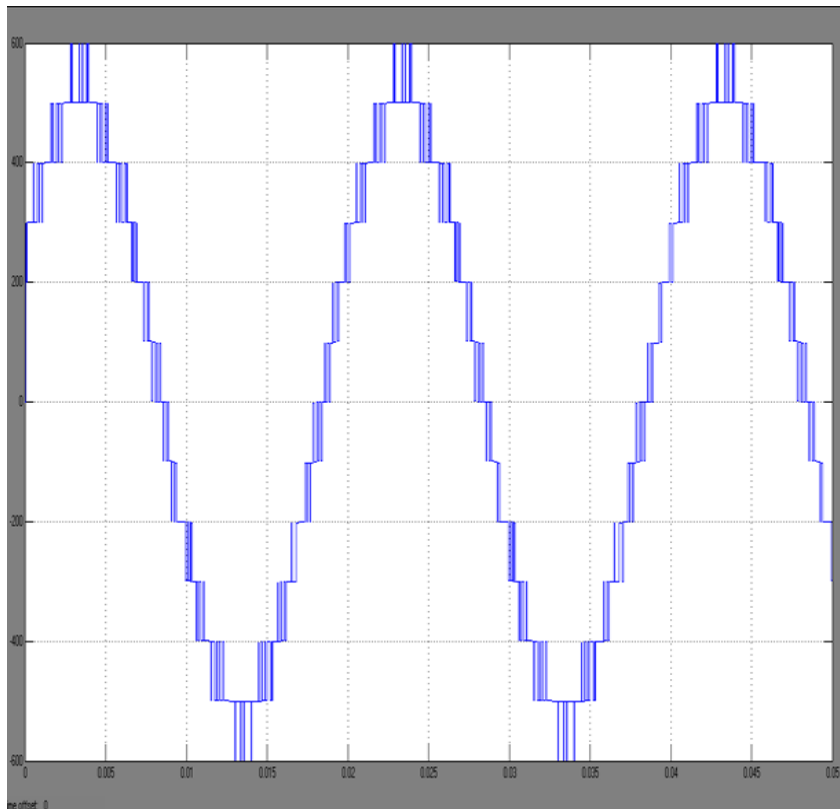
Figure 6 Simulation Result for Output voltage generated by PDPWMtechnique

Phase voltage of Three Phase PDDCMLI
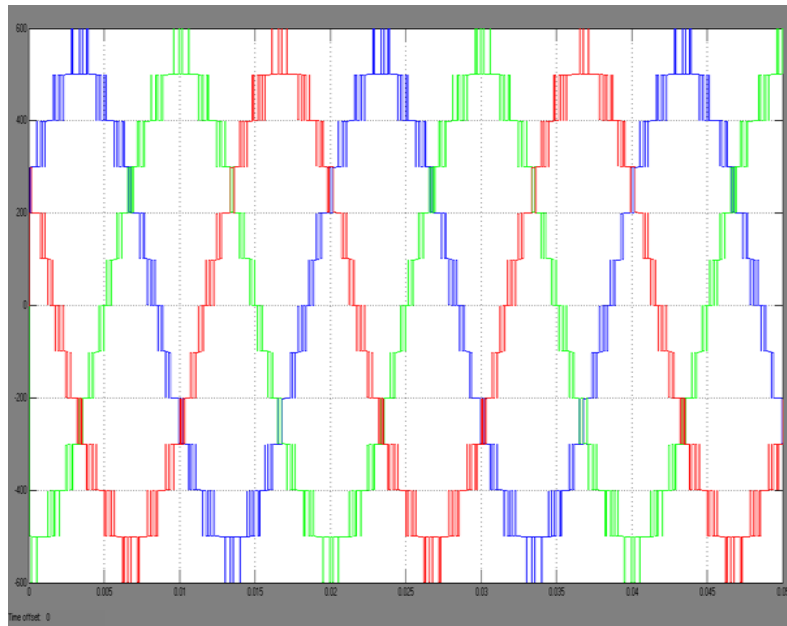
Figure 7 Phase voltage of Three Phase PDDCMLI

FFT plot for Simulation Result output voltage of PDPWM technique
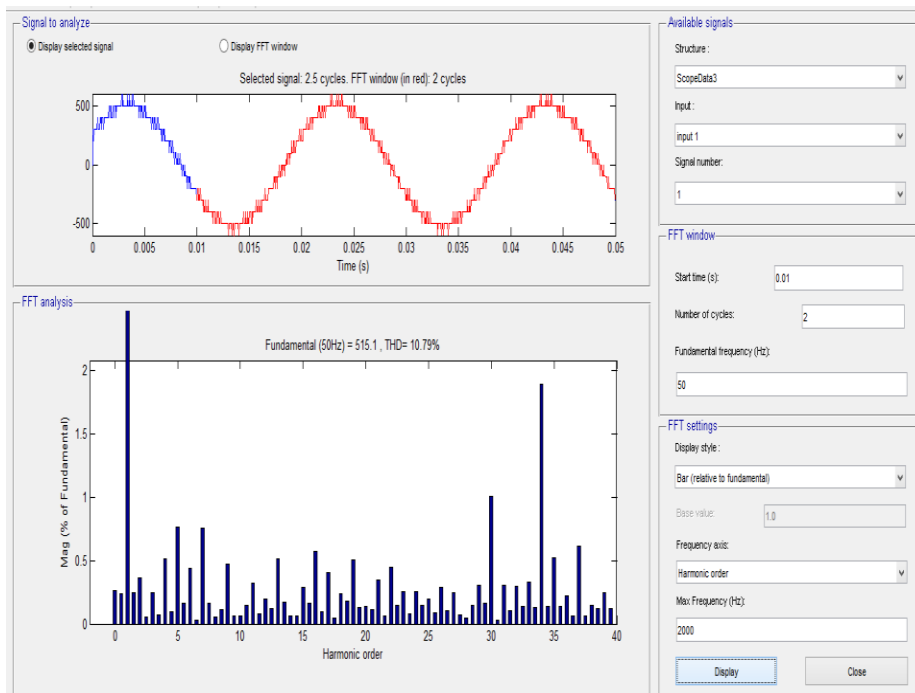
Figure 8 FFT plot for Simulation Result output voltage of PDPWM technique

TABLE % THD comparison for different LEVELS

It has shown that decrease in voltage THD in moving from three levelstoseven level inverter. It has shown that number of level increase output voltage THD is decrease.

Output Voltage level of NPCI	THD	Fundamental Component
Five level	16.30	346.5
Seven Level	10.79	515.1

VI.　CONCLUSION

A SPWM technique is proposed for three-level and five-level NPC inverter. The main feature of the modulation scheme lies in its ability to eliminate the harmonics in the inverter output voltages.The harmonic content and THD of the inverter output voltage produced by the three and five levels are compared and it seamless for five level diode clamped inverter compared three level diode clamped multilevel inverter.

REFERENCES

[1] Xiaoming Yuan and Ivo Barbi "Fundamentals of a New Diode Clamping Multilevel Inverter", IEEETrans.on Power Electronics, Vol.15, No.4, 2000, pp.711-718.

[2] O. Bouhali, B. Francois, E. M. Berkouk, and C. Saudemont, "DC Link Capacitor Voltage Balancing in a Three-Phase Diode Clamped Inverter Controlled by a Direct Space Vector of Line-to-Line Voltages", IEEE Trans. on Power Electronics, Vol.22, No.5, 2007, pp.1636-1648.

[3] AnshumanShukla, ArindamGhosh and Avinash Joshi, "Control Schemes for DC Capacitor Voltages Equalization in Diode-Clamped Multilevel Inverter Based DSTATCOM", IEEE Trans. on Power Delivery, Vol.23, No.2, 2008, pp.1139-1149.

[4] Sergio BusquetsMonge, Joan Rocabert Pedro Rodriguez, Salvador Alepuz and JosepBordonau, "Multilevel Diode Clamped Converter for Photovoltaic Generators With Independent Voltage Control of Each Solar Array", IEEE Trans. on Industrial Electronics, Vol.55, No.7, 2008, pp.2713-2723.

[5] Mohan M. Renge and Hiralal M. Suryawanshi, "Five-Level Diode Clamped Inverter to Eliminate Common Mode Voltage and Reduce dv/dt in Medium Voltage Rating Induction Motor Drives", IEEE Trans. on Power Electronics, Vol.23, No.4, 2008, pp.1598-1607.

[6] Hideaki Fujita, and Naoya Yamashita, "Performance of a Diode-Clamped Linear Amplifier", IEEE Trans. on Power Electronics, Vol.23, No.2, 2008, pp.824-831.

[7] NatchpongHatti, Kazunori Hasegawa and Hirofumi Akagi, "A 6.6-KV Transformer less Motor Drive Using a Five-Level Diode- Clamped PWM Inverter For Energy Savings of Pumps and Blowers", IEEE Trans. on Power Electronics, Vol.24, No.3, 2009, pp.796-803.

[8] S.Srinivas, "Uniform Overlapped Multi-Carrier PWM for a Six-Level Diode Clamped Inverter", International Journal of Electrical and Electronics Engineering , 2009, pp.763-768.

[9] EnginOzdemir, SuleOzdemir and Leon M. Tolbert, "Fundamental-Frequency-Modulated Six-Level Diode-Clamped Multilevel Inverter for Three-Phase Stand-Alone Photovoltaic System" IEEE Trans. on Power Electronics, Vol.56, No.11, 2009, pp.4407-4415.

[10] BerrezzekFarid and BerrezzekFarid, "A Study of New Techniques of Controlled PWM Inverters", European Journal of Scientific Research, ISSN 1450-216X, Vol.32, No.1, 2009, pp.77-87.

[11] Anshumanshukla, ArindamGhosh and Avinash Joshi, "Flying-Capacitor-Based Chopper Circuit for DC Capacitor Voltage Balancing in Diode-Clamped Multileverl Inverter", IEEE Trans. on Industrial Electronics, Vol.57, 2010

The Effects of Yaji Extract On Liver Enzymes of Carbon Tetrachloride Induced Hepatotoxicity In Adult Wistar Rats

[1]Ezejindu D.N., [2]Aligwekwe A.U., [1]Haastrup I.
[1]Department of Anatomy, College of Health Sciences, Nnamdi Azikiwe University, Nnewi
[2]Department of Anatomy, Madonna University, Elele, River State.

Abstract: - Effects of yaji extract on liver enzymes of carbon tetrachloride induced hepatotoxicity were studied. Twenty wistar rats weighing between 155-220g were used. They were allocated into four groups of five animals each. Group A animals served as the control and received 0.6ml of distilled water. Group B received 0.5ml of yaji extract, group C received 0.5ml of yaji extract plus 0.3ml of carbon tetrachloride while group D received 0.3ml of carbon tetrachloride. The oral administration lasted for twenty-eight days. Twenty-four hours after the last administration, the animals were weighed and sacrificed using chloroform. The Liver weight were recorded. The evaluation of the liver enzymes (AST, ALP,ALT) were carried out using randox kit method. The mean alkaline phosphatase (ALP), alanine amino transferase (ALT) and aspartate aminotransferase (AST) levels of group D animals were significantly higher than the control.

Key words*: - Yaji, Liver enzymes, Carbon tetrachloride, Body weight, Wistar rats.*

I.   INTRODUCTION

There is the growing concern about the excessive consumption of a meat sauce called 'yaji' which is used to serve the meat delicacy called 'suya' in Nigeria [1].

Yaji is a complex mixture of spices and additives; its constituents are ginger, cloves, red pepper, black pepper, salt, white maggi (Ajinomoto) and groundnut powder; and their active ingredients on individual basis are known to be harmful if consumed in excess [2].

Suya is a popular, traditionally processed, ready to eat Nigerian meat product, which may be served or sold along streets in club houses, at picnics, parties, restaurants and institutions. It is a consumer fast food whose preparation and sales along the streets are usually not done under strict hygienic conditions because they are still done locally [3].

It identified as a mass consumer fast food whose preparation and sales along streets are usually not done under strict hygienic environment and can serve as source of contaminants to the meat product [4]. Suya as one of such intermediate moisture products that is easy to prepare and highly relished [5].

Hepatotoxicity implies chemicals driven liver damage. Biochemical markers are often used to indicate liver damage. Liver damage is further characterized into hepatocellular and cholestatic types. Certain medicinal agents when taken in overdose and sometimes even when introduce within therapeutic range may cause liver injury. More than 900 drugs have been implicated in causing liver injury [6,] and it is the most common reason for drugs tobe withdrawn from the market. Other chemical agents (hepatotoxins) such as those used in the laboratories and industries, natural chemicals and herbal remedies can also induce hepatotoxicity. Chemicals often cause sub-clinical injury to the liver which manifest only as abnormal liver enzyme tests. Carbon tetrachloride (CCl_4) is a well known hepato-destructive agent that is widely used to induce toxic liver injury in a range of laboratory animals [7].The hepatotoxicity of CCl_4 has been reported to be due to its biotransformation by cytochrome P450 system to produce trichloromethyl free radical (CCl_3) which readily reacts with molecular oxygen to form trichloromethyl peroxy radical [8].

CCl_3OO which exert their action on lipids membrane of endoplasmic reticulum to evoke lipid per oxidation [9].Therefore, there is need to search, evaluate, and scientifically validate the activities of medicinal plants.

The aim of this study is to evaluate the effect of yaji extract on carbon tetrachloride induced hepatotoxicity in the liver enzymes (AST, ALP, and ALT) of adult wistar rats.

II. MATERIALS AND METHOD

PLANT COLLECTION

The yaji was prepared according to the according to the method used by (2). The measured quantities include: Ajinomoto (150g), Black pepper (30g), Clove (39), Ginger (78g) and Groundnut cake powder (230g), Red pepper (22g) and Salt (100g). The total weight of these constituents summed up to 649g in Nnewi area of Anambra state in the month of June, 2013.

III. EXTRACTION OF PLANT MATERIAL

AQUEOUS EXTRACT

The constituents of yaji 649g was grinded using a ginger mill. The constituents were then macerated for 48hrs in 500ml of distilled water. The extract was strained through muslin and the filtrate then filtered through whatman No. 1 filter paper. The aqueous extract was concentrated on a rotary evaporator (Model type 349/2 Corning Ltd., England). The extractive value of the aqueous extract was 250mg/ml.

ANIMALS

Adult male wistar rats weighing 150-210g were obtained from the animal farm house, Department of Anatomy, Nnamdi Azikiwe University, Nnewi Campus. They were maintained under standard housing conditions and fed with standard rat chow (Growers mash) and provided with water ad libitum during the experiment. They were acclimatized for two weeks before the experiment.

EXPERIMENTAL DESIGN

Twenty (20) albino rats were divided into four (4) groups (A-D) of five animals each. Group A received 0.6ml of distilled water, Group B received 0.5ml of yaji extract, Group C received 0.3ml of CCl_4 **,** Group D received 0.5ml of yaji extract plus 0.3ml of CCl_4 and administration lasted for 28 days. All administration was by oral route. Twenty-four hours after the last administration, the animals were weighed and sacrificed using chloroform. Liver tissue was collected, weighed and fixed in zenker's fluid for histological studies.

Twenty-fours post CCl_4 administration, about 5ml of blood was collected from animals in all the groups by cardiac puncture under the ether anesthesia into a dry glass container. The blood was allowed to clot and sera separated from the cells and stored frozen until analyzed for liver enzymes. The animals were euthanized while still under under anesthesia and their liver excised, washed in cold saline and fixed with 10% formal saline for histopathological studies.

MORPHOMETRIC ANALYSIS OF LIVER WEIGHTS

The results obtained from calculations of relative liver weight of the various groups are presented in table 1. The relative liver weight for group D (carbon tetrachloride administered) were significantly higher (P<0.001) than that of the group A (control) and other experimental groups (B and C). The values for groups B and C were similar to the group A, (control).

Comparison of mean relative liver weight for group A, (control) and experimental groups (B, C and D)

Table 1 (Mean ± SEM given for each measurement)

	GROUP A	GROUP B	GROUP C	GROUP D
LIVER WEIGHT	4.90±0.045	4.60±0.085	4.25±0.161	7.23±0.625

The bar chart representation of the relative liver weight of the various groups. The group D (carbon tetrachloride administered) were significantly higher (P<0.001) than the control group (A) and groups B and C as shown in Figure 1.
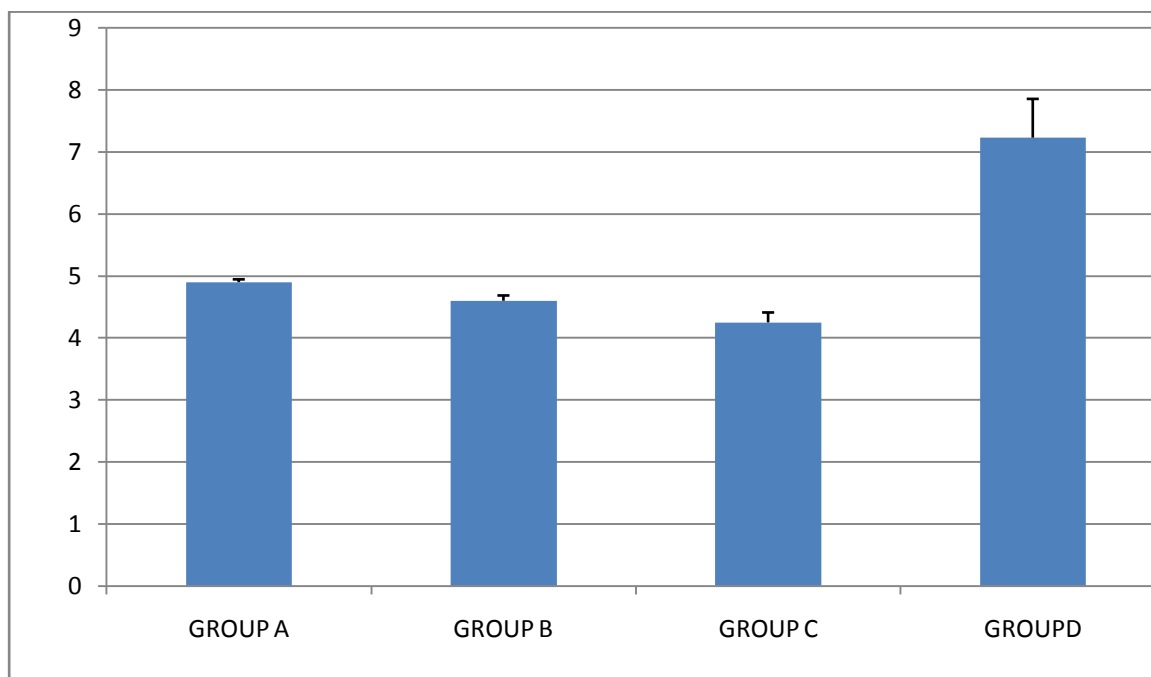
Relative liver weight of different groups

Activities Of Serum Levels Of Aspartate Aminotransferase (Ast), Alanine Aminotransferase (Alt) And Alkaline Phosphotase (Alp)

Table 2 (Mean ± SEM given for each measurement)

	GP.A (CONTROL)	GP.B 0.55ML OF EXTRACT	GP.C 0.3ML OF CAROTENOID	GP.D 0.41ML OF CCL$_4$	F-RATIO	SIGNIFICANCE
AST	76.60±28.50	71.31±10.34	67.55±11.51	243.64±5.72	58.04	<0.0001
ALT	48.00±13.54	47.00±3.39	44.50_+10.12	85.33±7.01	11.20	<0.0001
ALP	461.19±30.22	320.84±84.63	377.88±36.81	668±45.55	6.38	< 0.0012

From the results obtained from calculations of aspartate aminotrasferase (AST), alanine aminptransferase (ALT) and alkaline phosphotase (ALP), there were a significant decrease (P<0.001) in the AST activity levels at all doses of the drugs relative to the control (A) except in group D treated with carbon tetrachloride (CCL$_4$). The group D activity level statistically were significantly higher (P<0.001) than the control (A) and groups B and C.

The alanine aminotransferase (ALT) activity levels showed a significant decrease (P<0.001) in groups B and C relative to the control (A) except in group D treated with carbon tetrachloride (CCL$_4$). The alkaline phosphotase (ALP) level in group D were significantly higher than the control group (A) and groups B and C.

The alkaline phosphotase (ALP) activity levels in groups B and C were significantly lower (P<0.001) than the control (A). The alkaline phosphatase activity levels in group D were significantly higher (P<0.001) than the control (A) and groups B and C.

IV.   DISCUSSION

Yaji is composed of the spices- ginger, clove, red pepper, black pepper, white maggi (Ajinomoto) and salt [2] which on individual basis are known to be harmful. Some of the constituent exhibit antioxidant and hypolipidemic properties [10].Others exhibit chemical, physiological and pharmacological properties [11], and are also capable of inducing tissue damage.

Our findings show that the extract has the potency to normalize the elevated liver marker enzyme levels and maintain the synthetic function of the when compared with the control.

This indicates restoration of the normal functional status of the liver. The significant elevations in the liver marker enzymes such as ALT, AST and ALP, as well as decrease in albumin levels in CCl$_4$ control when

compared with normal, suggest liver injury, since these are reliable indices of liver toxicity [12]. Albumin is produced entirely by the liver and constitutes about 60% of the total serum protein. In liver damage, the synthetic capacity of the liver is reduced and consequently, synthses of albumin, clotting factors and so on are affected. The mechanism of CCl_4 induced liver injury involves oxidative stress. Injury is through the free radical (CCl_3 and CCl_3 00) of its metabolism which may cause lipid peroxidation and subsequent injury [13]. Several studies on extraranal lesions, such as hepatic cirrhosis and myelofibrosis have reported a close correlation between mast cells and fibrosis [14].

The result of the study are summarized in table 2. The activities of aspartate aminotranferase (AST) and alanine aminotranferase (ALT) were determined in serum because analysis of liver function enzymes are used as indicators of biomedical changes in tissues in response to treatment [15]. This result indicates a significant decrease in the aspartate to the control. This means that the group is not affected by the yaji received compared to the control. Therefore, extract of yaji combined with carbon tetrachloride suppressed the toxic effect of carbon tetrachloride on the liver tissues. Also, there was significant increase in alanine aminotransferase (ALT) activities which was similar to the control signify that the carotenoid was not toxic to the ALT enzyme. This decrease in the serum aspartate aminotranferase (AST) activity level observed in this study indicated that at the subcellular level, the liver cells may have been affected by the yaji since AST is found in the mitochondria, and cytoplasm. Also, the increase in serum alanine aminotranferase (ALT) level observed in this study indicated that the cytoplasm of the liver cells may have been affected by the drugs since ALT is found in the cytoplasm.

From the present study, the mean alkaline phosphatase (ALP), alanine amino transferase (ALT) and aspartate aminotransferase (AST) levels of group D animals were significantly higher than the control. It is therefore recommended that further studies be carried out on the spleen and the kidney.

V.   REFERENCES

[1]   Nwaopara, A.O., C.I.P. Anibeze and F.C. Akpuaka, (2010). Histological signs of neurodegeneration in the cerebrum of rats fed with diet containing *Yaji*: The complex Nigerian suya meat sauce. Asian J. Med. Sci., 2(1): 16 -21.
[2]   Nwaopara A.O, L.C. Anyanwu, C.A. Oyinbo, I.C. Anaikot, (2004). The histological changes in pancreas of wister rats fed with diets containing Yaji (Local meat sauce) .J. Exp. Clin. Anat., 3(2):44-47.
[3]   Igene JO, Mohammed ID (1983). Consumers' attitudes towards 'suya' meat product. Ann. Borno. 1. Retrieved 20th October, 2009 from http://www.pjbs.org/pjnonline/fin512.pdf.
[4]   Uzeh, R.E., R.E. Ohenhen and O.O. Adeniji, (2006). Bacterial contamination of tsire-suya, a nigerian meat product. Pak. J. Nutr., 5(5): 458-460.
[5]   Omojola AB (2008). Yield and organoleptic characteristics of Suya (an intermediate moisture meat) prepared from three different muscles of a matured bull African J. Biotech. 7(13): 2254-2257.
[6]   Friedman SE, Grendell JH, McQuaid KR (2003): Current diagnosis and treatment gastroenterology. Lang medical Books/ McGraw-Hill New York pp: 664-679.
[7]   Reyes-Gordillo K, Segovia J, Shibayama, M, Vergara, P, Moreno MG, Muriel P (2007): Curriculum protects against acute liver damage in the rats by inhibiting NF-KB, proinflammatory cytokines production and oxidative stress. Biochem Biophysics Acta. 1770: 989-996.
[8]   Raucy JL, Kraner JC, Lasker (1993) : Bioactivation of halogenated hydrocarbons by cytochrome P450. EI. Grit Review of Toxicology 23:1-20.
[9]   Recknagel RO, Glende, EA, Dolk JA, Waller RL (1989):Mechanism of carbontetrachloride toxicity. Pharmacological Therapy 43: 139-54.
[10]   Manjunatha H, Srinivasan K (2008). Hypolipidemic and antioxidant potency of heat processed turmeric and red pepper in experimental Rats. Afr. J. Food Sci. 2: 1-6.
[11]   Govindarajan VS, Sathyanarayana MN (1991).Capsicum production, Technology, Chemistry and quality. Part V. Impact on physiology, pharmacology, nutrition and metabolism: structure, pungency, pain and desensitization sequences. Crit. Rev. Food Sci. Nutr. 29: 435–474.
[12]   Omoniyi KY, Matthew CI (2006): Protective effects of Zingiber officinale against carbon tetrachloride and acetaminophen-induced hepatotoxicity in rats. Phytotherapeutic Research. 20:997-1002.
[13]   Sies H (1997) : Oxidative stress: Oxidants and antioxidants. Experimental Physiology 82 (2): 291-295.
[14]   Eddy, A.A., (2001a). Mast cells find their way to the kidney.Kidney Int., 60: 375–377.
[15]   Key A., Anderson J.T., Grande F. (1957). Prediction of serum cholesterol responses of man to changes in fats in the diet, lancet 11. 959-966.

Research Paper   Open Access

Ground Water Quality Assessment in the Basement Complex Areas of Kano State Nigeria

Adamu G.K, Rabi'u Tukur, Aliyu Ibrahim Kankara
Department of Geography and Regional Planning Federal University Dutsin-Ma, P.M.B 5001 Dutsin-Ma, Katsina State Nigeria

Abstract: - The research aimed at assessing the quality of underground water for safe drinking in the basement complex region of Kano state. In achieving this aim a total of twenty (20) boreholes were selected at random across the state. Thirteen (13) relevant parameters on the test of water quality were taken into consideration. The research found out that underground water in the area is safe for drinking due natural filtration process that the water undergo, because, the soil chemistry and mineralogy alters the chemistry of the water there by making it safe for drinking by meeting the standard requirement of World Health Organisation (WHO) 1984. It is therefore recommended that, more boreholes should be constructed through the intervention of both government and other relevant organsations. Also surface water source should also be improve to reduce the burden that underground water source might have encountered.

Key Words: - *Borehole, Geology, Resource, Safe drinking, Underground Water, Water Chemistry.*

I.   INTRODUCTION

Nigeria's increasingly urban population coupled with the desire to raise standard of living among the populace have increased the pressure on natural resources particularly water. This is witnessed by the efforts of various governmental agencies in providing water for domestic, industrial and agricultural uses. Therefore, efficient development of groundwater resources is of particular importance in northern Nigeria where due to the low rainfall and the length of dry season surface water sources are often inadequate. Correspondingly, this promoted the assessment of available groundwater resources in various parts of the country. A number of such studies for instance Dupreeze and Barber (1965) wrote on the distribution and chemical quality of groundwater in Chad and Basement complex of northern Nigeria. Egboka 1983, Ogunkoye 1986 and Ako 1988 also wrote on parameters such as water quality, aquifer transitivity, age of groundwater, table depth to surface and relative location of groundwater as potential resources.

The provision of groundwater supply in Kano state as part of a coordinated development programme for rural development is seen as an essential service imperative to the entire state's development (Macdonald's and Partners, 1986). Three governmental organisations were responsible for provision of groundwater for the entire state; namely, Water Resources Engineering and Construction Agency (WRECA), Kano State Water Board, Ministry of Water Resources. In addition, a number of local governments are also promoting their own groundwater supply programmes. Groundwater exploitation by these agencies is carried out by sinking of hand-dug, concrete limed wells and drilling of abstraction boreholes all located in geologies. However, despite the efforts of these organizations, it is estimated that out of the 7,500 hand dug wells in the state in 1981, about 3,300 had either fallen into disrepair or were in need of being re-evacuated due to collapse/slumping-cave-in e.t.c. Thus, village water supply sources essentially that consisted of seasonal streams, rainfall pools and other such reservoirs. These sources are invariably polluted and constitute hazards to health (Imerbore et al 1987). In alleviating the hardships endured by rural population, the objective of the international drinking water supply and sanitation decade will have been considerably satisfied (WHO 1990).

Groundwater has many advantages over surface water when obtained from deep sources, it undergoes natural filtration e.g. removal of bacteria and odour, also groundwater chemistry and temperature are much less. However, the long residence time of groundwater brings it into intimate contact with the country coprolite and rocks so that it tends to have higher concentration of dissolved solids than surface water and at times contains

inorganic matter in concentration. Groundwater quality could vary by such spatially varying factors as lithology, texture and structure of the rocks (Ogunkoya 1986), and in areas with heavily polluted atmosphere, rain water quality is heavily altered (Horning et al, 1990).

This study investigates quality of groundwater for safe drinking, by testing parameters like PH, Electrical conductivity (EC) and Ionic concentration of Calcium (Ca), Magnesium (Mg), Iron (Fe), Chlorine (Cl), Nitrate (NO_3), Ammonium Nitrate (NH_3N), Sulphate(II)oxide (SO_4^{2-}), Silconoxide (SiO_2), Floride (F^-), Carbondioxide (CO_2) and Total Dissolve Solids (TDS) from various Precambrian Basement Complex rocks in Kano State.

II.   STUDY AREA

The Nigeria Basement Complex is believed to have had structural complexity as a result of multiple folding, igneous and metamorphic activities. Kogbe (1977), the Basement Complex areas of Kano State are no exception to the above assertion. It occupies the middle and south-western portion of the entire state, roughly about 2/3 of the area. The boundary with the sedimentary area is generally well defined, although in few areas there is transition zone in which sediments are shallow. In the basement complex, the rock types encountered were predominantly granites with magmatites, gneisses and schist, and minor occurrences of quartzite, volcanic basalt and rhyolite. All these rocks belong to the Pre-Cambrian Basement Complex group. The elevation of the region above main sea level ranges from about 400 meters at the north-eastern margin to over 1200 meters at the southern tip, that is, the highest elevation occurs in the south. Elevations decrease both northwards and north-eastwards. The region is part of the high plains of the Hausa land (Motimore 1973), except for the section east of the hydrological divide the rock structure texture, lithology, mineralogy, relief and landforms are closely linked and described under conceptualization.

The state lies within the tropical savannah zone of Nigeria. Temperatures are high throughout the year, the mean maximum temperature is between 27°-35° C and the mean minimum temperature is between 16-21° C. The annual rainfall varies from 1200mm in the south to 650mm in the north. Indeed, there are two main seasons – rainy season starts by May or June and ends in October or November while dry season is from November to April.

III.   METHODOLOGY

Samples of water were collected from boreholes drilled into the various Basement Complex rocks in the State. In all, twenty boreholes were randomly sampled – five from each of quartzite, granite, gneiss and schist areas. Total of thirteen parameters were chosen base on those found to be relevant to the study area (Macdonald's et al, 1986) and taking into consideration World Health Organisation Current (1984) Geneva reviewed chemical parameters in drinking water standard for developing countries, hence, justify reason for the choice.

The PH value of all the samples were taken shortly after collection, using a PH Meter, while electrical conductivity of the water samples was measured with a Conductivity Bridge Meter.

The Calcium (Ca^{2+} and Magnesium (Mg^{2+}) concentration were determined using the atomic absorption spectrophotometer. The total iron concentration was determined by calorimetric method using throglycollic acid which reduces iron (III) to iron (II) and forms a reddish purple. In the case of chloride concentration, it was determined by titration with a standard solution of silver nitrate using an indicator of 8% potassium chromate solution, the appearances of red precipitate signifies the titration end point. The total silica was determined in all samples by colorimetric method using acidified sodium molybdate ($Na_2 MaO_2$) and acidified stannous chloride solution ($SnCl_2O$). The intensity of the blue colour formed was matched with the Standard Aquameck Silica Colour Scale and corresponding concentration read off in mg/1.

In all samples sulphate (SO_4) concentration was determined turbidinate method while the nitrate nitrogen and ammoniac nitrogen were determined by calorimetric method respectively.

Finally, the total hardness was determined by titration with sodium dihydrogen ethylendiamine tetracetate dehydrate – (E.D.T.A. – Salt, $N_{a2} H_2 C_{10} H_{12} O8 H_2 2HO_2$) using Eriochrome black T as indicator. The samples were analysed at Water Resources Engineering and Construction Agency (WRECA) Chalawa Quality Control Laboratory, Kano.

The data collected for this research includes the lithologic or geology of the twenty (20) boreholes taken as samples. There are depth drilled, borehole yields rock at zone of abstraction or fracture (screen position) and Rock Samples encountered from the surface to the bottom of each borehole sample.

The statistical tools that would be employed in this study are both descriptive and inferential mean and standard deviation is also used in the analyses of the data.

RESULT PRESENTATION DISCUSSION AND ANALYSIS

Table 1: Chemical Water Quality Parameters of the Boreholes

Borehole No	PH	EC	Ca^{2+}	Mg^{2+}	Fe	Cl^-	NO_3-N	NH_2-N	SO_4^{2-}	S_1O_2	F^-	CO_2	TDS
1	7.6	150	23.49	10.41	0.05	7.40	3.95	1.20	0.95	0.90	0.06	0.01	160
2	6.4	45	8.00	0.0	0.01	5.00	3.00	0.10	0.50	1.00	0.07	0.15	45.0
3	6.6	32	3.60	4.38	0.01	4.94	1.20	0.62	0.71	1.78	0.15	0.11	40.0
4	5.7	44	2.70	4.38	0.50	2.47	0.00	0.08	0.50	0.50	0.01	0.04	45.0
5	6.0	45	21.63	7.67	0.00	9.87	0.00	0.50	0.30	1.20	0.05	0.62	35.0
6	6.8	100	9.22	4.41	0.02	3.95	2.10	0.10	0.60	1.50	1.50	0.06	0.00
7	6.8	95	9.91	2.19	0.10	5.92	2.30	0.00	0.50	1.60	0.02	0.08	100
8	6.0	64	6.31	4.00	0.01	5.43	0.20	0.62	0.65	2.60	0.30	0.06	68
9	6.3	74	53.17	14.79	0.20	24.60	2.10	0.05	2.86	1.60	0.05	0.16	80
10	6.3	150	36.00	10.95	0.07	5.12	0.12	0.00	0.00	1.50	0.03	0.24	160
11	5.5	70	55.88	14.79	0.01	35.6	2.05	0.00	0.00	0.90	0.05	0.07	85
12	6.4	140	31.54	20.18	0.10	5.43	0.07	0.00	0.00	2.05	0.02	0.20	130
13	6.5	150	10.81	6.02	0.00	6.91	1.50	0.00	0.00	0.90	0.07	0.02	162
14	7.1	110	63.08	51.98	0.00	57.74	2.60	0.14	0.60	0.90	0.04	0.09	120
15	6.0	195	95.53	40.08	0.05	99.1	4.20	0.00	0.00	1.05	0.04	0.16	254
16	6.5	45	19.25	6.54	0.01	8.65	2.50	0.12	0.06	1.05	0.08	0.13	50
17	6.7	154	53.12	41.45	0.01	46.8	0.04	0.14	___	1.10	0.08	0.65	160
18	6.5	120	2.20	3.40	0.08	37.6	4.50	0.16	0.80	3.50	0.03	0.16	125
19	6.3	190	19.83	9.31	0.02	7.40	2.60	0.20	0.30	1.70	0.05	0.20	200
20	6.3	120	2.70	3.29	0.00	4.40	0.28	0.00	0.05	1.50	0.05	0.02	130

Source; Laboratory Analysis 2013

Table 2: Mean and Standard Deviation of the Various Chemical Parameters

Rock Type		PH	EC	Ca	Mg	Fe	Cl^-	NO_3-N	NH_2N	SO_4^2	SiO_2	F	CO_2	TDS
QZ	☐	6.7	63.2	11.9	5.4	0.1	5.9	1.6	0.5	0.6	111	0.1	0.2	65.0
	δ	0.6	49	9.9	3.9	0.1	2.8	1.7	0.5	0.2	0.4	0.1	0.2	53.3
GR	☐	6.6	123.4	39.2	16.8	0.04	45.9	1.6	0.1	0.4	1.3	0.1	0.1	133.5
	δ	0.3	45.3	35.9	16.0	0.05	86.1	1.3	0.14	0.7	0.7	0.2	0.1	50.8
SCT	☐	6.6	126	34.2	13	0.03	7.5	0.9	0.0	0.02	1.3	0.3	0.04	113
	δ	0.2	20.8	17.3	2.2	0.01	0.4	0.3	0.0	0.03	1.1	0.5	0.05	11.5
GN	☐	6.7	125	18.0	8.0	0.2	10.0	0.9	0.04	0.01	1.7	0.1	0.1	129
	δ	0.3	56.3	9.6	6.8	0.2	8.4	0.3	0.07	0.01	0.6	0.04	0.1	55

Source: Data Analysis 2013
Key;

Borehole Number	Geology of the Area found	Abbreviation of the Geologic Formation
1 – 5	Quartzite	QZ
6 – 10	Granite	GR
11 – 15	Schist	SCT
16 – 20	Gneiss	GN

Table 1 and 2 show the pattern of the groundwater quality parameters of the four rock types where samples are obtained for this study. They show that values for conductivity, alkalinity and Total Dissolve Solids (TDS) appeared to be lower in quartzite areas while those in granites, schist and gneiss appear to have similar patterns with no apparent striking differences. The patterns of PH and free carbon dioxide (CO_2) also portray similar range of concentration in the four rock types.

PH values ranged from an average 6.7 in granite area to 7.6 in areas under schist with lowest individual values of 6.0 in (borehole No 8 and 15) granitic areas, and highest 7.6 in quartzite area (borehole No 1) though with little concentration of bases and carbons, PH could be reasonably said to be constant, thus within the general acceptance range. Conductivity ranges between averages of 63.2m[sm-1] in quartzite areas to 126m[sm-1] in Schist areas. Conductivity peaks are observed mainly in schist, gneiss and granite areas, highest individual sample value is 195m[sm-1] (borehole No 15) in granitic area.

Free carbon dioxide was lowest in gneiss areas ($\dot{X}$ = 0.1 Mg/L) and normally higher in quartzite areas ($\dot{X}$ = 0.2 Mg/L). Generally, low values were recorded in all the various geologic areas.

Nitrate-Nitrogen (NO_3-N) concentration were similar and showed a decreasing trend from a maximum of 4.2 Mg/L on a granite area (borehole No 15) to nil in areas under lain by schist.

Calcium values range from an average of 11.9 Mg/L in gneiss areas to 39.0 Mg/L in areas underlain by granite rocks. The highest individual value of 95.53 Mg/L (borehole No 15) occurred in granite areas while the lowest value of 2.2 Mg/L was recorded for the same area. Generally, samples from gneiss areas tend to have

much lower values of calcium concentration. Peak and minimum values tend to occur in quartzite, granite and schist areas.

Magnesium values were lower in quartzite areas with an average concentration of 5.4 Mg/L, and an average value of 16.8 Mg/L was recorded in a granite area. The samples with the highest individual value of 41.45 Mg/L (Borehole No 17) occurred in a granite area and a nil value was recorded in quartzite and schist areas.

Chlorine concentration ranges from an average of ($\dot{X}$ =4.00 Mg/L) in schist area t ($\dot{X}$ =45.9 Mg/L) in granite areas. Individual sample concentration in al thirty-one boreholes ranges from 4.00 Mg/L in gneiss area to 74.8 Mg/L (borehole No 23) in older granite areas.

As indicated in table 2, the concentration of sulphate, silicate and floride generally have low values without any significant difference. The result thus, shows that there are differences in the various geologies and chemical parameters of thirty-one borehole waters analysed. More importantly ionic concentrations of Magnesium (mg), Calcium (Ca) were found; consequently conductivity and PH tend to have linkage with underlying rock types (geology) of the area.

IV.   DISCUSSION

The quality of groundwater is commonly determined by factors other than the source rocks. Other factors such as the chemistry of the saprolite (Ogunkoye 1986) through which groundwater percolated, nature of chemical reactions between the water and the minerals in associated rocks and saprolite and the velocity of the water body are very essential though rare in occurrence. In basement complex areas, groundwater can move from one aquifer to another and the quality may be modified by each in turn. These notwithstanding the background value of the chemical elements in groundwater should have some direct bearing to the geology of the environment from which it is taken. This is especially true where the water accumulates and remains fairly long enough to attain chemical equilibrium with the country rocks and saprolite (Freez and Cherry 1979). Thus, one may expect the concentration of a particular iron in water from similar or identical geological background to be similar.

The Nigerian basement complex is achieved to have had structural complexity as a result of multiple folding, igneous and metamorphic activities (Kogbe 1977). Kano State basement complex is no exception to this observation. Complex foliations and lineation exist among the different of the rock types and in addition to these differences of rock mineralogy exist over small depths, thus affecting chemical composition of groundwater. Borehole-geology obtained from the thirty one samples goes to confirm this assertion. For instance, in borehole number one in a quartzite area (table 1) shows existence of laterite from 0-3 meters, 3-16 meters decomposed granite and at fourty three meters in quartzite. Similarly, in a typical gneiss area (borehole No 3) looking at the geology or drillers log, one could observe; 0:15m laterites plus silt, 15-31m pink granite and 31-48m fractured gneiss. Even though the hand pump is tapping groundwater from purely gneiss area one would expect water seeping from upper layers of pink granite to contain some dissolved materials inherent in granite hence may influence the chemistry of such waters.

The PH of the water samples from rock types ranges from an average of 6.7 to 6.0 in granite and schist areas respectively. In borehole No 8 and 15 granite areas, comparatively could be said to be neutral even though there are some bases and calcium especially in quartzite areas. Using the criteria of Taylor (1958) one could suggest that all the thirty-one samples tasted are free from inorganic or organic acid.

V.   CONCLUSION AND RECOMMENDATION

Due to the natural filtration process of the soil and weathered material, water by the time it reaches the water table is practically always of a good chemical quality and on comparing the results of the analyses with the US and WHO drinking water standards; the water is safe for domestic consumption.

The geology of the study area and the degree of weathering, influence the ground water chemistry, because of different mineralogy and degree of weathering. Consequently, different minerals are eventually weathered and leached down to the water table thereby altering the groundwater chemistry.

Calcium is the most dissolved action in water while floride, chloride and iron are the least dissolved irons. The extremely low concentration of nitrate-nitrogen (N03-N) in all the samples suggests that there are little or no pollutions from sewage sources.

No aquifer study is ever complete; therefore, as more groundwater quality data become available, the understanding of the subject should develop further and mathematical model should be evolve in order to gain insight to the complexities underlying the study of groundwater quality in any particular area.

The recent establishment of the Federal Ministry of Water Resources is very endearing development in Nigeria. The ministry shall in addition to other duties, provide the much needed leadership in the harnessing and management of the country's water resources.

However, it is considered that this study has identified the important features of groundwater quality in parts of the Basement Complex Areas of Kano State. Therefore, the government, Nongovernmental organisations and wealthy individuals come to the aid of maintaining the existing boreholes and sinking of new ones, for this will help to reduce the vulnerability people may have as result of poor drinking water.

REFERENCES

[1]. Ako, B. D. 1988, Groundwater Prospecting in Basement Complex of South Western Nigeria. Unpublished Ph.D Thesis

[2]. Dupreez, J. W. and Barber, W. 1965, The Distribution and Chemical Quality of Groundwater in Northern Nigeria. Geo Survey Nigeria Bulletin N0 36, pp. 67

[3]. Freeze, R. A. and Cherry, J. A. 1979, Groundwater Prentice Hall, New York, pp. 604

[4]. Imerbore, A. M. A. Obot, E. A. and Etozic I. E. 1987. Report of the Study of Water Resources Development Projects in Nigeria. Institute of Ecology, University of Ife, Ile-Ife, Nigeria

[5]. Kenneth, D. S. 1977, "Water Quality Variations for Pumping Boreholes". Journal on Groundwater vol. 15, No 2 Fresno Press Limited, California, USA

[6]. Horning, M., Reynolds, B., Stevens , P. A. and Aughes, S. 1990, Water Quality Changes from Input to Stream, pp. 223-240; In Acid Water in Wells. Edward, R.W. et al (eds). Kluwer Academic Publication, Amsterdam

[7]. Macdonalds and Partners 1986, Rural Water Supplies Final Report. Volume I Main Report, Sir Macdonalds Press Limited, Demeter, England pp. 123-153

[8]. Ogunkoye, O. O. 1986, Quality of Flows as an Index of Aquifer Yield in the Basement Complex Area South Western Nigeria. Journal of Environment Management pp. 291-300. Academic Press London Limited.

[9]. World Health Organization, Group on the Water Quality Studies, 1984. Geneva, a Guide for Collection and Interpretation of Water Quality Data. Geneva, Vol. 3, pp. 18-20

| Research Paper | Open Access |

Optimized Modulo Multiplier Based On R.N.S

Manjula.S.Doddamane, G.Parameshappa
Dept of Electronics and Communication JSSATE Bengaluru, India

Abstract: - To implement long and repetitive multiplications of cryptographic and signal processing algorithm we often adopt residue number system. In this paper a new low power and low modulo multiplier foe well established $\{2^n-1, 2^n, 2^n+1\}$ based is proposed .Radix-8 Booth encoding technique is used in the proposed modulo 2^n-1 and modulo 2^n+1 multipliers. In the proposed modulo 2^n-1 multiplier, the number of partial products is lowered to $[n/3]+1$. For modulo 2^n+1 multiplication ,the aggregate bias due to the hard multiple and the modulo reduced partial product generation is composed of multiplier dependent dynamic bias and multiplier-independent static bias .In the proposed modulo 2^n+1 multiplier , the number of partial products is lowered to $n/3+6$ .For different modulo 2^n-1 and modulo 2^n+1 multiplier our proposed modulo multiplier consumes less area and has minimum power dissipation over radix-4 Booth encoded and non-encoded modulo multiplier.

I. INTRODUCTION

Residue Number System (RNS) is adopted in high speed digital signal processors and cryptographic application. RNS is defined by a set of co-prime moduli and is represented as non-positional number representation .The residue of modulo is represented as P=XoY is (p1,p2,--pn)=(|x1oy1|L1,|x2oy2|L2----------|xnoyn|Ln) ,where pi is computed from xi and yi in the modulo channel corresponding to Li for i=1,2…,N. In any operation carry is generated and carry chain slows down the VLWL(Very Long Word Length).The addition and multiplication is effectively broken in RNS ,into smaller digits so that carry chain can be avoided. The main barrier in implementing VLWL arithmetic is with limited space and constrained battery specification, so that it can used for smart cards and Radio Frequency Identification (RFID) tags.

RNS are especially useful in algorithms where multiplication and addition dominate .It distributes a long integer multiplication into several shorter and independent modulo .So arithmetic circuits required for digits are smaller and faster. As RNS is most suited for applications involving repetitive computations like repeated modulo multiplications in cryptographic algorithm and multiply-add operations in signal processing algorithm, the research emphasis has shifted markedly in recent years to the area-power efficient implementation of concurrent modulo arithmetic operations in RNS.

In this paper, we propose a new radix-8 Booth encoded modulo $\mathbf{2^n}\text{-}\mathbf{1}$ multiplier and radix-8 Booth encoded modulo $\mathbf{2^n}\text{+}\mathbf{1}$ multiplier. Our objective is to minimize the area and power consumption of VLWL multiplication in RNS based on moduli $\mathbf{2^n}\text{-}\mathbf{1}$ and $\mathbf{2^n}\text{+}\mathbf{1.}$ Both the proposed modulo hard multiple generators (HMGs) employ only prefix levels and are by far the most area-delay-power efficient customized adders for this application. In the proposed modulo multiplier, one partial product per radix-8 Booth encoded multiplier digit is generated. As the hard multiple is generated in an unbiased form, no further correction term is incurred. Thus, the number of modulo-reduced partial products in modulo multiplier is lowered , which is the best achievable partial product count using radix-8 Booth encoding scheme. So the hardware's required for implementing the proposed multiplier modulo $\mathbf{2^n}\text{-}\mathbf{1}$ and modulo $\mathbf{2^n}\text{+}\mathbf{1}$ is less due to which we can minimize size of the multiplier block.

II.　　MODULO-REDUCED PARTIAL PRODUCTS FOR RADIX-8 BOOTH ENCODED MULTIPLICATION

This section presents the preliminaries of radix-8 Booth encoded modulo 2^n-1 multiplication using binary representation with dual zeros for modulo 2^n+1 arithmetic and diminished-1 representation for modulo arithmetic. Mathematically, the modulo 2^n-1 and modulo 2n+1 multiplications can be expressed.

For modulo 2^n-1

$$|P|_m = X.Y = \sum_{i=0}^{n-1} X.yi\, 2^i \qquad \text{if } m = 2^n\text{-1}$$

(1)

For modulo 2^n+1

$$|P|_m = X.Y + X + Y$$
$$= \sum_{i=0}^{n-1} X.yi.2^i + X + Y \qquad \text{if } m = 2^n + 1$$

where X,Y and P represent multiplicand , multiplier and product respectively By adopting Radix-8 Booth encoding ,the product can be computed from only n/3+1 modulo reduced partial products and (1) can be expressed as

for modulo 2^n-1

$$|P|_m = X.Y = \sum_{i=0}^{n/3} X.di\, 2^{3i} \qquad \text{if } m = 2^n\text{-1}$$

(2)

for modulo 2^n+1

$$|P|_m = \sum_{i=0}^{n/3} X.di.2^{3i} + X + Y \qquad \text{if } m = 2^n + 1$$

can be further simplified to

for modulo 2^n-1

$$|P|_m = \sum_{i=0}^{n/3}. PP_i \qquad \text{if } m = 2^n\text{-1}$$

(3)

for modulo 2^n+1

$$|P|_m = \sum_{i=0}^{n/3}(PPi + ki) + X + Y \qquad \text{if } m = 2^n + 1$$

III.　　PROPOSED MODULO AND MODULO HARD MULTIPLE GENERATORS (HMGs)

A . Modulus 2^n-1

As is congruent to zero modulo , 2^n-1 zero can be represented by an -bit binary string of all zeros or all ones in modulo 2^n-1 arithmetic. Thus, a modulo addition of two operands, A and B is equivalent to an -bit addition of ,A,B and cout i.e.,

$$|G+H|_{2n\text{-}1} = |G+H|_{2n} \qquad \text{if } G+H < 2^n$$
$$|G+H+1|_{2n} \qquad \text{if } G+H > 2^n$$
$$|G+H+C_{out}|_{2n}$$

(4)

where C_{out} is the carry output resulting from the addition of G and H . As is added to the sum of G and H at the position, modulo 2^n-1 addition is commonly referred to as end-around-carry (EAC) addition.This modulo 2^n-1 adder can be implemented by a parallel-prefix structure with three operator stages, namely pre-processing, prefix-computation and post-processing .The pre-processing stage computes the generate (gi), propagate(pi) and half-sum (hi)bits for i=0 to n-1.

$$g_i = a_i . b_i$$
$$p_i = a_i + b_i$$
$$h_i = a_i \oplus b_i$$

(5)

The prefix-computation stage uses the prefix operators (•) on (g_i, p_i) to calculate the carry bits c_i for the EAC addition. For $i=0$ to $n-1$.

$$c_i=(g_i,p_i)\circledast\text{-------}(g_0,p_0)\circledast(g_{n-1},p_{n-1})\circledast\text{-----}\circledast(g_{i+1},p_{i+1}) \tag{6}$$

where $(g_i,p_i) \circledast (g_j,p_j)=(g_i+p_i.g_j,pi,p_j)$

The modified n/2 generate and propagate bits pairs (g_i,p_i) are required in the prefix computation stage of modulo $2^n\text{-}1$ is given as

$$
\begin{aligned}
g_i&=x_{n-1}(x_0+x_{n-2}) &&\text{for i=0 to n-1}\\
p_i&=x_{n-1}+x_0.\ x_{n-2} &&\text{for i=0 to n-1}\\
h_i&=x_i\oplus x_{i-1} &&\text{for i=0 to n-1}
\end{aligned} \tag{7}
$$

The post-processing stage computes the sum bit for $i=0$ to $n-1$ i.e.,

$$s_i=h_i\oplus c_{i-1} \tag{8}$$
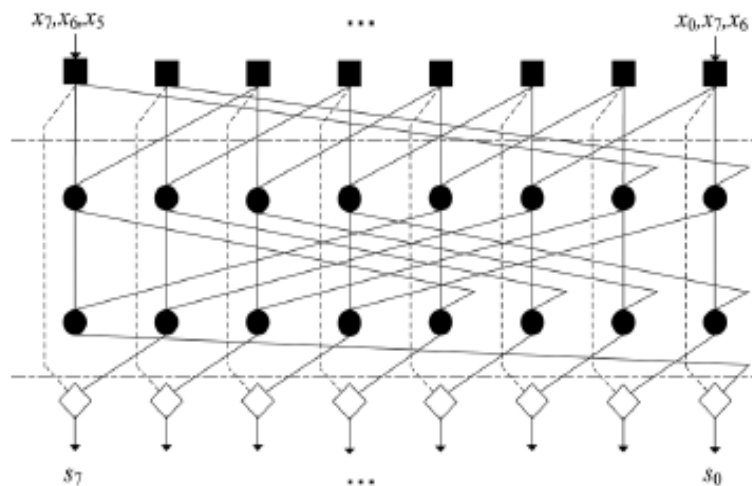
Fig1.Hard Multiple generator for modulo $2^n\text{-}1$

B. Modulus $2^n\text{+}1$

A modulo $2^n\text{+}1$ addition of two diminished-1 represented operands, and , is equivalent to an -bit addition of G and H with

$$
\begin{aligned}
&|S+1|_{2n+1}=|G+H+1|_{2n+1}\\
&|G+H+\overline{Cout}|_{2n}
\end{aligned} \tag{8}
$$

where $C_{ou}t$ is the carry output from the addition of G and H . As $\overline{Cout}$ is added to the sum of and at the LSB position, modulo addition is commonly referred to as complementary-end around- carry (CEAC) addition .The pre-processing and post-processing stages of the parallel prefix modulo $2^n\text{+}1$ adder are identical to those of the modulo$2^n\text{-}1$ adder but the carry equation is implemented differently in the prefix-computation stage due to CEAC addition

$$c_i=(g_i,p_i)\text{ }\circledast\text{ -------- }\circledast(g_0,p_0)\text{ }\circledast\overline{(g_{n-1},p_{n-1})}\text{ }\circledast\text{------}\circledast(g_{i+1},p_{i+1}) \tag{9}$$

where $(g_i,p_i) \circledast (g_i,p_i)=(g_i+p_i.g_i,pi,p_i)$
$(\overline{p_i},\ \overline{g_i}) \circledast (\overline{p_i}\ ,\overline{g_i})=(\overline{p_i}+\overline{g_i}.\overline{p_i}\ ,\overline{g_i}.\overline{g_i})$
$(g_i\ ,p_i)\text{ }\circledcirc(g_j\ ,\ p_j)=(g_i+p_i.g_j,pi,p_j)(p_i+g_i\ p_j,g_i.g_j)$

The modified prefix operator for modulo 2^n+1 (g_i,p_i) is given as

$$g_i = \overline{x}_{n-1} \cdot (x_0 + \overline{x}_{n-2}) \qquad \text{for i=0 to n-1}$$
$$p_i = \overline{x}_{n-1} + x_0 \cdot \overline{x}_{n-2} \qquad \text{for i=0 to n-1}$$
$$h_i = x_i \oplus x_{i-1} \qquad \text{for i=0 to n-1} \qquad (10)$$

Fig 2.Hard multiple generator for modulo 2^n+1

IV.   PROPOSED MODULO 2^n-1 AND MODULO 2^n+1 MULTIPLIERS

The Booth Encoder (BE) produces a signed digit represented by a sign bit and one-hot encoded magnitude bits denoted by m1i,m2i,m3i,m4i and from four consecutive multiplier bit. The generation PPi of in BE, BS and HMG blocks for the moduli **2^n+1** and **2^n-1** . A bank of identical BS blocks is required to generate a single PPi. Specifically for modulo **2^n+1** multiplier, the outputs of the BS blocks at the least-significant 3i bit positions are inverted to implement the CCLS operation

The modulo-reduced partial product accumulation (MPPA) differs significantly for modulo **2^n-1** and modulo **2^n+1** multipliers. For modulo **2^n-1** multiplier, the number of modulo-reduced partial products to be accumulated is n/3+1. Since modulo addition can be efficiently implemented by EAC addition, the CSA for its MPPA is shown in Fig. 6 for .n=8

(a)   (b)
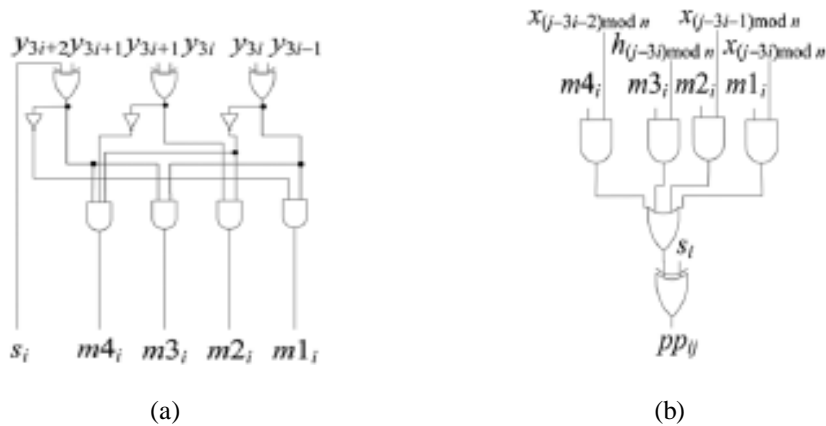
Fig 3 (a)Booth encoder and (b)Booth selector
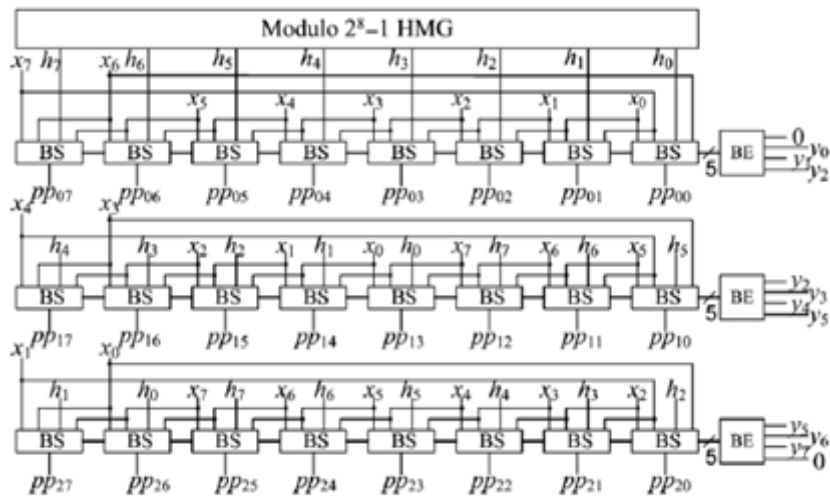
Fig 4.Modulo 2^n-1PP$_i$ generation
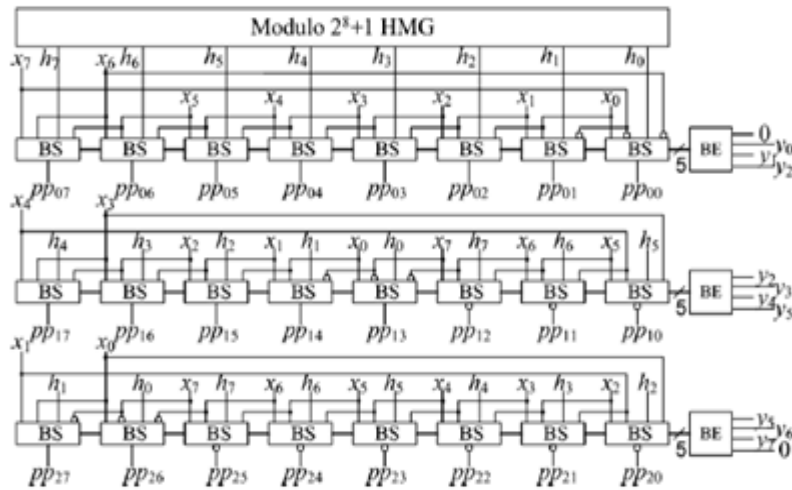
Fig 5.Modulo 2^n+1PP$_i$ generation
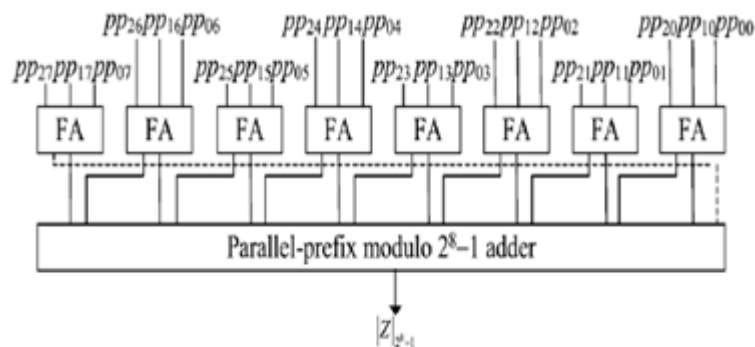
Fig 6.Modulo 2^n-1 reduced partial product accumulation

For modulo **2^n-1** multiplier, the number of modulo-reduced partial products and biasing constant to be accumulated is n/3+6. Since modulo addition can be efficiently implemented by CEAC addition, the CSA for its MPPA is shown in Fig. 7 for .n=8

we need to compute the bias constant that is

$$K1 = \sum_{i=0}^{n/3} \overline{m2_i \lor m3_i} \cdot 2^{3i} + \overline{m3_i \lor m4_i} \cdot 2^{3i+1}$$

$$K2 = \sum_{i=0}^{n/3} ((m2_i \lor m4_i) \land s_i) \cdot 2^{3i+1} + \sum_{i=0}^{\frac{n}{3}-1} ((m3_i \lor m4_i) \land s_i) \cdot 2^{3i+2}$$

$$K3 = \sum_{i=1}^{n/3} 2^{3i} + \sum_{i=0}^{n/3} \overline{s_i} \, 2^{3i+1} + \sum_{i=0}^{n/3} s_i \, 2^{3i+1}$$

$$(10)$$

The final product is given by

$$|P|_{2n+1} = \sum_{i=0}^{n/3} PPi + X + Y + K1 + K2 + K3 \qquad (11)$$
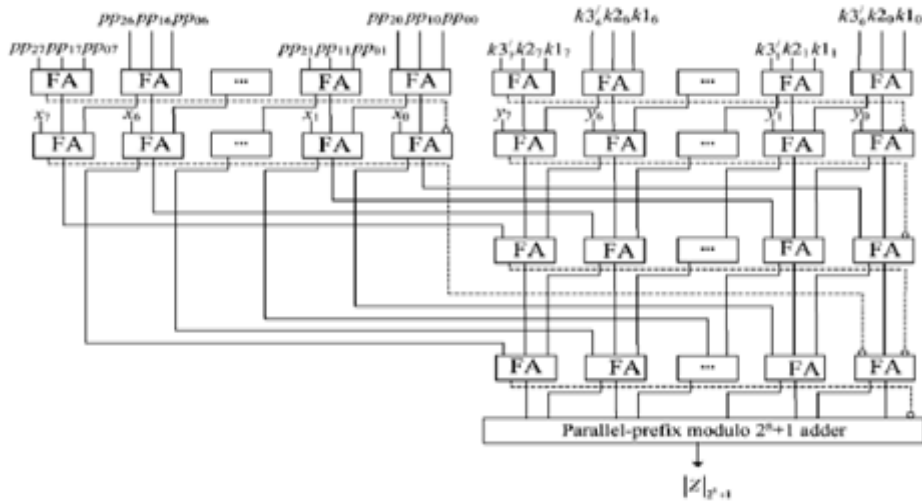
Fig 7. Modulo 2^n+1 reduced partial product accumulation

V. SIMULATION RESULT
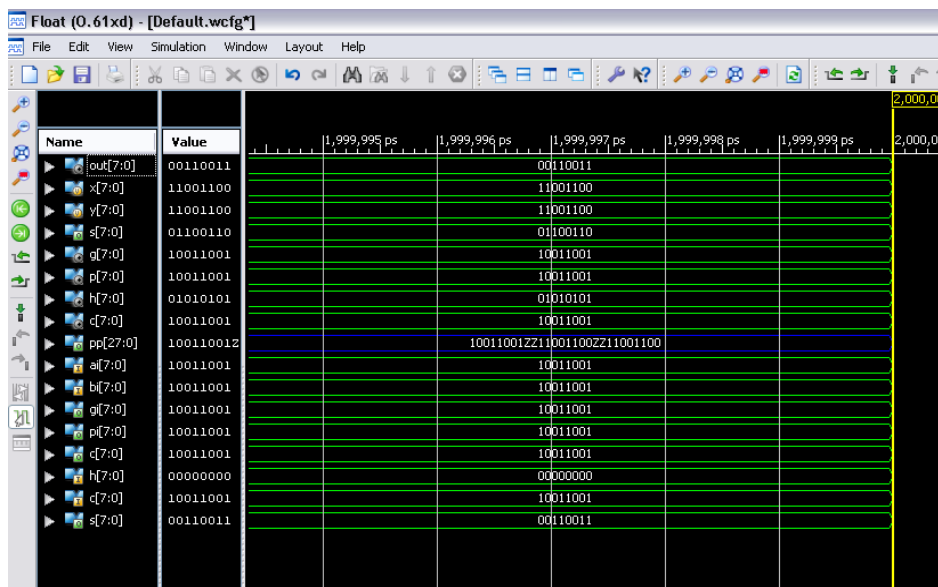
Fig 8 For Modulo2^n-1 multiplier
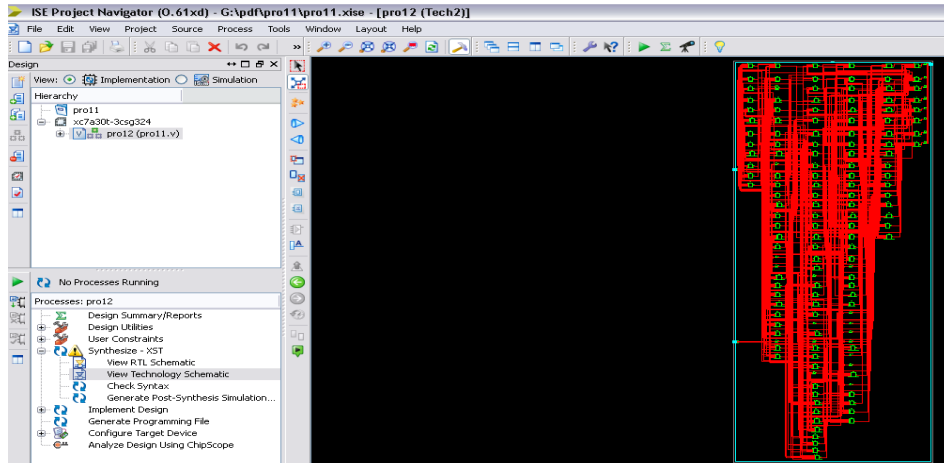
Fig 9.Technology schematic for modulo 2^n-1
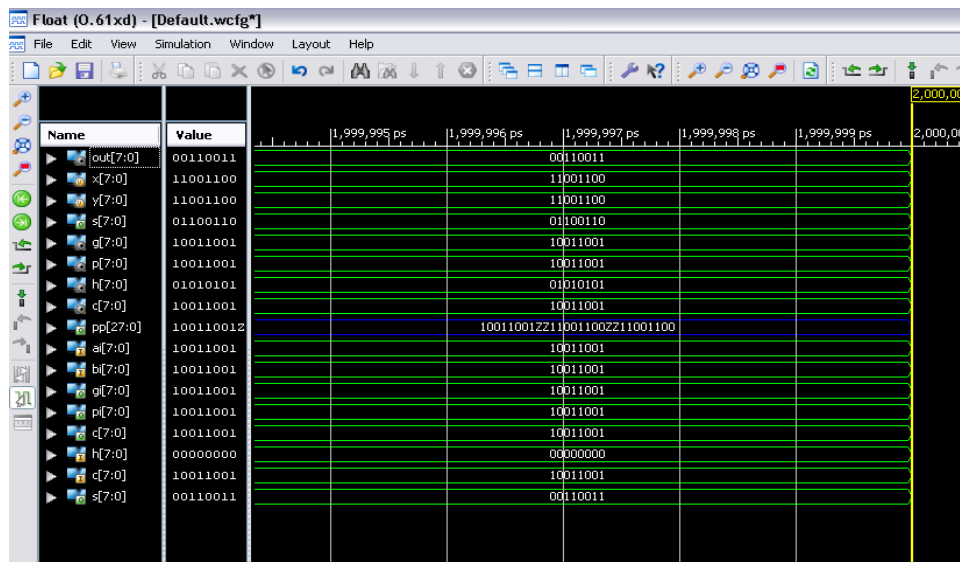
Fig 10 .For Modulo2^n+1 multiplier
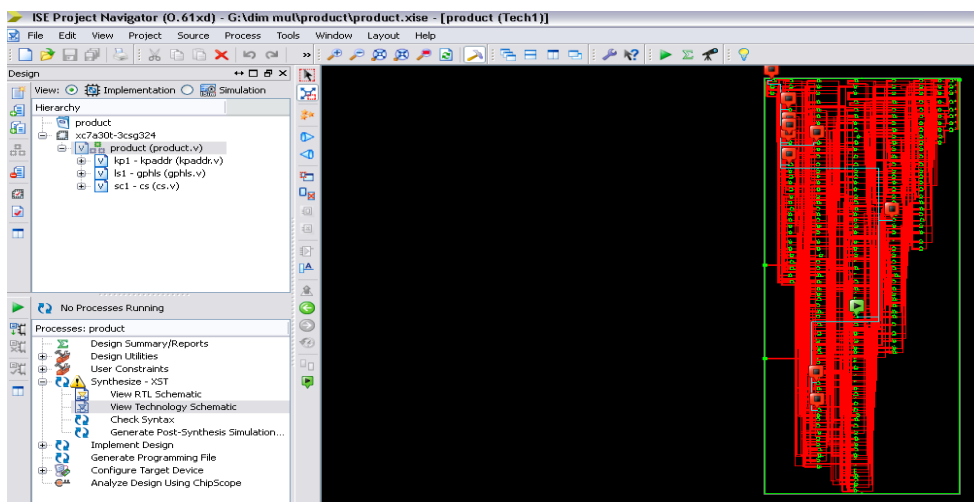
Fig 11.Technology schematic for modulo 2^n+1

VI.PERFORMANCE COMPARISION

The proposed multiplier is synthesized in Xilinx ISE simulator cadence tool to find optimized area and power dissipation for modulo 2^n-1 and modulo 2^n+1 .The modulo multipliers is compared with different modulo multiplier that can be seen below

TABLE 1.Area of modulo 2^n-1

n	PROPOSED MULTIPLIER	[2]	[3]
8	1189	1147	988
16	4270	4249	3921
32	14961	15966	15301

TABLE 2 .Power dissipation of modulo 2^n-1

n	PROPOSED MULTIPLIER (n W)	[2] (n W)	[3](n W)
8	47910.969	61227.246	48260.121
16	29334.151	337299.160	316111.870
32	1457361.477	1799592.653	1746144.796

TABLE 3. Area of modulo 2^n+1

n	PROPOSED MULTIPLIER	[5]	[6]
8	2358	1926	1710
16	6750	6813	6233
32	20745	24810	23099

TABLE 4. Power dissipation of modulo 2^n+1

n	PROPOSED MULTIPLIER (n W)	[5] (n W)	[6](n W)
8	103190.856	104933.202	78377.144
16	478557.460	525754.151	446820.961
32	2023247.140	2307567.659	2173617.139

VII.   CONCLUSION

The Optimized modulo 2^n-1 and modulo2^n+1 multipliers employing radix-8 Booth encoding scheme were proposed. The hardware cost of hard multiple generation was minimized by customizing the parallel-prefix modulo 2^n-1   and modulo 2^n+1 adders for the efficient computation of hard multiples . The area-delay-power metrics of the proposed modulo multipliers were evaluated and compared against radix-4 Booth encoded and non-encoded modulo multipliers. the simulation of multiplier is done in Xilinx and synthesis in cadence In RNS multiplier based on moduli 2^n-1   and , 2^n+1   the proposed multipliers lower both the implementation area and the total power dissipation.

REFERENCES

[1].   Z.Wang.G.A.Jullien and W.C.Miller ."An algorithm for Multiplication modulo 2^n-1   ."in Proc 39th IEEE Midwest Symp.circuit Syst ,Ames ,IA Aug 1996pp 1301-1304

[2].   R. Zimmermann ,"Efficient VLSI implementation of modulo addition and multiplication" ,in proc 14th IEEE Symp Computer Arithmetic ,Adelaide ,Australia apr 1999,pp 158-167.

[3].   C. Efstathiou, H. T. Vergos, and D. Nikolos, "Modified Booth modulo2^n-1   multipliers," IEEE Trans. Comput., vol. 53, no. 3, pp. 370–374, Mar. 2004.

[4].   Z.Wang, G. A. Jullien, andW. C.Miller, "An efficient tree architecture for modulo 2^n+1 multiplication," J. VLSI Signal Process., vol. 14, no. 3, pp. 241–248, Dec. 1996.

[5].   C. Efstathiou, H. T. Vergos, G. Dimitrakopoulos, and D. Nikolos, "Efficient diminshed-1 modulo 2^n+1 multipliers," IEEE Trans. Comput., vol. 54, no. 4, pp. 491–496, Apr. 2005.

[6].   J.W.Chen R.H.Yao " Efficient modulo 2^n+1 multipliers for diminished -1 representation."

[7].   Y. Ma, "A simplified architecture for modulo 2^n+1 multiplication," IEEE Trans. Comput., vol. 47, no. 3, pp. 333–337, Mar. 1998.

[8].   L. Sousa and R. Chaves, "A universal architecture for designing efficient modulo 2^n+1 multipliers," IEEE Trans. Circuits Syst. I, Reg.Papers, vol. 52, no. 6, pp. 1166–1178, Jun. 2005.

[9].   J. W. Chen and R. H. Yao, "Efficient modulo 2^n+1 multipliers fordiminished-1 representation," IET Circuits, Devices Syst., vol. 4, no. 4,pp. 291–300, Jul. 2010.

[10].   L. Leibowitz, "A simplified binary arithmetic for the Fermat number transform," IEEE Trans. Acoustics, Speech Signal Process., vol. 24,no. 5, pp. 356–359, Oct. 1976.

[11].   H. T. Vergos and C. Efstathiou, "Design of efficient modulo 2^n+1 multipliers," IET Comput. Digital Tech., vol. 1, no. 1, pp. 49–57, Jan.2007.

[12].   G.W. Bewick, "Fast Multiplication: Algorithms 2^n-1   and2^n+1 Implementation,"Ph.D. dissertation, Stanford Univ, Stanford, CA, 1994.

[13].   B. S. Cherkauer and E. G. Friedman, "A hybrid radix-4/radix-8 low power signed multiplier architecture," IEEE Trans. Circuits Syst. II, Analog.Digit. Signal Process., vol. 44, no. 8, pp. 656–659, Aug. 1997.

[14].   M. J. Flynn and S. F. Oberman, Advanced Computer Arithmetic Design. New York: Wiley, 2001.

[15].   R. Muralidharan and C. H. Chang, "Radix-8 Booth encoded modulo 2^n-1   multipliers with adaptive delay for high dynamic range residue number system," IEEE Trans. Circuits Syst.I, Reg. Papers, vol. 58, no. 5, pp. 982–993, Jun.2011

Research Paper | Open Access

Design of Three Phase Solar-Based 4.5kw Ac Power Inverter Station

Dr.J.C. Onuegbu, Dr.F.O. Enemuoh, Dr. E. A. Anazia
Department of Electrical Engineering Nnamdi Azikiwe University, Awka, Nigeria

Abstract: - The design model of a 4.50Kilowatt, 3-phase, 50 hertz solar-based power generating station was examined by the paper. The power station is a dual source input generating station using 8 series connected 100A, 12V batteries per phase as backup, the solar panels being the main frame. An inverter of 12Volt direct current input voltage was incorporated to supply an output of 3-phase, 220Volts and 50 hertz alternating current. A charging circuit was installed to monitor charging level and to preserve the accumulator's life span. The paper also looked into the solar-based power station component design model. The batteries therein are back-up and the system will ensure 24-hours reliable power supply. The setup has a normally closed switching relay ready to pickup the auxiliary battery supply within a few milliseconds after the solar source voltage drops below a stipulated level. The three phase a.c. voltage was achieved using standby on-line circuit with cascaded 741-based flip-flop at the base of the transistor drivers of the 3-phase power transformer. This model circuit reduced the load on each phase winding and facilitated reliable and uninterruptible power supply. The delta-wye connected transformer will guarantee proper phase shift of 120 degrees that will emulate alternating current voltage similar to the conventional generator voltage.

I. INTRODUCTION

Renewable energy has come to compliment the insufficient and epileptic supply of the energy needs of the 21st century. The new found knowledge in Engineering and Technology has made it possible to harness the abundant energy resource of the sun to generate electricity [1]. The paper is on the design of three-input three phase inverter. The presented paper tried to utilize three energy sources, namely: solar panel, lead–acid accumulators and electricity (if available) to provide safe, reliable and efficient source of electricity to an average middle class family. Solar-based electricity power system supplies one of the cleanest sources of energy. It is safe, noiseless and cheap on the long run. The work being presented was based on On-line bypass mode of operation [2]. This means that the solar cell and the mains supply are complimenting each other but the accumulator is constantly fitted at the supply terminal. The relay which feeds the solar panel into the charging circuit is powered separately from a rectified 12 volts dc supply from the mains Fig. 1.0. This makes the solar panel to give way whenever there is availability of electricity.

Three phase design model was applied in this UPS to ease the load on the MOSFETs. The 4500watts total power rating of the system was distributed among the three phases. The design was done in such a way that the damage of any one pulse generator does not result to total blackout. Instead, when any of the three pulse generators goes bad, only two phases will be affected and can be isolated from the system while the remaining two pulses continue to supply one phase voltage that is distributed equally on the three secondary windings. Finally, the manoeuvrability and ease of trouble shooting of the device is guaranteed by the choice of simple and cheap components.

II. DESIGN OF UPS TRANSFORMER

Design data
Input Voltage: V_1 = 12 Volts dc
Output Voltage: V_2 = 220 Volts ac
Operating frequency: f = 50Hz

Stacking factor: $K_w = 0.80$
Current density: $J_1 = 8.1A/mm^2$ or $8.1*10^2 A/cm^2$ (for primary winding)
Current density: $J_2 = 2.7A/mm^2$ or $2.7*10^2 A/cm^2$ (for secondary winding) [3]
Maximum flux density: $B_m = 1.2$ Tesla (assumed)

III.   DEFINITION OF MAIN PARAMETERS

Input current: $I_1 = 4500/12 = 375A$ or $125A/phase$
Output current: $I_2 = 4500/220 = 20.5A$ or $6.83A/phase$
Voltage per turn: $V_t = C\sqrt{S} = 1.0\sqrt{1.5} = 1.22V$
where $C = \sqrt{4.44*f*r*10^3}$ and r - permeance of iron core, $r = \Phi/I_1 N_1$ [4]
For shell type transformers: C= (1.0 to 1.2)
The maximum magnetic flux: $\Phi_m = V_t/4.44f = 1.22/4.44*50 = 0.0055$ Weber
Net core section: $A_i = \Phi_m/B_m = 0.0055/1.2 = 0.0046m^2 = 46cm^2$
Gross core area: $A_g = A_i/K_w = 46cm^2/0.80 = 57.5$ cm^2
Diameter of circumscribed circle: $d = \sqrt{A_g/0.5} = \sqrt{57.5/0.5} = 10.72cm$
Lamination thickness: (L_T) = Width of lamination $(W_L) = \sqrt{A_g} = \sqrt{57.5} = 7.6$ cm
The area of window A_w will be defined using the equation that defines the power rating of a three phase transformer.
Power rating of three phase transformer is defined by the expression:
$S = 3.33*f*A_i*B_m* A_w*K_w*J_1$ [5], from where the area of window becomes:
$A_w = S/3.33*f*A_i*B_m*K_w*J_1 = 4500/3.33*50*46*10^{-4}*1.2*0.8*8.1*6 = 0.000756m^2$ or $7.56cm^2$. This will give a window area of: A_w = (4.5cm by 1.68cm).

IV.   NUMBER OF TRANSFORMER TURNS

Number of turns of the primary windings $N_1 = V_{in}/V_t = 12/1.22 = 9.64 \approx 10$ turns. Number of turns of the secondary windings $N_2 = V_2/V_t = 220/1.22 = 180.3 \approx 181$ turns.

V.   CONDUCTOR CROSS-SECTIONAL AREA

Primary winding conductor: $A_1 = I_1/J_1 = 125/8.1 = 15.43mm^2$. The diameter of the primary winding conductor: $d_1 = \sqrt{4*A_1/\pi} = \sqrt{4*15.43/\pi} = 4.43mm$ (2.5*2mm wire). This will give 20 turns of two parallel wires. The primary winding conductor: $A_2 = I_2/J_2 = 6.83/2.7 = 2.53mm^2$. The diameter of the secondary winding conductor: $d_2 = \sqrt{4*A_2/\pi} = \sqrt{4*2.53/\pi} = 1.80mm$.

VI.   POWER SUPPLY CIRCUIT

The major device in the power supply circuit is the battery charger. There are three different voltage inputs to the oscillator. The battery is the default power source and then the solar panel and the mains ac can be selected alternately using a relay RL. This three-input inverter is designed for reliability and comfort aimed at guaranteed 24-hour availability of electricity. As shown in Fig. 1.0, the relay feeds directly from the mains source, where the normally open contact (A) is connected to the rectified voltage and the normally closed contact (B) is connected to the solar panel [6]. The arrangement is such that the UPS will always take source from the battery.
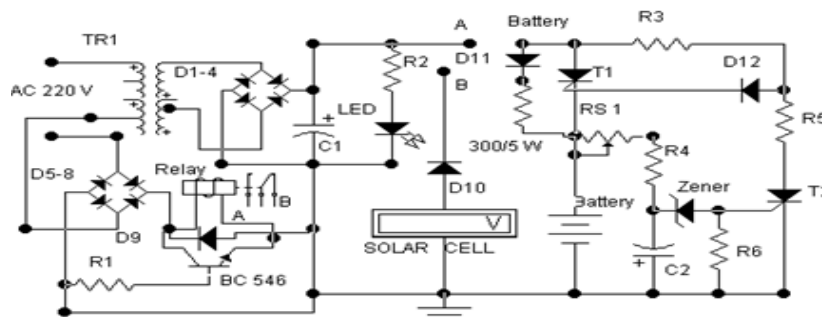
Fig. 1.0 Power supply and Battery charging circuit [7]

When there is no ac, the relay is de-energized and it goes back to the normally closed contact which links the solar panel to the charging circuit. To power the station using accumulators, the number of accumulators required is calculated as shown: 100Amperes-Hour/I_1 = 100Amperes-Hour/375A = 0.27hour or 16 minutes (for one accumulator). To sustain the solar-based power station for 6hours at 4500 watts, an imaginary

2250AH lead-acid accumulator is needed, which is approximately:

2250AH/100A = 22.5 ≈ 23 batteries. If each 100AH battery at 12 volts gives 100*12 = 1200watts-hour, then 23 batteries will give: 1200*23 = 27600watts-hour or 4600watts-6hour. The 23 batteries will be arranged in parallel since only 12 volts is required for the power station inverter [8].

VII.   BATTERY CHARGING CIRCUIT

The battery charging circuit contains two thyristors T_1 and T_2. T_1 is biased through the diode D_{12} to conduction to link the positive terminal of the battery to the rectified 15 Volts from the ac supply to start charging. When the battery is charged to a value specified by the variable resistor RS, usually 14.5 Volts [9], the zener diode as shown in Fig. 1 goes into conduction and sends biasing voltage to the gate of the thyristor T_2 which also goes into conduction and grounds the battery through the resistors R_4 and R_6. The resistor R_7 is used to stabilize the break over voltage of the zener diode while the capacitor C_2 is used to prevent zero resistance grounding of the battery through R_5. The voltage at the zener diode is controlled by the discharge time of the capacitor C_2.

VIII.   SOLAR PANEL AREA

The area of the solar panel required to power this station can be gotten from assumption using the solar constant (I_{sc} =1353watts/m^2) [10, 11]. For 4500watts, the needed area is 4500/ I_{sc} = 3.326 m^2 ≈ 4.0 m^2 solar panels connected in parallel.

IX.   THE MULTIVIBRATOR

The multivibrator is a simple 5-resistor Wien bridge circuit designed on the principle of 741 op-amp with 2 capacitor interface to facilitate the oscillation [12]. Fig. 2.0 shows a sine wave oscillator on the bases of which the inverter was built. C_1 and C_2 define the shape of the output waveform while RS is used to tune the device to oscillation. The numerous MOSFETs involved in the output circuit of the inverter makes it imperative to incorporate driver circuit at the output terminals of the 741 op-amps.

The op-amps were used to generate independent sine-wave frequency that went into the base of the MOSFETs through the driver circuit. To get 3-phase output voltage, the three independent output waveforms were shifted in phase by the use of six diodes to produce 3-phase ac voltage with neutral. As shown in Fig. 4.0**,** the output transformer can be connected in delta for loads that feed on line voltage.
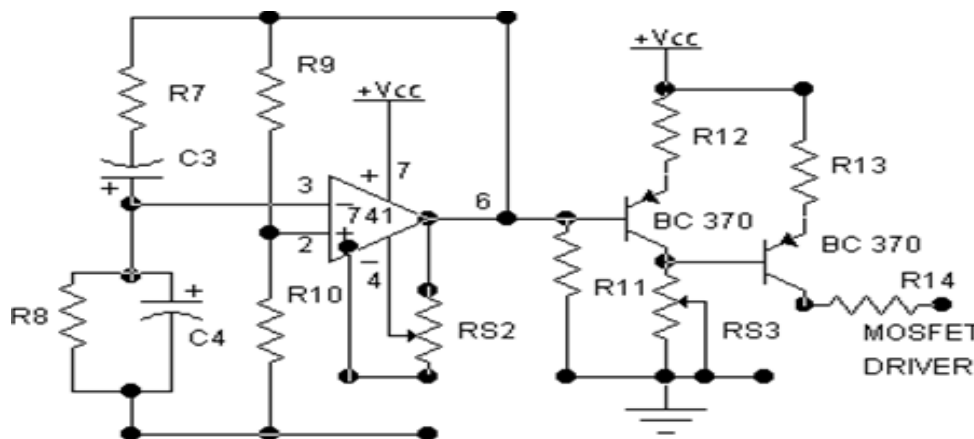
Fig. 2.0 Multivibrator circuit

From fig. 2.0, $V^+ = V^-$, $C_1 = C_2 = C_3$, $R_1 = R_4 = R$; $R_3 = 2R_1$

Where $V^+ = (R_1||C)V_o/(R_1||C)+R_1+ C = R_1*(V_o/ Cs)/(R_1+(1/ Cs))/[R_1*(1/Cs)/R_1+1/Cs+ R_1+1/Cs] =$

$R_1*Vo/(R_1*Cs +1)/[R_1/(R_1*Cs +1)+ 1/Cs + R_1$

And $V^- = R_1*V_o/(R_1 +2R_1) = R_1*V_o/3R_1 = V_o/3$

Now, $V^+ = V^-$, ∴ $R_1*V_o/(R_1*Cs +1)/[R_1/(R_1*Cs +1)+ 1/Cs + R_1 = V_o/3$

Therefore, $3R_1/Cs*R_1+1 = (R_1/Cs*R_1+1) +1/Cs+R_1$

$2R_1/1+Cs*R_1 = (1/Cs+R_1) = 1+Cs*R_1/Cs$ or $2Cs*R_1 = (1/Cs+R_1)^2$

$1+2Cs*R_1 + (Cs*R_1)^2$

$0 = 1+C^2s^2R_1^2$; $C^2s^2R_1^2 = -1$; $s^2 = -1/C^2R_1^2$; $s = (-1/C^2R_1^2)^{1/2} = j/R_1*C$. At $s = j\omega$; $f_o= 1/2\pi R_1C = 0.159/RC$, Hz. This is the output signal frequency of the op-amp. The input impedance of 741 op-amp is 2MΩ with output impedance of 75Ω [13].

X.   THE POWER MOSFETS

The power MOSFETs used in the power output is IRFZ44 with the following properties: V-mos = 60Volts, 50A, 150 watts. Its equivalent are BUK556-60, 2SK2049 and 2SK 2499 [14]. IRFZ44 MOSFET has higher theoretical output power than the practical output power. Using a push-pull amplifier circuit with an efficiency of about 78% [15], the theoretical output power can be calculated as:

$P_{max} = Vce_{max}I_{op} = 60*2.5 = 150$ watts.

Output power $P_{op} = V_{op}*I_{op}*\eta$,

where efficiency of a push-pull amplifier, $\eta = P_{ac}/P_{dc}$

$P_{ac} = Vcc*Ic_{max}/2$

$P_{dc} = 2Vcc*Ic_{max}/\pi$

$\eta = P_{ac}/P_{dc} = (Vcc*Ic_{max}/2)/(2*Vcc*Ic_{max}/\pi) = \pi/4 = 0.785$

$\therefore$ output power $P_{op} = 220*2.5*0.785 = 431.8$ watts
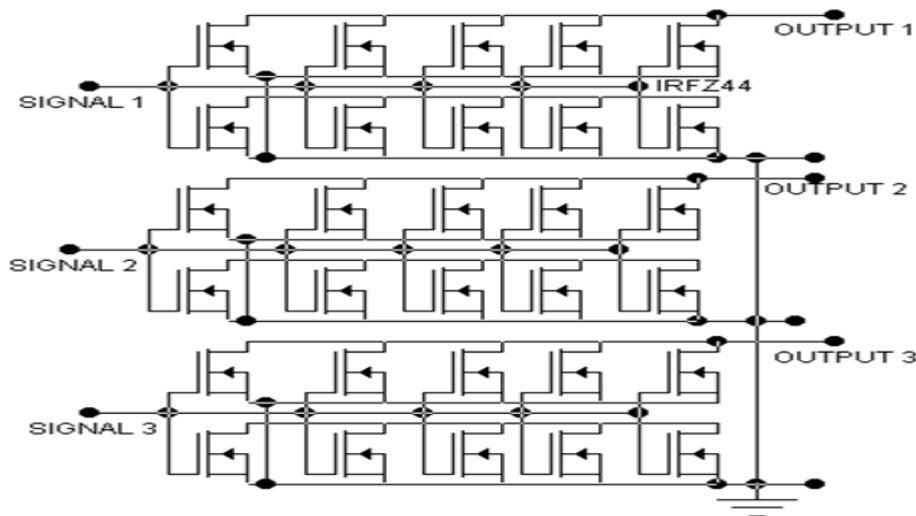
Fig. 3.0 MOSFET arrangement for output voltage transformer

A look at the power rating of the solar-based power station shows that the 4500watts will require 4500/150 =30 pieces of IRFZ44 or 10 pieces of IRFZ44 per phase cascaded as shown in Fig. 3.0.Figure 4(a) shows a Δ/Y connected inverter transformer requiring three input signals with center tapped V_{cc} to give out three phase voltage. Figures 4(b) and 4(c) show wye-wye connection of inverter transformer with phase shift using diodes. The circuit of 4(c) will require 4 sinusoidal signal inputs while the other two circuits of 4(a) and 4(b) will require 3 sinusoidal signal inputs to generate a 3-phase circuit. The output of Fig. 3.0 forms the input of Fig. 4 (a, b and c) arranged as appropriate.
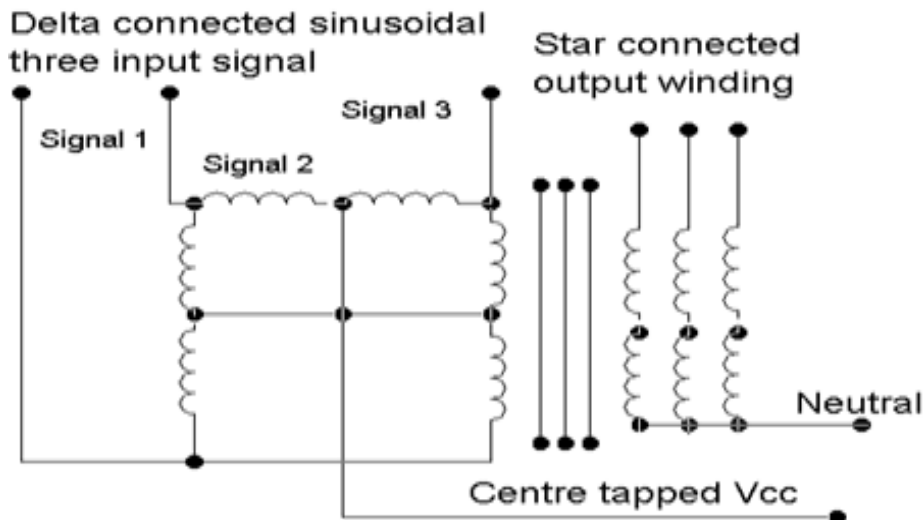
Fig. 4.0(a) 3-phase delta-wye connected transformer without diodes
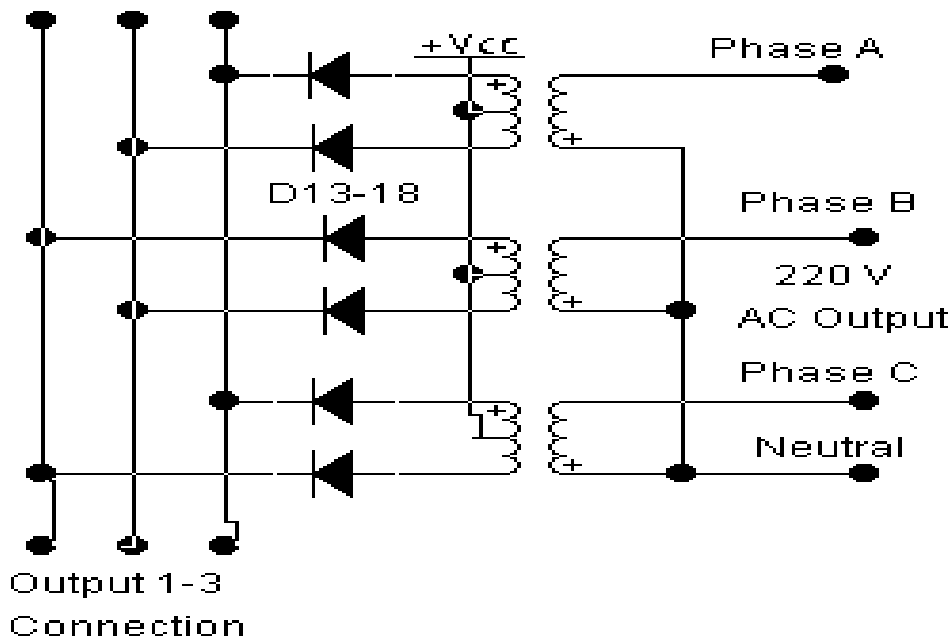
Fig. 4.0(b) 3-phase wye-wye connected transformer with 6 diodes
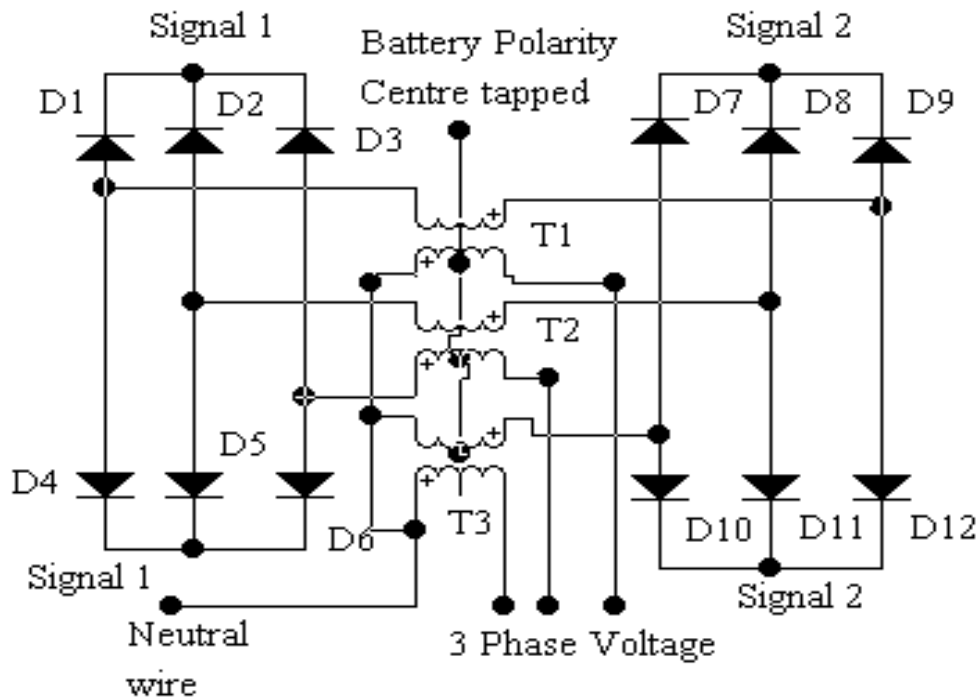
Fig. 4.0(c) 3-phase wye-wye connected transformer with 12 diodes

XI.   CONCLUSION

The modeled UPS which was meant to support a load of 4500 watts for 6 hours can be extended to 24 hours service at a load of 1150 watts. The usual high harmonic associated with singles phase systems has been reduced by the use delta-wye connected transformer. Again, mass and weight of inverters have been grossly reduced by the compactness of three phase inverter. The problem of heat removal is obvious and that is the reason for the incorporation of a small dc fan to cool the power MOSFET bank. The number of cascaded MOSFETs will be reduced with the availability of MOSFETs with higher power rating. The economic application of this type of renewable energy resource will be realizable in combination with the introduction of energy saving bulbs.

REFERENCES

[1].   World energy; Looking Ahead to 2020. Report by the Conservation Commission of the World Energy Conference 1978, Mid-County Press London, SW15.
[2].   Onuegbu J. C., Anazia E. A. and Okafor T. C. Comparative analysis of discrete based UPS topologies. Journal of Electrical and Telecommunication System   Research. Nnamdi Azikiwe University, Awka. Vol. 3 No. 3, 2009, pp29-36.
[3].   Paul Horowitz and Winfield Hill., The art of Electronics. Cambridge University Press, 1989 pp 284293.
[4].   Pearman P., Electrical Machinery and transformer Technology. Saunders College Publication, 1994, pp 387-444.
[5].   Handbook of PV System Design Practices. Sandia National Laboratories USA, 1973.
[6].   Horowitz S. H. and Shadke A. G., power system Relaying. Research studies Press, 1996, 2nd Edition, pp 7-12.
[7].   John Markus, Sourcebook of Electronic circuits. McGraw-Hill Book Company, USA, 1968, pp75 and 491-496.
[8].   Robert Simon, Solar electricity. A practical guide to designing and installing small photovoltaic systems. Prentice Hall, New York, USA 1977.
[9].   Nikitin V. A., Radio Construction Handbook. M. Patriot, Moscow, 1990, 108th Edition. pp 52-54.
[10].   John A. Duffie and William A. Beckman, Solar Energy Thermal Processes. John Wiley Inc., USA, 1974.
[11].   Handbook of PV System Design Practices. Sandia National Laboratories, USA, 1973.
[12].   Forest M. Mims III., Engineers Mini-notebook. A Siliconcepts ^{TM} Book, USA, 1991 1st Ed. pp 47.
[13].   Up-date World's Transistors-Diodes, Thyristors and IC's Comparison tables A-Z. Tech. Pub. PTE Ltd, Singapore, 2001 Vol. 1, pp 775.
[14].   Kasatkin A. S. and Nemtsov M. V., Electrical Engineering. Mir Publishers Moscow, 1990, 2nd Printing. pp 278-281.
[15].   Nagrat I. J. and Kothanri D. P., Power System Engineering. Tata McGraw Hill Ltd, New Delhi, 2004, pp 25 and 26.

Research Paper   Open Access

Exhaust Gas Analysis and Parametric Study of Ethanol Blended Gasoline Fuel in Spark Ignition Engine

Jitendra kumar[1], N.A Ansari[2], Vikas Verma[3], Sanjeev Kumar[4]

[1] *M.Tech Scholar, Department of Mechanical Engineering, Delhi Technological University, New Delhi-110042, India,*

[2] *Asst. Professor, Department of Mechanical Engineering, Delhi Technological University, New Delhi-110042, India,*

[3] *PhD. Scholar, Department of metallurgical and materials engineering, IIT Roorkee , Uttarakhand, -247667, India*

[4] *Asst. Professor, Department of Mechanical Engineering, KIMT, U.P Moradabad -244001U.P, India,*

Abstract: *- It is well known that the future availability of energy resources, as well as the need for reducing CO_2 emissions from the fuels used has increased the need for the utilization of regenerative fuels. This research is done taking commercial gasoline as reference which is originally blended with 5% ethanol. Hence 5%, 10%, 15%, 20% ethanol blended with Gasoline initially was tested in SI engines. Physical properties relevant to the fuel were determined for the four blends of gasoline. A four cylinder, four stroke, varying rpm, Petrol (MPFI) engine was tested on blends containing 5%,10%,15%,20% ethanol and performance characteristics, and exhaust emissions were evaluated. Even though higher blends can replace gasoline in a SI engine, results showed that there is a reduction in exhaust gases, such as HC, O_2, CO, CO_2 and increase in Brake Thermal Efficiency on blending. Hence we can conclude from the result that using 10% ethanol blend is most effective and we can utilize it for further use in SI engines with little constraint on material used to sustain little increase in pressure.*

Keywords: *- Spark Ignition Engine, Ethanol, Brake Thermal Efficiency, Emission, Gasoline etc.*

I.   INTRODUCTION

Rising fuel prices and increased oil consumption along with the lack of sustainability of oil-based fuels have generated an interest in alternative, renewable sources of fuel for internal combustion engines, namely alcohol-based fuels. Currently ethanol is the most widely used renewable fuel with up to 10% by volume blended in to gasoline for regular engines or up to 85% for use in Flex-Fuel vehicles designed to run with higher concentrations of ethanol. Ethanol can also be used as a neat fuel in spark-ignition (SI) engines or blended up to 40% with Diesel fuel for use in compression-ignition (CI) engines [1-2]. Ethanol was introduced as a replacement for methyl tertiary butyl ether (MTBE) when it was realized that MTBE leaked onto the ground at filling stations resulting in the contamination of large quantities of groundwater. Ethanol is biodegradable, less detrimental to ground water, and has an octane number much higher than gasoline as well as having a positive effect on vehicle emissions [3].There are lots of gases in the environment which are causing pollution and greenhouse effect and the major contributor is the transport sector due to the heavy, and increasing, traffic levels. In spite of ongoing activity to promote efficiency, the sector is still generating significant increases in CO_2 emissions. As transport levels are expected to rise, especially in developing countries, fairly drastic political decisions may have to be taken to eradicate this problem in the future. Furthermore, the dwindling supply of petroleum. Today, the transport sector is a major contributor to net emissions of greenhouse gases, of which carbon dioxide is particularly important. The carbon dioxide emissions originate mainly from the use of fossil fuels; mostly gasoline and diesel oil in road transportation systems, although some originates from other types of fossil fuels such as natural gas and Liquefied Petroleum Gas (LPG). If international and national goals (such as those set out in the Kyoto protocol) for reducing net emissions of carbon dioxide are to be met, the use of fossil fuels in the transport sector has to be substantially reduced. This can be done, to some extent, by

increasing the energy efficiency of engines and vehicles and thus reducing fuel consumption on a volume per unit distance travelled basis. However, since the total transportation work load is steadily increasing such measures will not be sufficient if we really want to reduce the emissions of carbon dioxide.

1.1 Ethanol as a Blend

In the medium term ethanol produced from grain will probably be the most important alternative fuel for replacing gasoline and in the long term ethanol produced from cellulose might take over from grain ethanol. Today, ethanol accounts for a substantial part of the alternative fuel market. From an international perspective, most research up to 1990 was focused on blends of methanol and gasoline, but some studies were carried out on ethanol-gasoline blends. Since these studies were carried out in the USA, it can be assumed that they mainly included vehicles with efficient emission control systems, but at the same time technical features of cars in the USA have historically differed, at least in part, from those in Sweden. It should also be noted that for a longtime 10% ethanol has been added to commercial gasoline in many parts of the world. In the US there is considerable experience of adding higher proportions of ethanol to gasoline than those allowed by gasoline regulations in Sweden (Europe). The primary advantage of adding a bio based alcohol to gasoline is that it reduces net CO_2 emissions but it also has other positive effects, such as increasing the octane value of the fuel and reducing the benzene content of the exhaust gases. The use of alcohol blended gasoline and neat fuel alcohols as substitutes for neat gasoline have become matters of interest in many countries. The International Energy Agency (IEA), established in 1974, follows the development, and data and other experience from various trials have been presented and discussed at symposia organized by the International Symposium on Alcohol Fuels (ISAF).

1.2 Co-products of ethanol

The co-products that results when making ethanol are dependent on the medium used to produce the ethanol. Table 1 shows a summary of the co-products and what they are used for.

Table 1. Summary of by-products/co-products made through ethanol production.

SI.No.	By-Products/Co-Products	Used For
1	Flour, Corn Oil, Corn Meal, Corn Grits	Used in producing food for human consumption
2	Fibrotein TM	Used as a high fibre and protein food additive
3	Corn Gluten Meal and Corn Gluten Feed	Used as high protein animal feed additives
4	Amino Acids	Used as animal feed additives
5	Dry Distiller's Grains	Used as high protein and energy animal feed
6	Carbon Dioxide	Used as a refrigerant, in carbonated beverages, to help vegetable crops grow more rapidly in greenhouses, and to flush oil wells

In practice, about two-thirds of each tone of grain (i.e., the starch) is converted to ethanol. The remaining by-product is a high protein livestock feed which is particularly well suited for ruminant animals such as cattle and sheep. This by product is also known as Distillers' Dried Grains, DDGS. The protein in this material is utilized more efficiently in ruminant nutrition than are other high-protein feed ingredients such as soybean meal. This by-product of ethanol production is particularly good for Canadian dairy, beef and sheep production. It improves the competitive position globally of producers of these farm commodities. The manure from livestock can be used as a major source of fertilizer in grain crop production. Carbon dioxide is another by-product produced when making ethanol. Carbon dioxide, given off in great quantities during fermentation will be collected and cleaned of any residual alcohol, compressed and sold as an industrial commodity.

II.   LITERATURE SURVEY

Fikret Yuksel et.al [4] one of the major problems for the successful application of gasoline–alcohol mixtures as a motor fuel is the realization of a stable homogeneous liquid phase. To overcome this problem, a new carburetor was designed. With the use of this new carburetor, not only the phase problem was solved but also the alcohol ratio in the total fuel was increased. By using ethanol–gasoline blend, the availability analysis of a spark-ignition engine was experimentally investigated. Sixty percent ethanol and 40% gasoline blend was exploited to test the performance, the fuel consumption, and the exhaust emissions. As a result of this study, it was seen that a new dual fuel system could be serviceable by making simple modifications on the carburetor and these modifications would not cause complications in the carburetor system.Ceviz M.A et al. [5] investigated

the effects of using ethanol–unleaded gasoline blends on cyclic variability and emissions in a spark-ignited engine. Results of this study showed that using ethanol–unleaded gasoline blends as a fuel decreased the coefficient of variation in indicated mean effective pressure, and CO and HC emission concentrations, while increased CO_2 concentration up to 10vol. % ethanol in fuel blend. On the other hand, after this level of blend a reverse effect was observed on the parameters aforementioned. The 10vol. % ethanol in fuel blend gave the best results.Altun Sehmus et al. [6] experimentally investigated the effect of unleaded gasoline and unleaded gasoline blended with 5% and 10% of ethanol or methanol on the performance and exhaust emissions of a spark-ignition engine. The engine tests were performed by varying the engine speed between 1000 and 4000 rpm with 500 rpm period at three fourth throttle opening positions. The results showed that brake specific fuel consumption increased while brake thermal efficiency, emissions of carbon monoxide (CO) and hydrocarbon (HCs) decreased with methanol-unleaded gasoline and ethanol-unleaded gasoline blends. It was found that a 10% blend of ethanol or methanol with unleaded gasoline works well in the existing design of engine and parameters at which engines are operating.Amit Pal et al. [7] operated a Kirloskar, four stroke, 7.35kW, twin cylinder, DI diesel engine in dual fuel mode (with substitution of up to 75% diesel with CNG). The results of this experiment of substituting the diesel by CNG at different loads showed significant reduction in smoke, 10 to 15 % increase in power, 10 to 15 %reduction in fuel consumption and 20 to 40 % saving in fuel cost (considering low cost of CNG). The most exciting result was about 33% reduction in engine noise which may prolong the engine life significantly and the consequent sound levels of giant diesel engine reduced to that of a similarly sized gasoline engine.Hubballi P.A et al. [8] investigated experimentally the effect of Denatured spirit (DNS) and DNS-Water blends as fuels in a four cylinder four stroke SI engine. Performance tests were conducted to study Brake Thermal Efficiency (BThE), Brake Power (BP), Engine Torque (T) and Brake Specific Fuel Consumption (BSFC). Exhaust emissions were also investigated for carbon monoxide (CO), hydrocarbons (HC), oxides of nitrogen (NO_x) and carbon dioxide (CO_2). The results of the experiments reveled that, both DNS and DNS95W5 as fuels increase BThE, BP, engine torque and BSFC. The CO, HC, NO_x and CO_2 emissions in the exhaust decreased. The DNS and DNS95W5 as fuels produced the encouraging results in engine performance and mitigated engine exhaust emissions.N. Seshaiah et al. [9] tested the variable compression ratio spark ignition engine designed to run on gasoline with pure gasoline, LPG (Isobutene), and gasoline blended with ethanol 10%, 15%, 25% and 35% by volume. Also, the gasoline mixed with kerosene at 15%, 25% and 35% by volume without any engine modifications has been tested and presented the result. Brake thermal and volumetric efficiency variation with brake load is compared. CO and CO_2 emissions have been also compared for all tested fuels. It is observed that the LPG is a promising fuel at all loads lesser carbon monoxide emission compared with other fuels tested. Using ethanol as a fuel additive to the mineral gasoline, (up to 30% by volume) without any engine modification and without any loses of efficiency, it has been observed that the petrol mixed with ethanol at 10% by volume is better at all loads and compression ratios.

III.   EXPERIMENTAL SETUP

3.1 Descriptions

The setup consists of four cylinder, four stroke, Petrol (MPFI) engine connected to eddy current type dynamometer for loading. It is provided with necessary instruments for combustion pressure and crank-angle measurements. These signals are interfaced to computer through engine indicator for P-V diagrams. Provision is also made for interfacing airflow, fuel flow, temperatures and load measurement. The set up has stand-alone panel box consisting of air box, fuel tank, manometer, fuel measuring unit, transmitters for air and fuel flow measurements, process indicator and engine indicator. Rotameters are provided for cooling water and calorimeter water flow measurement.

The setup enables study of engine performance for brake power, indicated power, frictional power, BMEP, IMEP, brake thermal efficiency, indicated thermal efficiency, Mechanical efficiency, volumetric efficiency, specific fuel consumption, A/F ratio and heat balance. Windows based Engine Performance Analysis software package "Engine soft" is provided for online performance evaluation.
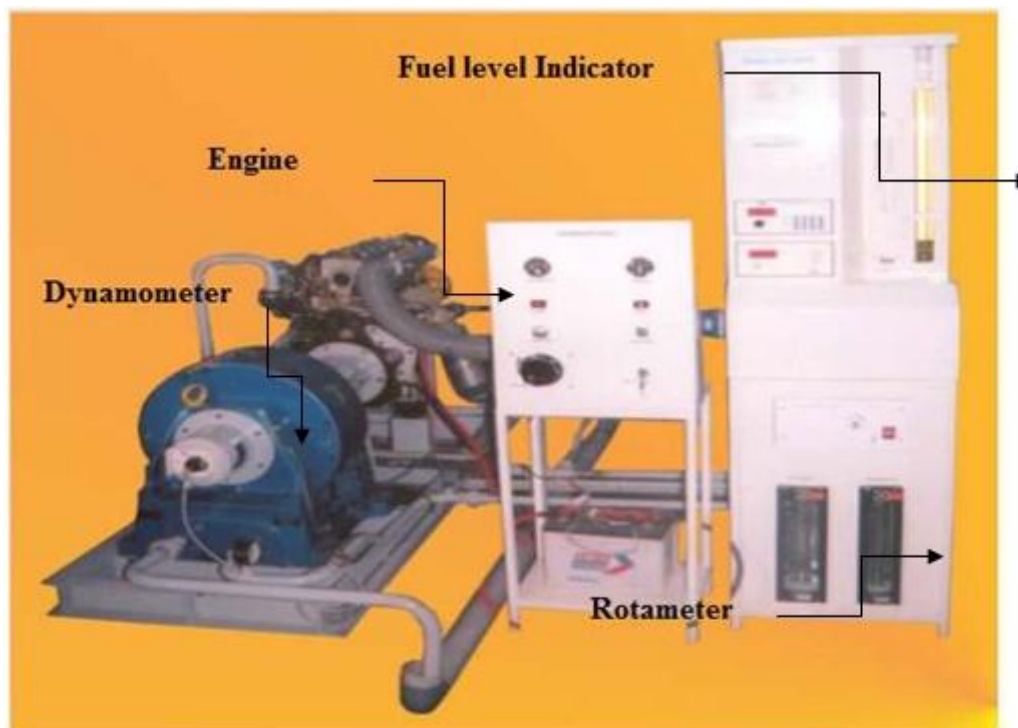
Figure 1.Diagram of Setup used

3.2 Specification

Table 2.Specification

S.NO	Equipment	Sub-parts
1	Product	Engine test setup 4 cylinder, 4 stroke, Petrol(Computerized)
2	Product code	233
3	Engine	Make Maruti, Model Wagon-R MPFI, Type 4 Cylinder, 4Stroke, Petrol (MPFI), water cooled, Power 44.5Kw at6000 rpm, Torque 59 NM at 2500rpm, stroke 61mm,bore 72mm, 1100 cc,CR 9.4:1
4	Dynamometer	Type eddy current, water cooled, with loading unit
5	Propeller shaft	With universal joints
6	Air box	M S fabricated with orifice meter and manometer(Orifice dia 40 mm)
7	Fuel tank	Capacity 15 lit with glass fuel metering column
8	Calorimeter	Type Pipe in pipe
9	Piezo sensor	Range 5000 PSI, with low noise cable
10	Crank angle sensor	Resolution 1 Deg, Speed 5500 RPM with TDC pulse
11	Engine indicator	Input Piezo sensor, crank angle sensor, No of channels 2, Communication RS232
12	Digital milivoltmeter	Range 0-200mV, panel mounted
13	Temperature sensor	Type RTD, PT100 and Thermocouple, Type K
14	Temperature transmitter	Type two wire, Input RTD PT100, Range 0–100 Deg C, Output 4–20 mA and Type two wire, Input Thermocouple, Range 0–1200 Deg C, Output 4–20 mA
15	Load indicator	Digital, Range 0-50 Kg, Supply 230VAC
16	Load sensor	Load cell, type strain gauge, range 0-50 Kg
17	Fuel flow transmitter	DP transmitter, Range 0-500 mm WC
18	Airflow transmitter	Pressure transmitter, Range (-) 250 mm WC

19	Rotameter	Engine cooling 100-1000 LPH; Calorimeter 25-250 LPH
20	Pump	Type Monoblock
21	Add on card	Resolution12 bit, 8/16 input, Mounting PCI slot
22	Software	"Enginesoft" Engine performance analysis software

IV.   RESULT AND DISCUSSION

Gasoline Blends having 5%, 10%, 15% and 20% Ethanol is prepared. Brake thermal efficiency, HC exhaust was plotted in parts per million, O_2, CO, CO_2 were plotted on volume percentage basis. These curves are plotted firstly at no load and then at constant rpm of 3000 and 4000. The density and Lower calorific value of blends are first calculated and then fed in the software set up configuration to get the desired results. The results obtained were noted and then curves were plotted as shown below to have a clear understanding of the variations of different parameters by using different blends.

4.1 No Load Test
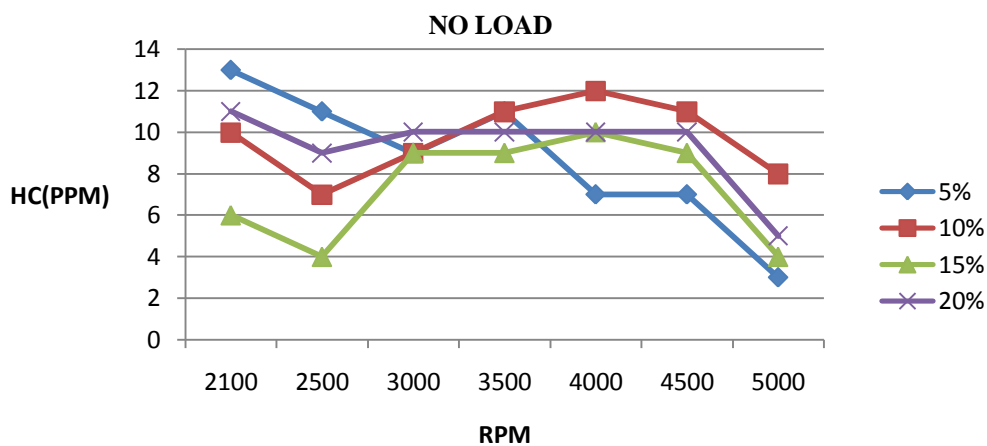
Figure 3.HC exhaust variation with blends at different rpm.
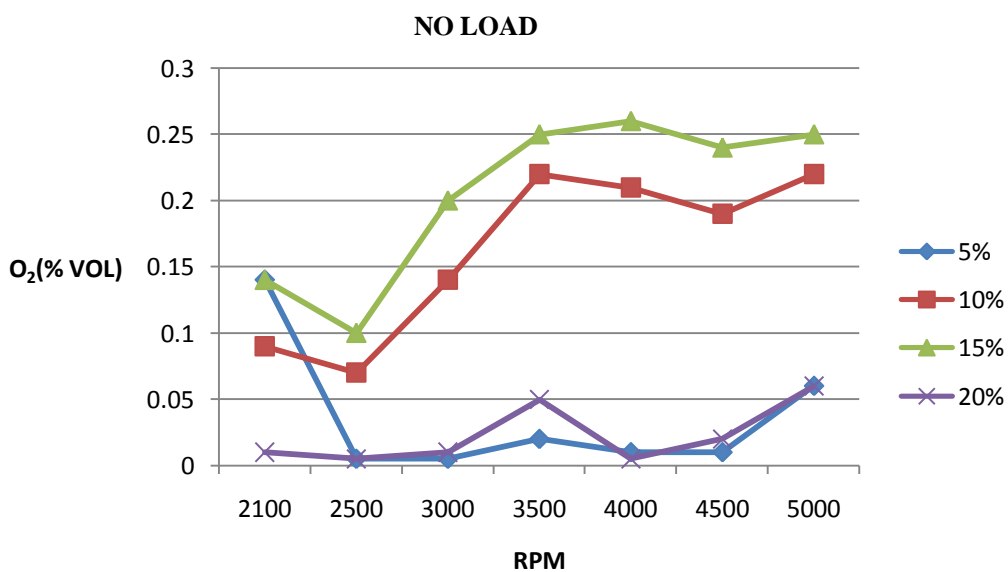
Figure 4.O_2 exhaust variation with blends at different rpm.
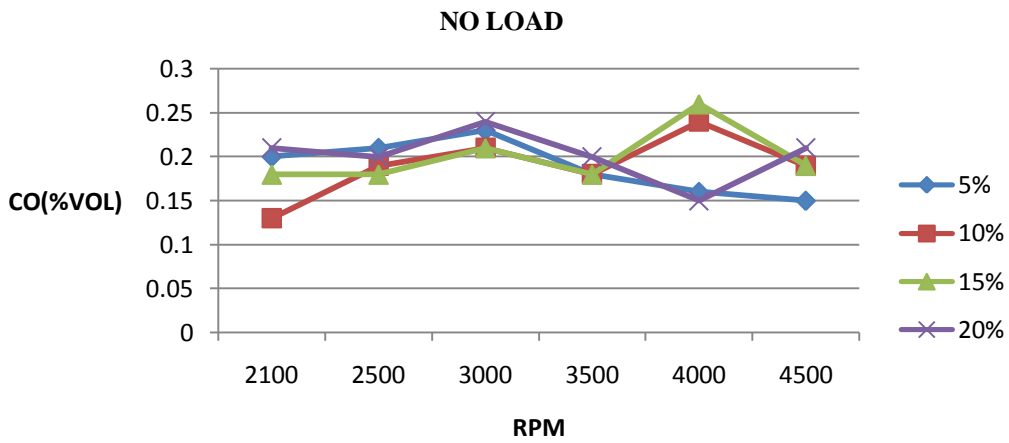
NO LOAD

Figure 5.CO variation with blends at different rpm.
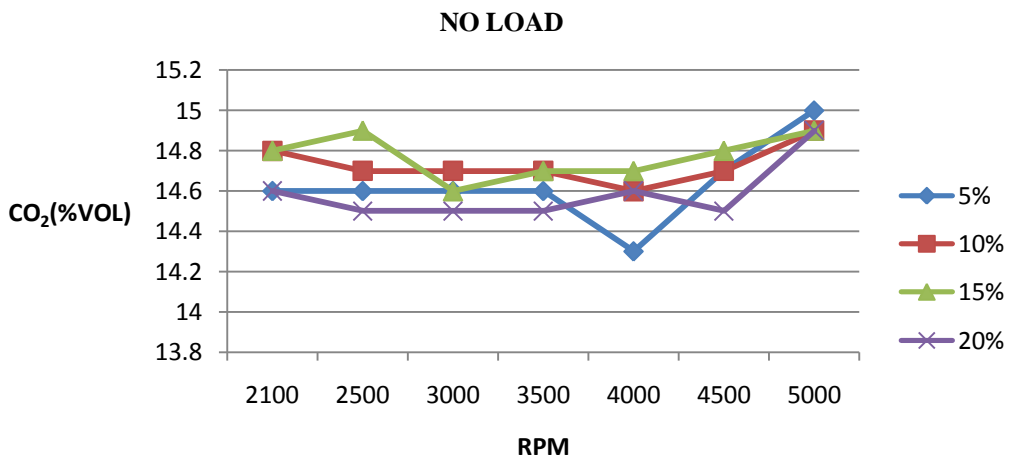
NO LOAD

Figure 6.CO$_2$ variation with blends at different rpm.
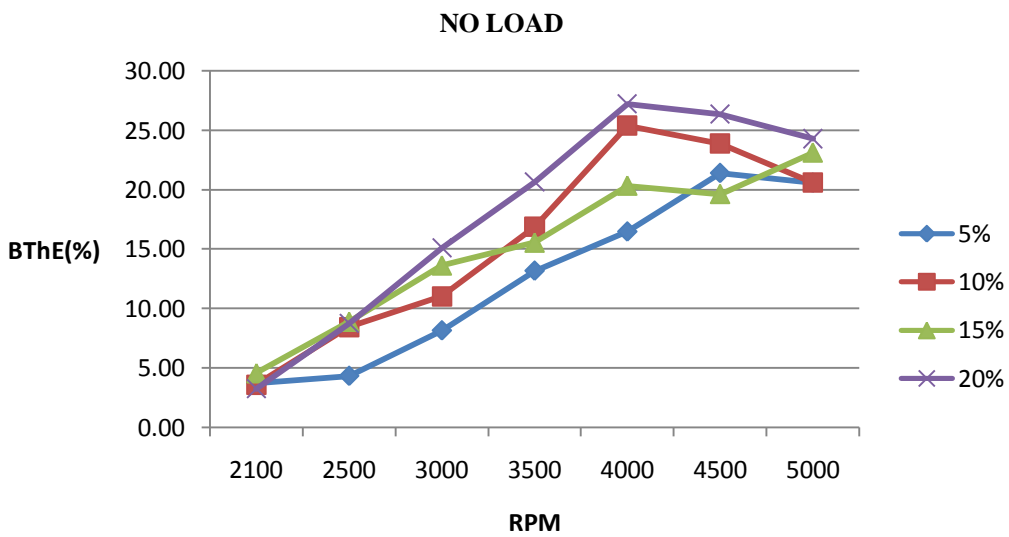
NO LOAD

Figure 7.Brake Thermal efficiency variations with blends at different rpm.

At no Load conditions some points are clear which are given below.

➢ HC emission decreases as blending increases up to 4000 rpm with respect to E5 and is lowest at 2500 rpm. For 10% blend HC emission reduces by 23.08% at 2100 rpm in comparison to commercial Gasoline.

➢ O_2 Percentage increases as blending increases from 5% and is highest between 2500 rpm to 3500 rpm.

➢ CO_2 increases up to 4000 rpm when blending increased from 5% and is highest at 2500rpm. For 10% blend it increases by 0.68% at 2500 rpm in comparison to commercial Gasoline.

➢ CO decreases as blending is increased and is lowest at 2100 rpm. For 10% blend, it reduces by 35% in comparison to commercial Gasoline.

➢ Brake Thermal Efficiency increases on blending. Brake Thermal Efficiency reaches a maximum at around 4500 rpm and then starts decreasing. In comparison to commercial Gasoline it increases by 11.6% for 10% blend, 8.1% for 15%blend and 23.37% for 20%blend at 4500 rpm.

4.2 Constant rpm Test
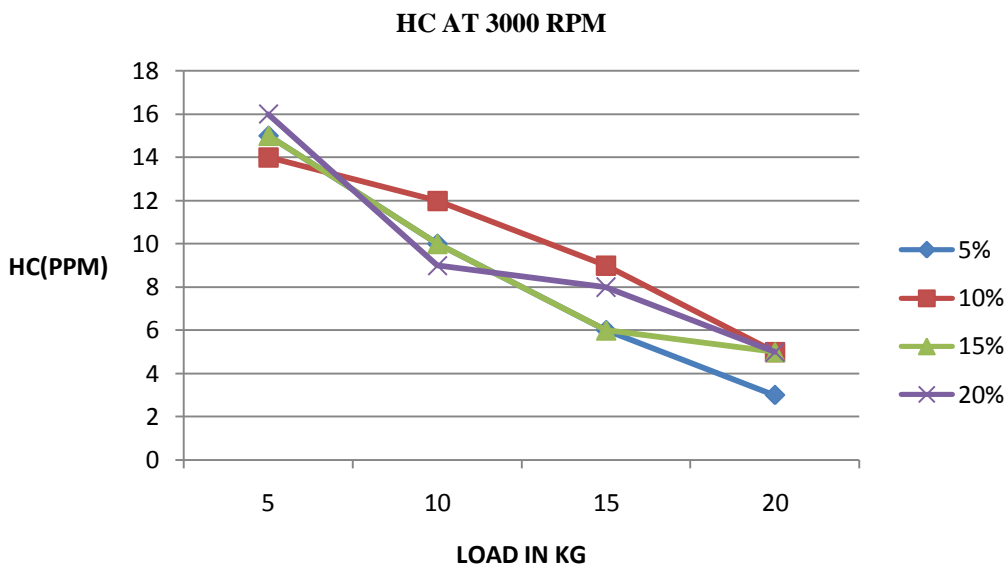
HC AT 3000 RPM

Figure 8.Variation of HC emission with load at 3000 rpm
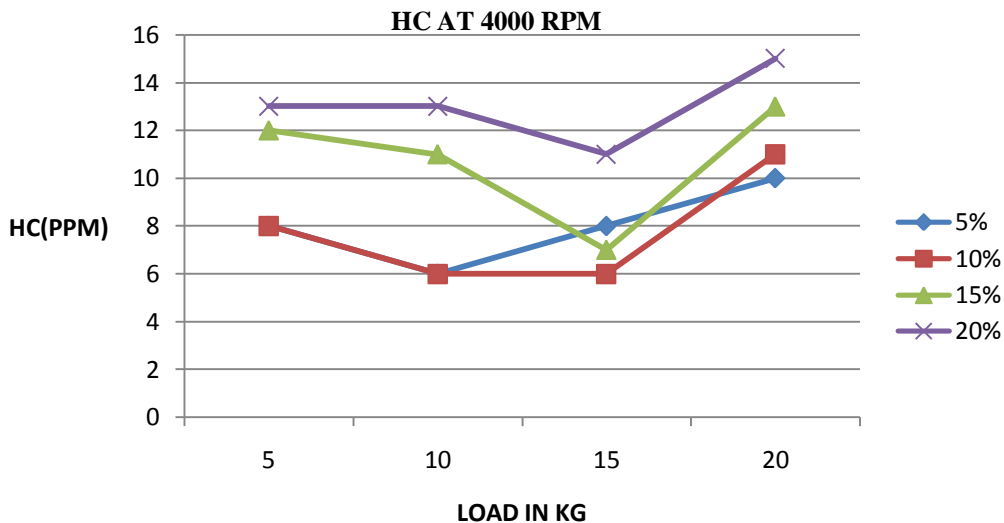
HC AT 4000 RPM

Figure 9.Variation of HC emission with load at 4000 rpm
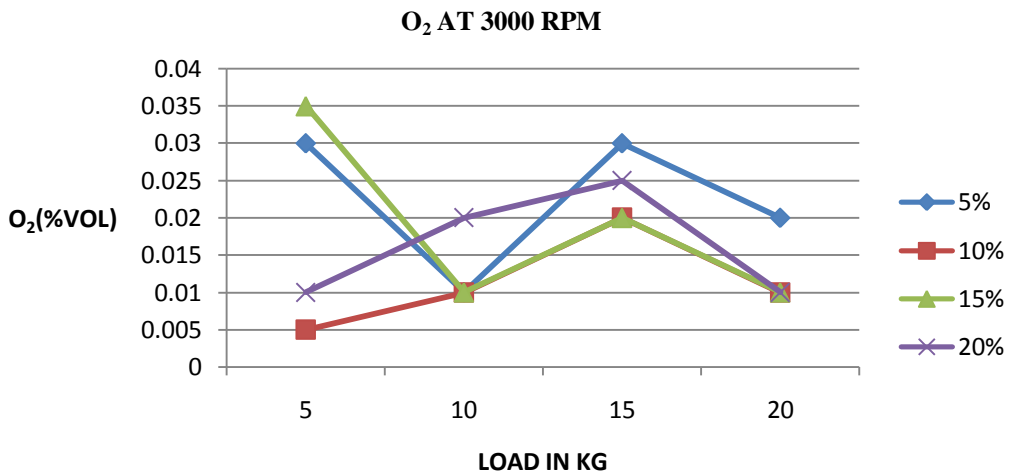
O$_2$ AT 3000 RPM

Figure 10. Variation of O$_2$ emission with load at 3000 rpm
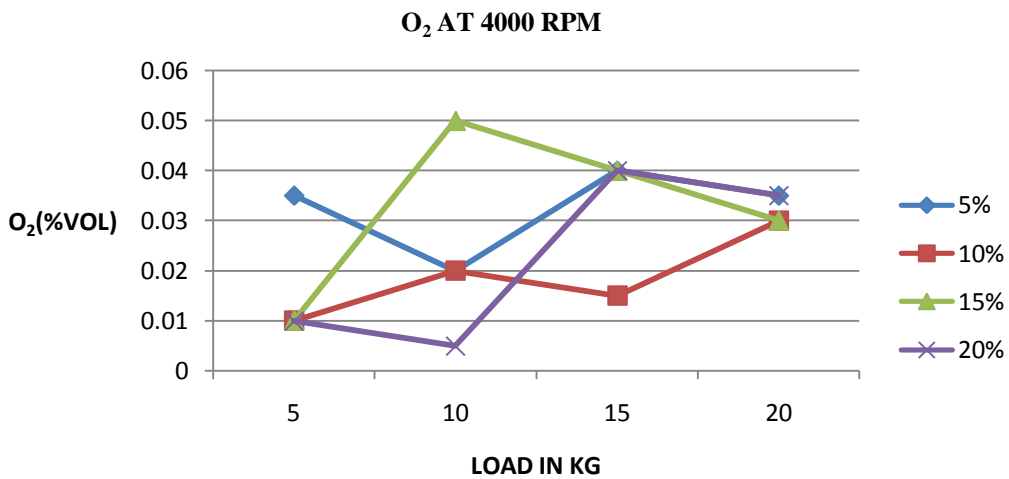
O$_2$ AT 4000 RPM

Figure 11. Variation of O$_2$ emission with load at 4000 rpm
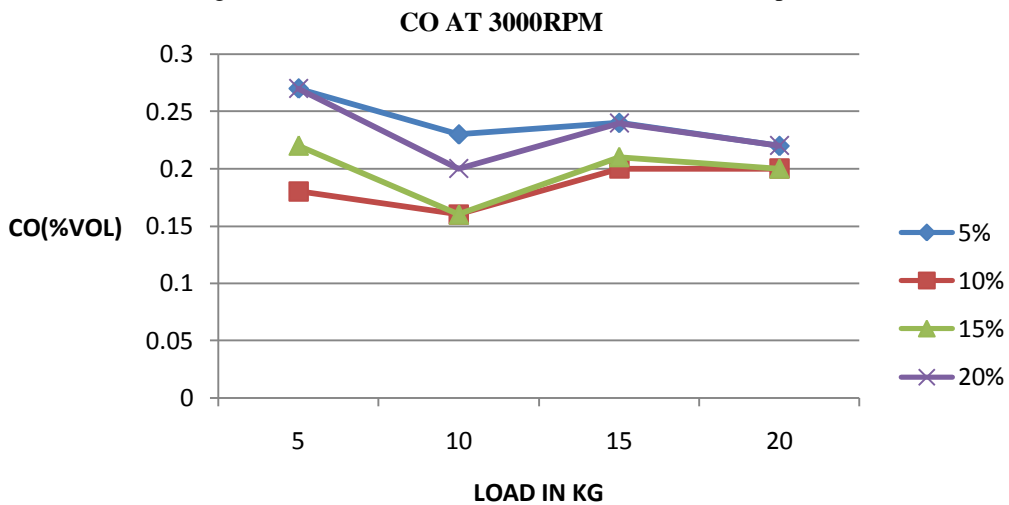
CO AT 3000RPM

Figure 12. Variation of CO emission with load at 3000 rpm
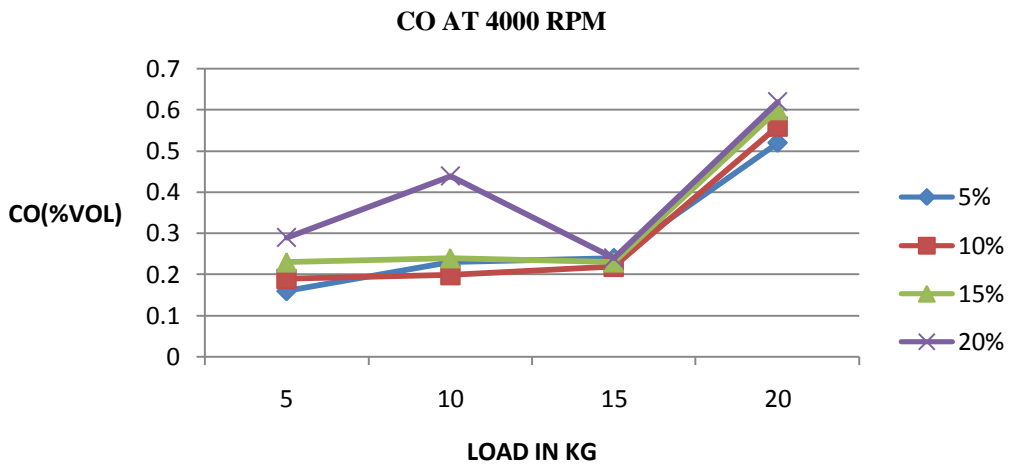
CO AT 4000 RPM

Figure 13. Variation of CO emission with load at 4000 rpm
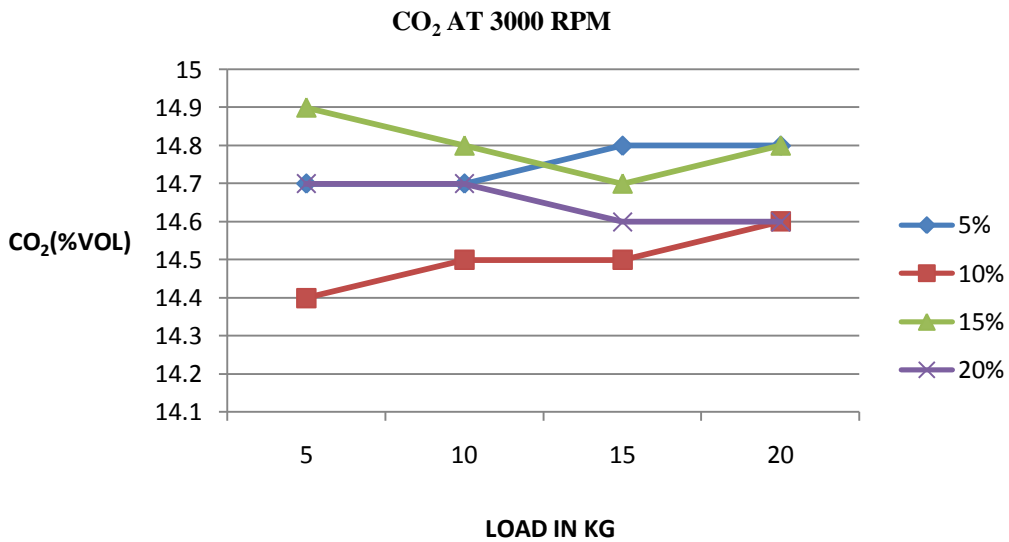
CO₂ AT 3000 RPM

Figure 14. Variation of CO_2 emission with load at 3000 rpm
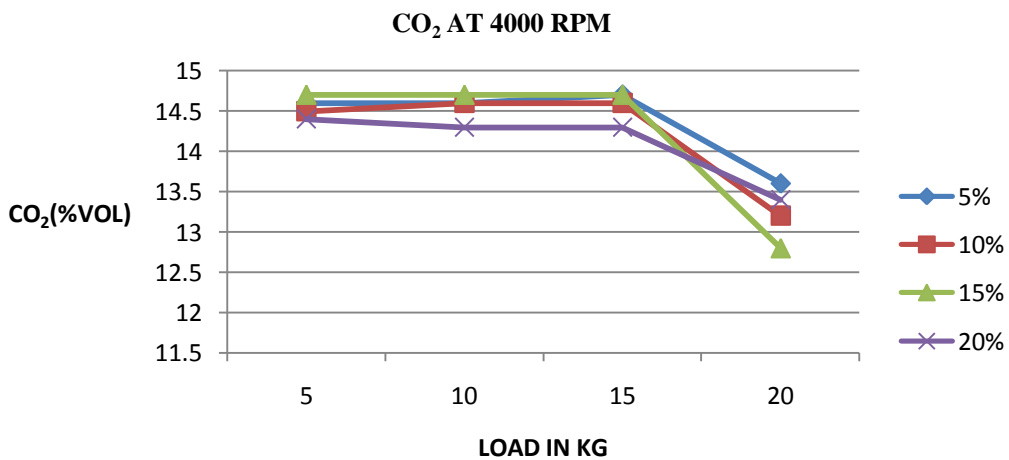
CO₂ AT 4000 RPM

Figure 15. Variation of CO_2 emission with load at 4000 rpm
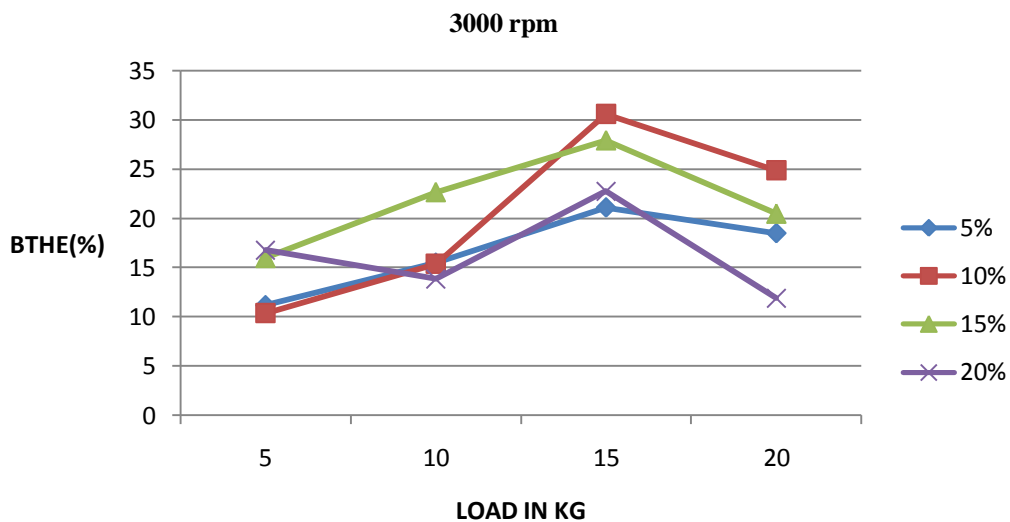
3000 rpm

Figure 16. Variation of Brake Thermal Efficiency with load at 3000 rpm
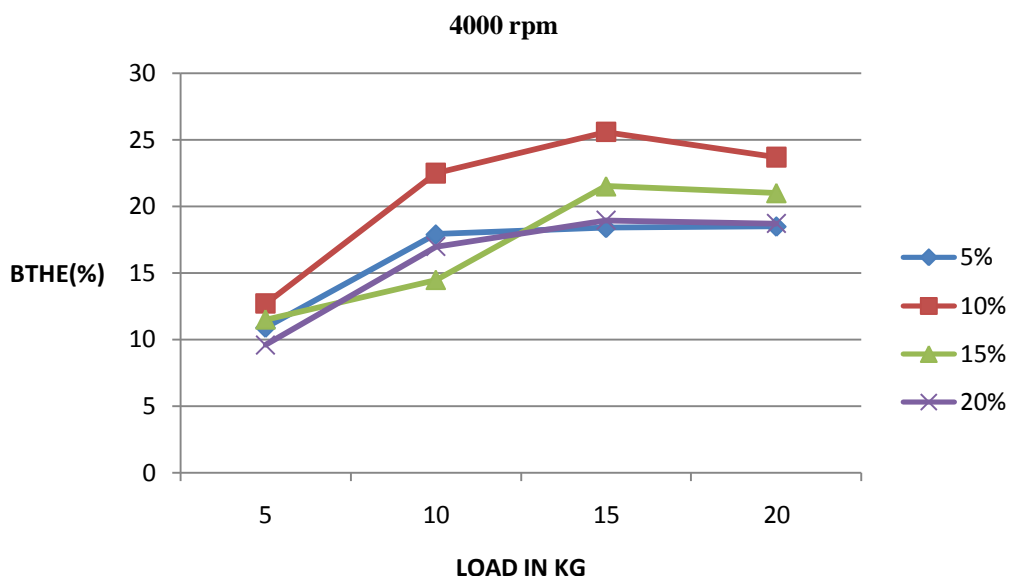
4000 rpm

Figure 17. Variation of Brake Thermal Efficiency with load at 4000 rpm

At Constant RPM some ponts are clear which are given below.

➢ HC emission increases with blending and is more at 3000 rpm compared to 4000 rpm for low loads. At 5kg load, it increases by 6.67% for 10%blend at 3000 rpm and increases by 25% for 10% blend at 4000 rpm with respect to commercial Gasoline.

➢ CO_2 generally decreases with blending and is generally more for 3000 rpm as compared to 4000 rpm. At 5kg load, it decreases by 2.04% for 10%blend at 3000 rpm and decreases by 2.94% for 10% blend at 4000 rpm with respect to commercial Gasoline.

➢ CO is less for 3000 rpm as compared to 4000 rpm.At 5kg load, it decreases by 33.33% for 10% blend at 3000 rpm and increases by 18.75% for 10% blend at 4000 rpm with respect to commercial Gasoline.

➢ O_2 Percentage decreases with blending and is less for 3000 rpm.

➢ Brake Thermal Efficiency increases on blending.It reaches a maximum at 15 kg load and is generally higher for 3000 rpm than 4000rpm.At 20kg load, it increases by 45% for 10%blend, 32.2% for 15% blend, 7.91% for 20% blend at 3000 rpm and increase by 39.1% for 10% blend, 17% for 15% blend and 2.99 % for 20% blend at 4000 rpm with respect to commercial Gasoline.

V.   CONCLUSION

From the results, it can be concluded that Ethanol blends are quite successful in replacing pure Gasoline in Spark Ignition Engine. Results clearly show that there is a decrease in exhaust emissions, increase in Brake Thermal Efficiency. So from the curves it is seen that 10% ethanol blended Gasoline is the best choice for use in the existing Spark Ignition Engines without any modification to reduce exhaust and increase Efficiency. A little consideration has to be taken on material used as maximum pressure inside cylinder is increased by blending. A balance has to be made between Specific Fuel Consumption and Efficiency to take care of users using blend as more fuel will be consumed due to blending of Ethanol with gasoline.

REFERENCES

[1]   *Demain, A. L., "Biosolutions to the energy problem," Journal of Industrial Microbiology & Biotechnology. 36(3): 319-332, 2009*

[2]   *Festal, G. W., "Biofuels – Economic Aspects," Chemical Engineering & Technology. 31(5):715-720, 2008.*

[3]   *Wallner, T., Miers, S. A., and McConnell, S., "A Comparison of Ethanol and Butanol as Oxygenates Using a Direct-Injection, Spark-Ignition Engine," Journal of Engineering for Gas Turbines and Power. 131(3): 2009.*

[4]   *Yuksel Fikret, Yuksel Bedri, the use of ethanol–gasoline blend as a fuel in a SI engine, Renewable energy 29 (2004) 1181–1191.*

[5]   *Ceviz M.A, Yuksel F., effects of ethanol–unleaded gasoline blends on cyclic variability and   emissions in an si engine, applied thermal engineering 25 (2005) 917–925.*

[6]   *Altun Sehmus, Hakan F. Oztop, exhaust emissions of methanol and ethanol-Unleaded gasoline blends in a spark-ignition engine, applied energy, 86 (2009), pp. 630–639.*

[7]   *Pal Amit, S. Maji, Sharma O.P. and Babu M.K.G., "Vehicular Emission Control Strategies for the Capital City of Delhi", India, January 16-18, 2004, SAE Paper no 2004-28-0051.*

[8]   *Hubballi P.A. and BabuT.P.Ashok, effect of aqueous denatured spirit on engine Performance and exhaust emissions, SAE 2004-28-0036.*

[9]   *N. Seshaiah, "Efficiency and exhaust gas analysis of variable compression ratio spark Ignition engine fuelled with alternative fuels" international journal of energy and Environment. Volume 1, Issue 5, 2010 pp.861-870.*

[10]   *Science fair projects encyclopedia, 2004; launder, 2001.*

.

| Research Paper | Open Access |

The Theoretical Science of Research

Subbarayan Peri

Director, and Principal, Institute of Advanced Studies in Education Rashtriya Sanskrit University, TIRUPATI-517 507, India.

Abstract: - The science of research is unique among sciences in many respects. All other sciences are reared by it, but it has never been viewed as a science so far in this world. Had it been developed as an independent science, the world would have advanced by some centuries than what it did and had. The science of research is an integral part of the emerging 'learning science' along with it counter-parts the science of education. Every systematic science has its elements i.e. paraphernalia —assumptions, theories, laws, dimensions, taxonomy et.hoc. which designate that science as 'systematic science'. So the first step in construing the theoretical science of research is to explore its paraphernalia. Again, every science exists in two essential forms; pure and applied. Astonishingly, the applied form of the research science is so popular, but it's pure from is un-identified and unknown. The present paper aims at to iterate the need of theoretical science of research. The strategy— since education is our twin science and that it developed as a full-fledged science with robust theoretical form and frame, we need its help, at least in the formative stages to visualize 'the theoretical science of research'. The paraphernalia are presented in this paper.

I. INITIATION

A metaphor would suit to explain the context, as well my intent very clear.

The metaphor—There is a platinum mixed gold throne full of costly stones. On it a peerless and priceless prince prays. Around him are there mighty ministers: finance, education, social welfare, warfare, software, aviation, mines, and the like. Every minister had with him treasures of knowledge, affect, and skill of his portfolio. Billions of populations composed of different races, communities, continents, casts, cults et. hoc. are approaching the ministers. All the people are getting what they desire. All the ministers including the two prime ministers are happy and prospering day by day. Centuries are rolling....... There stood a humble person, a tailor with an indigenous tape tight to his hand wants to measure his physical get-up and mental make-up (personality) of the precious prince. It is surprising – neither the joyful benefactor masses, nor the ministers, nor the prime ministers, except the humble tailor are caring the prince. Mutually thanking cabinet and the people are dancing individually and in groups. In fact, the cabinet is a part of the thick population. The prince bestows all the property to the masses through the cabinet. But, anybody noticed the prince? No, never! None of them bothered for his needs— could the tiny tailor do his job? You are the judges!

Analyse the scene

The prince is the science of research, the tiny tailor is me, and the tight tape is the psychometric. All the sciences are being under the reign of the science of research, but no science cares for the development of the RSc. This happens since centuries together. Now, let's do the job—is the intention of this paper. Scientists could hire the services of the RSc as a house-maid, but could never recognize her as the, queen of all sciences alas! More than that, let's understand; if philosophy and mathematics are the king and queen of sciences, RSc is the emperor!

II.　　RATIONALE FOR RESEARCH THEORY

Research theory is the theory of the purpose, application and interpretation of research i.e. learning from inquiry. It is largely an umbrella term, being comprised of a number of theories, rather than a single explanation of— why and how do people research, the process of research, and assessment of research. Rather, it is affected by several factors, including theoretical perspective and epistemological premises. There is no one, clear and universal explanation of how we research and subsequent guide-lines as to how we should research. Rather, there are a range of theories, each with their background in a different psychological, learning and epistemological tradition. To understand research then, we have to understand the theories and rationale behind them. In research, the meaning of the term 'theory' ranges from being connected to scientific knowledge, academic subjects and to empirical and pragmatic knowledge such as research foundations and methodology.

The dualism of theory and practice, which is reflected in the dictionary definition is also evident in the theory of research, where theory is often understood as being all that is not practice. This could be why the term 'theoretical' is regularly used to denote academic as opposed to field experiments, and laboratory research practices. In one perspective, theory is understood to be normative for practice and in the other perspective theory is understood to be derived from practice. The first implies practice having to adapt to theory. Here the term theory attaches itself to scientific knowledge, the knowledge one acts on in practice is thus understood here as being synonymous with applied scientific knowledge. The second that theory is defined through practice— theory is almost understood to be verbalized practice, it becomes a kind of pragmatic guide for actions, where the ideal is a connection between theory and practice that is as close as possible, i.e. theory should fit practice like a glove fits a hand. We are not limiting the definition of theory of research to any one of the above perspective, but a harmonious composite of the two. If the first perspective is synthesis, the second one is analysis, and both in coherence make the sense of the 'theory of research'.

2.1. The common assumptions are as follows
- That practical and theoretical knowledge is coherent, convertible and compatible.
- The assumption that the theoretical and practical domains are of such a nature that a connection is possible.
- That there is one specific theory that applies to one given practice. This assumption is deduced from the conceptions that practice is either 'the realisation of the theoretical aspect', or that theory is derived from practice.
- That theory is directly converted into practice and vice versa.
- That practice is rule based and describable in general terms— derived from the conception that the generality, predictability and regularity, which is a characteristic of theory, is also a characteristic of practice.

Research theory seeks to know, understand and prescribe research practices. Research theory includes many topics, such as— fundamental, applied, and action research, research methods from experimental to historical, research systems designs, experimental designs, dependent, independent, and intervening variables, qualitative and quantitative analysis, instruments, sample, statistical techniques, interpretational ways, generalization modes et.hoc. learning (both learning from inquiry), research policy, organization and leadership. Research thought is informed by many disciplines— anthropology, biology, computers science, economics, education, history, linguistics, neurology, philosophy, psychology, and sociology. Its applications are found in all sciences without any single exception.

Normative theories of research provide the norms, goals, and standards of research, while the descriptive theories of research provide descriptions or explanations of the processes of research. Research psychology is an empirical science that provides descriptive theories of research behaviors of researchers and research out-comes. Examples of theories of research in psychology are: constructivism, behaviorism, cognitive, motivational theory, post-modernism.

There may be any number of theories of research, like cultural theory of research considers how research occurs through the totality of cultures of the globe on the whole, east or west. Other examples are the behaviorist theory of research that comes from research psychology and the functionalist theory of education that comes from sociology of research.

2.2. Theories, in general are used for the following main reasons:
1. Help explain a puzzling or complex issue and to predict its occurrence in the future: Research behavior is a latent variable so there is no clear and universal way to explain, measure, predict, and control it. To help explain this process, therefore, theories based on differing epistemological positions have been developed to explain the procedure.
2. Allow the transfer of information in one setting to that of another: The complex and comprehensive conceptual explanations provided within the framework of a theory can be applied in different settings. Theories provide different "lenses" through which to look at complicated problems and social issues,

focusing their attention on different aspects of the data and providing a framework within which to conduct their analysis (Reeves, Albert, Kuper, & Hodges, 2008).

3. Theories provide greater opportunities for improvement by design: By providing information about the mechanisms underlying learning from inquiry and performance, an awareness of theories and can help us to design environments to improve potential research. They enable us for building capacity of researchers. Refer section (10) for translation of research theory into practice.

This is the general statement on the theory of research. Now we try to devote our discussion taking the guide-lines into consideration. Out of the total 12 sections of this paper first 09 sections are devoted to the first perspective (theory/foundations) and last three (9, 10 and 11) sections for the practical (empirical) perspective of the theory of research.

III.   CHARACTERISTICS OF A SYSTEMATIC SCIENCE:

i). Society's demand for more

Wholeness-orientation in RSc implies a deviation from traditional disciplinary research that is not well suited. The position of RSc is quite different from other sciences, which depend on it. There are however, no established systematic principles that can meet the demand for wholeness orientation of RSc. To be frank, so far no systematic efforts are observed to systematize RSc itself. "From a philosophy of research perspective, any science is seen as an interactive learning process with both a cognitive and a social communicative aspect. This means, first of all, that science plays a role in the world that it studies. A science that influences its own subject area, such as agricultural science, is named a systemic science (Alroe and Kristensen, 2000)". In the same way, could we designate RSc as systematic science, like agriculture, health, or education? The answer is definitely, non-affirmative. The researcher has in his mind very broad aim to forge a 'systematic science of research' with all its paraphernalia of a systematic science – assumptions, foundations, principles, schools, laws, approaches, methods, taxonomy et.hoc. Again, the quality of any science reflects in all its phases; objectives, process, and products leading to the total quality assurance. Any systematic science, naturally, wants to achieve the quality out-puts. The proposed systematic RSc should also be able to deliver the quality products.

ii). we never supposed research as a science,

and suppose if we accept it as a science, what would be its position in the row of sciences; natural, social or human. There are many sciences available today in the world, a part from the pseudoscience. All sciences are classified into three categories; natural, social, and human sciences. The exact sciences are sharp in their theories, methods, and results, but they are of no use, if not applicable/acceptable to the society. It is the society to consume the applied products, and in turn it has to encourage the development of exact sciences to march ahead for perfection. The second category is more nearer to the needs of the society, but they are not perfect from the view point of their vigour of experimentation, methods, and products. By and large, they depend on second hand methods of research; quasi-experimental. Generalization, which is the crux of research cannot be possible in these sciences. The human sciences cannot go for generalization. Objectivity cannot be expected in the case of human sciences. However, our main point is that all these sciences are under the influence of RSc. Any science, strong or weak, but is in the gamut of the science of research. Research component is inbuilt in every science. Evidently, unless any science is equipped with the research component, it would definitely, be a dead science.

iii). One more characteristic of the science of research is it's dependability on some subject.

All subjects though being developed by research, RSc cannot have independent existence. So a referral subject is always required. RSc shares the characteristic with its co-science, education. Unless there is content, there is no teaching or research at all. Notwithstanding, the subjects dependency, today, education is an independent discipline, like engineering, medicine or agriculture, physics, physiology, psychology, or pharmacology.

iv). RSc shares many things with the science of education.

The subject matter of both the sciences is the same, 'learning'. I proposed that both education and research are the two legitimate fields of the 'science of learning', their core being 'learning'. At the same time see the difference; if a content known to somebody is learnt by us, it is designated as is teaching, while a content unknown to anybody in the world up to that point of time that is research. It is surprising, if the two poles of education— teacher and the taught are reduced into one pole, it is research! Education and research represent the two hemi-spheres of the brain, the left for teaching (by reasoning and training for reasoning) and the right for research (intuition). Both are the tendencies of human mind. Inquisitiveness is the base. If inquisitiveness is unveiled by somebody who knows it already, it is teaching. But, if inquisitiveness is unveiled by himself, it is research. Finally, leaning from instruction is designated as teaching, while learning from inquiry is designated

as research. In another way, let's see: education is acquirement of knowledge, affect, and skills of a subject, research is enhancement and or create of the acquired knowledge, affect, and skills of a subject. "The emerging science of learning is a merger or rather an amalgam of two behavioristic, cognitive, and brain sciences—the science of education, and the science of research (Peri, 2013)".

v). Both ESc and RSc work on complementary basis

mastery gained from instruction helps to probe further to invent, and today's inventions are tomorrow's curriculum. Teaching pushes the teacher and the taught to invent. The inventor teaches his inventions by virtue of his self-actualization. He cannot keep quite, but in practice he really, thumps-up! Scholarship is the common denominator for both of them. They both are the brain-activities, involving in teaching behaviour and research behaviour respectively. The process of teaching and research are assessed by their end-products, mostly. In case of teaching, the assessment is by the achievement of the students, while in research by peer-evaluation (as on date). Of course, I am developing research assessment procedures which are content-free and other than peer evaluation.

3.1. Some characteristics of RSc

The above discussion could derive some characteristics of RSc as listed below—

- Inquisitiveness is the parent of the science of research.
- The science of research is a natural product, like the breathing.
- It is found abundant in nature.
- The human mind has the tendency of inquiry and establishing facts.
- Research behavior is endowed in the human nature.
- Activity of the right brain, like intuition is inclusive of the activities of the left-brain.
- The science of research is always dependent on some other subject.
- Philosophy and mathematics are the two eyes of the science of research.
- The science of research is one sub-field of the emerging science, the learning science.
- Concentration and commitment are the two fundamental principles of the science of research.
- Intuition is the key concept in the study of the science of research, just as S—R bond for the
- behaviourists, and whole of Gestalts, but beyond them.
- Theory to run after applications for its construction.
- Research science is the study of research behaviours of researchers.

IV.   WHY PEOPLE DO RESEARCH

How researchers are motivated? is the genuine question often come across the discussions. There are three sets of reasons; psychological (hedonism, inquisitiveness, self-actualization, meta-motivation, peak-experiences), economical (wants, and incentives) and social (necessarily, social status, status symbol).

4.1. Types of researchers

There are many types of researchers. Formal and informal, freelancers and hired, hobby, habituated, and addicted, accident and occupational, trained and untrained, professional and non-professional et.hoc.

V.   INDUCTION

5.1. Subject matter of the science of research

Is it a descriptive science? a process science? or a product oriented one? Or an exact science? What should be our answer to the question, what it studies?

a).

My immediate, spontaneous, Un-inhibited and straight forward answer is, it is the "study of the research behaviors of the researchers". Research behaviors of the researchers are the building blocks or rather fundamental units of the RSc, whereby we can understand, measure, predict, and control the research as a whole. Are there attempts to define, explore, and explain the research behaviors? The answer is clear 'no'. When our sister science has grown to the level of an independent science or discipline with its constructs viz. teaching behaviours, why can't we advance with similar constructs? This the most important point where we should start our attack.

b).

Again, if you ask me the question, What is the subject matter of the RSc, it is the study of learning with special reference to learning from inquiry. The higher order learning (obtained from insight to creativity) is the

subject matter of the science of research. To be more specific, learning by intuition is the subject matter of the RSc. A lot of research is required on this issue for the development of the science of research as a conscious and formal effort . Intuition is the key concept in the research process and research behavior. There are three sources of literature in support:

i) A school of ancient Indian philosophers, Vedantins studied nididhyasana and practiced in their curriculum. Nididhyasana via. upsana is the technique of inculcation of intuition.

ii) Blooms and Flanders could show a way that intuition to be an objective of research, and finally

iii) computational models of learning also support it.

Of course, a great deal of literature is available on this issue. However, there is need to balance the use of the subjective and esoteric intuition and objective and scientific method in the science of research.

c).
Study of scientific method is another subject area of the RSc.

5.2. Theory of science of Research

Education or teaching theory mainly rests on learning theories. It's quite natural because, learning is the subject matter of teaching. Same thing holds good for research theory also. But, the most unfortunate thing is that we never tried for 'a theory of research'. Extensive literature on learning theories and their applicability for teaching has been witnessed and recorded. Right from beginning of the 20th century from the efforts of Thorndike much work was done. In fact, today we are in a position to control the learning of a given individual. Thanks to educational psychology. The education theory is supported by cognitive, behavioristic, humanistic, constructivism and post-modernism contributions to learning. Both tough-minded (behaviorism) and tender-minded (humanistic) psychologies supported our understanding of learning from their theoretical back-up. We are applying them to education, but never to research. In fact, constructivism and post-modernism learning theories are more useful for research than for teaching. The individual has to construct his own authentic knowledge is the main caption of constructivism. Is it easy for a matured scholar or for a immature novice or sophomore to construct his own authentic knowledge? Where does the constructivism hold better? But, we never tried constructivism in the case of research. In sixties Skinner has used the concepts 'shaping the behavior' and Bloom, 'teaching behavior' , learning out-comes et.hoc. and teaching theory woes much to these concepts, but we didn't try to apply or coin such constructs to understand learning from inquiry. As a result there is no any research theory under the surface of the earth. The root cause of non-development of any research theory is that we couldn't come out of the tunnel vision of 'learning', viewing it as only teaching-learning process, but never thought beyond that. While appreciating the efforts of educational psychologists for their commendable contributions to teaching, we have to find fault with them for their short-sightedness or limited-sightedness. In 2000 in one of my research papers I commented: Who is the last bench, last seat occupier in the class of universal scientists? My spontaneous, immediate, un-inhibited response is 'psychologist'. Being a psychologist why do you speak so? is the question from my friends circles. "Psychologists are late born and lazy. They are fed and led by their elder brothers, who are far, further, fore-goers in predicting and controlling the behaviors of their clients— plasma, plants, and planets. They, psychologists don't know that they have a behavior unless pointed out by somebody. They discard their characterstic and unique legitimate subject of study, the study of consciousness (the most precious substance than any other entity in the world) out of passion for pretty purposes, study of overt-behavior". Let it be, of course, I have my pride of being a psychologist that we are successful in prediction, and control of our clients— teachers, engineers, scientists, linguists, administrators, leaders et.id. The success of educational psychologists is that: given an individual and defined content, they are in a position to inculcate the desired knowledge to a predetermined degree within the specified time to that individual. Yes, it is their success story.

5.3. My expectation of educational psychologists is— they could estimate the quality of research out-comes of a given researcher as they did for teachers. The days are not far away, soon we could do it with the concept of 'research values'. I am developing a strategy to assess the quality of researcher, and research products in "PERI" units. In future, any researcher could select research out-comes from the list of standardized research out-comes to guide his research at three nodes; selecting objectives, conducting the experiment and evaluating the out-comes then and there. At the same time, through-out the gamut, 'the research values (RV)' will help him to navigate his research to achieve better quality of research. RV of any product of research is estimated by the quantity and quality research out-comes embedded in that research product. The unit of research value is 'Peri', just like Helmholtz, Volts, or Ohms. Here-after, evaluation of the quality of research is assessed in 'Peris', just as the quality of the metal gold is expressed in 'carrots'. It takes care of many unanswered queries and practices in the field of research. Finally, the need of the hour is forging the RSc is to establish 'a research theory', may

be or may not be on the same grounds of educational theory. This is an unique and peculiar state of affairs—theory to run after applications for its construction. As said earlier, applied form of the RSc is so popular, while its theoretical form is un-identified and unknown.

VI.   APPROACHES TO THE SCIENCE OF RESEARCH

For every science there shall be two approaches, in general traditional and scientific. Traditional is mostly carried from its formative stages with their cumulative efforts, while the scientific takes over at one fine moment and influence the growth of that science towards perfection. In general, both approaches would be complementary in nature in nurturing that science. This mutual functioning is quite common in all sciences.

6.1.

At times, the indigenous research insights are flourished in the light of the scientific approach, and sometimes the scientific thought delivers a new insight under the traditional. We find many examples for the first statement, but limited to the second. I quote one latest example to the indigenous insight to be developed in the light of scientific approach. John Biggs, an influential educationalist of our century, posed one query with the caption, "The paradox of the China's learners". Biggs (1992) contends, "Students from the Confucian heritage (China, Japan and Korea) are stereotyped in the West for passively memorising. Well, that's the way they're taught, isn't it, to memorise large amounts of material in preparation for gruelling examinations in harsh, overcrowded classrooms? But hey, don't they also out-shine Western students in international comparisons of academic achievement, in science and mathematics achievement especially? And don't these students disproportionately gain first class honours in our universities? You can't do that by rote memorisation. So are we wrong about what constitutes 'good teaching' and about the evils of rote memorising? Or are Sino-Japanese brains genetically better than ours?" This hypothesis needs a lot of research out-put by scientists! Personally, I too agree with John Biggs. I studied the Sanskrit grammar under a guru, my father traditionally. In the Hindu tradition the father ought to be guru to his sons. Again, rote memorization is a part and parcel of learning the Paninian Sanskrit grammar (though the guru teaches the meaning of aphorisms, at that age and stage of developmental we cannot understand them). So, rote memory is the forced choice, but after advancement the entire text would be at tip-of-tongue and we would form the gestalt of the grammar). Though no scientific study is attempted, we witnessed transfer of training from the knowledge of the Sanskrit grammar to other learning. Good Sanskrit scholar's proficiency of English is unparallel than his counter parts. This is my observation since six decades with hundreds of cases, indeed. In education they continued to accept the traditional approach since centuries together, and recently accepted the scientific approach (with Skinner, Bloom and Flanders et.hoc).

6.2.

We should take note that in general, in any process there appears three approaches – traditional, scientific, and combination of the two. Peri (2011) define traditional approach as, "Handing over the knowledge, affect, and skills of the subject from generation to generation successively and successfully". In teaching this process is being carried out by teacher-taught activity. I define scientific approach as "Understanding, measuring, predicting, and controlling the phenomena under taken for study". Though there is apparent conflict among the first two streams, they are always complimentary in their nature and yield the best results when we try for the third approach. For clear understanding of any phenomena both are indispensable parts of the whole. But, as long as we depend on only one among them, either traditional or scientific approach we enjoy the lop-sided understanding. If we apply this principle of approaches to the RSc, we have only approach, the traditional. It is our first duty to develop the scientific approach to the science of research. So far, it is unavailable, indeed! Scientific approach is possible through understanding the elements of research, building-blocks i.e. units of research behaviors. This is dealt with in section (9).

VII.   DIMENSIONS OF SCIENCE OF RESEARCH

We call them as dimensions, references, foundations, or family in a net-work. Those sciences, which share some commonality with respect to their subject matter, methods, processes, procedures or in their nature with akin sciences are called as dimensions, references or foundations etc. For example, education is a social science. It's an abstract science. It shares its components with philosophy, psychology, sociology, and economics. So the four sciences are said to be the foundations of the science of education. I define RSc as, "study of research behavior of researchers'' in relation to the wants and needs of the society, but under the frame work of the broadest perspective beyond the wants of an individual, total individual, and universal social organization". The definition may be explained as: individual has wants (economics), he behaves as a unit (psychology), he behaves as an integral part of the whole, the social organization (sociology), and finally, with universal perspective (philosophy). The science of research has five foundations viz sociological, philosophical, psychological, economical, and educational. Among the five, each one has got its own significance in

visualizing and developing the science of research. Research is from the society, by the society, and for the society. Philosophy directs the research, the psychology is the real process of research, and economics economizes the research resources, efforts, process and products. The educational foundations serves two functions viz. (a) sustenance of research trends, content for generations together and (b) facilitate enhancement of the research methods and content to keep up-to-date in flow of time. In fact, by its very nature RSc is at a higher level with respect to its abstractness. Further, its loci are so vast to embrace all sciences— physical, natural, social, and human. Then what should be the dimensions of the science of research?

VIII. PRINCIPLES OF SCIENCE OF RESEARCH

As a matter of fact all principles of learning apply to the research also, as research is also a kind of learning. Thus Thorndike's laws of learning viz. readiness, use-and-disuse, effect along with latest list; primacy, recency, intensity, freedom and requirement are accepted principles of research. In addition, I have added; scholarship, favourable attitude to the theme of research, and life, humanness, sensitivity to issues, fraternity, fore-sightedness and self-esteem to the above list. In general, the principles accepted for research are: systematic, discipline, verifiable, cautious, value-free, excellence, honesty, integrity, co-operation, and accountability. However, for the science of research, the first two basic principles are concentration and commitment (CC). I need to comment on my fraternity in this context. We belong to the family of educational psychologists. Our fathers are the great B.F. Skinner, Carl Rogers, Jerome. S. Bruner, Albert Bandura, B.S. Bloom et.id. We did a great service to the society; educating the progeny. But, we left what we ought to do as primary, but attempt what needs to be secondary. There are two doublets— i) attention and concentration; and ii) motivation and commitment. Among them, to me it appears both attention and motivation is at lower level paving way for higher ones; concentration and commitment. But, we, educational psychologists or to the matter of fact, psychologists, in general, did tremendous job on attention and motivation and totally left the other important couplet; concentration and commitment. Both concentration and commitment are productive skills. For a detailed discussion on this issue refere my papers referred to in the references, Peri (2007).

IX. TOWARDS TAXONOMY OF RESEARCH

Any systematic science will have its systematic. It is otherwise known as taxonomy. The entire science has been analyzed up to the least possible division to get the building-blocks. The nature of these building blocks is studied in isolation and in permutations and combinations. This process gives rise to a systematic understanding of the subject. This in short, is the philosophy of taxonomy. The life of the life sciences is their taxonomy. Dimitri Mendeleev's periodic law is the basis of taxonomy of chemistry. The study of sub-atomic particles is the taxonomy in physics. Taxonomy injects scientific temper and treatment to any science. Our sister science, education has a well developed taxonomy of educational objectives constructed by Bloom, Simson, and Krathowhol. In 1982 John Biggs developed SOLO taxonomy for the cognitive domain. In 2001 Bloom's taxonomy has been revised to include and reflect the timely changes and trends by Anderson and Krathowhol. We needn't emphasize that educational taxonomy improved the educational practices to an astonishing level. Its influence is felt throughout the world. It is the Bloom's taxonomy which gave a clear statement on the teaching process in toto, comprehending objectives, process, and evaluation of teaching, bringing all the components of teaching under one umbrella. It helps the teachers to identify the objectives of teaching before teaching, guides the process of instruction at the time of its execution, and provides objective evaluation then and there itself. It is a pre-sketch of the proposed teaching explaining what, how, and gains of teaching. While, Flanders focus is on the real and exact scene of teaching, studying the teaching behaviours of teachers' in co-ordination with the learning behaviours of the students. These two attempts discovered the scientific approach of teaching. Thus teaching enjoys the two essential and well collaborated approaches i.e. traditional and scientific. Today, after Bloom and Flanders we are in a position to follow the two complimentary approaches in teaching. This is the reason, why I say teaching is in advantageous position of enjoying both the approaches, while the research lacks in the second approach. Ultimately, research is subjected to subjective assessment with its essential evils, ballistic and personal judgements. But coming to our own story of RSc, we didn't attempt taxonomy of research objectives, which would have presented clarity of the research objectives, process, and products in whole-someness. I proposed a taxonomy of research in 2007 and now, I am at it.

X. RESEARCH SYSTEMS DESIGNS (FROM THEORY TO PRACTICE)

All sensible sciences have their strategies to culminate the theories into practice. The architect has his blue-print beforehand for all practical purposes. The economist has his annual plans of budget. A teacher has his annual, semester, unit plans and finally 'instructional designs before he proceeds to the class room teaching with clarity of objectives, teaching-learning activities, and evaluation. My pre-caution to you is don't be confused between experimental designs in research with research systems designs. In research we have experimental and quasi-experimental designs to run the experiment, but nothing more. Research systems designs are blue-prints

for the entire planning of the research undertaken. At present, our research process is en-capsule between project (research) proposal and report. Meanwhile, at each and every stage of your research process what you are doing is not known to the outer world or for himself also sometimes. We require 'research systems designs (like instructional systems designs for teaching)' for planning, execution, and evaluation of research from point-to-point and stage-by-stage. How do you design them? It is possible by developing taxonomy of research only. The purpose of this proposal is to develop HRSD based on Prof. Peri's taxonomy of research, and to attempt an effective research training development modules for researchers. Hypothetical research design is the practice of creating research experiences to enhance knowledge, affect and skill of a subject more efficient, and effective with efficacy. The process consists broadly of determining the current state and needs of the researcher, defining the end goal of research, and creating some 'intervention' to assist in the transition. Ideally, the process is informed by tested theories of learning science and may take place in research and development based settings. "Emerging science of learning is a merger, or rather amalgam of two sciences—education and research (Peri, 2013)". As a field of learning science, both ISD and HRSD are historically and traditionally rooted in cognitive and behavioral psychology, and recently in constructivism and post-modernism. The contrast of the instructional and research designs is that—

i) ISD is for teaching-learning process (learning from instruction) and HRSD is for research process (learning from inquiry).

ii) if ISD has the Bloom's taxonomy as its theory, the HRSD has Professor Peri's taxonomy of research objectives as its theory.

Educationalists have developed ISD to culminate the theory/ies of education into real teaching-learning process, and it's a success story beyond any doubt hence, now, an attempt to develop HRSD to culminate theory of research into practice.

Strategy to develop HRSD: The position of HRSD is in-between research proposal and research reporting, which are familiar to the world of research. Its step-by-step analysis, but leading to the final goal. It's the micro-approach to research. In general, if the research proposal is too broad and vague, the HRSD is pin-pointed and focused by its nature. As the first step, RP are identified with the objectives, hypotheses or any other criteria as to the wish of the researcher. The entire research is divided into several smaller units, and each unit is subdivided into chewable chalk-lets viz. RPs. Each RP is taken up for process, one-by-one till the end point. As the second step, RA includes— research designs, methods, data-collection (includes variables, tool, sample, and analysis). Finally, summary and conclusion are made at the end of the HRSD.

10.1. Proposed Lay-out of Peri's HRSD

I). Preliminaries: General statement of— objectives, specifications, hypotheses, research activities, data-collection (experimental design, methods, tool, sample) analysis, and generalizations.

II. Table: Showing PRs and RAs and Research Process:

S.N	Obj/specification	Research Point	Research Activities	Timeframe	Evaluation
1	From Peri's taxonomy	RP (i)	RA (a, f, o......)	06months	***
n	-do-	RP (n)	RA (b, j, o........)	03months	***

Objective type questions framed on Research Questions are posed to ensure out-comes of research objectives. or significance of the research hypotheses are questioned.

III). Concluding remarks: 1, 2, 3, 4, 5,

10.2. Advantages

1. Transparency and clarity of the research process, 2. Establishes a clear communication across a host of stake-holders—researcher, supervisor, evaluator, funding agency, policy-makers, and public on objectives/process/products of research, 3. Serve as blue-print, 4. The researcher can spot out himself where his research is? and its progress, like railway time table, 5. Immediate feed-back at the end of every RP makes the researcher confident via. sense of achievement, 6. The adjudicator is also in a position to verify the progress of the work at any given time, 7. Since research specifications are the fundamental units of the research, the quality of researcher and research products could be objectively estimated, 8. Again, since research specifications are units of research which are content-free, it helps to estimate the quality of research over a wide spectrum of subjects and disciplines; physics, philology, political science, music et.id, and 9. The final visible advantage is that we could 'develop research design development program' scientifically.

XI.   ASSESSMENT OF RESEARCH

Lack of a strong theory reflects in all segments of that science—understanding, measuring, predicting, and control. This is true in the case of the science of research. Absence of fundamental theory of a science reflects in its assessment. Anyhow, let us survey the methods of assessment of Research available today. If we penetrate deep into the literature on research on Research, we notice the entire focus on evaluative studies. Just like teachers have more tendencies to test the students, rather to teach, so also the researchers! Of course, it's the human nature. The studies on the philosophy, theory, process of Research are limited while on evaluation are out-rated. The agencies and governments are more interested in the methodology of rating the individual, departmental/ school/ and university potentiality of research. The unhappy out-come is more concentration on quantitative studies establishing indices with strong mathematical support. It is so unhappy that attempts on subjective peer-evaluation have not gained momentum. Actually, researchers would have taken rigours studies on the serious defects of the peer-evaluation viz. its ballistic, and subjectivity or on some supporting evaluative methods.

The International Network for Quality Assurance Agencies in Higher Education (INQAAHE) is a world-wide association of some 200 organisations that are active in the theory and practice of quality assurance in higher education. The greater majority of its members are quality assurance agencies that operate in many different ways. However, the Network also welcomes (as associate or institution members) other organisations that have an interest in quality assurance (QA) in higher education (HE). INQAAHE thus offers its members the many benefits of being part of such an active group of workers in QA in H E. This body of like-minded folk provides an enormous reassurance, support and assistance in our daily QA work. But, finally in all above mentioned cases they couldn't over-come the major weakness – lion's share to the peer- evaluation with its serious defects – high degree of ballistic and subjectivity.

Both NGO and GO agencies play a crucial role in guiding, and enforcing the policies and practices of not only doctoral degree award, but in rating a particular university department/school/university or research organization–government, non-government. They act as authorities to sanction funding for research projects and monitor the research at all levels. We know very well that there are research projects running into billions of dollars sanctioned by UNO and governments. The basic remains the same–on what base they sanction billions and how do they evaluate the proposal, how do they evaluate the mid-term, and the final? The answer is the Peer-evaluation. Is peer-evaluation is pool-proof? No. Then! No answer? We measure the depth of the subject matter and expressive ability of students with essay type questions and supplement it with the objective type to down grade bias and to assess the steep understanding of the concept/theory and its applications. We assess the specific learning out-come to the minute level where subjectivity is equated to zero level. But, in contrast we have not identified and listed the Research Out-comes at all. Isn't?

11.1. There are two divisions of assessment of Research

qualitative and quantitative. Under the sub-head qualitative there is only one entry, viz. peer-review. Though there are other entries, like credibility of the publisher, credibility of the author, they are peripheral one. They have their limitations and demerits. Among the quantitative there are many, for e.g. number of papers, articles, chapters, monographs, text books, reference books etc. Recently, some more measures like bibliometric, scientiometric, impact factor, citation index, etc. are found. In other words, the peer-review is an internal, while the others are external. The gap between the two sets of measures is unhealthy, yet attempts are not found in this direction. I contemplate on a method which would be quantitative and qualitative as well and friendly to the existing methods and could get along with them with the base of RVs. It is not totally from the thread out my mind, but following the foot prints. Our identical twin, Education which is far further fore-runner in the race of assessment will definitely, provide a clue.

XII.   SUMMARY AND CONCLUSION

Rationale for the research theory was presented at the out-set. Just like any other science, say physics, the RSc would have taken its structure, strength, and soul as a theoretical science. Despite being a member of the LSc, it is unfortunate it didn't solidify as a systematic science as its twin science, ESc. We can follow the not exactly finger prints, but foot-prints of the well established theory of ESc to evolve our theoretical science of research, for both ESc and RSc have many things in common, including their subject matter i.e. 'learning'. With the same reason we can adapt a majority of essentials characteristics of a science— its paraphernalia of elements; assumptions, theories, principles, laws, taxonomy, dimensions et.id as per their applicability to our concern science, the RSc. Some important characteristics which we could construct, develop, and establish are: theories of research based on learning theories, dimensions, taxonomy, and hypothetical research systems designs corresponding to education theory, dimensions of education, approaches to education, taxonomy of educational objectives, and instructional systems designs. In all the above developments much care has taken in respect of— what to be taken, what to be taken with necessary changes, and what not to be taken to abandon

blind follow-up. It could be concluded that there is actuate need to shape, forge, and establish 'the theoretical scince of research' like any other theoretical science (for example theoretical physics) to strengthen the RSc, and there by the galaxy of sciences, including the emerging learning science.

REFERENCES

[1].   Alrøe, H. F., and. Kristensen, E. S. (2000) "Research, values and ethics in organic agriculture — examples from sustainability, precaution, nature quality, and animal welfare." In Two Systems — One World, Proc. of EurSafe 2000, Congress on Agricultural and Food Ethics (Edited by P. Robinson). Centre for Bioethics and Risk.

[2].   Assagilio, R. (1971). Psycho-synthesis. New York. Viking.

[3].   Biggs, J. and Kevin Collis. (1982). Evaluating the Quality of Learning: The SOLO Taxonomy . New York: Academic Press.

[4].   Bloom, B.S. (1956).   Taxonomy of Educational Objectives: Classification of Educational Goals, Hand Book I, Cognitive Domain, New York: Me Kay.

[5].   Elliott, K.C. (2010)   'Scientific judgement and the limits of conflict-of-interest policies', Accountability in Research, 15: 1-29.

[6].   Fritz Capra. (1984). The Tao of physics. 8th Reprint. Bontom books.

[7].   Gange, R. M. (1964). The implications of instructional objectives for learning in Lindavall, C.M (ed.), Defining educational objectives. Pittsburgh. University of Pittsburgh press.

[8].   Goleman, D. (1985). Eastern psychologies. In Calvin.S, and Hall, and Gardener Lindezy (eds.), Theories of personality. Wiley Eastern.

[9].   Kamiya, J. Conscious brain waves. Psychology Today, 1968,1: 127-154.

[10].   Maslow, A.H. (1972). The farther Reaches of human nature. New York: Viking Compass Edition.

[11].   Landsheer, De, V. (1990). Taxonomy of Educational Objectives in the Psycho-motor Domain. Vol.3. Washington: Gryphon House.

[12].   Maslow, A.H. (1966). The psychology of science: A Reconnaissance. New York: Haper & Row.

[13].   Maslow, A.H. (1962). Lessons from the peak experience. Journal of Humanistic psychology, 1962, 2: 9-18.

[14].   Max Muller, Friedrich. (1999). 10th edition. The six systems of Indian philosophy. New Delhi. Associated publishing house.

[15].   Patanjali. (1910).   The Yoga Sutras. The Ramakrishna Mission. Kolkatta.

[16].   Peri, S. R. (2013). Creativity as an object of taxonomy of research. In press.

[17].   Peri, S. R. (2013). Intuition as an objective in taxonomy of research. (accepted).

[18].   Peri, S. R. (2013). Developing Hypothetical Research Systems Designs. In press.

[19].   Peri, S. R. (2012). Foundations of the science of research. Voice of research, 1:2, 41-46.

[20].   Peri' S.R. (2012). Trends in Indian Educational Research. Keynote addressed for the annual research meet, Center of advanced study in education and psychology, M S University, Baroda. Feb 19-21.

[21].   Peri, S.R.   (2011). Upasana – a technique for Meta-learning. Report of sabbatical leave project submitted to the R.S.University.Tirupati.

[22].   Peri, S.R.   (2011). Learning by Verbal Testimony—a learning theory from the classical Indian philosophy/psychology.

[23].   Peri, S.R. (2011). Upasana – a technique for trans-personal learning. VDM Publications.

[24].   Peri, S. R. (2011). Research outcomes. Inaugural address. Centre of Advanced Study in Psychology and Education, M.S. University, Baroda. Feb, 28th.

[25].   Peri, S.R. (2010).   Research Out-Comes as Units of Research Ability. Baroda. Keynote addressed for the annual research meet, Center of advanced study in education and psychology, M S University. Feb 28-March 2.

[26].   Peri, S.R. (2009). Standardization of Research Assessment Battery. Proposal accepted for a place in the IOE, University of London, London.

[27].   Peri, S.R.   (2009). Research Education—Zeitgeist. Accepted for 117th Annual Conference APA, Toronto, Canada. August, 6th to 9th.

[28].   Peri, S. R. (2008). Learning by Verbal Testimony. Lecture delivered in Academic Staff College. M.A.M. Urdu University, Hyderabad. 17th, August.

[29].   Peri, S.R.   (2008). Assessing Research Ability. Paper presented at International Workshop on "Emerging Frameworks and Issues for S & T recruitments" Organized by the Society for Reliability Engineering, Quality and Operation Management (SREQOM), Recruitment and Assessment Centre (RAC) D.R.D.O, Delhi. September 18th.

[30].   Peri, S.R. (2008). Upasana-technique for Meta-learning. Report of the Sabbatical leave. Tirupati. Rasshtriya Sanskrit University.

[31]. Peri, S.R. (2007). Taxonomy of Research, Proceeding of the Interaction Conference on Higher Education (ICAH-07), Bangalore, July 12-14.

[32]. Peri, S.R. (2007). Upasana-technique of Meta-learning. Xvii International Vedanta Congress. Miami University, Oxford, OH, USA, September, 20-23.

[33]. Peri, S.R. (2007). Concentration as criteria for selection of personnel. International conference on selection of personnel. Organized by the Defense Institute of Psychological Research, Govt. of India. New Delhi. November, 18th -21st, 18-26.

[34]. Peri, S.R. (2007). Psychology of Commitment. International conference on selection of personnel. Organized by the Defense Institute of Psychological Resarch, Govt. of India. New Delhi. November, 18th -21st, Vol. II, 20-28.

[35]. Peri, S.R. (2006). Learning by Aptvakyam. Association of Indian Universities Journal. Special Issue. March.

[36]. Peri, S.R. (2006). Sravana-Manana-Nididhyasana-Taxonomy of Educational Objectives of Ancient India. Association of Indian Universities Journal. Special Issue. March.

[37]. Peri, S. R. (2004). Sravana-Manana-Nidhidhyasana. In J.S.Rajput (ed.) Encyclopedia of Indian Education, New-Delhi. National Council of Educational Research and Training. 1581-83.

[38]. Peri, S. R. (2004). Indian Concept of Self-concept. Siksha Vasistam. Puri. Felicitation Committee, Samsmrti.

[39]. Peri, S. R. (2000). A lee learning strategy-From Indian Philosophy. Perspectives in Education. Vol.16 Special issue.19-26.

[40]. Peri, S. R. (1985). A Study of Relationship between Teacher Effectiveness, Ability to publish, and Self-concept", an unpublished Ph.D. dissertation submitted to the Andhra University, Visakhapattanam, India.

[41]. Reeves, Albert, Kuper, & Hodges, 2008). Education theory. Retrieved from www.ucdoer.ie/index.php/Education_Theory -

[42]. Rayner, S. (2011) Researching Style: epistemology, paradigm shifts and research interest groups. Learning and Individual Differences, 21(2), 255-262.

[43]. Rayner, S. (2007) What next? Developing global research and applied practice the field of cognitive and learning styles. In, Lassen, L., Bostrom, L. & Knoop, H. K. (Eds) Laering og Laeringsstile. Om unikke of faelles veje I paedagogikken (pp 165 -183). Virum, Denmark: Dansk Psykologisk Forlag.

[44]. Sinha, J. (1959). Indian psychology. Kolkatta. Sinha publishing house.

[45]. Stagner, S. (1988). A history of psychological theories. Macmillan In

[46]. www.nesochina.org/...education.../quality-assurance - China

[47]. en.wikipedia.org/.../United_States_National_Research_Council

[48]. www.ugc.ac.in/orgn/naac.html

[49]. en.wikipedia.org/wiki/Research_Assessment_Exercise

[50]. en.wikipedia.org/wiki/Excellence_in_Research_for_Australia

[51]. www.unesco.org/education/.../highlights/.../vroeijenseiijn.doc - France

[52]. en.wikipedia.org/.../United_States_National_Research_Council

[53]. en.wikipedia.org/wiki/Fundamental_science

[54]. www.scienceandyou.org/articles/ess_09.shtml

[55]. www.Buzzedu.com/Middlesex

[56]. www.umsl.edu/~keelr/3210/3210_lectures/what_is_soc_theory.html

[57]. www.sims.berkeley.edu

[58]. www.ucdoer.ie/index.php/Education_Theory .

[59]. en.wikipedia.org/wiki/Education_theory .

Research Paper   Open Access

Image Classifying Registration and Dynamic Region Merging

Himadri Nath Moulick, Moumita Ghosh
CSE, Aryabhatta Institute of Engg & Management, Durgapur, PIN-713148, India
CSE, University Institute Of Technology,(The University of Burdwan) Pin -712104,India

Abstract: - In this paper, we address a complex image registration issue arising when the dependencies between intensities of images to be registered are not spatially homogeneous. Such a situation is frequently encountered in medical imaging when a pathology present in one of the images modifies locally intensity dependencies observed on normal tissues. Usual image registration models, which are based on a single global intensity similarity criterion, fail to register such images, as they are blind to local deviations of intensity dependencies. Such a limitation is also encountered in contrast enhanced images where there exist multiple pixel classes having different properties of contrast agent absorption. In this paper, we propose a new model in which the similarity criterion is adapted locally to images by classification of image intensity dependencies. Defined in a Bayesian framework, the similarity criterion is a mixture of probability distributions describing dependencies on two classes. The model also includes a class map which locates pixels of the two classes and weights the two mixture components. The registration problem is formulated both as an energy minimization problem and as a Maximum A Posteriori (MAP) estimation problem. It is solved using a gradient descent algorithm. In the problem formulation and resolution, the image deformation and the class map are estimated at the same time, leading to an original combination of registration and classification that we call image classifying registration. Whenever sufficient information about class location is available in applications, the registration can also be performed on its own by fixing a given class map. Finally, we illustrate the interest of our model on two real applications from medical imaging: template-based segmentation of contrast-enhanced images and lesion detection in mammograms. We also conduct an evaluation of our model on simulated medical data and show its ability to take into account spatial variations of intensity dependencies while keeping a good registration accuracy.   And the addresses the automatic image segmentation problem in a region merging style. With an initially over-segmented image, in which the many regions (or super-pixels) with homogeneous color are detected, image segmentation is performed by iteratively merging the regions according to a statistical test. There are two essential issues in a region merging algorithm: order of merging and the stopping criterion. In the proposed algorithm, these two issues are solved by a novel predicate, which is defined by the sequential probability ratio test (SPRT) and the minimal cost criterion. Starting from an over-segmented image, neighboring regions are progressively merged if there is an evidence for merging according to this predicate. We show that the merging order follows the principle of dynamic programming. This formulates image segmentation as an inference problem, where the final segmentation is established based on the observed image. We also prove that the produced segmentation satisfies certain global properties. In addition, a faster algorithm is developed to accelerate the region merging process, which maintains a nearest neighbor graph (NNG) in each iteration. Experiments on real natural images are conducted to demonstrate the performance of the proposed dynamic region merging algorithm.

I.   INTRODUCTION

Image registration is a central issue of image processing, which is particularly encountered in medical applications [1]–[5]. Medical image registration is critical for the fusion of complementary information about patient anatomy and physiology, for the longitudinal study of a human organ over time and the monitoring of disease development or treatment effect, for the statistical analysis of a population variation in comparison to a

so-called digital atlas, for image-guided therapy, etc. Image registration consists in mapping domains of several images onto a common space and results in some corrections of geometric differences between the images. Most of classical registration techniques rely upon the assumption that there exists a relationship between intensities of images to be registered and that this relationship remains the same all over the image domains [6]–[11]. This assumption is typically made when applying registration techniques based on intensity criteria such as the sum of squared differences, the correlation ratio, the correlation coefficient or the mutual information [10]. But such an assumption is not always satisfied. As an example, let us mention the medical imaging case when a contrast agent is used to enhance some pathological tissues (lesions) [12], [13]. After enhancement, intensities of normal tissues and lesions are likely to differ, even though they can be the same before enhancement. So, a same intensity before enhancement may correspond to several intensities after enhancement. Hence, with contrast-enhanced imaging modalities, the relationship between image intensities is neither unique, nor spatially invariant. It mainly depends on the type of observed tissues. In such cases, ignoring the spatial context may lead to locally establishing an inaccurate or even inconsistent correspondence between homologous geometric structures. This issue was documented in [13], [14],

where it is shown that such non-rigid registration would wrongly change the size of non-deformed contrast-enhanced structures. In the literature, there have been several works dealing with image registration in the presence of multiple pixel classes. These works can mainly be divided into two categories: those based on robust estimation and mixture models, and those combining registration and classification (or segmentation). Robust estimation is a statistical approach which has been widely applied to image processing [15]. This approach involves the definition of outliers, which are characterized as elements deviating from a normal model, detected and possibly rejected [16]–[19]. Applied to optical flow estimation and image registration [20]–[25], robust estimation helps to reduce the influence of large insignificant image differences on the optical flow or the deformation estimation. However, these approaches offer poor characterizations of outliers, which are usually described as pixels generating large image differences. They cannot deal with complex situations arising from medical imaging applications. More general robust estimation approaches are based on mixture models [18] and characterize outliers by some specific probability distributions [26]–[34]. In optical flow computation, a mixture model was used to distinguish between several layers of movements and an outlier class [31]. In image registration, some authors used a mixture model in which image differences generated by outliers are represented by a mixture component [29], [30]. Similar approaches could be used in medical image registration considering medical lesions as outliers [26]–[28]. However, the main and important difference with the model we introduce in this paper is that the mixture models proposed above do not use any spatial and geometric information about the pixel classes but only pixel-independent mixing proportions. In other approaches, spatial informations derived from segmentation were used to adapt regionally the similarity criterion describing intensity relationships [35]–[38]. Such segmentation-based approaches require a preliminary segmentation of the images which, obviously, cannot always be obtained. For instance, in dynamic contrast-enhanced sequences, the image segmentation has to be estimated from the registered images [39]. Image segmentation has also been combined with atlas-based registration in Bayesian frameworks [40], [41], where mixture models were used to represent pixel intensities of different anatomical structures. In other works, Markov random fields were employed to describe a label map of pixel classes. The registration and the segmentation were then computed by the Maximum A Posteriori (MAP) estimation [42]–[44]. In such approaches, one can incorporate prior information about the lesion shape and localization. However, the proposed methods used simple characterizations of intensity variations. In this paper, we deal with the issue of registering images whose intensity relationship is spatially dependent. We propose a new technique where the registration is simultaneously combined to a pixel classification. This classification provides some spatial information about intensity relationships. We use

Mixture models to take into account complex intensity changes and Markov random fields to label pixels. The paper is organized as follows. Section 2 describes the theoretical foundation of the proposed new method. Then, the numerical aspects are discussed in Section 3. In Section 4, experiments are conducted both on simulated and on real data to evaluate the method performance. Finally, some conclusions and possible extensions of the proposed approach are discussed in the last section. Image segmentation is a fundamental yet still challenging problem in computer vision and image processing. In particular, it is an essential process for many applications such as object recognition, target tracking, content-based image retrieval and medical image processing, etc. Generally speaking, the goal of image segmentation is to partition an image into a certain number of pieces which have coherent features (color, texture, etc.) and in the meanwhile to group the meaningful pieces together for the convenience of perceiving [61]. In many practical applications, as a large number of images are needed to be handled, human interactions involved in the segmentation process should be as less as possible. This makes automatic image segmentation techniques more appealing. Moreover, the success of many high-level segmentation techniques (e.g. class-based object segmentation [82, 83]) also demands sophisticated automatic segmentation techniques. Dating back over decades, there is a large amount of literature

on automatic image segmentation. For example, the edge detection algorithms [74-79] are based on the abrupt changes in image intensity or color, thus salient edges can be detected. However, due to the resulting edges are often discontinuous or over-detected, they can only provide candidates for the object boundaries. Another classical category of segmentation algorithms is based on the similarities among the pixels within a region, namely region-based algorithms. In order to cluster the collection of pixels of an image into meaningful groups of regions or objects, the region homogeneity is used as an important segmentation criterion. Many cut criteria in graph theory have been studied for this purpose. The most widely used cut criteria include normalized cut [88], ratio cut [9], minimum cut [10] and so on. The aim of these algorithms is to produce a desirable segmentation by achieving global optimization of some cost functions. However, these cost functions only provide a

Characterization of each cut rather than the whole regions. Another problem is that the optimization processes are often computationally inefficient for many practical applications. In recent years, the success of combinatorial graph cut methods [71-72] has been attracting significant research attention. These methods utilize the user input information along with the cut criteria in optimization and nearly global optima can be achieved in linear computational time. As a matter of fact, for most cut-based energy functionals a single optimal partition of an image is not easy to obtain. It makes a possibility of finding different level-based explanations of an image. From this aspect, there are methods [81-82] tackling the image segmentation as a hierarchical bottom-up problem. In region-based methods, a lot of literature has investigated the use of primitive regions as a preprocessing step for image segmentation [83-85]. The advantages are twofold. First, regions carry on more information in describing the nature of objects. Second, the number of primitive regions is much fewer than that of pixels in an image and thus largely speeds up the region merging process. Starting from a set of primitive regions, the segmentation is conducted by progressively merging the similar neighboring regions according to a certain predicate, such that a certain homogeneity criterion is satisfied. In previous works, there are region merging algorithms based on statistical properties [66, 72-73, 70-71], graph properties [87-89, 74-75] and spatio-temporal similarity [80]. Although the segmentation is obtained by making local decisions, some techniques [66-71] have shown satisfying results with efficient implementation. Most region merging algorithms do not have some desirable global properties, even though some recent works in region merging address the optimization of some global energy terms, such as the number of labels [90] and the area of regions [91]. As a good representation of morphological segmentation, watershed transform [92] can also be classified as region-based segmentation methods. The intuitive idea comes from geography, where watersheds are the dividing lines of different catchment basins. The major drawback of watershed transform is the over-segmentation of the image. To overcome this problem, one solution is "flooding" from the selected markers [76-78] such that only the most important regional minima are saved for the segmentation. The other [79] is based on a hierarchical process, where the catchment basins of the watershed image are merged until they belong to almost homogeneous regions. In this paper, we implement the segmentation algorithm in a region merging style for its merit of efficiency, where similar neighboring regions are iteratively merged according to a novel merging predicate. As stated above, homogeneity criteria (cues) are essential to the region merging process. Although a good enough cue is needed in order to obtain a valuable segmentation, our work does not focus on finding a more complex region model. Instead, we model the cues by a function of random variables. In this way, the properties of cues are not mainly concerned, but the reliability of the cues. In many traditional segmentation algorithms (e.g. [63-69]), the reliability is predetermined and thus researchers often try to use more reliable cues for implementation. In contrast, some statistical segmentation methods are able to calculate the reliability of cues, for example, using the parametric probability models [80-81]. But they cannot be used in a general scenario. Another statistical method [76] directly uses the statistical property of image data (e.g., colors) to identify the region border. Particularly, a homogeneity criterion is proposed based on the expectation of pixel colors inside a region, which naturally leads to a merging predicate. In the recent work of region merging [72], a likelihood ratio test is applied as the measure of region similarity. The probability of adjacent regions and that of their merging are both computed. To minimize both probabilities of error, the optimal merging will take place along with the largest decreasing of the likelihood ratio.

II.   THE BAYESIAN FRAMEWORK

Let m and n be two integers, and $\Omega_d = \{0, ..., m-1\} \times \{0, ..., n-1\}$ be a discrete grid of size N = m n. Observed images are real-valued functions defined on d. They can be interpolated on the continuous domain $\Omega = [0, m-1] \times [0, n-1]$ naturally associated to the grid d. For convenience, elements of Ω_d are ordered and will be denoted xi for i = 1, $\cdots$, N. The registration of two images I and J consists in finding a mapping _ : ϕ : $\Omega \rightarrow \Omega$ for which the

deformed image Iφ := I$^\phi$ of the so-called source image I is as similar as possible to the so-called target image J.

In a Bayesian framework, the mapping _ is usually obtained as a MAP estimate (see [45] and references therein). Specific to this framework, images and deformations are assumed to be some realizations of random fields indexed on Ω_d and Ω, respectively. For each point xi of Ω_d, I(xi) and J(xi) are realizations of two real-valued random variables and, for each point x of , Ω, (x) is a realization of a random vector with values in . The relationships between the intensities of the registered images are then statistically described by a probability distribution of J given I, ϕ and a set of parameters θ (this conditional distribution is denoted by π (J | I, $I, \phi; \theta$)). Usually, the variables J(xi) are assumed to be independent conditionally to the variables Iφ(xi). Hence, ($\pi(J \mid I, \phi; \theta)$) can be written as

$$\pi(J \mid I, \phi; \theta) = \prod_{i=1}^{N} \pi(J(x_i) \mid I^{\phi}(x_i); \theta). \tag{1}$$

Because of noise, and also because it is a very generic choice, it is possible to assume that the intensity differences between J(x) and Iφ(x) follow a Gaussian distribution with mean μ and variance σ^2 at each pixel x $\in \Omega_d$, leading to the distribution

$$\pi(J(x) \mid I^{\phi}(x); \theta) =$$

$$\frac{1}{\sqrt{2\pi}\sigma} \exp\left(-\frac{1}{2\sigma^2}(J(x) - I^{\phi}(x) - \mu)^2\right), \tag{2}$$

with $\theta = (\mu, \sigma)$ In this definition, it is worth noticing that the mean μ and the variance σ^2 do not depend on any position x. Consequently, the intensity relationship between images is spatially homogeneous. Let us further mention that, similarly to this particular Gaussian distribution, distributions associated to other usual criteria (e.g. correlation ratio, correlation coefficient, or mutual information) are also homogeneous. Besides, a prior probability distribution is set on the mappings _ in order to favour smooth deformations as solutions of the registration problem. Let $\phi = \mathrm{id} + u$ be written as the sum of the identity map id and a displacement field u, seen as an element of a Hilbert space H equipped with an inner product a($\cdot$, $\cdot$). Let then ˜H be a finite-dimensional approximation subspace of H which is spanned by a basis $\mathcal{B} = (\psi_i)_{i=1}^{n_e}$, with ne $\in$ N$*$. In ˜H, a displacement u is uniquely determined by a vector of coefficients $\mathbf{b} = (\beta_i)_{i=1}^{n_e}$ such that $u = \sum_{i=1}^{n_e} \beta_i \cdot \psi_i$. In the following, the deformations ϕ are assumed to be expanded into the subspace ˜H and identified with their decomposition coefficients b. We will also use the notation Ib instead of Iφ. Several choices are possible for the basis B: Fourier basis, sine and cosine transform basis functions, B-splines, piecewise affine or trilinear basis functions, wavelets (see [46] for a review), etc. We consider an inner product on ˜H, given by $a(u,u) = \mathbf{b}^T A \mathbf{b}$, where bT is the transpose of b, and A is a symmetric positive-definite matrix. On ˜H, we then define a centered multivariate normal distribution with covariance matrix A^{-1} given by

$$\pi(\mathbf{b}) = (2\pi)^{-\frac{n_e}{2}} \sqrt{\det(A^{-1})} e^{-\frac{1}{2}\mathbf{b}^T A \mathbf{b}}. \tag{3}$$

This prior distribution is used as a regularity term to enforce the smoothness of the deformations ϕ. A usual choice for a($\cdot$, $\cdot$) is the bilinear form

$$a(u,v) = \frac{1}{2} \int_{\Omega} \sum_{i,j=1}^{2} \frac{\lambda}{2} \left(\frac{\partial u_i(x)}{\partial y_i} \frac{\partial v_j(x)}{\partial y_j} \right) dy +$$

$$\frac{1}{2} \int_{\Omega} \sum_{i,j=1}^{2} \frac{\mu}{4} \left(\frac{\partial u_i(x)}{\partial y_j} + \frac{\partial v_j(x)}{\partial y_i} \right)^2 dy, \tag{4}$$

defined for $\lambda > 0$ and μ > 0, which is an inner product on the Sobolev space $H^1(\Omega; \mathbb{R}^2)$ and is related to the linearized strain energy of elastic materials [47]–[50]. We choose here the elastic regularization without aiming at a specific application, but knowing that this term enables to deal with many medical imaging applications. Other regularity terms could be better adapted to specific applications. They can be easily introduced in the proposed model. Other choices include the membrane energy [51], the bending energy [52], etc. The matrix A can also be estimated from the data using for instance EM algorithms with stochastic approximation [53], [54].

III.   THE TWO-CLASS REGISTRATION MODEL

We now outline our new model. It is an extension of the model described in the previous section. The main feature is the introduction and the estimation of a pixel classification to take into account the spatial variations of the statistical relationships between the intensities of J and Iφ.

Intensity relationships In Equation (2), the probability distribution $\pi(J(x)|I^b(x); \theta)$ describing the intensity relationship is spatially homogeneous. We now assume that the pixels of image J can be divided into two classes (labeled 0 and 1) where the intensity relationships are different and denoted respectively by $\pi_j(J(x)|I^b(x); \theta_j)$, $j \in \{0, 1\}$. Let also L(x) be the probability for a pixel x to belong to the class 1. Then, the intensity relationship at pixel x is described by the mixture distribution

$$\pi(J(x)|I^b(x), L(x); \theta) = \pi_0(J(x)|I^b(x); \theta_0)\,(1 - L(x))$$
$$+ \pi_1(J(x)|I^b(x); \theta_1)\,L(x), \tag{5}$$

where $\theta = (\theta_0, \theta_1)$. Let us denote Li = L(xi) and L = (L1, · · · ,LN)T the vector of class probabilities on grid pixels. Assuming the conditional independence on grid points, we obtain the global conditional distribution

$$\pi(J|I^b, \mathbf{L}; \theta) = \prod_{i=1}^{N} \Big(\pi_0(J(x_i)|I^b(x_i); \theta_0)\,(1 - L_i) +$$
$$\pi_1(J(x_i)|I^b(x_i); \theta_1)\,L_i \Big). \tag{6}$$

In an application of our model to lesion detection, the classification aims at distinguishing pixels on a lesion (class 1) from those outside any lesion (class 0). In contrast-enhanced images, the enhancement is more important on lesions than it is on normal tissues, leading to higher image differences on lesions. Assuming that the distributions are Gaussian on both classes, we can define distributions π_0 and π_1 as in Equation (2) using two different sets of parameters: $\theta_0 = (\mu_0, \sigma_0)$ π_0 and $\theta_1 = (\mu_1, \sigma_1)$ with μ1 > μ0. Another possibility is, as in robust estimation, to consider elements of class 1 as outliers of class 0 and put no specific information on class 1 by defining π_1 as the uniform distribution

$$\pi_1(J(x)|I^b(x); \theta_1) = \frac{1}{N_{gl}}, \tag{7}$$

where Ngl is the number of possible gray-levels of J. Finally, we define a prior distribution on the class map L itself in order to introduce some constraints on the spatial homogeneity of the pixels of a same class. For that purpose, we equip the grid Ω_d with a neighborhood system (either a 4 or 8 neighborhood system) and assume that the class map L is a Markov random field on it [55]. We have considered two prior distributions on L. The first one is a Gaussian model, given by

$$\pi(\mathbf{L}) = \frac{1}{Z} \exp \Big(-\alpha_1 \sum_{i=1}^{N} L_i^2$$
$$-\alpha_2 \sum_{\{i,j=1,\cdots,N; x_i \sim x_j\}} (L_i - L_j)^2 \Big), \tag{8}$$

where xi ∼ xj means that xi and xj are neighboring pixels, Z is a normalization constant, $\alpha_1 > 0$ and $\alpha_2 > 0$. The second model, which is a particular case of the Gaussian model when L is binary with range {0, 1}, is the Bernoulli model

$$\pi(\mathbf{L}) = \frac{1}{Z} \exp\left(-\alpha_1 \sum_{i=1}^{N} L_i + \alpha_2 \sum_{\{i,j=1,\cdots,N; x_i \sim x_j\}} L_i L_j\right) \quad (9)$$

where $\alpha_1 > 0$ and $\alpha_2 > 0$. If we let X = 2L − 1, this model is equivalent to the Ising model [56].In models (10) and (11), the parameter α_1 restricts the amount of pixels of the class 1, whereas the parameter α_2 enforces the spatial homogeneity of the classes.

Parameters The distributions defined above involve several parameters. In our application, we used the prior deformation distribution defined by Equation (4) and set manually the Lame constants λ and μ from experiments. We also set manually the mean μ0 and the variance σ_0 of the Gaussian distribution π_0 of the class 0, and the weights α_1 and α_2 of the Gaussian or Bernoulli model in Equations (10) and (11). The other parameters, which are the mean μ1 and the variance σ_1 of the Gaussian distribution π_1 on class 1, are estimated from the data. We assume that μ1 belongs to an interval [μmin, μmax] and σ_1 to another interval [_min, _max] and put, as a prior, uniform independent distributions of μ1 and σ_1 on these intervals. The parameter vector θ is decomposed as $\theta = (\theta_0, \theta_1)$), where $\theta_0 = (\mu_0, \sigma_0)$ is known and $\theta_1 = (\mu_1, \sigma_1)$ This parameter θ_1 is then estimated, together with the deformation and the classification by solving the following MAP estimation problem:

$$(\tilde{\mathbf{b}}, \tilde{\mathbf{L}}, \tilde{\theta}_1) = \arg\max_{\mathbf{b}, \mathbf{L}, \theta_1} \pi(J|I, \mathbf{L}, \mathbf{b}; \theta_0, \theta_1)\, \pi(\mathbf{b})\, \pi(\mathbf{L})\, \pi(\theta_1). \quad (10)$$

As before, this is equivalent to the minimization of an energy of the form

$$\mathcal{E}(\mathbf{b}, \mathbf{L}, \theta_1) = S(I, J, \mathbf{b}, \mathbf{L}; \theta) + H(\mathbf{b}) + R(\mathbf{L}), \quad (11)$$

under the constraint that $\mu_1 \in [\mu_{min}, \mu_{max}]$ and $\sigma_1 \in [\sigma_{min}, \sigma_{max}]$.

IV. THE REGION MERGING PREDICATE

Automatic image segmentation can be phrased as an inference problem [60]. For example, we might observe the colors in an image, which are caused by some unknown principles. In the context of image segmentation, the observation of an image is given but the partition is unknown. In this respect, it is possible to formulate the inference problem as finding some representation of the pixels of an image, such as the label that each pixel is assigned. With these labels, an image is partitioned into a meaningful collection of regions and objects. The Gestalt laws in psychology [66-67] have established some fundamental principles for this inference problem. For example, they imply some well-defined perceptual formulations for image segmentation, such as homogeneous, con tinuity and similarity. In the family of region merging techniques, some methods have used statistical similarity tests [86, 89] to decide the merging of regions, where a predicate is defined for making local decisions. These are good examples of considering the homogeneity characteristics within a region, from which we can see that an essential attribute for region merging is the consistency of data elements in the same region. In other words, if neighboring regions share a common consistency property, they should belong to the same group. However, most of the existing region merging

Algorithms cannot guarantee a globally optimal solution of the merging result. As a consequence, the region merging output is over-merged, under-merged or a hybrid case. In this section, we propose a novel predicate which leads to certain global properties for the segmentation result. The proposed predicate is based on measuring the dissimilarity between pixels along the boundary of two regions. For the convenience of expression, we use the definition of region adjacency graph (RAG) [30] to represent an image. Let G = (V, E) be an undirected graph, where vi∈V is a set of nodes corresponding to image elements (e.g. super-pixels or regions). E is a set of edges connecting the pairs of neighboring nodes. Each edge (vi,vj)∈E has a corresponding weight w((vi,vj)) to measure the dissimilarity of the two nodes connected by that edge. In the context of region merging, a region is represented by a component R ⊆ V. We obtain the dissimilarity between two neighboring regions R1, R2 ⊆ V as the minimum weight edge connecting

them. That is,

$$S(R_1, R_2) = \min_{v_i \in R_1, v_j \in R_2, (v_i, v_j) \in E} w((v_i, v_j)) \tag{12}$$

The graph structure of an example partition is shown in Fig. 1, where the image has 7 regions and its RAG is shown on the right. The advantage of RAG is that it can provide a "spatial view" of the image.
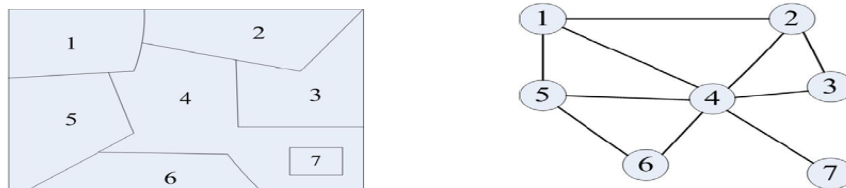
Fig 1. An example of region partition and the corresponding region adjacency graph (RAG).
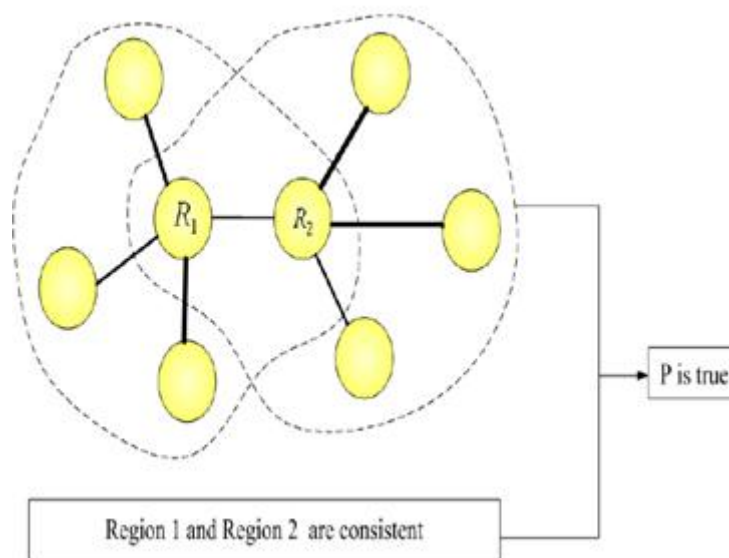
Fig 2. An example that the predicate P between R1 and R2 is true.

The thickness of lines indicates the weights of the edges. The most similar pair of regions is connected by an edge with the minimal weight.

Since the merging predicate will decide whether there is an evidence of merging between the pair of regions, it involves two aspects: a dissimilarity measure which is used to determine the candidate region for merging, and the consistency property which checks if the regions are homogenous. We define the following region merging predicate P:

$$P(R_1, R_2) = \begin{cases} true & \text{if (a) } S(R_1, R_2) = \min_{R_i \in \Omega_1} S(R_1, R_i) = \min_{R_j \in \Omega_2} S(R_2, R_j); \text{ and} \\ & \text{(b) } R_1 \text{ and } R_2 \text{ are consistent} \\ false & \text{otherwise} \end{cases} \tag{13}$$

where Ω1 and Ω 2 are the neighborhood sets of R1 and R2, respectively.[77] The merging predicate on regions R1 and R2 could thus be "merge R1 and R2 if and only if they are the most similar neighbors in each other's neighborhood and follow the principle of consistency." The condition (a) is stronger than that of only requiring the connecting edge between R1 and R2 to be the minimal one in either of the neighborhood. This leads to an interesting property of the proposed region merging algorithm, i.e., the candidates of the pairs of regions for merging are uniquely decided by the given graph. We shall see hereafter that such a condition uniquely decides the pairs of regions to be merged at a given merging level. Moreover, in Section V we will prove that there is always at least one pair of regions which satisfies condition (a). Clearly, without condition (b), all the regions will be merged into one big region at the end of region merging process. Therefore, condition (b) acts as a stopping criterion. Fig. 2 illustrates an example when the predicate P between regions R1 and R2 is true.

1. Consistency Test of Cues

In order to obtain the homogenous regions in region merging, the proposed predicate P in Eq. (13) checks the consistency of regions. Region information is usually presented by the cues extracted from the observed data. The choice of cues can be intensity, color, texture and so on. If we view the cue as a random variable, the distribution of the cue depends on the consistency of pairs of regions. In this paper, we formulate the evaluation of the region consistency as a sequential test process. Suppose parameter θ is related to the distribution of random cues x. More specifically, we gather information of parameter θ by observing random variables in successive steps. Since every sample of the cues carries statistical information on parameter θ, we may collect the information at the end of observation. This is one of the interesting problems studied in sequential analysis, where θ is called a hypothesis. In the context of region merging, two hypotheses are involved in the evaluation task: a pair of regions is "consistent", and is "inconsistent", which are denoted by a null hypothesis H0: $\theta = \theta 0$ against an alternative hypothesis H1: $\theta = \theta 1$, respectively. The property of the hypotheses is a hidden state that is not directly observable, but is statistically linked to the observable cues. To decide whether or not a pair of regions belongs to the same group, we look for the solution of its hypothesis test. An efficient and popular procedure for integrating the statistical evidence is the sequential probability ratio test (SPRT) which was proposed by Wald [78]. SPRT shows that the solution to the hypothesis can be found by making the smallest number of observations and satisfying the bounds on the predefined probabilities of two errors. SPRT is purely sequential in nature, i.e., continuing sampling on the instances of a random variable will eventually lead to a reliable inference about parameter θ. The application of SPRT to the consistency test of cues is described as follows. We observe the distribution of random cues x in a sequence until a likelihood ratio δ goes out of the interval (B, A) for the first time by a random walk, where the real numbers A and B satisfy B<0<A. The sequence of successive likelihood ratio δi is:

$$\delta_i = \log \frac{P_0(x_i \mid \theta_0)}{P_1(x_i \mid \theta_1)}, \quad i = 1, 2, \cdots, N$$

(14)

where P0(x| $\theta 0$) and P1(x| $\theta 1$) are the distributions of visual cues. P0(x| $\theta 0$) and P1(x| $\theta 1$) should be different so as to make a convincing decision. We use the Gaussian distribution model to approximate the cue distributions. The two conditional probabilities are given as follows:

$$\begin{cases} P_0(x \mid \theta_0) = \lambda_1 \exp(-(I_b - I_{a+b})^T S_I^{-1}(I_b - I_{a+b})) \\ P_1(x \mid \theta_1) = 1 - \lambda_2 \exp(-(I_b - I_a)^T S_I^{-1}(I_b - I_a)) \end{cases}$$

(15)

where Ia and Ib are the average color of sampled data in regions a and b respectively, and Ia+b is the average value of samples' union. SI is the covariance matrix of the regions, and $\lambda 1$ and $\lambda 2$ are scalar parameters. If each test is independent, the composition of the likelihood ratios is the sum of the individual δi:

$$\delta = \sum_{i=1}^{N} \delta_i$$

(16)

where N is the first integer for which $\delta \geq A$ or $\delta \leq B$. We can see that the solution to the hypothesis is decided by the relationship between δ, an upper limit and a lower limit, denoted by A and B, respectively. If δ goes out of one of these limits, the hypothesis is made and thus the test stops. Otherwise, the test is carried on with a new random sampling.

Algorithm 1: consistency test of cues

Preset $\lambda 1$;

Let $\lambda 2 =1$, $\alpha=0.05$, $\beta=0.05$;

Compute parameters:

N0: be a constant greater than max{E{$\delta \mid \theta 0$}, E{$\delta \mid \theta 1$}};

A=log(1-β)/α , B=logβ(1-α);

P0(x| $\theta 0$), P1(x| $\theta 1$) are computed using Eq. (4).

Input: a pair of neighboring regions.

Output: the decision D that the two regions are "consistent" (D=1) or "inconsistent" (D=0).

1. Set evidence accumulator δ and the trials counter n to be 0.

2. Randomly choose m pixels in each of the pair of regions, where m equals the half size of the region.

3. Calculate the distributions of visual cues x using Eq. (4) based on these pixels.

4. Update the evidence accumulator

$$\delta = \delta + \log \frac{P_0(x_i \mid \theta_0)}{P_1(x_i \mid \theta_1)}.$$

5. If n≤N0 If δ ≥ A, return D=1 (consistent)
If δ ≤ B, return D=0 (inconsistent)
If n>N0
If δ ≥ 0, return D=1 (consistent)
If δ <0, return D=0 (inconsistent)
6. Go back to step 2.

2. The dynamic region merging algorithm

In this section, we explain the proposed region merging algorithm as a dynamic region merging (DRM) process, which is proposed to minimize an objective function with the merging predicate P defined in Eq. (13). As mentioned in Section I, the proposed DRM algorithm is started from a set of over-segmented regions. This is because a small region can provide more stable statistical information than a single pixel, and using regions for merging can improve a lot the computational efficiency. For simplicity and in order to validate the effectiveness of the proposed DRM algorithm, we use the watershed algorithm [71] (with some modification) to obtain the initially over-segmented regions (please refer to Section VI-A for more information), yet using a more sophisticated initial segmentation algorithm (e.g. mean-shift [62]) may lead better final segmentation results. Given an over-segmented image, there are many regions to be merged for a meaningful segmentation. By taking the region merging as a labeling problem, the goal is to assign each region a label such that regions belong to the same object will have the same label. There are two critical labels for a region Ri: the initial label li 0, which is decided by the initial segmentation, and the final label li n, which is assigned to the region when the merging process stops. In our problem, the final label li n for a given region is not unique, which means that the same initialization li 0 could lead to different solutions. This uncertainty mainly comes from the process of SPRT with a given decision error. The test of consistency/inconsistency depends on the error probabilities of the cue decisions α and β. In general, these decisions are precise for homogenous regions. If a region contains a small part of non-homogenous data, the SPRT might add a few more times of tests to verify its decision. With reasonably small error probabilities, the segmentation results will be more reliable. According to our observation, in most cases, the segmentation result is stable for a given image and it can be guaranteed that all the results satisfy the merging predicate P defined in Eq. (2). In the process of region merging, the label of each region is sequentially transited from the initial one to the final one, which is denoted as a sequence

$$(l_i^0, l_i^1, \ldots, l_i^n)$$

. To find an optimal sequence of merges which produce a union of optimal labeling for all regions, the minimization of a certain objective function F is required. According to predicate P, the transition of a region label to another label corresponds to a minimal edge weight that connects the two regions. In this case, a sequence of transitions will be defined on a set of local minimum weights, i.e., in each transition the edge weight between the pair of merged regions should be the minimal one in the neighborhood. As a result, the objective function F used in this work is defined as the measure of transition costs in the space of partitions. In other words, as the whole image is a union of all regions, F is the sum of transition costs over all regions. That is:

$$F = \sum_{R_i} F_i$$

(17)

Where Fi is the transition costs of one region Ri in the initial segmentation. Minimizing F in Eq. (17) is a combinatorial optimization problem and finding its global solution is in general a hard task. Since the exhaustive search in the solution space is impossible, an efficient approximation method is desired. The solution adopted here is based on the stepwise minimization of F, where the original problem is broken down into several sub-problems by using the dynamic programming (DP) technique [73]. The DP is widely used to find the (near) optimal solution of many computer vision problems. The principle of DP is to solve a problem by studying a collection of sub-problems. Indeed, there have been some works in image segmentation that benefit from this efficient optimization technique, such as DP snake [64-65]. In the proposed DRM algorithm, we apply DP on discrete regions instead of line segments. The minimization problem for region Ri starting at labeling li 0 is defined as:

$$\min F_i(l_i^0, \cdots, l_i^n) = \min F_i(l_i^0, l_i^{n-1}) + d_{n-1,n}$$
$$= \min F_i(l_i^0, l_i^{n-2}) + d_{n-2,n-1} + d_{n-1,n}$$
$$= \cdots$$
$$= \sum_{k=0}^{n-1} d_{k,k+1}$$

(18)

Where $F_i(l_i^0,\ l_i^1,\ldots,\ l_i^n)$ is the transition cost from l_i^0 to l_i^n, dk,k+1 is the minimal edge weight between the regions with labeling l_i^k and l_i^{k+1}, respectively. In conjunction with Eq. (12), we have

$$d_{k,k+1} = \min_{R_{k+1}\in\Omega_k} S(R_k, R_{k+1})$$

(19)

The overall path length from l_i^0 to l_i^n n is the sum of minimum edges dk,k+1 for each node in that path. This problem reduces to a search for a shortest path problem, whose solution can be found at a finite set of steps by the Dijkstra's algorithm in polynomial time. At this point, a minimization process of objective function F is exactly described by the predicate P defined in Eq. (13), where P is true if the nodes are connected by the edge with the minimal weight in their neighborhood. It means that the closest neighbors will be assigned to the same label, which is the cause of the merging. In Fig. 3, an example process of region merging is shown by embedding it into a 3D graph. Between two adjacent layers there is a transition which indicates the costs of a path. Clearly, this is also a process of label transitions.[92] The neighborhood of the highlighted region (in red) is denoted as the black nodes in the graph and the closest neighbor is denoted as the red nodes. The directed connections with the lowest cost between adjacent layers are made (shown as blue arrows). Note that the connectivity between regions in the same layer is represented by the RAG, which is not explicitly shown in Fig.3.
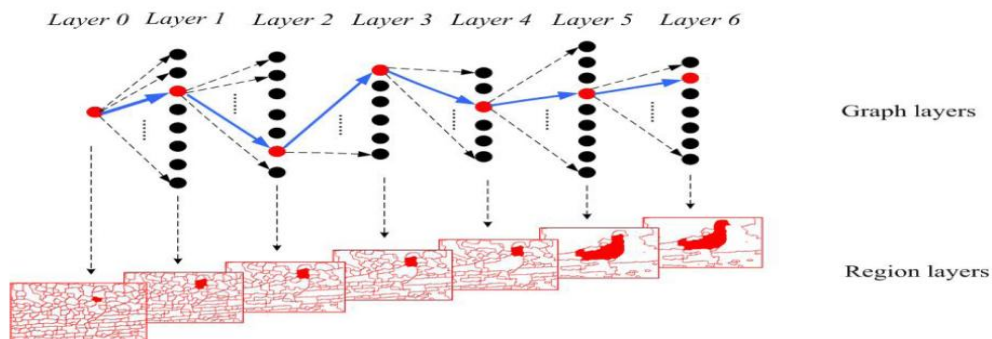
Fig 3. The dynamic region merging process as a shortest path in a layered graph.

The upper row shows the label transitions of a graph node. The lower row shows the corresponding image regions of each label layer. Starting from layer 0, the highlighted region (in red) obtains a new label from its closest neighbor (in red). If the region is merged with its neighbor, they will be assigned to the same label. The shortest path is shown as the group of the directed edges (in blue).

Algorithm 2: segmentation by dynamic region merging
Input: the initially over segmented image S0.
Output: region merging result.
1. Set i=0.
2. For each region in segmentation Si, use **Algorithm 1** to check the value of predicate P with respect to its neighboring regions.
3. Merge the pairs of neighboring regions whose predicate P is true, such that segmentation Si+1 is constructed.
4. Go back to step 2 until Si+1 = Si.
5. Return Si.

V.   CONCLUSIONS

In this paper, we have proposed a Bayesian approach to perform simultaneously image registration and pixel classification. The proposed technique is well-suited to deal with image pairs that contain two classes of pixels with different inter-image intensity relationships. We have shown through different experiments that the model can be applied in many different ways. For instance if the class map is known, then it can be used for template-based segmentation. If the full model is used (estimation of the class map, the registration and the parameters of the distribution of the outliers), then it can be applied to lesion detection by image comparison. In

this paper, we proposed a novel method for segmenting an image into distinct components. The proposed algorithm is implemented in a region merging style. We defined a merging predicate P for the evidence of a merging between two neighboring regions. This predicate was defined by the sequential probability ratio test (SPRT) and the maximum likelihood criterion. A dynamic region merging (DRM) was then presented to automatically group the initially over-segmented many small regions. Although the merged regions are chosen locally in each merge stage, some global properties are kept in the final segmentations. For the computational efficiency, we introduced an accelerated algorithm by using the data structure of region adjacency graph (RAG) and nearest neighbor graph (NNG). Experiments on natural images showed the efficiency of the proposed algorithm. There are several potential extensions to this work, such as the introduction of global refinement and user interaction, etc. Those will be further investigated in our future work.

REFERENCES

[1]. L. Brown, "A survey of image registration techniques," ACM Computing Surveys, vol. 24, pp. 325–376, 1992.

[2]. D. Hill, P. Batchelor, M. Holden, and D. J. Hawkes, "Medical image registration," Physics in Medicine and Biology, vol. 46, no. 3, pp. R1–R45, 2001.

[3]. J. Maintz and M. Viergever, "A survey of medical image registration," Medical Image Analysis, vol. 2(1), pp. 1–36, 1998.

[4]. P. Pluim, J. Maintz, and M. Viergever, "Mutual-information based registration of medical images : a survey," IEEE Transactions on Medical Imaging, vol. 22, no. 8, pp. 986–1004, 2003.

[5]. J. Modersitzki, Numerical Methods for Image Registration, ser. Numerical Mathematics And Scientific Computation, C. S. G. H. Golub and E. Suli, Eds. Oxford University Press, 2004.

[6]. R. Woods, J. Mazziotta, and S. R. Cherry, "MRI-PET registration with automate algorithm," Journal of Computer Assisted Tomography, vol. 17, no. 4, pp. 536–46, Jul-Aug 1993.

[7]. T. M. Buzug and J. Weese, "Voxel-based similarity measures for medical image registration in radiological diagnosis and image guided surgery," Journal of Computing and Information Technology, vol. 6, no. 2, pp. 165–179, 1998.

[8]. A. Roche, G. Malandain, X. Pennec, and N. Ayache, "The correlation ratio as a new similarity measure for multimodal image registration," in First Int. Conf. on Medical Image Computing and Computer-Assisted Intervention (MICCAI'98). vol. LNCS 1496. Cambridge, USA: Springer Verlag, October 1998, pp. 1115–1124.

[9]. C. Studholme, D. Hill, and D. J. Hawkes, "An overlap invariant entropy measure of 3D medical image alignment," Pattern Recognition, vol. 1, no. 32, pp. 71–86, 1999.

[10]. A. Roche, G. Malandain, and N. Ayache, "Unifying Maximum Likelihood Approaches in Medical Image Registration," International Journal of Computer Vision of Imaging Systems and Technology, vol. 11, pp. 71–80, 2000.

[11]. G. Malandain, "Les mesures de similarit´e pour le recalage des images m´edicales," Habilitation `a Diriger des Recherches, Universit´e de Nice Sophia-Antipolis, 2006.

[12]. P. Hayton, M. Brady, L. Tarassenko, and N. Moore, "Analysis of dynamic MR breast images using a model of contrast enhancement," Medical Image Analysis, vol. 1, pp. 207–224, 1997.

[13]. C. Tanner, J. A. Schnabel, D. Chung, M. J. Clarkson, D. Rueckert, D. Hill, and D. J. Hawkes, "Volume and shape preservation of enhancing lesions when applying non-rigid registration to a time series of contrast enhancing MR breast images," in MICCAI '00: Proceedings of the Third International Conference on Medical Image Computing and Computer- Assisted Intervention, London, UK, 2000, pp. 327–337.

[14]. T. Rohlfing and C. R. Maurer, Jr., "Intensity-based non-rigid registration using adaptive multilevel free-form deformation with an incompressibility constraint," in Proceedings of Fourth International Conference on Medical Image Computing and Computer-Assisted Intervention (MICCAI 2001), ser. Lecture Notes in Computer Science, W. Niessen and M. A. Viergever, Eds., vol. 2208. Berlin: Springer-Verlag, 2001, pp. 111–119. N. Sebe and M. Lew, Robust Computer Vision: Theory and Applications. Series: Computational Imaging and Vision, 2003, vol. 26.

[15]. P. Rousseeuw and A. Leroy, Robust Regression and Outlier Detection. Wiley, New York, 1987.

[16]. F. Hampel, E. Ronchetti, P. Rousseeuw, and W. Stahel, Robust Statistics: The Approach Based on Influence Functions. Wiley, New York, 1986.

[17]. D. Hawkins, Identifications of Outliers. Chapman & Hall, London, New York, 1980.

[18]. P. Huber, Robust Statistics. Wiley, New York, 1981.

[19]. F. Richard, "A new approach for the registration of images with inconsistent differences," in Proc. of the Int. Conf. on Pattern Recognition, ICPR, vol. 4, Cambridge, UK, 2004, pp. 649–652.

[20].   C. Nikou, F. Heitz, and J.-P. Armspach, "Robust voxel similarity metrics for the registration of dissimilar single and multimodal images," Pattern Recognition, vol. 32, pp. 1351–1368, 1999.

[21].   J. Kim, "Intensity based image registration using robust similarity measure and constrained optimization: Applications for radiation therapy," Ph.D. dissertation, University of Michigan, 2004.

[22].   M. Black, "Robust incremental optical flow," Ph.D. dissertation, Yale University, New Haven, CT, USA, 1992.

[23].   P. Meer, D. Mintz, A. Rosenfeld, and D. Kim, "Robust regression methods for computer vision: A review," International Journal of Computer Vision, vol. 6, no. 1, pp. 59–70, 1991.

[24].   M. Black and A. Rangarajan, "On the unification of line processes, outlier rejection, and robust statistics with applications in early vision," International Journal of Computer Vision, vol. 19, no. 1, pp. 57–91, 1996.

[25].   N. S. Netanyahu and I. Weiss, "Analytic outlier removal in line fitting," in 12th IAPR International Conference on Computer Vision and Image Processing, vol. 2B, 1994, pp. 406–408.

[26].   P. Schroeter, J.-M. Vesin, T. Langenberger, and R. Meuli, "Robust parameter estimation of intensity distributions for brain magnetic resonance images," IEEE Transactions on Medical Imaging, vol. 17, no. 2, pp. 172–186, 1998.

[27].   P. S. Torr, R. Szeliski, and P. Anandan, "An Integrated Bayesian Approach to Layer Extraction from Image Sequences," IEEE Transactions on Pattern Analysis and Machine Intelligence, vol. 23, no. 3, pp. 297–303, 2001.

[28].   D. Hasler, L. Sbaiz, S. Susstrunk, and M. Vetterli, "Outlier modeling in image matching," IEEE Transactions on Pattern Analysis and Machine Intelligence, pp. 301–315, 2003.

[29].   P. Biber, S. Fleck, and W. Straßer, "A probabilistic framework for robust and accurate matching of point clouds," in 26th Pattern Recognition Symposium (DAGM 04), 2004.

[30].   A. Jepson and M. Black, "Mixture models for optical flow computation," in IEEE Conference on Computer Vision andPattern Recognition, 1993, pp. 760–761.

[31].   M. Hachama, A. Desolneux, and F. Richard, "Combining registration and abnormality detection in mammography," in Workshop on Biomedical Image Registration, (WBIR'2006), ser. Lecture Notes in Computer Science, J. Pluim, B. Likar, and F. Gerritsen, Eds., vol. 4057. Springer, 2006, pp. 178–185.

[32].   H. Hachama, F. Richard, and A. Desolneux, "A mammogram registration technique dealing with outliers," in Proc. of the IEEE International Symposium on Biomedial Imaging (ISBI'2006), 2006, pp. 458–461.

[33].   M. Hachama, F. Richard, and A. Desolneux, "A probabilistic approach for the simultaneous mammogram registration and abnormality detection," in International Workshop on Digital Mammography (IWDM'2006), ser. Lecture Notes in Computer Science, S. Astley, M. Brady, C. Rose, and R. Zwiggelaar, Eds., vol. 4046. Springer, 2006, pp. 205–212.

[34].   N. Rougon, A. Discher, and F. Preteux, "Region-driven statistical non-rigid registration: application to model-based segmentation and tracking of the heart in perfusion MRI," in Proceedings SPIE Conference on Mathematical Methods in Pattern and Image Analysis, vol. 5916, San Diego, August 2005, pp. 148–159.

[35].   C. Studholme, D. Hill, and D. J. Hawkes, Eds., Incorporating Connected Region Labeling into Automated Image Registration Using Mutual Information, ser. Proceedings of the IEEE workshop on Mathematical Methods in Biomedical Image Analysis, San Francisco Ca. IEEE Computer Society Press, 1996.

[36].   J. Chappelow, B. Bloch, N. Rofsky, E. Genega, R. Lenkinski, W. DeWolf, and A. Madabhushi, "Elastic registration of multimodal prostate mri and histology via multiattribute combined mutual information." Med Phys, vol. 38, no. 4, pp. 2005–18, 2011.

[37].   P. Patel, J. Chappelow, J. Tomaszewski, M. Feldman, M. Rosen, N. Shih, and A. Madabhushi, "Spatially weighted mutual information (SWMI) for registration of digitally reconstructed ex vivo whole mount histology and in vivo prostate MRI," in IEEE International Conference of Engineering in Medicine and Biology Society (EMBS), 30 2011-sept. 3 2011, pp. 6269 –6272.

[38].   M. Hachama, A. Desolneux, C. Cuenod, and F. Richard, "A classifying registration technique for the estimation of enhancement curves of DCE-CT scan sequences," Medical Image Analysis, vol. 14, no. 2, pp. 185 – 194, 2010.

[39].   J. Ashburner and K. Friston, "Unified segmentation," NeuroImaging, vol. 26, pp. 839–851, 2005.

[40].   K. Pohl, J. Fisher, W. Grimson, R. Kikinis, and W. Wells, "A Bayesian model for joint segmentation and registration," NeuroImage, vol. 31, no. 1, pp. 228–239, 2006.

[41].   P. Wyatt and A. Noble, "MAP MRF Joint Segmentation and Registration of Medical Images," Medical Image Analysis, vol. 7, no. 4, pp. 539–552, 2003.

[42]. C. Xiaohua, M. Brady, J. L.-C. Lo, and N. Moore, "Simultaneous segmentation and registration of contrast-enhanced breast MRI," in Information Processing in Medical Imaging, 2005, pp. 126–137.

[43]. Y. Zheng, J. Yu, C. Kambhamettu, S. Englander, M. Schnall, and D. Shen, "De-enhancing the Dynamic Contrast-Enhanced Breast MRI for Robust Registration," in MICCAI, ser. Lecture Notes in Computer Science, N. Ayache, S. Ourselin, and A. Maeder, Eds., vol. 4791. Springer, 2007, pp. 933–941.

[44]. D. Mumford, "The Bayesian rationale for energy functionals," Geometry-driven Diffusion in Computer Vision, vol. 46, pp. 141–153, 1994.

[45]. C. A. Glasbey and K. V. Mardia, "A review of image-warping methods," Journal of Applied Statistics, vol. 25, no. 2, pp. 155–171, April 1998.

[46]. C. Broit, "Optimal registration of deformed images," Ph.D. dissertation, University of Pennsylvania, Philadelphia, 1981.

[47]. R. Bajcsy, R. Lieberson, and M. Reivich, "Computerized system for the elastic matching of deformed radiographic images to idealized atlas images," Journal of Computer Assisted Tomography, vol. 7, 1983.

[48]. R. Bajcsy and S. Kovacic, "Multiresolution elastic matching," Computer Vision, Graphics, and Image Processing, vol. 46, no. 1, pp. 1–21, 1989.

[49]. M. Miller, G. Christensen, Y. Amit, and U. Grenander, "Mathematical textbook of deformable neuroanatomies," Proc. Of the National Academy of Sciences, vol. 90, pp. 11 944–11 948, 1993.

[50]. Y. Amit, U. Grenander, and M. Piccioni, "Structural image restoration through deformable templates," American Statistical Association, vol. 86, no. 414, June 1991.

[51]. F. L. Bookstein, "Principal warps: Thin-plate splines and the decomposition of deformations," IEEE Transactions on Pattern Analysis and Machine Intelligence, vol. 11, no. 6, pp. 567–585, 1989.

[52]. S. Allassonni`ere, Y. Amit, and A. Trouv´e, "Towards a coherent statistical framework for dense deformable template estimation," Journal Of The Royal Statistical Society Series B, vol. 69, no. 1, pp. 3–29, 2007.

[53]. F. Richard, A. Samson, and C. Cuenod, "A SAEM algorithm for the estimation of template and deformation parameters in medical image sequences," Statistics and Computing, vol. 19, no. 4, pp. 465–478, 2009.

[54]. S. Geman and D. Geman, "Stochastic relaxation, Gibbs distributions, and the Bayesian restoration of images," IEEE Transactions on Pattern Analysis and Machine Intelligence, vol. 6, pp. 721–741, 1984.

[55]. B. Chalmond, Modelling and inverse problems in image analysis, ser. Applied mathematical sciences, Kindle, Ed. Springer, 2003, vol. 155.

[56]. M. Staring, S. Klein, and J. Pluim, "Nonrigid registration with tissue-dependent filtering of the deformation field," Physics in Medicine and Biology, vol. 52, pp. 6879–6892, 2007.

[57]. P. G. Ciarlet, The Finite Element Method for Elliptic Problems. Amsterdam: North-Holland Publishing Co., 1978.

[58]. J. Bonnans, J. Gilbert, C. Lemar´echal, and C. Sagastiz´abal, Numerical Optimization – Theoretical and Practical Aspects, ser. Universitext. Springer Verlag, Berlin, 2006.

[59]. D.A. Forsyth and J. Ponce, Computer Vision: A Modern Approach. Prentice Hall, 2002

[60]. L. Ladicky, C. Russell, P. Kohli, P. Torr. Associative Hierarchical CRFs for Object Class Image Segmentation. In: ICCV 2009.

[61]. F, Lecumberry, A, Pardo and G. Sapiro. Simultaneous object classification and segmentation with high-order multiple shape models. IEEE Transactions on Image Processing. pp: 625 - 635, 2010.

[62]. R.C. Gonzalez and R.E. Woods. Digital Image Processing. Addison Wesley, Reading, MA, 1992.

[63]. J. Canny. A Computational Approach to Edge Detection, IEEE Trans. Pattern Analysis and Machine Intelligence, vol. 8, pp. 679-698, 1986.

[64]. B. Paul, L. Zhang and X. Wu, "Canny edge detection enhancement by scale multiplication," IEEE. Trans. on Pattern Analysis and Machine Intelligence, vol. 27, pp. 1485-1490, Sept. 2005.

[65]. L. Zhang, B. Paul, et al, "Edge detection by scale multiplication in wavelet domain," Pattern Recognition Letters, vol. 23, pp. 1771-1784, 2002.

[66]. J. Shi and J. Malik. Normalized Cuts and Image Segmentation. IEEE Transactions on Pattern Analysis and Machine Intelligence (PAMI) 2000.

[67]. S. Wang, J. M. Siskind. Image Segmentation with Ratio Cut, IEEE Transactions on Pattern Analysis and Machine Intelligence, 25(6):675-690, 2003.

[68]. Z. Wu and R. Leahy. An optimal graph theoretic approach to data clustering Theory and its application to image segmentation. IEEE Transactions on Pattern Analysis and Machine Intelligence. November 1993.

[69]. H. D Cheng, Y. Sun. A hierarchical approach to color image segmentation using homogeneity. IEEE Transactions on Image Processing. Volume: 9 , Issue: 12, page(s): 2071-2082, 2000.

[70]. S. Lee; M.M. Crawford. Unsupervised multistage image classification using hierarchical clustering with a bayesian similarity measure. IEEE Transactions on Image Processing. Page(s): 312 -320, 2005.

[71]. A. Moore, S. J. D. Prince, J. Warrell, U. Mohammed, and G. Jones. Superpixel lattices. CVPR, 2008.

[72]. A. Moore, S. J. D. Prince, J. Warrell, U. Mohammed, and G. Jones. Scene shape priors for superpxiel segmentation. ICCV, 2009.

[73]. A. Moore, S. Prince . "Lattice Cut" - Constructing superpixels using layer constraints. CVPR 2010.

[74]. R. Nock and F. Nielsen. Statistic region merging. IEEE Trans. on Pattern Analysis and Machine Intelligence, vol 26, pages 1452-1458, 2004.

[75]. K. Haris and S. N. Estradiadis and N. Maglaveras and A. K. Katsaggelos. Hybrid image segmentation using watersheds and fast region merging. IEEE Transactions on Image Processing, vol 7, pp. 1684-1699, Dec. 1998.

[76]. P.F. Felzenszwalb and D.P. Huttenlocher. Efficient Graph-Based Image SegmentationInternational Journal of Computer Vision. Vol. 59, Number 2, September 2004.

[77]. B. Peng, L. Zhang and J. Yang, Iterated Graph Cuts for Image Segmentation. In Asian Conference on Computer Vision, 2009.

[78]. Moscheni, F. Bhattacharjee, S. Kunt, M. Spatio-temporal segmentation based on region merging. IEEE Transactions on Pattern Analysis and Machine Intelligence. Vol. 20, pages: 897-915. Sep 1998.

[79]. J. Ning, L. Zhang, D. Zhang and C. Wu. Interactive Image Segmentation by Maximal Similarity based Region Merging. Pattern Recognition, vol. 43, pp. 445-456, Feb, 2010.

[80]. F. Calderero, F. Marques. Region merging techniques using information theory statistical measures. IEEE Transactions on Image Processing. Volume: 19 , Issue: 6. page(s): 1567-1586, 2010.

[81]. F. Calderero, F. Marques. General region merging approaches based on information theory statistical measures. The 15th IEEE International Conference on Image Processing (ICIP). pp: 3016-3019, 2008.

[82]. H. Liu, Q. Guo, M, Xu, I. Shen. Fast image segmentation using region merging with a k-Nearest Neighbor graph. IEEE Conference on Cybernetics and Intelligent Systems. Page(s): 179-184, 2008.

[83]. Y. Shu, G. A. Bilodeau, F. Cheriet. Segmentation of laparoscopic images: integrating graph-based segmentation and multistage region merging. The 2nd Canadian Conference on Computer and Robot Vision, 2005.

[84]. I.E. Gordon, Theories of Visual Perception, first ed. John Wiley and Sons, 1989.

[85]. K. Koffka. Principles of Gestalt Psychology. New York: Harcourt, Brace and World. 1935.

[86]. A. Wald. Sequential Analysis. Wiley Publications in Statistics, Third ed. Wiley, 1947.

[87]. Z. Wu, Homogeneity testing for unlabeled data: A performance evaluation, CVGIP: Graph. Models Image Process., vol. 55, pp. 370-380, Sept. 1993.

[88]. A. Trémeau and P. Colantoni. Regions adjacency graph applied to color image segmentation. IEEE Transactions on Image Processing. Vol. 9, pp. 735-744, 2000.

[89]. L. Vincent, P. Soille, Watersheds in digital spaces: an efficient algorithm based on immersion simulations, IEEE Transactions on Pattern Analysis and Machine Intelligence 13 (6) 583–598, 1991.

[90]. D. Comanicu, P. Meer. Mean shift: A robust approach toward feature space analysis. IEEE Trans. On Pattern Analysis and Machine Intelligence, 24, 603-619, May 2002.

[91]. Bellman, Richard, Dynamic Programming, Princeton University Press, 1957.

Research Paper   Open Access

Biomedical Image Processing with Morphology and Segmentation Methods for Medical Image Analysis

Joyjit Patra[1], Himadri Nath Moulick[2], Arun Kanti Manna[3]
[1](C.S.E, Aryabhatta Institute Of Engineering And Management,Durgapur,West Bengal,India)
[2](C.S.E, Aryabhatta Institute Of Engineering And Management,Durgapur,West Bengal,India)
[3](C.S.E,Modern Institue Of Engineering & Technology,Bandel,Hoogly,West Best Bengal,India)

*Abstract: - Modern three-dimensional (3-D) medical imaging offers the potential and promise for major advances in science and medicine as higher fidelity images are produced.It has developed into one of the most important fields within scientific imaging due to the rapid and continuing progress in computerized medical image visualization and advances in analysis methods and computer-aided diagnosis[1],and is now,for example,a vital part of the early detection,diagnosis, and treatment of cancer.The challenge is to effectively process and analyze the images in order to effectively extract, quantify,and interpret this information to gain understanding and insight into the structure and function of the organs being imaged.The general goal is to understand the information and put it to practical use.A multitude of diagnostic medical imaging systems are used to probe the human body.They comprise both microscopic (viz. cellular level) and macroscopic (viz.organ and systems level) modalities.Interpretation of the resulting images requires sophisticated image processing methods that enhance visual interpretation and image analysis methods that provide automated or semi-automated tissue detection,measurement, and characterization [2–4].In general,multiple transformations will be needed in order to extract the data of interest from an image,and a hierarchy in the processing steps will be evident, e.g., enhancement will precede restoration,which will precede analysis,feature extraction,and classification[5].Often,these are performed sequentially, but more sophisticated tasks will require feedback of parameters to preceding steps so that the processing includes a number of iterative loops.Segmentation is one of the key tools in medical image analysis.The objective of segmentation is to provide reliable, fast, and effective organ delineation.While traditionally, particularly in computer vision, segmentation is seen as an early vision tool used for subsequent recognition, in medical imaging the opposite is often true. Recognition can be performed interactively by clinicians or automatically using robust techniques, while the objective of segmentation is to precisely delineate contours and surfaces. This can lead to effective techniques known as "intelligent scissors" in 2D and their equivalent in 3D. This paper divided as follows. starts off with a more "philosophical" section setting the background for this study. We argue for a segmentation context where high-level knowledge, object information, and segmentation method are all separate. we survey in some detail a number of segmentation methods that are well-suited to image analysis, in particular of medical images.We illustrate this, make some comparisons and some recommendations. we introduce very recent methods that unify many popular discrete segmentation methods and we introduce a new technique. we give some remarks about recent advances in seeded, globally optimal active contour methods that are of interest for this study. we compare all presented methods qualitatively. We then conclude and give some indications for future work.
Nonlinear filtering techniques are becoming increasingly important in image processing applications, and are often better than linear filters at removing noise without distorting image features. However, design and analysis of nonlinear filters are much more difficult than for linear filters. One structure for designing nonlinear filters is mathematical morphology, which creates filters based on shape and size characteristics. Morphological filters are limited to minimum and maximum operations that introduce bias into images. This precludes the use of morphological filters in applications where accurate estimation of the true gray level is necessary.
This work develops two new filtering structures based on mathematical morphology that overcome the limitations of morphological filters while retaining their emphasis on shape. The linear combinations of morphological filters eliminate the bias of the standard filters, while the value-and-criterion filters allow a*

variety of linear and nonlinear operations to be used in the geometric structure of morphology. One important value-and-criterion filter is the Mean of Least Variance (MLV) filter, which sharpens edges and provides noise smoothing equivalent to linear filtering. To help understand the behavior of the new filters, the deterministic and statistical properties of the filters are derived and compared to the properties of the standard morphological filters. In addition, new analysis techniques for nonlinear filters are introduced that describe the behavior of filters in the presence of rapidly fluctuating signals, impulsive noise, and corners. The corner response analysis is especially informative because it quantifies the degree to which a filter preserves corners of all angles.Examples of the new nonlinear filtering techniques are given for a variety of medical images, including thermographic, magnetic resonance, and ultrasound images. The results of the filter analyses are important in deciding which filter to use for a particular application. For thermography, accurate gray level estimation is required, so linear combinations of morphological operators are appropriate. In magnetic resonance imaging (MRI), noise reduction and contrast enhancement are desired. The MLV filter performs these tasks well on MR images. The new filters perform as well or better than previously established techniques for biomedical image enhancement in these applications.

I.　　INTRODUCTION

The major strength in the application of computers to medical imaging lies in the use of image processing techniques for quantitative analysis. Medical images are primarily visual in nature; however, visual analysis by human observers is usually associated with limitations caused by interobserver variations and errors due to

fatigue, distractions, and limited experience. While the interpretation of an image by an expert draws from his/her experience and expertise, there is almost always a subjective element. Computer analysis, if performed with the appropriate care and logic, can potentially add objective strength to the interpretation of the expert. Thus,it becomes possible to improve the diagnostic accuracy and confidence of even an expert with many years of experience.Imaging science has expanded primarily along three distinct but related lines of investigation: segmentation, registration and visualization [6]. Segmentation, particularly in three dimensions, remains the holy grail of imaging science. It is the important yet elusive capability to accurately recognize and delineate all the individual objects in an image scene. Registration involves finding the transformation that brings different images of the same object into strict spatial (and/or temporal) congruence.And visualization involves the display, manipulation, and measurement of image data. A common theme throughout this book is the differentiation and integration of images. On the one hand, automatic segmentation and classification of tissues provide the required differentiation, and on the other the fusion of complementary images provides the integration required to advance our understanding of life processes and disease. Measurement of both form and function, of the whole image and at the individual pixel level, and the ways to display and manipulate digital images are the keys to extracting the clinical information contained in biomedical images.The need for new techniques becomes more pressing as improvements in imaging technologies enable more complex objects to be imaged and simulated.

The approach required is primarily that of problem solving. However, the understanding of the problem can often require a significant amount of preparatory work.The applications chosen for this book are typical of those in medical imaging; they are meant to be exemplary, not exclusive. Indeed, it is hoped that many of the solutions presented will be transferable to other problems. Each application begins with a statement of the problem, and includes illustrations with real-life images. Image processing techniques are presented, starting with relatively simple genericmethods, followed bymore sophisticated approaches directed at that specific problem.The benefits and challenges in the transition from research to clinical solution are also addressed.Biomedical imaging is primarily an applied science, where the principles of imaging science are applied to diagnose and treat disease, and to gain basic insights into the processes of life.The development of such capabilities in the research.laboratory is a time-honored tradition. The challenge is to make new techniques available outside the specific laboratory that developed them, so that others can use and adapt them to different applications. The ideas, skills and talents of specific developers can then be shared with a wider community and this will hopefully facilitate the transition of successful research technique into routine clinical use.Nonlinear methods in signal and image processing have become increasingly popular over the past thirty years.There are two general families of nonlinear filters: the homomorphic and polynomial filters, and the order statistic and morphological filters [1]. Homomorphic filters were developed during the 1970's and obey a generalization of the superposition principle [2]. The polynomial filters are based on traditional nonlinear system theory and use Volterra series. Analysis and design of homomorphic and polynomial filters resemble traditional methods used

for linear systems and filters in many ways.The order statistic and morphological filters, on the other hand, cannot be analyzed efficiently using generalizations of linear techniques.The median filter is an example of an order statistic filter, and is probably the oldest [3, 4] and most widely used order statistic filter. Morphological filters are based on a form of set algebra known as mathematical morphology. Most morphological filters use extreme order statistics (minimum and maximum values) within a filter window, so they are closely related to order statistic filters [5, 6].While homomorphic and polynomial filters are designed and analyzed by the techniques used to define them, order statistic filters are often chosen by more heuristic methods. As a result, the behavior of the median filter and other related filters was poorly understood for many years. In the early 1980's, important results on the statistical behavior of the median filter were presented [7], and a new technique was developed that defined the class of signals invariant to median filtering, the root signals [8, 9]. Morphological filters are derived from a more rigorous mathematical background [10-12], which provides an excellent basis for design but few tools for analysis. Statistical and deterministic analyses for the basic morphological filters were not published until 1987 [5, 6, 13].The understanding of the filters' behavior achieved by these analyses is not complete, however, so further study may help determine when morphological filters are best applied.

II.   MEDIAN FILTER ROOT SIGNALS

The median filter is an order statistic (stack) filter that replaces the center value in the filter window with the median of the values in the window. If the values in the window are updated as the filter acts on the signal, it is called a recursive median filter. Non-recursive median filtering, which is far more common than recursive median filtering, always acts on the original values in the signal. For a signal $f(\mathbf{x})$ and a filter window W, the non-recursive median filter is denoted as shown in equation (1) below:

$$\text{med}(f; W)(\mathbf{x}) = \text{median}\{f(\mathbf{y}): \quad \mathbf{y} \in W_{\mathbf{x}}\}$$
$$\text{where} \quad W_{\mathbf{x}} = \{\mathbf{x} + \mathbf{a}: \quad \mathbf{a} \in W\} \text{ is the window } W \text{ centered at } \mathbf{x}. \quad \dots\dots\dots(1)$$

Repeated application of the median filter is denoted by a superscript; for example, med3(f; W) denotes the result of three iterations of the non-recursive median filter with window W over the signal f. The root signal set of the 1-D median filter for finite-length signals consists only of signals that are everywhere locally monotonic of length $n + 2$, where W is $2n+1$ points long $W = 2n(+1)$[8, 9]. This means that any section of a finite-length median root signal of at least $n + 2$ points is monotonic (nonincreasing or nondecreasing). This result assumes the signal is padded appropriately with constant regions to obtain the filter output near the ends, as described previously. Gallagher and Wise [9] stated the same result slightly differently: a finite-length median root signal consists only of constant neighborhoods and edges. A constant neighborhood is an area of constant value of at least length $n + 1$ (just over half the length of W) and an edge is a monotonic region of any length between two constant neighborhoods.This root signal set indicates that the median filter preserves slowly varying regions and sharp edges, but alters impulses and rapid oscillations. For infinite-length signals, Tyan [8] showed that another type of root signal exists for the non-recursive median filter. These root signals, the "fastfluctuating" roots, consist solely of rapid oscillations between two values. Nowhere in these signals is there even one monotonic region of length $n + 1$. For example, the infinite-length signal ..., 1, 0, 1, 0, 1, 0, 1, 0, ... is a root of the nonrecursive median filter with a window width of $4k+1$, where k is any positive integer. Although this type of signal is seldom encountered in practical applications, sections of a finite-length signal that fluctuate quickly (even if they are not bi-valued) are often passed by the median filter without much smoothing. An example of this situation is shown in Figure 1. The original signal has an oscillation in it, and when filtered by a 5-wide median filter only the first and last two peaks in the oscillation are smoothed.
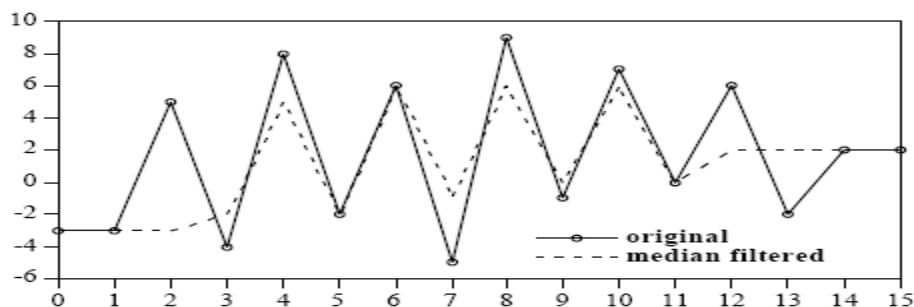

Figure 1. Oscillatory signal filtered by a 5-wide non-recursive median filter.

Gallagher and Wise [9] showed that repeated iteration of the non-recursive median filter on a signal of length L reduces the signal to a root signal in at most $(L–2)/2$ passes. This result comes from the observation that on the first pass, the first and last values must be unchanged; on succeeding passes, the area at the beginning and end of the signal that is unchanged by filtering is at least one point longer. Figure 1 also illustrates how oscillatory signals are reduced to a root a few points at a time from either end. The root signal resulting from repeated iteration of the non-recursive median filter is denoted med∞(f; W). Although the number of passes required to reduce most signals to a median root is fairly small, in some instances the number of passes required is very large.The recursive median filter yields a root signal from any input signal in a single pass; however, the resulting root is usually not as good a representation of the original signal as med∞(f; W). This is because the recursive filter allows signal values to propagate along the signal sequence, so that the output value at any point is not necessarily related to the values currently in the filter window.The recursive median filter is rarely used in practice for this reason. Figure 2 is an example of 5-wide recursive median filtering on the same signal as in Figure1. The result is a root signal, but it is very different from the result of nonrecursive median filtering.
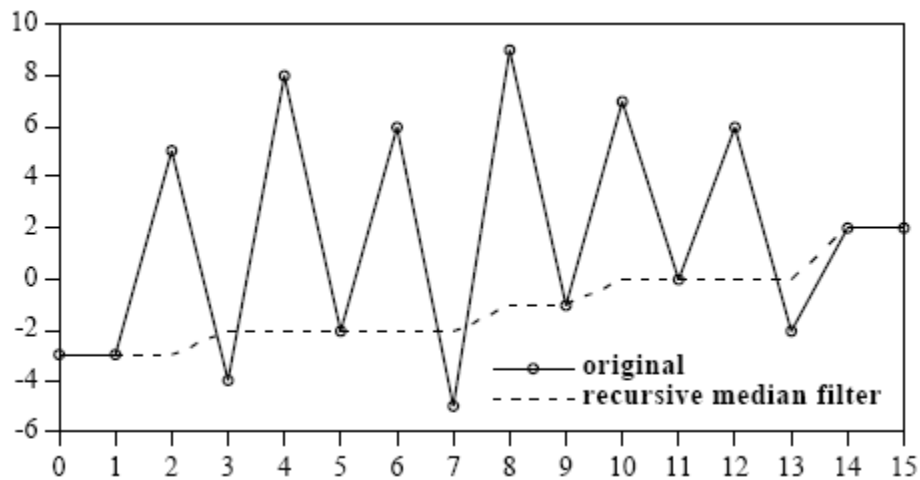

Figure 2. Oscillatory signal filtered by a 5-wide recursive median filter.

III.   INEAR COMBINATIONS OF MORPHOLOGICAL OPERATORS

Since the complementary morphological operators (OC and CO; opening and closing; erosion and dilation) are equally and oppositely biased, an obvious way to try to remove the bias is by simply taking the average of the two operators. For symmetric input noise distributions, an evenly weighted average clearly should give an unbiased result; however, for asymmetric distributions an unequally weighted average of the two operators may work better for removing the bias.This chapter describes the various types of linear combinations of morphological operators and illustrates how they alleviate some of the bias problems of standard morphological filters. Theorems describing the root signal sets of these linear combinations are presented, and approximations for the statistical properties of the filters are also given and compared to the properties of the standard morphological filters.

Midrange Filter
The midrange filter is defined as the average of the maximum and the minimum values in a filter window, the midpoint of the range of values in the window. Since the erosion is a sliding minimum operation acting over the window N and dilation is a sliding maximum operation acting over the same window, another form of the midrange filter is the average of the two basic morphological operators, erosion and dilation. The midrange filter is a wellknown estimator in the order statistics literature; see, for example, [25-27]. The midrange filter is optimal in the mean square sense among all filters that are linear combinations of order statistics for removing uniformly distributed noise from a constant signal [26]. The midrange filter is also the maximum likelihood estimator for uniformly distributed noise [26].The notation for the midrange filter is given in equation (9) below.

$$\text{midr}(f, N) = \frac{1}{2}(f \boxminus \tilde{N} + f \boxminus \tilde{N})$$

…………(2)

Pseudomedian Filter

The pseudomedian filter was originally defined in 1985 by Pratt, Cooper, and Kabir [28]. They defined the filter in one dimension to be the average of the maximum of the minima of $n+1$ subwindows within an overall window and the minimum of the maxima of the same subwindows. Each subwindow is $n+1$ points long, and is within an overall window of length $2n+1$. This structure corresponds to that of morphological opening and closing: the subwindows are the structuring elements N, and the overall window is W. Pratt recast the definition of the pseudomedian filter in his 1991 text [29] by forming the "maximin" and "minimax" functions, which he averages to find the pseudomedian. The maximin and minimax functions are equivalent to morphological opening and closing. The 1-D pseudomedian filter is therefore the average of the opening and closing, as noted previously by this author [30]. Pratt defined a two-dimensional pseudomedian filter in a manner that does not correspond to 2-D opening and closing; however, other work by the author [31, 32] generalized the pseudomedian filter to two dimensions in a manner corresponding to the definition of the pseudomedian as the average of opening and closing. The notation for pseudomedian filter is given in equation (10) below.

$$\text{pmed}(f, N) = \frac{1}{2}(f_N + f^N)$$

…………..(3)

Pseudomedian Filter

The deterministic behavior of the pseudomedian filter is quite different from that of the midrange filter. Theorem 3.15 below proves that the root signal set of the pseudomedian filter for bounded signals includes only signals that consist entirely of constant neighborhoods and edges.

Theorem 3.15: A bounded root signal of the pseudomedian filter consists only of constant neighborhoods and edges.

Proof: Suppose $f(\mathbf{x})$ is a root signal of the pseudomedian filter with structuring element N of length $|N| = n+1$; that is, $f(\mathbf{x}) = \text{pmed}(f(\mathbf{x}); N)$.

This proof will proceed by defining three possible cases for the root signals. The opening and closing of the signal may be equal at all points, or may be unequal at all points, or may be equal at some points and unequal at others. The case where opening and closing are equal at all points corresponds to the root signals consisting of constant neighborhoods and edges. The other two cases show that there are not roots where the opening and closing are unequal at all points or where opening and closing are equal at some points and unequal at other points.

Case I: $f_N(\mathbf{x}) = f^N(\mathbf{x})$ for all $\mathbf{x}$.

Together, the definition of the pseudomedian filter and the above assumption imply that

$$f_N(\mathbf{x}) = f^N(\mathbf{x}) = f(\mathbf{x})$$

for all $\mathbf{x}$.

$f(\mathbf{x})$ of the pseudomedian filter is everywhere LOMO($n+2$); that is, $f(\mathbf{x})$ consists only of constant neighborhoods and edges.

Case II: $fN(\mathbf{x}) \neq f N(\mathbf{x})$ for all $\mathbf{x}$.

First, assume that there exists a point $\mathbf{x}1$ such that $f(\mathbf{x}_1) = (f \mathbf{K} \ \tilde{N})(\mathbf{x}_1)$. By Theorem 6, $fN(\mathbf{x}1) = f(\mathbf{x}1)$. Then, by the definition of the pseudomedian filter, $fN(\mathbf{x}1) = f N(\mathbf{x}1)$, which is a contradiction. Similarly, if there is a point $\mathbf{x}2$ such that $f(\mathbf{x}_2) = (f \mathbf{D} \ \tilde{N})(\mathbf{x}_2)$ then $f N(\mathbf{x}2) = f(\mathbf{x}2)$. Again, $fN(\mathbf{x}2) = f N(\mathbf{x}2)$, which is a contradiction. Therefore, for Case II there can be no point $\mathbf{x}$ where $f(\mathbf{x})$ is equal to the erosion, dilation, opening, or closing at $\mathbf{x}$. $fN(\mathbf{x})$ and $f N(\mathbf{x})$ are then infinitely long and n-monotonic everywhere. $f N(\mathbf{x}) \geq fN(\mathbf{x})$, so the closing and opening must be both increasing or both decreasing, since any infinite n-monotonic increasing signal must be greater than any infinite n-monotonic decreasing signal as $\mathbf{x} \to +\infty$ and less than any infinite n-monotonic decreasing signal as $\mathbf{x} \to -\infty$. The average of two signals that are n-monotonic and either both increasing or both decreasing is a signal that is n-monotonic. Therefore, the pseudomedian of a signal $f(\mathbf{x})$ that satisfies $fN(\mathbf{x}) \neq f N(\mathbf{x})$ for all $\mathbf{x}$ is an $n$monotonic signal. However, if $f(\mathbf{x})$ is n-monotonic, then $fN(\mathbf{x}) = f(\mathbf{x}) = f N(\mathbf{x})$, which is a contradiction of $fN(\mathbf{x}) \neq f N(\mathbf{x})$. Therefore, there exist no root signals of the pseudomedian filter that satisfy Case II.

Seed-Driven Segmentation

Segmentation is a fundamental operation in computer vision and image analysis. It consists of identifying regions of interests in images that are semantically consistent.Practically, this may mean finding individual white blood cells amongst red blood cells; identifying tumors in lungs; computing the 4D hyper-surface of a beating heart, and so on. Applications of segmentation methods are numerous. Being able to reliably and readily characterize organs and objects allows practitioners to measure them, count them and identify them. Many images analysis problems begin by a segmentation step, and so this step conditions the quality of the end results. Speed and ease of use are essential to clinical practice. This has been known for quite some time, and so *numerous* segmentation methods have been proposed in the literature [57]. However, segmentation is a difficult problem. It usually requires high-level knowledge about the objects under study. In fact, semantically consistent, high-quality segmentation, in general, is a problem that is indistinguishable from strong Artificial Intelligence and has probably no exact or even generally agreeable solution. In medical imaging, experts often disagree amongst themselves on the placement of the 2D contours of normal organs, not to mention lesions. In 3D, obtaining expert opinion is typically difficult, and almost impossible if the object under study is thin, noisy and convoluted, such as in the case of vascular systems. At any rate, segmentation is, even for humans, a difficult, time-consuming and error-prone procedure.

Image Analysis and Computer Vision

Segmentation can be studied from many angles. In computer vision, the segmentation task is often seen as a low-level operation, which consists of separating an arbitrary scene into reasonably alike components (such as regions that are consistent in terms of color, texture and so on). The task of grouping such component into semantic objects is considered a different task altogether. In contrast, in image analysis, segmentation is a high-level task that embeds high-level knowledge about the object. This methodological difference is due to the application field. In computer vision, the objective of segmentation (and grouping) is to recognize objects in an arbitrary scene, such as persons, walls, doors, sky, etc. This is obviously extremely difficult for a computer, because of the generality of the context, although humans do generally manage it quite well. In contrast, in image analysis, the task is often to *precisely* delineate some objects sought in a particular setting known in advance. It might be for instance to find the contours of lungs in an X-ray photograph. The segmentation task in image analysis is still a difficult problem, but not to the same extent as in the general vision case. In contrast to the vision case, experts might agree that a lesion is present on a person's skin, but may disagree on its exact contours [45]. Here, the problem is that the boundary between normal skin and lesion might be objectively difficult to specify. In addition, sometimes there does exist an object with a definite physical contour (such as the inner volume of the left ventricle of the heart). However, imaging modalities may be corrupted by noise and partial volume effects to an extent that delineating the precise contours of this physical object in an image is also objectively difficult.

Objects Are Semantically Consistent

However, in spite of these difficulty, we may assume that, up to some level of ambiguity, an object (organ, lesion, etc) may still be specified somehow. This means that semantically, an object possess some consistency.When we point at a particular area on an image, we expect to be, again with some fuzziness, either inside or outside the object This leads us to the realize that there must exist some mathematical indicator function, that denotes whether we are inside or outside of the object with high probability. This indicator function can be considered like a series of constraints, or labels. They are sometimes called *seeds* or *markers*, as they provide starting points for segmentation procedures, and they mark where objects are and are not. In addition, a *metric* that expresses the consistency of the object is likely to exist. A gradient on this metric may therefore provide object contour information. Contours may be weak in places where there is some uncertainty, but we assume they are not weak everywhere (else we have an ambiguity problem, and our segmentation cannot be precise). The metric may simply be the image intensity or color, but it may express other information like consistency of texture for instance. Even though this metric may contain many descriptive elements (as a vector of descriptors for instance), we assume that we are still able to compute a gradient on this metric [61]. This is the reason why many segmentation methods focus on contours, which are essentially discontinuities in the metric. Those that focus on regions do so by defining and utilizing some consistency metric, which is the same problem expressed differently. The next and final step for segmentation is the actual contour placement, which is equivalent to object delineation. This step can be considered as an optimization problem, and this is the step on which segmentation methods in the literature focus the most. We will say more about this in Sect. 3.2 listing some image segmentation categories.

Desirable Properties of Seeded Segmentation Methods

We come to the first conclusion that to provide reliable and accurate results, we must rely on a segmentation procedure and not just an operator. Object identification and constraints analysis will set us in good stead to achieve our results, but not all segmentation operators are equivalent.We can list here some desirable properties of interactive segmentation operators. • It is useful if the operator can be expressed in an energy or cost optimization formulation. It is then amenable to existing optimizationmethods, and this entails a number of benefits. Lowering the cost or the energy of the formulation can be done in several ways (e.g. continuous or discrete optimization), which results in different characteristics and compromises, say between memory resources and time. Optimizationmethods improve all the time through the work of researchers,and so our formulations will benefit too.

• It is desirable if the optimization formulation can provide a solution that is at least locally optimal, and if possible globally optimal, otherwise noise will almost certainly corrupt the result.

• The operator should be fast, and provide guaranteed convergence, because it will be most likely restarted several times, in order to adjust parameters. Together with this requirement, the ability to segment many objects at once is also desirable, otherwise the operator will need to be restarted as many time as there are objects in the image. This may not be a big problem if objects do not overlap and if bounding boxes can be drawn around them, because the operator can then be run only within the bounding box, but this is not the general case.

• The operator should be bias-free: e.g. with respect to objects size or to the discretization grid or with respect to initialization.

• The operator should be flexible: it is useful if it can be coupled with topology information for instance, or with multi-scale information.

• It should be generic, not tied to particular data or image types.

• It should be easy to use. This in practice means possessing as few parameters as possible. Of course one can view constraints setting as an enormous parameter list, but this is the reason why we consider this step as separate. Such a method certainly does not yet exist to our knowledge, although some might be considered to come close. We describe some of them in the next section.

Pixel Selection

Pixel selection is likely the oldest segmentation method. It consists of selecting pixels solely based on their values and irrespective of their spatial neighborhood. The simplest pixel selection method is humble thresholding, where we select pixels that have a gray-level value greater or smaller than some threshold value. This particular method is of course very crude, but is used frequently nonetheless. Multiple thresholding uses several values instead of a single value; color and multispectral thresholding using vectors of values and not just scalars. By definition all histogram-based methods for finding the parameters of the thresholding, including those that optimize a metric to achieve this [54], are pixel selection methods.Statistical methods (e.g. spectral classification methods) that include no spatial regularization fall into this category as well. This is therefore a veritable plethora of methods that we are including here, and research is still active in this domain. Of course, thresholding and related methods are usually very fast and easily made interactive, which is why they are still used so much. By properly pre-processing noisy, unevenly illuminated images, or by other transforms, it is surprising how many problems can be solved by interactive or automated thresholding. However, this is of course not always the case, hence the need for more sophisticated methods.

Contour Tracking

It was realized early on that (1) human vision is sensitive to contours and (2) there is a duality between simple closed contours and objects. A simple closed contour (or surface) is one that is closed and does not self-intersect. By the Jordan theorem, in the Euclidean space, any such contour or surface delineates a single object of finite extent. There are some classical difficulties with the Jordan theorem in the discrete setting [52], but they can be solved by selecting proper object/background connectivities, or by using a suitable graph, for instance, the 6-connected hexagonal grid or the Khalimsky topology [22, 40]. A contour can be defined locally (it is a frontier separating two objects (or an object and its background in the binary case)), while an object usually cannot (an object can have an arbitrary extent). A gradient (first derivative) or a Laplacian (second derivative) operator can be used to define an object border in many cases, and gradients are less sensitive to illumination conditions than pixel values. As a result, contour detection through the use of gradient or Laplacian operators became popular, and eventually led to the Marr–Hildreth theory [44]. Given this, it is only natural that most segmentation method use contour information directly in some ways, and we will revisit this shortly. Early methods used *only* this information to detect contours and then tried to combine them in some way. By far the most popular and successful version of this approach is the Canny edge detector [9]. In his classical paper, Canny proposed a closed-form optimal 1D edge detector assuming the presence of additive white Gaussian

noise, and successfully proposed a 2D extension involving edge tracking using non-maxima suppression with hysteresis.One problem with this approach is that there is no optimality condition in 2D, no topology or connectivity constraints and no way to impose markers in the final result. All we get is a series of contours, which may or may not be helpful. Finding a suitable combination of detected contours (which can be incomplete) to define objects is then a combinatorial problem of high complexity. Finally, this approach extends even less to 3D.Overall, in practical terms, these contour tracking methods have been superseded by more recent methods and should not be used without good reasons. For instance, more recent minimal-path methods can be applied to contour tracking methods, although they are much more sophisticated in principle [3, 14]. In this class of methods belongs also the "intelligent scissors" types. There were many attempts in previous decades to provide automated delineating tools in various image processing software packages, but a useful contribution was provided relatively recently by Mortensen [48]. This method is strictly interactive, in the sense that it is designed for human interaction and feedback. "Intelligent scissor" methods are useful to clinicians for providing ground truth data for instance. Such methods are still strictly 2D. As far as we know, no really satisfying 3D live-wire/intelligent scissor method is in broad use today [5]. However, minimal surfaces methods, which we will describe, in some ways do perform this extension to nD [30].

Continuous Optimization Methods

In the late 1980s, it was realized that contour tracking methods were too limited for practical use. Indeed, getting closed contours around objects were difficult to obtain with contour tracking. This meant that detecting actual objects was difficult except in the simplest cases.

Active Contours

Researchers, therefore, proposed to start from already-closed loops, and to make them evolve in such a way that they would converge towards the true contours of the image. Thus were introduced *active contours*, or *snakes* [39]. The formulation of snakes takes the following continuous-domain shape:

$$E_{\text{snake}} = \int_0^1 \left\{ E_{\text{internal}}(\mathbf{v}(s)) + E_{\text{data}}(\mathbf{v}(s)) + E_{\text{constraints}}(\mathbf{v}(s)) \right\} ds.$$

………………….(4)

where $\mathbf{v}(s)$ is a parametric representation of the contour.
This model is very flexible. It contains internal terms, image data terms and constraints terms :
• The first term, the internal energy, contains a curvature term and a "rubber band"energy. The former tends to smooth the resulting contour following a thin plate,while the latter tends to make it shrink around features of interest. Other terms such as kinetic energy can be added too, which makes it possible for the snake to avoid noisy zones and flat areas.
• The second term, the data energy, attracts the active contours towards points of interest in the image: typically, image contours (zones of high gradient), lines or termination points.
• The last term, the constraint term, is optional, but allows interaction with the snake by defining zones of attraction and repulsion.

To solve this equation, the Euler–Lagrange of (3.1) is worked out (typically in closed form), and a gradient descent algorithm is used. All the terms are combined in a linear combination, allowing them to be balanced according to the needs of the user. Due to its flexibility, the active contour modelwas very popular in the literature as well as in applications. It fits very well into the interactive segmentation paradigm because constraints can be added very easily, and it can be quite fast because it uses a so-called Lagrangian framework. The contour itself is discretized at regular interval points and evolves according to (3.1). Convergence towards a local minimum of the energy is guaranteed, but may require many iterations. In practice, there are some difficulties: the snake energy is flexible but difficult to tune. Because of the contour evolution, points along the contour tend to spread out or bunch up, requiring regular and frequent resampling. There can also be topological difficulties, for instance causing the snake to self-intersect. The snake is also sensitive to its parametrization and to initialization. Finally, even though a local optimum is guaranteed, in practice, it may not be of good quality due to noise sensitivity.

One major difficulty with snakes is that they can be extended to 3D viatriangulation, but such extensions can be complicated, and topological problems plaguing snakes in 2D are usually more difficult to avoid in 3D. However, 3D active surfaces are still widely used, because they make it easy to improve or regularize a triangulated surface obtained by other means. For instance, the brain segmentation software FreeSurfer includes such a method. To distinguish them from other models we are going to introduce now, snake-like active contours or surfaces are sometimes called *parametric deformable models*.

Level Sets

One way to avoid altogether some of the problems brought about by the way parametric deformablemodels are discretized, is to embed the contour into a higherdimensional manifold. This idea gave rise to *level sets*, proposed by Osher and Sethian in 1988 [53]. Remarkably, this is around the same time when active contours
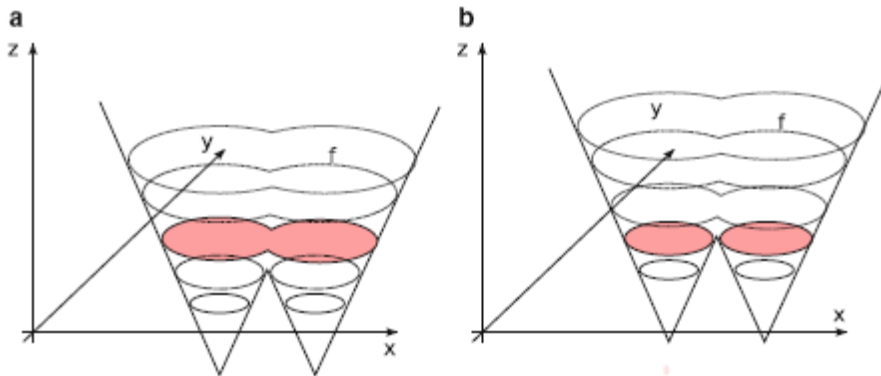

Fig.3 Embedding and evolving a curve as a level set of a higher-dimension function. The zerolevel of function is shown in color, representing a 2D contour.

To evolve the contour, the whole function evolves. Note that topology changes can occur in the contour, while the embedding surface shows no such effect were proposed. However level sets were initially proposed for computational fluid dynamics and numerical simulations. They were applied to imaging somewhat later [43, 62]. A contour is represented on the surface *S* of an evolving regular function□by its zero level-set, which is simply the threshold of the function□at zero. By using sufficiently regular embedding functions □, namely signed distance transforms from an initial contour, it was possible to propose effective evolution equations to solve similar problems to Lagrangian active contours. The main advantages of the level-sets method were that contour resampling was no longer necessary, and contour self-intersection (shock solutions) was avoided because level sets were able to change topology easily. This means practically that it was possible at least in theory to initialize a segmentation by drawing a box around a series of object of interest, and the level set could find a contour around each of them. This was seen as a major benefit by the vision community.The level set Eulerian formulation (where the whole space is discretized) is thoughtto offer better theoretical guarantees than the Lagrangian framework of previous non-embedded formulations, and the simulation of function evolution is a wellresearched topic with many usable and interesting results. Finally, the formulation is dimension independent. Level sets work virtually unchanged in 3D or more, which is a major benefit. There are also a number of drawbacks. First, the level set formulation is more
expensive than earlier active contour formulations. It requires the iterative solving of PDEs in the whole space, which is expensive. In practice, it is possible to limit the computation in a narrow band around the contour, but this is still more costly than if they were limited to the contour itself, and requires the resampling that was sought to be avoided. The surface *S* of function □is implicitly represented by the function itself, but it requires more space than the contour. In 3D or more, this may be prohibitive. Some contour motions are not representable (e.g. contour rotation), but this is a minor problem. More importantly, the fact that level-sets can undergo topology changes is actually a problem in image analysis, where it is useful to know that a contour initialized somewhere will converge to a single simple closed contour. In some cases, a contour can split or even disappear completely, leading to undesirable results.

$$\psi_t + F|\nabla \psi_t| = 0,$$

……………………….(5)

where *F* is the so-called speed function. Malladi and Sethian proposed the following for *F*:

$$F = \frac{1 - \varepsilon \kappa}{1 + |\nabla I|} + \beta \left(\nabla \psi . \nabla |\nabla I| \right).$$

…….(6)

The first part of the equation is a term driving the embedding function ψ towards contours of the image with some regularity and smoothing controlled by the curvature κ. The amount of smoothing is controlled by the parameter $\sum$. The second term is a "balloon" force that tends to expand the contour. It is expected that the contour initially be placed inside the object of interest, and that this balloon force should be reduced or eliminated after some iterations, controlled by the parameter β. We see here that even though this model is relatively simple for a level-set one, it already has a few parameters that are not obvious to set or optimize.

Geodesic Active Contours

An interesting attempt to solve some of the problems posed by overly general level sets was to go back and simplify the problem, arguing for consistency and a geometric interpretation of the contour obtained. The result was the geodesic active contour (GAC), proposed by Caselles et al. in 1997 [10]. The level set formulation is the following:

$$\psi_t = |\nabla\psi|\,\mathrm{div}\left(g(I)\frac{\nabla\psi}{|\nabla\psi|}\right).$$

.......(7)

This equation is virtually parameter-free, with only a g function required. This function is a *metric* and has a simple interpretation: it defines at point x the cost of a contour going through x. This metric is expected to be positive definite, and in most cases is set to be a scalar functional with values in R+. In other words, the GAC equation finds the solution of:

$$\mathrm{argmin}_C \int_C g(s)\,\mathrm{d}s,$$

......(8)

where C is a closed contour or surface. This is the minimal closed path or minimal closed surface problem, i.e. finding the closed contour (or surface) with minimum weight defined by g. In addition to simplified understanding and improved consistency, (3.4) has the required form for Weickert's PDE operator splitting [28, 68],allowed PDEs to be solved using separated semi-implicit schemes for improved efficiency. These advances made GAC a reference method for segmentation, which is now widely used and implemented in many software packages such as ITK. The GAC is an important interactive segmentation method due to the importance of initial contour placement, as with all level-sets methods. Constraints such as forbidden or attracting zones can all be set through the control of function g, which has an easy interpretation. As an example, to attract the GAC towards zones of actual image contours, we could set

$$g \equiv \frac{1}{1+|\nabla I|^p},$$

........(9)

With $p = 1$ or 2. We see that for this function, g is small (costs little) for zones where the gradient is high. Many other functions, monotonically decreasing for increasing values for ∇I, can be used instead. One point to note, is that GAC has a so-called *shrinking bias*, due to the fact that the globally optimal solution for (3.5) is simply the null contour (the energy is then zero). In practice, this can be avoided with balloon forces but the model is again non-geometric. Because GAC can only find a local optimum, this is not a serious problem, but this does mean that contours are biased towards smaller solutions.

RandomWalkers

In order to correct some of the problems inherent to graph cuts, Grady introduced the RandomWalker (RW) in 2004 [29,32].We set ourselves in the same framework as in the Graph Cuts case with a weighted graph, but we consider from the start a multilabel problem, and, without loss of generality, we assume that the edgeweights are all normalized between 0 and 1. This way, they represent the probability that a random particle may cross a particular edge to move from a vertex to a neighboring one. Given a set of starting points on this graph for each label, the algorithm considers the probability for a particle moving freely and randomly on this weighted graph to reach any arbitrary unlabelled vertex in the graph before any other coming from the other

labels. A vector of probabilities, one for each label, is therefore computed at each unlabeled vertex. The algorithm considers the computed probabilities at each vertex and assigns the label of the highest probability to that vertex. Intuitively, if close to a label starting point the edge weights are close to 1, then its corresponding "random walker" will indeed walk around freely, and the probability to encounter it will be high. So the label is likely to spread unless some other labels are nearby. Conversely, if somewhere edge weights are low, then the RW will have trouble crossing these edges. To relate these observations to segmentation, let us assume that edge weights are high within objects and low near edge boundaries. Furthermore, suppose that a label starting point is set within an object of interest while some other labels are set outside of it. In this situation, the RW is likely to assign the same label to the entire object and no further, because it spreads quickly within the object but is essentially stopped a the boundary. Conversely, the RW spreads the other labels outside the object, which are also stopped at the boundary. Eventually, the whole image is labeled with the object of interest consistently labeled with a single value.

Watershed

While there are many variations on discrete segmentationmethods, we will consider one last method: the Watershed Transform (WT). It was introduced in 1979 by Beucher and Lantu´ejoul [6] by analogy to the topography feature in geography. It can be explained intuitively in the following manner: consider a gray-level image to be a 3D topographical surface or terrain. A drop of water falling onto this surface would follow a descending path towards a local minimum of the terrain.The set of points, such that drops falling onto them would flow into the same minimum, is called a *catchment basin*. The set of points that separate catchment basins form the *watershed line*. Finally, the transform that takes an image as input and produces its set of watershed lines is called the *Watershed Transform*. To use
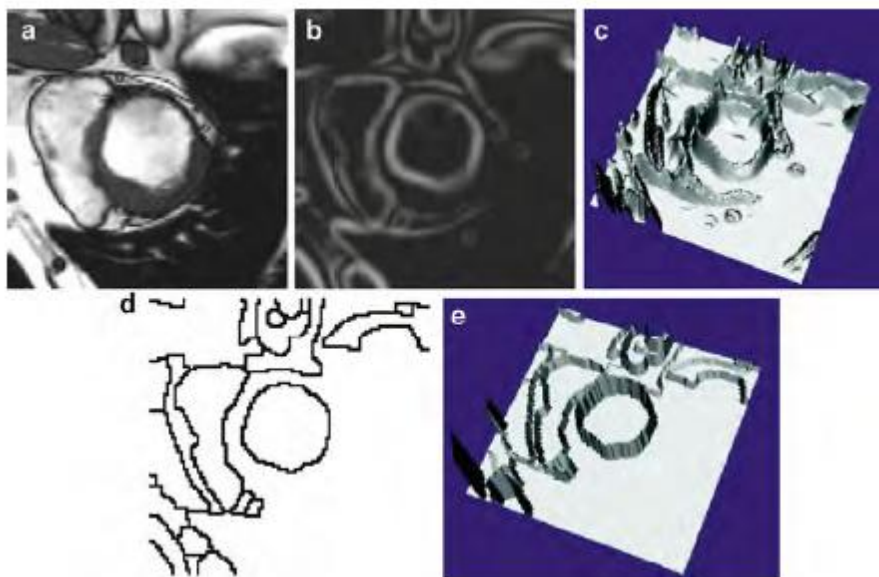

Fig. 4 Watershed segmentation: (**a**) anMRI image of the heart, (**b**) its smoothed gradient, (**c**) the gradient seen as a topographic surface, (**d**) Watershed of the gradient, and (**e**) topographical view of the watershed

this transform in practical segmentation settings, we must reverse the point of view somewhat. Assume now that labels are represented by lakes on this terrain and that by some flooding process, the water level rises evenly. The set of points that are such that waters from different lakes meet is also called the watershed line. Now this watershed line is more constrained, because there are only as many lines as necessary to separate all the lakes. This intuitive presentation is useful but does not explain why theWT is useful for segmentation. As the "terrain", it is useful to consider the magnitude of the gradient of the image. On this gradient image, interior objects will have values close to zero and will be surrounded by zones of high values: the contours of the objects. They can therefore be assimilated to catchment basins, and the WT can delineate them well (see Fig. 4).The WT is a seeded segmentation method, and has many interesting interpretations.If we consider the image again as a graph as in the GC setting, then on this graph the set of watershed lines from the WT form a graph cut. The edges of this tree can be weighted with a functional derived from a gradient exactly as in the GC case. Computing the WT can be performed in many efficient ways [46, 67], but an interesting one is to consider the Maximum Spanning Forest (MSF) algorithm [19]. In this algorithm, the classical graph algorithm for maximum

spanning tree (MST) is run on the graph of the image, following for instance Kruskal's algorithm [41,59], with the following difference: when an edge selected by the MST algorithm is connected with a seed, then all vertices that are connected with it become also labeled with this seed, and so on recursively. However, when an edge selected by the MST algorithm would be connecting two different seeds, the connection is simply not performed. It is easy to show that (1) eventually all edges of the graph are labeled with this algorithm; (2) the set of edge that are left connected form a graph cut separating all the seeds; and (3) the labels are connected to the seeds by subtrees. The result is a MSF, and the set of unconnected edges form a watershed line. The MSF algorithm can be run in quasi-linear time [20].

A Unifying Framework

We propose to optimize the following general discrete energy:

$$\operatorname{argmin}_x E(x) = \sum_{u \in \mathscr{V}} w_u^p |x_u - y_u|^q + \sum_{(u,v) \in \mathscr{E}} w_{u,v}^p |x_u - x_v|^q,$$

…………………………….(10)

The *p* and *q* terms are integer exponents. In cases where the optimal x_- is not binary, we threshold it in the end as in (3.13). An analysis of the influence of *p* and *q* provides us with Table 1. In this table, we find some well-known algorithms, such as previously mentioned GR and RW, in addition to the Shortest Path Forests algorithm [20], that uses forests of shortest path leading to seeds as segmentation criteria. Most of the other cases are not interesting (Voronoi diagrams, for instance), but the case $q = 1$ or 2 and $p \rightarrow \infty$ is novel and interesting: this is the Power Watershed algorithm [15].

Table 1 Our generalized scheme for image segmentation includes several popular segmentation algorithms as special cases of the parameters *p* and *q*.The power watershed are previously unknown in the literature, but may be optimized efficiently with a MSF calculation

$q \backslash p$	0	Finite	∞
1	Collapse to seeds	Graph cuts	Power watershed $q = 1$
2	ℓ_2 norm Voronoi	Random walker	Power watershed $q = 2$
∞	ℓ_1 norm Voronoi	ℓ_1 norm Voronoi	Shortest path forest

Power Watershed

Among the drawbacks of traditional watershed as described in Sect. 3.2.5.3 are the following: (1) watershed has no energy interpretation and is purely a segmentation algorithm; (2) watershed segmentations are not unique: for the same seed placement and edge weights, the same definition can provide different results; (3) watershed
results tend to leak in the presence of weak boundaries.We intend to solve all three problems.

An analysis of the convergence of (3.14) in the case $q = 1$ or 2 and $p \rightarrow \infty$ led us to the algorithm shown below. This algorithm is illustrated where we compare qualitatively the results of PW with the other classical discrete segmentation algorithms, namely GC, RW, SPF and the classical WT in the form of a MSF. More details on the Power Watershed algorithm can be found in [16]. We show the PW algorithm performs very well in terms of quantitative results, that qualitatively PW is devoid of size bias and grid artifacts, while being only slightly.

Algorithm: power watershed algorithm, optimizing $p \rightarrow \infty$, $q \geq 1$

Data: A weighted graph $\square(V, E)$ and a reference image *y* containing seed information

Result: A **potential function** *x* and a labeling *s* associating a label to each vertex.
Set *x* values as unknown except seed values. Sort the edges of *E* by decreasing order of weight.

while *any node has an unknown potential* **do**
Find an edge (or a plateau) *EMAX* in *E* of maximal weight; denote by *S* the set of nodes connected by *EMAX*.
if *S contains any nodes with known potential* **then**
Find *xS* minimizing (3.14) (using the input value of *q*) on the subset *S*
with the weights in *EMAX* set to $w_{ij} = 1$, all other weights set to $w_{ij} = 0$
and the known values of *x* within *S* fixed to their known values.
Consider all *xS* values produced by this operation as known.

else

Merge all of the nodes in S into a single node, such that when the value of x for this merged node becomes known, all merged nodes are assigned the same value of x and considered known. Set $si = 1$ if $xi \geq 12$ and $si = 0$ otherwise.
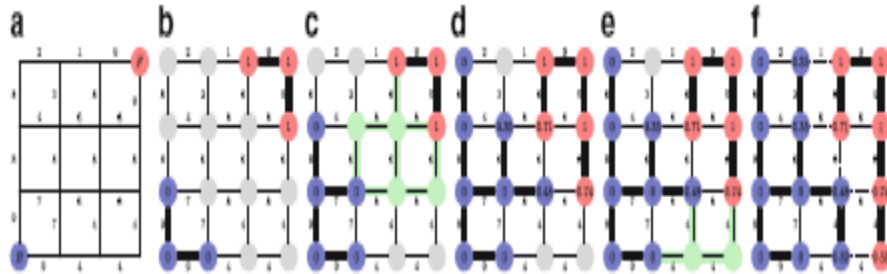

Fig. 5. Illustration of the different steps for Algorithm in the case $q = 2$. The values on the nodes correspond to x, their color to s. The bold edges represents edges belonging to a Maximum Spanning Forest. (**a**) A weighted graph with two seeds, all maxima of the weight function are seeded, (**b**) First step, the edges of maximum weight are added to the forest, (**c**) After several steps,the next largest edge set belongs to a plateau connected to two labeled trees, (**d**) Minimize (3.14) on the subset (considering the merged nodes as a unique node) with $q = 2$ (i.e., solution of the Random Walker problem), (**e**) Another plateau connected to three labeled vertices is encountered, and (**f**) Final solutions x and s obtained after few more steps. The q-cut, which is also an MSF cut, is represented in *dashed lines*

slower than standard watershed and much faster than either GC or RW, particularly in 3D. The PW algorithm provides a unique unambiguous result, and an energy interpretation for watershed, which allows it to be used in wider contexts as a solver, for instance in filtering [17] and surface reconstruction. One chief advantage of PW with respect with GC for instance, is its ability to compute a globally optimal result in the presence of multiple labels. When segmenting multiple objects this can be important.
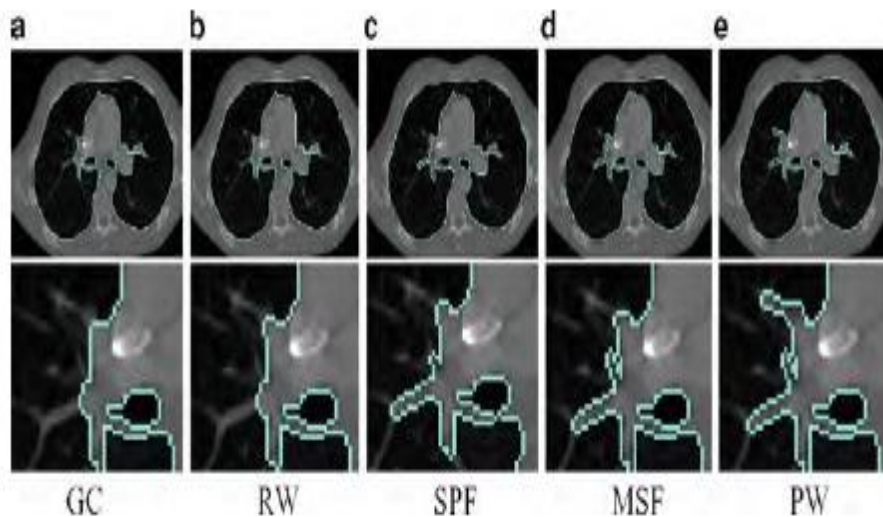

Fig. 6. Slides of a 3D lung segmentation. The foreground seed used for this image is a small rectangle in one slice of each lung, and the background seed is the frame of the image (**a**) GC (**b**) RW(**c**) SPF (**d**) MSF (**e**) PW

IV.   RESULTS

Comparisons of four different filters at $\alpha = 0$ and at $\alpha = 45°$ are shown in Figures 8 and 9, respectively. The four filters are the square-shaped median, LOCO, and averaging filters and the plus-shaped median filter. Significant differences among the responses of these filters are easily observed. The corner "passband" and "stopband" information for these filters are collected in Table below. The "perfect rejection" and "perfect preservation" bands correspond to regions of $\square$ where $r(\square, \alpha) = 0$ and $r(\square, \alpha) = 1$ respectively.

Figure 7. Comparison of fractional corner preservation of square-shaped median, LOCO, and averaging filters and the plus-shaped median filter at corner rotations α= 0.
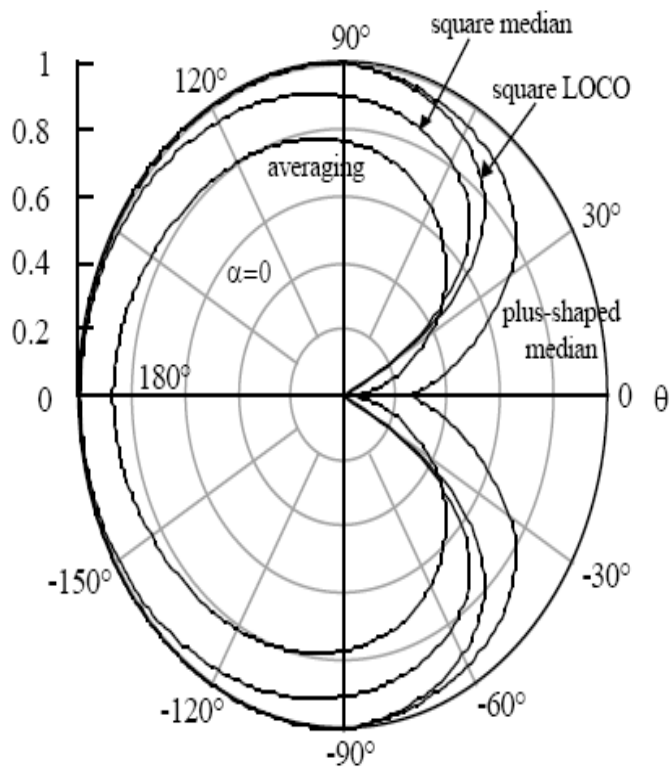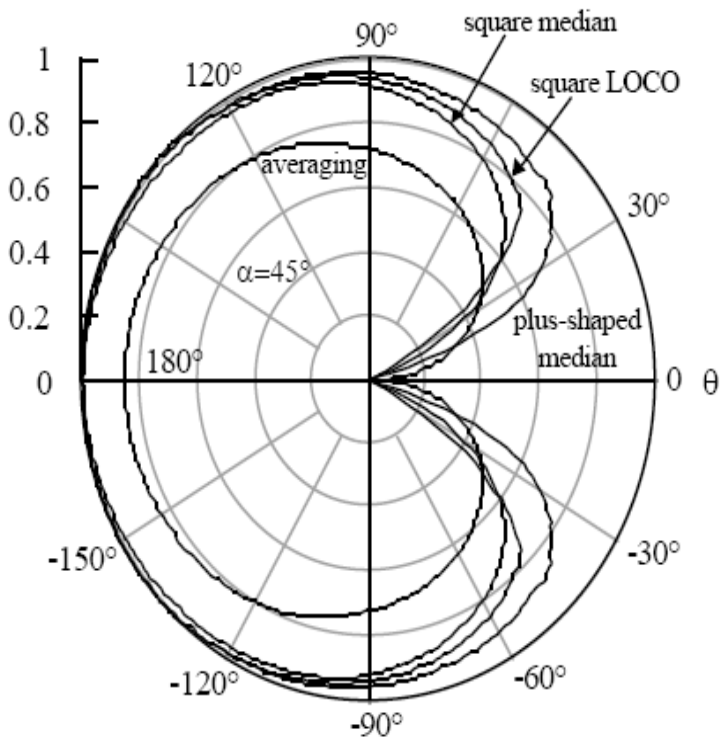

Figure 8. Comparison of fractional corner preservation of square-shaped median, LOCO, and averaging filters and the plus-shaped median filter at corner rotations α= 45°.

Table 2. Comparison of filter corner responses.

Filter (Shape)	Rotation	Perfect Rejection ($r = 0$) $\theta \leq$	Stopband $s < -10.7$dB ($r < .293$) $\theta \leq$	Transition Band Width	Passband $s > -3$dB ($r > .707$) $\theta \geq$	Perfect Preservation ($r = 1$) $\theta \geq$
Median (Square)	$\alpha = 0$	27°	31°	17°	48°	180°
	$\alpha = 45°$	19°	27°	22°	49°	180°
LOCO (Square)	$\alpha = 0$	27°	31°	12°	43°	90°
	$\alpha = 45°$	27°	32°	12°	44°	135°

The values in Table above indicate that the square-shaped LOCO filter has the sharpest transition between corner removal and corner preservation for $\alpha = 0$, and that its response changes the least when α changes from 0 to 45°. Thus, the LOCO filter is the closest of these four filters to an "ideal" filter with a very small transition band and a corner response that changes little for different corner orientations. However, there are usually many considerations taken into account other than just the response at corners when selecting a two-dimensional filter. For example, the degree of noise reduction offered by the filters in Table varies, as does the type of noise they perform best against. Also, the corner response characteristics of opening, OC, CO, and the LOCO filter are all identical, despite obvious visual differences among the results of the filters in real image processing applications. Clearly, the corner response is not a complete description of the behavior of a filter. Although the corner response technique is a valuable analysis tool, it does not indicate how to design a filter with given corner response characteristics. The cutoff angles of filters vary with the angle of rotation α and the shape of the filter, but usually the cutoff angle cannot be drastically changed for a given filter. Also,the fractional preservation $r(\square, \alpha)$ only indicates the amount of area preserved, not any change in the shape of that area. Some filters, especially the median and morphological filters, achieve partial preservation of corners by changing the shape of the corners: the median filter rounds off sharp corners, while morphological operators tend to make corners look more like their structuring element. Thus a 45° corner filtered by open-closing with a square structuring element is 75% preserved [$r(45°,0) = 0.75$], but the result may look like a more obtuse angle because this operation tends to clip corners to make them as close to right angles as possible.

V.　CONCLUSION

This chapter introduced three new methods for analyzing the behavior of nonlinear filters. These analysis techniques demonstrate some important differences among the morphological, median, averaging, and MLV filters. Continuous time analysis yields the peak response of filters to periodic signals of different frequencies. This analysis highlights the differences between the morphological and non-morphological filters in the presence of rapidly fluctuating periodic signals or noise. The breakdown point gives a measure of the resistance of a filter to large outliers in its input. Using order statistics to limit the range of outputs of a filter allows custom filters with almost any breakdown point to be designed.The last technique developed in this chapter analyzes the behavior of twodimensional filters at corners. This method finds the fraction of corners of different angles and orientations preserved by a filter, and is important because it is one of very few techniques available to analyze the behavior of filters on twodimensional structures. The corner response of a filter gives an indication of whether the filter is more likely to preserve details and sharp features in an image or remove them. The analysis techniques introduced in this chapter provide a significant improvement in understanding the behavior of nonlinear filters, especially their response to high frequency periodic signals, impulse noise, and two-dimensional corners. In conclusion, we argue that seeded or interactive segmentation is useful in medical imaging. Compared with model-based segmentation, seeded segmentation is more robust in actual image analysis applications, as opposed to computer vision. The ability to separate seeds/markers, use contour information, and perform contour optimization are very useful, as these elements generally result in a higher likelihood of good results. From this point of view, we argue that segmentation is a process and not merely an operator.In general, the literature focuses on contour placement optimization at the expense of the other two components, with some rare exceptions. This is unfortunate but understandable with respect to seeds/markers, because they are highly application dependent. The choice of methods for obtaining contour information is also limited, and this is probably a good area for future research. One conclusion of this study is that contour placement optimization methods are important. More recent methods focus on optimization robustness, which is important. For someone not yet experienced in medical segmentation, simpler, more robust methods should be

preferred over complex ones. Among those, power-watershed is a good candidate because of its combination of speed, relative robustness, ability to cope with multiple labels, absence of bias and availability (the code is easily available online). The random walker is also a very good solution, but is not generally and freely available. We have not surveyed or compared methods that encompass shape constraints. We recognize that this is important in some medical segmentation methods, but this would require another study altogether.

REFERENCES

[1]   Adams, R., Bischof, L.: Seeded region growing. IEEE Trans. Pattern Anal. Mach. Intell. **16**(6), 641–647 (1994)

[2]   Appleton, B.: Globally minimal contours and surfaces for image segmentation. Ph.D. thesis, University of Queensland (2004). Http://espace.library.uq.edu.au/eserv/UQ:9759/ba thesis.pdf

[3]   Appleton, B., Sun, C.: Circular shortest paths by branch and bound. Pattern Recognit. **36**(11), 2513–2520 (2003)

[4]   Appleton, B., Talbot, H.: Globally optimal geodesic active contours. J. Math. Imaging Vis. **23**, 67–86 (2005)

[5]   Ardon, R., Cohen, L.: Fast constrained surface extraction by minimal paths. Int. J. Comput. Vis. **69**(1), 127–136 (2006)

[6]   Beucher, S., Lantu´ejoul, C.: Use of watersheds in contour detection. In: International Workshop on Image Processing. CCETT/IRISA, Rennes, France (1979)

[7]   Boykov, Y., Kolmogorov, V.: An experimental comparison of min-cut/max- flow algorithms for energy minimization in vision. PAMI **26**(9), 1124–1137 (2004)

[8]   Boykov, Y., Veksler, O., Zabih, R.: Fast approximate energy minimization via graph cuts. IEEE Trans. Pattern Anal. Mach. Intell. **23**(11), 1222–1239 (2001)

[9]   Canny, J.: A computational approach to edge detection. IEEE Trans. Pattern Anal.Mach. Intell. **8**(6), 679–698 (1986)

[10]   Caselles, V., Kimmel, R., Sapiro, G.: Geodesic active contours. Int. J. Comput. Vis. **22**(1), 61–79 (1997)

[11]   Chambolle, A.: An algorithm for total variation minimization and applications. J. Math. Imaging Vis. **20**(1–2), 89–97 (2004)

[12]   Chan, T., Bresson, X.: Continuous convex relaxation methods for image processing. In: Proceedings of ICIP 2010 (2010). Keynote talk, http://www.icip2010.org/file/Keynote/ICIP

[13]   Chan, T., Vese, L.: Active contours without edges. IEEE Trans. Image Process. **10**(2), 266–277 (2001)

[14]   Cohen, L.D., Kimmel, R.: Global minimum for active contour models: A minimal path approach. Int. J. Comput. Vis. **24**(1), 57–78 (1997). URL citeseer.nj.nec.com/cohen97global. html

[15]   Couprie, C., Grady, L., Najman, L., Talbot, H.: Power watersheds: A new image segmentation framework extending graph cuts, random walker and optimal spanning forest. In: Proceedings of ICCV 2009, pp. 731–738. IEEE, Kyoto, Japan (2009)

[16]   Couprie, C., Grady, L., Najman, L., Talbot, H.: Power watersheds: A unifying graph-based optimization framework. IEEE Transactions on Pattern Analysis and Machine Intelligence, **33**(7), 1384–1399 (2011)

[17]   Couprie, C., Grady, L., Talbot, H., Najman, L.: Anisotropic diffusion using power watersheds. In: Proceedings of the International Conference on Image Processing (ICIP), pp. 4153–4156. Honk-Kong (2010)

[18]   Couprie, C., Grady, L., Talbot, H., Najman, L.: Combinatorial continuous maximum flows. SIAM J. Imaging Sci. (2010). URL http://arxiv.org/abs/1010.2733. In revision

[19]   Cousty, J., Bertrand, G., Najman, L., Couprie, M.:Watershed cuts: Minimum spanning forests and the drop of water principle. In: IEEE Transactions on Pattern Analysis and Machine Intelligence, pp. 1362–1374. (2008)

[20]   Cousty, J., Bertrand, G., Najman, L., Couprie, M.: Watershed cuts: Thinnings, shortest-path forests and topological watersheds. IEEE Trans. Pattern Anal. Mach. Intell. **32**(5), 925–939 (2010)

[21]   Cserti, J.: Application of the lattice Green's function for calculating the resistance of an infinite network of resistors. Am. J. Phys. **68**, 896 (2000)

[22]   Daragon, X., Couprie, M., Bertrand, G.: Marching chains algorithm for Alexandroff- Khalimsky spaces. In: SPIE Vision Geometry XI, vol. 4794, pp. 51–62 (2002)

[23]   Dougherty, E., Lotufo, R.: Hands-on Morphological Image Processing. SPIE press, Bellingham (2003)

[24]   Doyle, P., Snell, J.: Random Walks and Electric Networks. Carus Mathematical Monographs, vol. 22, p. 52. Mathematical Association of America, Washington, DC (1984)

[25]   Ford, J.L.R., Fulkerson, D.R.: Flows in Networks. Princeton University Press, Princeton, NJ (1962)

[26]   Geman, S., Geman, D.: Stochastic relaxation, gibbs distributions, and the bayesian restoration of images. PAMI **6**, 721–741 (1984)

[27] Goldberg, A., Tarjan, R.: A new approach to the maximum-flow problem. J. ACM **35**, 921–940 (1988)

[28] Goldenberg, R., Kimmel, R., Rivlin, E., Rudzsky, M.: Fast geodesic active contours. IEEE Trans. Image Process. **10**(10), 1467–1475 (2001)

[29] Grady, L.: Multilabel random walker image segmentation using prior models. In: Computer Vision and Pattern Recognition, IEEE Computer Society Conference, vol. 1, pp. 763–770 (2005). DOI http://doi.ieeecomputersociety.org/10.1109/CVPR.2005.239

[30] Grady, L.: Computing exact discrete minimal surfaces: Extending and solving the shortest path problem in 3D with application to segmentation. In: Computer Vision and Pattern Recognition, 2006 IEEE Computer Society Conference, vol. 1, pp. 69–78. IEEE (2006)

[31] Grady, L.: Random walks for image segmentation. IEEE Trans. Pattern Anal. Mach. Intell. **28**(11), 1768–1783 (2006)

[32] Grady, L., Funka-Lea, G.: Multi-label image segmentation for medical applications based on graph-theoretic electrical potentials. In: Computer Vision and Mathematical Methods in Medical and Biomedical Image Analysis, pp. 230–245. (2004)

[33] Grady, L., Polimeni, J.: Discrete Calculus: Applied Analysis on Graphs for Computational Science. Springer Publishing Company, Incorporated, New York (2010)

[34] Grady, L., Schwartz, E.: Isoperimetric graph partitioning for image segmentation. Pattern Anal. Mach. Intell. IEEE Trans. **28**(3), 469–475 (2006)

[35] Guigues, L., Cocquerez, J., Le Men, H.: Scale-sets image analysis. Int. J. Comput. Vis. **68**(3), 289–317 (2006)

[36] Horowitz, S., Pavlidis, T.: Picture segmentation by a directed split-and-merge procedure. In: Proceedings of the Second International Joint Conference on Pattern Recognition, vol. 424, p. 433 (1974)

[37] Iri, M.: Survey of Mathematical Programming. North-Holland, Amsterdam (1979)

[38] Kakutani, S.: Markov processes and the Dirichlet problem. In: Proceedings of the Japan Academy, vol. 21, pp. 227–233 (1945)

[39] Kass, M., Witkin, A., Terzopoulos, D.: Snakes: Active contour models. Int. J. Comput. Vis. **1**, 321–331 (1988)

[40] Khalimsky, E., Kopperman, R., Meyer, P.: Computer graphics and connected topologies on finite ordered sets. Topol. Appl. **36**(1), 1–17 (1990)

[41] Kruskal, J.J.: On the shortest spanning subtree of a graph and the travelling salesman problem. Proc. AMS **7**(1) (1956)

[42] Levinshtein, A., Stere, A., Kutulakos, K., Fleet, D., Dickinson, S., Siddiqi, K.: Turbopixels: Fast superpixels using geometric flows. Pattern Anal. Mach. Intell. IEEE Trans. **31**(12), 2290–2297 (2009)

[43] Malladi, R., Sethian, J., Vemuri, B.: Shape modelling with front propagation: A level set approach. IEEE Trans. Pattern Anal. Mach. Intell. **17**(2), 158–175 (1995)

[44] I. Pitas and A. N. Venetsanopoulos, *Nonlinear Digital Filters: Principles and Applications*. Boston: Kluwer Academic, 1990.

[45] A. V. Oppenheim and R. W. Schafer, *Discrete-Time Signal Processing*. Englewood Cliffs, New Jersey: Prentice Hall, 1989.

[46] J. W. Tukey, *Exploratory Data Analysis*. Reading, Massachusetts: Addison-Wesley, 1971.

[47] R. P. Borda and J. D. Frost, Jr., "Error reduction in small sample averaging through the use of the median rather than the mean," *Electroencephalography and Clinical Neurophysiology*, vol. 25, pp. 391- 392, 1968.

[48] P. Maragos and R. W. Schafer, "Morphological filters—Part I: Their settheoretic analysis and relations to linear shift-invariant filters," *IEEE Trans. Acoust., Speech, Signal Process.*, vol. 35, no. 8, pp. 1153-1169,

[49] 1987.P. Maragos and R. W. Schafer, "Morphological filters—Part II: Their relations to median, order-statistic, and stack filters," *IEEE Trans. Acoust., Speech, Signal Process.*, vol. 35, no. 8, pp. 1170-1184, 1987.

[50] B. I. Justusson, "Median filtering: Statistical properties," in *Two- Dimensional Digital Signal Processing II: Transforms and Median Filtering*, T. S. Huang, Editor. Berlin: Springer-Verlag, 1981. pp. 161- 196.

[51] S. G. Tyan, "Median filtering: Deterministic properties," in *Two- Dimensional Digital Signal Processing II: Transforms and Median Filtering*, T. S. Huang, Editor. Berlin: Springer-Verlag, 1981. pp. 197- 217.

[52] N. C. Gallagher, Jr. and G. L. Wise, "A theoretical analysis of the properties of the median filter," *IEEE Trans. Acoust., Speech, Signal Process.*, vol. 29, no. 6, pp. 1136-1141, 1981.

[53] G. Matheron, *Random Sets and Integral Geometry*. New York: Wiley, 1974. 53. J. Serra, *Image Analysis and Mathematical Morphology*, Vol. 1. London: Academic, 1982.

[54] J. Serra, Editor. *Image Analysis and Mathematical Morphology*, Vol. 2: Theoretical Advances. London: Academic, 1988.

[55] R. L. Stevenson and G. R. Arce, "Morphological filters: Statistics and further syntactic properties," *IEEE Trans. Circuits Syst.*, vol. 34, no. 11, pp. 1292-1305, 1987.

[56] G. Gerig, O. Kübler, R. Kikinis, and F. A. Jolesz, "Nonlinear anisotropic filtering of MRI data," *IEEE Trans. Med. Imag.*, vol. 11, no. 2, pp. 221- 232, 1992.

[57] 57. S. R. Sternberg, "Biomedical image processing," *IEEE Computer*, vol. 16, no. 1, pp. 22-34, 1983.

[58] S. R. Sternberg, "Grayscale morphology," *Comp. Vision, Graphics, Image Process.*, vol. 35, pp. 333-355, 1986.

[59] P. D. Wendt, E. J. Coyle, and N. C. Gallagher, "Stack filters," *IEEE Trans. Acoust., Speech, Signal Process.*, vol. 34, no. 4, pp. 898-911, 1986.

[60] J. P. Fitch, E. J. Coyle, and N. C. Gallagher, "Median filtering by threshold decomposition," *IEEE Trans. Acoust., Speech, Signal Process.*, vol. 32, pp. 1183-1188, 1984.

[61] J. P. Fitch, E. J. Coyle, and N. C. Gallagher, "Threshold decomposition of multidimensional ranked order operations," *IEEE Trans. Circuits Syst.*, vol. 32, pp. 445-450, 1985.

[62] E. J. Coyle and J.-H. Lin, "Stack filters and the mean absolute error criterion," *IEEE Trans. Acoust., Speech, Signal Process.*, vol. 36, no. 8, pp. 1244-1254, 1988.

[63] H. A. David, *Order Statistics*, 1st ed. New York: Wiley, 1970.

[64] R. V. Hogg and A. T. Craig, *Introduction to Mathematical Statistics*. 4th ed. New York: Macmillan, 1978.

[65] L. Koskinen, J. Astola, and Y. Neuvo, "Morphological filtering of noisy images," in *Visual Communications and Image Processing '90*, M. Kunt, Editor, *Proc. SPIE*, vol. 1360, pp. 155-165, 1990.

[66] J. Astola, L. Koskinen, and Y. Neuvo, "Statistical properties of discrete morphological filters," in *Mathematical Morphology in Image Processing*, E. R. Dougherty, Editor. New York: Marcel Dekker, 1993. pp. 93-120.